

# GENETIC ANALYSIS OF ANIMAL MODELS TO UNDERSTAND THE GENOMIC ARCHITECTURE OF SUBSTANCE USE DISORDERS

EDITED BY: Gary T. Hardiman, Roberto Ciccocioppo, Peter Kalivas and Amy C. Lossie

PUBLISHED IN: Frontiers in Psychiatry, Frontiers in Genetics and Frontiers in Neuroscience





# frontiers

## Frontiers eBook Copyright Statement

The copyright in the text of individual articles in this eBook is the property of their respective authors or their respective institutions or funders. The copyright in graphics and images within each article may be subject to copyright of other parties. In both cases this is subject to a license granted to Frontiers.

The compilation of articles constituting this eBook is the property of Frontiers.

Each article within this eBook, and the eBook itself, are published under the most recent version of the Creative Commons CC-BY licence.

The version current at the date of publication of this eBook is CC-BY 4.0. If the CC-BY licence is updated, the licence granted by Frontiers is automatically updated to the new version.

When exercising any right under the CC-BY licence, Frontiers must be attributed as the original publisher of the article or eBook, as applicable.

Authors have the responsibility of ensuring that any graphics or other materials which are the property of others may be included in the CC-BY licence, but this should be checked before relying on the CC-BY licence to reproduce those materials. Any copyright notices relating to those materials must be complied with.

Copyright and source acknowledgement notices may not be removed and must be displayed in any copy, derivative work or partial copy which includes the elements in question.

All copyright, and all rights therein, are protected by national and international copyright laws. The above represents a summary only. For further information please read Frontiers' Conditions for Website Use and Copyright Statement, and the applicable CC-BY licence.

ISSN 1664-8714

ISBN 978-2-83250-367-6

DOI 10.3389/978-2-83250-367-6

## About Frontiers

Frontiers is more than just an open-access publisher of scholarly articles: it is a pioneering approach to the world of academia, radically improving the way scholarly research is managed. The grand vision of Frontiers is a world where all people have an equal opportunity to seek, share and generate knowledge. Frontiers provides immediate and permanent online open access to all its publications, but this alone is not enough to realize our grand goals.

## Frontiers Journal Series

The Frontiers Journal Series is a multi-tier and interdisciplinary set of open-access, online journals, promising a paradigm shift from the current review, selection and dissemination processes in academic publishing. All Frontiers journals are driven by researchers for researchers; therefore, they constitute a service to the scholarly community. At the same time, the Frontiers Journal Series operates on a revolutionary invention, the tiered publishing system, initially addressing specific communities of scholars, and gradually climbing up to broader public understanding, thus serving the interests of the lay society, too.

## Dedication to Quality

Each Frontiers article is a landmark of the highest quality, thanks to genuinely collaborative interactions between authors and review editors, who include some of the world's best academicians. Research must be certified by peers before entering a stream of knowledge that may eventually reach the public - and shape society; therefore, Frontiers only applies the most rigorous and unbiased reviews. Frontiers revolutionizes research publishing by freely delivering the most outstanding research, evaluated with no bias from both the academic and social point of view. By applying the most advanced information technologies, Frontiers is catapulting scholarly publishing into a new generation.

## What are Frontiers Research Topics?

Frontiers Research Topics are very popular trademarks of the Frontiers Journals Series: they are collections of at least ten articles, all centered on a particular subject. With their unique mix of varied contributions from Original Research to Review Articles, Frontiers Research Topics unify the most influential researchers, the latest key findings and historical advances in a hot research area! Find out more on how to host your own Frontiers Research Topic or contribute to one as an author by contacting the Frontiers Editorial Office: [frontiersin.org/about/contact](https://frontiersin.org/about/contact)

# GENETIC ANALYSIS OF ANIMAL MODELS TO UNDERSTAND THE GENOMIC ARCHITECTURE OF SUBSTANCE USE DISORDERS

Topic Editors:

**Gary T. Hardiman**, Queen's University Belfast, United Kingdom

**Roberto Ciccocioppo**, University of Camerino, Italy

**Peter Kalivas**, Medical University of South Carolina, United States

**Amy C. Lossie**, National Institutes of Health (NIH), United States

**Citation:** Hardimanm G. T., Ciccocioppo, R., Kalivas, P., Lossie, A. C., eds. (2022). Genetic Analysis of Animal Models to Understand the Genomic Architecture of Substance Use Disorders. Lausanne: Frontiers Media SA.  
doi: 10.3389/978-2-83250-367-6

# Table of Contents

- 05    *Developmental Alcohol Exposure in Drosophila: Effects on Adult Phenotypes and Gene Expression in the Brain***  
Sneha S. Mokashi, Vijay Shankar, Rebecca A. MacPherson,  
Rachel C. Hannah, Trudy F. C. Mackay and Robert R. H. Anholt
- 17    *Confirmation of a Causal Taar1 Allelic Variant in Addiction-Relevant Methamphetamine Behaviors***  
Tamara J. Phillips, Tyler Roy, Sara J. Aldrich, Harue Baba, Jason Erk,  
John R. K. Mootz, Cheryl Reed and Elissa J. Chesler
- 35    *The Gut Microbiome and Substance Use Disorder***  
Jordan T. Russell, Yanjiao Zhou, George M. Weinstock and Jason A. Bubier
- 43    *Individual Differences in Different Measures of Opioid Self-Administration in Rats Are Accounted for by a Single Latent Variable***  
Yayi Swain, Niels G. Waller, Jonathan C. Gewirtz and Andrew C. Harris
- 51    *On the Use of Heterogeneous Stock Mice to Map Transcriptomes Associated With Excessive Ethanol Consumption***  
Robert Hitzemann, Denesa R. Lockwood, Angela R. Ozburn and  
Tamara J. Phillips
- 65    *Genetic Differences in Dorsal Hippocampus Acetylcholinesterase Activity Predict Contextual Fear Learning Across Inbred Mouse Strains***  
Sean M. Mooney-Leber, Dana Zeid, Prescilla Garcia-Trevizo,  
Laurel R. Seemiller, Molly A. Bogue, Stephen C. Grubb, Gary Peltz and  
Thomas J. Gould
- 77    *Genetic Modifiers of Oral Nicotine Consumption in Chrna5 Null Mutant Mice***  
Erin Meyers, Zachary Werner, David Wichman, Hunter L. Mathews,  
Richard A. Radcliffe, Joseph H. Nadeau and Jerry A. Stitzel
- 89    *Neurofilament Light Chain Is a Promising Biomarker in Alcohol Dependence***  
Yanfei Li, Ranran Duan, Zhe Gong, Lijun Jing, Tian Zhang, Yong Zhang and  
Yanjie Jia
- 98    *Mitochondria-Related Nuclear Gene Expression in the Nucleus Accumbens and Blood Mitochondrial Copy Number After Developmental Fentanyl Exposure in Adolescent Male and Female C57BL/6 Mice***  
Cali A. Calarco, Megan E. Fox, Saskia Van Terheyden, Makeda D. Turner,  
Jason B. Alipio, Ramesh Chandra and Mary Kay Lobo
- 111    *Network-Based Discovery of Opioid Use Vulnerability in Rats Using the Bayesian Stochastic Block Model***  
Carter Allen, Brittany N. Kuhn, Nazzareno Cannella, Ayteria D. Crow,  
Analyse T. Roberts, Veronica Lunerti, Massimo Ubaldi, Gary Hardiman,  
Leah C. Solberg Woods, Roberto Ciccocioppo, Peter W. Kalivas and  
Dongjun Chung

- 124 Behavioral and Gene Regulatory Responses to Developmental Drug Exposures in Zebrafish**  
Aleksandra M. Mech, Munise Merteroglu, Ian M. Sealy, Muy-Teck Teh, Richard J. White, William Havelange, Caroline H. Brennan and Elisabeth M. Busch-Nentwich
- 148 What Have We Learned (or Expect to) From Analysis of Murine Genetic Models Related to Substance Use Disorders?**  
Gary Peltz and Yalun Tan
- 158 Ankk1 Loss of Function Disrupts Dopaminergic Pathways in Zebrafish**  
Adele Leggieri, Judit García-González, Jose V. Torres-Perez, William Havelange, Saeedeh Hosseinian, Aleksandra M. Mech, Marcus Keatinge, Elisabeth M. Busch-Nentwich and Caroline H. Brennan
- 174 Genome-Wide Association Study on Three Behaviors Tested in an Open Field in Heterogeneous Stock Rats Identifies Multiple Loci Implicated in Psychiatric Disorders**  
Mustafa Hakan Gunturkun, Tengfei Wang, Apurva S. Chitre, Angel Garcia Martinez, Katie Holl, Celine St. Pierre, Hannah Bimschleger, Jianjun Gao, Riyan Cheng, Oksana Polesskaya, Leah C. Solberg Woods, Abraham A. Palmer and Hao Chen
- 188 Functional Genomic Analysis of Amphetamine Sensitivity in Drosophila**  
Caline S. Karam, Brenna L. Williams, Irina Morozova, Qiaoping Yuan, Rony Panarsky, Yuchao Zhang, Colin A. Hodgkinson, David Goldman, Sergey Kalachikov and Jonathan A. Javitch
- 199 Beyond Genes: Inclusion of Alternative Splicing and Alternative Polyadenylation to Assess the Genetic Architecture of Predisposition to Voluntary Alcohol Consumption in Brain of the HXB/BXH Recombinant Inbred Rat Panel**  
Ryan Lusk, Paula L. Hoffman, Spencer Mahaffey, Samuel Rosean, Harry Smith, Jan Silhavy, Michal Pravenec, Boris Tabakoff and Laura M. Saba
- 219 Cocaine-Induced Locomotor Activation Differs Across Inbred Mouse Substrains**  
Christiann H. Gaines, Sarah A. Schoenrock, Joseph Farrington, David F. Lee, Lucas J. Aponte-Collazo, Ginger D. Shaw, Darla R. Miller, Martin T. Ferris, Fernando Pardo-Manuel de Villena and Lisa M. Tarantino
- 230 Glucocorticoid Receptor-Regulated Enhancers Play a Central Role in the Gene Regulatory Networks Underlying Drug Addiction**  
Sascha H. Duttke, Patricia Montilla-Perez, Max W. Chang, Hairi Li, Hao Chen, Lieselot L. G. Carrette, Giordano de Guglielmo, Olivier George, Abraham A. Palmer, Christopher Benner and Francesca Telese



# Developmental Alcohol Exposure in *Drosophila*: Effects on Adult Phenotypes and Gene Expression in the Brain

Sneha S. Mokashi<sup>†</sup>, Vijay Shankar<sup>†</sup>, Rebecca A. MacPherson, Rachel C. Hannah, Trudy F. C. Mackay and Robert R. H. Anholt\*

Department of Genetics and Biochemistry and Center for Human Genetics, Clemson University, Greenwood, SC, United States

## OPEN ACCESS

### Edited by:

Gary T. Hardiman,  
Queen's University Belfast,  
United Kingdom

### Reviewed by:

Joseph Andrew Seggio,  
Bridgewater State University,  
United States  
Yong-Kyu Kim,  
Northwestern University, United States

### \*Correspondence:

Robert R. H. Anholt  
ranholt@clemson.edu

<sup>†</sup>These authors have contributed  
equally to this work

### Specialty section:

This article was submitted to  
Psychopharmacology,  
a section of the journal  
Frontiers in Psychiatry

Received: 22 April 2021

Accepted: 07 June 2021

Published: 22 July 2021

### Citation:

Mokashi SS, Shankar V,  
MacPherson RA, Hannah RC,  
Mackay TFC and Anholt RRH (2021)  
Developmental Alcohol Exposure in  
*Drosophila*: Effects on Adult  
Phenotypes and Gene Expression in  
the Brain.  
Front. Psychiatry 12:699033.  
doi: 10.3389/fpsy.2021.699033

Fetal alcohol exposure can lead to developmental abnormalities, intellectual disability, and behavioral changes, collectively termed fetal alcohol spectrum disorder (FASD). In 2015, the Centers for Disease Control found that 1 in 10 pregnant women report alcohol use and more than 3 million women in the USA are at risk of exposing their developing fetus to alcohol. *Drosophila melanogaster* is an excellent genetic model to study developmental effects of alcohol exposure because many individuals of the same genotype can be reared rapidly and economically under controlled environmental conditions. Flies exposed to alcohol undergo physiological and behavioral changes that resemble human alcohol-related phenotypes. Here, we show that adult flies that developed on ethanol-supplemented medium have decreased viability, reduced sensitivity to ethanol, and disrupted sleep and activity patterns. To assess the effects of exposure to alcohol during development on brain gene expression, we performed single cell RNA sequencing and resolved cell clusters with differentially expressed genes which represent distinct neuronal and glial populations. Differential gene expression showed extensive sexual dimorphism with little overlap between males and females. Gene expression differences following developmental alcohol exposure were similar to previously reported differential gene expression following cocaine consumption, suggesting that common neural substrates respond to both drugs. Genes associated with glutathione metabolism, lipid transport, glutamate and GABA metabolism, and vision feature in sexually dimorphic global multi-cluster interaction networks. Our results provide a blueprint for translational studies on alcohol-induced effects on gene expression in the brain that may contribute to or result from FASD in human populations.

**Keywords:** behavioral genetics, single cell RNA sequencing, transcriptomics, model organism, fetal alcohol spectrum disorder, interaction networks

## INTRODUCTION

Prenatal exposure to ethanol can trigger a wide range of adverse physiological, behavioral, and cognitive outcomes, collectively termed fetal alcohol spectrum disorder (FASD) (1–4). Fetal alcohol syndrome (FAS) has the most severe manifestations of all FASDs, including craniofacial dysmorphologies, neurocognitive deficiencies, and behavioral disorders such as hyperactivity, attention deficit disorder and motor coordination anomalies (1, 5–7). FAS/FASD

is the most common preventable pediatric disorder, often diagnostically confounded with autism spectrum disorder (8). Time, dose, and frequency of exposure are often unknown, and manifestations of FASD are diverse and become evident long after exposure. The Centers for Disease Control and Prevention found that 1 in 10 pregnant women report alcohol use and more than 3 million women in the USA are at risk of exposing their developing fetus to alcohol, despite warning labels on alcoholic beverages that indicate possible effects on prenatal development (9). Adverse consequences of fetal alcohol exposure extend throughout the lifespan.

Determining the effects of developmental alcohol exposure on adult phenotypes and gene expression in the adult brain is challenging in human populations, but can be addressed in model organisms. *Drosophila melanogaster* is an excellent model to study developmental effects of alcohol exposure, as we can control the genetic background and environmental conditions for large numbers of individuals without regulatory restrictions and at low cost. Importantly, flies exposed to alcohol experience loss of postural control, sedation, and development of tolerance (10–13), resembling human alcohol intoxication. Previous studies on the effects of developmental alcohol exposure in *Drosophila* showed reduced viability and delayed development time (14, 15), reduced adult body size (14) and disruption of neural development (16). Developmental exposure to alcohol was associated with reduction in the expression of a subset of insulin-like peptides and the insulin receptor (14), dysregulation of lipid metabolism and concomitant increased oxidative stress (17), and reduced larval food intake due to altered neuropeptide F signaling (18).

Here, we show that developmental alcohol exposure in *Drosophila* results in decreased viability, reduced sensitivity to ethanol, and disrupted sleep and activity patterns. Single cell RNA sequencing on adult fly brains following developmental alcohol exposure shows widespread sexually dimorphic changes in gene expression. These changes in gene expression resemble changes observed previously following cocaine exposure (19), indicating common neuronal and glial elements that respond to alcohol and cocaine consumption.

## MATERIALS AND METHODS

### *Drosophila* Stocks and Exposure to Ethanol

*Drosophila melanogaster* of the wild type Canton S (B) strain were maintained on cornmeal/yeast/molasses-agar medium supplemented with yeast at 25°C on a 12 h light: dark cycle with 50% humidity, in controlled adult density vials to prevent overcrowding. We allowed 5 males and 5 females to mate for 2 days and aged their progeny for 3–5 days after eclosion. We then placed 50 males and 50 females into large egg collection cages on grape juice agar and yeast paste. We acclimatized the flies to the cages for 24 h with grape juice plate changes every 12 h, and collected up to 12-h old eggs with a blunt metal needle. We placed the eggs on cornmeal-agar-molasses medium (control) or on cornmeal-agar-molasses medium containing 10% (v/v) ethanol

(ethanol) without yeast. We collected 50 eggs per vial and set up 10–15 vials per condition per collection week over a 48-h period (Figure 1). After eclosion, flies were transferred to control medium without yeast and aged as indicated for the relevant experiments. Unless otherwise indicated, all behavioral assays were performed in a controlled environment at 25°C.

### Viability

The number of flies that emerged from vials into which 50 eggs had been placed were counted and the data were analyzed using the “PROC GLM” command (Type III) in SAS v3.8 (Cary, NC) according to the model  $Y = \mu + T + \varepsilon$ , where  $Y$  is the number of eclosed flies,  $\mu$  is the population mean,  $T$  is the fixed effect of treatment (flies reared on control or ethanol medium), and  $\varepsilon$  is the residual error.

### Ethanol Sensitivity

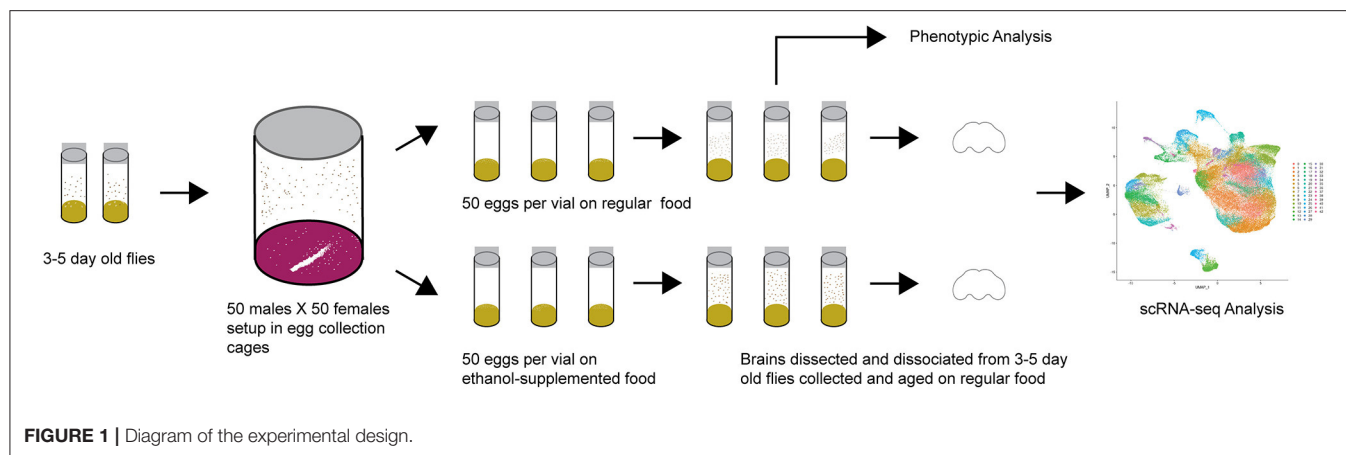
We measured ethanol sedation time as described previously (20) on 44–48 3–5 day old flies per sex per treatment. Ethanol sedation time was assessed between 8:30 a.m. and 11:30 a.m. The number of seconds required for flies to lose postural control was analyzed using the “PROC GLM” command (Type III) in SAS v3.8 according to the model  $Y = \mu + T + S + TxS + \varepsilon$ , where  $Y$  is the time to sedation,  $\mu$  is the population mean,  $T$  is the fixed effect of treatment (control or ethanol medium),  $S$  is the fixed effect of sex, and  $\varepsilon$  is the residual error.

### Sleep and Activity

Flies reared on either control or ethanol medium were placed in *Drosophila* Activity Monitors (DAM) (TriKinetics, Waltham, MA) containing a 5% sucrose, 2% agar medium at 1–2 days of age, and monitored for 7 days on a 12 h light-dark cycle. Activity was recorded as counts every time the fly interrupts an infrared beam. Sleep was defined as at least 5 min of inactivity. Only data from flies that survived the entire testing period were included, resulting in 57–64 flies per sex per treatment for analysis. Raw DAM monitor data were run in ShinyR-DAM (21), and the outputs were downloaded and parsed according to phenotype (e.g., day/night, sleep/activity, bout length/bout count) for subsequent statistical analyses. The data were analyzed using the “PROC MIXED” command (Type III) in SAS v3.8 according to the model  $Y = \mu + T + S + TxS + Rep(TxS) + \varepsilon$ , where  $Y$  is the sleep or activity phenotype,  $\mu$  is the population mean,  $T$  is the fixed effect of treatment (control or ethanol medium),  $S$  is the fixed effect of sex,  $Rep$  is the random effect of replicate and  $\varepsilon$  is the residual error. Reduced models were also performed for each sex.

### Brain Dissociation and Single Cell RNA Sequencing

For single cell RNA sequencing, we collected duplicate samples of 20 brains for each sex from flies reared on control or ethanol medium. We dissociated the brains as previously described after incubation with 450  $\mu$ l of collagenase solution [50  $\mu$ l of fresh 25 mg/ml collagenase (Gibco) in sterile water + 400  $\mu$ l of Schneider's medium] for 30 min followed by stepwise trituration - P200 pipette 5 times, 23G needle pre-wetted with PBS + BSA



5 times, and 27G pre-wetted needle 5 times (19). The resulting suspension was passed through a pre-wetted 10  $\mu$ m strainer (Celltrics, Görlitz, Germany) with gentle tapping. We counted live cells using a hemocytometer with trypan blue exclusion and proceeded with GEM generation using the Chromium controller (10X Genomics, Pleasanton, CA) for samples with >500 live cells/ $\mu$ l. We prepared libraries in accordance with 10X Genomics v3.1 protocols. We determined fragment sizes using Agilent TapeStation kits (Agilent, Santa Clara, CA)—d5000 for amplified cDNA and d1000 for libraries. We measured the concentrations of amplified cDNA and final libraries using a Qubit 1X dsDNA HS kit (Invitrogen, Waltham, MA) and a qPCR based library quantification kit (KAPA Biosystems, Roche, Basel, Switzerland). We used 12 cycles for the cDNA amplification and 12 cycles for indexing PCR. We sequenced the final libraries on an Illumina NovaSeq6000.

## Single Cell RNA Sequencing Data Analysis and Bioinformatics

We used the *mkfastq* pipeline within Cell Ranger v3.1 (10X Genomics, Pleasanton, CA) to convert BCL files from the sequence run folder to demultiplexed FASTQ files. We used the *mkref* pipeline to index the release 6 version of the *D. melanogaster* reference GCA\_000001215.4 from NCBI Genbank. For alignment, we used the *count* pipeline within Cell Ranger v3.1 with the expected cell count parameter set to 5,000 cells. We imported raw expression counts output for each sample from the Cell Ranger pipeline and analyzed these data using the Seurat v3 package in R (22). We normalized counts by regularized negative binomial regression using the *scTransform* pipeline (23). We performed integration of samples using the SCT method. *RunUMAP* and *FindNeighbors* functions were used with 10 dimensions to ordinate expression space and reduce data dimensionality. To identify cell-type clusters, we used unsupervised clustering using the *FindClusters* function and assigned the origin of clustered cells based on well-established biomarkers.

We used the Pearson residuals output from the *scTransform* pipeline as input for differential expression calculation (23). We used the MAST algorithm as the testing methodology in the *FindMarkers* function for each cluster to calculate differential

expression, which allows for the incorporation of the cellular detection rate, defined as a fraction of genes expressed in each cell, as a covariate (24). *P*-values for differential expression were adjusted for multiple-hypothesis testing using a Bonferroni correction, and adjusted *p*-values that are <0.05 were considered statistically significant.

Interaction networks were produced using the unique list of differentially expressed genes aggregated from all clusters and the stringApp (25) within Cytoscape (26).

The code for all analyses can be found here: [https://github.com/vshanka23/The-Drosophila-Brain-after-developmental-ethanol-exposure-at-Single-Cell-Resolution/blob/main/Rcode\\_for\\_analysis.R](https://github.com/vshanka23/The-Drosophila-Brain-after-developmental-ethanol-exposure-at-Single-Cell-Resolution/blob/main/Rcode_for_analysis.R)

## RESULTS

### Effects of Developmental Alcohol Exposure on Adult Phenotypes

Exposure of flies to ethanol during the embryonic and larval stages resulted in an 8.9% reduction in viability compared to flies reared on control medium (**Figure 2A**). The adult flies exposed to ethanol during development did not show any overt morphological abnormalities. We next asked whether developmental alcohol exposure would alter sensitivity to acute alcohol exposure as adults. We reared developing flies on ethanol medium and transferred the adults to control medium immediately after eclosion. The flies that developed on ethanol medium showed reduced sensitivity (longer sedation times) to acute alcohol exposure in both sexes, indicating increased tolerance to acute alcohol exposure compared to flies that developed on control medium (**Figure 2B**).

Children with FASD often have disturbed sleep (27, 28). Therefore, we used the *Drosophila* Activity Monitor system to assess the effects of developmental alcohol exposure on adult activity and sleep patterns and found that exposure to alcohol during development had sex-specific effects on these phenotypes. Overall activity in males was not affected by the ethanol treatment, but females exposed to ethanol were more active (**Figure 2C** and **Supplementary Table 1**). Ethanol exposure reduced sleep during the day in both sexes (**Figure 2D**), and day sleep in males was fragmented, with an increase in

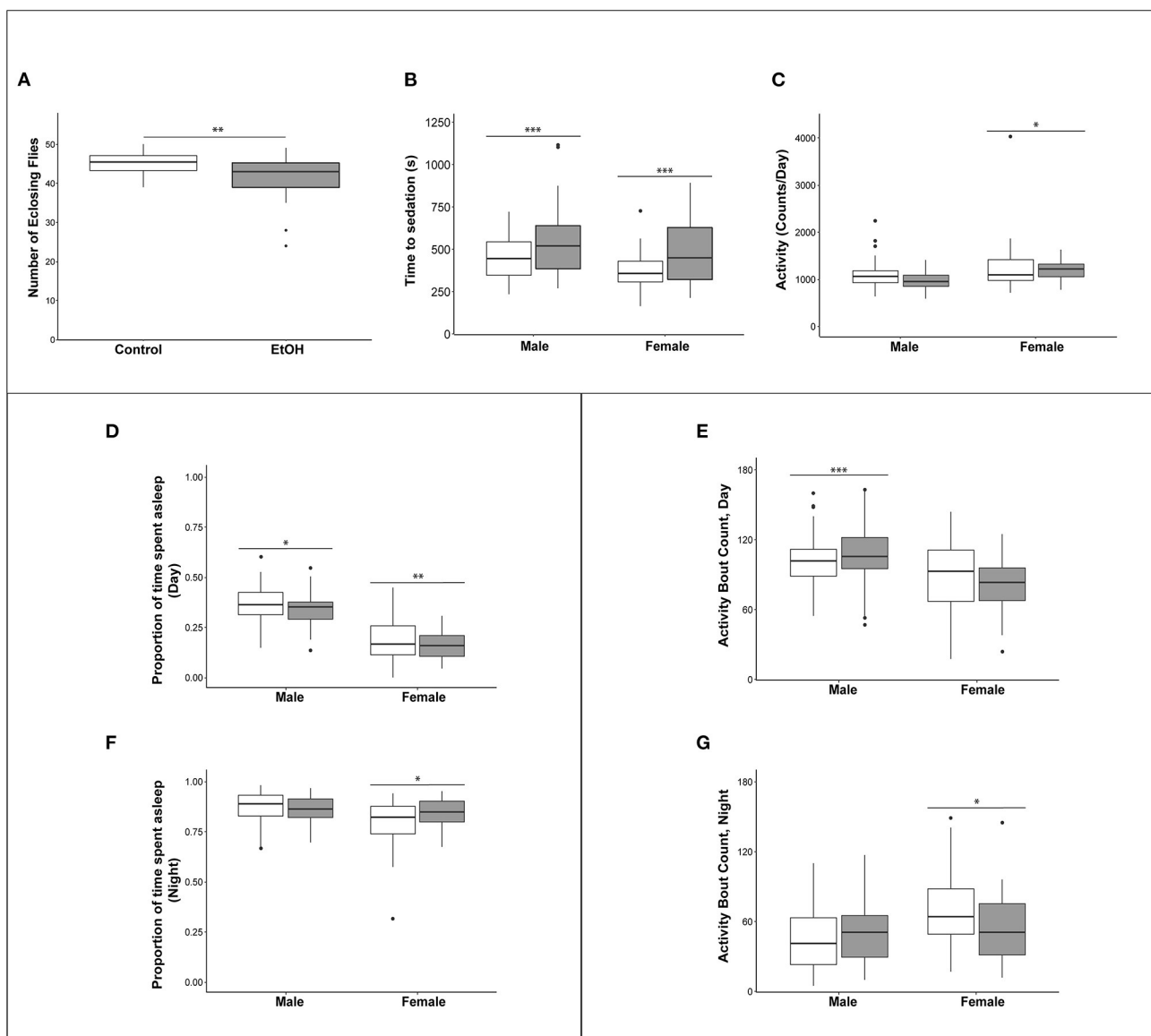


**FIGURE 2 |** Effects of developmental alcohol exposure on viability and behavioral phenotypes in adult flies. **(A)** Boxplots of viability ( $n = 12$  reps of 50 embryos per treatment), **(B)** Ethanol sensitivity ( $n = 43$ – $49$ , 3–5 day old flies per sex per treatment), **(C)** Activity, **(D)** Proportion of daytime sleep, **(E)** Activity bouts during the day, **(F)** Proportion of night time sleep, **(G)** Activity bouts during the night. Day hours are from 7 a.m. to 7 p.m., lights on 7 h after hour zero. Gray boxes indicate flies reared on medium supplemented with 10% (v/v) ethanol and white boxes indicate control flies grown on regular medium.  $n = 57$ – $64$  flies per sex per treatment for all sleep and activity phenotypes. \* $p < 0.05$ , \*\* $p < 0.01$ , \*\*\* $p < 0.001$ . Actograms are shown in **Supplementary Figure 1**.

activity bouts (**Figure 2E**). In contrast, females compensated for increased activity and reduced daytime sleep with extended periods of night sleep (**Figure 2F**) with a reduced number of activity bouts (**Figure 2G** and **Supplementary Figure 1**; **Supplementary Table 1**).

## Effects of Developmental Alcohol Exposure on Gene Expression in the Brain

We performed single cell RNA sequencing to assess the effects of developmental alcohol exposure on gene expression in the brain in males and females, with two replicates per sex and

treatment (**Figure 1**). We obtained a total of 108,571 cells across all samples, which corresponds to  $\sim 10\%$  of all cells in a *Drosophila* brain (**Supplementary Table 2**). We visualized these data using the Uniform Manifold Approximation and Projection (UMAP) non-linear dimensionality reduction method (29), which showed that all samples were uniformly represented (**Figure 3** and **Supplementary Table 2**). Unsupervised clustering of the dataset generated 43 cell clusters, which represent the major regions of the *Drosophila* brain, including neuronal and glial populations, and all major neurotransmitter cell types (**Figure 4** and **Supplementary Table 3**). We identified seven

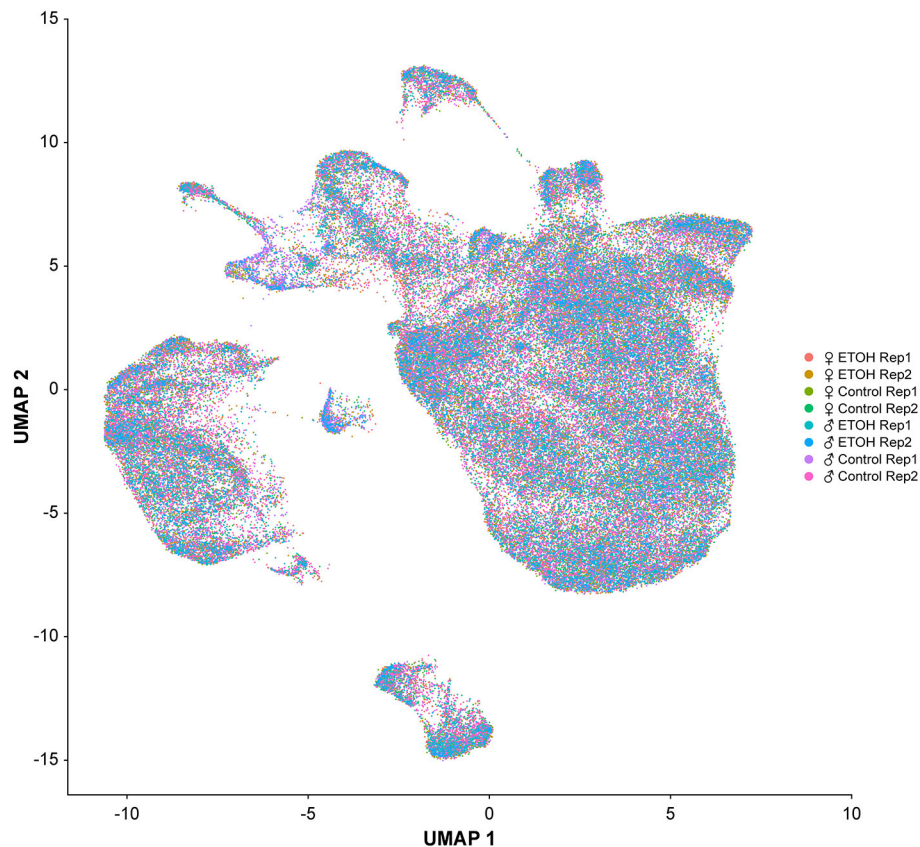


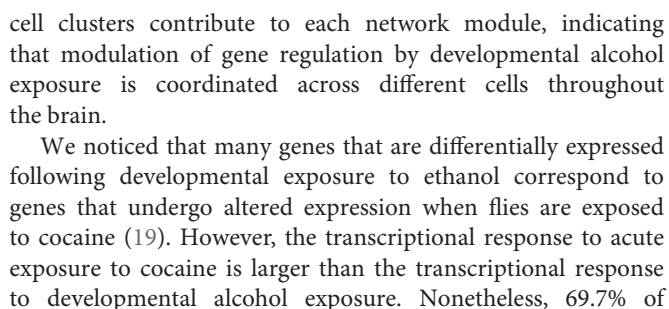
**FIGURE 3 |** Uniformity across samples of single cell transcriptomes. Gene expression patterns of single cells ( $n = 108,571$ ) from all eight samples are represented in low dimensional space using a graph-based, non-linear dimensionality reduction method (UMAP). Individual dots represent the transcriptome of each cell and the colors of the dots represent the samples to which the cells belong.

distinct populations of GABAergic neurons, two subpopulations of Kenyon cells of the mushroom bodies (integrative centers for experience-dependent modulation of behavior), and several distinct populations of glia, including two separate clusters of astrocytes as well as surface glia that form the blood-brain barrier (Figure 4).

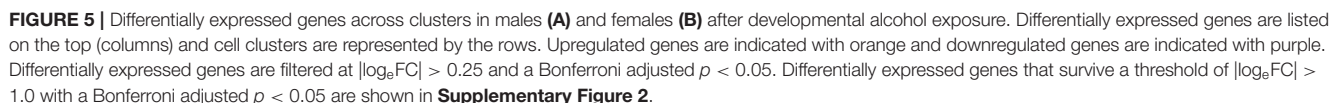
We combined all differentially expressed genes from all clusters and performed differential expression analyses. We found 119 transcripts in males and 148 transcripts in females with altered abundances after developmental alcohol exposure at a Bonferroni adjusted  $p < 0.05$ . We identified 61 upregulated and 25 downregulated genes in males, and 57 upregulated and 34 downregulated genes in females at a threshold of  $|\log_2FC| > 0.25$  (Figure 5 and Supplementary Tables 4, 5). Increasing the stringency to  $|\log_2FC| > 1.0$  (Bonferroni adjusted  $p < 0.05$ ) retained 36 upregulated and 10 downregulated genes in males and 32 upregulated and 20 downregulated genes in females (Supplementary Figure 2). Differential expression patterns are sexually dimorphic, as observed previously for cocaine-induced modulation of gene expression (19), with only 32 differentially expressed genes in common between the sexes. Changes in gene expression in the mushroom

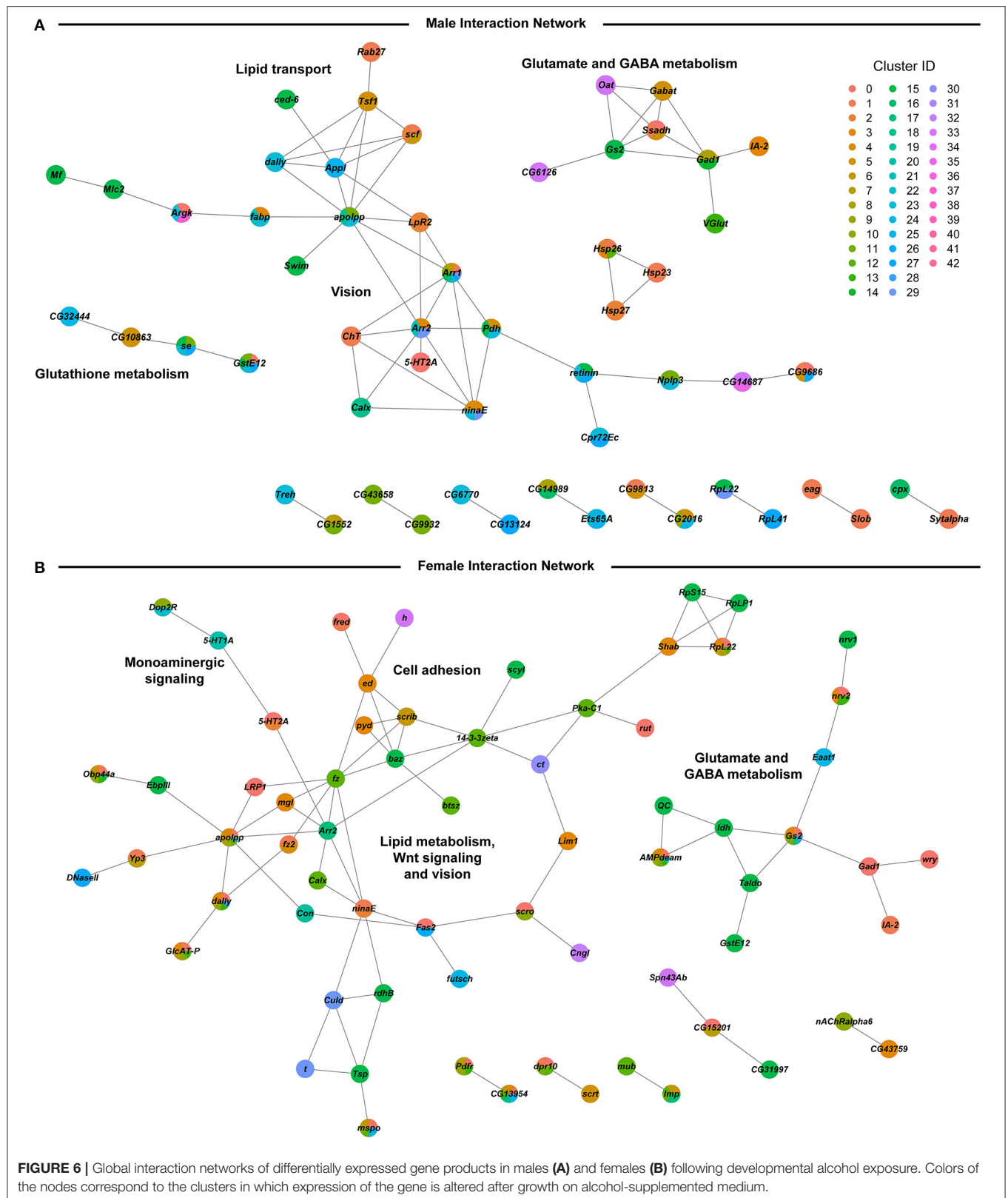
bodies, represented by cluster C12, are primarily observed in females. Developmental alcohol exposure modulates expression of several genes in glia, represented by clusters C5, C15, C23, C24, and C33, in a sexually dimorphic pattern (Figure 5). Especially noteworthy is the prominent differential expression of *lncRNA:CR31451*, a long non-coding RNA of unknown function, in multiple neuronal populations. This transcript is globally upregulated in males but downregulated in females (Figure 5 and Supplementary Figure 2). Among all differentially expressed genes, ~58% have human orthologs (DIOPT score  $\geq 3$ ; Supplementary Table 6).

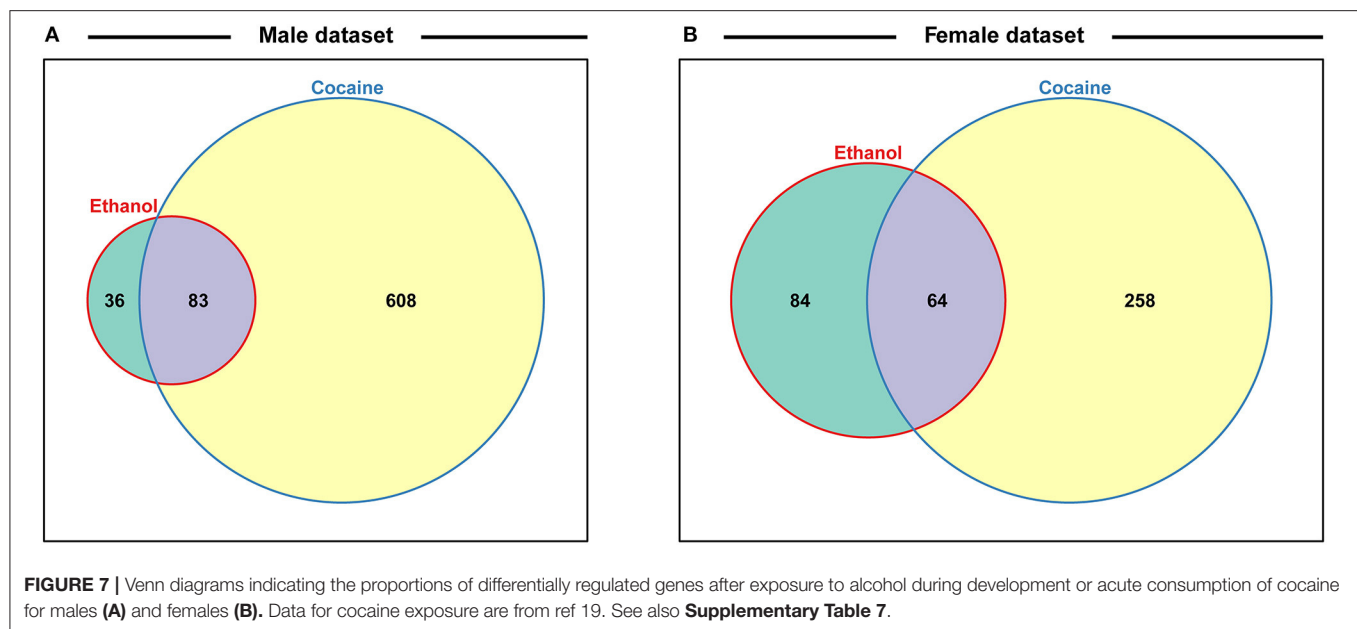
We assessed global interaction networks of differentially expressed gene products across all cell clusters for males and females separately (Figure 6). The male interaction network is composed of modules associated with glutathione metabolism, lipid transport, glutamate and GABA metabolism, and vision (Figure 6A). The female interaction network also contains modules associated with glutamate and GABA metabolism, lipid metabolism, and vision, but the composition of these modules is distinct from their male counterparts. In addition, the female network features modules associated with monoaminergic signaling, cell adhesion, and Wnt signaling (Figure 6B). Multiple



differentially expressed genes in males and 43.2% of differentially expressed genes in females in our data overlap with differentially expressed genes after consumption of cocaine (**Figure 7** and **Supplementary Table 7**), although the magnitude and direction of differential expression of common genes between the two treatments varies by cell type (**Supplementary Table 8**). Gene ontology enrichment analyses of this common set of genes in each sex highlights gene ontology categories associated with development and function of the nervous system (**Supplementary Table 9**) (31).







## DISCUSSION

We characterized the consequences of developmental alcohol exposure in *Drosophila* on viability, behavioral phenotypes, and gene expression in the brain. Characteristic features of FASD in humans include craniofacial dysmorphologies and cognitive impairments. Although we did not perform detailed morphometric measurements, we did not observe any overt morphological aberrations, and cognitive impairments are challenging to assess in *Drosophila*. Nevertheless, flies exposed to alcohol during embryonic and larval development showed changes in activity and sleep patterns (Figures 2C–G), consistent with previously observed effects of larval ethanol exposure on adult circadian rhythms (32, 33) and reminiscent of activity and sleep disturbances seen in children with FASD (27, 28). We also find that growth on alcohol supplemented medium results in reduced ethanol sensitivity of adult flies, in agreement with a previous study (Figure 2B) (14).

We hypothesize that the effects of developmental alcohol exposure on changes in gene expression in the *Drosophila* central nervous system will converge on evolutionarily conserved cellular processes. *Drosophila* is advantageous for studies on gene expression at single cell resolution because we can survey the entire brain in a single analysis, unlike studies in rodents, and pooling multiple brains of the same genotype averages individual variation. The power to detect changes in gene expression in our study is improved by only considering changes in gene expression that are consistent across replicates.

We observed changes in gene expression in adult flies, even though exposure to alcohol occurred only during the larval stages and briefly after eclosion, after which adults were collected and maintained on regular medium without alcohol. It is possible that developmental alcohol exposure may result in epigenetic

modifications that give rise to altered gene expression patterns into adulthood (34).

We observe changes in gene expression in diverse neuronal and glial cell populations (Figure 5). Since we are not able to sample all cells of the brain, it is likely that some neuronal or glial cell populations are not represented in our data. However, the major regions of the *Drosophila* brain and all major neurotransmitter cell types are represented (Figure 4 and Supplementary Table 3). The effects of developmental alcohol exposure are sexually dimorphic, similar to previously observed changes in transcript abundances following consumption of cocaine (19). Sexual dimorphism is also a hallmark of FASD, with different effects of fetal alcohol exposure on neural development and cognitive abilities between males and females (35–38). Although different genes are affected in males and females, gene ontology analysis indicates that they converge on the same biological processes, related to development and function of the nervous system (Supplementary Table 8). The considerable overlap between differentially expressed genes in response to alcohol and cocaine suggests common neural substrates that respond to toxic exposures. Genes associated with immune defense and xenobiotic detoxification, including the glutathione pathway, feature in interaction networks of differentially expressed gene products (Figure 6).

*lncRNA:CR31451* shows large sexually antagonistic responses to developmental alcohol exposure in many neuronal cell populations. Whereas, a previous study documented expression of this gene in glia (39), we only observe differential gene expression of *lncRNA:CR31451* in neurons under the conditions of our study (Figure 5). Future studies are needed to assess whether this gene product fulfills a regulatory function that affects multiple neurotransmitter signaling processes and whether its sex-antagonistic response to alcohol exposure could

in part cause the differential gene expression patterns seen in males and females.

Our observations of extensive changes in gene expression in glia in response to developmental alcohol exposure are in accordance with the role of glia in FASD. Fetal alcohol exposure leads to impaired astrocyte development and differentiation, which gives rise to microencephaly (40, 41). In addition, ethanol exposure increases permeability of the blood brain barrier (42), which in *Drosophila* is formed by the surface glia (43). Among the glial genes that show altered expression after developmental alcohol exposure in *Drosophila* are *GILT1*, which contributes to the immune defense response to bacteria (44), *Gs2* and *Eaat1*, which are involved in glutamine synthesis and transport of glutamate in astrocytes (45, 46), *GstE12* and *se*, which are involved in glutathione metabolism (47), and *fabp* and *apolpp*, which function in lipid metabolism (48, 49).

GABA signaling and glutamate signaling neuronal cell populations feature prominently in our data (Figure 4). Glutamate is also a precursor for the biosynthesis of glutathione, which is produced in glia and protects against oxidative stress and detoxification of xenobiotics (50). Developmental alcohol exposure interferes with glutamate and GABA signaling because ethanol is both an antagonist to the NMDA glutamate receptor and mimics GABA (51). Consequently, fetal alcohol exposure results in neuronal apoptosis during the rapid brain growth spurt during which the astrocytes play a major role (51, 52). Evolutionarily conserved neural processes that respond to developmental alcohol exposure in *Drosophila* thus provide a blueprint for translational studies on alcohol-induced effects on gene expression in the brain that may contribute to or result from FASD in human populations.

## DATA AVAILABILITY STATEMENT

The datasets for this study can be found in the GEO repository under accession number GSE172231.

## AUTHOR CONTRIBUTIONS

SM and RH maintained fly stocks, reared flies on developmental alcohol, measured viability, and performed brain dissociation. RM measured and analyzed ethanol sensitivity and sleep and activity phenotypes. SM performed RNA sequencing. SM and VS analyzed the RNA sequencing data. SM, TM, and RA conceived of the experiments. SM, VS, RM, TM, and RA wrote the manuscript. TM and RA provided resources. All authors contributed to manuscript revision, read, and approved the submitted version.

## FUNDING

This work was supported by grants GM128974 and DA041613 from the National Institutes of Health to TFCM and RRHA. The funding sources were not involved in the study design; collection, analysis, or interpretation of data;

writing of the report, or decision to submit the article for publication.

## SUPPLEMENTARY MATERIAL

The Supplementary Material for this article can be found online at: <https://www.frontiersin.org/articles/10.3389/fpsy.2021.699033/full#supplementary-material>

**Supplementary Figure 1** | Actograms showing average number of counts per fly per minute from females grown on (A) ethanol-supplemented food (10% v/v) and (B) regular food, and males grown on (C) ethanol-supplemented food (10% v/v) and (D) regular food. Actograms correspond to data collected for sleep and activity phenotypes shown in Figures 2D–G. Day hours are from 7:00 a.m. to 7:00 p.m., lights on 7 h after hour zero. Bin length = 5 min.

**Supplementary Figure 2** | Differentially expressed genes across clusters in males (A) and females (B) after developmental alcohol exposure. Differentially expressed genes are listed on the top (columns) and cell clusters are represented by the rows. Upregulated genes are indicated with orange and downregulated genes are indicated with purple. Differentially expressed genes are filtered at  $|\log_2FC| > 1.0$  and a Bonferroni adjusted  $p < 0.05$ .

**Supplementary Table 1** | ANOVA tables for viability, ethanol sensitivity, sleep, and activity.

**Supplementary Table 2** | Sequencing statistics. F denotes females and M denotes males. C indicates control medium and E ethanol-supplemented medium. The numbers indicate replicates 1 and 2.

**Supplementary Table 3** | Genes used to annotate cell clusters.

**Supplementary Table 4** | List of differentially expressed genes in each cluster in males. Each sheet corresponds to the male analyses for the given cluster. “Avg\_diff” is conditionally formatted to indicate up- and down-regulation of expression in ethanol compared to regular food (red: up-regulated, green: down-regulated and yellow: no difference). p\_val: raw  $p$ -value from the differential expression analysis for the given gene in the corresponding cluster. avg\_diff: the difference in the  $\log(e)$  transformed average expression of the given gene in the corresponding cluster (sheet) between the two conditions (ethanol compared to regular food). Values above zero indicate up-regulation of expression due to developmental exposure to ethanol, and likewise, values below zero represent down-regulation of expression due to ethanol. p\_val\_adj: Bonferroni adjusted  $p$ -value. The DE matrix sheet is a summary of differentially expressed genes (columns) and the clusters in which they are differentially expressed (rows) with orange indicating upregulation and purple indicating downregulation at  $|\text{avg\_diff}|$  thresholds of 0.25 and 1. The All DE per cluster sheet and the All DE sheet are summaries of all the differentially expressed genes.

**Supplementary Table 5** | List of differentially expressed genes in each cluster in females. Each sheet corresponds to the female analyses for the given cluster. “Avg\_diff” is conditionally formatted to indicate up- and down-regulation of expression in ethanol compared to regular food (red: up-regulated, green: down-regulated and yellow: no difference). p\_val: raw  $p$ -value from the differential expression analysis for the given gene in the corresponding cluster. avg\_diff: the difference in the  $\log(e)$  transformed average expression of the given gene in the corresponding cluster (sheet) between the two conditions (ethanol compared to regular food). Values above zero indicate up-regulation of expression due to developmental exposure to ethanol, and likewise, values below zero represent down-regulation of expression due to ethanol. p\_val\_adj: Bonferroni adjusted  $p$ -value. The DE matrix sheet is a summary of differentially expressed genes (columns) and the clusters in which they are differentially expressed (rows) with orange indicating upregulation and purple indicating downregulation at  $|\text{avg\_diff}|$  thresholds of 0.25 and 1. The All DE per cluster sheet and the All DE sheet are summaries of all the differentially expressed genes.

**Supplementary Table 6** | Human orthologs of differentially expressed genes.

**Supplementary Table 7** | Common differentially expressed genes upon developmental alcohol exposure and acute exposure to cocaine.

**Supplementary Table 8 |** Comparison of cell type-specific differentially expressed genes between developmental ethanol exposure and acute cocaine exposure. Meta-comparison sheet contains the mapping of clusters and cell types between the two datasets as well as the methodology and summary of the comparisons. The rest of the sheets contain the list of statistically significantly differentially expressed genes, their Log<sub>2</sub> fold change values, the calculations of

the comparisons between the two datasets for each cell type-category. The comparisons were done for each cell type-category separately for the male and female datasets.

**Supplementary Table 9 |** Gene ontology analysis of differentially expressed genes identified both after developmental exposure to alcohol and acute intake of cocaine.

## REFERENCES

- Jones K, Smith D. Recognition of the fetal alcohol syndrome in early infancy. *Lancet*. (1973) 302:999–1001. doi: 10.1016/S0140-6736(73)91092-1
- Hoyme HE, May PA, Kalberg WO, Kodituwakku P, Gossage JP, Trujillo PM, et al. A practical clinical approach to diagnosis of fetal alcohol spectrum disorders: clarification of the 1996 Institute of Medicine criteria. *Pediatrics*. (2005) 115:39–47. doi: 10.1542/peds.2004-0259
- Roozen S, Peters GJ, Kok G, Townend D, Nijhuis J, Curfs L. Worldwide prevalence of fetal alcohol spectrum disorders: a systematic literature review including meta-analysis. *Alcohol Clin Exp Res*. (2016) 40:18–32. doi: 10.1111/acer.12939
- Kaminen-Ahola N. Fetal alcohol spectrum disorders: genetic and epigenetic mechanisms. *Prenat Diagn*. (2020) 40:1185–92. doi: 10.1002/pd.5731
- Clarren SK, Smith DW. The fetal alcohol syndrome. *Lancet*. (1978) 298:1063–7. doi: 10.1056/NEJM19780512981906
- Pulsifer MB. The neuropsychology of mental retardation. *J Int Neuropsychol Soc*. (1996) 2:159–76. doi: 10.1017/S1355617700001016
- Eckardt MJ, File SE, Gessa GL, Grant KA, Guerri C, Hoffman PL, et al. Effects of moderate alcohol consumption on the central nervous system. *Alcohol Clin Exp Res*. (1998) 22:998–1040. doi: 10.1111/j.1530-0277.1998.tb03695.x
- Lange S, Rehm J, Anagnostou E, Popova S. Prevalence of externalizing disorders and Autism Spectrum Disorders among children with Fetal Alcohol Spectrum Disorder: systematic review and meta-analysis. *Biochem Cell Biol*. (2018) 96:241–51. doi: 10.1139/bcb-2017-0014
- Tan CH, Denny CH, Cheal NE, Sniezek JE, Kanny D. Alcohol use and binge drinking among women of childbearing age - United States, 2011–2013. *MMWR*. (2015) 64:1042–6. doi: 10.15585/mmwr.mm6437a3
- Morozova TV, Goldman D, Mackay TFC, Anholt RRH. The genetic basis of alcoholism: multiple phenotypes, many genes, complex networks. *Genome Biol*. (2012) 13:239. doi: 10.1186/gb-2012-13-2-239
- Morozova TV, Mackay TFC, Anholt RRH. Genetics and genomics of alcohol sensitivity. *Mol Genet Genomics*. (2014) 289:253–69. doi: 10.1007/s00438-013-0808-y
- Scholz H. Unraveling the mechanisms of behaviors associated with AUDs using flies and worms. *Alcohol Clin Exp Res*. (2019) 43:2274–84. doi: 10.1111/acer.14199
- Petrucelli E, Kaun KR. Insights from intoxicated *Drosophila*. *Alcohol*. (2019) 74:21–7. doi: 10.1016/j.alcohol.2018.03.004
- McClure KD, French RL, Heberlein U. A *Drosophila* model for fetal alcohol syndrome disorders: role for the insulin pathway. *Dis Model Mech*. (2011) 4:335–46. doi: 10.1242/dmm.006411
- Morozova TV, Hussain Y, McCoy LJ, Zhirnov EV, Davis MR, Pray VA, et al. A *Cyclin E* centered genetic network contributes to alcohol-induced variation in *Drosophila* development. *G3*. (2018) 8:2643–53. doi: 10.1534/g3.118.200260
- Scepanovic G, Stewart BA. Analysis of *Drosophila* nervous system development following an early, brief exposure to ethanol. *Dev Neurobiol*. (2019) 79:780–93. doi: 10.1002/dneu.22718
- Logan-Garbisch T, Bortolazzo A, Luu P, Ford A, Do D, Khodabakhshi P, et al. Developmental ethanol exposure leads to dysregulation of lipid metabolism and oxidative stress in *Drosophila*. *G3*. (2014) 5:49–59. doi: 10.1534/g3.114.015040
- Guevara A, Gates H, Urbina B, French R. Developmental ethanol exposure causes reduced feeding and reveals a critical role for Neuropeptide F in survival. *Front Physiol*. (2018) 9:237. doi: 10.3389/fphys.2018.00237
- Baker BM, Mokashi SS, Shankar V, Hatfield JS, Hannah RC, Mackay TFC, et al. The *Drosophila* brain on cocaine at single cell resolution. *Genome Res*. (2021). doi: 10.1101/gr.268037.120s. [Epub ahead of print].
- Sass TN, MacPherson RA, Mackay TFC, Anholt RRH. A high-throughput method for measuring alcohol sedation time of individual *Drosophila melanogaster*. *J Vis Exp*. (2020) 158:e61108. doi: 10.3791/61108
- Cichewicz K, Hirsh J. ShinyR-DAM: a program analyzing *Drosophila* activity, sleep and circadian rhythms. *Commun Biol*. (2018) 1:1–5. doi: 10.1038/s42003-018-0031-9
- Butler A, Hoffman P, Smibert P, Papalexi E, Satija R. Integrating single-cell transcriptomic data across different conditions, technologies, and species. *Nat Biotechnol*. (2018) 36:411–20. doi: 10.1038/nbt.4096
- Hafemeister C, Satija R. Normalization and variance stabilization of single-cell RNA-seq data using regularized negative binomial regression. *Genome Biol*. (2019) 20:296. doi: 10.1186/s13059-019-1874-1
- Finak G, McDavid A, Yajima M, Deng J, Gersuk V, Shalek AK, et al. MAST: a flexible statistical framework for assessing transcriptional changes and characterizing heterogeneity in single-cell RNA sequencing data. *Genome Biol*. (2015) 16:278. doi: 10.1186/s13059-015-0844-5
- Doncheva NT, Morris J, Gorodkin J, Jensen LJ. Cytoscape stringApp: network analysis and visualization of proteomics data. *J Proteome Res*. (2018) 18:623–32. doi: 10.1021/acs.jproteome.8b00702
- Shannon P, Markiel A, Ozier O, Baliga NS, Wang JT, Ramage D, et al. Cytoscape: a software environment for integrated models of biomolecular interaction networks. *Genome Res*. (2003) 13:2498–504. doi: 10.1101/gr.1239303
- Hanlon-Dearman A, Chen ML, Olson HC. Understanding and managing sleep disruption in children with fetal alcohol spectrum disorder. *Biochem Cell Biol*. (2018) 96:267–74. doi: 10.1139/bcb-2017-0064
- Kamara D, Beauchaine TP. A review of sleep disturbances among infants and children with neurodevelopmental disorders. *Rev J Autism Dev Disord*. (2020) 7:278–94. doi: 10.1007/s40489-019-00193-8
- Becht E, McInnes L, Healy J, Dutertre C, Kwok IWH, Ng LG, et al. Dimensionality reduction for visualizing single-cell data using UMAP. *Nat Biotechnol*. (2019) 37:38–44. doi: 10.1038/nbt.4314
- Thurmond J, Goodman JL, Strelets VB, Attrill H, Gramates LS, Marygold SJ, et al. FlyBase 2.0: the next generation. *Nucleic Acids Res*. (2019) 47:D759–65. doi: 10.1093/nar/gky1003
- Thomas PD, Campbell MJ, Kejariwal A, Mi H, Karlak B, Daverman R, et al. PANTHER: a library of protein families and subfamilies indexed by function. *Genome Res*. (2003) 13:2129–41. doi: 10.1101/gr.772403
- Seggio JA, Possidente B, Ahmad ST. Larval ethanol exposure alters adult circadian free-running locomotor activity rhythm in *Drosophila melanogaster*. *Chronobiol Int*. (2012) 29:75–81. doi: 10.3109/07420528.2011.635236
- Ahmad ST, Steinmetz SB, Bussey HM, Possidente B, Seggio JA. Larval ethanol exposure alters free-running circadian rhythm and *per* locus transcription in adult *D. melanogaster period* mutants. *Behav Brain Res*. (2013) 241:50–5. doi: 10.1016/j.bbr.2012.11.035
- Kobor MS, Weinberg J. Focus on: epigenetics and fetal alcohol spectrum disorders. *Alcohol Res Health*. (2011) 34:29–37.
- May PA, Tabachnick B, Hasken JM, Marais AS, de Vries MM, Barnard R, et al. Who is most affected by prenatal alcohol exposure: boys or girls? *Drug Alcohol Depend*. (2017) 177:258–67. doi: 10.1016/j.drugalcdep.2017.04.010
- Coleman LG Jr, Oguz I, Lee J, Styner M, Crews FT. Postnatal day 7 ethanol treatment causes persistent reductions in adult mouse brain volume and cortical neurons with sex specific effects on neurogenesis. *Alcohol*. (2012) 46:603–12. doi: 10.1016/j.alcohol.2012.01.003
- Weinberg J, Sliwowska JH, Lan N, Hellemans KG. Prenatal alcohol exposure: foetal programming, the hypothalamic-pituitary-adrenal axis and sex differences in outcome. *J Neuroendocrinol*. (2008) 20:470–88. doi: 10.1111/j.1365-2826.2008.01669.x

38. Kelly SJ, Leggett DC, Cronise K. Sexually dimorphic effects of alcohol exposure during development on the processing of social cues. *Alcohol Alcohol.* (2009) 44:555–60. doi: 10.1093/alcal/a/gp061
39. Davie K, Janssens J, Koldere D, De Waegeneer M, Pech U, Kreft L, et al. A single-cell transcriptome atlas of the aging *Drosophila* brain. *Cell.* (2018) 174:982–98.e20. doi: 10.1016/j.cell.2018.05.057
40. Wilhelm CJ, Guizzetti M. Fetal alcohol spectrum disorders: an overview from the glia perspective. *Front Integr Neurosci.* (2016) 9:65. doi: 10.3389/fnint.2015.00065
41. Guerri C, Pascual M, Renau-Piqueras J. Glia and fetal alcohol syndrome. *Neurotoxicol.* (2001) 22:593–9. doi: 10.1016/S0161-813X(01)00037-7
42. Tufa U, Ringuette D, Wang XF, Levi O, Carlen P. Two-photon microscopy imaging of blood brain barrier leakage in fetal alcohol disorder mice. In: *Optics in the Life Sciences Congress*. OSA Technical Digest (2017). doi: 10.1364/BODA.2017.JTu4A.9
43. DeSalvo MK, Hindle SJ, Rusan ZM, Orng S, Eddison M, Halliwill K, et al. The *Drosophila* surface glia transcriptome: evolutionary conserved blood-brain barrier processes. *Front Neurosci.* (2014) 8:346. doi: 10.3389/fnins.2014.00346
44. Kongton K, McCall K, Phongdara A. Identification of gamma-interferon-inducible lysosomal thiol reductase (GILT) homologues in the fruit fly *Drosophila melanogaster*. *Dev Comp Immunol.* (2014) 44:389–96. doi: 10.1016/j.dci.2014.01.007
45. Parinejad N, Peco E, Ferreira T, Stacey SM, van Meyel DJ. Disruption of an EAAT-mediated chloride channel in a *Drosophila* model of ataxia. *J Neurosci.* (2016) 36:7640–7. doi: 10.1523/JNEUROSCI.0197-16.2016
46. Chen WT, Yang HY, Lin CY, Lee YZ, Ma SC, Chen WC, et al. Structural insight into the contributions of the N-terminus and key active-site residues to the catalytic efficiency of glutamine synthetase 2. *Biomolecules.* (2020) 10:1671. doi: 10.3390/biom10121671
47. Saisawang C, Wongsantichon J, Ketterman AJ. A preliminary characterization of the cytosolic glutathione transferase proteome from *Drosophila melanogaster*. *Biochem J.* (2012) 442:181–90. doi: 10.1042/BJ20111747
48. Palm W, Sampaio JL, Brankatschk M, Carvalho M, Mahmoud A, Shevchenko A, et al. Lipoproteins in *Drosophila melanogaster* – assembly, function, and influence on tissue lipid composition. *PLoS Genet.* (2012) 8:e1002828. doi: 10.1371/journal.pgen.1002828
49. Gerstner JR, Vanderheyden WM, Shaw PJ, Landry CF, Yin JC. Fatty-acid binding proteins modulate sleep and enhance long-term memory consolidation in *Drosophila*. *PLoS ONE.* (2011) 6:e15890. doi: 10.1371/journal.pone.0015890
50. Sedlak TW, Paul BD, Parker GM, Hester LD, Snowman AM, Taniguchi Y, et al. The glutathione cycle shapes synaptic glutamate activity. *Proc Natl Acad Sci USA.* (2019) 116:2701–6. doi: 10.1073/pnas.1817885116
51. Olney JW, Wozniak DE, Jevtovic-Todorovic V, Farber NB, Bittigau P, Ikonomidou C. Glutamate and GABA receptor dysfunction in the fetal alcohol syndrome. *Neurotox Res.* (2002) 4:315–25. doi: 10.1080/1029842021000010875
52. Tsai G, Gastfriend DR, Coyle JT. The glutamatergic basis of human alcoholism. *Am J Psychiatry.* (1995) 152:332–40. D doi: 10.1176/ajp.152.3.332

**Conflict of Interest:** The authors declare that the research was conducted in the absence of any commercial or financial relationships that could be construed as a potential conflict of interest.

Copyright © 2021 Mokashi, Shankar, MacPherson, Hannah, Mackay and Anholt. This is an open-access article distributed under the terms of the Creative Commons Attribution License (CC BY). The use, distribution or reproduction in other forums is permitted, provided the original author(s) and the copyright owner(s) are credited and that the original publication in this journal is cited, in accordance with accepted academic practice. No use, distribution or reproduction is permitted which does not comply with these terms.



# Confirmation of a Causal *Taar1* Allelic Variant in Addiction-Relevant Methamphetamine Behaviors

Tamara J. Phillips<sup>1,2\*</sup>, Tyler Roy<sup>3</sup>, Sara J. Aldrich<sup>1</sup>, Harue Baba<sup>1</sup>, Jason Erk<sup>1</sup>, John R. K. Mootz<sup>1</sup>, Cheryl Reed<sup>1</sup> and Elissa J. Chesler<sup>3</sup>

<sup>1</sup> Department of Behavioral Neuroscience and Methamphetamine Abuse Research Center, Oregon Health & Science University, Portland, OR, United States, <sup>2</sup> Veterans Affairs Portland Health Care System, Portland, OR, United States, <sup>3</sup> The Jackson Laboratory and Center for Systems Neurogenetics of Addiction, Bar Harbor, ME, United States

## OPEN ACCESS

### Edited by:

Peter Kalivas,  
Medical University of South Carolina,  
United States

### Reviewed by:

Sammanda Ramamoorthy,  
Virginia Commonwealth University,  
United States  
Ryan K. Bachtell,  
University of Colorado Boulder,  
United States

### \*Correspondence:

Tamara J. Phillips  
phillipt@ohsu.edu

### Specialty section:

This article was submitted to  
Psychopharmacology,  
a section of the journal  
Frontiers in Psychiatry

**Received:** 15 June 2021

**Accepted:** 02 August 2021

**Published:** 26 August 2021

### Citation:

Phillips TJ, Roy T, Aldrich SJ, Baba H, Erk J, Mootz JRK, Reed C and Chesler EJ (2021) Confirmation of a Causal *Taar1* Allelic Variant in Addiction-Relevant Methamphetamine Behaviors.  
Front. Psychiatry 12:725839.  
doi: 10.3389/fpsy.2021.725839

Sensitivity to rewarding and reinforcing drug effects has a critical role in initial use, but the role of initial aversive drug effects has received less attention. Methamphetamine effects on dopamine re-uptake and efflux are associated with its addiction potential. However, methamphetamine also serves as a substrate for the trace amine-associated receptor 1 (TAAR1). Growing evidence in animal models indicates that increasing TAAR1 function reduces drug self-administration and intake. We previously determined that a non-synonymous single nucleotide polymorphism (SNP) in *Taar1* predicts a conformational change in the receptor that has functional consequences. A *Taar1*<sup>m1J</sup> mutant allele existing in DBA/2J mice expresses a non-functional receptor. In comparison to mice that possess one or more copies of the reference *Taar1* allele (*Taar1*<sup>+/+</sup> or *Taar1*<sup>+/m1J</sup>), mice with the *Taar1*<sup>m1J/m1J</sup> genotype readily consume methamphetamine, express low sensitivity to aversive effects of methamphetamine, and lack sensitivity to acute methamphetamine-induced hypothermia. We used three sets of knock-in and control mice in which one *Taar1* allele was exchanged with the alternative allele to determine if other methamphetamine-related traits and an opioid trait are impacted by the same *Taar1* SNP proven to affect MA consumption and hypothermia. First, we measured sensitivity to conditioned rewarding and aversive effects of methamphetamine to determine if an impact of the *Taar1* SNP on these traits could be proven. Next, we used multiple genetic backgrounds to study the consistency of *Taar1* allelic effects on methamphetamine intake and hypothermia. Finally, we studied morphine-induced hypothermia to confirm prior data suggesting that a gene in linkage disequilibrium with *Taar1*, rather than *Taar1*, accounts for prior observed differences in sensitivity. We found that a single SNP exchange reduced sensitivity to methamphetamine conditioned reward and increased sensitivity to conditioned aversion. Profound differences in methamphetamine intake and hypothermia consistently corresponded with genotype at the SNP location, with only slight variation in magnitude across genetic backgrounds. Morphine-induced hypothermia was not dependent on *Taar1* genotype. Thus, *Taar1*

genotype and TAAR1 function impact multiple methamphetamine-related effects that likely predict the potential for methamphetamine use. These data support further investigation of their potential roles in risk for methamphetamine addiction and therapeutic development.

**Keywords:** aversion, CRISPR-Cas9, hypothermia, knock-in, morphine, pleiotropic, selective breeding, two-bottle choice

## INTRODUCTION

Considerable research has focused on drug use disorders as motivational disorders involving inherent or drug-induced reward pathway function. Human and animal research supports a critical role for circuitry underlying sensitivity to rewarding and reinforcing drug effects in risk for continued use, neuroadaptation and relapse. Less is known about factors that reduce risk for addiction such as, for example, the protective role of sensitivity to aversive or adverse drug effects. Although there is important research in this area for alcohol (1–4), it has not been a focus of psychostimulant research or therapeutic development for psychostimulant addiction. To address initial sensitivity to drug aversive effects in humans requires knowledge of initial drug effects and the inclusion of individuals in studies who have tried a drug, but did not continue to use because they found the effects to be unpleasant. This is not the typical research performed in the addiction field; rather individuals suffering from a substance use disorder, or with a significant history of drug use, are compared to individuals with a low to modest drug history. Concerns about potential long-term consequences on behavior and in the brain, of even relatively low-level exposure to drugs like methamphetamine (MA) (5–14), raise concerns about conducting such research in drug-naïve humans. However, the study of drug avoiders could lead to the identification of a new class of therapeutics. Animal models of drug use have an important role in this area of study, because drug history can be controlled and initial responses readily measured.

Bidirectional selective breeding has the explicit goal of creating animal lines that exhibit a low vs. high level of a particular characteristic. We bred mice for level of voluntary MA intake and created MA high drinking (MAHDR) and MA low drinking (MALDR) lines of mice that consume binge-like levels of MA or avoid consuming MA, respectively (15–18). Using this model, we determined that a single nucleotide polymorphism (SNP) at position 229 in the trace amine-associated receptor 1 gene (*Taar1*) accounts for 60% of the heritable variance in MA intake (19–21). The non-synonymous SNP (rs33645709) is found in DBA/2J mice sourced from The Jackson Laboratory (JAX), but not in DBA/2 mice sourced from other suppliers (22) or in any of the 28 other strains that have been genotyped at this genetic location (23, 24). This coding variant changes a proline to a threonine in the second transmembrane domain of the receptor (24). Multiple lines of evidence, beginning with quantitative trait locus mapping and culminating in the use of a CRISPR-Cas9-derived knock-in (KI) model on the MAHDR background, definitively determined that this *Taar1* SNP impacts level of MA consumption (21). Thus, mice homozygous for the

*Taar1*<sup>m1J</sup> allele consume more MA on average than mice that possess one or two copies of the reference *Taar1*<sup>+</sup> allele.

In addition to identifying genetic differences related to the bidirectional selection response, selectively bred lines provide information about genetically correlated traits, defined as phenotypes that are impacted by one or more of the genes that influence the selection trait. Several MA-related traits reliably differentiate the MA drinking (MADR) lines. These include rewarding and aversive traits, as well as a physiological trait, MA-induced hypothermia, proposed to be among the aversive effects of MA that inhibit MA intake (20, 25, 26). Herein, we report studies performed in three sets of matched KI and control line mice in which one *Taar1* allele was exchanged with the alternative allele. First, MAHDR-*Taar1*<sup>+/+</sup> KI and control mice were studied for tastant intake and preference, and sensitivity to two traits hypothesized to be pleiotropically influenced by *Taar1*: sensitivity to MA-induced conditioned place preference and conditioned taste aversion. Based on previous findings (16, 18, 21, 22, 27), we predicted that the KI and control mice would not differ in saccharin or quinine intake or preference, KI of the *Taar1*<sup>+</sup> allele would decrease sensitivity to MA-induced conditioned place preference, and KI of the *Taar1*<sup>+</sup> allele would increase sensitivity to MA-conditioned taste aversion. Next, KI mice generated on the MADR progenitor C57BL/6J and DBA/2J background strains were studied for MA intake and MA-induced hypothermia to examine replication of *Taar1* effects on different genetic backgrounds. These traits have already been confirmed to be impacted by *Taar1* in the MAHDR KI and control lines (21).

Finally, previous data in MADR mice suggest that a difference in sensitivity to morphine-induced hypothermia was not a pleiotropic effect of *Taar1*, but more likely due to a linked polymorphism (25). To confirm this, we examined this trait in the MAHDR-*Taar1*<sup>+/+</sup> KI and control mice and predicted comparable morphine-induced hypothermia.

## MATERIALS AND METHODS

### Subjects

Subjects were male and female MAHDR-*Taar1*<sup>+/+</sup> KI, DBA/2J-*Taar1*<sup>+/+</sup> KI, C57BL/6J-*Taar1*<sup>m1J/m1J</sup> KI, and control lines matched to each KI line (MAHDR-*Taar1*<sup>m1J/m1J</sup>, DBA/2J-*Taar1*<sup>m1J/m1J</sup>, and C57BL/6J-*Taar1*<sup>+/+</sup>). The MAHDR KI mice were created at the Oregon Health & Science University Transgenic Mouse Models Shared Resource, utilizing CRISPR-Cas9 technology to replace the *Taar1*<sup>m1J</sup> allele with the reference *Taar1*<sup>+</sup> allele; controls were derived from those mice in which the *Taar1*<sup>m1J</sup> allele was not successfully excised and replaced; thus, they retained the *Taar1*<sup>m1J/m1J</sup> genotype. Details can be

found in Stafford et al. (21). The identical process was applied at JAX (Bar Harbor, ME, USA) to generate the same KI on a pure DBA/2J inbred strain background, or to replace the reference *Taar1*<sup>+</sup> allele with the *Taar1*<sup>m1J</sup> allele on a pure C57BL/6J inbred strain background.

Mice participating in the current studies were either born within the VA Portland Health Care System (VAPORHCS) Veterinary Medical Unit or within a breeding colony at JAX; location for each study is indicated in experiment descriptions. Breeders (pairs at VAPORHCS; harems at JAX) were maintained in standard acrylic plastic shoebox cages on corncob bedding (The Andersons, Maumee, Ohio; VAPORHCS) or pine shavings (Hancock Lumber, Bethel, Maine; JAX), with wire lids and filter tops. Breeding cages resided on Thoren racks under a standard 12:12 light:dark cycle, and mice were weaned at 21 ± 2 days of age into same-sex groups of 2–4 per cage. During breeding and experiments, mice were maintained in climate-controlled rooms under a standard 12:12 light:dark cycle with lights on at 0600h, and free access to water (tap water at the VAPORHCS; filtered and acidified at JAX) and rodent block food (Purina 5001 or 5LOD PicoLab Rodent Diet; Animal Specialties, Woodburn, Oregon at the VAPORHCS; NIH315K52 chow Lab Diet 6%PM Nutrition, St. Louis MO, USA at JAX); exceptions are noted in experimental methods. All animal care and testing procedures were approved by the VAPORHCS or JAX Institutional Animal Care and Use Committee, and were conducted in compliance with the National Institutes of Health Guidelines for Care and Use of Laboratory Animals. Group sizes for each experiment are given in the figure captions.

## Genotyping

All KI and control offspring used in these studies were genotyped for *Taar1* using an rtPCR method developed in our laboratory for the relevant *Taar1* SNP, based on a standard Taqman (ThermoFisher Scientific) assay in which fluorescent probes were used for differentiation (22).

## Drugs

(+)-Methamphetamine hydrochloride was purchased from Sigma-Aldrich (St. Louis, MO, USA) or obtained from the National Institutes of Health, National Institute on Drug Abuse drug supply program (Rockville, MD, USA) and dissolved in tap water for drinking or in sterile 0.9% saline (Baxter Healthcare Corp., Deerfield, IL, USA) for injection. Sodium chloride for conditioned taste aversion studies, and saccharin and quinine for novel tastant intake studies, were purchased from Sigma-Aldrich and dissolved in tap water. Morphine was obtained from the NIDA Drug Supply program (Rockville, MD, USA) and dissolved in sterile saline. Saline vehicle served as a 0 dose control treatment for MA and morphine injection studies. All injections were delivered intraperitoneally (IP) in a volume of 10 ml/kg.

## Experiment 1: Novel Tastant Intake and Preference in MAHDR-*Taar1*<sup>+/+</sup> KI and MAHDR-*Taar1*<sup>m1J/m1J</sup> Control Mice

We characterized saccharin (SACC) and quinine (QUIN) intake and preference to investigate whether a difference in tastant intake or preference corresponds with the difference in MA intake found in a previous study between the MAHDR-*Taar1*<sup>+/+</sup> KI and MAHDR-*Taar1*<sup>m1J/m1J</sup> control mice (21). This study was conducted at the VAPORHCS using methods consistent with our previous studies in the MADR mice (16, 18). Male and female mice were weighed, singly-housed, and given access to two water-filled 25-ml graduated cylinders fitted with stoppers and sipper tubes for 2 consecutive days to familiarize them with drinking fluid from these tubes. Using a counterbalanced design, mice were then offered water vs. SACC and then water vs. QUIN or the two tastants in the alternate order. Tastants were offered 24 h/day in two increasing concentrations for 4 days each and mice were weighed every 4 days; therefore, the two-bottle choice tastant phase included days 3–18. The positions of the water and tastant tubes were alternated every 2 days, the SACC concentrations were 1.6 and 3.2 mM, and the QUIN concentrations were 0.015 and 0.03 mM, consistent with our previous studies (16, 18). Consumption was measured each day in ml. Mice were tested at an average age of 81 ± 1 days, with a range of 77–87 days.

## Experiment 2: MA-Induced Conditioned Place Preference Testing in MAHDR-*Taar1*<sup>+/+</sup> KI and MAHDR-*Taar1*<sup>m1J/m1J</sup> Control Mice

Group housed (2–4 per cage) male and female MAHDR-*Taar1*<sup>+/+</sup> KI and MAHDR-*Taar1*<sup>m1J/m1J</sup> control mice were tested for sensitivity to conditioned place preference induced by 0.5 mg/kg MA, a dose that has produced consistent preference in MAHDR and no preference in MALDR mice (16, 18). This study was conducted at the VAPORHCS using our established unbiased place conditioning procedure. Custom-built conditioning boxes (30 cm × 15 cm × 15 cm; San Diego Instruments, San Diego, CA USA) were housed in sound attenuating, illuminated and ventilated chambers. Each conditioning box had a removable central black wall used to sequester the animal to the left or right half of the chamber during conditioning trials; the wall was removed during preference tests. Removable floor panels with unique textures served as conditioning cues. One floor was composed of 2.3 mm stainless steel rods mounted 6.4 mm apart (the “grid” floor); the other was a stainless steel sheet with 6.4 mm round holes on 9.5 mm staggered centers (the “hole” floor). Animal location was detected by photocell beam interruptions and automatically converted to time spent on a particular floor type; photocell beam interruptions were also recorded as a measure of locomotor activity.

The study began on a Monday and excluded weekends, and mice were returned to group housing (2–4 per cage) each day after testing. Mice were moved to the procedure room each day 1 h before conditioning or testing. Initial preference for the cues was determined in a 30-min test; mice were injected with saline immediately prior to placement in the box. Beginning

24 h later, there were 12 alternating conditioning trials (one daily), six immediately after saline, and six immediately after 0.5 mg/kg MA treatment that were 15 min in duration. Half of the mice had MA paired with the grid floor and half with the hole floor, with left/right placement of floor types counterbalanced. A 30-min “drug-free” preference test was performed the day after the last conditioning trial; mice were treated with saline immediately prior to placement in the box. Finally, a 30-min “drug-present” preference test was performed 2 days after the drug-free preference test (after a weekend break); mice were treated with MA immediately prior to placement in the box. Mice were tested at an average age of  $91 \pm 1$  days, with a range of 73–107 days; mice were tested between 1000 and 1400 h.

### Experiment 3: MA-Induced Conditioned Taste Aversion Testing in MAHDR-*Taar1*<sup>+/+</sup> KI and MAHDR-*Taar1*<sup>m1J/m1J</sup> Control Mice

Male and female MAHDR-*Taar1*<sup>+/+</sup> KI and MAHDR-*Taar1*<sup>m1J/m1J</sup> control mice were tested for sensitivity to conditioned taste aversion induced by 2 mg/kg MA, a dose that has produced consistent differences in mice with different *Taar1* genotypes (22, 27). This study was conducted at the VAPORHCS using our established procedures. A novel 0.2 M NaCl solution was offered as the conditioned cue just prior to MA treatment to create an association with the interoceptive effects of MA. Briefly, mice were weighed, singly-housed, and familiarized to drinking water from a 10-ml graduated cylinder fitted with a sipper tube (study days –1 and 0). Water access was then limited to 2 h per day for a 4-day acclimation period to induce motivation to drink the novel NaCl solution at a particular time of each day (study days 1–4). Beginning on day 5, the NaCl solution was offered for 1 h every other day for 6 presentations (days 5, 7, 9, 11, 13, and 15). No treatment was given after the first presentation, which was a trial intended to reduce neophobia. On the remaining NaCl access days, with the exception of the last, saline or MA was injected immediately after the drinking period. NaCl consumption was measured in ml. To ensure proper hydration, 3 h post-injection, mice were given access to water for 30 min, and they had 2 h water access on days between trials. Mice were tested at an average age of  $93 \pm 1$  days, with a range of 82–112 days; NaCl access occurred at 0900–1000 h.

### Experiments 4 and 5: Two-Bottle Choice Methamphetamine Intake in DBA/2J-*Taar1*<sup>+/+</sup> KI and DBA/2J-*Taar1*<sup>m1J/m1J</sup> Control, and in C57BL/6J-*Taar1*<sup>m1J/m1J</sup> KI and C57BL/6J-*Taar1*<sup>+/+</sup> Control Mice

A two-bottle choice MA vs. water drinking procedure, similar to that used to characterize voluntary MA intake in our previous studies was used (15–18). This study was conducted at JAX. One day prior to testing, male and female mice were singly housed and offered two water-filled 50 ml polypropylene centrifuge tubes (item number 430291; Corning, Corning, NY) fitted with rubber

stoppers (Fisher Scientific, Pittsburgh, PA, USA) and single ball-bearing stainless steel sipper tubes (Sta Pure Systems, Carnegie, PA, USA) to provide experience with consuming fluid from these tubes. On test days 2–5, mice were offered one water tube and a tube containing a 10 mg/L solution of MA in water. On days 6–17, the tubes contained water vs. 20 mg/L, then 40 mg/L, and then 80 mg/L MA, with each MA concentration offered for 4 consecutive days. During the MA phase, mice had access to MA 24 h/day and tubes were weighed prior to cage placement and again every 48 h. Changes in MA concentration were accompanied by fresh tubes and switching of the position of the water vs. MA tube to account for potential side bias in fluid intake. Mice were weighed on days 1 and 17 of the study, and weights on those days were averaged to approximate mg/kg MA consumed. Two separate studies were conducted. The first included DBA/2J-*Taar1*<sup>+/+</sup> KI and DBA/2J-*Taar1*<sup>m1J/m1J</sup> control mice, tested at an average age of  $72 \pm 2$  days, with a range of 56–88 days. The other included C57BL/6J-*Taar1*<sup>m1J/m1J</sup> KI and C57BL/6J-*Taar1*<sup>+/+</sup> control mice, tested at an average age of  $75 \pm 1$  days, with a range of 55–88 days.

### Experiments 6 and 7: MA-Induced Body Temperature Changes in DBA/2J-*Taar1*<sup>+/+</sup> and DBA/2J-*Taar1*<sup>m1J/m1J</sup> Control, and in C57BL/6J-*Taar1*<sup>m1J/m1J</sup> KI and C57BL/6J-*Taar1*<sup>+/+</sup> Control Mice

Male and female mice were tested for the effect of 2 mg/kg MA on core body temperature using our established procedures. This MA dose consistently produces hypothermia in MALDR mice and other mice that possess *Taar1*<sup>+</sup>, a response that is absent in MAHDR mice and other mice that lack TAAR1 function (20, 22). This study was conducted at the VAPORHCS using our established procedures. Mice were moved to the procedure room at 0800–0830 h, weighed, isolated in acrylic plastic cubicles to prevent huddling-associated body temperature changes, and left undisturbed for 1 h to acclimate to the testing environment, maintained at a temperature of  $21 \pm 1^\circ\text{C}$ . A baseline temperature was then obtained at 0900–0930 h, designated as time 0 (T0), using a 5 mm glycerin-coated rectal probe attached to a Thermalert TH-8 digital thermometer (Sensortek, Clifton, New Jersey). Mice were then immediately treated with saline or 2 mg/kg MA and returned to their holding cubicles. Temperatures were subsequently obtained at T30, T60, T90, T120, T150, and T180 min post-injection. Experiment 6 included DBA/2J-*Taar1*<sup>+/+</sup> KI and DBA/2J-*Taar1*<sup>m1J/m1J</sup> control mice, tested at an average age of  $92 \pm 1$  days, with a range of 62–122 days. Experiment 7 included C57BL/6J-*Taar1*<sup>m1J/m1J</sup> KI and C57BL/6J-*Taar1*<sup>+/+</sup> control mice, tested at an average age of  $82 \pm 1$  days, with a range of 62–108 days.

### Experiment 8: Morphine-Induced Body Temperature Changes in MAHDR-*Taar1*<sup>+/+</sup> KI and MAHDR-*Taar1*<sup>m1J/m1J</sup> Control Mice

Male and female MAHDR-*Taar1*<sup>+/+</sup> KI and MAHDR-*Taar1*<sup>m1J/m1J</sup> control mice were tested for sensitivity to the hypothermic effect of 15 and 30 mg/kg morphine. These doses

were chosen from our previous research in the MADR lines (25). This study was conducted at the VAPORHCS, and experimental details were identical to those described for experiments 6 and 7. Mice were tested at an average age of  $85 \pm 1$  days, with a range of 65–109 days.

## Statistics

Data were analyzed using factorial ANOVA with repeated measures as appropriate. Independent grouping factors are described with the results for each study. Complex interactions involving more than 2 factors were first examined by 2-way ANOVA at each level of the third factor. Significant 2-way interactions were examined for simple main effects and means were compared using the Newman-Keuls *post-hoc* test. The number of *post-hoc* comparisons was reduced by assessing changes from one mean to the next for concentration, time, and trial effects, or between first and subsequent trials.

## RESULTS

### Baseline Data

Baseline body weight data collected across studies, along with age ranges, are summarized in **Table 1**. Although there were some significant differences between genotypes in baseline body weight, differences were not consistently found across studies, suggesting that they were specific to the particular groups of animals included in a given experiment. Thus, C57BL/6J-*Taar1*<sup>m1J/m1J</sup> KI and C57BL/6J-*Taar1*<sup>+/+</sup> control mice had equivalent body weights in both studies in which they were tested; DBA/2J-*Taar1*<sup>+/+</sup> KI and DBA/2J-*Taar1*<sup>m1J/m1J</sup> control mice differed in body weight in one, but not the other experiment; and MAHDR-*Taar1*<sup>+/+</sup> KI and MAHDR-*Taar1*<sup>m1J/m1J</sup> control mice had comparable body weights in two studies and differed in the remaining two. When significant, mean differences ranged from 1.1 to 2.2 g. Total volume of water consumed was recorded prior to tastant access in Experiment 1 and there was no significant difference between the genotypes (mean  $\pm$  SEM =  $5.8 \pm 0.2$  ml vs.  $6.0 \pm 0.2$  ml for KI and Control, respectively). Other measures, including total volume of fluid consumed, baseline locomotor activity level, and baseline body temperature are reported with the experiments during which these data were collected.

### Experiment 1: Novel Tastant Intake and Preference in MAHDR-*Taar1*<sup>+/+</sup> KI and MAHDR-*Taar1*<sup>m1J/m1J</sup> Control Mice

Data for each tastant were analyzed separately by repeated measures factorial ANOVA grouped on mouse line and sex, with concentration as the repeated measure.

#### SACC Intake, Preference, and Total Volume Consumed

MAHDR-*Taar1*<sup>+/+</sup> KI and MAHDR-*Taar1*<sup>m1J/m1J</sup> control mice did not differ in SACC intake or preference (calculated as ml from tastant tube/total ml consumed). The initial analysis of SACC intake data (**Figure 1A**) identified significant effects of sex [ $F_{(1,44)} = 4.7, p = 0.036$ ] and SACC concentration [ $F_{(1,44)} = 124.2, p <$

0.0001]. Female mice consumed more SACC than males (mean  $\pm$  SEM =  $106.6 \pm 10.4$  mg/kg vs.  $77.9 \pm 6.6$  mg/kg, respectively), and mice consumed more SACC when it was offered at the higher concentration. These outcomes were not dependent on mouse line. For SACC preference (**Figure 1B**) and total volume consumed from the water plus SACC tubes (**Figure 1C**), there were no significant effects of line, sex, or concentration.

#### QUIN Intake, Preference, and Total Volume Consumed

MAHDR-*Taar1*<sup>+/+</sup> KI mice consumed more QUIN and had a higher QUIN preference ratio, compared to MAHDR-*Taar1*<sup>m1J/m1J</sup> control mice. The initial analysis of QUIN intake data (**Figure 1D**) identified a significant line  $\times$  QUIN concentration interaction [ $F_{(1,44)} = 13.9, p = 0.0005$ ]. There were no effects of sex. Follow-up analyses indicated that more QUIN was consumed by mice of both lines when the concentration was increased. The lines consumed comparable amounts of QUIN at the lower concentration, but MAHDR-*Taar1*<sup>+/+</sup> KI mice consumed more QUIN than MAHDR-*Taar1*<sup>m1J/m1J</sup> control mice when the QUIN concentration was increased ( $p = 0.001$ ). For QUIN preference (**Figure 1E**), there was a significant main effect of line [ $F_{(1,44)} = 6.2, p = 0.02$ ], with MAHDR-*Taar1*<sup>+/+</sup> KI mice exhibiting higher preference than MAHDR-*Taar1*<sup>m1J/m1J</sup> control mice. For total volume consumed (**Figure 1F**), there was a significant line  $\times$  concentration interaction [ $F_{(1,44)} = 11.6, p = 0.001$ ] that was associated with smaller volumes consumed by MAHDR-*Taar1*<sup>+/+</sup> KI mice when the lower vs. higher QUIN concentration was offered ( $p < 0.0001$ ;  $4.9 \pm 0.2$  vs.  $5.8 \pm 0.2$  for the 0.015 and 0.03 mM concentrations, respectively). However, there were no significant differences between the lines in total volume consumed at either concentration.

### Experiment 2: MA-Induced Conditioned Place Preference Testing in MAHDR-*Taar1*<sup>+/+</sup> KI and MAHDR-*Taar1*<sup>m1J/m1J</sup> Control Mice

Data analyses considered percent time spent on the drug-paired floor during the pre-test, drug-free test and drug-present test, as measures of initial floor type bias, preference for floor cues induced by prior association with MA, and preference for MA-associated floor cues when tested during the associative state (**Figure 2A**). Locomotor activity data collected during these tests were also analyzed (**Figure 2B**). Data were analyzed by repeated measures factorial ANOVA grouped on mouse line and sex, with test day as the repeated measure.

#### Place Preference

Floor cues were initially equally preferred, and MA induced a conditioned preference in MAHDR-*Taar1*<sup>m1J/m1J</sup> control mice, but not MAHDR-*Taar1*<sup>+/+</sup> KI mice. There was a significant line  $\times$  test day interaction [ $F_{(2,184)} = 3.54, p = 0.03$ ], but no significant effects of sex. For initial preference, there was no significant difference between the lines for percent time spent on the assigned drug-paired floor, and values were near 50%, indicating that the floor types were approximately equally preferred before conditioning. For the drug-free preference test,

**TABLE 1** | Body weight and age range data for each study.

Exp number	Study description	Mouse model	Age range (days)	Body weight (g $\pm$ SEM)		Mouse line comparison
				KI	Control	
(1)	Tastant intake	MAHDR- <i>Taar1</i> <sup>+/+</sup> KI vs. Control	77–87	25.1 $\pm$ 0.7	25.7 $\pm$ 0.7	KI = Control
(2)	MA conditioned place preference	MAHDR- <i>Taar1</i> <sup>+/+</sup> KI vs. Control	73–107	25.7 $\pm$ 0.4	27.9 $\pm$ 0.4***	KI < Control
(3)	MA conditioned taste aversion	MAHDR- <i>Taar1</i> <sup>+/+</sup> KI vs. Control	82–112	26.8 $\pm$ 0.6	27.9 $\pm$ 0.6	KI = Control
(4)	MA intake	DBA/2J- <i>Taar1</i> <sup>+/+</sup> KI vs. Control	56–88	21.2 $\pm$ 0.7	20.5 $\pm$ 0.7	KI = Control
(5)	MA intake	C57BL/6J- <i>Taar1</i> <sup>m1J/m1J</sup> KI vs. Control	55–88	23.0 $\pm$ 0.5	23.8 $\pm$ 0.3	KI = Control
(6)	MA body temperature	DBA/2J- <i>Taar1</i> <sup>+/+</sup> KI vs. Control	62–122	25.2 $\pm$ 0.4	27.0 $\pm$ 0.4**	KI < Control
(7)	MA body temperature	C57BL/6J- <i>Taar1</i> <sup>m1J/m1J</sup> KI vs. Control	62–108	24.0 $\pm$ 0.2	23.9 $\pm$ 0.2	KI = Control
(8)	Morphine body temperature	MAHDR- <i>Taar1</i> <sup>+/+</sup> KI vs. Control	65–109	26.1 $\pm$ 0.3	27.1 $\pm$ 0.3*	KI < Control

Exp, experiment; g, gram; KI, knock-in; MA, methamphetamine; MAHDR, methamphetamine high drinking mice; SEM, standard error of the mean; *Taar1*<sup>+/+</sup>, homozygous reference trace amine-associated receptor 1 genotype; *Taar1*<sup>m1J/m1J</sup>, homozygous mutant trace amine-associated receptor 1 genotype; \* $p < 0.05$ , \*\* $p < 0.01$ , \*\*\* $p < 0.001$  for the difference between mouse lines.

there was a significant difference between the lines ( $p = 0.02$ ), with the MAHDR-*Taar1*<sup>m1J/m1J</sup> controls spending more time on the drug-paired floor than the MAHDR-*Taar1*<sup>+/+</sup> KI mice. A similar outcome was obtained for the drug-present preference test, with MAHDR-*Taar1*<sup>m1J/m1J</sup> controls spending significantly more time on the drug-paired floor than the MAHDR-*Taar1*<sup>+/+</sup> KI mice ( $p = 0.007$ ).

Evidence for MA-conditioned preference is indicated by a difference between percent time on the initial test day vs. the two post-conditioning preference test days. For MAHDR-*Taar1*<sup>m1J/m1J</sup> control mice, there was a significant effect of test day [ $F_{(2,94)} = 21.4$ ,  $p < 0.0001$ ], and *post-hoc* mean comparisons indicated that percent time was greater after MA conditioning when mice were tested under both drug-free and drug-present states ( $ps < 0.001$ ). For MAHDR-*Taar1*<sup>+/+</sup> KI mice, there was no significant effect of test day; thus, there was no evidence for MA-induced conditioned place preference in these mice.

### Locomotor Activity During Preference Testing

There was a significant sex  $\times$  test day interaction [ $F_{(2,184)} = 3.42$ ,  $p = 0.03$ ]. Activity levels were comparable for males and females during the initial and drug-free preference tests, but males were significantly more active than females during the drug-present test ( $p = 0.03$ ;  $3,753 \pm 119$  and  $3,319 \pm 157$  for males and females, respectively). Sex differences were not dependent on line, but there was a significant line  $\times$  test day interaction [ $F_{(2,184)} = 5.49$ ,  $p = 0.005$ ]. Activity levels were comparable between the two genotypes during the initial preference test. Both genotypes increased their activity during the subsequent 2 tests (all  $ps < 0.001$ ), with the highest level of locomotion during the drug-present test and greater activity in MAHDR-*Taar1*<sup>+/+</sup> KI, compared to MAHDR-*Taar1*<sup>m1J/m1J</sup> control mice ( $p = 0.02$  and  $0.053$  on the drug-free and drug-present test day, respectively).

### Locomotor Activity During Conditioning

Locomotor activity level data during saline and MA conditioning trials were analyzed for sex, line, and conditioning trial effects. For saline trial data (Figure 3A), there were significant effects of sex [ $F_{(1,92)} = 7.75$ ,  $p = 0.007$ ] and trial [ $F_{(5,460)} = 10.58$ ,  $p < 0.0001$ ]. Males were more active than females and activity levels declined significantly from trial 1 to 2 ( $p < 0.001$ ), and were then stable. For MA trial data (Figure 3B), there were no significant sex effects, but there was a significant line  $\times$  trial interaction [ $F_{(5,460)} = 2.57$ ,  $p = 0.026$ ]. The mouse lines had comparable activity levels after the first MA treatment, then MAHDR-*Taar1*<sup>+/+</sup> KI mice were more active than MAHDR-*Taar1*<sup>m1J/m1J</sup> control mice on subsequent trials. Although there was a significant effect of trial within each line ( $ps < 0.001$ ), significant sensitization to the locomotor stimulant effect of MA was found after fewer treatments in MAHDR-*Taar1*<sup>+/+</sup> KI mice.

### Experiment 3: MA-Induced Conditioned Taste Aversion Testing in MAHDR-*Taar1*<sup>+/+</sup> KI and MAHDR-*Taar1*<sup>m1J/m1J</sup> Control Mice

MAHDR-*Taar1*<sup>+/+</sup> KI mice, but not MAHDR-*Taar1*<sup>m1J/m1J</sup> control mice, exhibited sensitivity to MA-induced conditioned taste aversion (Figure 4). NaCl intake data were analyzed by repeated measures factorial ANOVA grouped on mouse line, sex, and treatment (saline or 2 mg/kg MA), with test trial as the repeated measure. There was a significant three-way interaction of line, treatment, and trial [ $F_{(4,176)} = 14.73$ ,  $p < 0.0001$ ], but no significant effect of sex. For the MAHDR-*Taar1*<sup>m1J/m1J</sup> control mice, there was a significant effect of trial [ $F_{(4,88)} = 4.76$ ,  $p = 0.002$ ], but no effect of treatment; rather than a conditioned reduction in NaCl intake, these

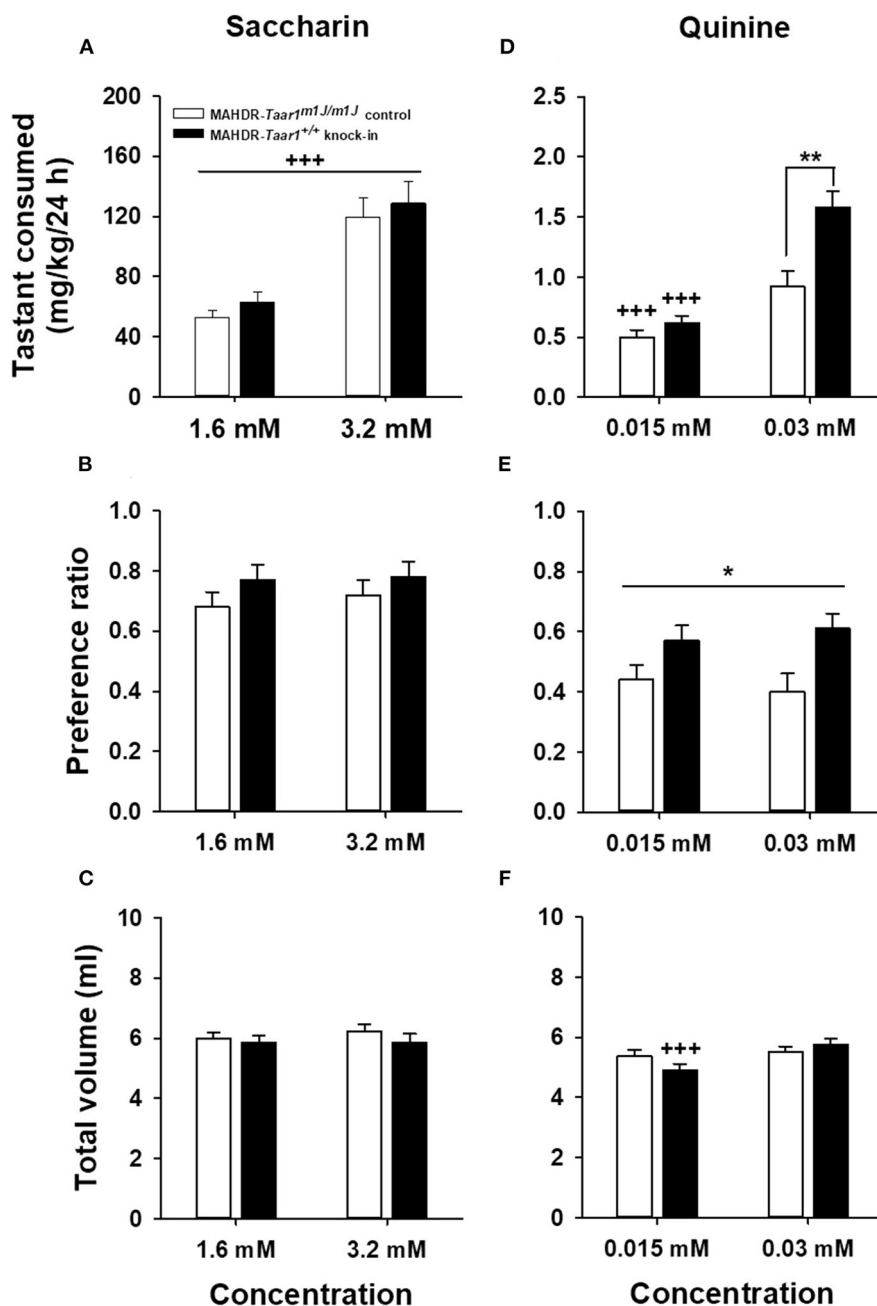
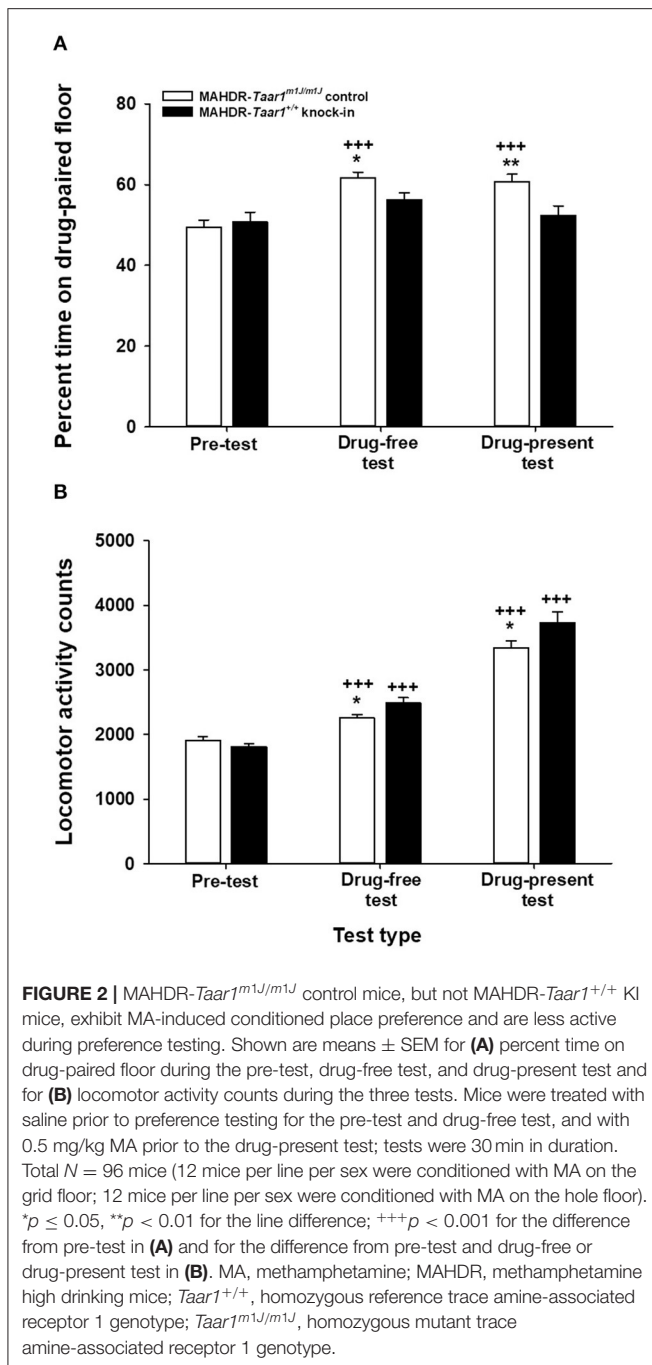


**FIGURE 1 |** Novel saccharin and quinine tastant intake and preference in MAHDR-*Taar1*<sup>+/+</sup> KI and MAHDR-*Taar1*<sup>m1J/m1J</sup> control mice. Shown are means  $\pm$  SEM for (A) saccharin consumed (mg/kg/24 h), (B) saccharin preference ratio (ml from saccharin tube/total ml consumed), (C) total volume (ml/24 h) consumed (water + saccharin solution) during access to each saccharin concentration, (D) quinine consumed (mg/kg/24 h), (E) quinine preference ratio (ml from quinine tube/total ml consumed), and (F) total volume consumed (water + quinine solution) during quinine access. Tastants were offered vs. water for 4-day periods at increasing concentrations in counterbalanced order. Total  $N = 48$  mice (12 mice per sex for the MAHDR-*Taar1*<sup>+/+</sup> KI; 10 female MAHDR-*Taar1*<sup>m1J/m1J</sup> control mice, and 14 male MAHDR-*Taar1*<sup>m1J/m1J</sup> control mice). \* $p < 0.05$ , \*\* $p < 0.01$  for the main effect of mouse line (E) or for the line difference at the indicated concentration (D); \*\*\* $p < 0.001$  for the main effect of concentration (A) or for the concentration difference for the indicated mouse line (D,F). MAHDR, methamphetamine high drinking mice; *Taar1*<sup>+/+</sup>, homozygous reference trace amine-associated receptor 1 genotype; *Taar1*<sup>m1J/m1J</sup>, homozygous mutant trace amine-associated receptor 1 genotype.

mice consumed significantly more NaCl during trials 3–5, compared to trial 1 ( $p = 0.04$ ,  $0.04$ , and  $0.0008$ , for trials 3, 4, and 5, respectively; Figure 4A). For the MAHDR-*Taar1*<sup>+/+</sup> KI mice, there was a significant trial  $\times$  treatment

interaction [ $F_{(4,88)} = 34.4$ ,  $p < 0.0001$ ]; there was no significant effect of trial for the saline treatment group, but there was for the MA treatment group ( $p < 0.0001$ ). *Post-hoc* comparisons indicated that NaCl intake was lower for trials 2–5,



compared to trial 1 (all  $ps < 0.001$ ; **Figure 4B**), supporting the development of a conditioned taste aversion in MAHDR-Taar1<sup>+/+</sup> KI mice.

#### Experiment 4: Two-Bottle Choice Methamphetamine Intake in DBA/2J-Taar1<sup>+/+</sup> KI and DBA/2J-Taar1<sup>m1J/m1J</sup> Control Mice

DBA/2J-Taar1<sup>m1J/m1J</sup> control mice consumed more MA and exhibited greater MA preference, compared to

DBA/2J-Taar1<sup>+/+</sup> KI mice (**Figure 5**). Average MA intake, preference and total volume intake data were analyzed by repeated measures factorial ANOVA grouped on mouse line, sex, and MA concentration. For MA intake (**Figure 5A**), there was a significant line  $\times$  MA concentration interaction [ $F_{(3,78)} = 5.9$ ,  $p = 0.001$ ], but no effect of sex. DBA/2J-Taar1<sup>m1J/m1J</sup> control mice consumed more MA than DBA/2J-Taar1<sup>+/+</sup> KI mice at all MA concentrations. Intake significantly increased as MA concentration was increased for DBA/2J-Taar1<sup>m1J/m1J</sup> control mice ( $ps < 0.0001$ ), with a statistical trend for KI mice ( $p = 0.06$ ); results for mean comparisons are shown in **Figure 5A**.

For MA preference (**Figure 5B**), there was a main effect of line [ $F_{(1,78)} = 12.9$ ,  $p = 0.001$ ], with DBA/2J-Taar1<sup>m1J/m1J</sup> control mice exhibiting a greater MA preference ratio, compared to DBA/2J-Taar1<sup>+/+</sup> KI mice. There was also a significant main effect of concentration [ $F_{(3,78)} = 5.8$ ,  $p = 0.001$ ]; preference declined with increasing concentration. For total volume consumed (**Figure 5C**), the only significant effect was MA concentration [ $F_{(3,84)} = 7.7$ ,  $p = 0.0001$ ]; total volume increased with increasing MA concentration.

#### Experiment 5: Two-Bottle Choice Methamphetamine Intake in C57BL/6J-Taar1<sup>m1J/m1J</sup> KI and C57BL/6J-Taar1<sup>+/+</sup> Control Mice

C57BL/6J-Taar1<sup>m1J/m1J</sup> KI mice consumed more MA and exhibited greater MA preference than C57BL/6J-Taar1<sup>+/+</sup> control mice (**Figure 6**). MA intake, preference and total volume intake data were analyzed as described for Experiment 4. For MA intake (**Figure 6A**), there was a significant line  $\times$  concentration interaction [ $F_{(3,129)} = 19.4$ ,  $p < 0.0001$ ]. C57BL/6J-Taar1<sup>m1J/m1J</sup> KI mice consumed more MA than C57BL/6J-Taar1<sup>+/+</sup> control mice at all MA concentrations, except 10 mg/L (there was a strong statistical trend,  $p = 0.07$ ). Although there was an increase in intake in both lines across concentration, the increase was steeper in the C57BL/6J-Taar1<sup>m1J/m1J</sup> KI mice (see mean comparison results in **Figure 6A**). There was also a significant line  $\times$  sex interaction [ $F_{(1,129)} = 5.4$ ,  $p = 0.025$ ]. However, this interaction was due to a magnitude effect, as there was a significant difference in MA intake between the KI and control mice ( $ps < 0.001$ ) for both males and females ( $5.2 \pm 0.6$  mg/kg and  $2.7 \pm 0.4$  for KI vs. control males;  $7.5 \pm 0.6$  and  $2.5 \pm 0.4$  for KI vs. control females), but the difference was 1.9 fold in males and 3 fold in females.

For MA preference (**Figure 6B**), there was a significant line  $\times$  concentration interaction [ $F_{(3,132)} = 5.5$ ,  $p = 0.001$ ], with significantly greater MA preference in C57BL/6J-Taar1<sup>m1J/m1J</sup> KI mice compared to C57BL/6J-Taar1<sup>+/+</sup> control mice for the 40 and 80 mg/L concentrations ( $ps < 0.001$ ). There was no significant effect of sex. MA preference decreased in the control mice across increasing concentrations ( $p < 0.0001$ ; see **Figure 6B** for mean comparisons), but remained stable in the KI mice. For total volume consumed (**Figure 6C**), there was a significant line  $\times$  sex interaction [ $F_{(1,144)} = 13.9$ ,  $p = 0.0006$ ], and a significant effect of concentration [ $F_{(3,129)} = 3.3$ ,  $p = 0.02$ ]. However, there were no significant increases in fluid consumption from one concentration to the next higher

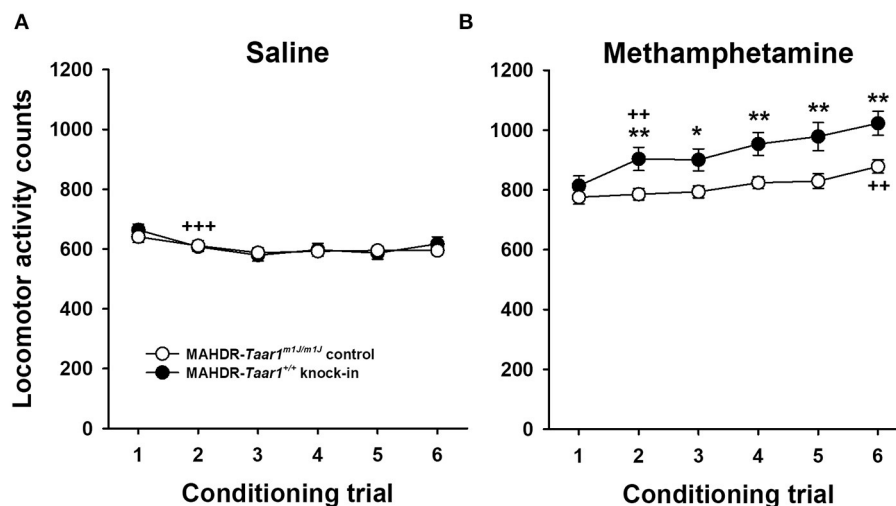


**FIGURE 3 |** Locomotor activity levels of saline-treated and acute MA-treated MAHDR-Taar1<sup>+/+</sup> KI and MAHDR-Taar1<sup>m1J/m1J</sup> control mice are comparable, but locomotor sensitization is more rapid in MAHDR-Taar1<sup>+/+</sup> KI mice. Shown are mean  $\pm$  SEM locomotor activity counts on each day of conditioning with either (A) saline or (B) MA. Mice were treated with saline or 0.5 mg/kg MA immediately prior to each 15-min conditioning trial. Mice were the same animals that generated the data in Figure 2. \* $p < 0.05$ , \*\* $p < 0.01$  for the line difference; ++ $p < 0.01$ , +++ $p < 0.001$  for the difference from the previous conditioning trial. MA, methamphetamine; MAHDR, methamphetamine high drinking mice; Taar1<sup>+/+</sup>, homozygous reference trace amine-associated receptor 1 genotype; Taar1<sup>m1J/m1J</sup>, homozygous mutant trace amine-associated receptor 1 genotype.

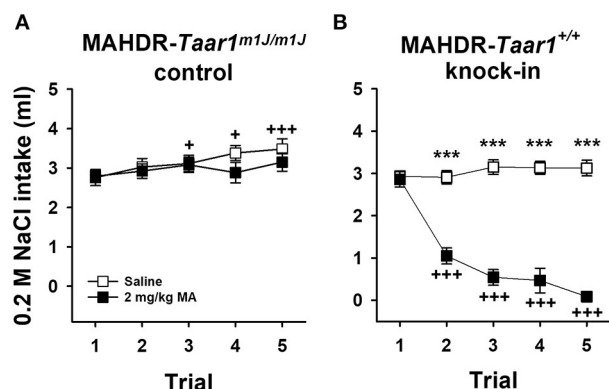


**FIGURE 4 |** MAHDR-Taar1<sup>+/+</sup> KI mice, but not MAHDR-Taar1<sup>m1J/m1J</sup> control mice, exhibit MA-induced conditioned taste aversion. Shown are means  $\pm$  SEM for 0.2 M NaCl intake in (A) MAHDR-Taar1<sup>m1J/m1J</sup> control mice and (B) MAHDR-Taar1<sup>+/+</sup> KI mice. Consumption trials were separated by 48 h, and saline or 2 mg/kg MA injections (IP) were given immediately after 1 h NaCl access for trials 1–4. Total  $N = 48$  mice (6 per line per sex per treatment). \*\*\* $p < 0.001$  for the difference between treatment groups; + $p < 0.05$ , +++ $p < 0.001$  for the difference compared to trial 1, collapsed on treatment (A) or within the MA treatment group (B). MA, methamphetamine; MAHDR, methamphetamine high drinking mice; NaCl, sodium chloride; Taar1<sup>+/+</sup>, homozygous reference trace amine-associated receptor 1 genotype; Taar1<sup>m1J/m1J</sup>, homozygous mutant trace amine-associated receptor 1 genotype.

concentration. The line  $\times$  sex interaction was due to significantly more total volume consumed by female C57BL/6J-Taar1<sup>m1J/m1J</sup> KI mice, compared to female C57BL/6J-Taar1<sup>+/+</sup> control mice

(27.6  $\pm$  1.2 vs. 22.0  $\pm$  0.9, respectively;  $p = 0.0004$ ), but no significant difference between male mice of the KI and control lines (22.7  $\pm$  1.2 vs. 24.7  $\pm$  0.8, respectively;  $p = 0.17$ ).

### Experiment 6: MA-Induced Body Temperature Change in DBA/2J-Taar1<sup>+/+</sup> KI and DBA/2J-Taar1<sup>m1J/m1J</sup> Control Mice

DBA/2J-Taar1<sup>+/+</sup> KI mice displayed MA-induced hypothermia, whereas DBA/2J-Taar1<sup>m1J/m1J</sup> control mice exhibited MA-induced hyperthermia (Figure 7). An interaction with sex was associated with a longer duration of the difference in body temperature response between the two lines in females than in males. Thus, the sex difference did not impact the conclusion regarding the impact of the genetic manipulation. The following analyses support our conclusions. Body temperature data were first analyzed by repeated measures factorial ANOVA grouped on line, sex and treatment (saline or 2 mg/kg MA), with time as the repeated measure. There was a significant four-way interaction [ $F_{(5,365)} = 4.3$ ,  $p = 0.0009$ ]. Because our main interest is in differences between the mouse lines in MA response, we performed ANOVAs to determine if there were effects of line, treatment and time within each sex. In both the males and females, there was a significant line  $\times$  treatment  $\times$  time interaction [ $F_{(5,180)} = 6.4$ ,  $p < 0.0001$  for males;  $F_{(5,185)} = 11.3$ ,  $p < 0.0001$  for females]. For both male and female DBA/2J-Taar1<sup>m1J/m1J</sup> control mice, there was a treatment  $\times$  time interaction [ $F_{(5,90)} = 7.1$ ,  $p < 0.0001$  for males;  $F_{(5,95)} = 9.2$ ,  $p < 0.0001$  for females]. Mean differences are indicated in Figures 7A,B. There were no differences in body temperature between the treatment groups at T0. Female DBA/2J-Taar1<sup>m1J/m1J</sup> control mice treated with MA had

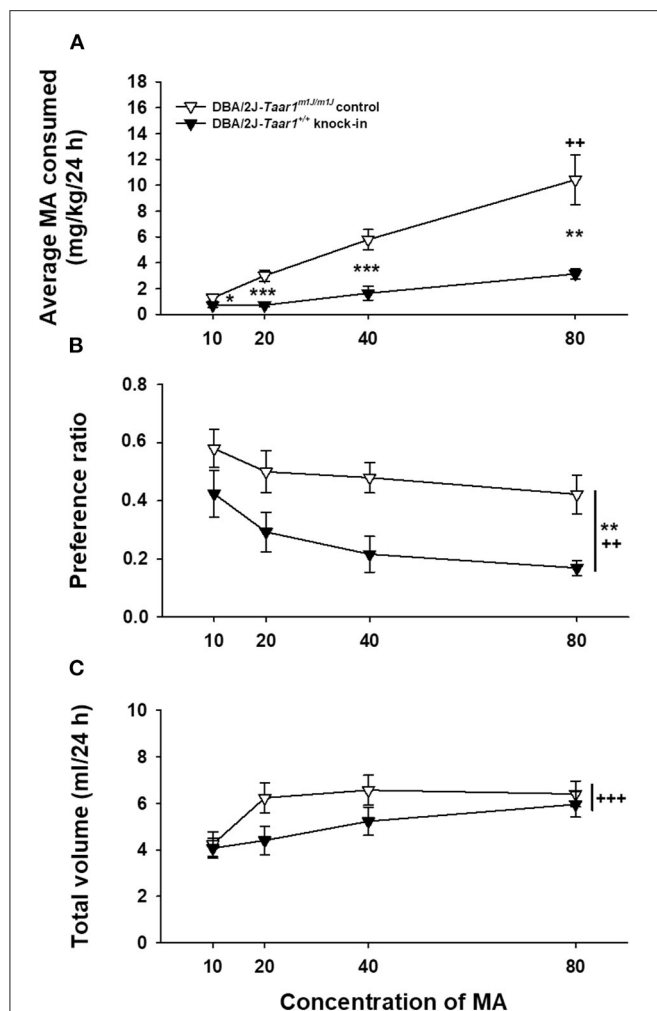


**FIGURE 5** | DBA/2J-*Taar1*<sup>m1J/m1J</sup> control mice consume more MA and exhibit greater MA preference, compared to DBA/2J-*Taar1*<sup>+/+</sup> KI mice. Shown are means  $\pm$  SEM for (A) average MA consumed (mg/kg/24 h), (B) preference ratio (ml from MA tube/total ml consumed), and (C) total volume consumed (ml/24 h) during two-bottle choice of water and ascending concentrations of MA. Each concentration was offered for a 4-day period. Total  $N = 32$  mice (eight per mouse line per sex); \* $p < 0.05$ , \*\* $p < 0.01$ , \*\*\* $p < 0.001$  for the difference between mouse lines for a given concentration (A) or collapsed on concentration (B); ++ $p < 0.01$ , +++ $p < 0.001$  for the effect of concentration compared to the previous concentration (A) or for the main effect of concentration (B,C). MA, methamphetamine; *Taar1*<sup>+/+</sup>, homozygous reference trace amine-associated receptor 1 genotype; *Taar1*<sup>m1J/m1J</sup>, homozygous mutant trace amine-associated receptor 1 genotype.

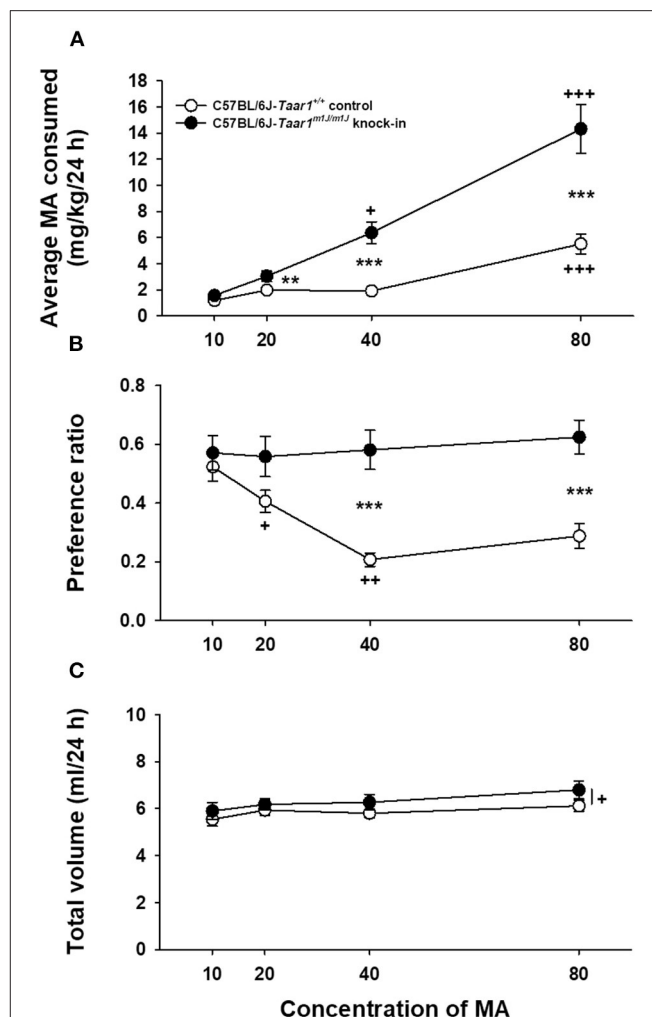
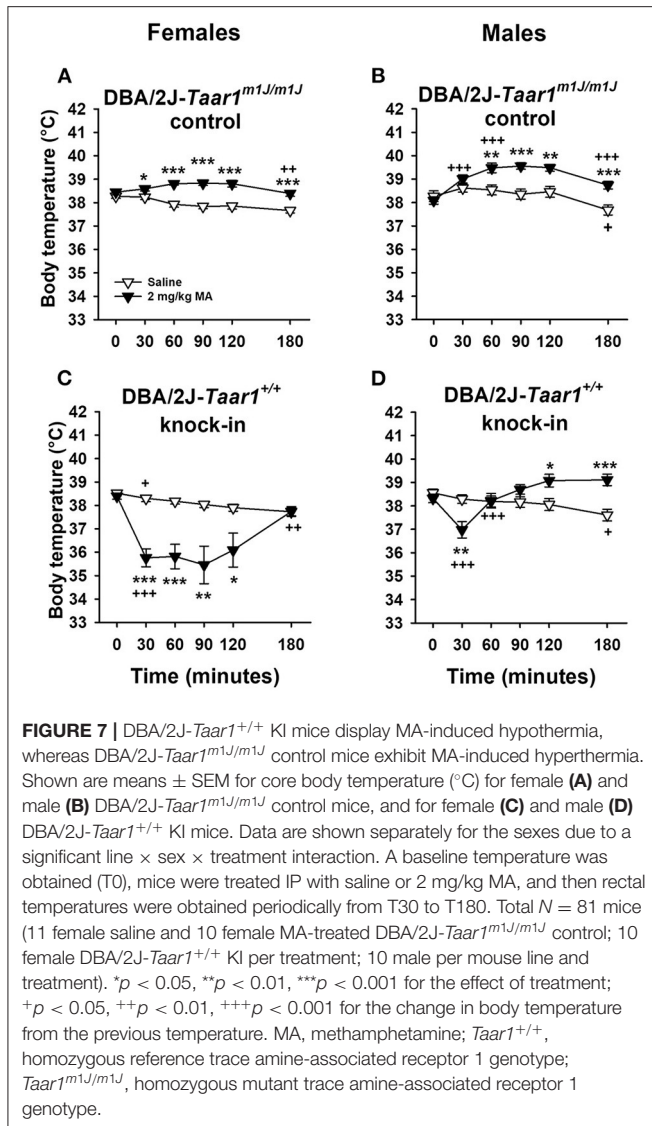


**FIGURE 6** | C57BL/6J-*Taar1*<sup>m1J/m1J</sup> KI mice consume more MA and exhibit greater MA preference than C57BL/6J-*Taar1*<sup>+/+</sup> control mice. Shown are means  $\pm$  SEM for (A) average MA consumed (mg/kg/24 h), (B) preference ratio (ml from MA tube/total ml consumed), and (C) total volume consumed (ml/24 h) during two-bottle choice of water and ascending concentrations of MA. Each concentration was offered for a 4-day period. Total  $N = 47$  (eight mice per sex for the C57BL/6J-*Taar1*<sup>m1J/m1J</sup> KI; 16 male C57BL/6J-*Taar1*<sup>+/+</sup> control mice, and 15 female C57BL/6J-*Taar1*<sup>+/+</sup> control mice. \*\* $p < 0.01$ , \*\*\* $p < 0.001$  for the difference between mouse lines; + $p < 0.05$ , ++ $p < 0.01$ , +++ $p < 0.001$  for the effect of concentration compared to the previous concentration (A,B) or for the main effect of concentration (C). MA, methamphetamine; *Taar1*<sup>+/+</sup>, homozygous reference trace amine-associated receptor 1 genotype; *Taar1*<sup>m1J/m1J</sup>, homozygous mutant trace amine-associated receptor 1 genotype.

significantly higher body temperatures at T30–T180 than their saline-treated counterparts. A similar difference was found in males, beginning at T60. For both male and female DBA/2J-*Taar1*<sup>+/+</sup> KI mice, there was a treatment  $\times$  time interaction [ $F_{(5,90)} = 18.9$ ,  $p < 0.0001$  for males;  $F_{(5,90)} = 8.8$ ,  $p < 0.0001$  for females]. Mean differences are indicated in Figures 7C,D. There were no differences in body temperature between the treatment groups at T0. Female DBA/2J-*Taar1*<sup>+/+</sup> KI mice exhibited long-lasting hypothermia from T30–T120, whereas males exhibited

significant MA-induced hypothermia only at T30. The MA-treated males had significantly higher body temperatures than saline-treated males at T120 and T180.

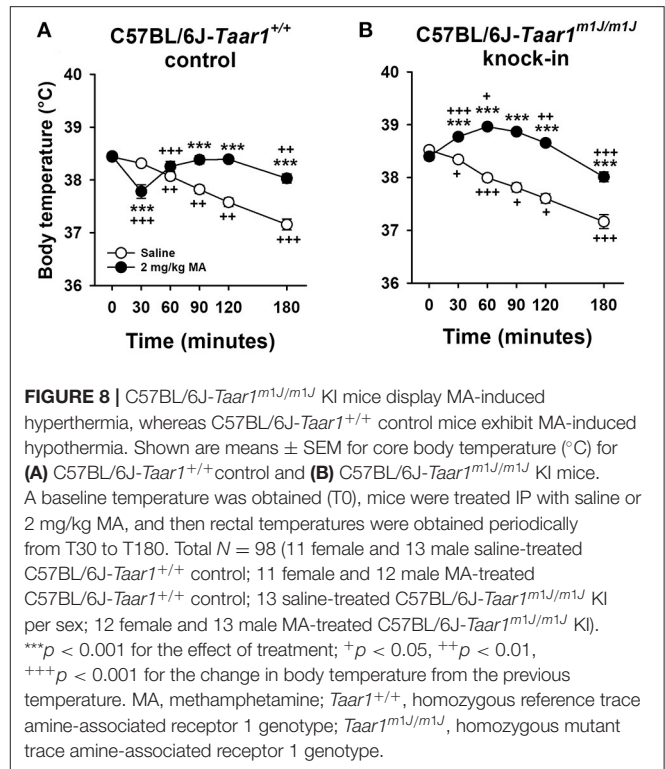
We next examined the data for line, sex and time differences within each treatment condition. Data are presented in Supplementary Figure 1. For the saline-treated mice, there was a significant effect of time [ $F_{(5,185)} = 18.9$ ,  $p < 0.0001$ ], but no significant effect of line or sex. Body temperature changes



were examined by comparing adjacent means (i.e., change from the prior time point). Body temperature at T180 was significantly lower than at T120 ( $p < 0.0001$ ). For the MA-treated mice, there was a significant 3-way interaction of line, sex and time [ $F_{(5,180)} = 3.8$ ,  $p = 0.003$ ]. There were no differences in body temperature between the lines for the MA-treatment group at T0. Female DBA/2J-*Taar1*<sup>+/+</sup> KI mice had lower body temperatures than female DBA/2J-*Taar1*<sup>m1J/m1J</sup> control mice after MA treatment at T30–T180. A similar difference was found in males at T30–T90. Significant changes across time are indicated in Supplementary Figure 1.

### Experiment 7: MA-Induced Body Temperature Change in C57BL/6J-*Taar1*<sup>m1J/m1J</sup> KI and C57BL/6J-*Taar1*<sup>+/+</sup> Control Mice

C57BL/6J-*Taar1*<sup>m1J/m1J</sup> KI mice displayed MA-induced hyperthermia, whereas C57BL/6J-*Taar1*<sup>+/+</sup> control mice



exhibited MA-induced hypothermia (Figure 8). The following analyses support this summary. Body temperature data were first analyzed by repeated measures factorial ANOVA grouped on line, sex, and treatment (saline or 2 mg/kg MA), with time as the repeated measure. There were two significant three-way interactions; a line  $\times$  treatment  $\times$  time interaction [ $F_{(5,450)} = 20.0$ ,  $p < 0.0001$ ] and a sex  $\times$  treatment  $\times$  time interaction [ $F_{(5,450)} = 7.0$ ,  $p < 0.0001$ ]. There were no interactions of sex with line, indicating that line differences were not sex-dependent.

To examine the line  $\times$  treatment  $\times$  time interaction, data were examined for treatment effects within each line. For the C57BL/6J-*Taar1*<sup>+/+</sup> control mice (Figure 8A), there was a significant treatment  $\times$  time interaction [ $F_{(5,225)} = 34.7$ ,  $p < 0.0001$ ]. MA produced significant hypothermia at T30, and the declining temperatures that occurred in the saline group across time were reduced in the MA-treated mice; thus, they had higher body temperatures at T90–T180. For the C57BL/6J-*Taar1*<sup>m1J/m1J</sup> KI mice (Figure 8B), there was a significant treatment  $\times$  time interaction [ $F_{(5,245)} = 37.2$ ,  $p < 0.0001$ ]. MA-treated mice had higher body temperatures than saline-treated mice at all time points except T0.

We next examined the data for line and time differences within each treatment condition. Data are presented in Supplementary Figure 2. For the saline group, there was a significant effect of time [ $F_{(5,240)} = 140.8$ ,  $p < 0.0001$ ], but no body temperature differences between the mouse lines. For the MA treatment group, there was a significant line  $\times$  time interaction [ $F_{(5,230)} = 23.0$ ,  $p < 0.0001$ ], and the mouse lines differed in body temperature at all time points except

T0 and T180. Significant changes across time are indicated in **Supplementary Figure 2**.

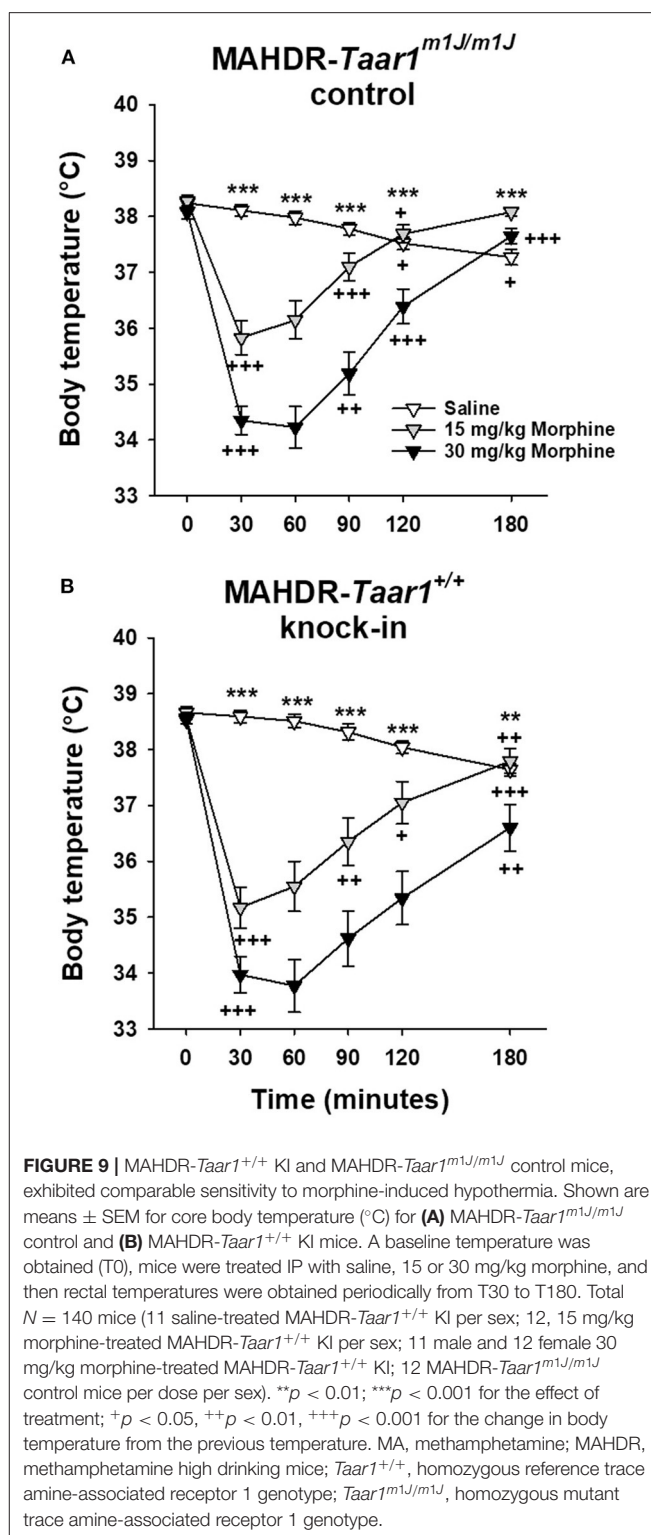
### Experiment 8: Morphine-Induced Body Temperature Changes in MAHDR-*Taar1*<sup>+/+</sup> KI and MAHDR-*Taar1*<sup>m1J/m1J</sup> Control Mice

MAHDR-*Taar1*<sup>+/+</sup> KI and MAHDR-*Taar1*<sup>m1J/m1J</sup> control mice, exhibited comparable sensitivity to morphine-induced hypothermia (**Figure 9**). The following statistical outcomes support this conclusion. In the initial 4-way repeated measures ANOVA, the only significant effects involving line were line  $\times$  morphine dose [ $F_{(2,129)} = 3.2, p = 0.04$ ] and line  $\times$  time [ $F_{(5,645)} = 3.6, p = 0.003$ ] interactions. However, further examination of the effect of line at each morphine dose, identified no statistically significant differences, and examination of the line  $\times$  time interaction identified a significant line difference in body temperature only at T0 ( $p < 0.0001$ ), with a higher temperature in MAHDR-*Taar1*<sup>+/+</sup> KI than MAHDR-*Taar1*<sup>m1J/m1J</sup> control mice of only 0.4°C. Although line did not interact with morphine dose and time, data were analyzed separately for each line to demonstrate that morphine induced significant hypothermia. The outcomes of these analyses are represented in **Figures 9A,B**. Within each line, there was no effect of dose at T0, but there were significant dose effects at all other time points, supporting morphine-induced hypothermia.

In addition, there was a sex  $\times$  treatment  $\times$  time interaction [ $F_{(10,645)} = 2.2, p = 0.02$ ]. When data were examined for sex differences, there was a significant sex  $\times$  time interaction for the 0 [ $F_{(5,220)} = 2.6, p = 0.03$ ] and 30 mg/kg [ $F_{(5,225)} = 3.8, p = 0.002$ ] dose groups, but not the 15 mg/kg dose group. Further examination of the effect of sex at each time point for the saline treatment dose, identified no statistically significant differences. For the 30 mg/kg dose group, females had lower temperatures than males at T30 ( $p = 0.004$ ) and T60 ( $p = 0.03$ ), reflecting greater morphine-induced hypothermia. The temperature difference was 1.2°C at T30 and 1.3°C at T60; however, this sex effect was not dependent on line and thus, did not impact conclusions regarding the genetic manipulation.

## DISCUSSION

Our research provides new and conclusive evidence indicating that a *Taar1* SNP with a key role in MA intake also impacts sensitivity to MA-induced conditioned place preference, conditioned taste aversion and hypothermia. Furthermore, we demonstrate impacts of *Taar1* genotype on multiple genetic backgrounds and significant reciprocal effects of allele exchange by CRISPR-Cas9. Low MA intake is associated with low sensitivity to MA reward and high sensitivity to aversive effects of MA. Furthermore, we confirm prior evidence indicating that a gene in linkage disequilibrium with *Taar1* is responsible for a difference in sensitivity to morphine-induced hypothermia in the MADR mouse lines. **Table 2** summarizes our key findings.



### Pleiotropic Effects of *Taar1* on MA-Related Traits in MAHDR Mice

MAHDR mice were selectively bred for high levels of voluntary MA intake using a two-bottle choice water vs. MA solution procedure. Subsequent investigation established that taste does

**TABLE 2 |** Summary of results for *Taar1* genotype effects for all experiments.

Exp	Trait	Background	Tastant or Drug, Dose or Conc.	<i>Taar1</i> <sup>+/+</sup> vs. <i>Taar1</i> <sup>m1J/m1J</sup>
(1)	Intake	MAHDR	SACC, 1.6 and 3.2 mM	=
	Preference	MAHDR	SACC, 1.6 and 3.2 mM	=
	Total volume	MAHDR	SACC, 1.6 and 3.2 mM	=
(1)	Intake	MAHDR	QUIN, 0.015 and 0.03 mM	≥
	Preference	MAHDR	QUIN, 0.015 and 0.03 mM	>
	Total volume	MAHDR	QUIN, 0.015 and 0.03 mM	=
(2)	CPP baseline	MAHDR	Saline	=
	CPP	MAHDR	MA, 0.5 mg/kg then saline test	<
	CPP drug-present	MAHDR	MA, 0.5 mg/kg then 0.5 mg/kg test	<
(3)	CTA	MAHDR	MA, 0 and 2 mg/kg	>
(4)	Intake	DBA/2J	MA, 10–80 mg/L	<
	Preference	DBA/2J	MA, 10–80 mg/L	<
	Total volume	DBA/2J	MA, 10–80 mg/L	=
(5)	Intake	C57BL/6J	MA, 10–80 mg/L	<
	Preference	C57BL/6J	MA, 10–80 mg/L	<
	Total volume	C57BL/6J	MA, 10–80 mg/L	<*
(6)	Hypothermia	DBA/2J	MA, 0 and 2 mg/kg	>
	Hyperthermia	DBA/2J	MA, 0 and 2 mg/kg	<
(7)	Hypothermia	C57BL/6J	MA, 0 and 2 mg/kg	>
	Hyperthermia	C57BL/6J	MA, 0 and 2 mg/kg	<
(8)	Hypothermia	MAHDR	Morphine, 0, 15, and 30 mg/kg	=

\*This difference was found in females only; Conc., concentration; CPP, conditioned place preference; CTA, conditioned taste aversion; Exp, experiment; MA, methamphetamine; MAHDR, methamphetamine high drinking line; QUIN, quinine; SACC, saccharin; *Taar1*<sup>+/+</sup>, homozygous reference trace amine-associated receptor 1 genotype; *Taar1*<sup>m1J/m1J</sup>, homozygous mutant trace amine-associated receptor 1 genotype.

not provide an explanation for the difference in MA intake between the MADR lines (16, 18), the MAHDR mice will voluntarily consume binge-like levels of MA (17), and baseline measures, including locomotor activity, measures of learning and memory, body weight, and body temperature, do not systematically differentiate the lines (26). Furthermore, the lines do not differ in responses to cocaine or alcohol, but they do differ in responses to fentanyl, morphine and amphetamine-like drugs, including MDMA (25, 28–30). The current studies investigated whether the *Taar1* SNP that impacts MA intake also plays a part in the reliable differences in MA-induced conditioned place preference, conditioned taste aversion and hypothermia we have observed between the MADR lines (16, 18, 20, 27). Our results confirm an impact of this polymorphism on all three traits.

MAHDR mice consume less morphine and exhibit greater morphine-induced hypothermia than MALDR mice (25, 28). Both *Taar1* and the  $\mu$ -opioid receptor gene, *Oprm1*, are on mouse chromosome 10, 17 Mb apart. We speculated that the differences in morphine consumption and hypothermia were associated with linkage disequilibrium and more likely an effect of different *Oprm1* alleles inherited from the DBA/2J and C57BL/6J strains, known to impact morphine preference (31,

32). When we examined *Taar1* and *Oprm1* genotype in MADR line mice tested for morphine-induced hypothermia, there was correspondence of magnitude of hypothermia with *Oprm1*, but not *Taar1*, genotype (25). The current data in the MAHDR KI model are consistent with the conclusion that the *Taar1* SNP is not responsible for the difference in morphine-induced hypothermia between the MADR lines, and that another gene(s) is responsible. We have not tested the MAHDR KI mice for all of the traits previously examined in the MADR lines, but would not expect the KI and control lines to differ for cocaine or alcohol responses. We did observe an unexpected difference in quinine intake in experiment 1, but it was the MA-avoiding line that consumed more quinine, so this result does not provide an explanation for higher consumption of bitter-tasting MA. Future studies will track the reliability of this outcome by repeating the study in all of the KI models.

Finally, the results for locomotor activity in the MAHDR KI and control mice agree with our prior findings in the MADR lines that also did not differ in acute locomotor response to 0.5 mg/kg MA. However, the differences found here between the lines, with *Taar1*<sup>+/+</sup> mice exhibiting greater locomotor activity on subsequent MA treatment trials than *Taar1*<sup>m1J/m1J</sup> mice, were not found for the MALDR and MAHDR lines (16). Although it is possible that this difference is related to *Taar1* genotype, existing studies indicate that mice without *Taar1* function would be more likely to exhibit the greater stimulant response (see section Other examples of single gene identification for addiction-related traits), opposite to our finding. However, differences in those studies were found for higher doses of MA. It is possible that a genetic background difference played a role in the current outcome. Dose-response studies and studies in the other KI and control lines would benefit interpretation.

## Genetic Background Effects

Previous data support an impact of *Taar1* genotype on MA intake and other MA-related traits in multiple mouse models, derived from the DBA/2J and C57BL/6 strains that served as the progenitors of the MADR lines (22). Because many polymorphisms differentiate these strains, more definitive attribution of a trait difference to the *Taar1* SNP is provided by KI models in which the SNP is specifically manipulated. Thus, we generated multiple CRISPR-Cas9 KI models to provide conclusive evidence of the impact of the *Taar1* SNP and examine potential genetic background effects. In addition, robust effects were observed when the mutant *Taar1* allele was replaced with the reference allele in MAHDR mice (21), but we did not know whether such robust effects would be observed for the reciprocal manipulation. Results for MA intake and preference aligned with *Taar1* genotype across all of the KI models. Thus, *Taar1*<sup>m1J/m1J</sup> mice of both MAHDR and DBA/2J backgrounds consumed more MA and exhibited greater MA preference than their *Taar1*<sup>+/+</sup> controls [see (21) and Table 2]. Likewise, results for MA treatment-induced temperature changes were aligned with *Taar1* genotype across all of the KI models, with *Taar1*<sup>+/+</sup> controls exhibiting hypothermic responses that did not occur in *Taar1*<sup>m1J/m1J</sup> mice [see (20) and Table 2].

Although there were similar general outcomes, there were some qualitative differences in results across the models. Because MA intake data for the DBA/2J and C57BL/6 genetic backgrounds were not collected simultaneously, they could not be subjected to direct comparative analysis, but some observations may be worth noting. The effect of exchanging the reference *Taar1* allele with the mutant allele in C57BL/6J mice was an increase in MA intake that peaked at about 14 mg/kg for the 80 mg/L MA concentration, whereas the DBA/2J mice, which naturally possess the mutant *Taar1* genotype consumed about 10 mg/kg MA at the 80 mg/L concentration. Furthermore, the MA intake of mice possessing the *Taar1*<sup>+/+</sup> genotype on the C57BL/6J vs. DBA/2J background was 5 mg/kg, compared to 3 mg/kg, for the highest MA concentration. This may indicate that there are other genetic variants promoting MA intake in the C57BL/6J strain even in the presence of the protective *Taar1*<sup>+/+</sup> genotype. This is supported by somewhat higher MA preference in *Taar1*<sup>+/+</sup> mice of the C57BL/6J background. However, the lower overall MA preference of mice with the *Taar1*<sup>+/+</sup> genotype, compared to those with the *Taar1*<sup>m1J/m1J</sup> genotype, was clear on both backgrounds. In previous studies, results were compared under identical conditions for DBA/2J and MAHDR mice for MA intake in a binge drinking procedure and for the effect of binge-level drinking followed by withdrawal on depression-like outcomes. MAHDR mice consumed almost twice as much MA as DBA/2J mice. In addition, MAHDR mice displayed greater depression-like symptoms after withdrawal, which may have been related to their higher MA intake (33). Higher MA intake of the MAHDR mice, compared to the DBA/2J, could be due to the presence of C57BL/6J alleles in the MAHDR mice that are permissive for MA intake.

Another apparent difference found in the current studies was a greater reduction over time in body temperature of saline-treated C57BL/6J mice, compared to DBA/2J mice, during isolate housing. This did not impact our ability to detect MA-induced hypothermia, because that effect tends to be most robust within the first 30 min after administration, but it did clearly demonstrate the ability of MA treatment to inhibit the progressive reduction in body temperature.

Rarely have we found sex differences that interact with line in our previous studies of MA-related traits. A significant line  $\times$  sex  $\times$  time interaction was observed in the examination of MA effects on body temperature in the DBA/2J KI and control line study, but not the C57BL/6J study. Examination of the patterns of response in **Figures 7, 8** indicate a strong similarity in male DBA/2J mice with the overall outcome for the C57BL/6J mice. However, female DBA-*Taar1*<sup>+/+</sup> KI mice had a markedly prolonged hypothermic response to the 2 mg/kg dose of MA that is more reminiscent of our previous data in MALDR mice (20) and the MAHDR-*Taar1*<sup>+/+</sup> KI mice (21), although sex differences were not found in those studies. We have speculated that greater sensitivity to hypothermic drug effects may be protective against further drug intake and drug toxicity, and could serve as a marker for reduced psychostimulant addiction risk (25, 34, 35). Additional data are needed to determine if this is a replicable finding worth pursuing.

## Other Examples of Single Gene Identification for Addiction-Related Traits

The successful identification of single gene effects on complex traits, including addiction-related phenotypes, is increasing. Drug-induced stimulation has been of considerable focus, because feelings of stimulation or euphoria in humans appear to contribute to the potential for escalated use (36). Recent data confirmed *Hnrnp1* as a quantitative trait gene for sensitivity to MA-induced stimulation (37). Similar to the way in which *Taar1* was identified, *Hnrnp1* was first implicated in a quantitative trait locus analysis (38), and then gene editing was used to produce a deletion in the first coding exon of the gene and substantiate its role. Not only did this deletion reduce sensitivity to MA stimulation, it also decreased MA-induced reinforcement, reward and dopamine release (39). It is of interest that MA-induced stimulation also tends to be greater in *Taar1*<sup>m1J/m1J</sup> and *Taar1* knock-out mice, both of which lack TAAR1 function and consume more MA or exhibit greater MA reward and reinforcement (16, 18, 20, 40–43). Another study focused on a region of the cannabinoid-1 receptor gene associated with drug and alcohol addiction (44, 45). Deletion using CRISPR-Cas9 technology reduced expression of the cannabinoid-1 receptor in the hippocampus and also reduced alcohol intake (46). Thus, in recent years, several addiction-relevant genes have been identified using genetic mapping and rapid deletion and KI techniques.

The *Taar1* SNP is a spontaneously occurring mutation that arose in the JAX DBA/2J mice between 2001 and 2003 (22). Such mutations are not rare. For example, a single base pair deletion arose in intron 3 of the C57BL/6J *Gabra2* gene adjacent to a splice acceptor site that results in global reduction of mRNA and protein level expression, compared to levels found in other inbred mouse strains. When CRISPR-Cas9 was used to repair the deletion, mRNA and protein levels were restored (47). GABRA2 variation has been implicated in alcoholism and drug abuse in human populations (48–52). It is possible that this gene also plays a role in the high alcohol consumption found in C57BL/6J mice, compared to many other strains [e.g., (53, 54)].

Finally, based on previous data supporting an association of the glutamate receptor subunit gene, ionotropic N-methyl-D-aspartate 3A (*GRIN3A*), with nicotine dependence, 16 SNPs were examined in a Chinese Han population. A single SNP association was identified and gene editing was performed in cultured cells using CRISPR-Cas9 to demonstrate a regulatory function impacting mRNA and protein expression that could be related to differential susceptibility to nicotine dependence (55). The obvious question arises as to whether human TAAR1 variants impact risk for MA addiction. In the mouse, a key feature of *Taar1* involvement in MA intake appears to be initial sensitivity to adverse effects of MA, such as conditioned aversion and hypothermia. In fact, the MALDR mice bred for low MA intake consume a comparable amount the first time MA is offered, precipitously reducing their intake in the next drinking session, presumably after experiencing negative subjective effects (42, 56). The predictive outcome of negative first experiences with amphetamines have not often been studied in humans,

although there are a few laboratory-based studies. The general outcome for acute amphetamine and methylphenidate, the two drugs most studied in healthy non-addicted young adults, have documented variation in ratings of arousal, liking and anxiety. Most report positive mood effects, but some report unpleasant effects, and these outcomes predict subsequent session choices of whether or not to take the drug again [see (36)]. None of this research has examined genetic relationships. A recent study by Loftis et al. (57) identified a synonymous *TAAR1* SNP that was associated with higher MA craving in individuals with active MA dependence and in remission, compared to controls with no history of substance dependence. When examined in cell culture, cells transfected with this variant had 40% higher TAAR1 protein expression, compared to cells transfected with the wild-type allele, but no change in protein function. It would be interesting to test this variant in a rodent model of MA craving.

## Potential Shortcomings and Limitations of the Current Work

MA consumption was measured slightly differently at JAX in the DBA/2J and C57BL/6J KI and control mice, compared to the way in which it was measured in our previous studies of the MADR lines and MAHDR KI and controls at the VAPORHCS. At JAX, mice were given access to MA for 24 h/day vs. the 18 h/day established procedure at the VAPORHCS. The JAX method is procedurally simpler, since bottles do not need to be manipulated during the course of the day, as they do for the 18 h/day procedure. Although this reduces our ability to directly compare MA intake amounts across studies conducted at the two locations, there is no issue with evaluating genotype effects using either procedure, as can be seen here and in our data for the MAHDR KI and control mice (21). In fact, a previous study found that MA intake was lower when offered to MAHDR mice for 24 h/day, compared to 18 h/day, but that the difference in MA intake between MAHDR and MALDR mice remained robust (58).

Our MA-induced conditioned place preference, conditioned taste aversion and hypothermia studies examined the effects of only a single MA dose in each case. The dose used was chosen from previous dose-response studies to reliably produce the effects examined here (16, 18, 20, 27). Furthermore, we have found mice with the *Taar1*<sup>m1J/m1J</sup> genotype to be insensitive to the aversive and hypothermic effects of a wide range of MA doses (20, 27); thus, we do not believe that testing additional doses would change the general outcome of the associations described here. Likewise, mice possessing the *Taar1*<sup>+</sup> allele have exhibited little to no sensitivity to rewarding or reinforcing effects of MA (16, 42).

Our KI mice are produced by separate breeding pairs from those that produce our control mice; thus, the mice are not littermates. However, that is also the case for all mice that possess each of these genotypes, with the exception of non-inbred crosses. For example, the *Taar1*<sup>m1J</sup> mutation is found in homozygous form in DBA/2J mice and in some strains of the C57BL/6J × DBA/2J recombinant inbred (BXD RI) series (21, 22, 24, 25). F2 crosses of these mice result in the 3

possible *Taar1* genotypes: *Taar1*<sup>+/+</sup>, *Taar1*<sup>+/m1J</sup>, *Taar1*<sup>m1J/m1J</sup>. *Taar1* genotype—phenotype correlations for MA intake in F2 mice, raised with mixed *Taar1* genotypes among littermates, are comparable to those for MADR line individuals and BXD RI strains (22).

## CONCLUSIONS AND FUTURE DIRECTIONS

The *Taar1* SNP at position 229 accounts for 60% of the genetic variance in MA intake in the selectively bred MADR lines (19, 21). Additional research is underway to identify other genes that impact MA intake, including the identification of relevant gene networks [e.g., (15, 19)]. Variance in MA intake in mice with functional TAAR1 is low, whereas variance in mice lacking TAAR1 function is high (17, 22). Data herein and in our published papers indicate that TAAR1 agonist effects of MA are aversive, and we hypothesize that these effects mask rewarding MA effects, strongly inhibiting MA intake. Greater knowledge about the mechanisms by which TAAR1 agonism induces aversion could be leveraged to identify more efficacious treatments for methamphetamine addiction. Because TAAR1 is located intracellularly, MA must be transported into the cell, for example by the dopamine transporter, to gain access. TAAR1 is localized to distinct cellular compartments and signals through different Gα proteins. Thus, cytoplasmic TAAR1 signals via Gαs and adenylyl cyclase, whereas TAAR1 localized to the endoplasmic reticulum signals via Gα13, stimulating the GTPase, RhoA (59). The involvement of these different mechanisms in different aspects of TAAR1 effects is currently unknown, as is the circuitry underlying TAAR1 agonist-induced aversion. The lateral habenula (LHb) encodes negative prediction errors and punishment signals, and LHb activation results in aversive behaviors (60–62). Further, acute MA induces expression of the immediate early gene, *fos* (63), and lesions of the LHb increase amphetamine-induced stimulation (64). Based on data indicating that glutamate-mediated synaptic plasticity differentiates the MADR lines (15), and data demonstrating differences between the MADR lines in glutamate responses to MA (65, 66), future studies are planned to examine TAAR1 regulation of glutamate synapses in ventral tegmental area dopamine neurons and dorsal raphe serotonin neurons, arising from LHb afferents (67).

Because mice that lack functional TAAR1 are deficient in the opposing aversion mechanism, they have the capacity to experience MA reward. Individual variability in the strength of the rewarding effect may be responsible for residual variability in MA intake in the MAHDR line. Another source of individual variability is genetic modifiers of the *Taar1*<sup>m1J</sup> effect in homozygous individuals. We are examining this in the heterogeneous stock—collaborative cross mice developed by our collaborator, Dr. Robert Hitzemann, at the VAPORHCS, which are the product of an 8-way cross of mouse strains representing 89% of the genetic variability present in mice (68, 69). We recently reported the successful selective breeding of mice for higher and lower amounts

of MA intake from a population of individuals that are all homozygous for the *Taar1*<sup>m1J</sup> allele (70). These lines will allow us to perform transcriptome analyses to identify genetic differences that result in resistance to the enhancing effect of the homozygous *Taar1*<sup>m1J</sup> genotype on MA intake, information that could lead to the identification of a new class of therapeutics.

We previously found that although *Oprm1* is not a quantitative trait gene for MA intake (71), it serves as a hub when added to a network of differentially expressed genes derived from nucleus accumbens, prefrontal cortex and ventral midbrain samples from the MALDR and MAHDR lines (19). We confirmed herein that *Taar1* does not impact sensitivity to morphine-induced hypothermia; rather, *Oprm1* likely underlies differential sensitivity to this morphine effect in the MADR lines. This may also be the case for the differential morphine intake of the MADR lines (28), though we have not yet examined this trait in the KI mice. Buprenorphine reduced MA intake in MAHDR mice without impacting total fluid consumption. Lower doses were effective, but higher doses known to have  $\mu$ -opioid receptor antagonist effects were ineffective, as was the  $\mu$ -opioid receptor antagonist, naltrexone (28). Morphine, on the other hand, reduced MA intake, but also total fluid intake (71). This suggests that a partial agonist could serve as a treatment to reduce MA intake. To determine whether *Oprm1* plays a role in the effectiveness of buprenorphine, we intend to test BXD RI strain mice that have the high MA intake *Taar1*<sup>m1J/m1J</sup> genotype, but are homozygous for either the DBA/2J or C57BL/6J *Oprm1* allele. If *Oprm1* allele is irrelevant, than effects on MA intake should be comparable across strains.

Finally, it should be noted that *Taar1* agonists and partial agonists are being explored as therapeutics for MA addiction and other neuropsychiatric conditions (72), and have shown promise in animal models (73–75). Of course, the strategy of increasing TAAR1-mediated activity with direct agonists requires a functional receptor, and thus, is not an approach we have been able to take in our genetic mouse models of absent TAAR1 function. However, we have collected data in mice possessing the *Taar1*<sup>+</sup> allele, and confirmed that TAAR1-specific agonists have strong aversive effects (Shabani and Phillips, unpublished data). It is possible that TAAR1 agonists reduce MA intake via a substitution mechanism (75), but also possible that agonists activate aversion circuitry that reduces the potency of MA reward. We are not aware of reports directly characterizing the subjective effects of TAAR1 agonists in humans.

## REFERENCES

1. Barkley-Levenson AM, Cunningham CL, Smitasin PJ, Crabbe JC. Rewarding and aversive effects of ethanol in High Drinking in the Dark selectively bred mice. *Addict Biol.* (2015) 20:80–90. doi: 10.1111/adb.12079
2. Cunningham CL. Genetic relationships between ethanol-induced conditioned place aversion and other ethanol phenotypes in 15 inbred mouse strains. *Brain Sci.* (2019) 9:209. doi: 10.3390/brainsci9080209
3. Fritz BM, Cordero KA, Barkley-Levenson AM, Metten P, Crabbe JC, Boehm SL, et al. Genetic relationship between predisposition for binge alcohol consumption and blunted sensitivity to adverse effects of alcohol in mice. *Alcohol Clin Exp Res.* (2014) 38:1284–92. doi: 10.1111/acer.12385
4. Rhodes JS, Ford MM, Yu CH, Brown LL, Finn DA, Garland T Jr, et al. Mouse inbred strain differences in ethanol drinking to intoxication. *Genes Brain Behav.* (2007) 6:1–18. doi: 10.1111/j.1601-183X.2006.00210.x
5. Davidson C, Lee TH, Ellinwood EH. Acute and chronic continuous methamphetamine have different long-term behavioral and neurochemical consequences. *Neurochem Int.* (2005) 46:189–203. doi: 10.1016/j.neuint.2004.11.004
6. Narita M, Miyatake M, Shibasaki M, Tsuda M, Koizumi S, Narita M, et al. Long-lasting change in brain dynamics induced by methamphetamine: enhancement of protein kinase C-dependent astrocytic response and behavioral sensitization. *J Neurochem.* (2005) 93:1383–92. doi: 10.1111/j.1471-4159.2005.03097.x

## DATA AVAILABILITY STATEMENT

The original contributions presented in the study are included in the article/**Supplementary Materials**, further inquiries can be directed to the corresponding author/s.

## ETHICS STATEMENT

The animal study was reviewed and approved by Institutional Animal Care and Use Committee of the VA Portland Health Care System, Portland, OR or the Institutional Animal Care and Use Committee of The Jackson Laboratory, Bar Harbor, ME.

## AUTHOR CONTRIBUTIONS

TP: experimental design, development of mouse models, statistical analysis, data interpretation, and manuscript writing and revision. TR, SA, HB, JE, and JM: data acquisition, entry, and verification of accuracy. CR: development of experimental protocols, supervision of technical staff, statistical analysis, figure preparation, drafting of methods and results, and manuscript editing. EC: experimental design, development of mouse models, and manuscript editing. All authors contributed to the article and approved the submitted version.

## FUNDING

The funding sources for this research were NIH NIDA U01 DA041579 and R01 DA046081 (TP, SA, HB, JE, and CR), P50 DA018165 (TP, HB, JE, and CR), P50 DA039841 (EC and TR), and T32DA007262 (JM); NIH NIAAA R24 AA020245 (TP, JE, and CR); Department of Veterans Affairs I01 BX002106 (TP and JE) and the VA Research Career Scientist Program (TP).

## ACKNOWLEDGMENTS

The authors gratefully acknowledge the assistance of the Scientific Services at The Jackson Laboratory, in particular Genetic Engineering Technology service.

## SUPPLEMENTARY MATERIAL

The Supplementary Material for this article can be found online at: <https://www.frontiersin.org/articles/10.3389/fpsy.2021.725839/full#supplementary-material>

7. Nishioku T, Shimazoe T, Yamamoto Y, Nakanishi H, Watanabe S. Expression of long-term potentiation of the striatum in methamphetamine-sensitized rats. *Neurosci Lett.* (1999) 268:81–4. doi: 10.1016/S0304-3940(99)00386-9
8. Pierce RC, Kalivas PW. A circuitry model of the expression of behavioral sensitization to amphetamine-like psychostimulants. *Brain Res Brain Res Rev.* (1997) 25:192–216. doi: 10.1016/S0165-0173(97)00021-0
9. Richetto J, Feldon J, Riva MA, Meyer U. Comparison of the long-term consequences of withdrawal from repeated amphetamine exposure in adolescence and adulthood on information processing and locomotor sensitization in mice. *Eur Neuropsychopharmacol.* (2013) 23:160–70. doi: 10.1016/j.euroneuro.2012.04.005
10. Robinson TE, Becker JB, Presty SK. Long-term facilitation of amphetamine-induced rotational behavior and striatal dopamine release produced by a single exposure to amphetamine: sex differences. *Brain Res.* (1982) 253:231–41. doi: 10.1016/0006-8993(82)90690-4
11. Schmidt ED, Tilders FJ, Binnekade R, Schoffeleer AN, De Vries TJ. Stressor- or drug-induced sensitization of the corticosterone response is not critically involved in the long-term expression of behavioural sensitization to amphetamine. *Neuroscience.* (1999) 92:343–52. doi: 10.1016/S0306-4522(98)00725-8
12. Schmidt ED, Schoffeleer AN, De Vries TJ, Wardeh G, Dogterom G, Bol JG, et al. A single administration of interleukin-1 or amphetamine induces long-lasting increases in evoked noradrenaline release in the hypothalamus and sensitization of ACTH and corticosterone responses in rats. *Eur J Neurosci.* (2001) 13:1923–30. doi: 10.1046/j.0953-816x.2001.01569.x
13. Tenn CC, Kapur S, Fletcher PJ. Sensitization to amphetamine, but not phencyclidine, disrupts prepulse inhibition and latent inhibition. *Psychopharmacology (Berl).* (2005) 180:366–76. doi: 10.1007/s00213-005-2253-z
14. Vanderschuren LJ, Schmidt ED, De Vries TJ, Van Moorsel CA, Tilders FJ, Schoffeleer AN. A single exposure to amphetamine is sufficient to induce long-term behavioral, neuroendocrine, and neurochemical sensitization in rats. *J Neurosci.* (1999) 19:9579–86. doi: 10.1523/JNEUROSCI.19-21-09579.1999
15. Hitzemann R, Iancu OD, Reed C, Baba H, Lockwood DR, Phillips TJ. Regional analysis of the brain transcriptome in mice bred for high and low methamphetamine consumption. *Brain Sci.* (2019) 9:155. doi: 10.3390/brainsci9070155
16. Shabani S, McKinnon CS, Reed C, Cunningham CL, Phillips TJ. Sensitivity to rewarding or aversive effects of methamphetamine determines methamphetamine intake. *Genes Brain Behav.* (2011) 10:625–36. doi: 10.1111/j.1601-183X.2011.00700.x
17. Shabani S, Houlton SK, Hellmuth L, Mojica E, Mootz JR, Zhu Z, et al. A mouse model for binge-level methamphetamine use. *Front Neurosci.* (2016) 10:493. doi: 10.3389/fnins.2016.00493
18. Wheeler JM, Reed C, Burkhart-Kasch S, Li N, Cunningham CL, Janowsky A, et al. Genetically correlated effects of selective breeding for high and low methamphetamine consumption. *Genes Brain Behav.* (2009) 8:758–71. doi: 10.1111/j.1601-183X.2009.00522.x
19. Belknap JK, McWeeney S, Reed C, Burkhart-Kasch S, McKinnon CS, Li N, et al. Genetic factors involved in risk for methamphetamine intake and sensitization. *Mamm Genome.* (2013) 24:446–58. doi: 10.1007/s00335-013-9484-9
20. Harkness JH, Shi X, Janowsky A, Phillips TJ. Trace amine-associated receptor 1 regulation of methamphetamine intake and related traits. *Neuropsychopharmacology.* (2015) 40:2175–84. doi: 10.1038/npp.2015.61
21. Stafford AM, Reed C, Baba H, Walter NA, Mootz JR, Williams RW, et al. Taar1 gene variants have a causal role in methamphetamine intake and response and interact with *Oprm1*. *Elife.* (2019) 8:e46472. doi: 10.7554/eLife.46472.022
22. Reed C, Baba H, Zhu Z, Erk J, Mootz JR, Varra NM, et al. A spontaneous mutation in Taar1 impacts methamphetamine-related traits exclusively in DBA/2 mice from a single vendor. *Front Pharmacol.* (2018) 8:993. doi: 10.3389/fphar.2017.00993
23. Keane TM, Goodstadt L, Danecsek P, White MA, Wong K, Yalcin B, et al. Mouse genomic variation and its effect on phenotypes and gene regulation. *Nature.* (2011) 477:289–94. doi: 10.1038/nature10413
24. Shi X, Walter NA, Harkness JH, Neve KA, Williams RW, Lu L, et al. Genetic polymorphisms affect mouse and human trace amine-associated receptor 1 function. *PLoS One.* (2016) 11:e0152581. doi: 10.1371/journal.pone.0152581
25. Mootz JRK, Miner NB, Phillips TJ. Differential genetic risk for methamphetamine intake confers differential sensitivity to the temperature-altering effects of other addictive drugs. *Genes Brain Behav.* (2020) 19:e12640. doi: 10.1111/gbb.12640
26. Phillips TJ, Shabani S. An animal model of differential genetic risk for methamphetamine intake. *Front Neurosci.* (2015) 9:327. doi: 10.3389/fnins.2015.00327
27. Shabani S, McKinnon CS, Cunningham CL, Phillips TJ. Profound reduction in sensitivity to the aversive effects of methamphetamine in mice bred for high methamphetamine intake. *Neuropharmacology.* (2012) 62:1134–41. doi: 10.1016/j.neuropharm.2011.11.005
28. Eastwood EC, Phillips TJ. Morphine intake and the effects of naltrexone and buprenorphine on the acquisition of methamphetamine intake. *Genes Brain Behav.* (2014) 13:226–35. doi: 10.1111/gbb.12100
29. Eastwood EC, Phillips TJ. Opioid sensitivity in mice selectively bred to consume or not consume methamphetamine. *Addict Biol.* (2014) 19:370–9. doi: 10.1111/adb.12003
30. Gubner NR, Reed C, McKinnon CS, Phillips TJ. Unique genetic factors influence sensitivity to the rewarding and aversive effects of methamphetamine versus cocaine. *Behav Brain Res.* (2013) 256:420–7. doi: 10.1016/j.bbr.2013.08.035
31. Doyle GA, Furlong PJ, Schwebel CL, Smith GG, Lohoff FW, Buono RJ, et al. Fine mapping of a major QTL influencing morphine preference in C57BL/6 and DBA/2 mice using congenic strains. *Neuropsychopharmacology.* (2008) 33:2801–9. doi: 10.1038/npp.2008.14
32. Doyle GA, Schwebel CL, Ruiz SE, Chou AD, Lai AT, Wang MJ, et al. Analysis of candidate genes for morphine preference quantitative trait locus Mop2. *Neuroscience.* (2014) 277:403–16. doi: 10.1016/j.neuroscience.2014.07.020
33. Shabani S, Schmidt B, Ghimire B, Houlton SK, Hellmuth L, Mojica E, et al. Depression-like symptoms of withdrawal in a genetic mouse model of binge methamphetamine intake. *Genes Brain Behav.* (2019) 18:e12533. doi: 10.1111/gbb.12533
34. Miner NB, Elmore JS, Baumann MH, Phillips TJ, Janowsky A. Trace amine-associated receptor 1 regulation of methamphetamine-induced neurotoxicity. *Neurotoxicology.* (2017) 63:57–69. doi: 10.1016/j.neuro.2017.09.006
35. Miner NB, Phillips TJ, Janowsky A. The role of biogenic amine transporters in trace amine-associated receptor 1 regulation of methamphetamine-induced neurotoxicity. *J Pharmacol Exp Ther.* (2019) 371:36–44. doi: 10.1124/jpet.119.258970
36. de Wit H, Phillips TJ. Do initial responses to drugs predict future use or abuse? *Neurosci Biobehav Rev.* (2012) 36:1565–76. doi: 10.1016/j.neubiorev.2012.04.005
37. Ruan QT, Yazdani N, Reed ER, Beierle JA, Peterson LP, Luttik KP, et al. 5' UTR variants in the quantitative trait gene *Hnrnp1* support reduced 5' UTR usage and hnRNP H protein as a molecular mechanism underlying reduced methamphetamine sensitivity. *FASEB J.* (2020) 34:9223–44. doi: 10.1096/fj.202000092R
38. Yazdani N, Parker CC, Shen Y, Reed ER, Guido MA, Kole LA, et al. *Hnrnp1* is a quantitative trait gene for methamphetamine sensitivity. *PLoS Genet.* (2015) 11:e1005713. doi: 10.1371/journal.pgen.1005713
39. Ruan QT, Yazdani N, Blum BC, Beierle JA, Lin W, Coelho MA, et al. A mutation in *Hnrnp1* that decreases methamphetamine-induced reinforcement, reward, and dopamine release and increases synaptosomal hnRNP H and mitochondrial proteins. *J Neurosci.* (2020) 40:107–30. doi: 10.1523/JNEUROSCI.1808-19.2019
40. Lindemann L, Meyer CA, Jeanneau K, Bradaia A, Ozmen L, Bluethmann H, et al. Trace amine-associated receptor 1 modulates dopaminergic activity. *J Pharmacol Exp Ther.* (2008) 324:948–56. doi: 10.1124/jpet.107.132647
41. Miller GM. The emerging role of trace amine-associated receptor 1 in the functional regulation of monoamine transporters and dopaminergic activity. *J Neurochem.* (2011) 116:164–76. doi: 10.1111/j.1471-4159.2010.07109.x
42. Shabani S, Dobbs LK, Ford MM, Mark GP, Finn DA, Phillips TJ. A genetic animal model of differential sensitivity to methamphetamine reinforcement. *Neuropharmacology.* (2012) 62:2169–77. doi: 10.1016/j.neuropharm.2012.01.002
43. Wolinsky TD, Swanson CJ, Smith KE, Zhong H, Borowsky B, Seeman P, et al. The trace amine 1 receptor knockout mouse: an animal model with relevance to schizophrenia. *Genes Brain Behav.* (2007) 6:628–39. doi: 10.1111/j.1601-183X.2006.00292.x

44. Chen X, Williamson VS, An SS, Hettema JM, Aggen SH, Neale MC, et al. Cannabinoid receptor 1 gene association with nicotine dependence. *Arch Gen Psychiatry*. (2008) 65:816–24. doi: 10.1001/archpsyc.65.7.816
45. Pava MJ, Woodward JJ. A review of the interactions between alcohol and the endocannabinoid system: implications for alcohol dependence and future directions for research. *Alcohol*. (2012) 46:185–204. doi: 10.1016/j.alcohol.2012.01.002
46. Hay EA, McEwan A, Wilson D, Barrett P, D'Agostino G, Pertwee RG, et al. Disruption of an enhancer associated with addictive behaviour within the cannabinoid receptor-1 gene suggests a possible role in alcohol intake, cannabinoid response and anxiety-related behaviour. *Psychoneuroendocrinology*. (2019) 109:104407. doi: 10.1016/j.psyneuen.2019.104407
47. Mulligan MK, Abreo T, Neuner SM, Parks C, Watkins CE, Houseal MT, et al. Identification of a Functional Non-coding Variant in the GABA (A) Receptor  $\alpha 2$  subunit of the C57BL/6J mouse reference genome: major implications for neuroscience research. *Front Genet*. (2019) 10:188. doi: 10.3389/fgenet.2019.00188
48. Agrawal A, Edenberg HJ, Foroud T, Bierut LJ, Dunne G, Hinrichs AL, et al. Association of GABRA2 with drug dependence in the collaborative study of the genetics of alcoholism sample. *Behav Genet*. (2006) 36:640–50. doi: 10.1007/s10519-006-9069-4
49. Enoch MA, Schwartz L, Albaugh B, Virkkunen M, Goldman D. Dimensional anxiety mediates linkage of GABRA2 haplotypes with alcoholism. *Am J Med Genet B Neuropsychiatr Genet*. (2006) 141b:599–607. doi: 10.1002/ajmg.b.30336
50. Lappalainen J, Krupitsky E, Remizov M, Pchelina S, Taraskina A, Zvartau E, et al. Association between alcoholism and gamma-amino butyric acid  $\alpha 2$  receptor subtype in a Russian population. *Alcohol Clin Exp Res*. (2005) 29:493–8. doi: 10.1097/01.ALC.0000158938.97464.90
51. Li D, Sulovari A, Cheng C, Zhao H, Kranzler HR, Gelernter J. Association of gamma-aminobutyric acid A receptor  $\alpha 2$  gene (GABRA2) with alcohol use disorder. *Neuropsychopharmacology*. (2014) 39:907–18. doi: 10.1038/npp.2013.291
52. Villafuerte S, Strumba V, Stoltenberg SF, Zucker RA, Burmeister M. Impulsiveness mediates the association between GABRA2 SNPs and lifetime alcohol problems. *Genes Brain Behav*. (2013) 12:525–31. doi: 10.1111/gbb.12039
53. Belknap JK, Crabbe JC, Young ER. Voluntary consumption of ethanol in 15 inbred mouse strains. *Psychopharmacology (Berl)*. (1993) 112:503–10. doi: 10.1007/BF02244901
54. Yoneyama N, Crabbe JC, Ford MM, Murillo A, Finn DA. Voluntary ethanol consumption in 22 inbred mouse strains. *Alcohol*. (2008) 42:149–60. doi: 10.1016/j.alcohol.2007.12.006
55. Chen J, Liu Q, Fan R, Han H, Yang Z, Cui W, et al. Demonstration of critical role of GRIN3A in nicotine dependence through both genetic association and molecular functional studies. *Addict Biol*. (2020) 25:e12718. doi: 10.1111/adb.12718
56. Eastwood EC, Barkley-Levenson AM, Phillips TJ. Methamphetamine drinking microstructure in mice bred to drink high or low amounts of methamphetamine. *Behav Brain Res*. (2014) 272:111–20. doi: 10.1016/j.bbr.2014.06.035
57. Loftis JM, Lasarev M, Shi X, Lapidus J, Janowsky A, Hoffman WE, et al. Trace amine-associated receptor gene polymorphism increases drug craving in individuals with methamphetamine dependence. *PLoS One*. (2019) 14:e0220270. doi: 10.1371/journal.pone.0220270
58. Stafford AM, Reed C, Phillips TJ. Non-genetic factors that influence methamphetamine intake in a genetic model of differential methamphetamine consumption. *Psychopharmacology (Berl)*. (2020) 237:3315–36. doi: 10.1007/s00213-020-05614-9
59. Underhill SM, Hullihen PD, Chen J, Fenollar-Ferrer C, Rizzo MA, Ingram SL, et al. Amphetamines signal through intracellular TAAR1 receptors coupled to G $\alpha$ (13) and G $\alpha$ (S) in discrete subcellular domains. *Mol Psychiatry*. (2021) 26:1208–23. doi: 10.1038/s41380-019-0469-2
60. Hikosaka O. The habenula: from stress evasion to value-based decision-making. *Nat Rev Neurosci*. (2010) 11:503–13. doi: 10.1038/nrn2866
61. Matsumoto M, Hikosaka O. Lateral habenula as a source of negative reward signals in dopamine neurons. *Nature*. (2007) 447:1111–5. doi: 10.1038/nature05860
62. Matsumoto M, Hikosaka O. Two types of dopamine neuron distinctly convey positive and negative motivational signals. *Nature*. (2009) 459:837–41. doi: 10.1038/nature08028
63. Wirtshafter D, Asin KE, Pitzer MR. Dopamine agonists and stress produce different patterns of Fos-like immunoreactivity in the lateral habenula. *Brain Res*. (1994) 633:21–6. doi: 10.1016/0006-8993(94)91517-2
64. Gifuni AJ, Jozaghi S, Gauthier-Lamer AC, Boye SM. Lesions of the lateral habenula dissociate the reward-enhancing and locomotor-stimulant effects of amphetamine. *Neuropharmacology*. (2012) 63:945–57. doi: 10.1016/j.neuropharm.2012.07.032
65. Lominac KD, Quadir SG, Barrett HM, McKenna CL, Schwartz LM, Ruiz PN, et al. Prefrontal glutamate correlates of methamphetamine sensitization and preference. *Eur J Neurosci*. (2016) 43:689–702. doi: 10.1111/ejn.13159
66. Szumlanski KK, Lominac KD, Campbell RR, Cohen M, Fultz EK, Brown CN, et al. Methamphetamine addiction vulnerability: the glutamate, the bad, and the ugly. *Biol Psychiatry*. (2017) 81:959–70. doi: 10.1016/j.biopsych.2016.10.005
67. Quina LA, Tempest L, Ng L, Harris JA, Ferguson S, Jhou TC, et al. Efferent pathways of the mouse lateral habenula. *J Comp Neurol*. (2015) 523:32–60. doi: 10.1002/cne.23662
68. Iancu OD, Darakjian P, Walter NA, Malmanger B, Oberbeck D, Belknap J, et al. Genetic diversity and striatal gene networks: focus on the heterogeneous stock-collaborative cross (HS-CC) mouse. *BMC Genomics*. (2010) 11:585. doi: 10.1186/1471-2164-11-585
69. Roberts A, Pardo-Manuel de Villena F, Wang W, McMillan L, Threadgill DW. The polymorphism architecture of mouse genetic resources elucidated using genome-wide resequencing data: implications for QTL discovery and systems genetics. *Mamm Genome*. (2007) 18:473–81. doi: 10.1007/s00335-007-9045-1
70. Reed C, Stafford AM, Mootz JRK, Baba H, Erk J, Phillips TJ. A breeding strategy to identify modifiers of high genetic risk for methamphetamine intake. *Genes Brain Behav*. (2021) 20:e12667. doi: 10.1111/gbb.12667
71. Eastwood EC, Eshleman AJ, Janowsky A, Phillips TJ. Verification of a genetic locus for methamphetamine intake and the impact of morphine. *Mamm Genome*. (2018) 29:260–72. doi: 10.1007/s00335-017-9724-5
72. Dodd S, Carvalho AF, Puri BK, Maes M, Bortolasci CC, Morris G, et al. Trace amine-associated receptor 1 (TAAR1): a new drug target for psychiatry? *Neurosci Biobehav Rev*. (2021) 120:537–41. doi: 10.1016/j.neubiorev.2020.09.028
73. Cotter R, Pei Y, Mus L, Harmeier A, Gainetdinov RR, Hoener M, et al. The trace amine-associated receptor 1 modulates methamphetamine's neurochemical and behavioral effects. *Front Neurosci*. (2015) 9:39. doi: 10.3389/fnins.2015.00039
74. Liu J, Wu R, Li JX. TAAR1 and psychostimulant addiction. *Cell Mol Neurobiol*. (2020) 40:229–38. doi: 10.1007/s10571-020-00792-8
75. Pei Y, Asif-Malik A, Hoener M, Canales JJ. A partial trace amine-associated receptor 1 agonist exhibits properties consistent with a methamphetamine substitution treatment. *Addict Biol*. (2017) 22:1246–56. doi: 10.1111/adb.12410

**Conflict of Interest:** The authors declare that the research was conducted in the absence of any commercial or financial relationships that could be construed as a potential conflict of interest.

**Publisher's Note:** All claims expressed in this article are solely those of the authors and do not necessarily represent those of their affiliated organizations, or those of the publisher, the editors and the reviewers. Any product that may be evaluated in this article, or claim that may be made by its manufacturer, is not guaranteed or endorsed by the publisher.

Copyright © 2021 Phillips, Roy, Aldrich, Baba, Erk, Mootz, Reed and Chesler. This is an open-access article distributed under the terms of the Creative Commons Attribution License (CC BY). The use, distribution or reproduction in other forums is permitted, provided the original author(s) and the copyright owner(s) are credited and that the original publication in this journal is cited, in accordance with accepted academic practice. No use, distribution or reproduction is permitted which does not comply with these terms.



# The Gut Microbiome and Substance Use Disorder

Jordan T. Russell<sup>1</sup>, Yanjiao Zhou<sup>1</sup>, George M. Weinstock<sup>2</sup> and Jason A. Bubier<sup>3\*</sup>

<sup>1</sup> School of Medicine, University of Connecticut Health Center, Farmington, CT, United States, <sup>2</sup> The Jackson Laboratory for Genomic Medicine, Farmington, CT, United States, <sup>3</sup> The Jackson Laboratory, Bar Harbor, ME, United States

## OPEN ACCESS

### Edited by:

Gary T. Hardiman,  
Queen's University Belfast,  
United Kingdom

### Reviewed by:

Drew D. Kiraly,  
Icahn School of Medicine at Mount  
Sinai, United States  
Donald Michael Kuhn,  
Wayne State University, United States

### \*Correspondence:

Jason A. Bubier  
Jason.Bubier@jax.org

### Specialty section:

This article was submitted to  
Neurogenetics,  
a section of the journal  
Frontiers in Neuroscience

**Received:** 15 June 2021

**Accepted:** 12 August 2021

**Published:** 31 August 2021

### Citation:

Russell JT, Zhou Y, Weinstock GM  
and Bubier JA (2021) The Gut  
Microbiome and Substance Use  
Disorder. *Front. Neurosci.* 15:725500.  
doi: 10.3389/fnins.2021.725500

Substance use disorders (SUDs) remain a significant public health challenge, affecting tens of millions of individuals worldwide each year. Often comorbid with other psychiatric disorders, SUD can be poly-drug and involve several different substances including cocaine, opiates, nicotine, and alcohol. SUD has a strong genetic component. Much of SUD research has focused on the neurologic and genetic facets of consumption behavior. There is now interest in the role of the gut microbiome in the pathogenesis of SUD. In this review, we summarize current animal and clinical evidence that the gut microbiome is involved in SUD, then address the underlying mechanisms by which the gut microbiome interacts with SUD through metabolomic, immune, neurological, and epigenetic mechanisms. Lastly, we discuss methods using various inbred and outbred mice models to gain an integrative understanding of the microbiome and host genetic controls in SUD.

**Keywords:** substance use disorder, addiction, microbiome, animal models, gut-brain axis

## INTRODUCTION

Substance use disorder (SUD) is a mental condition affecting the brain and is characterized in part by chronic dependence despite negative social, mental, and physical health consequences. Addiction represents the most severe form of SUD, with affected individuals often incapable of maintaining abstinence despite the will to discontinue substance use. Importantly, the effects of addiction can persist beyond cessation of substance use, suggesting that lasting physiological changes in the brain are involved (Koob et al., 2008). An expansive list of substance classes are related to SUD, ranging from legal forms, including alcohol, to illicit or controlled forms, including cocaine and opioids. Alcohol use disorder (AUD) remains the most prevalent SUD, however, poly-drug use within individuals is not uncommon (Lipari and Van Horn, 2017).

Addictive substances can affect multiple pathways controlling brain function. Alteration of the dopaminergic system is one common mechanism shared by all substances in the establishment of recurrent substance use (Nestler, 2005). Notably, substance misuse leads to increased levels of dopamine release and chronic signal imbalance in D2-like dopamine receptors in the ventral striatum, particularly in the nucleus accumbens (Koob and Le Moal, 2001; Nestler, 2005). Termed the mesolimbic pathway, substances of misuse operate to “hijack” the host reward system critical for pleasurable response and reinforcement to rewarding stimuli, as well as memory and emotional processes. Furthermore, the chronic use of these substances leads to neuroplasticity and structural reorganizations, and drug-specific changes in neurotransmitter transporters and receptors (Bliss et al., 2003; Kauer, 2004). Despite the central role of dopamine in SUD, other neurotransmitters such as serotonin and gamma-aminobutyric acid (GABA) also play an important role in SUD,

depending on the dosage and frequency of substance use, as well as intrinsic biological factors such as host genetics (Prom-Wormley et al., 2017).

Previous human linkage studies have shown that children of individuals affected by SUD are at a greater risk for SUD, suggesting a genetic component to the risk of developing the disorder (Kreek et al., 2004). SUD involving cocaine confers the highest genetic risk of any substance, estimated at approximately 70% heritability (Goldman et al., 2005). Numerous genetic loci have been implicated in the heritability of risk for cocaine SUD, most notably genes involved in dopamine transport (*Drd2*, *Drd4*) and metabolism (*Dbh*) (Table 1). AUD also show strong genetic factors with variants in genes involved in alcohol metabolism (*Adh1b*, *Aldh2*) and diverse variants of smaller effect in dopaminergic systems (Table 1). However, discordant SUD rates found in identical twins suggest that genetics alone does not entirely explain the incidence of SUD (Agrawal and Lynskey, 2008). Aside from socio-economic factors studied extensively (Stone et al., 2012), there is intense interest in examining the role of the gut microbiome in SUD. The gut microbiota are a diverse population of microorganisms that constantly interact with the central nervous system (CNS) through complicated metabolomic, immune, neurological, and epigenetic pathways, making them potential sources of environmental influence on SUD.

Although methods for investigating the microbiome in various diseases have made tremendous advancements in the last decade (Quigley and Gajula, 2020), studies of SUD in humans remain challenging because of the difficulty in controlling for complex experimental variables (for example, diet and host genotype). Model organisms such as mice provide excellent opportunities for studying the microbiome and its interaction with the host due to greater control over genetic and environmental confounders. In addition, mice of diverse but known genetic backgrounds can be harnessed to interrogate complex interactions between host genotype and the gut microbiota that may be important for risk of developing SUD (Poltorak et al., 2018). This review will provide a concise overview of recent insights on mechanisms of interaction between the gut microbiota and CNS, in addition to methodological considerations for studying the gut microbiome in SUD in animal models.

## THE GUT-BRAIN AXIS AND SUBSTANCE USE

The human gastrointestinal tract is home to a large community of microbiota on the order of trillions of cells. Likewise, the collective gene content of the microbiome encodes a staggering amount of functional potential, with an estimated 150 times greater number of genes than that of the human or mouse genome (Grice and Segre, 2012). Despite a core microbiome, fluctuations in composition

are often observed after administering antibiotics, non-antibiotic medication, and diet intervention (Caporaso et al., 2011). This deviation from an individual-defined normal or “healthy” microbiome in the context of disease is termed dysbiosis, and a significant body of evidence has linked the dysbiotic microbiome as a contributor of disease and recently mental health (Shreiner et al., 2015; Capuco et al., 2020). There are multiple potential facets of gut host-microbe interactions to explain these disease associations, requiring much interdisciplinary research focus. Emerging evidence suggests prominent roles in host-microbe immune interaction, crosstalk between the gut and brain *via* neurotransmitters, and a role for bacterial metabolites including short-chain fatty acids (SCFA) in the pathophysiology of SUD. A summary of representative studies of the microbiome and SUD in animal models is provided in Table 2. For a comprehensive summary see the recent review by Angoa-Pérez and Kuhn (2021).

## INTERACTIONS BETWEEN THE MICROBIOTA AND THE IMMUNE SYSTEM IN SUD

The gut microbiota produce an immense number of foreign antigens to which the host immune system must tolerate under normal homeostasis (Swiatczak and Cohen, 2015). The intestinal epithelium provides a physical barrier between the microbiota and immune cells, largely regulating the immune response to commensal microbes. Evidence suggests increased intestinal barrier permeability (leaky gut) in SUD, particularly AUD (Leclercq et al., 2014). Alcohol consumption has long been associated with developing a leaky gut through oxidative stress, which allows for increased translocation of bacterial products into the lamina propria. Here, microbial antigens can interact directly with gut-localized dendritic cells and macrophages and upregulate multiple pro-inflammatory cytokines production, leading to a heightened local and systemic inflammatory response.

Immune cytokines have modulatory effects on behavior. Levels of pro-inflammatory cytokines, including IL-1 $\beta$ , TNF- $\alpha$ , and IL-8, are increased in response to numerous substances of abuse (Meckel and Kiraly, 2019). Interestingly, this pro-inflammatory response to substance use is akin to the response to bacterial lipopolysaccharide (LPS) through signaling *via* toll-like receptor 4 (Northcutt et al., 2015). This pro-inflammatory response further implicates the interaction between the gut microbiota and the immune system in SUD pathology. It was observed that alcohol and opiates use leads to an enrichment of pro-inflammatory Proteobacteria in the gut. Likewise, anti-inflammatory responses are altered in instances of substance use which leads to an unbalanced neuroimmune response. Anti-inflammatory cytokines such as IL-10 have been shown to modulate and even reverse anxiety behaviors related to substance use (Patel et al., 2021). Furthermore, IL-10 could entirely diminish the escalation of alcohol intake by modulating GABA signaling in the amygdala. Thus, the link between the gut

**TABLE 1** | Substances involved in SUD and addiction, their mechanism of action and genetic risk loci for development of SUD/addiction.

Substance	Mechanism of action	Risk loci for developing SUD/addiction	References
Alcohol (ethanol)	Acts on multiple targets within the CNS including GABA synapse, glutamate signaling, and other neurotransmitters or receptors that indirectly control release of dopamine.	Variants in alcohol dehydrogenase (ADH1B); acetaldehyde dehydrogenase (ALDH2); small effect variants in reward pathway genes including dopamine receptor D2 ( <i>Drd2</i> ).	Boileau et al., 2003; Roberto and Varodayan, 2017; Edenberg and McClintick, 2018; Kranzler et al., 2019
Stimulants (e.g., cocaine, amphetamine)	Cocaine targets dopamine transporters, blocking dopamine re-uptake in dopaminergic neurons. Other stimulants such as amphetamines act to stimulate release of dopamine directly.	Dopamine transport and metabolism ( <i>Drd2</i> , <i>Drd4</i> , <i>Dbh</i> ); norepinephrine transporter ( <i>Slc6a2</i> ); 53 B-like family gene ( <i>Fam53b</i> ).	Noble et al., 1993; Volkow et al., 1999; Xu et al., 2000; Kahlig and Galli, 2003; Avelar et al., 2013
Opioids (e.g., heroin or pharmaceutical opioids)	Target the mu-opioid receptor MOR, leading to the activation of neurons containing MORs and subsequent dopamine release.	Variants in the mu-opioid receptor gene ( <i>Oprm1</i> ); potassium gated channels ( <i>Kcnc1</i> , <i>Kcng2</i> ); repulsive guidance molecule ( <i>Rgma</i> ).	Gelernter et al., 2014; Cheng et al., 2018; Valentino and Volkow, 2018; Zhou et al., 2020
Nicotine (tobacco)	Acts directly on nicotine receptors leading to dopamine release, or by activating other receptors indirectly.	Variants in the cholinergic nicotinic receptor gene locus ( <i>Chrna1/b1</i> ).	D'Souza and Markou, 2011; Hancock et al., 2018
Cannabis (marijuana)	Targets cannabinoid receptor CB1, indirectly stimulating dopamine release mediated through GABA and glutamate.	Variants near the forkhead box P2 gene ( <i>Foxp2</i> ); cholinergic nicotine receptor ( <i>Chrna2</i> ); epoxide hydrolase 2 ( <i>Ephx2</i> ).	Draycott et al., 2014; Demontis et al., 2019; Johnson et al., 2020

microbiota and the immune system *via* neuroimmune pathways are important research areas in SUD and addiction.

## MICROBIOTA-DERIVED NEUROTRANSMITTERS

Neurotransmitters intuitively play a critical role in the development and maintenance of all forms of SUD. Numerous bacteria have been described as capable of producing a number of neurotransmitters including GABA, serotonin, and dopamine (Yano et al., 2015; Strandwitz, 2018). A culture study showed that *Bacillus* species can produce dopamine. Furthermore, germ-free and antibiotic-treated mice have shown that the gut microbiota influences the production and turnover of dopamine outside the CNS (Strandwitz, 2018). Similar fluctuations in GABA levels are observed in mice treated with antibiotics (Yunes et al., 2020). *Lactobacillus*, *Bifidobacteria*, and *Bacteroides* species were identified to have the capability to produce GABA (Barrett et al., 2012; Strandwitz et al., 2019). Mice given specific GABA-producing *Lactobacillus* or *Bifidobacteria* have shown altered behavioral phenotypes (Yunes et al., 2020). Curiously, neurotransmitters produced by the gut microbiota may not under normal circumstances directly affect the brain, as whether these molecules cross the blood–brain barrier is still debated (Boonstra et al., 2015). However, increasing evidence has shown that the blood–brain barrier can fluctuate between states of increased permeability (Braniste et al., 2014). It may also be that

the gut microbiota, rather than producing neurotransmitters themselves, affect neurotransmitter production or receptor expression indirectly *via* signals delivered through the vagus nerve (Bravo et al., 2011). Studies are ongoing to identify the full breadth of neurotransmitter-producing strains in the gut microbiome and the mechanisms by which microbial messages influence host behavior in the context of SUD.

## GUT MICROBIOME MEDIATED EPIGENETIC MECHANISMS

Substance use leads to changes in gene expression in the brain in critical signaling pathways in the reward circuitry (Walker et al., 2018). Regulation of gene activation and repression is controlled in part epigenetically by adding and removing histone post-translational modifications. Common modifications include acetylation and methylation, which work to activate or silence gene expression, respectively. Importantly, these modifications are reversible; they can be added or removed by dedicated enzymes for this process, based on cellular cues. Histone acetylation, which leads to gene activation by opening the chromatin structure, increases at the nucleus accumbens in response to drug use for most substances (Renthall and Nestler, 2009). Alcohol is a unique case because the byproduct of ethanol metabolism is acetate itself. Acetate derived from alcohol metabolism post-consumption is readily incorporated into the brain, and in mice is associated with spatial

**TABLE 2 |** Summary of representative studies using animal models in SUD and microbiome research.

Substance	Observations	References
Alcohol	Antibiotic treatment reduced voluntary alcohol intake by 70% in high-drinker rats; vagotomy led to similar reduction in alcohol consumption.	Ezquer et al., 2021
	Tigecycline antibiotic treatment reduced ethanol intake in male and female dependent/non-dependent C57B/6J mice.	Bergeson et al., 2016
	Transplantation of microbiota from alcohol-fed mice to controls led to similar alcohol withdrawal-induced anxiety behavior in recipients.	Xiao et al., 2018
Cocaine	Treatment with non-absorbable antibiotics for 2 weeks led to behavioral changes (enhanced reward, sensitization) in response to cocaine stimulation compared with controls in male C57BL/6J mice; microbiota depletion altered transcriptional activity in the nucleus accumbens; replacement of SCFAs reversed the antibiotic effect on behavior in response to cocaine.	Kiraly et al., 2016
Opioids	Intermittent and continuous treatment with morphine led to significant changes in the gut microbiota of male C57BL/6J mice; <i>Lactobacillus</i> were reduced and <i>Ruminococcus</i> were enriched after morphine exposure; antibiotic treatment led to increased drug tolerance and alterations in drug reward behaviors.	Lee et al., 2018
Nicotine	Nicotine altered the gut microbiota of C57BL/6 mice with sex-specific differences; nicotine led to decreased weight in males but not females; oxidative stress and DNA repair pathways were enriched in the microbiome after nicotine treatment; neurotransmitters (GABA) and precursor metabolites (glutamate) were significantly altered by nicotine treatment.	Chi et al., 2017
Cannabis	Differential gut microbiota composition in germ-free (Swiss Webster and B6.129P2(SJL)-Myd88 <sup>tm1.1Defr</sup> ) and conventional (C57BL/6 and B6.Cg-Lep <sup>ob</sup> /J) mice linked to expression of cannabinoid receptor CB1; modulation of CB1 expression is linked to gut permeability and leakage of pro-inflammatory LPS, also characteristic of the neuroimmune pathologies observed in SUD.	Muccioli et al., 2010

memory and preference for the rewarding stimulus of alcohol (Mews et al., 2019). Inhibition or deletion of genes involved in acetylation, histone acetyltransferase (HAT), and histone

deacetylase (HDAC) leads to alterations in sensitivity and drug-related behaviors (Cadet, 2016). These lines of evidence implicate the epigenetics of the brain in chronic SUD and addiction, and

current research is focusing on the specific genetic loci affected by epigenetic alteration in response to substance use.

The gut microbiota produces large quantities of SCFAs, predominantly acetate, propionate, and butyrate, through carbohydrate metabolism and the breakdown of dietary fiber (Dalile et al., 2019). Butyrate, a potent HDAC inhibitor, can modulate host epigenetics through similar pathways as those affected by substance use (Simon-O'Brien et al., 2015). The microbial contribution to epigenetic modification may be important not only for current SUD but also the risk of developing SUD before initial drug intake, by predisposition toward the activation of addiction and reward pathways in the brain (Meckel and Kiraly, 2019).

## STUDYING THE MICROBIOME IN SUD USING INBRED MICE

The use of laboratory rodents to study the neurobiological aspects of SUD has been well documented, and the use of animal research to study the environmental effects of the microbiome is expanding rapidly (Fowler and Kenny, 2012; Meckel and Kiraly, 2019). Mouse models prove useful for investigating the interactions between host genetics and the gut microbiome in substance use. For example, C57BL/6 (B6) mice consume sufficient alcohol levels to mimic binge-like drinking episodes, making this strain a popular choice for modeling binge alcohol intake (Thiele et al., 2014). Further work in this model strain investigates links between alcohol consumption, the gut microbiota, host gene expression, and drinking-related phenotypes. Furthermore, rodent models of selectively inbred “high drinkers” have been proposed for the use of screening drugs aimed at reducing binge-like drinking behaviors (Crabbe et al., 2017). Using single or selectively inbred strains effectively isolates environmental variables of interest for experimentation by controlling for genetic variation in the host. Considering the complex diversity of the microbiota, isolating the microbial effects while controlling for host genetics is prudent. Despite the utility of inbred strains in isolating environmental effects, this method does not fully consider both the genetic and environmental complexity of SUD in humans, underpinning the critical issue of translatability of rodent models.

## DIVERSITY OUTBRED MOUSE MODELS

Much effort has been placed on developing recombinant-inbred mouse strains to capture greater genetic diversity in strains that are more applicable to complex disorders such as SUD in humans. In 2004, a large multi-institutional initiative led to the creation of the collaborative cross (CC) strains by crossing among a set of eight mouse strains which represent >90% of the genetic diversity of *Mus musculus* and its subspecies (Threadgill et al., 2011). Because CC mice originate from founder strains with defined genomes, this panel provides a high degree of genetic diversity that can be accurately mapped with genotyping techniques (Srivastava et al., 2017). Expanding further on

the CC mouse panel are the diversity outbred (DO) strains, which provide even greater genetic and phenotypic diversity by outbreeding, producing unique individual heterozygous mice (Churchill et al., 2012).

There are numerous advantages to utilizing DO mice for mapping phenotypic traits to host genotype. Because they originate from the same founder strains as the CC panel, their genomes are well defined and suited for fine-detail trait mapping (Svenson et al., 2012). Furthermore, DO mice traits can be recovered from inbred CC lines to test for allelic effects. Research into benzene toxicity in DO mice revealed that harnessing this genetic heterogeneity in the mouse better reflected the diverse reactions to benzene exposure seen in humans (French et al., 2015). Efforts using heterogeneous stock (HS) mice, with similar genetic backgrounds as DO mice, have correlated genes with sex-specific ethanol preference and chronic consumption phenotypes, and similar results have been corroborated in DO mice (Hitzemann et al., 2020). In the context of SUD, DO mice may be used to study the interaction between host genes, the environment (i.e., microbiome), and phenotypic differences between strains that reflect similar genetic diversity in humans.

## REPRODUCIBILITY THROUGH A CONTROLLED ENVIRONMENT

Despite considerable effort, reproducibility in microbiome research using animal models remains challenging. Careful considerations must be made when studying the relationship between genetics, phenotype, and the microbiome in an animal. Microbiome differences in mice can be seen based on external factors such as vendor, environmental and facility conditions, and co-housing with other mice (Justice and Dhillon, 2016). When controlling for genetics by using inbred strains, mouse-to-mouse variation in microbiome composition is observed. A consistent methodology plays a crucial role in the reproducibility of microbiome research in animals, as circadian rhythm can also have confounding effects for sampling at different times of the day (Thaiss et al., 2014). In order to reduce confounding individual variation of the microbiota, strategies for the rotation of mice and mixing of bedding may be used so that all mice in the experiment are normalized to the same common microbiota. Furthermore, greater reproducibility can be achieved by defining a standard microbiota composition for a given model or experiment (Witjes et al., 2020). Thus, experimental replication is more likely to be achieved by knowing the target microbiota important for obtaining similar outcomes.

Though defining a normal microbiota for an experiment or model organism may lead to a greater likelihood of reproducibility, it raises the question of translatability since a standardized microbiome is not realistic in humans. Here the concept of increased reproducibility is at odds with the fact that human disorders such as SUD are not simply defined systems. Just as genetically diverse DO mice better reflect the natural heterogeneity seen in humans, so too is there value in assessing natural variation in the microbiome. The advent of “wildlings” by implanting lab-strain mouse embryos into wild mice provides

a useful tool for studying a more naturally derived microbiome in an effort to enhance translatability (Rosshart et al., 2019). Ultimately, the choice to standardize and how will depend on the experimental question; whether there is a necessity to study the full breadth of genetic and microbial heterogeneity such as that in humans, to discover interactions between host and microbe, or to isolate as best as possible specific genetic and environmental factors for studying direct effects.

## DISCUSSION

Addiction and substance use research has seen renewed enthusiasm with a focus on the innate gut microbiota. Numerous studies have proposed a connection between the gut microbiota and the CNS *via* the gut-brain axis, providing a mechanism by which these microbes influence the host. Often drug use is associated with dysbiosis of the gut microbiome, and these changes may be critical to the establishment and maintenance of addiction by altering signals between the gut and the brain. Thus, a probiotic intervention has garnered much interest as a novel form of therapy for SUD. Recent evidence shows promising effects of probiotics in treating other mental disorders, including anxiety and depression, both of which are often comorbid with SUD (Abildgaard et al., 2017; Hadizadeh et al., 2019; Kim and Kim, 2019; Liu et al., 2020). Fecal microbial transplant is also an area of intense research. Studies in mice have shown that transplantation of fecal microbiota of individuals diagnosed with AUD leads to altered social and anxiety behaviors and increased preference toward alcohol (Zhao et al., 2020). Reciprocally, transplantation of microbiota from healthy donors reduced anxiety and depressive behaviors in mice exposed to alcohol (Xu et al., 2018). More research is needed to validate the effects of FMT for other addictive substances and whether dysbiosis perpetuates the chronic nature of addiction. Future work will focus on untangling the mechanisms of gut microbiota modulation on the host addiction behaviors to identify target

pathways and functions for potential probiotic therapeutics, such as those focused on SCFA production.

Gut microbiome dysbiosis is evident after chronic and acute substance use. However, more research is needed into whether the gut microbiome may also serve as a source of environmental risk for the development of SUD and addiction or be used as a predictor of future SUD. Furthermore, interactions between host genetics and gut microbiota deserve greater attention. Recent evidence has suggested that host genetics can have strong effects on the composition and function of the gut microbiome (Goodrich et al., 2014; Abildgaard et al., 2017; Kim and Kim, 2019; Korach-Rechtman et al., 2019; Liu et al., 2020). Using animal models from diverse genetic backgrounds will pave the way toward understanding complex interactions between genetic traits and the microbiota, especially given that genetically diverse mice respond differently to probiotic interventions (McVey Neufeld et al., 2018). Lastly, researchers must consider the balance between the reproducibility of using inbred mouse strains to test specific hypotheses versus the translatability of genetically diverse mice, as both methods will be critical to not only bolstering our understanding of the microbiome in SUD and addiction but also its applicability to a diverse human population.

## AUTHOR CONTRIBUTIONS

JR drafted the initial version of the manuscript. YZ, GW, and JB contributed to and edited the final manuscript. All authors approved the final manuscript.

## FUNDING

JR, YZ, and JB were funded by R21 AA027858 and YZ, GW, and JB were funded by U01DA043809. JR was also funded by Ruth L. Kirschstein T32 NRSA award 5T32AA007290-38.

## REFERENCES

- Abildgaard, A., Elfving, B., Hokland, M., Wegener, G., and Lund, S. (2017). Probiotic treatment reduces depressive-like behaviour in rats independently of diet. *Psychoneuroendocrinology* 79, 40–48. doi: 10.1016/j.psyneuen.2017.02.014
- Agrawal, A., and Lynskey, M. T. (2008). Are there genetic influences on addiction: evidence from family, adoption and twin studies. *Addiction* 103, 1069–1081. doi: 10.1111/j.1360-0443.2008.02213.x
- Angoa-Pérez, M., and Kuhn, D. M. (2021). Evidence for Modulation of Substance Use Disorders by the Gut Microbiome: hidden in Plain Sight. *Pharmacol. Rev.* 73, 571–596. doi: 10.1124/pharmrev.120.000144
- Avelar, A. J., Juliano, S. A., and Garriss, P. A. (2013). AMPHETAMINE AUGMENTS VESICULAR DOPAMINE RELEASE IN THE DORSAL AND VENTRAL STRIATUM THROUGH DIFFERENT MECHANISMS. *J. Neurochem.* 125, 373–385. doi: 10.1111/jnc.12197
- Barrett, E., Ross, R. P., O'Toole, P. W., Fitzgerald, G. F., and Stanton, C. (2012).  $\gamma$ -Aminobutyric acid production by culturable bacteria from the human intestine. *J. Appl. Microbiol.* 113, 411–417. doi: 10.1111/j.1365-2672.2012.05344.x
- Bergeson, S. E., Nipper, M. A., Jensen, J., Helms, M. L., and Finn, D. A. (2016). Tigecycline Reduces Ethanol Intake in Dependent and Non-Dependent Male and Female C57BL/6J Mice. *Alcohol. Clin. Exp. Res.* 40, 2491–2498. doi: 10.1111/acer.13251
- Bliss, T. V. P., Collingridge, G. L., Morris, R. G. M., Thomas, M. J., and Malenka, R. C. (2003). Synaptic plasticity in the mesolimbic dopamine system. *Philos. Trans. R. Soc. Lond. Ser. B Biol. Sci.* 358, 815–819. doi: 10.1098/rstb.2002.1236
- Boileau, I., Assaad, J.-M., Pihl, R. O., Benkelfat, C., Leyton, M., Diksic, M., et al. (2003). Alcohol promotes dopamine release in the human nucleus accumbens. *Synapse* 49, 226–231. doi: 10.1002/syn.10226
- Boonstra, E., de Kleijn, R., Colzato, L. S., Alkemade, A., Forstmann, B. U., and Nieuwenhuis, S. (2015). Neurotransmitters as food supplements: the effects of GABA on brain and behavior. *Front. Psychol.* 6:1520. doi: 10.3389/fpsyg.2015.01520
- Braniste, V., Al-Asmakh, M., Kowal, C., Anuar, F., Abbaspour, A., Tóth, M., et al. (2014). The gut microbiota influences blood-brain barrier permeability in mice. *Sci. Transl. Med.* 6:263ra158. doi: 10.1126/scitranslmed.3009759
- Bravo, J. A., Forsythe, P., Chew, M. V., Escaravage, E., Savignac, H. M., Dinan, T. G., et al. (2011). Ingestion of Lactobacillus strain regulates emotional behavior and central GABA receptor expression in a mouse via the vagus nerve. *PNAS* 108, 16050–16055. doi: 10.1073/pnas.1102999108
- Cadet, J. L. (2016). Dysregulation of Acetylation Enzymes in Animal Models of Psychostimulant use Disorders: evolving Stories. *Curr. Neuropharmacol.* 14, 10–16. doi: 10.2174/1570159X13666150121230133
- Caporaso, J. G., Lauber, C. L., Costello, E. K., Berg-Lyons, D., Gonzalez, A., Stombaugh, J., et al. (2011). Moving pictures of the human microbiome. *Genome Biol.* 12:R50. doi: 10.1186/gb-2011-12-5-r50

- Capuco, A., Urits, I., Hasoon, J., Chun, R., Gerald, B., Wang, J. K., et al. (2020). Gut Microbiome Dysbiosis and Depression: a Comprehensive Review. *Curr. Pain Headache Rep.* 24:36. doi: 10.1007/s11916-020-00871-x
- Cheng, Z., Zhou, H., Sherva, R., Farrer, L., Kranzler, H. R., and Gelernter, J. (2018). Genome-wide association study identifies a regulatory variant of *RGMA* associated with opioid dependence in European Americans. *Biol. Psychiatry* 84, 762–770. doi: 10.1016/j.biopsych.2017.12.016
- Chi, L., Mahbub, R., Gao, B., Bian, X., Tu, P., Ru, H., et al. (2017). Nicotine Alters the Gut Microbiome and Metabolites of Gut–Brain Interactions in a Sex-Specific Manner. *Chem. Res. Toxicol.* 30, 2110–2119. doi: 10.1021/acs.chemrestox.7b00162
- Churchill, G. A., Gatti, D. M., Munger, S. C., and Svenson, K. L. (2012). The diversity outbred mouse population. *Mamm. Genome* 23, 713–718. doi: 10.1007/s00335-012-9414-2
- Crabbe, J. C., Ozburn, A. R., Metten, P., Barkley-Levenson, A., Schlumbohm, J. P., Spence, S. E., et al. (2017). High Drinking in the Dark (HDID) mice are sensitive to the effects of some clinically relevant drugs to reduce binge-like drinking. *Pharmacol. Biochem. Behav.* 160, 55–62. doi: 10.1016/j.pbb.2017.08.002
- Dalile, B., Van Oudenhove, L., Vervliet, B., and Verbeke, K. (2019). The role of short-chain fatty acids in microbiota–gut–brain communication. *Nat. Rev. Gastroenterol. Hepatol.* 16, 461–478. doi: 10.1038/s41575-019-0157-3
- Demontis, D., Rajagopal, V. M., Thorgeirsson, T. E., Als, T. D., Grove, J., Leppälä, K., et al. (2019). Genome-wide association study implicates *CHRNA2* in cannabis use disorder. *Nat. Neurosci.* 22, 1066–1074. doi: 10.1038/s41593-019-0416-1
- Draycott, B., Loureiro, M., Ahmad, T., Tan, H., Zunder, J., and Laviolette, S. R. (2014). Cannabinoid Transmission in the Prefrontal Cortex Bi-Phasically Controls Emotional Memory Formation via Functional Interactions with the Ventral Tegmental Area. *J. Neurosci.* 34, 13096–13109. doi: 10.1523/JNEUROSCI.1297-14.2014
- D'Souza, M. S., and Markou, A. (2011). Neuronal Mechanisms Underlying Development of Nicotine Dependence: implications for Novel Smoking-Cessation Treatments. *Addict. Sci. Clin. Pract.* 6, 4–16.
- Edenberg, H. J., and McClintick, J. N. (2018). Alcohol dehydrogenases, aldehyde dehydrogenases and alcohol use disorders: a critical review. *Alcohol. Clin. Exp. Res.* 42, 2281–2297. doi: 10.1111/acer.13904
- Ezquer, F., Quintanilla, M. E., Moya-Flores, F., Morales, P., Munita, J. M., Olivares, B., et al. (2021). Innate gut microbiota predisposes to high alcohol consumption. *Addict. Biol.* 26:e13018. doi: 10.1111/adb.13018
- Fowler, C. D., and Kenny, P. J. (2012). Utility of genetically modified mice for understanding the neurobiology of substance use disorders. *Hum. Genet.* 131, 941–957. doi: 10.1007/s00439-011-1129-z
- French, J. E., Gatti, D. M., Morgan, D. L., Kissling, G. E., Shockley, K. R., Knudsen, G. A., et al. (2015). Diversity Outbred Mice Identify Population-Based Exposure Thresholds and Genetic Factors that Influence Benzene-Induced Genotoxicity. *Environ. Health Perspect.* 123, 237–245. doi: 10.1289/ehp.1408202
- Gelernter, J., Kranzler, H. R., Sherva, R., Koesterer, R., Almasy, L., Zhao, H., et al. (2014). Genome-Wide Association Study of Opioid Dependence: multiple Associations Mapped to Calcium and Potassium Pathways. *Biol. Psychiatry* 76, 66–74. doi: 10.1016/j.biopsych.2013.08.034
- Goldman, D., Oroszi, G., and Ducci, F. (2005). The genetics of addictions: uncovering the genes. *Nat. Rev. Genet.* 6, 521–532. doi: 10.1038/nrg1635
- Goodrich, J. K., Waters, J. L., Poole, A. C., Sutter, J. L., Koren, O., Blekman, R., et al. (2014). Human genetics shape the gut microbiome. *Cell* 159, 789–799. doi: 10.1016/j.cell.2014.09.053
- Grice, E. A., and Segre, J. A. (2012). The Human Microbiome: our Second Genome. *Annu. Rev. Genom. Hum. Genet.* 13, 151–170. doi: 10.1146/annurev-genom-090711-163814
- Hadizadeh, M., Hamidi, G. A., and Salami, M. (2019). Probiotic supplementation improves the cognitive function and the anxiety-like behaviors in the stressed rats. *Iran. J. Basic Med. Sci.* 22, 506–514. doi: 10.22038/ijbms.2019.33956.8078
- Hancock, D. B., Markunas, C. A., Bierut, L. J., and Johnson, E. O. (2018). Human Genetics of Addiction: new Insights and Future Directions. *Curr. Psychiatry Rep.* 20:8. doi: 10.1007/s11920-018-0873-3
- Hitzemann, R., Phillips, T. J., Lockwood, D. R., Darakjian, P., and Searles, R. P. (2020). Phenotypic and gene expression features associated with variation in chronic ethanol consumption in heterogeneous stock collaborative cross mice. *Genomics* 112, 4516–4524. doi: 10.1016/j.ygeno.2020.08.004
- Johnson, E. C., Demontis, D., Thorgeirsson, T. E., Walters, R. K., Polimanti, R., Hatoum, A. S., et al. (2020). A large-scale genome-wide association study meta-analysis of cannabis use disorder. *Lancet Psychiatry* 7, 1032–1045. doi: 10.1016/S2215-0366(20)30339-4
- Justice, M. J., and Dhillon, P. (2016). Using the mouse to model human disease: increasing validity and reproducibility. *Dis. Model Mech.* 9, 101–103. doi: 10.1242/dmm.024547
- Kahlig, K. M., and Galli, A. (2003). Regulation of dopamine transporter function and plasma membrane expression by dopamine, amphetamine, and cocaine. *Eur. J. Pharmacol.* 479, 153–158. doi: 10.1016/j.ejphar.2003.08.065
- Kauer, J. A. (2004). Learning Mechanisms in Addiction: synaptic Plasticity in the Ventral Tegmental Area as a Result of Exposure to Drugs of Abuse. *Annu. Rev. Physiol.* 66, 447–475. doi: 10.1146/annurev.physiol.66.032102.112534
- Kim, S.-K., and Kim, D. H. (2019). Lactobacillus mucosae and Bifidobacterium longum Synergistically Alleviate Immobilization Stress-Induced Anxiety/Depression in Mice by Suppressing Gut Dysbiosis. 29, 1369–1374. doi: 10.4014/jmb.1907.07044
- Kiraly, D. D., Walker, D. M., Calipari, E. S., Labonte, B., Issler, O., Pena, C. J., et al. (2016). Alterations of the Host Microbiome Affect Behavioral Responses to Cocaine. *Sci. Rep.* 6:35455. doi: 10.1038/srep35455
- Koob, G. F., Kandel, D., and Volkow, N. D. (2008). “Pathophysiology of Addiction” in *Psychiatry*, eds T. Allan, K. Jerald, J. A. Lieberman, M. B. First, and M. Mario (United States: John Wiley & Sons, Ltd). 354–378. doi: 10.1002/9780470515167.ch22
- Koob, G. F., and Le Moal, M. (2001). Drug Addiction, Dysregulation of Reward, and Allostasis. *Neuropsychopharmacol* 24, 97–129. doi: 10.1016/S0893-133X(00)00195-0
- Korach-Rechtman, H., Freilich, S., Gerassy-Vainberg, S., Buhnik-Rosenblau, K., Danin-Poleg, Y., Bar, H., et al. (2019). Murine Genetic Background Has a Stronger Impact on the Composition of the Gut Microbiota than Maternal Inoculation or Exposure to Unlike Exogenous Microbiota. *Appl. Environ. Microbiol.* 85, e00826–19. doi: 10.1128/AEM.00826-19
- Kranzler, H. R., Zhou, H., Kember, R. L., Vickers Smith, R., Justice, A. C., Damrauer, S., et al. (2019). Genome-wide association study of alcohol consumption and use disorder in 274,424 individuals from multiple populations. *Nat. Commun.* 10:1499. doi: 10.1038/s41467-019-09480-8
- Kreek, M. J., Nielsen, D. A., and LaForge, K. S. (2004). Genes associated with addiction. *Neuromol. Med.* 5, 85–108. doi: 10.1385/NMM:5:1:085
- Leclercq, S., Matamoros, S., Cani, P. D., Neyrinck, A. M., Jamar, F., Stärkel, P., et al. (2014). Intestinal permeability, gut-bacterial dysbiosis, and behavioral markers of alcohol-dependence severity. *Proc. Natl. Acad. Sci. U. S. A.* 111, E4485–E4493. doi: 10.1073/pnas.1415174111
- Lee, K., Vuong, H. E., Nusbaum, D. J., Hsiao, E. Y., Evans, C. J., and Taylor, A. M. W. (2018). The gut microbiota mediates reward and sensory responses associated with regimen-selective morphine dependence. *Neuropsychopharmacology* 43, 2606–2614. doi: 10.1038/s41386-018-0211-9
- Lipari, R. N., and Van Horn, S. L. (2017). “Trends in substance use disorders among adults aged 18 or older” *The CBHSQ Report. Rockville (MD): Substance Abuse and Mental Health Services Administration*. (United States: Substance Abuse and Mental Health Services Administration).
- Liu, Q. F., Kim, H.-M., Lim, S., Chung, M.-J., Lim, C.-Y., Koo, B.-S., et al. (2020). Effect of probiotic administration on gut microbiota and depressive behaviors in mice. *Daru* 28, 181–189. doi: 10.1007/s40199-020-00329-w
- McVey Neufeld, K.-A., Kay, S., and Bienenstock, J. (2018). Mouse Strain Affects Behavioral and Neuroendocrine Stress Responses Following Administration of Probiotic Lactobacillus rhamnosus JB-1 or Traditional Antidepressant Fluoxetine. *Front. Neurosci.* 12:294. doi: 10.3389/fnins.2018.00294
- Meckel, K. R., and Kiraly, D. D. A. (2019). potential role for the gut microbiome in substance use disorders. *Psychopharmacology* 236, 1513–1530. doi: 10.1007/s00213-019-05232-0
- Mews, P., Egervari, G., Nativio, R., Sidoli, S., Donahue, G., Lombroso, S. I., et al. (2019). Alcohol metabolism contributes to brain histone acetylation. *Nature* 574, 717–721. doi: 10.1038/s41586-019-1700-7
- Muccioli, G. G., Naslain, D., Bäckhed, F., Reigstad, C. S., Lambert, D. M., Delzenne, N. M., et al. (2010). The endocannabinoid system links gut microbiota to adipogenesis. *Mol. Syst. Biol.* 6:392. doi: 10.1038/msb.2010.46
- Nestler, E. J. (2005). Is there a common molecular pathway for addiction? *Nat. Neurosci.* 8, 1445–1449. doi: 10.1038/nn1578

- Noble, E. P., Blum, K., Khalsa, M. E., Ritchie, T., Montgomery, A., Wood, R. C., et al. (1993). Allelic association of the D2 dopamine receptor gene with cocaine dependence. *Drug Alcohol Depend* 33, 271–285. doi: 10.1016/0376-8716(93)90113-5
- Northcutt, A. L., Hutchinson, M. R., Wang, X., Baratta, M. V., Hiranita, T., Cochran, T. A., et al. (2015). DAT isn't all that: cocaine reward and reinforcement requires Toll Like Receptor 4 signaling. *Mol. Psychiatry* 20, 1525–1537. doi: 10.1038/mp.2014.177
- Patel, R. R., Wolfe, S. A., Bajo, M., Abeynaik, S., Pahng, A., Borgonetti, V., et al. (2021). IL-10 normalizes aberrant amygdala GABA transmission and reverses anxiety-like behavior and dependence-induced escalation of alcohol intake. *Prog. Neurobiol.* 199:101952. doi: 10.1016/j.pneurobio.2020.101952
- Poltorak, A., Apalko, S., and Sherbak, S. (2018). Wild-derived mice: from genetic diversity to variation in immune responses. *Mamm Genome* 29, 577–584. doi: 10.1007/s00335-018-9766-3
- Prom-Wormley, E. C., Ebejer, J., Dick, D. M., and Bowers, M. S. (2017). The genetic epidemiology of substance use disorder: a review. *Drug Alcohol Depend.* 180, 241–259. doi: 10.1016/j.drugalcdep.2017.06.040
- Quigley, E. M. M., and Gajula, P. (2020). Recent advances in modulating the microbiome. *F1000Res.* 9, F1000 Faculty Rev-46. doi: 10.12688/f1000research.20204.1
- Renthal, W., and Nestler, E. J. (2009). Histone Acetylation in Drug Addiction. *Semin. Cell. Dev. Biol.* 20, 387–394. doi: 10.1016/j.semcdb.2009.01.005
- Roberto, M., and Varodayan, F. (2017). Synaptic Targets: chronic Alcohol Actions. *Neuropharmacology* 122, 85–99. doi: 10.1016/j.neuropharm.2017.01.013
- Rosshart, S. P., Herz, J., Vassallo, B. G., Hunter, A., Wall, M. K., Badger, J. H., et al. (2019). Laboratory mice born to wild mice have natural microbiota and model human immune responses. *Science* 365:eaaw4361. doi: 10.1126/science.aaw4361
- Shreiner, A. B., Kao, J. Y., and Young, V. B. (2015). The gut microbiome in health and in disease. *Curr. Opin. Gastroenterol.* 31, 69–75. doi: 10.1097/MOG.000000000000139
- Simon-O'Brien, E., Alaux-Cantin, S., Warnault, V., Buttolo, R., Naassila, M., and Vilpoux, C. (2015). The histone deacetylase inhibitor sodium butyrate decreases excessive ethanol intake in dependent animals. *Addict. Biol.* 20, 676–689. doi: 10.1111/adb.12161
- Srivastava, A., Morgan, A. P., Najarian, M. L., Sarsani, V. K., Sigmon, J. S., Shorter, J. R., et al. (2017). Genomes of the Mouse Collaborative Cross. *Genetics* 206, 537–556. doi: 10.1534/genetics.116.198838
- Stone, A. L., Becker, L. G., Huber, A. M., and Catalano, R. F. (2012). Review of risk and protective factors of substance use and problem use in emerging adulthood. *Addict. Behav.* 37, 747–775. doi: 10.1016/j.addbeh.2012.02.014
- Strandwitz, P. (2018). Neurotransmitter modulation by the gut microbiota. *Brain Res.* 1693, 128–133. doi: 10.1016/j.brainres.2018.03.015
- Strandwitz, P., Kim, K. H., Terekhova, D., Liu, J. K., Sharma, A., Levering, J., et al. (2019). GABA-modulating bacteria of the human gut microbiota. *Nat. Microbiol.* 4, 396–403. doi: 10.1038/s41564-018-0307-3
- Svenson, K. L., Gatti, D. M., Valdar, W., Welsh, C. E., Cheng, R., Chesler, E. J., et al. (2012). High-Resolution Genetic Mapping Using the Mouse Diversity Outbred Population. *Genetics* 190, 437–447. doi: 10.1534/genetics.111.132597
- Swiatczak, B., and Cohen, I. R. (2015). Gut feelings of safety: tolerance to the microbiota mediated by innate immune receptors. *Microbiol. Immunol.* 59, 573–585. doi: 10.1111/1348-0421.12318
- Thaiss, C. A., Zeevi, D., Levy, M., Zilberman-Schapira, G., Suez, J., Tengeler, A. C., et al. (2014). Transkingdom Control of Microbiota Diurnal Oscillations Promotes Metabolic Homeostasis. *Cell* 159, 514–529. doi: 10.1016/j.cell.2014.09.048
- Thiele, T. E., Crabbe, J. C., and Boehm, S. L. (2014). Drinking in the Dark" (DID): a Simple Mouse Model of Binge-Like Alcohol Intake. *Current Protocols in Neuroscience* 68, 9.49.1–12. doi: 10.1002/0471142301.ns0949s68
- Threadgill, D. W., Miller, D. R., Churchill, G. A., and de Villena, F. P.-M. (2011). The collaborative cross: a recombinant inbred mouse population for the systems genetic era. *ILAR J.* 52, 24–31. doi: 10.1093/ilar.52.1.24
- Valentino, R. J., and Volkow, N. D. (2018). Untangling the complexity of opioid receptor function. *Neuropsychopharmacology* 43, 2514–2520. doi: 10.1038/s41386-018-0225-3
- Volkow, N. D., Wang, G. J., Fowler, J. S., Logan, J., Gatley, S. J., Wong, C., et al. (1999). Reinforcing effects of psychostimulants in humans are associated with increases in brain dopamine and occupancy of D(2) receptors. *J. Pharmacol. Exp. Ther.* 291, 409–415.
- Walker, D. M., Cates, H. M., Loh, Y.-H. E., Purushothaman, I., Ramakrishnan, A., Cahill, K. M., et al. (2018). Cocaine Self-administration Alters Transcriptome-wide Responses in the Brain's Reward Circuitry. *Biol. Psychiatry* 84, 867–880. doi: 10.1016/j.biopsych.2018.04.009
- Witjes, V. M., Boleij, A., and Halfman, W. (2020). Reducing versus Embracing Variation as Strategies for Reproducibility: the Microbiome of Laboratory Mice. *Animal* 10:2415. doi: 10.3390/ani10122415
- Xiao, H.-W., Ge, C., Feng, G.-X., Li, Y., Luo, D., Dong, J.-L., et al. (2018). Gut microbiota modulates alcohol withdrawal-induced anxiety in mice. *Toxicol. Lett.* 287, 23–30. doi: 10.1016/j.toxlet.2018.01.021
- Xu, F., Gainetdinov, R. R., Wetsel, W. C., Jones, S. R., Bohn, L. M., Miller, G. W., et al. (2000). Mice lacking the norepinephrine transporter are supersensitive to psychostimulants. *Nat. Neurosci.* 3, 465–471. doi: 10.1038/74839
- Xu, Z., Liu, Z., Dong, X., Hu, T., Wang, L., Li, J., et al. (2018). Fecal Microbiota Transplantation from Healthy Donors Reduced Alcohol-induced Anxiety and Depression in an Animal Model of Chronic Alcohol Exposure. *Chin. J. Physiol.* 61, 360–371. doi: 10.4077/CJP.2018.BAH633
- Yano, J. M., Yu, K., Donaldson, G. P., Shastri, G. G., Ann, P., Ma, L., et al. (2015). Indigenous bacteria from the gut microbiota regulate host serotonin biosynthesis. *Cell* 161, 264–276. doi: 10.1016/j.cell.2015.02.047
- Yunes, R. A., Poluektova, E. U., Vasileva, E. V., Odorskaya, M. V., Marsova, M. V., Kovalev, G. I., et al. (2020). A Multi-strain Potential Probiotic Formulation of GABA-Producing *Lactobacillus plantarum* 90sk and *Bifidobacterium adolescentis* 150 with Antidepressant Effects. *Probiotics Antimicrob. Proteins* 12, 973–979. doi: 10.1007/s12602-019-09601-1
- Zhao, W., Hu, Y., Li, C., Li, N., Zhu, S., Tan, X., et al. (2020). Transplantation of fecal microbiota from patients with alcoholism induces anxiety/depression behaviors and decreases brain mGluR1/PKC  $\epsilon$  levels in mouse. *BioFactors* 46, 38–54. doi: 10.1002/biof.1567
- Zhou, H., Rentsch, C. T., Cheng, Z., Kember, R. L., Nunez, Y. Z., Sherva, R. M., et al. (2020). Association of OPRM1 Functional Coding With Opioid Use Disorder. *JAMA Psychiatry* 77, 1072–1080. doi: 10.1001/jamapsychiatry.2020.1206

**Conflict of Interest:** The authors declare that the research was conducted in the absence of any commercial or financial relationships that could be construed as a potential conflict of interest.

**Publisher's Note:** All claims expressed in this article are solely those of the authors and do not necessarily represent those of their affiliated organizations, or those of the publisher, the editors and the reviewers. Any product that may be evaluated in this article, or claim that may be made by its manufacturer, is not guaranteed or endorsed by the publisher.

Copyright © 2021 Russell, Zhou, Weinstock and Bubier. This is an open-access article distributed under the terms of the Creative Commons Attribution License (CC BY). The use, distribution or reproduction in other forums is permitted, provided the original author(s) and the copyright owner(s) are credited and that the original publication in this journal is cited, in accordance with accepted academic practice. No use, distribution or reproduction is permitted which does not comply with these terms.



# Individual Differences in Different Measures of Opioid Self-Administration in Rats Are Accounted for by a Single Latent Variable

Yayi Swain<sup>1,2</sup>, Niels G. Waller<sup>2</sup>, Jonathan C. Gewirtz<sup>2,3</sup> and Andrew C. Harris<sup>1,2,4\*</sup>

<sup>1</sup> Hennepin Healthcare Research Institute, Minneapolis, MN, United States, <sup>2</sup> Department of Psychology, University of Minnesota, Minneapolis, MN, United States, <sup>3</sup> Department of Neuroscience, University of Minnesota, Minneapolis, MN, United States, <sup>4</sup> Department of Medicine, University of Minnesota, Minneapolis, MN, United States

## OPEN ACCESS

### Edited by:

Peter Kalivas,  
Medical University of South Carolina,  
United States

### Reviewed by:

Morgan H. James,  
Rutgers, The State University of New  
Jersey, United States  
Deena Marie Walker,  
Oregon Health and Science University,  
United States

### \*Correspondence:

Andrew C. Harris  
harr0547@umn.edu

### Specialty section:

This article was submitted to  
Addictive Disorders,  
a section of the journal  
Frontiers in Psychiatry

Received: 20 May 2021

Accepted: 10 August 2021

Published: 07 September 2021

### Citation:

Swain Y, Waller NG, Gewirtz JC and  
Harris AC (2021) Individual Differences  
in Different Measures of Opioid  
Self-Administration in Rats Are  
Accounted for by a Single Latent  
Variable. *Front. Psychiatry* 12:712163.  
doi: 10.3389/fpsy.2021.712163

Individual differences in vulnerability to addiction have been widely studied through factor analysis (FA) in humans, a statistical method that identifies “latent” variables (variables that are not measured directly) that reflect the common variance among a larger number of observed measures. Despite its widespread application in behavioral genetics, FA has not been used in preclinical opioid addiction research. The current study used FA to examine the latent factor structure of four measures of i.v. morphine self-administration (MSA) in rats (i.e., acquisition, demand elasticity, morphine/cue- and stress/cue-induced reinstatement). All four MSA measures are generally assumed in the preclinical literature to reflect “addiction vulnerability,” and individual differences in multiple measures of abuse liability are best accounted for by a single latent factor in some human studies. A one-factor model was therefore fitted to the data. Two different regularized FAs indicated that a one-factor model fit our data well. Acquisition, elasticity of demand and morphine/cue-induced reinstatement loaded significantly onto a single latent factor while stress/cue-induced reinstatement did not. Consistent with findings from some human studies, our results indicated a common drug “addiction” factor underlying several measures of opioid SA. However, stress/cue-induced reinstatement loaded poorly onto this factor, suggesting that unique mechanisms mediate individual differences in this vs. other MSA measures. Further establishing FA approaches in drug SA and in preclinical neuropsychopathology more broadly will provide more reliable, clinically relevant core factors underlying disease vulnerability in animal models for further genetic analyses.

**Keywords:** opioid self-administration, factor analysis, individual differences, behavioral economics, multivariate methods

## INTRODUCTION

Individual differences in susceptibility to addiction in humans have been studied widely through factor analysis (FA), a statistical method that identifies “latent” variables (variables that are not measured directly) that reflect the common variance among a larger number of observed measures. In contrast to “bottom-up” approaches evaluating a wide range of measures e.g. (1), FA is

a theory-driven statistical method that uses well-defined indicators from a common behavioral domain (2). These models provide both insights into the relationship between different facets of addiction- and dependence-related symptomatology (3), and a relatively parsimonious account of disease comorbidity (4). For example, FA approaches have revealed that liability to alcohol abuse is associated both with a general drug abuse vulnerability factor and with several factors that are specific to this form of addiction (e.g., genetic variants in alcohol metabolizing enzymes) (5–7).

Factor analytic approaches have been widely used in the clinical literature to explore the factor structure underlying various addiction measures. Such structures may have both vertical and horizontal dimensions. The vertical dimension essentially represents hierarchical relationships between concrete traits or behaviors and higher-order, more abstract, or general “latent” factors. The horizontal dimension represents the degree of similarity between factors within a single level of the hierarchy (8). Elaboration of such two-dimensional factor structure may yield one or more robust endophenotypes that can be used to identify genomic loci associated with core features of substance use disorders (9, 10).

In animal addiction research, FA approaches could be useful in identifying the underlying associations between, and uniqueness of, different addiction-related behavioral measures, developing more reliable measures of addiction, and uncovering their underlying genomic and neurobiological substrates (11). Such approaches have rarely been employed in this area, however, despite the fact that the drug self-administration (SA) paradigm models a variety of aspects of addiction (e.g., acquisition, relapse, etc.) within individual subjects, thereby lending itself to multivariate statistical analyses. In one previous study, an exploratory FA revealed three addiction vulnerability measures—(a) SA despite punishment, (b) progressive ratio (PR) breakpoint, and (c) drug-seeking during no-drug periods—as loading onto a single latent factor underlying cocaine SA in rats, whereas extinction loaded onto a separate factor (12). However, despite the dramatic impact of opioid addiction on public health (13), no preclinical studies have applied FA to opioid SA.

The primary goal of this study was to use FA to examine the latent factor structure between four measures of i.v. opioid (morphine) SA in rats (i.e., acquisition, demand elasticity, morphine/cue-induced reinstatement, stress/cue-induced reinstatement), using data from a previously published study (14). The four SA measures were selected due to their common use in preclinical studies and to the relevance of each to different aspects of addiction (15–18).

In animal research, there is frequently the implicit assumption that a variety of different SA variables all have relevance to addiction vulnerability. This is consistent with findings in humans showing that individual differences in multiple measures of abuse liability are best accounted for by a single latent factor (19–21). Therefore, in the current study, a one-factor model was fitted to the data, with the single latent factor conceptualized as the “addiction” factor.

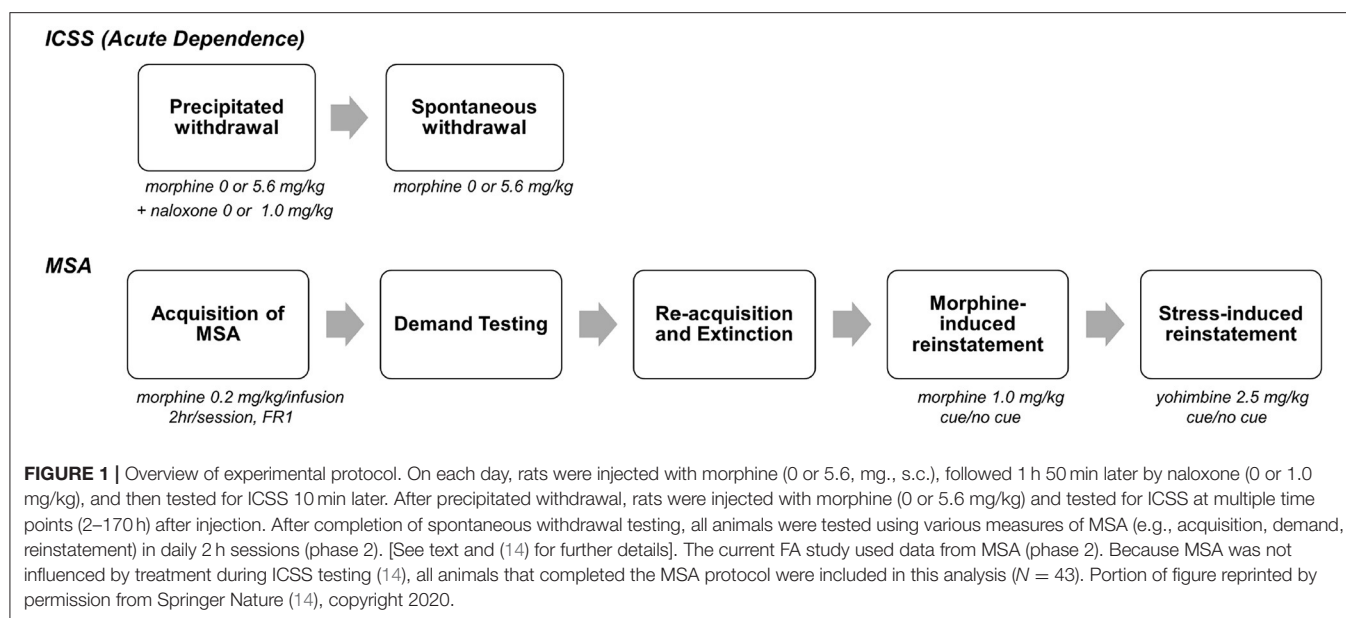
It has been proposed that the minimum sample size required for FA ranges between  $N = 50$ – $250$  (22–26). Conducting small

sample-size FA may result in many issues that are otherwise uncommon in large sample-size analyses, such as Heywood cases denoting negative estimated variances (22, 27). Preclinical addiction studies have typically employed relatively small sample sizes, which pose a challenge to the use of FA. Therefore, the secondary goal of this study was to test the utility of a novel approach to conducting FA on preclinical data that allows for smaller sample sizes to be used. Several proposed (28–30) “regularization methods” can effectively address the challenges of conducting small sample FA by reducing the number of estimated model parameters. In this study, we utilized two robust regularization methods in conjunction with a method to obtain a robust correlation matrix from our data (31) to demonstrate the feasibility of conducting FA in a small preclinical dataset. By applying these iterative statistical procedures to our data, we aimed to understand the core dimensions underlying the morphine SA (MSA) model.

## MATERIALS AND METHODS

### Overview of Experimental Protocol

Data from a recent study (14) were used for the current analyses. The goal of that study was to evaluate whether withdrawal-induced anhedonia as measured using elevated intracranial self-stimulation (ICSS) thresholds predicted individual differences in subsequent MSA. **Figure 1** shows an overview of the experimental protocol, which is described in detail in Swain et al. (14). Briefly, male Sprague-Dawley rats that were trained in an ICSS paradigm underwent naloxone (NX)-precipitated and/or spontaneous withdrawal from acute morphine (MOR) injections or received control (saline, SAL) injections. This resulted in four experimental groups: MOR + NX ( $n = 29$ ), MOR + SAL, SAL + NX, SAL + SAL ( $n = 10$ – $11$  each). During the subsequent MSA protocol, all rats acquired MSA (0.2 mg/kg/infusion) under a fixed ratio (FR) 1 schedule of reinforcement for at least 10 daily sessions and until MSA was stable. Rats then underwent demand testing in which the FR response requirement was progressively increased every 3–4 sessions as follows: FR 2, 3, 6, 12, 24, and doubled thereafter until infusion rates were reduced by  $>90\%$  compared to FR 1. Rats then re-acquired MSA under an FR 1 schedule for at least 5 sessions and until infusions/session were stable and subsequently underwent extinction of MSA in the absence of the cue light previously paired with morphine infusions for at least 10 sessions and until active lever pressing was stable. Rats were then tested for drug-induced reinstatement (with morphine injection prior to the SA session) and finally, stress-induced reinstatement (with injection of the pharmacological stressor yohimbine prior to the SA session), both in the presence and absence of the visual cue paired with morphine, and with appropriate within-subject control conditions (1 session per experimental/control condition) [see (14) for more details on animals, apparatus and experimental protocol]. Since a history of MOR and/or NX injections during ICSS testing did not have a significant effect on subsequent MSA, rats from all groups that completed all phases of the study were included in the data analyses ( $N = 43$ ). These



experiments conformed to appropriate NIH and institutional ethical / biosafety standards see (14).

## Overview of Factor Model

We tested a one-factor model with one latent variable (the “addiction” factor) and four observed variables from the MSA model: acquisition, elasticity of demand ( $\alpha$ ), and morphine/cue- and stress/cue-induced reinstatement with visual cue light present. These measures were chosen due to the distinct aspects of addiction-like behavior they are often thought to capture and their common application in drug SA research. Acquisition was defined as the average number of infusions across the first 10 days of MSA. An exponential demand function was fitted to data from the FR escalation protocol to obtain the  $\alpha$  statistic, as described in previous studies (14, 16).  $\alpha$  refers to the rate of change in consumption with increases in unit price (elasticity of demand), with higher  $\alpha$  values indicating lower reinforcement efficacy. Reinstatement was measured as the difference between the number of active and inactive lever presses over each of the 2-h reinstatement test sessions after the challenge (i.e., morphine or yohimbine) drug injection, with cue light present. The use of difference scores to measure reinstatement controls for potential non-specific (e.g., motoric) effects of treatments (14, 32–34). These reinstatement conditions were analyzed because they produced more robust reinstatement than either the challenge drug (morphine or yohimbine) alone or the cue alone (see Results). A higher number of infusions during acquisition, lower elasticity of demand ( $\alpha$ ), and higher reinstatement scores reflect greater abuse liability for each of these measures.

## Statistical Analyses

All statistical analyses were performed in GraphPad Prism (GraphPad Software, San Diego, California USA) and R ver. 4.0.4 (35). A one-factor model was hypothesized to show good model-fit with each of the SA measures showing high factor loadings,

indicating a common “addiction” factor underlying all tested SA measures.

Three distinct methods were used for extracting factor loadings. Given the small sample size of our data set and several outlying values (to be discussed later), we used two distinct factor extraction algorithms that are known to yield robust factor loadings in small sets of non-normal data. The first method involves computing Mahalanobis distances for all data points and then identifying the number of multivariate outliers via a series of chi-squared tests ( $\alpha = 0.1$ ). Next, we used the minimum covariance determinant [MCD: MASS package (31, 36)] method to produce a robust estimator of multivariate scatter and center to remove the multivariate outliers and generate a robust correlation matrix. This robust correlation matrix was factor analyzed with a regularized least squares estimator [fareg function; (37)]. Robust least squares estimation does not assume data multinormality and aims to minimize residuals between the observed and reproduced correlations under the proposed factor model (38). Model fit was tested via the correlation root mean square residual (CRM) statistic:

$$CRM = \sqrt{\frac{1}{t-p} \sum_{i < j} (\rho_{ij} - \rho_{ij}^0)^2},$$

with  $t$  denoting the number of non-redundant population variances and co-variances among the  $p$  observed variables,  $\rho_{ij}$  denoting the correlation between variables  $i$  and  $j$ , and  $\rho_{ij}^0$  denoting the model-implied population correlation under the theoretical model (39). CRM is commonly used in FA and structural equation modeling (SEM) as a model fit statistic, with smaller numbers indicating better model fit. Finally, effect size of overall model misfit was determined by the  $\Gamma_1$  statistic, defined as

$$\Gamma_1 = \frac{p}{tr(\Sigma \Sigma_0^{-1})^2},$$

where  $\Sigma$  denotes a population covariance matrix,  $\Sigma_0$  denotes the population covariance under the null hypothesis, and  $tr$  denotes the trace operator (the trace of a square matrix equals the sum of its diagonal elements). Parametric bootstrap standard errors (SE) were computed for the factor loadings using 5,000 bootstrap samples (40).

The second robust method for analyzing the data used regularized FA as described by Jung et al. [(29, 30); implemented in the `fareg` function; (37)]. Both least squares (LS) and maximum likelihood (MLE) regularized FA were used to estimate robust factor loadings for testing the 1-factor model. Previous work suggests that these methods work well in small samples of non-normally distributed data (27, 29, 30) and thus were well-suited for the current study.

To further demonstrate the advantages of the robust correlation and robust factor analytic methods, a third analysis was implemented using principal axis factoring, a traditional factor extraction method, with the complete data set of 43 rats [using the `faMain` function in the R `fungible` library (37)]. This method was not expected to perform well given the small sample size of our data set and the existence of several multivariate outliers. To allow comparison with the other analyses, we also computed the CRMR index for this analysis.

## RESULTS

### MSA

Detailed behavioral results from the MSA protocol are reported in Swain et al. (14). Briefly, rats reliably acquired MSA, exhibiting a clear preference for the active over inactive response lever (**Figure 2A**). Increases in FR requirement resulted in a progressive reduction in morphine consumption that was well-described by an exponential demand function ( $R^2 = 0.84$ ) (**Figure 2B**). After MSA reacquisition and extinction in the absence of the morphine-associated cue light, rats reliably reinstated active lever responding following a priming dose of morphine in the absence of the cue light (MOR + NO CUE; **Figure 2C**), response-contingent presentation of the cue light (VEH + CUE), or combined exposure to morphine and the cue light (MOR + CUE). Similar findings were observed when reinstatement was induced by the pharmacological stressor yohimbine (**Figure 2D**).

### FA

All variables were standardized to keep their scales consistent. The factor loadings from each analysis are shown in **Table 1**.

For the two regularized FA analyses, 5 multivariate outliers ( $\alpha = 0.1$ ) were identified from the chi-squared test using Mahalanobis distance. Subsequently, these 5 multivariate outliers were excluded from the robust correlation matrix computation using MCD ( $N = 38$ ) (31). Using the robust correlation matrix with LS estimation, the first regularized FA revealed that acquisition, elasticity of demand and morphine/cue-induced reinstatement showed high factor loadings (all  $|\text{loadings}| \geq 0.58$ ) on a single common factor, whereas stress/cue-induced reinstatement showed low factor loading on this dimension

(loading = 0.27) (**Table 1**). Bootstrap SEs for factor loadings of acquisition, elasticity of demand and morphine/cue-induced reinstatement were also lower (SE = 0.14 for all three) compared to SE of the factor loading for stress/cue-induced reinstatement (SE = 0.22). The second regularized FA using MLE factoring (on the same robust correlation matrix) produced similar results. Acquisition, elasticity of demand and morphine/cue-induced reinstatement showed high factor loadings on a single dimension (all  $|\text{loadings}| \geq 0.59$ ), and stress/cue-induced reinstatement again showed a low factor loading (loading = 0.28) (**Table 1**). Similar SEs were also observed, where acquisition, elasticity of demand and morphine/cue-induced reinstatement showed lower SEs (all SEs  $\leq 0.14$ ) compared to stress/cue-induced reinstatement (SE = 0.23). Overall, based on the CRMR and  $\Gamma_1$  values, the one-factor model showed excellent model fit (CRMR = 0.03,  $\Gamma_1 = 1$  for both analyses).

As expected, the results from the principal axis factoring ( $N = 43$ ) were less robust. Although acquisition, morphine/cue-induced reinstatement and stress/cue-induced reinstatement showed positive factor loading values (all  $|\text{loadings}| \geq 0.27$ ), the loading for elasticity of demand was outside of theoretical bounds with a  $|\text{loading}| = 1.03$  (**Table 1**). Since factor loadings in the standardized 1-factor model can be interpreted as correlations, values outside of the  $-1$  to  $1$  interval are indicative of a Heywood case. As noted earlier, this mathematically illogical result can occur when common factor extraction methods are applied to small sample data sets. The fact that the principal axis method produced a Heywood case in our data provides further justification for our choice to use robust methods for factor extraction. Therefore, it was not surprising that the one-factor principal axis solution did not fit the data well as indicated by CRMR = 0.07.

## DISCUSSION

Our data demonstrated that a single latent addiction factor fits four distinct MSA measures. This indicates that acquisition, elasticity of demand, morphine/cue-induced reinstatement, and stress/cue-induced reinstatement all in some way measure a common construct, akin to a general factor of addiction vulnerability. These findings support the implicit assumption in the preclinical literature that these different SA measures are related to abuse liability. This one-factor model is also consistent with the clinical literature that often posits a single latent factor to underlie multiple measures of addiction (19–21).

In terms of individual factor loadings, results from both regularized FAs implicated elasticity of demand as the variable most reliably strongly associated with the addiction factor, with a stable, high factor loading across both analyses. Previous studies have demonstrated the value of behavioral economics in studying individual differences in vulnerability to addiction to opioids and other drugs in both humans and animals (14, 16, 41–43). For example, elasticity of demand predicts a variety of other measures of cocaine and opioid SA in rats (41, 42). The high factor loading for  $\alpha$  in the current study complements these findings and further

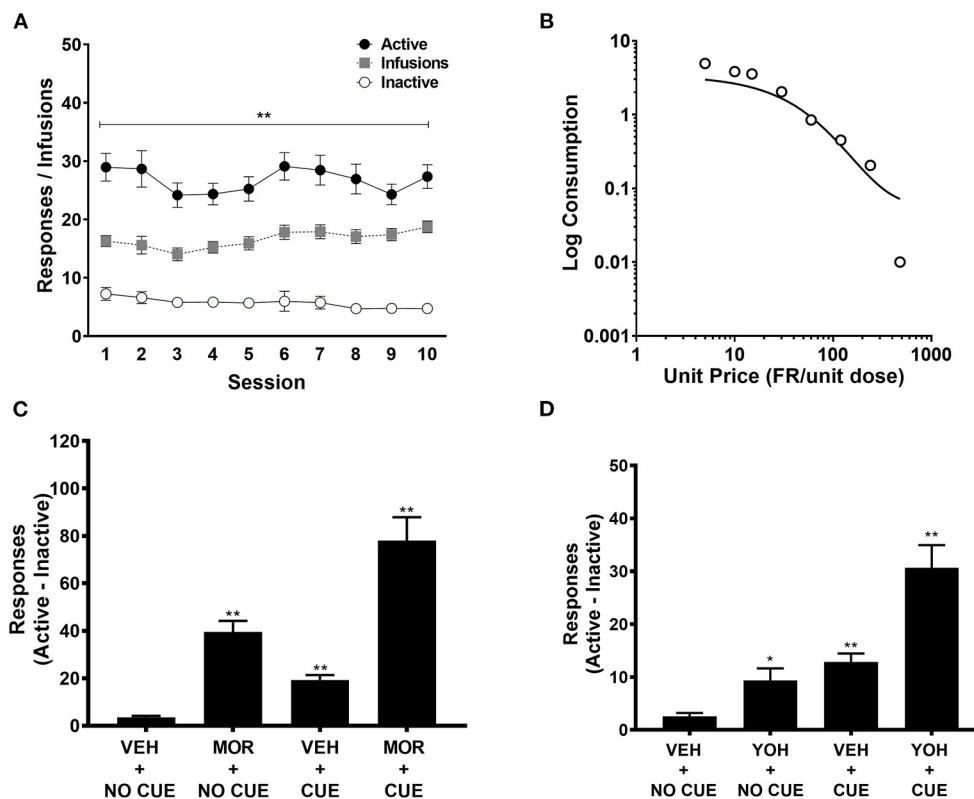


**FIGURE 2 |** Active and inactive lever pressing during acquisition ( $n = 43$ ), (A); exponential demand curve for morphine intake during demand testing ( $n = 43$ ) (B); difference scores between active and inactive lever pressing during morphine-induced ( $n = 43$ ) (C) and yohimbine-induced ( $n = 43$ ) (D) reinstatement. These data are derived from Swain et al. (14), but are here pooled across groups irrespective of treatment prior to MSA. MOR, Morphine; YOH, Yohimbine; VEH, Vehicle. Data points represent mean  $\pm$  SEM. \*Significant difference compared to inactive lever pressing or VEH+NO CUE responding,  $p < 0.05$ ; \*\* $p < 0.01$ .

**TABLE 1 |** Estimates for factor loadings from 3 analyses, with bootstrapped standard errors for the factor loadings from the two robust methods in parenthesis.

SA measures	Factor loadings		
	Robust LS	Robust MLE	Principal axis
Acquisition	0.58 (0.14)	0.59 (0.08)	0.48
Demand	-0.63 (0.14)	-0.64 (0.13)	-1.03
Morphine/cue-induced reinstatement	0.62 (0.14)	0.63 (0.14)	0.32
Stress/cue-induced reinstatement	0.27 (0.22)	0.28 (0.23)	0.27

Robust LS, regularized FA using least squares estimates with MCD robust correlation matrix excluding 5 multivariate outliers; Robust MLE, regularized FA using maximum likelihood estimates with robust correlation matrix excluding 5 multivariate outliers; Principal Axis, traditional principal axis factor extraction.

demonstrates the utility of this demand function for studying drug addiction.

In contrast, stress/cue-induced reinstatement did not load onto the addiction factor. Stress-induced reinstatement differed from the other three measures in that it (1) involved stress, which can induce relapse via partially distinct biological mechanisms (44), and (2) was tested in the absence of morphine. To evaluate whether either of these features could account for our findings, we tested an additional model (see **Supplemental Materials**), in which we added cue-induced reinstatement, and replaced elasticity of demand ( $\alpha$ ) with

intensity of demand ( $Q_0$ ), an alternative behavioral economic measure that reflects the maximum level of consumption at zero price. Neither cue-induced reinstatement or  $Q_0$  involve acute stress, while  $Q_0$  is derived from data collected in the presence of morphine. Neither of these measures showed high factor loading, suggesting that neither the presence of stress, nor the absence of morphine, can alone account for the poor loading of stress-induced reinstatement onto the addiction factor. Further research using more complex models is needed to elaborate the factor-analytic structure of MSA. This could include evaluation of whether stress/cue-induced reinstatement,

cue-induced reinstatement, and Qo load onto a single, additional latent factor or are each associated with different sources of variance.

Utilizing different regularized FA methods with robust correlations in direct comparison with a traditional principal axis factoring method, we have demonstrated the feasibility of these statistical tools in analyzing sample sizes that are realistic targets for preclinical studies where traditional FA methods might fail. These methods help address some major statistical challenges in small sample size factor analyses such as Heywood cases, which was observed using the traditional factor extraction method (45, 46). Moreover, the regularization methods used in the current study have been shown to provide good recovery of underlying factor structures in simulation data, increasing confidence in the interpretation of our results (29, 30).

Though statistical methods such as regularization enable complex multivariate analyses of small sample sizes, there are inherent limitations of such analyses, such as sampling bias, that could not be fully addressed in this study. Future studies could include a larger preclinical sample for analyses where cross-validation is warranted, such as regularized factor analytic methods using least absolute shrinkage and selection operator (LASSO) penalization (28, 47). Additionally, with a larger preclinical sample, a higher count of observed variables could be included in the model, allowing for examination of more complex multi-factor models.

A further limitation of this study is that some rats had prior morphine and/or naloxone experience, and all rats underwent ICSS surgery and training. However, no significant difference was found on any SA measure between rats with morphine and/or naloxone experience compared to saline controls. Furthermore, despite their history of ICSS testing, rats from the current study showed similar acquisition and demand compared to rats from a previous study that did not have a history of ICSS testing (14, 16). The fixed order of assessment of the MSA outcomes also represents a potential limitation. While some measures (e.g., acquisition) inevitably precede others in a SA model, when possible future studies should counterbalance the phases (e.g., stress-induced and morphine-induced reinstatement) to control for any potential order effects.

Notwithstanding these limitations, the current study represents a first step in using robust FA to understand the factor structure of opioid SA. As such, our study identifies a single factor that contributes to four common opioid SA measures, revealing the common and unique information each of the measures could contribute to preclinical addiction literature. Elasticity

of demand most reliably represents the common “addiction” factor. Therefore, future studies examining individual differences in opioid SA may be rendered most informative by selectively examining this variable. More generally, exploring relationships beyond prevailing bivariate correlations in preclinical behavioral studies may further our understanding of addiction vulnerability and its neurobiological basis and lead to better prevention and treatment.

## DATA AVAILABILITY STATEMENT

The original contributions presented in the study are included in the article/**Supplementary Material**, further inquiries can be directed to the corresponding author.

## ETHICS STATEMENT

The animal study was reviewed and approved by Institutional Animal Care and Use Committee (IACUC), Hennepin Health Research Institute.

## AUTHOR CONTRIBUTIONS

YS contributed to experimental design, conducted behavioral studies on which these findings are based, conducted statistical analyses, and contributed to writing and revision of the manuscript. NW conducted statistical analyses and contributed to revision of the manuscript. JG and AH contributed to experimental design and writing and revision of the manuscript. All authors contributed to the article and approved the submitted version.

## FUNDING

Supported by NIH/NIDA grant R21 DA037728 (JG and AH), NIDA U01 DA051993 (JG and AH), the Hennepin Healthcare Research Institute (formerly Minneapolis Medical Research Foundation) Translational Addiction Research Program (AH), Hennepin Healthcare Research Institute Career Development Award (AH), and NIDA training grant T32 DA007097 (YS).

## SUPPLEMENTARY MATERIAL

The Supplementary Material for this article can be found online at: <https://www.frontiersin.org/articles/10.3389/fpsy.2021.712163/full#supplementary-material>

## REFERENCES

- Quinn RK, James MH, Hawkins GE, Brown AL, Heathcote A, Smith DW, et al. Temporally specific miRNA expression patterns in the dorsal and ventral striatum of addiction-prone rats. *Addict Biol.* (2018) 23:631–42. doi: 10.1111/adb.12520
- McDonald RP, Mulaik SA. Determinacy of common factors: a nontechnical review. *Psychol Bull.* (1979) 86:297–306.
- Gillespie NA, Neale MC, Prescott CA, Aggen SH, Kendler KS. Factor and item-response analysis DSM-IV criteria for abuse of and dependence on cannabis, cocaine, hallucinogens, sedatives, stimulants and opioids. *Addiction.* (2007) 102:920–30. doi: 10.1111/j.1360-0443.2007.01804.x
- Neale MC, Kendler KS. Models of comorbidity for multifactorial disorders. *Am J Human Genet.* (1995) 57:935.
- Krueger RF, Hicks BM, Patrick CJ, Carlson SR, Iacono WG, McGue M. Etiologic connections among substance dependence, antisocial

- behavior, and personality: modeling the externalizing spectrum. *J of Abnormal Psych.* (2002) 111:411–24. doi: 10.1037/0021-843X.111.3.411
6. Tsuang MT, Lyons MJ, Meyer JM, Doyle T, Eisen SA, Goldberg J, et al. Co-occurrence of abuse of different drugs in men: the role of drug-specific and shared vulnerabilities. *Arch General Psychiatr.* (1998) 55:967–72. doi: 10.1001/archpsyc.55.11.967
  7. Luczak SE, Glatt SJ, Wall TL. Meta-analyses of ALDH2 and ADH1B with alcohol dependence in Asians. In: Marlatt GA, and K. Witkiewitz, editors. *Addictive Behaviors: New Readings on Etiology, Prevention, Treatment*. Washington, DC: American Psychological Association (2009). p. 677–712.
  8. Goldberger LR, Velicer WF. Principles of exploratory factor analysis. *Diff. Normal Abnormal Personal.* (2006) 2:209–337.
  9. Hicks BM, Schalet BD, Malone SM, Iacono WG, McGue M. Psychometric and genetic architecture of substance use disorder and behavioral disinhibition measures for gene association studies. *Behavior Genet.* (2011) 41:459–75. doi: 10.1007/s10519-010-9417-2
  10. Palmer RH, Brick L, Nugent NR, Bidwell LC, McGeary JE, Knopik VS, et al. Examining the role of common genetic variants on alcohol, tobacco, cannabis and illicit drug dependence: genetics of vulnerability to drug dependence. *Addiction.* (2015) 110:530–7. doi: 10.1111/add.12815
  11. Swain Y, Gewirtz JC, Harris AC. Behavioral predictors of individual differences in opioid addiction vulnerability as measured using i.v. self-administration in rats. *Drug Alcohol Depend.* (2021) 221:108561. doi: 10.1016/j.drugalcdep.2021.108561
  12. Deroche-Gamonet V, Belin D, Piazza PV. Evidence for addiction-like behavior in the rat. *Science.* (2004) 305:1014–7. doi: 10.1126/science.1099020
  13. Center for Behavioral Health Statistics Quality. *Results From the 2019 National Survey on Drug Use and Health: Detailed Tables*. Substance Abuse and Mental Health Services Administration, Rockville, MD (2020).
  14. Swain Y, Muelken P, Skansberg A, Lanzdorf D, Haave Z, LeSage MG, et al. Higher anhedonia during withdrawal from initial opioid exposure is protective against subsequent opioid self-administration in rats. *Psychopharmacology.* (2020) 237:2279–91. doi: 10.1007/s00213-020-05532-w
  15. Belin D, Mar AC, Dalley JW, Robbins TW, Everitt BJ. High impulsivity predicts the switch to compulsive cocaine-taking. *Science.* (2008) 320:1352–5. doi: 10.1126/science.1158136
  16. Swain Y, Muelken P, LeSage MG, Gewirtz JC, Harris AC. Locomotor activity does not predict individual differences in morphine self-administration in rats. *Pharmacol Biochem Behav.* (2018) 166:48–56. doi: 10.1016/j.pbb.2018.01.008
  17. Banna KM, Back SE, Do P, See RE. Yohimbine stress potentiates conditioned cue-induced reinstatement of heroin-seeking in rats. *Behav Brain Res.* (2010) 208:144–8. doi: 10.1016/j.bbr.2009.11.030
  18. Sinha R. How does stress increase risk of drug abuse and relapse? *Psychopharmacology.* (2001) 158:343–59. doi: 10.1007/s002130100917
  19. Blanco C, Rafful C, Wall MM, Jin CJ, Kerridge B, Schwartz RP. The latent structure and predictors of non-medical prescription drug use and prescription drug use disorders: a national study. *Drug Alcohol Depend.* (2013) 133:473–9. doi: 10.1016/j.drugalcdep.2013.07.011
  20. Lennox R, Dennis ML, Scott CK, Funk R. Combining psychometric and biometric measures of substance use. *Drug Alcohol Depend.* (2006) 83:95–103. doi: 10.1016/j.drugalcdep.2005.10.016
  21. Lynskey MT, Agrawal A. *Psychometric Properties of DSM Assessments of Illicit Drug Abuse and Dependence: Results From the National Epidemiologic Survey on Alcohol and Related Conditions (NESARC)* (2007).
  22. de Winter JC, Dodou D. Factor recovery by principal axis factoring and maximum likelihood factor analysis as a function of factor pattern and sample size. *J Appl Statist.* (2012) 39:695–710. doi: 10.1080/02664763.2011.610445
  23. Cattell RB. *The Scientific Use of Factor Analysis*. New York, NY: Plenum (1978).
  24. Gorsuch RL. *Factor Analysis, 2nd Edn.* Hillsdale, NJ: Erlbaum (1983).
  25. Guilford JP. *Psychometric Methods, 2nd Edn.* New York, NY: McGraw-Hill (1954).
  26. Kline P. *Psychometrics and Psychology*. London: Academic Press (1979).
  27. Cooperman AW, Waller NG. *Heywood You Go Away!* Examining causes, effects, and treatments for Heywood cases in exploratory factor analysis. In press (2021).
  28. Jacobucci R, Grimm KJ, McArdle JJ. Regularized structural equation modeling. *Structural Equation Model.* (2016) 23:555–66. doi: 10.1080/10705511.2016.1154793
  29. Jung S, Lee S. Exploratory factor analysis for small samples. *Behav Res Methods.* (2011) 43:701–9. doi: 10.3758/s13428-011-0077-9
  30. Jung S, Takane Y. Regularized common factor analysis. In: Shigemasa K, editor. *New Trends in Psychometrics*. Tokyo: Universal Academy Press (2008). p. 141–9.
  31. Rousseeuw PJ, Driessen KV. A fast algorithm for the minimum covariance determinant estimator. *Technometrics.* (1999) 41:212–23.
  32. Cipitelli A, Karlsson C, Shaw JL, Thorsell A, Gehlert DR, Heilig M. Suppression of alcohol self-administration and reinstatement of alcohol seeking by melanin-concentrating hormone receptor 1 (MCH1-R) antagonism in Wistar rats. *Psychopharmacology.* (2010) 211:367–75. doi: 10.1007/s00213-010-1891-y
  33. Le AD, Harding S, Juzysch W, Funk D, Shaham Y. Role of alpha-2 adrenoceptors in stress-induced reinstatement of alcohol seeking and alcohol self-administration in rats. *Psychopharmacology.* (2005) 179:366–73. doi: 10.1007/s00213-004-2036-y
  34. Tran-Nguyen LT, Fuchs RA, Coffey GP, Baker DA, O'Dell LE, Neisewander JL. Time-dependent changes in cocaine-seeking behavior and extracellular dopamine levels in the amygdala during cocaine withdrawal. *Neuropsychopharmacology.* (1998) 19:48–59. doi: 10.1016/S0893-133X(97)00205-4
  35. R Core Team. *R: A Language and Environment for Statistical Computing*. R Foundation for (2021).
  36. Venables WN, Ripley BD. *Modern Applied Statistics With 4th Edon*. Springer, NYL (2002). Available online at: <https://www.stats.ox.ac.uk/pub/MASS4/>
  37. Waller NG. *fungible: Psychometric Functions from the Waller Lab. version 1.95.4.8* (2020).
  38. Beauducel A, Herzberg PY. On the performance of maximum likelihood versus means and variance adjusted weighted least squares estimation in CFA. *Struct Equation Model.* (2006) 13:186–203. doi: 10.1207/s15328007sem1302\_2
  39. Maydeu-Olivares A, Shi D, Rosseel Y. Assessing fit in structural equation models: a monte carlo evaluation of RMSEA versus SRMR confidence intervals and tests of close fit. *Struct Equation Model.* (2018) 25:389–402. doi: 10.1080/10705511.2017.1389611
  40. Efron B, Tibshirani RJ. *An Introduction to the Bootstrap (Chapman and Hall/CRC Monographs on Statistics and Applied Probability)*. New York, NY: Chapman and Hall/CRC (1994).
  41. Fragale JE, Pantazis CB, James MH, Aston-Jones G. The role of orexin-1 receptor signaling in demand for the opioid fentanyl. *Neuropsychopharmacology.* (2019) 44:1690–7. doi: 10.1038/s41386-019-0420-x
  42. Mohammadkhani A, Fragale JE, Pantazis CB, Bowrey HE, James MH, Aston-Jones G. Orexin-1 receptor signaling in ventral pallidum regulates motivation for the opioid remifentanyl. *J Neurosci.* (2019) 39:9831–40. doi: 10.1523/JNEUROSCI.0255-19.2019
  43. Worley MJ, Shoptaw SJ, Bickel WK, Ling W. Using behavioral economics to predict opioid use during prescription opioid dependence treatment. *Drug Alcohol Depend.* (2015) 148:62–8. doi: 10.1016/j.drugalcdep.2014.12.018
  44. Reiner DJ, Fredriksson I, Lofaro OM, Bossert JM, Shaham Y. Relapse to opioid seeking in rat models: behavior, pharmacology and circuits. *Neuropsychopharmacology.* (2019) 44:465–77. doi: 10.1038/s41386-018-0234-2
  45. Heywood HB. On finite sequences of real numbers. *Proc R Soc London.* (1931) 134:486–501.
  46. Kolenikov S, Bollen KA. Testing negative error variances: is a Heywood case a symptom of misspecification? *Sociol Methods Res.* (2012) 41:124–67. doi: 10.1177/0049124112442138

47. Tibshirani R. Regression shrinkage and selection via the lasso. *J R Statist Soc.* (1996) 58:267–88. doi: 10.1111/j.2517-6161.1996.tb02080.x

**Conflict of Interest:** The authors declare that the research was conducted in the absence of any commercial or financial relationships that could be construed as a potential conflict of interest.

**Publisher's Note:** All claims expressed in this article are solely those of the authors and do not necessarily represent those of their affiliated organizations, or those of

the publisher, the editors and the reviewers. Any product that may be evaluated in this article, or claim that may be made by its manufacturer, is not guaranteed or endorsed by the publisher.

Copyright © 2021 Swain, Waller, Gewirtz and Harris. This is an open-access article distributed under the terms of the Creative Commons Attribution License (CC BY). The use, distribution or reproduction in other forums is permitted, provided the original author(s) and the copyright owner(s) are credited and that the original publication in this journal is cited, in accordance with accepted academic practice. No use, distribution or reproduction is permitted which does not comply with these terms.



# On the Use of Heterogeneous Stock Mice to Map Transcriptomes Associated With Excessive Ethanol Consumption

Robert Hitzemann<sup>1</sup>, Denesa R. Lockwood<sup>1\*</sup>, Angela R. Ozburn<sup>1,2</sup> and Tamara J. Phillips<sup>1,2</sup>

<sup>1</sup> Department of Behavioral Neuroscience and Portland Alcohol Research Center, Oregon Health & Science University, Portland, OR, United States, <sup>2</sup> Veterans Affairs Portland Health Care System, Portland, OR, United States

We and many others have noted the advantages of using heterogeneous (HS) animals to map genes and gene networks associated with both behavioral and non-behavioral phenotypes. Importantly, genetically complex *Mus musculus* crosses provide substantially increased resolution to examine old and new relationships between gene expression and behavior. Here we report on data obtained from two HS populations: the HS/NPT derived from eight inbred laboratory mouse strains and the HS-CC derived from the eight collaborative cross inbred mouse strains that includes three wild-derived strains. Our work has focused on the genes and gene networks associated with risk for excessive ethanol consumption, individual variation in ethanol consumption and the consequences, including escalation, of long-term ethanol consumption. Background data on the development of HS mice is provided, including advantages for the detection of expression quantitative trait loci. Examples are also provided of using HS animals to probe the genes associated with ethanol preference and binge ethanol consumption.

**Keywords:** RNA-Seq—RNA sequencing, alcohol use disorder (AUD), genetic variability, gene networks, excessive ethanol consumption

## OPEN ACCESS

### Edited by:

Peter Kalivas,  
Medical University of South Carolina,  
United States

### Reviewed by:

Mark J. Ferris,  
Wake Forest School of Medicine,  
United States  
Anushree N. Karkhanis,  
Binghamton University, United States

### \*Correspondence:

Denesa R. Lockwood  
denesaruth@gmail.com

### Specialty section:

This article was submitted to  
Addictive Disorders,  
a section of the journal  
Frontiers in Psychiatry

**Received:** 15 June 2021

**Accepted:** 30 August 2021

**Published:** 12 October 2021

### Citation:

Hitzemann R, Lockwood DR,  
Ozburn AR and Phillips TJ (2021) On  
the Use of Heterogeneous Stock Mice  
to Map Transcriptomes Associated  
With Excessive Ethanol Consumption.  
Front. Psychiatry 12:725819.  
doi: 10.3389/fpsy.2021.725819

## INTRODUCTION TO HS MICE

McClearn and Rodgers (1) observed that among five inbred mouse strains there was a marked difference in ethanol preference (2-bottle choice, water vs. 10% ethanol). Of the strains tested, the C57BL/6 (B6) showed the highest preference. This experiment, with numerous variations, has been repeated hundreds of times [e.g., (2)] with the B6 strain consistently showing a high preference. Further, the B6 strain shows the highest binge ethanol consumption when tested in the Drinking-In the-Dark (DID) model (3). These data have cast a long shadow on ethanol research resulting in the almost exclusive use of the B6 strain to test for mechanisms of ethanol action and for new therapeutic treatments. This monoculture focus has some obvious advantages including replicability across laboratories and the ability to use genetically modified mice, which are almost exclusively on a B6 or largely B6 background, for hypothesis testing. These and related advantages are substantial. However, the major disadvantage of using the B6 strain or even B6 diallel crosses (e.g., B6 × DBA/2 [D2]) is that the biology extracted may not be generally applicable. Thus, important pathways are missed due to the lack of genetic diversity and further, individual variation, a key component of some analyses, will be substantially reduced. One solution to these problems is the use of outbred mice and heterogeneous stocks (HS) [see e.g., (4, 5)].

The first widely used mouse HS appears to be the HS/Ibg, described by McClearn et al. (6). This HS was a cross of 8 laboratory mouse strains; the cross was begun at Berkeley before the mice were transferred to the Institute for Behavioral Genetics (Boulder), hence the Ibg designation. For an 8-way cross there are >40,000 possible breeding funnels. Rather than dealing with this issue, the colony was formed balancing for the Y chromosome from each of the founder strains. The colony was maintained at ~40 families. These mice served as the founders for a number of alcohol-related selected lines including the Long Sleep/Short Sleep, Withdrawal Sensitive Prone(WSP)/Withdrawal Sensitive Resistant (WSR), the FAST/SLOW and the High Alcohol Preference/Low Alcohol Preference lines (7–10). Here, we briefly focus on the replicate WSP/WSR selected lines; the lines were selectively bred for withdrawal severity after cessation of 3 days of ethanol vapor exposure. Crabbe et al. (11) discussed the consilience of the mouse genetic models with human genetics in some detail. It was concluded that the overlap was greatest for tolerance and withdrawal and that for both mice and humans, these phenotypes had independent genetic risk. From the perspective of alcohol use disorder, the question naturally arises as to whether the WSP and WSR lines differ in ethanol consumption. Previous studies in animals with a B6xD2 genotype [see details in Metten et al. (12)] suggested a strong negative genetic relationship between withdrawal and consumption, although there are exceptions (13). In the WSP/WSR lines derived from HS founders, the situation appears more complex. Crabbe et al. (13) found, as predicted, the WSR-2 line had significantly higher preference than the WSP-2 line, but the opposite line difference was found for the WSP-1 and WSR-1 lines. Regarding drinking in the dark (DID), a model of binge consumption (see below), both WSP lines consumed more ethanol and had higher BECs than the WSR lines; thus, greater genetically-determined withdrawal severity predicted higher ethanol consumption, opposite to previous findings (12). Turning things around, the High DID-1 and –2 selected lines (selectively bred from HS/NPT founders—see below) do not differ in withdrawal severity after cessation of vapor inhalation. There are many interpretations of these data. However, we simply wish to make the point that lessons learned from simple crosses may not apply to HS and vice-versa.

In 1991, Gerry McClearn suggested to one of us (RH) that there was a need for a new HS. Two of the HS/Ibg founder strains (Is/Bi and RIII were no longer available for testing) and random genetic drift over the >25 years of breeding was likely to have significantly distorted allele frequencies. Our interest at the time was not in ethanol-related behaviors, but rather in haloperidol-induced catalepsy [see e.g., (14)] and in developing haloperidol response selected lines. The 6 HS/Ibg founders available for testing were skewed to very haloperidol responsive strains. Two non-responsive strains (CBA/J and LP/J) were chosen to fill out the 8 founders for developing a new HS. However, it should be noted that the 8 strains included 2 representatives each from 4 different phylogenetic clades [see Figure 1b in (3)]. The new HS was formed by pseudo-random breeding at the Northport VA, hence the NPT designation. The first report on the HS/NPT is found in Hitzemann et al. (15). For more than 25 years, the HS/NPT have been maintained as 48 families using a circle

breeding design. HS/NPT were first used in ethanol research to fine map a QTL for ethanol-induced locomotor activation on chromosome 2 (16).

Breeding pairs from each of the 48 HS/NPT families were shipped in 2000 to Jonathan Flint (Oxford, U.K). Over the next several years >2,400 animals were phenotyped for a variety of physiological and behavioral traits (17). Valdar et al. (18) examined the genetic and environmental effects on 88 of these traits and mapped the QTLs for 97 traits to a reasonably high resolution (19). Huang et al. (20) mapped eQTLs in a subset of the tested animals; data were obtained for the hippocampus, liver and lung. Although these authors noted a large number of hybridization artifacts for detecting eQTLs, the data obtained remain an important feature in evaluating HS/NPT data. Of equal importance, the 8 HS/NPT founders were among the 17 strains initially sequenced as part of the Mouse Genomes Project (21).

Twenty years ago, members of the Complex Trait Consortium (CTC), later renamed the Complex Trait Community, began a series of meetings to develop the Collaborative Cross [CC] (22). The CC was proposed as a large panel of recombinant inbred (RI) strains derived from a genetically diverse HS. The initial plans were to develop more than 1,000 RI strains. Much of the early CC planning sessions focused on determining the 8 strains that would be crossed to form the HS founders. How the final 8 strains were chosen could easily be the subject of another review. There was however, general agreement that three wild-derived strains (WSB/EiJ, CAST/EiJ, and PWK/PhJ) would be included, which in turn would boost the overall HS genetic diversity to more than 90% of what is available in *Mus musculus* [see (23)]. In 2005, we began crossing the 8 CC founder strains. Thirty-two unique breeding funnels were used and each funnel was bred in duplicate [see (24) for breeding details]. Of the 64 breeding funnels, 3 produced no offspring, but each was unique. The 32 families were expanded to 48 and have been bred continuously since 2007 using a circle breeding design. This HS was designated the HS-CC (25).

The Diversity Outbred HS were formed by crossing 144 of the partially inbred CC lines [see (26) for breeding details]. The DO colony is maintained as a panel of ~175 breeding pairs; all matings are randomized with avoidance of sibling matings. The HS-CC and DO were compared in (27). Of particular note, a meiotic drive locus on chromosome 2 has been eliminated from the DO but not the HS-CC. However, this difference does not appear to have affected the high ethanol preference found in both the HS-CC and DO. Given the larger DO breeding population, genetic drift in the DO compared to the HS-CC will be slower. Compared to the HS/NPT, ethanol preference in the HS-CC and DO is 3–4 times higher. The reason for the higher preference in both populations would appear to be at least partially associated with the fact that in addition to the B6 strain, the PWK/PhJ founder strain also has a high ethanol preference (28).

## TRANSCRIPTOMICS IN HS POPULATIONS

Sandberg et al. (29) were the first to detect differences in genome-wide brain gene expression between 2 inbred mouse strains (B6 and 129S6/SvEvTac). Several differentially expressed (DE) genes aligned with known behavioral quantitative trait loci

(bQTLs). For example, *Kcnj9* was DE and is located on distal chromosome 1 in a region where bQTLs had been identified for locomotor activity, alcohol and pentobarbital withdrawal, open-field emotionality, and certain aspects of fear-conditioned behavior. This study was unable to determine whether or not the elements regulating *Kcnj9* expression were located within the bQTL intervals and/or near the gene locus. However, it is possible to make such links by combining gene expression and genotype data. Jansen and Nap (30) termed this approach “genetical genomics.” This approach was quickly adopted to examine gene expression in *Arabidopsis*, *Drosophila*, yeast, and the mouse [see (31) and references therein]. The expression QTLs (eQTLs) can be classified as either *cis* (mapping near the gene locus) or *trans* (mapping elsewhere in the genome) (32). When bQTLs and *cis*-eQTLs overlap, the *cis*-eQTL genes are inferred as causal genes [see e.g., (32)].

This general strategy from the perspective of HS populations has evolved in several important ways. First and beginning with Talbot et al. (33), mapping QTLs, including eQTLs in advanced HS populations has become relatively straightforward. QTL intervals of 1–2 Mbp can be routinely obtained and a haplotype signature for each QTL can be extracted. Behavioral and gene expression data are generally available for the founder strains, which facilitates the mapping process. Rather than using relatively expensive microarrays, very cost effective genotype information can now be obtained by low density genome-wide sequencing, which builds upon the detailed founder strain sequence information. Second, mouse microarrays used probes based on B6 sequence. Because of hybridization errors, this was problematic even for di-allele crosses and resulted in false positive eQTLs [see e.g., (34)]. For HS populations, the hybridization artifacts increase dramatically. RNA-Seq essentially solved this problem. However, RNA-Seq has its own set of problems and biases, which have been detailed elsewhere [e.g., (4, 35)]. Importantly for expression analysis in HS populations, alignment errors can occur. Although most RNA-Seq experiments use polyA+ RNA libraries, ribosome depleted RNA libraries can be used to also look at the expression of non-coding RNAs. Third, regardless of whether one uses microarrays or RNA-Seq for genome-wide studies, one is making thousands of comparisons. The number of independent comparisons is fewer than the number of genes detected since gene expression can be collapsed into modules with similar expression patterns. Perhaps the most widely used algorithm to detect these modules is the Weighted Gene Co-expression Network Analysis (WGCNA) (36), although there are many others. In the WGCNA, the general procedure is to extract the module eigengene (first principal component) and determine how well the eigengene aligns with the phenotype of interest. Since the number of modules formed is generally relatively small (e.g., 30–40), the multiple comparison penalty is greatly reduced. This approach is relevant to HS animals for at least two reasons. One, given that RNA-Seq is the preferred technology to analyze gene expression in HS populations, it should be noted that because of the difference in variance structure (compared to microarray data), RNA-Seq datasets have an advantage when constructing co-expression networks (37). Two, the expression variances in HS animals are higher than

those found for diallel crosses of laboratory mouse strains (37). Although it may seem superficially counter-intuitive, increased variance will, up to a point, improve co-expression detection. Finally we note that the network based approaches allow one to differentiate hub and leaf nodes. Module hub nodes are generally defined as those in the top 10–20 percent of module connectivity, while the leaf nodes are those that collectively contribute the bottom 10 percent of connectivity.

Although not explicitly stated in the argument for developing the CC (22), one could imagine that by including the 3 wild-derived strains, splicing complexity would greatly increase. Related arguments could be used for developing any HS population. Zheng et al. (38) examined the splicing issue with paired-end sequencing (>160,000,000 reads/strain) of the ventral striatum in the 8 CC founder strains. Mapped junctions were >360,000 for all strains; but only 50% of these junctions were annotated. Strain specific splicing (SSS) events were those detected in only one strain. Sixty-four thousand strain-specific junctions were identified when all junctions were considered; however, for junctions with  $\geq 3$  or  $\geq 10$  read coverage, the numbers dropped to an average of  $\sim 3,000$  and 500, respectively. The wild-derived strains, CAST/EiJ and PWK/PhJ, were demonstrated to have the highest percentages of strain-specific junctions. Some of these junctions were confirmed using qPCR. From the perspective of genetic diversity and splicing, this study should be seen as a starting point. The read density would likely need to be an order of magnitude higher to reliably detect rare splice junctions and rare SSS events. Further, any survey would need to include multiple brain regions.

## HS4 MICE AND MULTIPLE-CROSS MAPPING

We briefly introduce here the HS4, a relatively short-lived HS population (2001–2011). The HS4 was formed by crossing the B6, D2, BALB/cJ, and LP/J strains. Breeding details for the HS4 are found in Iancu et al. (24). It is important to note that a HS derived from only 4 strains can easily be completely balanced, while for an 8-way cross this is practically impossible (see above). A comparison of eQTL mapping in a B6xD2 F<sub>2</sub>, the HS4 and HS-CC is found in Iancu et al. (24). Two analysis methods were compared: HAPPY (39) and EMMA (40); the methods were also combined to produce joint method (JM). Single-marker (SM) QTL analysis tests for association between genotype at individual markers and the phenotype of interest here, gene expression. EMMA implements a variant of SM analysis. One essential feature of EMMA is to efficiently control for sample relatedness. HAPPY integrates information from several markers, and estimates the probability of descent from each of the founder strains and evaluates if there are significant phenotype differences between alleles inherited from the different progenitor strains. Perhaps the key observation from these analyses was the superior performance of the HS4 for detecting both *cis* and *trans* effects on gene expression when compared to the F<sub>2</sub> and HS-CC. The superior performance was true regardless of the method used.

The HS4 were part of a project we and others termed multiple cross mapping (MCM). A summary of this project is found in Hitzemann et al. (41). Our interest in MCM was triggered by the observation that an open-field activity QTL was independently detected in three different mouse F<sub>2</sub> intercrosses (B6xD2; B6xA; B6xBALB/c) (42–44); however, the QTL was not detected in D2xBALB/c or D2xLP crosses (45). We proposed that the information detected from multiple crosses could be used to sort microsatellite or SNP markers in order to detect chromosomal regions with the highest probability of containing QTLs. Empirically, the data described above suggested that there must be a region or regions on chromosome 1 where three strains (i.e., D2, BALB/c and A strains) are identical and different from the B6. Given that it was not possible to easily sequence the region(s) of interest, MCM appeared to be a reasonable approach. The down-side of MCM was that each cross required several hundred animals to be phenotyped and genotyped, whereas mapping in a HS would require fewer animals and provide greater precision [see Figure 15 in (41)]. With the advent of sequence data for the inbred mouse strains (21) and improvements in genotyping technology, including reduced costs, the MCM approach was no longer appropriate or necessary.

## HIGH DRINKING IN THE DARK (HDID) SELECTED LINES

Rhodes et al. (46) introduced the Drinking-In-the Dark (DID) procedure as a simple model of ethanol drinking to intoxicating blood ethanol concentrations (BECs). B6 mice regularly drank to BECs >1 mg/ml. Subsequently (3), DID was examined in a panel of inbred strains that included the 8 HS/NPT founders. The highest BECs (4 h DID trial) were obtained in the B6 and BALB/c strains, with males having somewhat higher BECs than females, even though females consumed higher amounts of ethanol. For all strains, the relationship between consumption and BECs was at best complex. Crabbe et al. (47) reported on the selection of the HDID-1 line; HS/NPT mice were the founders. The selection phenotype was the BEC at the end of a 4 h DID trial from the ingestion of a 20% ethanol solution. After 11 generations of selection, the BEC increased from 0.30 to 1.07 mg/ml. A replicate HDID selection (HDID-2) followed the HDID-1 selection. The lines were separated by 7 generations of breeding, but the selection response was largely identical [see Figure 3 in (48)]. Interestingly, the microstructure of drinking in the HDID-1 and -2 lines is different. HDID-1 mice drink in larger ethanol bouts than the HS founders, whereas HDID-2 mice drink in more frequent bouts (49). The observation that the two HDID lines appear superficially phenotypically similar but do show important differences is not unique to these replicate lines [see e.g., (50)]. In general, this should not be unexpected for a complex trait where no genes have a very large effect and where different allelic combinations can lead to a largely similar phenotype.

An issue we have indirectly addressed over the past few years is whether the transcriptional profiles associated with DID

and ethanol preference overlap. Related to this issue, when compared across panels of inbred strains, DID and 2-bottle choice preference consumption appear to show some genetic overlap (3). Crabbe et al. (51) examined this issue in greater detail by looking at preference consumption in HDID-1 and the founder HS/NPT mice. The conclusion reached was similar; preference and DID consumption showed some genetic overlap, but this depended on the assay being used.

## HDID SELECTED LINES AND GENE EXPRESSION

Iancu et al. (52) used the Illumina Mouse 8.2 array to examine gene expression in HDID-1, HDID-2, and HS/NPT mice ( $N = 48/\text{group}$  balanced for sex). An early version of the Mouse Universal Genotyping Array (MUGA) was used for genotyping; the MUGA contained 7,851 SNP markers, with an average spacing of  $325 \pm 191$  kb. After elimination of non-polymorphic or low frequency (below 2.5%) SNPs, the data contained 3,683 markers further analyzed using a marker by marker approach (53, 54). The genotype data extracted (Figure 1) illustrated two important points. One, compared to the HS/NPT founders, genetic variance was strikingly reduced in both of the selected lines, presumably the result of the inbreeding that occurs when using a relatively small number of families for selection. Two, the genotype data illustrated that the selected lines were genetically distinct. The QTL analysis confirmed this point. Five unique QTLs exceeding the adjusted LOD threshold of 10.6 were found in the HDID-1 line and three unique QTLs were found in the HDID-2 line. There were however, three common QTLs on chromosomes 4, 14, and 16, each of which were mapped to relatively good (<5 Mbp) resolution. Of relevance to subsequent discussions, the Chr 14 QTL contained only 1 gene, protocadherin 17; the haplotype signature of the QTL corresponds to the LP/J strain being different than the other 7 founder strains. The QTL on Chr 4 has a similar haplotype (LP/J different from other founders) and a similar position and haplotype to a startle response QTL reported previously (19).

The gene expression analyses reported in Iancu et al. (52) and especially the integration of the differential expression and network analyses, set a pattern that has been repeated in our subsequent studies. The DE genes are in general, poorly connected to the co-expression network; i.e., the DE genes are largely leaf nodes. This cannot be unexpected. Unless the change in expression is very large, to detect DE the variance must be low. In contrast, construction of the co-expression network depends on a robust but biologically relevant variance structure. There were marked differences between the HDID-1 vs. HS/NPT and HDID-2 vs. HS/NPT in terms of the number of DE (FDR < 0.1) transcripts (1,430 vs. 301). One hundred and four transcripts were differentially expressed in both comparisons; 94 of these had the same directionality. A majority of the DE transcripts (85 out of 94) were found among the gray-network module, which is reserved for the poorly connected transcripts. GO annotation

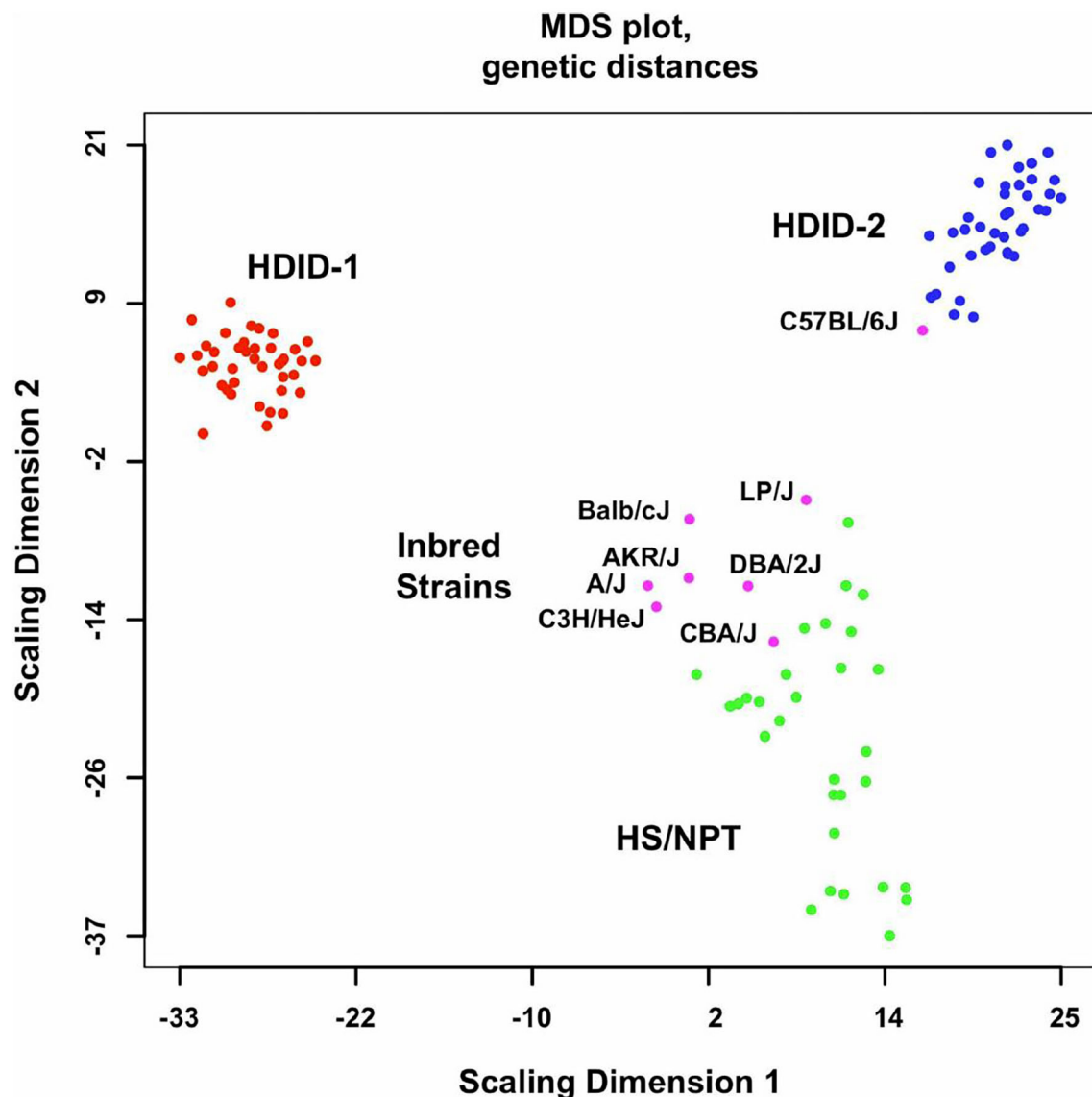


**FIGURE 1 |** Genome-wide genetic distances between the HDID-1 and -2 selected lines, HS/NPT animals and the inbred strains used to form the HS/NPT. Details of the animals used are found in the Methods in (52). Data are presented as a multidimensional scaling (MDS) plot. Note the greater dispersion in the HS/NPT animals when compared to the HDID-1 and HDID-2 selected lines and the differences between the two selected lines. Also note that among the inbred strains the C57BL/6J is distinct from the other 7 founders. Figure reprinted with permission from (52).

of the DE genes revealed significant enrichments in extracellular region part ( $p < 2 \times 10^{-3}$ ) and the extracellular matrix ( $p < 5 \times 10^{-3}$ ).

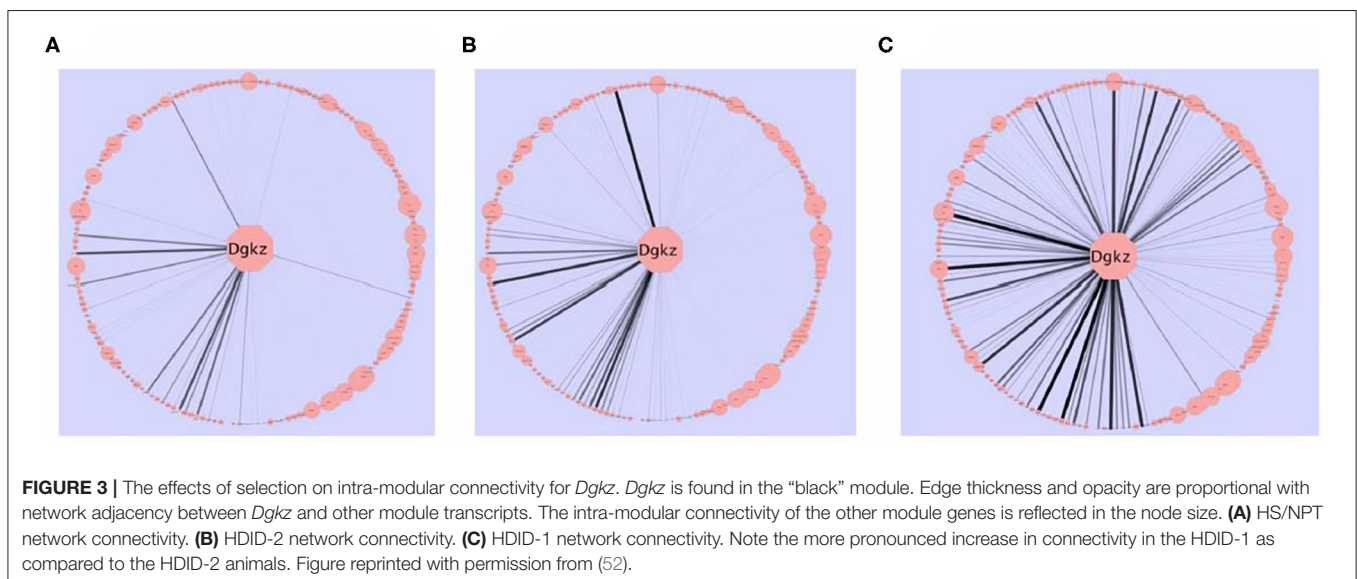
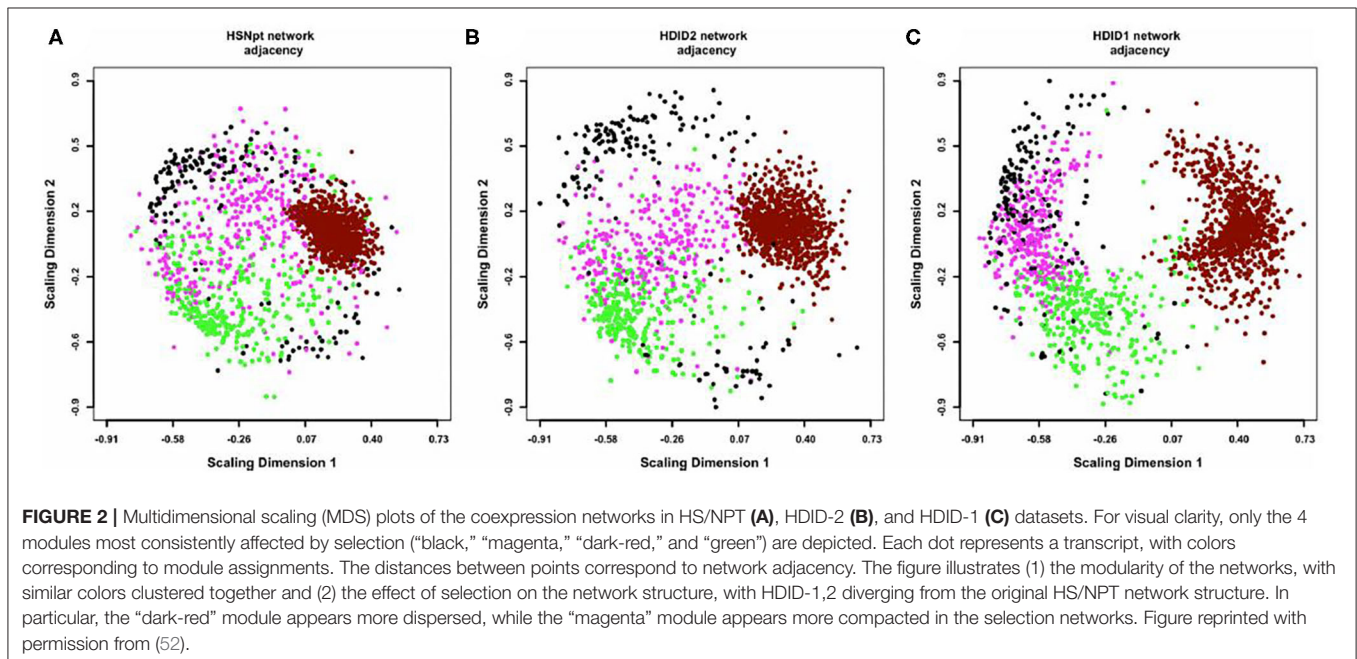
A consensus network approach (55) was used to evaluate the effects of selection on transcriptome organization. Based on previous empirical observations (25), we concluded that in order to form modules of very high quality, sample sizes of  $\sim >40$  are required [see Supplemental Table 2 in (52)]. With modules of high quality, module disruption is relatively easy to detect (module disruption may be either a significant increase or decrease in module connectivity). Separate networks were formed using the HS/NPT and each HDID

line's expression data; differences between these networks were evaluated against random changes. An empirical distribution of random changes was generated by constructing networks ( $N = 1,000$ ) using a mixture of samples from the HS/NPT and HDID animals. Bootstrapping and statistical significance assessment was performed over samples. Despite the genetic differences noted above, two of the co-expression modules (black and magenta [color has no meaning]) were similarly affected; i.e., the modules were significantly disrupted (see **Figure 2**). Both modules were highly enriched in neuronal genes (black module— $p < 3 \times 10^{-27}$ ; magenta module— $p < 3 \times 10^{-5}$ ). GO annotation of the black module revealed significant enrichments

in neurological system process ( $p < 5 \times 10^{-6}$ ), glutamate secretion ( $p < 7 \times 10^{-5}$ ), and neurotransmitter transport ( $p < 8 \times 10^{-5}$ ). GO annotation of the magenta module revealed significant enrichments in neuropeptide hormone activity ( $p < 2 \times 10^{-5}$ ), peptide receptor activity ( $p < 9 \times 10^{-5}$ ), and post-synaptic membrane ( $p < 2 \times 10^{-4}$ ). The progressive effects of selection on *Dgkz*, a gene found in the black module and known to be associated with glutamate neurotoxicity and brain trauma, are illustrated in **Figure 3**. Gene module connectivity was increased in the HDID-2 animals and further increased in the HDID-1. Examples of selected genes in the magenta module and significantly affected by selection are found in Table 1 in (52). We bring two points to the readers' attention. The first is that

both selections have affected a subgroup of GABA and glutamate related genes; this will be a familiar observation. The second point is the observation that selection affected the neuropeptide Y system. Manipulation of the neuropeptide Y system affects both DID and ethanol preference consumption [see (56) and references therein]. There is some evidence, at least for ethanol preference that these effects may be genotype-dependent (57).

Hoffman et al. (58) is the brain gene expression study focusing on ethanol preference that appears to be closest to Iancu et al. (52). Gene expression in HAP3 and LAP3 animals derived from HS/Ibg mice (59) were analyzed using Affymetrix microarrays. Although the analysis strategies were different, there appears to be no overlap of the DE genes detected in Iancu et al. (52).



Following on Iancu et al. (52), Iancu et al. (60) used RNA-Seq to compare the ventral striatal transcriptome of ethanol naïve HDID-2 mice and HS/NPT founders. Sample sizes were sufficient to analyze the male and female data separately. For females, the number of DE (FDR < 0.05) genes was 227; there was no significant GO enrichment for this grouping. For males, there were 1,525 DE genes, 836 and 689 genes were down- and up-regulated; 153 genes overlapped with the female grouping. Analysis of the down-regulated genes revealed significant enrichment in genes associated with extracellular matrix (ECM) organization and immune system process. No significant GO enrichment categories were detected for the up-regulated genes.

Beginning with Colville et al. (61) (see below), we introduced the differential variability (DV) metric into our analysis strategy [see (62–64)]. This computationally simple procedure identifies those genes that are likely to show a change in network connectivity. “For the DV metric, selection significantly (FDR < 0.05) increased the variability of 1,498 female genes and 766 male genes; 82 genes overlapped. Included in the overlapping subset were *Calb2*, *Gabrq*, *Nos1ap*, *Oxt*, *Pomc*, *Pvab*, *Slc6a11*, and *Trh*. For female genes with increased variance ( $N = 1,418$ ), there was significant enrichment in annotations that included extracellular space, plasma membrane part, signaling receptor activity, and extracellular matrix organization. For female genes with decreased variance ( $N = 80$ ), significant enrichment was detected for cytoskeleton of presynaptic active zone and axon part; genes involved included *Bsn*, *Pclo*, *Syn1*, *Myoc*, *Nav1*, *Tubb4a*, *Cplx2*, and *Ank3*. For male genes with increased variance ( $N = 663$ ), there were significant enrichments in GO categories that included modulation of synaptic transmission, voltage gated cation channel activity, plasma membrane part, and synapse part. Genes in the latter category included *Grin2a*, *Grin2b*, *Dlg4*, *Gabbr2*, *Grm2*, *Pdyn*, *Gabra1*, and *Camk2a*. For male genes with decreased variance ( $N = 103$ ), there were significant enrichments in GO categories associated with biological adhesion and extracellular part. From the perspective of the DV metric, which is closely aligned with network connectivity, the female and male data were largely mirror images” (64).

Additional analyses of this data set are found in Iancu et al. (60). However, the main observations are noted above. Two of these observations we wish to emphasize. The first is the involvement of neuroimmune systems, at least in males, in the DID phenotype. These data are consistent with the neuroimmune hypothesis of alcohol use disorder (AUD) (65). Sex differences in the alcohol-induced neuroimmune signaling are discussed elsewhere (64). The second point of emphasis are the data pointing to the involvement of the ECM. Alcohol and other drugs of abuse can have marked effects on ECM constituents [reviewed in (66–68)]. Ethanol has been shown to affect the brain expression of *tPA* (or *Plat*) (69, 70), *Mmp-9* (71), *Bcan* & *Ncan* (72), and *Tsp2* & *Tsp4* (73). Some data show that all elements of the brain ECM—the basement membrane, the interstitial ECM and the perineuronal nets—are affected by acute and/or chronic ethanol treatment (67). The evidence that changes in the brain ECM are associated with the *risk* for developing an AUD are less compelling. However, polymorphisms have been detected in

*Mmp-9m*, *Tnc* & *Tnr* in human alcoholics (74, 75). Genome-wide association studies (GWAS) have revealed a polymorphism in *Col6a3* associated with alcoholism (76). Our data illustrate that HDID risk is associated with ECM associated genes in both males and females.

A common observation in both basic science and clinical populations is that substantial individual variation is retained even in groups at high risk for excessive ethanol consumption. Interestingly, this individual variation is seen even within inbred mouse strains such as the B6 [see (77)]. We asked whether the genes associated with individual variation in HDID-1 mice are different from those associated with selection (risk) (78). Thirty-five HDID-1 mice (18 males and 17 females) phenotyped for their BECs at the end of a standard 4-day DID trial, were sacrificed 3 weeks later. RNA-Seq was used to analyze the striatal transcriptome. Pearson correlations were used to assess the relationships between gene expression and the BEC. Five hundred and fifty-seven genes (375 positive vs. 182 negative) met the criteria for inclusion in the gene set enrichment analysis. The most significant (FDR < 0.01) annotation enrichments were for the positively correlated genes [Table 2 in (78)]. Broadly, the enriched gene categories were associated with the regulation of synaptic function. Genes associated with the category included *Grik5*, *Syn1*, *Stxbp1*, *Stx1a*, *Rims4*, *Rims1*, and *Stx1b* *Camk2g*, *Chrm3*, *Crhbp*, *Gria3*, *Grin1*, *Strn4*, *Syngap1* and *Syt2*. These data generally differ from those reported by Mulligan et al. (77) for individual DID variation in B6 mice. Given the differences in experimental design, such differences cannot be unexpected. However, perhaps their most salient conclusion is consistent with our results. “One hypothesis that evolved from our modular network analysis is that striatal medium spiny neurons may react to acute alcohol consumption with transcriptional changes that may underlie subsequent changes in behavior, including alcohol preference, tolerance and dependence” (77).

## HS-CC AND ETHANOL PREFERENCE

HDID selection has only used HS/NPT founders. Thus, there is no way to actually know if a different and/or simpler founder cross would yield similar results. However, for ethanol preference, we do have data that gets very close to this issue (see below). For those unfamiliar with alcohol preference research, selection from B6xD2 intercross animals and/or data collected from BXD RI strains has yielded remarkably consistent preference results for almost 30 years [see e.g., (79–81)].

Colville et al. (82) examined the transcriptional changes across three brain regions associated with selection for ethanol preference (24h/7d, 10% ethanol vs. water) from HS-CC founders. The three brain regions examined were the nucleus accumbens shell, the prelimbic cortex, and the central nucleus of the amygdala (CeA). Sample sizes were moderate ( $N = \sim 30$ /region/line). The selection protocol was short-term, terminated after four generations of selection. In the “High” line, ethanol preference more than doubled to  $\sim 0.5$  whereas in the “Low” line preference was  $< 0.1$ . As expected [see (83)] there were a large number of transcriptional changes, unique to each

brain region. Here we focus on the changes that were common to all three regions [see Figure 3 in (82)]. *5730455P16Rik*, *Gdi2*, *Skiv2*, *Tsr1*, and *Glod4* were the only common DE genes. There were 30 common DV genes and this grouping was significantly enriched in genes associated with cell to cell signaling. Genes with this GO annotation included *Dlg2*, *Egr3*, *Gabbr2*, *Lnpep*, *Pcdhgb2*, *Pcdhac2*, *Sstr4*, and *Syt10*. The common DV genes were enriched in a common network module that differed in size across the three regions but shared common annotations. The three modules also shared 183 common genes. These common genes included several receptors; *Adra1a*, *Chrna7*, *Grin2b*, *Htr2a*, *Oprd1*, and *Sstr4*; 17 protocadherins including 14 of the 22 known protocadherins. Common hub nodes across regions included *Dlg2*, *Gatad2b*, *Pcdhac2*, *Tnks*, *Usp29*, and *Usp9x*.

**Figure 4** illustrates the coexpression and physical interaction partners for *Dlg2*. Key partners include a number of glutamate related genes: e.g., *Grin2b*, *Grid1*, *Dlg1*, *Dlg4*, and *Dlgap1*. These data extend the observations of Bell et al. (85) who noted when comparing ethanol naïve P and NP rats, there were a number of differences in glutamate signaling genes. Further, clinical studies

have shown that in family history positive (FHP) individuals there is an altered response to the NMDA antagonist ketamine (86, 87).

A statistic added in Colville et al. (82) was differential wiring (DW). DW was restricted to search for Pearson correlations between individual genes that differed by  $>0.5$ . This general procedure has been used to quantify network rewiring in both genomic (88) and neural imaging studies (89). We identified for each gene, the number of changed edges and then inquired as to whether some genes had a disproportionately high number of changed edges. For the latter, a binomial test was used to test for significance. There were 72 significant DW genes common to all three brain regions and this grouping included *Chrna7*, *Als2*, *Pppir9a*, *Strn*, *Kcna4*, *Kif1a*, and *Slc1a2*. *Slc1a2*, which encodes for the excitatory amino acid transporter 2 (EAAT2); the inhibition of EAAT2 has been reported to reduce ethanol consumption (90).

Keeping the Colville et al. (61, 82) data in perspective, we turn to Kozell et al. (81). Beginning with a B6xD2 F2 intercross founder population, these authors selectively bred for both high alcohol consumption and low acute withdrawal

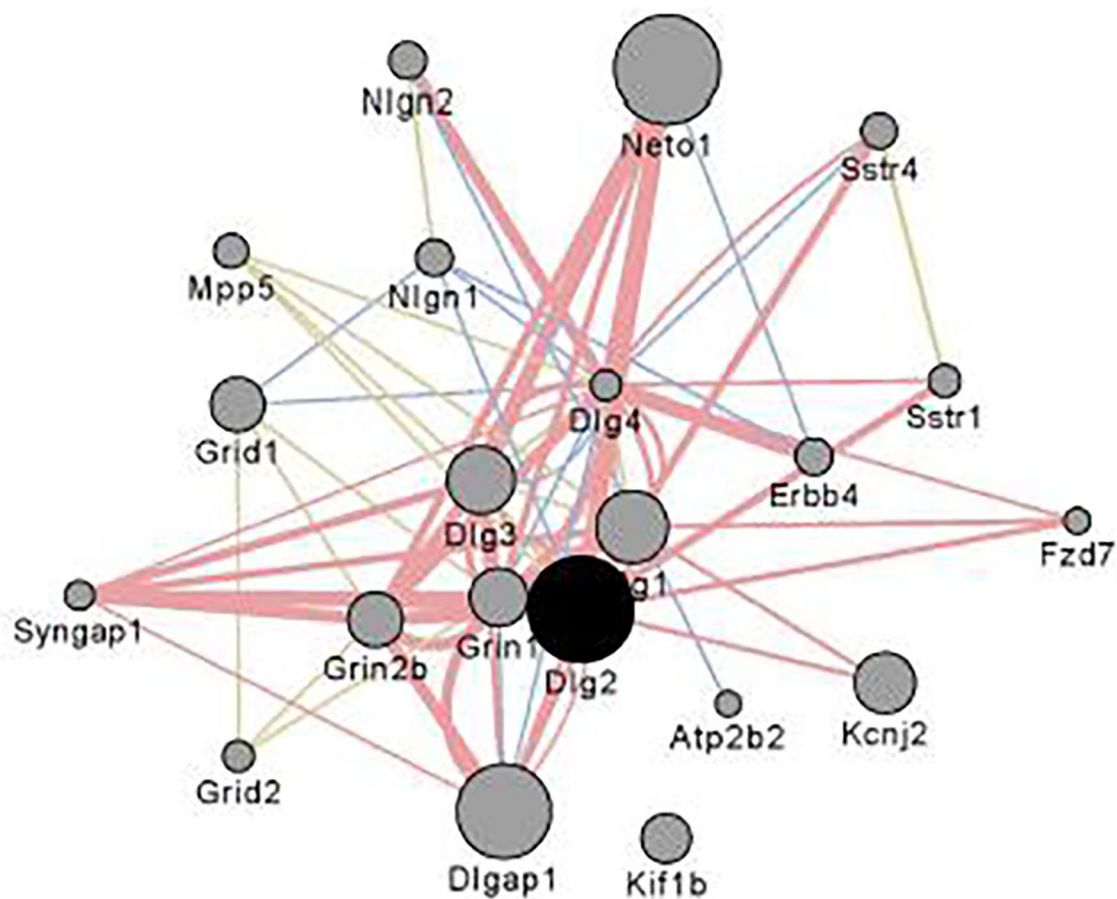


**FIGURE 4 |** Interaction partners for *Dlg2* extracted using Gene Mania (84) which was accessed as a Cytoscape plugin with default settings. Depicted are top 20 genes related to *Dlg2* through physical interactions, colocalizations, or sharing protein domains. *Dlg2* which encodes for PSD93, interacts with a number of genes and gene products associated with glutamate receptor activity including *Dlg4*, *Syngap1*, *Neto*, *Grin1*, *Grin2b*, *Dlgap1* & *Dlg3*. Figure reprinted with permission from (82).

(SOT line), or vice versa (NOT line). SOT is Old-English for habitual high alcohol user. Using randomly chosen fourth selected generation (S4) mice, RNA-Seq was employed to assess transcriptional differences in the ventral striatum between the SOT and NOT mice. Data were analyzed as described in Colville et al. (61, 82). For genes more highly expressed in the SOT line there was enrichment in genes associated with cell adhesion and post-synaptic membrane. The cell adhesion genes included 23 protocadherins, *Mpdz* & *Dlg2*. The post-synaptic membrane genes included *Gabrb3*, *Gphn*, *Grid1*, *Grin2b*, and *Grin2c* & *Grm3*. Thus, the SOT selection (81) and High preference line selection show overlapping transcriptional signatures. In contrast, the NOT line was enriched in genes with mitochondrial function.

The final study to be reviewed is Hitzemann et al. (68), which examined in HS-CC mice the effects of chronic (13 weeks) ethanol consumption [24h/7d 2-bottle choice] on CeA gene expression. Here we focus on the correlation of individual gene expression and week 13 ethanol preference. For females, the enriched annotations associated with cilium organization, extracellular region, and collagen-containing ECM. For males there were no significant annotation enrichments.

The majority (70%) of female genes correlated with preference were found in a single WGCNA network module. This module was enriched ( $p < 0.0001$ ) in genes with an astrocyte annotation and in annotations associated with the extracellular matrix and cilium. Among the female genes positively correlated with preference, 43 were top hub nodes. “Enrichr (91, 92) was used to search for key transcription factors among the top hub nodes. A key finding was that 19 of the top nodes were down-regulated in an orthodenticle homeobox 2 (*Otx2*) knockout mouse [GSE27630; (93)]. *Otx2* is often referred to as a master regulator, and known to have key roles in brain patterning and post-natal plasticity. *Otx2* is further required for generation of various neuronal subpopulations, including ocular motor and midbrain dopaminergic neurons (94, 95), and development and maintenance of perineuronal nets. In the adult brain, *Otx2* expression is largely localized to the choroid plexus (96). The OTX2 protein is captured by the perineuronal nets and accumulated in parvalbumin type GABA-ergic neurons throughout the brain (97). Our data indicate a low, but detectable expression of *Otx2* in the CeA, affected by ethanol exposure and predicted to have a role in the escalation of ethanol preference seen in HS-CC females, but not males, and in the observed sex differences in the transcriptional response” (68). Of related interest, Coles and Lasek (98) found that DID increased *Otx2* expression in the VTA; however, viral mediated down-regulation of *Otx2* did not affect ethanol consumption.

## DISCUSSION

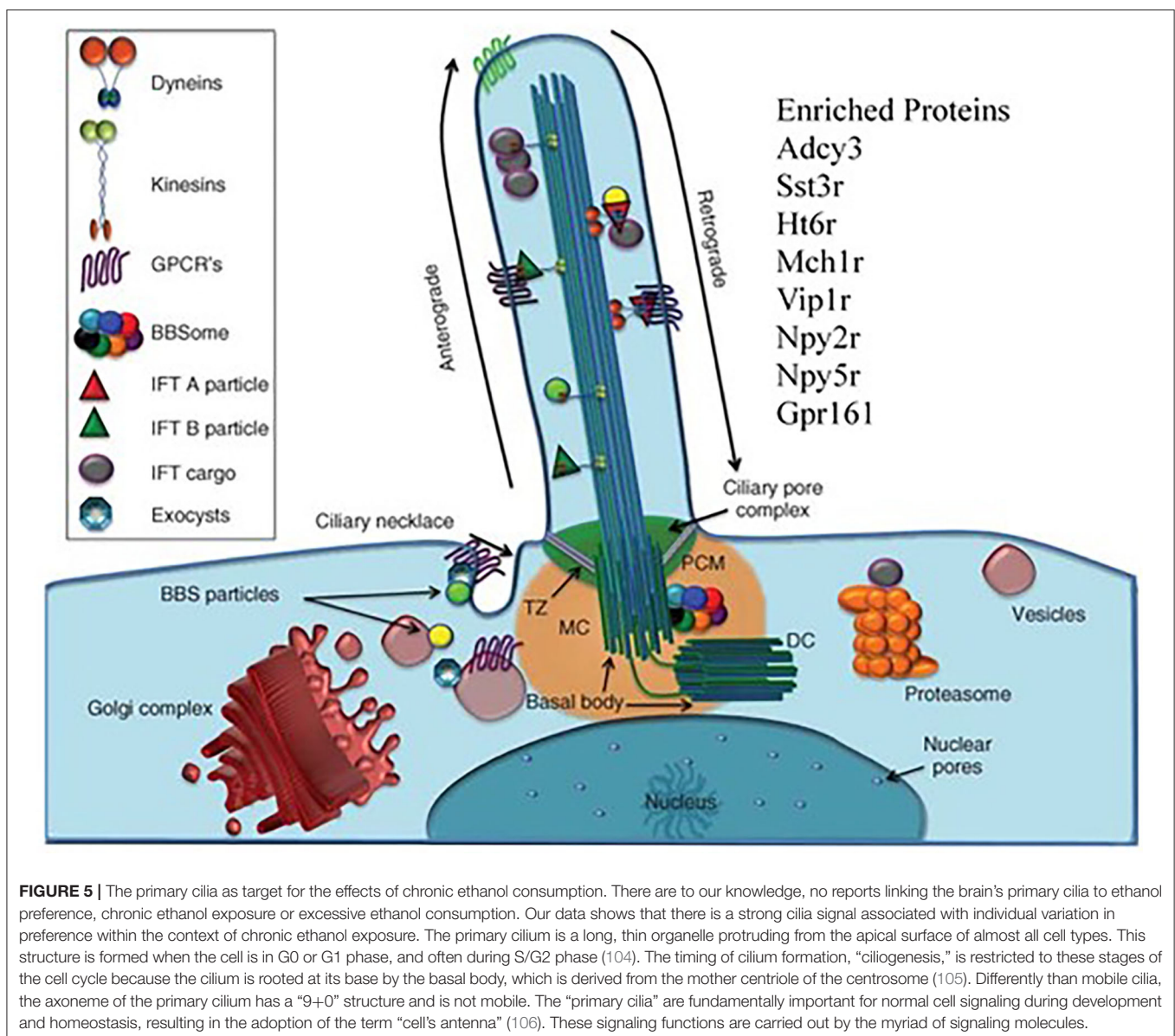
For more than 50 years, HS and other outbred rodent populations have been key to investigating the genetics and basic biology of ethanol phenotypes, including excessive ethanol consumption. To put the current use of HS animals in perspective it is useful to return to Gora-Maslek et al. (99) who observed that

a panel of BXD RI strains, even with a sparse genetic map, could be used to map drug-related QTLs. However, this study also illustrated a point that continues to complicate genomic research: gene effect sizes for essentially all complex traits are very small. To confirm a BXD generated QTL with an effect size of 5 percent (actually a very large effect!) would require ~600 B6xD2 F<sub>2</sub> intercross animals. While confirmation was possible, resolution of the QTL was poor, given the relatively low number of recombinations in the F<sub>2</sub> population. One suggested solution to this problem was to generate from the F<sub>2</sub> an advanced intercross that would build the recombination density [see e.g., (100)]. This solution introduced a new problem. Since it is practically impossible to generate an advanced intercross with a very large number of families, substantial relationships among individuals will develop over time and relatedness becomes a confounding factor. HS animals and selected lines have this same problem. As noted above, there are algorithms that deal with relatedness and importantly these are included in recent updates to r/QTL (101). Regardless of how one deals with the relatedness issue(s), it would seem that independent replication should be a convincing solution to the problem. For QTLs associated with ethanol preference and derived from B6xD2 crosses, replication has worked extremely well (79–81). However, replication in HS animals does not appear to be straightforward. As shown in Iancu et al. (52), the replicate HDID-1 and HDID-2 selections yielded only partially overlapping QTL results. These data suggest that with the increase in genetic diversity, different sets of genes can be employed to produce a similar phenotype, in this case high BECs. In addition, detailed analysis of the drinking behavior in the two selected lines revealed that there are differences—one favors larger bouts and the other favors more bouts to increase BECs. From a certain perspective, one could argue that these differences in genotype and phenotype are precisely the reasons one uses an HS population, to generate a diversity of results, detecting new pathways and mechanisms of action. However, one can also understand why this diversity is not universally appealing.

The argument that new mechanisms will be revealed as genetic diversity increases has rarely been tested under identical laboratory conditions. As noted above, Iancu et al. (24) examined eQTL expression in the striatum of F<sub>2</sub>, HS4 and HS-CC animals. This experiment was conducted using Illumina microarrays; in order to prevent hybridization artifacts, any probe sequence known to contain a SNP from one of the founder strains, was removed from the analysis. As noted previously, the detection of *cis* and *trans* eQTLs was the most reliable in the HS4. However, the detection of *trans* eQTLs was higher in the HS-CC. However, interpretation of these data are complicated by the complex kinship matrices among samples, which differ on a chromosome by chromosome basis. The question naturally arises as to how these and other changes in the regulation of gene expression will affect issues such as selection for a behavioral phenotype and the associated transcriptional changes. The only data we have for an ethanol phenotype (ethanol preference) are described above and suggest that there is likely overlap between the F<sub>2</sub> and HS-CC along dimensions related to glutamate synaptic transmission and cell adhesion. However, for a different phenotype, haloperidol-induced catalepsy, we have a very direct comparison among F<sub>2</sub>,

HS4 and HS-CC animals (102). Haloperidol-induced catalepsy is highly heritable ( $h^2 > 0.6$ ), and the mechanism of action is well-known (blockade of D<sub>2</sub> receptors), as is the target brain region (the striatum). Short-term selective breeding was used for all 3 populations and selection was stopped after 3 generations. The High and Low lines differed by 30 fold or more in the haloperidol ED<sub>50</sub>; the lines also differed in their response to raclopride and showed no difference in the response to the D<sub>1</sub> antagonist, SKF23390. Microarrays were used to analyze gene expression. The number of differentially expressed transcripts (FDR < 0.1) was significantly higher in the HS-CC compared with the F<sub>2</sub> and HS4 selections (445 vs. 113 and 33, respectively). There were no differentially expressed transcripts common to all 3 selections. A consensus network approach, previously described, was used to compare the effects of the 3 selections. A relatively large number

of transcripts significantly changed network connectivity: 458 (7.0%), 499 (7.6%), and 1,537 (23.4%) in F<sub>2</sub>, HS4 and HS-CC populations, respectively. However, as for differential expression, none of the differentially connected transcripts were shared in common across the 3 selections. Our analysis revealed that, for each selection, several modules significantly ( $Z < -2$ ) changed intra-modular connectivity structure: 4 modules in the F<sub>2</sub>, 12 in the HS4 and 21 in the HS-CC. There were 3 affected modules in common to all selections and in these the HS-CC showed the largest changes in connectivity. Importantly, and we believe this is the most *salient* point, there was no overlap among the 3 populations in the genes that showed a change in module connectivity. The common feature was the module(s) not the genes; the common modules were enriched in annotations associated with intracellular signaling and locomotor behavior.



The latter category included *Drd2*, *Chat*, and *Pde10a* & *Rgs9*. These data suggest that combining the results from populations at different levels of genetic diversity could be key to finding new (or old) targets for therapeutic manipulation.

Our last point is that working with HS animals may be beneficial in finding the truly unexpected. We return to Hitzemann et al. (68) which focused on the transcriptional changes associated with a 13 week preference trial. The unexpected observation was that in females the transcriptional features associated with week 13 preference were enriched in cilium annotations. Alcohol is known to affect the motile cilia in the brain's ventricles and other tissues [see e.g., (103)]. However, in the CeA and other brain regions there will only be primary cilia in neurons and astrocytes. There are a number of proteins localized in the neuronal primary cilia (Figure 5). These include ADCY3, SSTR3, and HT6R. There is some evidence that the manipulation of these cilium-specific molecules affects ethanol consumption. For example, de Bruin et al. (107) found that a highly selective HT6R antagonist (CMP 42) attenuated both nicotine- and alcohol-seeking behaviors in Wistar rats. Further, *Ht6r* knockout mice are less sensitive to alcohol-induced ataxia and sedation (108), and HT6R antagonists reduce cocaine self-administration, attenuate cue-induced reinstatement, attenuate the expression of cocaine-induced conditioned place preference, and reduce the acquisition and expression of nicotine-induced sensitization [see references in (109)]. The orphan receptor, GPR88, is enriched in striatal neuronal primary cilia (110). The GPR88 agonist, RTI-13951-33, significantly reduces alcohol self-administration and intake in female Long-Evans rats in a dose-dependent manner, without effects on locomotion and sucrose self-administration. However, given that the module is enriched in astrocyte annotation genes, it could be reasonably argued that our attention should focus on astrocyte primary cilia. However, as noted by Sterpka and Chen (111), "Presently, little is known about the function, signaling pathways, and structural dynamics of astrocytic primary cilia in the mature brain, although astrocytes fulfill a wide range of functions including providing trophic support, maintaining homeostasis, and protecting neurons from acute insults or brain injury (112). Since astrocytes can proliferate under certain pathological conditions (113), astrocytic primary cilia are not static but subject to dynamic changes."

## REFERENCES

- McClern GE, Rodgers DA. Differences in alcohol preference among inbred strains of mice. *Q J Stud Alcohol*. (1959) 20:691–5. doi: 10.15288/qjsa.1959.20.691
- Yoneyama N, Crabbe JC, Ford MM, Murillo A, Finn DA. Voluntary ethanol consumption in 22 inbred mouse strains. *Alcohol*. (2008) 42:149–60. doi: 10.1016/j.alcohol.2007.12.006
- Rhodes JS, Ford MM, Yu C-H, Brown LL, Finn DA, Garland T, et al. Mouse inbred strain differences in ethanol drinking to intoxication. *Genes Brain Behav*. (2007) 6:1–18. doi: 10.1111/j.1601-183X.2006.00210.x
- Hitzemann R, Bottomly D, Iancu O, Buck K, Wilmot B, Mooney M, et al. The genetics of gene expression in complex mouse crosses as a tool to study

the molecular underpinnings of behavior traits. *Mamm Genome*. (2014) 25:12–22. doi: 10.1007/s00335-013-9495-6

For most of the past 50 years, the use of HS mice largely has been limited to selective breeding; several examples of this approach in the context of ethanol research have been described. However, given that all the founder strains of existing HS populations have been deeply sequenced, it is now possible to precisely map QTLs in HS mice in much the same way one uses a GWAS approach to map human QTLs. The founders of the HS-CC and DO populations possess ~50 million SNPs. Thus, it is likely that there are allelic variants associated with the expression of every gene. Further, there are no rare alleles; absent the effects of genetic drift, the minimum allele frequency in an 8-way cross is 12.5%. With rare exception, because behavioral traits of interest are complex and polygenic, with no one gene accounting for a large percentage of the genetically-determined variance, sample sizes need to be scaled accordingly. Unlike human studies, the environment for mouse studies can be strictly controlled or modified in ways to test specific hypotheses. For some human disorders such as schizophrenia or major depressive disorder, a relevant mouse model seems unlikely. This challenge is considerably lessened for AUDs and substance abuse disorders and it is for such conditions that we believe HS mice will serve an important role in detecting new mechanisms of action that will lead to the development of new therapeutic approaches.

## AUTHOR CONTRIBUTIONS

RH wrote the first draft of the manuscript. All authors contributed to manuscript revision, read, and approved the submitted version.

## FUNDING

Funding sources were NIH NIAAA P60 AA 010760 (RH, AO, and TP), R01 AA 011034 (RH), U01 AA 013484 (RH), R24 AA020245 (RH and TP), U01 AA 013519 (AO), I01 BX 004699 (AO), and the Office of Research, Department of Veterans Affairs (AO and TP).

## ACKNOWLEDGMENTS

The studies described here reflect the contributions of numerous individuals who are noted in the respective publications.

- Solberg Woods LC, Mott R. Heterogeneous stock populations for analysis of complex traits. *Methods Mol Biol*. (2017) 1488:31–44. doi: 10.1007/978-1-4939-6427-7\_2
- McClern GE, Wilson JR, Meredith W. The use of isogenic and heterogenic mouse stocks in behavioral research. In *Contributions to Behavior-Genetic Analysis: The Mouse as a Prototype*. New York, NY: Appleton-Century-Crofts. p. 3–22.
- McClern GE, Kakihana R. Selective breeding for ethanol sensitivity: short-sleep and long-sleep mice. In: McClern GE, Deitrich RA, Erwin VG, editors. *Development of Animal Models as Pharmacogenetic Tools*. Rockville, MD: NIAAA Research Monograph. p. 147–59.

8. Crabbe JC, Kosobud A, Young ER, Tam BR, McSwigan JD. Bidirectional selection for susceptibility to ethanol withdrawal seizures in *Mus musculus*. *Behav Genet.* (1985) 15:521–36. doi: 10.1007/BF01065448
9. Shen EH, Harland RD, Crabbe JC, Phillips TJ. Bidirectional selective breeding for ethanol effects on locomotor activity: characterization of FAST and SLOW mice through selection generation 35. *Alcohol Clin Exp Res.* (1995) 19:1234–45. doi: 10.1111/j.1530-0277.1995.tb01606.x
10. Grahame NJ, Li TK, Lumeng L. Selective breeding for high and low alcohol preference in mice. *Behav Genet.* (1999) 29:47–57. doi: 10.1023/A:1021489922751
11. Crabbe JC, Kendler KS, Hitzemann RJ. Modeling the diagnostic criteria for alcohol dependence with genetic animal models. *Curr Top Behav Neurosci.* (2013) 13:187–221. doi: 10.1007/7854\_2011\_162
12. Metten P, Phillips TJ, Crabbe JC, Tarantino LM, McClearn GE, Plomin R, et al. High genetic susceptibility to ethanol withdrawal predicts low ethanol consumption. *Mamm Genome.* (1998) 9:983–990. doi: 10.1007/s003359900911
13. Crabbe JC, Spence SE, Huang LC, Cameron AJ, Schlumbohm JP, Barkley-Levenson AM, et al. Ethanol drinking in withdrawal seizure-prone and -resistant selected mouse lines. *Alcohol.* (2013) 47:381–9. doi: 10.1016/j.alcohol.2013.05.002
14. Kanes SJ, Hitzemann BA, Hitzemann RJ. On the relationship between D2 receptor density and neuroleptic-induced catalepsy among eight inbred strains of mice. *J Pharmacol Exp Ther.* (1993) 267:538–47.
15. Hitzemann B, Dains K, Kanes S, Hitzemann R. Further studies on the relationship between dopamine cell density and haloperidol-induced catalepsy. *J Pharmacol Exp Ther.* (1994) 271:969–76.
16. Demarest K, Koynier J, McCaughan J, Cipp L, Hitzemann R. Further characterization and high-resolution mapping of quantitative trait loci for ethanol-induced locomotor activity. *Behav Genet.* (2001) 31:79–91. doi: 10.1023/A:1010261909853
17. Solberg LC, Valdar W, Gauguier D, Nunez G, Taylor A, Burnett S, et al. A protocol for high-throughput phenotyping, suitable for quantitative trait analysis in mice. *Mamm Genome.* (2006) 17:129–46. doi: 10.1007/s00335-005-0112-1
18. Valdar W, Solberg LC, Gauguier D, Cookson WO, Rawlins JNP, Mott R, et al. Genetic and environmental effects on complex traits in mice. *Genetics.* (2006) 174:959–84. doi: 10.1534/genetics.106.060004
19. Valdar W, Solberg LC, Gauguier D, Burnett S, Klennerman P, Cookson WO, et al. Genome-wide genetic association of complex traits in heterogeneous stock mice. *Nat Genet.* (2006) 38:879–87. doi: 10.1038/ng1840
20. Huang MC, Chen CH, Chen CH, Liu SC, Ho CJ, Shen WW, et al. Alterations of serum brain-derived neurotrophic factor levels in early alcohol withdrawal. *Alcohol Alcohol.* (2008) 43:241–5. doi: 10.1093/alcalc/agn172
21. Keane TM, Goodstadt L, Danecsek P, White MA, Wong K, Yalcin B, et al. Mouse genomic variation and its effect on phenotypes and gene regulation. *Nature.* (2011) 477:289–94. doi: 10.1038/nature10413
22. Churchill GA, Airey DC, Allayee H, Angel JM, Attie AD, Beatty J, et al. The Collaborative Cross, a community resource for the genetic analysis of complex traits. *Nat Genet.* (2004) 36:1133–7. doi: 10.1038/ng1104-1133
23. Roberts A, Pardo-Manuel de Villena F, Wang W, McMillan L, Threadgill DW. The polymorphism architecture of mouse genetic resources elucidated using genome-wide resequencing data: implications for QTL discovery and systems genetics. *Mamm Genome.* (2007) 18:473–81. doi: 10.1007/s00335-007-9045-1
24. Iancu OD, Darakjian P, Kawane S, Bottomly D, Hitzemann R, McWeeney S. Detection of expression quantitative trait loci in complex mouse crosses: impact and alleviation of data quality and complex population substructure. *Front Genet.* (2012) 3:157. doi: 10.3389/fgene.2012.00157
25. Iancu OD, Darakjian P, Walter NA, Malmanger B, Oberbeck D, Belknap J, et al. Genetic diversity and striatal gene networks: focus on the heterogeneous stock-collaborative cross (HS-CC) mouse. *BMC Genomics.* (2010) 11:585. doi: 10.1186/1471-2164-11-585
26. Svenson KL, Gatti DM, Valdar W, Welsh CE, Cheng R, Chesler EJ, et al. High-resolution genetic mapping using the Mouse Diversity outbred population. *Genetics.* (2012) 190:437–47. doi: 10.1534/genetics.111.132597
27. Chesler EJ, Gatti DM, Morgan AP, Strobel M, Trepanier L, Oberbeck D, et al. Diversity outbred mice at 21: maintaining allelic variation in the face of selection. *G3.* (2016) 6:3893–902. doi: 10.1534/g3.116.035527
28. Bagley JR, Chesler EJ, Philip VM, Center for the Systems Genetics of Addiction, Jentsch JD. Heritability of ethanol consumption and pharmacokinetics in a genetically diverse panel of collaborative cross mouse strains and their inbred founders. *Alcohol Clin Exp Res.* (2021) 45:697–708. doi: 10.1101/2020.09.13.294769
29. Sandberg R, Yasuda R, Pankratz DG, Carter TA, Del Rio JA, Wodicka L, et al. Regional and strain-specific gene expression mapping in the adult mouse brain. *Proc Natl Acad Sci USA.* (2000) 97:11038–43. doi: 10.1073/pnas.97.20.11038
30. Jansen RC, Nap JP. Genetical genomics: the added value from segregation. *Trends Genet.* (2001) 17:388–91. doi: 10.1016/S0168-9525(01)02310-1
31. Dörner S, Lum L, Kim M, Paro R, Beachy PA, Green R. A genomewide screen for components of the RNAi pathway in *Drosophila* cultured cells. *Proc Natl Acad Sci USA.* (2006) 103:11880–5. doi: 10.1073/pnas.0605210103
32. Farris SP, Wolen AR, Miles MF. Using expression genetics to study the neurobiology of ethanol and alcoholism. *Int Rev Neurobiol.* (2010) 91:95–128. doi: 10.1016/S0074-7742(10)91004-0
33. Talbot CJ, Nicod A, Cherny SS, Fulker DW, Collins AC, Flint J. High-resolution mapping of quantitative trait loci in outbred mice. *Nat Genet.* (1999) 21:305–8. doi: 10.1038/6825
34. Walter NAR, McWeeney SK, Peters ST, Belknap JK, Hitzemann R, Buck KJ. SNPs matter: impact on detection of differential expression. *Nat Methods.* (2007) 4:679–80. doi: 10.1038/nmeth0907-679
35. Hitzemann R, Bottomly D, Darakjian P, Walter N, Iancu O, Searles R, et al. Genes, behavior and next-generation RNA sequencing. *Genes Brain Behav.* (2013) 12:1–12. doi: 10.1111/gbb.12007
36. Zhang B, Horvath S. A general framework for weighted gene co-expression network analysis. *Stat Appl Genet Mol Biol.* (2005) 4:17. doi: 10.2202/1544-6115.1128
37. Iancu OD, Kawane S, Bottomly D, Searles R, Hitzemann R, McWeeney S. Utilizing RNA-Seq data for de novo coexpression network inference. *Bioinformatics.* (2012) 28:1592–7. doi: 10.1093/bioinformatics/bts245
38. Zheng CL, Wilmot B, Walter NA, Oberbeck D, Kawane S, Searles RP, et al. Splicing landscape of the eight collaborative cross founder strains. *BMC Genomics.* (2015) 16:52. doi: 10.1186/s12864-015-1267-0
39. Mott R, Talbot CJ, Turri MG, Collins AC, Flint J. A method for fine mapping quantitative trait loci in outbred animal stocks. *Proc Natl Acad Sci USA.* (2000) 97:12649–654. doi: 10.1073/pnas.230304397
40. Kang HM, Zaitlen NA, Wade CM, Kirby A, Heckerman D, Daly MJ, et al. Efficient control of population structure in model organism association mapping. *Genetics.* (2008) 178:1709–23. doi: 10.1534/genetics.107.080101
41. Hitzemann R, Belknap JK, McWeeney SK. Quantitative trait locus analysis: multiple cross and heterogeneous stock mapping. *Alcohol Res Health.* (2008) 31:261–5.
42. Flint J, Corley R, DeFries JC, Fulker DW, Gray JA, Miller S, et al. A simple genetic basis for a complex psychological trait in laboratory mice. *Science.* (1995) 269:1432–5. doi: 10.1126/science.7660127
43. Gershenfeld HK, Neumann PE, Mathis C, Crawley JN, Li X, Paul SM. Mapping quantitative trait loci for open-field behavior in mice. *Behav Genet.* (1997) 27:201–10. doi: 10.1023/A:1025653812535
44. Koynier J, Demarest K, McCaughan J, Cipp L, Hitzemann R. Identification and time dependence of quantitative trait loci for basal locomotor activity in the BXD recombinant inbred series and a B6D2 F2 intercross. *Behav Genet.* (2000) 30:159–70. doi: 10.1023/A:1001963906258
45. Hitzemann R, Demarest K, Koynier J, Cipp L, Patel N, Rasmussen E, et al. Effect of genetic cross on the detection of quantitative trait loci and a novel approach to mapping QTLs. *Pharmacol Biochem Behav.* (2000) 67:767–72. doi: 10.1016/S0091-3057(00)00421-4
46. Rhodes JS, Best K, Belknap JK, Finn DA, Crabbe JC. Evaluation of a simple model of ethanol drinking to intoxication in C57BL/6J mice. *Physiol Behav.* (2005) 84:53–63. doi: 10.1016/j.physbeh.2004.10.007
47. Crabbe JC, Metten P, Rhodes JS, Yu C-H, Brown LL, Phillips TJ, et al. A line of mice selected for high blood ethanol concentrations shows drinking in the dark to intoxication. *Biol Psychiatry.* (2009) 65:662–70. doi: 10.1016/j.biopsych.2008.11.002

48. Crabbe JC, Phillips TJ, Belknap JK. The complexity of alcohol drinking: studies in rodent genetic models. *Behav Genet.* (2010) 40:737–50. doi: 10.1007/s10519-010-9371-z
49. Barkley-Levenson AM, Crabbe JC. Distinct ethanol drinking microstructures in two replicate lines of mice selected for drinking to intoxication. *Genes Brain Behav.* (2015) 14:398–410. doi: 10.1111/gbb.12225
50. Crabbe JC, Merrill CM, Belknap JK. Effect of acute alcohol withdrawal on sensitivity to pro- and anticonvulsant treatments in WSP mice. *Alcohol Clin Exp Res.* (1993) 17:1233–9. doi: 10.1111/j.1530-0277.1993.tb05235.x
51. Crabbe JC, Spence SE, Brown LL, Metten P. Alcohol preference drinking in a mouse line selectively bred for high drinking in the dark. *Alcohol.* (2011) 45:427–40. doi: 10.1016/j.alcohol.2010.12.001
52. Iancu OD, Oberbeck D, Darakjian P, Metten P, McWeeney S, Crabbe JC, et al. Selection for drinking in the dark alters brain gene coexpression networks. *Alcohol Clin Exp Res.* (2013) 37:1295–303. doi: 10.1111/acer.12100
53. Hitzemann R, Edmunds S, Wu W, Malmanger B, Walter N, Belknap J, et al. Detection of reciprocal quantitative trait loci for acute ethanol withdrawal and ethanol consumption in heterogeneous stock mice. *Psychopharmacology.* (2009) 203:713–22. doi: 10.1007/s00213-008-1418-y
54. Malmanger B, Lawler M, Coulombe S, Murray R, Cooper S, Polyakov Y, et al. Further studies on using multiple-cross mapping (MCM) to map quantitative trait loci. *Mamm Genome.* (2006) 17:1193–204. doi: 10.1007/s00335-006-0070-2
55. Langfelder P, Horvath S. WGCNA: an R package for weighted correlation network analysis. *BMC Bioinformatics.* (2008) 9:559. doi: 10.1186/1471-2105-9-559
56. Barkley-Levenson AM, Ryabinin AE, Crabbe JC. Neuropeptide Y response to alcohol is altered in nucleus accumbens of mice selectively bred for drinking to intoxication. *Behav Brain Res.* (2016) 302:160–70. doi: 10.1016/j.bbr.2016.01.015
57. Thiele TE, Miura GI, Marsh DJ, Bernstein IL, Palmiter RD. Neurobiological responses to ethanol in mutant mice lacking neuropeptide Y or the Y5 receptor. *Pharmacol Biochem Behav.* (2000) 67:683–91. doi: 10.1016/S0091-3057(00)00413-5
58. Hoffman PL, Saba LM, Flink S, Grahame NJ, Kechris K, Tabakoff B. Genetics of gene expression characterizes response to selective breeding for alcohol preference. *Genes Brain Behav.* (2014) 13:743–57. doi: 10.1111/gbb.12175
59. Oberlin B, Best C, Matson L, Henderson A, Grahame N. Derivation and characterization of replicate high- and low-alcohol preferring lines of mice and a high-drinking crossed HAP line. *Behav Genet.* (2011) 41:288–302. doi: 10.1007/s10519-010-9394-5
60. Iancu OD, Colville AM, Wilmot B, Searles R, Darakjian P, Zheng C, et al. Gender-specific effects of selection for drinking in the dark on the network roles of coding and noncoding RNAs. *Alcohol Clin Exp Res.* (2018) 42:1454–65. doi: 10.1111/acer.13777
61. Colville AM, Iancu OD, Oberbeck DL, Darakjian P, Zheng CL, Walter NA, et al. Effects of selection for ethanol preference on gene expression in the nucleus accumbens of HS-CC mice. *Genes Brain Behav.* (2017) 16:462–71. doi: 10.1111/gbb.12367
62. Ando T, Kato R, Honda H. Differential variability and correlation of gene expression identifies key genes involved in neuronal differentiation. *BMC Syst Biol.* (2015) 9:82. doi: 10.1186/s12918-015-0231-6
63. Mar JC, Matigian NA, Mackay-Sim A, Mellick GD, Sue CM, Silburn PA, et al. Variance of gene expression identifies altered network constraints in neurological disease. *PLoS Genet.* (2011) 7:e1002207. doi: 10.1371/journal.pgen.1002207
64. Hitzemann R, Bergeson SE, Berman AE, Bubier JA, Chesler EJ, Finn DA, et al. Sex differences in the brain transcriptome related to alcohol effects and alcohol use disorder. *Biol Psychiatry.* (2021). doi: 10.1016/j.biopsych.2021.04.016. [Epub ahead of print].
65. Mayfield J, Harris RA. The neuroimmune basis of excessive alcohol consumption. *Neuropsychopharmacology.* (2017) 42:376. doi: 10.1038/npp.2016.177
66. Lubbers BR, Smit AB, Spijker S, van den Oever MC. Neural ECM in addiction, schizophrenia, and mood disorder. *Prog Brain Res.* (2014) 214:263–84. doi: 10.1016/B978-0-444-63486-3.00012-8
67. Lasek AW. Effects of ethanol on brain extracellular matrix: implications for alcohol use disorder. *Alcohol Clin Exp Res.* (2016) 40:2030–42. doi: 10.1111/acer.13200
68. Hitzemann R, Phillips TJ, Lockwood DR, Darakjian P, Searles RP. Phenotypic and gene expression features associated with variation in chronic ethanol consumption in heterogeneous stock collaborative cross mice. *Genomics.* (2020) 112:4516–24. doi: 10.1016/j.ygeno.2020.08.004
69. Pawlak R, Melchor JP, Matys T, Skrzypiec AE, Strickland S. Ethanol-withdrawal seizures are controlled by tissue plasminogen activator via modulation of NR2B-containing NMDA receptors. *Proc Natl Acad Sci USA.* (2005) 102:443–8. doi: 10.1073/pnas.0406454102
70. Bahi A, Dreyer J-L. Involvement of tissue plasminogen activator “tPA” in ethanol-induced locomotor sensitization and conditioned-place preference. *Behav Brain Res.* (2012) 226:250–258. doi: 10.1016/j.bbr.2011.09.024
71. Wright JW, Masino AJ, Reichert JR, Turner GD, Meighan SE, Meighan PC, et al. Ethanol-induced impairment of spatial memory and brain matrix metalloproteinases. *Brain Res.* (2003) 963:252–61. doi: 10.1016/S0006-8993(02)04036-2
72. Coleman LG, Liu W, Oguz I, Styner M, Crews FT. Adolescent binge ethanol treatment alters adult brain regional volumes, cortical extracellular matrix protein and behavioral flexibility. *Pharmacol Biochem Behav.* (2014) 116:142–51. doi: 10.1016/j.pbb.2013.11.021
73. Risher M-L, Sexton HG, Risher WC, Wilson WA, Fleming RL, Madison RD, et al. Adolescent intermittent alcohol exposure: dysregulation of thrombospondins and synapse formation are associated with decreased neuronal density in the adult hippocampus. *Alcohol Clin Exp Res.* (2015) 39:2403–13. doi: 10.1111/acer.12913
74. Samochowiec A, Grzywacz A, Kaczmarek L, Bienkowski P, Samochowiec J, Mierzejewski P, et al. Functional polymorphism of matrix metalloproteinase-9 (MMP-9) gene in alcohol dependence: family and case control study. *Brain Res.* (2010) 1327:103–6. doi: 10.1016/j.brainres.2010.02.072
75. Zuo L, Zhang F, Zhang H, Zhang X-Y, Wang F, Li C-SR, et al. Genome-wide search for replicable risk gene regions in alcohol and nicotine co-dependence. *Am J Med Genet B Neuropsychiatr Genet.* (2012) 159B:437–44. doi: 10.1002/ajmg.b.32047
76. Adkins AE, Hack LM, Bigdeli TB, Williamson VS, McMichael GO, Mamdani M, et al. Genomewide association study of alcohol dependence identifies risk loci altering ethanol-response behaviors in model organisms. *Alcohol Clin Exp Res.* (2017) 41:911–28. doi: 10.1111/acer.13362
77. Mulligan MK, Rhodes JS, Crabbe JC, Mayfield RD, Harris RA, Ponomarev I. Molecular profiles of drinking alcohol to intoxication in C57BL/6J mice. *Alcohol Clin Exp Res.* (2011) 35:659–70. doi: 10.1111/j.1530-0277.2010.01384.x
78. Hitzemann R, Oberbeck D, Iancu O, Darakjian P, McWeeney S, Spence S, et al. Alignment of the transcriptome with individual variation in animals selectively bred for High Drinking-In-the-Dark (HDID). *Alcohol.* (2017) 60:115–20. doi: 10.1016/j.alcohol.2017.02.176
79. Belknap JK, Atkins AL. The replicability of QTLs for murine alcohol preference drinking behavior across eight independent studies. *Mamm Genome.* (2001) 12:893–9. doi: 10.1007/s00335-001-2074-2
80. Metten P, Iancu OD, Spence SE, Walter NAR, Oberbeck D, Harrington CA, et al. Dual-trait selection for ethanol consumption and withdrawal: genetic and transcriptional network effects. *Alcohol Clin Exp Res.* (2014) 38:2915–24. doi: 10.1111/acer.12574
81. Kozell LB, Lockwood D, Darakjian P, Edmunds S, Shepherdson K, Buck KJ, et al. RNA-Seq analysis of genetic and transcriptome network effects of dual-trait selection for ethanol preference and withdrawal using SOT and NOT genetic models. *Alcohol Clin Exp Res.* (2020) 44:820–30. doi: 10.1111/acer.14312
82. Colville AM, Iancu OD, Lockwood DR, Darakjian P, McWeeney SK, Searles R, et al. Regional differences and similarities in the brain transcriptome for mice selected for ethanol preference from HS-CC founders. *Front Genet.* (2018) 9:300. doi: 10.3389/fgene.2018.00300
83. Contet C. Gene expression under the influence: transcriptional profiling of ethanol in the brain. *Curr Psychopharmacol.* (2012) 1:301–14. doi: 10.2174/2211556011201040301

84. Warde-Farley D, Donaldson SL, Comes O, Zuberi K, Badrawi R, Chao P, et al. The GeneMANIA prediction server: biological network integration for gene prioritization and predicting gene function. *Nucleic Acids Res.* (2010) 38:W214–220. doi: 10.1093/nar/gkq537
85. Bell RL, Hauser SR, McClintick J, Rahman S, Edenberg HJ, Szumlanski KK, et al. Ethanol-Associated Changes in Glutamate Reward Neurocircuitry: A Minireview of Clinical and Preclinical Genetic Findings. *Prog Mol Biol Transl Sci.* (2016) 137:41–85. doi: 10.1016/bs.pmbts.2015.10.018
86. Petrakis IL, Limoncelli D, Gueorguieva R, Jatlow P, Boutros NN, Trevisan L, et al. Altered NMDA glutamate receptor antagonist response in individuals with a family vulnerability to alcoholism. *Am J Psychiatry.* (2004) 161:1776–82. doi: 10.1176/ajp.161.10.1776
87. Joslyn G, Ravindranathan A, Brush G, Schuckit M, White RL. Human variation in alcohol response is influenced by variation in neuronal signaling genes. *Alcohol Clin Exp Res.* (2010) 34:800–12. doi: 10.1111/j.1530-0277.2010.01152.x
88. Gill TM, Castaneda PJ, Janak PH. Dissociable roles of the medial prefrontal cortex and nucleus accumbens core in goal-directed actions for differential reward magnitude. *Cereb Cortex.* (2010) 20:2884–99. doi: 10.1093/cercor/bhq036
89. Hosseini SMH, Hoeft F, Kesler SR. GAT: a graph-theoretical analysis toolbox for analyzing between-group differences in large-scale structural and functional brain networks. *PLoS ONE.* (2012) 7:e40709. doi: 10.1371/journal.pone.0040709
90. Sari Y, Toalston JE, Rao PSS, Bell RL. Effects of ceftriaxone on ethanol, nicotine or sucrose intake by alcohol-preferring (P) rats and its association with GLT-1 expression. *Neuroscience.* (2016) 326:117–25. doi: 10.1016/j.neuroscience.2016.04.004
91. Kuleshov MV, Jones MR, Rouillard AD, Fernandez NF, Duan Q, Wang Z, et al. Enrichr: a comprehensive gene set enrichment analysis web server 2016 update. *Nucleic Acids Res.* (2016) 44:W90–97. doi: 10.1093/nar/gkw377
92. Chen EY, Tan CM, Kou Y, Duan Q, Wang Z, Meirelles GV, et al. Enrichr: interactive and collaborative HTML5 gene list enrichment analysis tool. *BMC Bioinformatics.* (2013) 14:128. doi: 10.1186/1471-2105-14-128
93. Johansson PA, Irmeler M, Acampora D, Beckers J, Simeone A, Götz M. The transcription factor Otx2 regulates choroid plexus development and function. *Development.* (2013) 140:1055–66. doi: 10.1242/dev.090860
94. Tripathi PP, Di Giovannantonio LG, Sanguinetti E, Acampora D, Allegra M, Caleo M, et al. Increased dopaminergic innervation in the brain of conditional mutant mice overexpressing Otx2: effects on locomotor behavior and seizure susceptibility. *Neuroscience.* (2014) 261:173–83. doi: 10.1016/j.neuroscience.2013.12.045
95. Sherf O, Nashelsky Zolotov L, Liser K, Tillemann H, Jovanovic VM, Zega K, et al. Otx2 Requires Lmx1b to control the development of mesodiencephalic dopaminergic neurons. *PLoS ONE.* (2015) 10:e0139697. doi: 10.1371/journal.pone.0139697
96. Planques A, Oliveira Moreira V, Dubreuil C, Prochiantz A, Di Nardo AA. OTX2 signals from the choroid plexus to regulate adult neurogenesis. *eNeuro.* (2019) 6:1–11. doi: 10.1101/243659
97. Spatzza J, Lee HHC, Di Nardo AA, Tibaldi L, Joliot A, et al. Choroid-plexus-derived Otx2 homeoprotein constrains adult cortical plasticity. *Cell Rep.* (2013) 3:1815–23. doi: 10.1016/j.celrep.2013.05.014
98. Coles C, Lasek AW. Binge-like ethanol drinking increases Otx2, Wnt1, and Mdk gene expression in the ventral tegmental area of adult mice. *Neurosci Insights.* (2021) 16:26331055211009850. doi: 10.1177/26331055211009850
99. Gora-Maslak G, McClearn GE, Crabbe JC, Phillips TJ, Belknap JK, et al. Use of recombinant inbred strains to identify quantitative trait loci in psychopharmacology. *Psychopharmacology.* (1991) 104:413–24. doi: 10.1007/BF02245643
100. Darvasi A, Soller M. A simple method to calculate resolving power and confidence interval of QTL map location. *Behav Genet.* (1997) 27:125–32. doi: 10.1023/A:1025685324830
101. Broman KW, Wu H, Sen S, Churchill GA. R/qtl: QTL mapping in experimental crosses. *Bioinformatics.* (2003) 19:889–90. doi: 10.1093/bioinformatics/btg112
102. Iancu OD, Oberbeck D, Darakjian P, Kawane S, Erk J, McWeeney S, et al. Differential network analysis reveals genetic effects on catalepsy modules. *PLoS ONE.* (2013) 8:e58951. doi: 10.1371/journal.pone.0058951
103. Omran AJA, Saternos HC, Althobaiti YS, Wisner A, Sari Y, Nauli SM, et al. Alcohol consumption impairs the ependymal cilia motility in the brain ventricles. *Sci Rep.* (2017) 7:13652. doi: 10.1038/s41598-017-13947-3
104. Plotnikova OV, Pugacheva EN, Golemis EA. Primary cilia and the cell cycle. *Methods Cell Biol.* (2009) 94:137–160. doi: 10.1016/S0091-679X(08)94007-3
105. Nigg EA, Stearns T. The centrosome cycle: Centriole biogenesis, duplication and inherent asymmetries. *Nat Cell Biol.* (2011) 13:1154–1160. doi: 10.1038/ncb2345
106. Singla V, Reiter JF. The primary cilium as the cell's antenna: signaling at a sensory organelle. *Science.* (2006) 313:629–633. doi: 10.1126/science.1124534
107. de Bruin NMWJ, McCreary AC, van Loevezijn A, de Vries TJ, Venhorst J, van Drimmelen M, et al. A novel highly selective 5-HT6 receptor antagonist attenuates ethanol and nicotine seeking but does not affect inhibitory response control in Wistar rats. *Behav Brain Res.* (2013) 236:157–65. doi: 10.1016/j.bbr.2012.08.048
108. Bonasera SJ, Chu H-M, Brennan TJ, Tecott LH. A null mutation of the serotonin 6 receptor alters acute responses to ethanol. *Neuropsychopharmacology.* (2006) 31:1801–13. doi: 10.1038/sj.npp.1301030
109. van Gaalen MM, Schettters D, Schoffemeer ANM, De Vries TJ. 5-HT6 antagonism attenuates cue-induced relapse to cocaine seeking without affecting cocaine reinforcement. *Int J Neuropsychopharmacol.* (2010) 13:961–5. doi: 10.1017/S1461145710000428
110. Marley A, Choy RW-Y, von Zastrow M. GPR88 reveals a discrete function of primary cilia as selective insulators of GPCR cross-talk. *PLoS ONE.* (2013) 8:e70857. doi: 10.1371/journal.pone.0070857
111. Sterpka A, Chen X. Neuronal and astrocytic primary cilia in the mature brain. *Pharmacol Res.* (2018) 137:114–21. doi: 10.1016/j.phrs.2018.10.002
112. Molofsky AV, Krenick R, Krenick R, Ullian EM, Ullian E, Tsai H, et al. Astrocytes and disease: a neurodevelopmental perspective. *Genes Dev.* (2012) 26:891–907. doi: 10.1101/gad.188326.112
113. Sofroniew MV, Vinters HV. Astrocytes: biology and pathology. *Acta Neuropathol.* (2010) 119:7–35. doi: 10.1007/s00401-009-0619-8

**Conflict of Interest:** The authors declare that the research was conducted in the absence of any commercial or financial relationships that could be construed as a potential conflict of interest.

**Publisher's Note:** All claims expressed in this article are solely those of the authors and do not necessarily represent those of their affiliated organizations, or those of the publisher, the editors and the reviewers. Any product that may be evaluated in this article, or claim that may be made by its manufacturer, is not guaranteed or endorsed by the publisher.

Copyright © 2021 Hitzemann, Lockwood, Ozburn and Phillips. This is an open-access article distributed under the terms of the Creative Commons Attribution License (CC BY). The use, distribution or reproduction in other forums is permitted, provided the original author(s) and the copyright owner(s) are credited and that the original publication in this journal is cited, in accordance with accepted academic practice. No use, distribution or reproduction is permitted which does not comply with these terms.



# Genetic Differences in Dorsal Hippocampus Acetylcholinesterase Activity Predict Contextual Fear Learning Across Inbred Mouse Strains

Sean M. Mooney-Leber<sup>1</sup>, Dana Zeid<sup>2</sup>, Prescilla Garcia-Trevizo<sup>2</sup>, Laurel R. Seemiller<sup>2</sup>, Molly A. Bogue<sup>3</sup>, Stephen C. Grubb<sup>3</sup>, Gary Peltz<sup>4</sup> and Thomas J. Gould<sup>2\*</sup>

<sup>1</sup> Department of Psychology, University of Wisconsin-Stevens Point, Stevens Point, WI, United States, <sup>2</sup> Department of Biobehavioral Health, The Pennsylvania State University, State College, PA, United States, <sup>3</sup> The Jackson Laboratory, Bar Harbor, ME, United States, <sup>4</sup> Department of Anesthesiology, Perioperative and Pain Medicine, Stanford University, Palo Alto, CA, United States

## OPEN ACCESS

### Edited by:

Peter Kalivas,  
Medical University of South Carolina,  
United States

### Reviewed by:

Dayan Kessler Knox,  
University of Delaware, United States  
Christina Jennifer Perry,  
Macquarie University, Australia

### \*Correspondence:

Thomas J. Gould  
tug70@psu.edu

### Specialty section:

This article was submitted to  
Molecular Psychiatry,  
a section of the journal  
Frontiers in Psychiatry

**Received:** 08 July 2021

**Accepted:** 21 September 2021

**Published:** 18 October 2021

### Citation:

Mooney-Leber SM, Zeid D, Garcia-Trevizo P, Seemiller LR, Bogue MA, Grubb SC, Peltz G and Gould TJ (2021) Genetic Differences in Dorsal Hippocampus Acetylcholinesterase Activity Predict Contextual Fear Learning Across Inbred Mouse Strains. *Front. Psychiatry* 12:737897. doi: 10.3389/fpsy.2021.737897

Learning is a critical behavioral process that is influenced by many neurobiological systems. We and others have reported that acetylcholinergic signaling plays a vital role in learning capabilities, and it is especially important for contextual fear learning. Since cholinergic signaling is affected by genetic background, we examined the genetic relationship between activity levels of acetylcholinesterase (AChE), the primary enzyme involved in the acetylcholine metabolism, and learning using a panel of 20 inbred mouse strains. We measured conditioned fear behavior and AChE activity in the dorsal hippocampus, ventral hippocampus, and cerebellum. Acetylcholinesterase activity varied among inbred mouse strains in all three brain regions, and there were significant inter-strain differences in contextual and cued fear conditioning. There was an inverse correlation between fear conditioning outcomes and AChE levels in the dorsal hippocampus. In contrast, the ventral hippocampus and cerebellum AChE levels were not correlated with fear conditioning outcomes. These findings strengthen the link between acetylcholine activity in the dorsal hippocampus and learning, and they also support the premise that the dorsal hippocampus and ventral hippocampus are functionally discrete.

**Keywords:** hippocampus, learning, acetylcholinesterase, genetics, fear conditioning

## INTRODUCTION

Learning is a complex behavioral process that relies on multiple neurobiological systems working in concert. The cholinergic system is one such system whose signaling modulates learning and memory networks (1, 2). For example, the acetylcholine muscarinic receptor (mAChR) antagonist scopolamine has been shown to impair learning in a contextual fear conditioning task (3, 4), spatial learning in the Morris Water Maze (5, 6), passive avoidance learning (6, 7), and object recognition learning (8). Other work has found that signaling via nicotinic acetylcholine receptors (nAChR) may modulate learning and memory.

Signaling via nAChR systems can enhance learning through interactions with other neurotransmitter systems. nAChR antagonism with mecamylamine, a non-selective nAChR ligand, does not impair fear conditioning (9, 10). However, mecamylamine paired with a subthreshold dose of an NMDA glutamate receptor antagonist disrupts fear conditioning (10). NMDA receptor signaling acts upstream of synaptic plasticity mediating several forms of learning and memory [for review see (11)]. Results of NMDA receptor and nAChR co-antagonism suggest that these two systems mediate similar learning-related processes, with the nAChR system perhaps subordinate to NMDA receptor signaling. In support, several studies have found that the administration of nicotine (a nAChR agonist) enhances learning (9, 12–14). In addition, nicotine reversed NMDA receptor antagonism-induced deficits in fear conditioning, and direct drug infusion experiments revealed that the dorsal hippocampus mediated this effect (15). Other studies have found that antagonism of nAChR receptors with mecamylamine alone was sufficient to impair learning (6, 16). Importantly, both of these studies used larger mecamylamine doses, and other work suggests that mecamylamine may act as an NMDA receptor antagonist at higher doses (17–19). Thus, impairment of learning via mecamylamine at higher doses may represent its influence on NMDA receptors directly instead of or in addition to actions at nAChRs. In sum, the cholinergic system is involved in learning, with the muscarinic subsystem directly mediating learning-associated cell signaling and the nicotinic system potentially interacting with glutamatergic signaling cascades to modulate learning.

Acetylcholine, the endogenous ligand of mAChRs and nAChRs, is primarily synthesized at axon terminals from choline and acetyl coenzyme A by choline acetyltransferase (ChAT). Acetylcholinesterase (AChE) works to rapidly metabolize acetylcholine into acetate and choline in the synaptic space (20). Manipulation of both acetylcholine synthesis and metabolism can alter learning (21, 22). Prevention of acetylcholine metabolism via AChE inhibition has been used to mitigate cognitive impairments associated with many neurodegenerative diseases (23–25).

A growing body of literature suggests that genetic variability in AChE-related genes could influence learning. Single nucleotide polymorphisms (SNP) in the *ACHE* gene, which encodes the acetylcholinesterase enzyme, have been identified in humans (26, 27). Valle et al. (28) reported that heritable variations in the *ACHE* gene may underlie individual differences in AChE expression and secretion. Genotype at a SNP found in the *ACHE* gene also predicted responsivity to cognitive-enhancing drug treatment in patients with dementia (29). Genetic variation impacting cholinergic signaling and associated cognition has also been reported in outbred and inbred rodent models (30, 31). Matson et al. (32) found significant differences in AChE activity in the brain cortex and red blood cells between 8 inbred mouse strains. Further, Schwegler et al. (33) reported that the density of cholinergic fibers within the hippocampus varied systematically by genetic background, which correlated with learning outcomes in two spatial learning tasks. Further evidence supporting the role of AChE in learning has been documented elsewhere (34).

These findings support that the presence of genetic variants related to cholinergic systems may have a measurable impact on learning outcomes.

Inbred mouse strains provide a powerful tool for identifying the genetic contributions to various behavioral outcomes since each inbred strain has a fixed homozygous genome. Fear conditioning is a simple form of learning that is often utilized to study cognitive performance in rodent models. Studies using large inbred mouse strain panels have demonstrated that learning capabilities in components of fear conditioning are, in part, driven by genetic background (35–37). Neuroanatomical contributors to fear conditioning have been identified (38). Specifically, the dorsal hippocampus is the primary processor of contextual information during fear conditioning (39), but it is not critically involved in cued fear conditioning (40). These neuroanatomical divisions can be leveraged to assess hippocampus-dependent and -independent learning in a fear conditioning model. Since cholinergic signaling within the hippocampus is vital for fear learning (4), genetic variation in acetylcholine signaling could contribute to inter-strain variation in fear conditioning.

Therefore, we examine genetic variability in AChE activity in three brain regions (dorsal hippocampus, ventral hippocampus, and cerebellum) in 20 inbred mouse strains. The dorsal and ventral hippocampus were separately examined due to their distinct roles in fear conditioning. Specifically, the dorsal hippocampus is primarily involved in cognitive processing, whereas the ventral hippocampus regulates stress and the emotional response to fear (41). The cerebellum was selected as a control due to its lack of participation in contextual or cued fear conditioning (42). Contextual and cued fear conditioning were used to understand how genetic variation in AChE activity correlated with strain differences in hippocampus-dependent learning. We hypothesized that learning capabilities and brain AChE activity would vary significantly between strains; and because of the prominent role that the hippocampus plays in fear learning, we predicted that hippocampal AChE activity levels would be correlated with fear conditioning.

## METHODS

### Subjects

Male 129S1/SvImJ, 129S4/SvJaeJ, 129S8/SvEvNimrJ, A/J, AKR/J, BALB/cJ, BTBRT<+>ltpr3<tf>/J, C3H/HeJ, C57BL/6J, CBA/J, DBA/1J, DBA/2J, FVB/NJ, LP/J, MA/MyJ, NZB/BINJ, SJL/J, SM/J, & SWR/J mice were obtained from Jackson Laboratory (Bar Harbor, ME). 129S2/SvPasCrl were obtained from Charles River (Wilmington, MA). Individual strain characteristics can be found on <https://mice.jax.org/> and [https://www.criver.com/\(129S2\)](https://www.criver.com/(129S2)). These mice were part of a larger project examining the influence of genetic background on sensitivity to drugs of abuse. All mice were 10–15 weeks of age for behavioral testing and tissue collection ( $n = 9$ –13 per strain). All mice were group-housed [with the exception of SJL/J, which were single-housed due to excessive social aggression characteristic of this strain; (43)] with a 12-h light/dark cycle and unlimited access to food and water. All behavioral testing occurred between

8:00 A.M. and 5:00 P.M. All procedures were conducted in accordance with the NIH Guide for the Care and Use of Laboratory Animals and approved by the Penn State University IACUC Committee.

## Saline Exposure

As mentioned previously, mice from this study served as saline controls for a larger project examining the impact of nicotine on learning and memory. As a result of their experimental assignment, mice used for the current study were exposed to chronic saline for 12 days. Saline was administered via subcutaneous osmotic minipumps (model #1002, Alzet Inc.; Cupertino, CA, USA). Surgical implantation and removal of the minipumps were performed under 3.5% isoflurane anesthesia using aseptic procedures. Pumps were removed 1 day prior to behavioral training.

## Apparatus

Fear conditioning training and testing for contextual fear learning occurred in four identical noise-attenuating chambers with metal bar grid flooring ( $18.8 \times 20 \times 18.3$  cm, MED Associates, St. Albans, VT, USA). Testing for cued fear learning was conducted in a separate room in four identical noise-attenuating chambers ( $20.32 \times 22.86 \times 17.78$  cm, MED Associates, St. Albans, VT, USA) designed to have distinct sensory cues (different chamber size, solid plastic flooring, background vanilla odor) to allow subjects to distinguish them from the training/context test chambers. Both sets of chambers were equipped with side-mounted speakers for cued stimuli presentation (85 dB white noise) and fans to provide ventilation and background noise (65 dB). Freezing behavior was recorded using cameras mounted to chamber ceilings (Ikegami, Tokyo, Japan) connected to Noldus media recording software (Noldus, Wageningen, Netherlands). Stimuli presentation during training and both testing sessions was controlled by Med-PC software and hardware (MED Associates, St. Albans, VT, USA).

## Fear Conditioning

Mice were trained and tested in both contextual and cued fear conditioning, as previously established in our laboratory (37). Briefly, for training, mice were placed in an operant chamber for a total of 5 min. The first 2 min of training consisted of a stimulus-free period (baseline) followed by 2 conditioned stimulus (CS; 30-s 85 dB white noise)—unconditioned stimulus (US; 2-s 0.45 mA foot shock) pairings presented 2 min apart, in which the US overlapped with the last 2-s of the CS. The 2-min period in between the two CS-US pairings served as the immediate or post-shock period. Two associations are formed during the training trial and are used to assess fear conditioning: (1) Between the tone CS and footshock US (cued fear conditioning) and (2) Between the footshock US and the context/environment (contextual fear conditioning). To assess the strength of these unique forms of learning and memory, mice were tested for both contextual and cued learning 24 h after training. To test contextual fear learning, mice were placed back inside the training chamber over a 5-min trial with no stimulus presentation. Cued testing occurred at least 1 h after context testing, for which mice were placed in a novel

chamber for a 3-min baseline assessment (pre-cue), followed by 3-min of CS exposure (cued). Chambers used for context and cued testing were not counterbalanced to be consistent with previous studies examining the impact of nicotine withdrawal on fear learning (37) and because contextual fear learning was the primary focus on this study. Novel cues (plastic flooring and vanilla scent) were present during cued testing to minimize generalization to the training chambers. All sessions were video recorded. Freezing behavior was tracked during all sessions via EthoVision XT (Noldus, Wageningen, Netherlands).

## Tissue Collection and AChE Activity

Twenty-four hours following the fear conditioning test, mice were sacrificed for the collection of hippocampus and whole cerebellum. Hippocampi were further dissected into dorsal and ventral sections (1:1 ratio). All tissue was flash frozen on dry ice and stored at  $-80^{\circ}\text{C}$  until further processing. Brain tissue from 5 to 6 mice was randomly selected from each strain. Tissue was homogenized in 1X RIPA buffer solution (R0278, Sigma Life Sciences, St. Louis, MO, USA) with HALT Protease and Phosphatase Inhibitor Cocktail at a ratio of 100:1 (78445, Fisher Scientific, Pittsburgh, PA, USA). Homogenates were spun down at 14,000 g at  $4^{\circ}\text{C}$  for 30 min. Total protein concentration of the supernatant was determined by DC Protein Assay (500-0112; Bio-Rad, Hercules, CA, USA). Each supernatant sample was further diluted in RIPA buffer to a standard 30  $\mu\text{g}$  total protein. AChE activity in diluted samples was measured using the Abcam Acetylcholinesterase Assay Kit (ab138871, Abcam, Cambridge, MA, USA) per manufacturer instructions. Inter- and intra-assay duplicate CV% were all  $<15\%$ .

## Mouse Phenome Database Gene Polymorphism Queries

To assess sequence variation in genes encoding AChE and other proteins relevant to cholinergic signaling, genes were surveyed using the Mouse Phenome Database SNP data retrieval tool (44). SNP and indel data were retrieved from the Sanger4 (45) data set because of its extensive genome coverage. However, only a subset of 13 strains was analyzed (DBA/1J, C57BL/6J, LP/J, BALB/cJ, DBA/2J, 129S1/SvImJ, CBA/J, C3H/HeJ, A/J, AKR/J, NZB/BINJ, FVB/NJ, BTBR T+ Itpr3tf/J) due to the other strains not being represented in the Sanger4 data set. These data were compiled with gene function and length data from Mouse Genome Informatics website [<http://www.informatics.jax.org/index.shtml> (June, 2021)] in **Supplementary File 1**.

## Heritability Estimates and Behavioral Correlations

Heritability estimates were based on within- and between-strain variance produced from one-way ANOVAs for each behavioral and biological outcome. Briefly, sum of squares between strains (between strain variance) was divided by the summation of sum of squares between and within-strains [within strain variance; (46)]. To explore potential genetic overlap between the collected behavioral and biological variables, strain mean Pearson  $r$  correlations between all fear conditioning and AChE activity variables were computed. Pearson  $r$  correlations

were also computed between AChE activity strain means and other behavioral phenotypes available through a custom dataset within Mouse Phenome Database [fear conditioning (Mooney1) and AChE data (Mooney2) collected for this study are available at <https://phenome.jax.org>]. A significance threshold of  $p < 0.01$  (based on Pearson  $r$ ) was applied to correlations calculated for AChE activity strain means in each brain region. As we were specifically interested in behavioral outcomes related to AChE activity, correlations significant at  $p < 0.01$  derived from behavioral assays are highlighted (see **Supplementary Tables 1–3**).

## Statistical Analysis

Separate one-way ANOVAs with strain as a between-subjects factor were utilized to examine conditioning variables (baseline, immediate, context, pre-cue, & cued freezing) and brain AChE activity levels (dorsal hippocampus, ventral hippocampus, and cerebellum). ANOVAs with a significant effect of strain were followed up with Tukey HSD *post-hoc*. If Levene's test of homogeneity of variance was violated, a Games-Howell *post-hoc* was conducted instead. Associations between fear conditioning behaviors and AChE activity were examined using a Pearson  $r$  correlation coefficient. All data analyses were conducted using SPSS 26 software (IBM, Chicago, USA). ANOVA results and within-dataset correlations were considered significant at  $p < 0.05$ . Strain AChE mean correlations with Mouse Phenome Database behavioral datasets were considered significant at  $p < 0.01$ . The significance threshold of  $p < 0.01$  was selected as a compromise between statistical lenience and stringency (47) to match the exploratory nature of these analyses.

## RESULTS

### Fear Conditioning

We examined multiple behavioral components of fear conditioning in 20 inbred strains. The range of freezing responses varied based on the following behaviors: baseline 0.48–19.15%, immediate 0.27–55.61%, context 6.96–77.18%, pre-cue 2.93–46.3%, and cued 21.54–84.14%. The resulting data was analyzed using one-way ANOVAs for the following: freezing during the baseline phase of fear conditioning training [**Figure 1A**;  $F_{(19,193)} = 12.81$ ,  $p < 0.001$ ], freezing during the immediate (post-shock) phase [**Figure 1B**;  $F_{(19,193)} = 20.27$ ,  $p < 0.001$ ], freezing to the conditioned context [**Figure 1C**;  $F_{(19,193)} = 33.12$ ,  $p < 0.001$ ], pre-cue freezing during the cued fear learning test [**Figure 1D**;  $F_{(19,193)} = 13.19$ ,  $p < 0.001$ ], and freezing to the conditioned cue [**Figure 1E**;  $F_{(19,193)} = 18.85$ ,  $p < 0.001$ ]. Each ANOVA revealed a significant main effect of strain. The calculated genetic heritability for freezing in each of these stages of fear conditioning were: baseline freezing 57.36%, immediate freezing 67.45%, context freezing 76.32%, pre-cue freezing 58.18%, and cued freezing 66.04%. *Post-hoc* outcomes examining strain differences can be found in **Supplementary Tables 4–8**.

### AChE Activity

We examined dorsal and ventral hippocampal and cerebellum AChE activity in 20 inbred strains. The range of AChE activity

levels varied by region: dorsal hippocampus 201.2–271.3 mU/ml, ventral hippocampus 222.5–325.1 mU/ml, and cerebellum 187–273 mU/ml. The resulting data was analyzed using separate one-way ANOVAs for dorsal hippocampus AChE activity [**Figure 2A**;  $F_{(19,99)} = 2.37$ ,  $p = 0.003$ ], ventral hippocampus AChE activity [**Figure 2B**;  $F_{(19,100)} = 4.25$ ,  $p < 0.001$ ] and whole cerebellum AChE activity [**Figure 2C**;  $F_{(19,99)} = 1.81$ ,  $p = 0.032$ ], which found a significant main effect for strain. Genetic heritability estimates were calculated as follows: dorsal hippocampus AChE activity 34.43%, ventral AChE activity 45.24%, and cerebellum AChE activity 26.15%. *Post-hoc* outcomes examining strain differences can be found in **Supplementary Tables 9–11**.

## Mouse Phenome Database Gene Polymorphism Queries

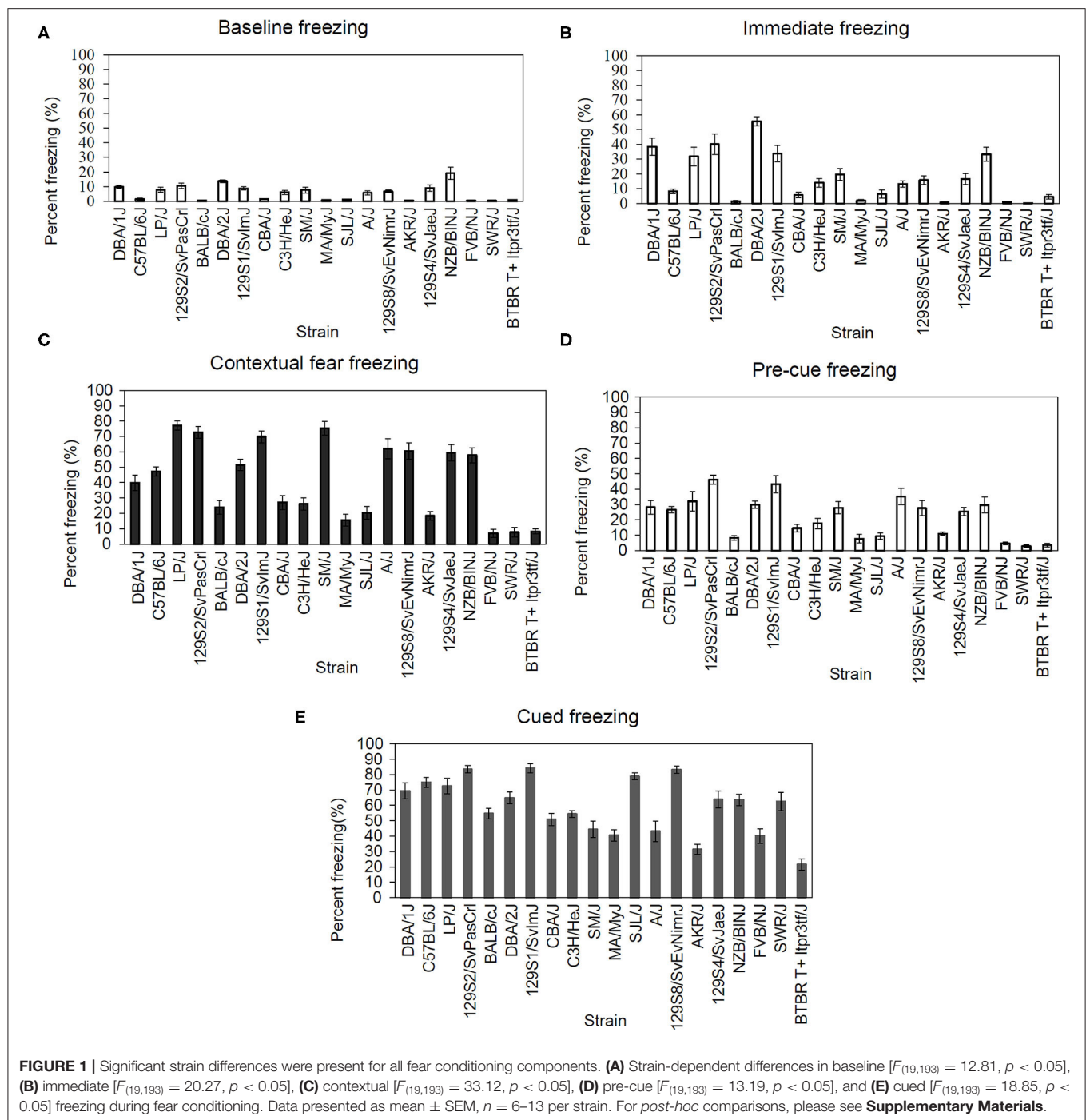
To identify genetic variants that could underlie the observed inter-strain differences in AChE activity and learning, we used the Mouse Phenome Database SNP data retrieval tool to examine inter-strain allelic differences in 28 genes related to cholinergic signaling. Their functions and SNPs are listed in **Supplementary File 1**. Notably, there were 18 polymorphisms within the *AChE* gene, including 5 indels. There were also many polymorphisms in other cholinergic signaling genes.

## Within-Dataset AChE Activity and Fear Conditioning Correlations

To examine potential genetic overlap between behavioral components of fear conditioning, strain mean correlations were calculated between all measured fear conditioning variables (**Table 1**). Freezing during the baseline of fear conditioning training positively correlated with immediate (post-shock) freezing during training [ $r_{(18)} = 0.87$ ,  $p < 0.001$ ], freezing to the conditioned context [ $r_{(18)} = 0.70$ ,  $p = 0.001$ ], and pre-cue [ $r_{(18)} = 0.73$ ,  $p < 0.001$ ] freezing, but not with freezing to the conditioned cue. Immediate (post-shock) freezing also positively correlated with freezing to context [ $r_{(18)} = 0.69$ ,  $p = 0.001$ ], pre-cue freezing during the cued fear learning test [ $r_{(18)} = 0.79$ ,  $p < 0.001$ ] and freezing to cue [ $r_{(18)} = 0.53$ ,  $p = 0.016$ ]. Context freezing also positively correlated with pre-cue freezing [ $r_{(18)} = 0.93$ ,  $p < 0.001$ ] and cue freezing [ $r_{(18)} = 0.54$ ,  $p = 0.013$ ] freezing. Finally, pre-cue freezing also correlated positively with cue freezing [ $r_{(18)} = 0.60$ ,  $p = 0.005$ ]. These results may point to shared genetic variance underlying freezing during different stages of fear conditioning.

Strain mean correlations were similarly calculated for AChE activity between brain regions (**Table 1**). From the three brain regions examined, only a positive correlation between dorsal and ventral hippocampus AChE activity levels was found [ $r_{(18)} = 0.52$ ,  $p = 0.019$ ]. Dorsal and ventral hippocampus AChE activity did not significantly correlate with cerebellum AChE activity. Significant covariance between dorsal and ventral hippocampus AChE activity implies potentially shared genetic factors impacting AChE activity levels between functionally distinct regions of the hippocampus.

Finally, we examined the relationship between strain means for brain AChE activity and freezing during fear conditioning.



Dorsal hippocampus AChE activity (**Figure 3**) negatively correlated with immediate (post-shock) freezing during fear conditioning training [**Figure 3B**;  $r_{(18)} = -0.53, p = 0.016$ ], freezing to the conditioned context [**Figure 3C**;  $r_{(18)} = -0.50, p = 0.026$ ], pre-cue freezing during cued test [**Figure 3D**;  $r_{(18)} = -0.58, p = 0.008$ ] and freezing to the conditioned cue [**Figure 3E**;  $r_{(18)} = -0.54, p = 0.015$ ] but not baseline freezing (**Figure 3A**). No significant correlations between ventral hippocampus or cerebellum AChE activity levels and any of the measured fear conditioning variables were found

(**Supplementary Figures 1, 2**). Thus, genetic factors underlying freezing during multiple stages of fear conditioning covary exclusively with dorsal hippocampus AChE activity, despite significant correlations between ventral and dorsal hippocampus AChE activity.

## Mouse Phenome Database Correlations

Brain AChE activity strain means were correlated with publicly available phenotypes using the Mouse Phenome Database. Only measures with mean data points for a

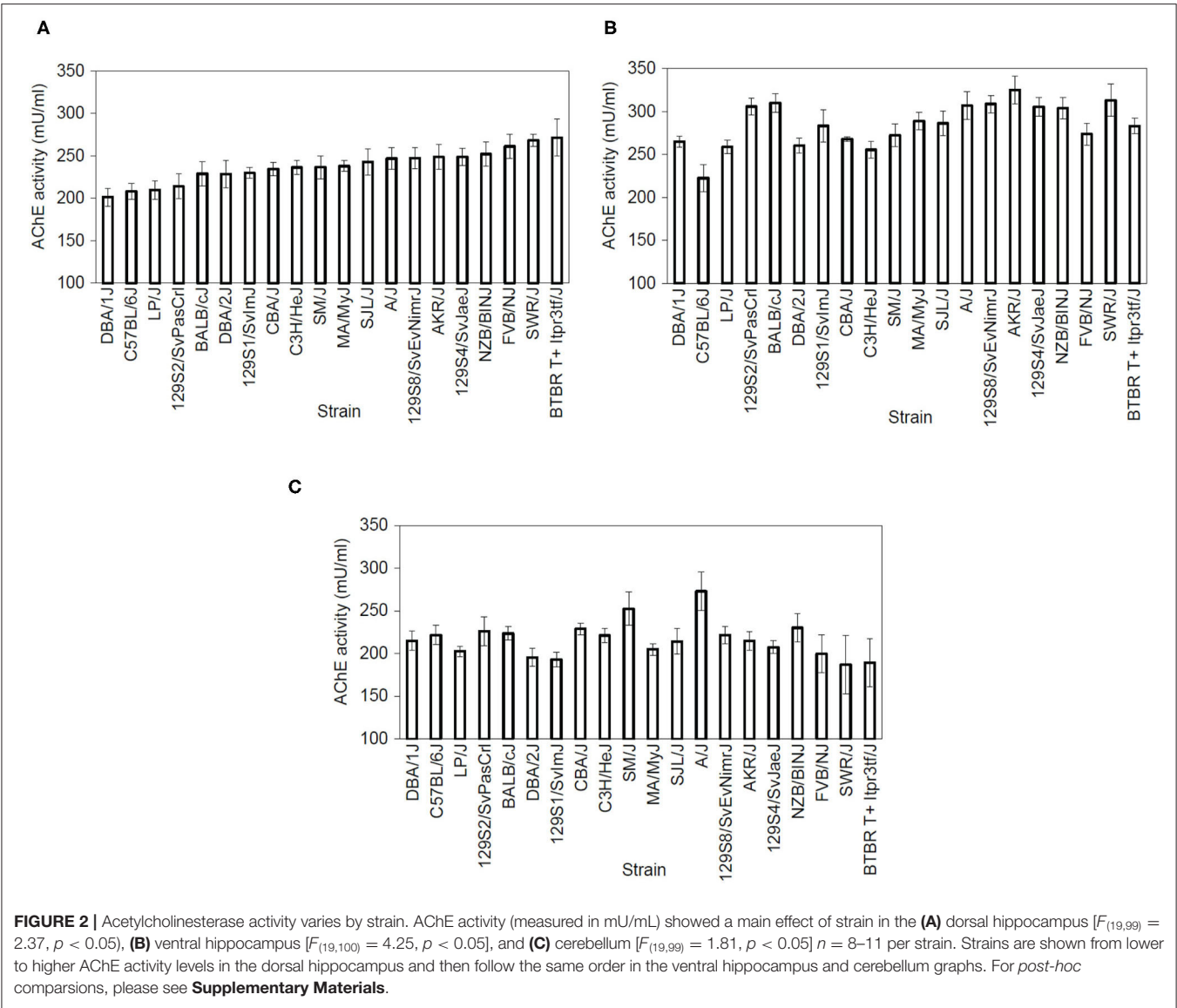
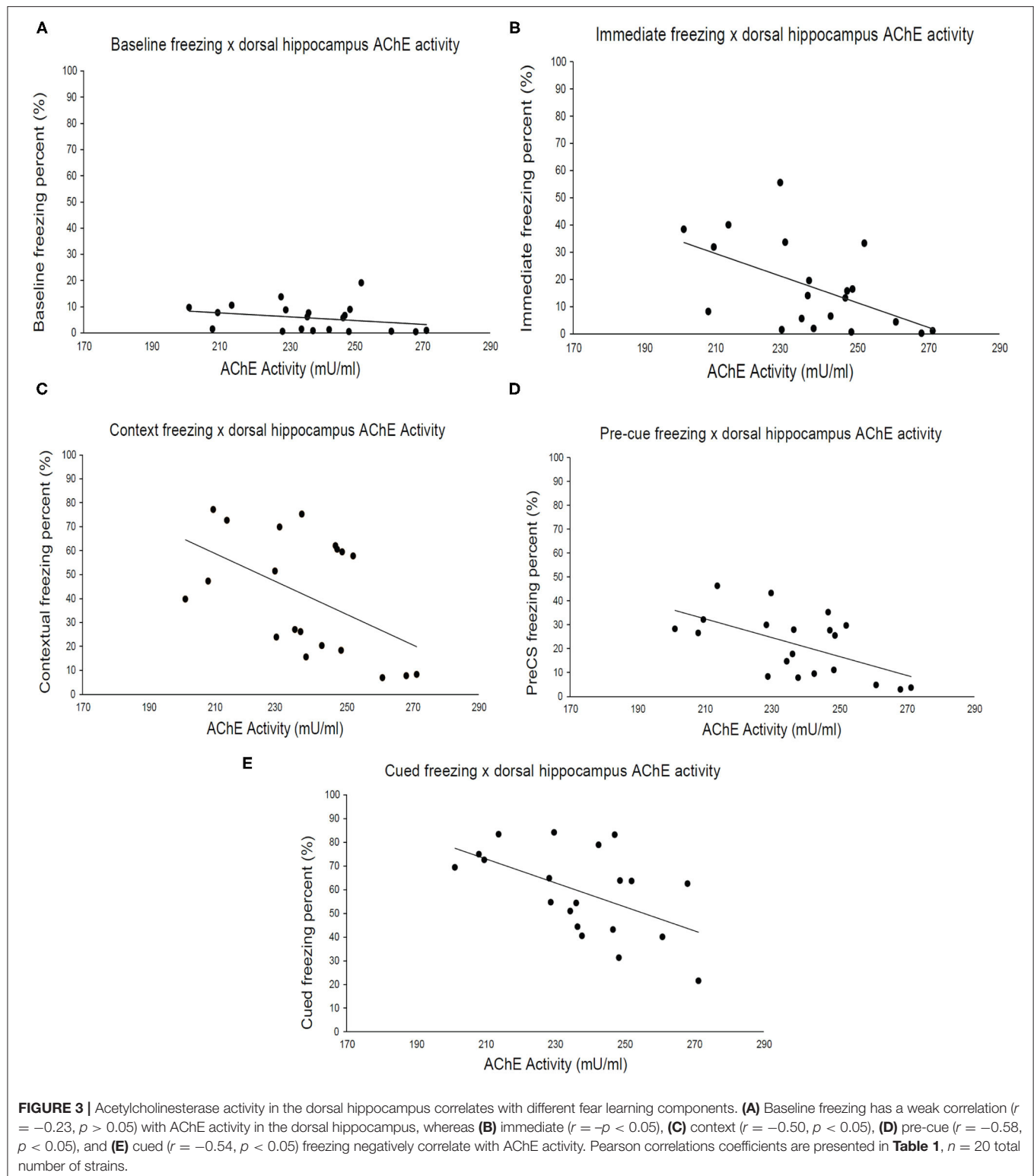


TABLE 1 | Pearson correlation coefficients of AChE activity when correlated with different components of fear learning.

	Baseline	Immediate	Context	Pre-cue	Cued	DH AChE	VH AChE	CB AChE
Baseline	1							
Immediate	<b>0.87**</b>	1						
Context	<b>0.70**</b>	<b>0.69**</b>	1					
Pre-CS	<b>0.73**</b>	<b>0.79**</b>	<b>0.93**</b>	1				
Cued	0.43	<b>0.53*</b>	<b>0.54*</b>	<b>0.6**</b>	1			
DH AChE	-0.23	<b>-0.53*</b>	<b>-0.5*</b>	<b>-0.58**</b>	<b>-0.54*</b>	1		
VH AChE	-0.02	-0.22	-0.09	-0.12	-0.14	<b>0.52*</b>	1	
CB AChE	0.16	-0.02	0.41	0.35	-0.08	-0.17	0.09	1

\*correlation is significant at 0.05 level; \*\*correlation is significant at the 0.01 level (two-tailed), based on strain means. Bold text represents significant values.



minimum of 8 strains overlapping with our own panel were utilized for MPD correlation analysis. Two thousand twenty-five total measures available in MPD were correlated with AChE activity in each of the tested brain regions

(dorsal and ventral hippocampus and cerebellum). We made the *a priori* decision to focus on the top ten significant correlations of AChE with behavioral variables for the purpose of this manuscript.

For dorsal hippocampus AChE activity strain mean correlations, 20 measures met the pre-determined significance cut-off ( $p < 0.01$ ; see **Supplementary Table 1**). Six of these phenotypes were classified as behavioral models, and three were cognitive assessments in the Barnes maze, as assessed by number of errors that positively correlated with AChE activity. For ventral hippocampus AChE activity (see **Supplementary Table 2**), 21 measures were considered to be significantly correlated (at  $p < 0.01$ ), with ten of those phenotypes corresponding to a behavioral measure. Specifically, for five out of the six correlated behaviors, AChE activity correlated positively with emotional behavioral responding in cued fear testing, light-dark box, and variants of the elevated maze. Lastly, 30 measures met the significance threshold for correlations with cerebellum AChE activity levels (see **Supplementary Table 3**). Nine of these corresponded to behavioral measurements. Of note, cerebellum AChE activity correlated positively with six measures of scheduled operant behavior, such as fixed-ratio responding.

## DISCUSSION

Here we report significant variation in fear conditioning and AChE activity in three brain regions across 20 inbred mouse strains. We found that these phenotypes were heritable, especially for freezing during the five stages of fear conditioning assessed (baseline, immediate, context, pre-cue, & cued). Correlation data generated within the current dataset indicate strong positive genetic relationships between freezing levels in various stages of fear conditioning and also between dorsal and ventral hippocampus AChE activity, in addition to a negative correlation between fear conditioning freezing and dorsal hippocampus AChE activity. Correlations of our strain means with publicly available datasets indicate that the dorsal hippocampus AChE activity levels may be more closely related to learning outcomes, whereas ventral hippocampus AChE activity may be better associated with other emotional processing outcomes. Collectively, these findings suggest a degree of heritability in fear learning and hippocampal AChE activity levels and that genetic variability associated with AChE activity in the dorsal hippocampus may contribute to learning in fear conditioning.

## AChE Activity

Using a panel of 20 inbred mouse strains, we found a significant variation of AChE activity in the dorsal hippocampus, ventral hippocampus, and cerebellum. These findings suggest that AChE activity varies by genetic background. Our genetic analysis identified at least 18 polymorphisms in the AChE gene among a subset of the tested strains. Although these polymorphisms did not clearly co-vary with learning or AChE activity in the current panel, they likely contribute in part to inbred strain variation in AChE efficiency and activity. Importantly, enzymatic activity can be modulated by variation in the enzyme itself (e.g., polymorphisms in the encoding gene leading to altered protein structure and changes in enzymatic activity), by distal regulatory genomic elements (e.g., polymorphisms in trans-regulatory elements targeting AChE gene expression), by interactions within the enzymatic

pathway (e.g., polymorphisms among broader genomic networks involved in cholinergic signaling), or by a combination of these factors. Our analysis found that related genes encoding choline acetyltransferase (ChAT), an important enzyme in acetylcholine synthesis (48, 49), RIC3, an acetylcholine receptor chaperone protein (50, 51), butyrylcholinesterase, another acetylcholine-metabolizing enzyme (52), and nicotinic acetylcholine receptor subunits (53) also contain numerous polymorphisms across strains. These polymorphisms could all potentially influence cholinergic signaling and represent possible mechanisms through which genetic differences across strains influence AChE activity and learning. Moreover, the large amount of cholinergic modulating genes exhibiting polymorphisms suggests that the observed phenotypic differences in learning may involve complex genotypic and regulatory interactions.

## Fear Conditioning

The current results are in line with previous findings of genetic variability in conditioned fear learning (37, 54, 55). Analyses of our inbred mouse strain panel indicated significant between-strain variation in freezing during multiple stages of fear conditioning (baseline, immediate, context, pre-cue, & cued). Moreover, these behaviors were highly heritable, all demonstrating  $>57\%$  heritability. Our fear conditioning paradigm measured two distinct associations: First, between the training context (contextual fear conditioning) and the US, and second, between the CS and US (cued fear conditioning). Here, we report a wide range of contextual fear conditioning across our inbred strain panel with some strains demonstrating high (LP/J, SM/J, 129S2, & 129S1,  $>68\%$  freezing) and some demonstrating low contextual fear conditioning (FVB/NJ, SWR/J, & BTBRT+,  $<10\%$  freezing). The differences in the mice that show high levels of freezing and the mice that show low levels of freezing during the context tests could suggest that the high and lower responders differ in hippocampus-dependent learning. In support, studies examining LP/J, SM/J, & 129S1 inbred mice have found high levels of learning in hippocampus-dependent tasks (56) including contextual fear conditioning (57, 58) relative to other tested strains. Similarly, FVB/NJ, SWR/J, and BTBRT+ strains exhibit low levels of hippocampus-dependent learning (35, 59–61). It should be noted that FVB/NJ and SWR/J strains possess a *Pde6b* gene mutation that leads to compromised visual acuity (62). However, work conducted by Bolivar et al. (36) indicated that retinal degeneration produced by this mutation did not impact contextual fear learning. Moreover, the C3H/HeJ strain shares a similar *Pde6b* mutation but displayed  $>20\%$  freezing, suggesting that factors outside of visual acuity contributed to the observed strain differences. Interestingly, the three strains with the lowest contextual fear learning also had the highest levels of dorsal hippocampus AChE activity. Low contextual fear conditioning in these strains may be explained in part by higher dorsal hippocampus AChE activity levels (discussed more below) as acetylcholine is critically involved in learning (63) but other differences could also contribute to the differences in fear conditioning.

In addition to contextual fear learning, we found significant between-strain variation in cued fear conditioning. Our results

indicate that the BTBRT+ strain exhibits poor cued fear conditioning (~21% freezing across trial), which is supported by other studies (64). BTBRT+ strain displays abnormal amygdala nuclei volume (65). Given the role of the amygdala in cued fear conditioning (39), it is possible that structural abnormalities within this region may account for the deficits reported here.

## Within-Dataset and Mouse Phenome Database Correlations

Strain mean correlations are useful for identifying potential relationships between the genetic influence of behavioral and biological outcomes. Here, we found that dorsal hippocampus AChE activity was significantly negatively correlated with freezing in all stages of fear conditioning except for baseline freezing. This finding suggests that genes that influence dorsal hippocampus AChE activity may contribute to variability in fear conditioning but not baseline levels of activity as assessed by freezing. Dong et al. (66) reported significant improvement in contextual fear conditioning in a mouse model of Alzheimer's disease following injections of AChE inhibitors physostigmine or donepezil. Moreover, nicotine withdrawal- and MK-801-induced deficits in contextual fear conditioning were prevented after administration of an AChE inhibitor (67–69). Notably, Csernansky et al. (67) observed inconsistent improvement in contextual fear conditioning via inhibition of AChE in saline-treated mice, suggesting that improvement in contextual fear conditioning via inhibition of AChE may be dependent on altered cholinergic signaling. The genetic association between dorsal hippocampus AChE activity and learning was further supported by our MPD analysis, which found that dorsal AChE activity strain means were positively correlated with the number of errors committed during the Barnes maze (see **Supplementary Table 1**), a hippocampus-dependent learning task. Qualitative support for this idea comes from the fact that the bottom three strains with the lowest freezing to the conditioned context (SWR/J, BTBRT+, and FVB/NJ) displayed the highest dorsal hippocampus AChE activity, indicating that enhanced AChE activity may impair contextual fear learning. Alternatively, it is possible that genetic differences in genes associated with AChE reflect or contribute to systemic alterations in cholinergic function, which is critical for learning (70, 71).

Both ventral hippocampus and cerebellum AChE activity failed to correlate with fear conditioning variables. Previous reports suggest that the dorsal and ventral hippocampus carry out distinct behavioral functions despite being a continuous anatomical structure (41). For instance, the dorsal hippocampus plays a role in spatial learning and memory (72, 73), whereas the ventral hippocampus is involved in emotional processing and stress responding (74). Although we did not examine more traditional behavioral paradigms of emotional processing (e.g., elevated plus maze or light dark box), strain mean correlations with external datasets in MPD indicated significant associations between ventral hippocampus AChE activity and behavioral

variables potentially representing emotional processing (see **Supplementary Table 2**). Interestingly, higher AChE activity in the ventral hippocampus was associated with greater frequency of urination and fecal boli in the light-dark box and elevated plus-maze. This suggests that increased AChE activity may predict greater levels of anxiety. It is worth noting that fear learning has emotional components and manipulation of ventral hippocampus functioning can influence fear learning (75). Moreover, recent findings from Giacomini et al. (76) suggest that inhibition of AChE via donepezil increases anxiety-like behavior in zebrafish in a dose-dependent manner. It is feasible that overlapping genes mediate ventral hippocampus AChE activity and anxiety-like behavior. However, the relationship between anxiety and AChE activity in the ventral hippocampus cannot be reliably surmised from the current data as there was no significant correlation with fear conditioning. Traditional measures of anxiety would need to be assessed to see if strain variability in the ventral hippocampus contributed to altered anxiety phenotypes.

## Limitations/Conclusions

The current study's goal was to examine genetic variation in fear conditioning, as well as AChE activity in the hippocampus and cerebellum. Our findings indicate that all five components of fear conditioning and AChE activity in three brain regions (dorsal and ventral hippocampus and cerebellum) significantly differed based on genetic background. Additionally, strain means correlational analysis found a negative relationship between the dorsal hippocampus AChE activity and fear conditioning, suggesting genetic variability in AChE activity contributes to differences in learning. While these findings have interesting implications for the role of AChE-related genetics in learning it is important to highlight their correlational nature. That is, the current study does not provide causal evidence that AChE differences may or may not be due to genetic differences. Future studies can also examine cholinergic markers in regions such as the amygdala, which is also importantly involved in fear conditioning (77). Additionally, correlations with publicly available datasets are limited by the number of overlapping strains. Moreover, it must be noted that all animals in the current study underwent surgical procedures, including osmotic minipump implantation (saline). Although animals were not subjected to drug exposure, it is possible that surgical stress may have influenced measured outcomes. Lastly, the scope of the current study is limited by using males only.

Collectively, our data provide further evidence that biological and behavioral outcomes are influenced by genetic background. Additionally, fear conditioning and dorsal hippocampus cholinergic signaling appear to be associated and mediated by common genetic factors. Additional research may help elucidate potential genetic targets influencing fear conditioning and AChE activity, as well as mechanisms possibly mediating the relationship between dorsal hippocampus AChE activity and fear conditioning.

## DATA AVAILABILITY STATEMENT

The original contributions presented in the study are included in the article/**Supplementary Material**, further inquiries can be directed to the corresponding author/s.

## ETHICS STATEMENT

The animal study was reviewed and approved by the Pennsylvania State University Institutional Animal and Care Use Committee.

## AUTHOR CONTRIBUTIONS

SM-L and DZ: conceptualization, data collection, analysis, and writing. PG-T and LS: data collection, analysis, and writing. MB: analysis and editing. SG: analysis. GP: funding and editing. TG: conceptualization, writing, editing, and funding. All authors contributed to the article and approved the submitted version.

## REFERENCES

- Fadda E, Cocco S, Stancampiano R. Hippocampal acetylcholine release correlates with spatial learning performance in freely moving rats. *Neuroreport*. (2000) 11:2265–9. doi: 10.1097/00001756-200007140-00040
- Takase K, Sakimoto Y, Kimura F, Mitsushima D. Developmental trajectory of contextual learning and 24-h acetylcholine release in the hippocampus. *Sci Rep*. (2014) 4:3738. doi: 10.1038/srep03738
- Anagnostaras SG, Maren S, Sage JR, Goodrich S, Fanselow MS. Scopolamine and Pavlovian fear conditioning in rats: dose-effect analysis. *Neuropsychopharmacology*. (1999) 21:731–44. doi: 10.1016/S0893-133X(99)00083-4
- Gale GD, Anagnostaras SG, Fanselow MS. Cholinergic modulation of pavlovian fear conditioning: effects of intrahippocampal scopolamine infusion. *Hippocampus*. (2001) 11:371–6. doi: 10.1002/hipo.1051
- Nakagawa Y, Takashima T. The GABA(B) receptor antagonist CGP36742 attenuates the baclofen- and scopolamine-induced deficit in morris water maze task in rats. *Brain Res*. (1997) 766:101–6. doi: 10.1016/S0006-8993(97)00529-5
- Gacar N, Mutlu O, Utkan T, Komsuoglu Celikyurt I, Gocmez SS, Ulak G. Beneficial effects of resveratrol on scopolamine but not mecamlamine induced memory impairment in the passive avoidance and morris water maze tests in rats. *Pharmacol Biochem Behav*. (2011) 99:316–23. doi: 10.1016/j.pbb.2011.05.017
- Rush DK. Scopolamine amnesia of passive avoidance: a deficit of information acquisition. *Behav Neural Biol*. (1988) 50:255–74. doi: 10.1016/S0163-1047(88)90938-7
- Dodart JC, Mathis C, Ungerer A. Scopolamine-induced deficits in a two-trial object recognition task in mice. *Neuroreport*. (1997) 8:1173–8. doi: 10.1097/00001756-199703240-00023
- Gould TJ, Wehner JM. Nicotine enhancement of contextual fear conditioning. *Behav Brain Res*. (1999) 102:31–9. doi: 10.1016/S0166-4328(98)00157-0
- Gould TJ, Lewis MC. Coantagonism of glutamate receptors and nicotinic acetylcholinergic receptors disrupts fear conditioning and latent inhibition of fear conditioning. *Learn Mem*. (2005) 12:389–98. doi: 10.1101/lm.89105
- Paoletti P, Bellone C, Zhou Q. NMDA receptor subunit diversity: impact on receptor properties, synaptic plasticity and disease. *Nat Rev Neurosci*. (2013) 14:383–400. doi: 10.1038/nrn3504
- Puma C, Deschaux O, Molimard R, Bizot JC. Nicotine improves memory in an object recognition task in rats. *Eur Neuropsychopharmacol*. (1999) 9:323–7. doi: 10.1016/S0924-977X(99)00002-4
- Ciamei A, Aversano M, Cestari V, Castellano C. Effects of MK-801 and nicotine combinations on memory consolidation in CD1 mice. *Psychopharmacology*. (2001) 154:126–30. doi: 10.1007/s002130000584
- Gould TJ, Wilkinson DS, Yildirim E, Blendy JA, Adoff MD. Dissociation of tolerance and nicotine withdrawal-associated deficits in contextual fear. *Brain Res*. (2014) 1559:1–10. doi: 10.1016/j.brainres.2014.02.038
- Andre JM, Leach PT, Gould TJ. Nicotine ameliorates NMDA receptor antagonist-induced deficits in contextual fear conditioning through high-affinity nicotinic acetylcholine receptors in the hippocampus. *Neuropharmacology*. (2011) 60:617–25. doi: 10.1016/j.neuropharm.2010.12.004
- Decker MW, Majchrzak MJ. Effects of systemic and intracerebroventricular administration of mecamlamine, a nicotinic cholinergic antagonist, on spatial memory in rats. *Psychopharmacology*. (1992) 107:530–4. doi: 10.1007/BF02245267
- O'dell TJ, Christensen BN. Mecamlamine is a selective non-competitive antagonist of N-methyl-D-aspartate- and aspartate-induced currents in horizontal cells dissociated from the catfish retina. *Neurosci Lett*. (1988) 94:93–8. doi: 10.1016/0304-3940(88)90276-5
- Snell LD, Johnson KM. Effects of nicotinic agonists and antagonists on N-methyl-D-aspartate-induced 3H-norepinephrine release and 3H-[1-(2-thienyl)cyclohexyl]-piperidine binding in rat hippocampus. *Synapse*. (1989) 3:129–35. doi: 10.1002/syn.890030204
- Mcdonough JH Jr, Shih TM. A study of the N-methyl-D-aspartate antagonistic properties of anticholinergic drugs. *Pharmacol Biochem Behav*. (1995) 51:249–53. doi: 10.1016/0091-3057(94)00372-P
- Soreq H, Seidman S. Acetylcholinesterase—new roles for an old actor. *Nat Rev Neurosci*. (2001) 2:294–302. doi: 10.1038/35067589
- Glick SD, Mittag TW, Green JP. Central cholinergic correlates of impaired learning. *Neuropharmacology*. (1973) 12:291–6. doi: 10.1016/0028-3908(73)90088-9
- Woodruff-Pak DS, Vogel III RW, Wenk GL. Galantamine: effect on nicotinic receptor binding, acetylcholinesterase inhibition, and learning. *Proc Natl Acad Sci USA*. (2001) 98:2089–94. doi: 10.1073/pnas.98.4.2089
- Ogura H, Kosasa T, Kuriya Y, Yamanishi Y. Comparison of inhibitory activities of donepezil and other cholinesterase inhibitors on acetylcholinesterase and butyrylcholinesterase *in vitro*. *Methods Find Exp Clin Pharmacol*. (2000) 22:609–13. doi: 10.1358/mf.2000.22.8.701373
- Wilkinson D, Murray J. Galantamine: a randomized, double-blind, dose comparison in patients with Alzheimer's disease. *Int J Geriatr Psychiatry*. (2001) 16:852–7. doi: 10.1002/gps.409

## FUNDING

This study was supported by the National Institutes of Health [T32GM108563 (LS), U01DA041632 (TG), F31DA049395 (DZ), and U01DA044399 (GP)], the Jean Phillips Shibley Endowment (TG), and Penn State University.

## ACKNOWLEDGMENTS

We would like to thank Sana Gadiwalla and Brendan Natwora for their technical assistance through the course of this study.

## SUPPLEMENTARY MATERIAL

The Supplementary Material for this article can be found online at: <https://www.frontiersin.org/articles/10.3389/fpsy.2021.737897/full#supplementary-material>

25. Howard R, Mcshane R, Lindesay J, Ritchie C, Baldwin A, Barber R, et al. Donepezil and memantine for moderate-to-severe Alzheimer's disease. *N Engl J Med*. (2012) 366:893–903. doi: 10.1056/NEJMoa1106668
26. Lockridge O, Norgren RBJr, Johnson RC, Blake TA. Naturally occurring genetic variants of human acetylcholinesterase and butyrylcholinesterase and their potential impact on the risk of toxicity from cholinesterase inhibitors. *Chem Res Toxicol*. (2016) 29:1381–92. doi: 10.1021/acs.chemrestox.6b00228
27. Reale M, Costantini E, Di Nicola M, D'angelo C, Franchi S, D'aurora M, et al. Butyrylcholinesterase and acetylcholinesterase polymorphisms in multiple sclerosis patients: implication in peripheral inflammation. *Sci Rep*. (2018) 8:1319. doi: 10.1038/s41598-018-19701-7
28. Valle AM, Radic Z, Rana BK, Mahboubi V, Wessel J, Shih PA, et al. Naturally occurring variations in the human cholinesterase genes: heritability and association with cardiovascular and metabolic traits. *J Pharmacol Exp Ther*. (2011) 338:125–33. doi: 10.1124/jpet.111.180091
29. Scacchi R, Gambina G, Moretto G, Corbo RM. Variability of AChE, BChE, and ChAT genes in the late-onset form of Alzheimer's disease and relationships with response to treatment with donepezil and rivastigmine. *Am J Med Genet B Neuropsychiatr Genet*. (2009) 150B:502–7. doi: 10.1002/ajmg.b.30846
30. Durkin T, Ayad G, Ebel A, Mandel P. Regional acetylcholine turnover rates in the brains of three inbred strains of mice: correlation with some interstrain behavioural differences. *Brain Res*. (1977) 136:475–86. doi: 10.1016/0006-8993(77)90072-5
31. Blaker WD, Cheney DL, Stoff DM. Interstrain comparison of avoidance behavior and neurochemical parameters of brain cholinergic function. *Pharmacol Biochem Behav*. (1983) 18:189–93. doi: 10.1016/0091-3057(83)90362-3
32. Matson LM, Lee-Stubbs RB, Cadieux CL, Koenig JA, Ardinger CE, Chandler J, et al. Assessment of mouse strain differences in baseline esterase activities and toxic response to sarin. *Toxicology*. (2018) 410:10–5. doi: 10.1016/j.tox.2018.08.016
33. Schwegler H, Boldyreva M, Linke R, Wu J, Zilles K, Crusio WE. Genetic variation in the morphology of the septo-hippocampal cholinergic and GABAergic systems in mice: II. Morpho-behavioral correlations. *Hippocampus*. (1996) 6:535–45. doi: 10.1002/(SICI)1098-1063(1996)6:5<535::AID-HIPO6>3.0.CO;2-H
34. Shaltiel G, Hanan M, Wolf Y, Barbash S, Kovalev E, Shoham S, et al. Hippocampal microRNA-132 mediates stress-inducible cognitive deficits through its acetylcholinesterase target. *Brain Struct Funct*. (2013) 218:59–72. doi: 10.1007/s00429-011-0376-z
35. Owen EH, Logue SF, Rasmussen DL, Wehner JM. Assessment of learning by the morris water task and fear conditioning in inbred mouse strains and F1 hybrids: implications of genetic background for single gene mutations and quantitative trait loci analyses. *Neuroscience*. (1997) 80:1087–99. doi: 10.1016/S0306-4522(97)00165-6
36. Bolivar VJ, Pooler O, Flaherty L. Inbred strain variation in contextual and cued fear conditioning behavior. *Mamm Genome*. (2001) 12:651–6. doi: 10.1007/s003350020039
37. Portugal GS, Wilkinson DS, Kenney JW, Sullivan C, Gould TJ. Strain-dependent effects of acute, chronic, and withdrawal from chronic nicotine on fear conditioning. *Behav Genet*. (2012) 42:133–50. doi: 10.1007/s10519-011-9489-7
38. Maren S. Neurobiology of pavlovian fear conditioning. *Annu Rev Neurosci*. (2001) 24:897–931. doi: 10.1146/annurev.neuro.24.1.897
39. Phillips RG, Ledoux JE. Differential contribution of amygdala and hippocampus to cued and contextual fear conditioning. *Behav Neurosci*. (1992) 106:274–85. doi: 10.1037/0735-7044.106.2.274
40. Hunsaker MR, Kesner RP. Dissociations across the dorsal-ventral axis of CA3 and CA1 for encoding and retrieval of contextual and auditory-cued fear. *Neurobiol Learn Mem*. (2008) 89:61–9. doi: 10.1016/j.nlm.2007.08.016
41. Fanselow MS, Dong HW. Are the dorsal and ventral hippocampus functionally distinct structures? *Neuron*. (2010) 65:7–19. doi: 10.1016/j.neuron.2009.11.031
42. Medina JF, Repa JC, Mauk MD, Ledoux JE. Parallels between cerebellum- and amygdala-dependent conditioning. *Nat Rev Neurosci*. (2002) 3:122–31. doi: 10.1038/nrn728
43. Smith AL, Corrow DJ. Modifications to husbandry and housing conditions of laboratory rodents for improved well-being. *ILAR J*. (2005) 46:140–7. doi: 10.1093/ilar.46.2.140
44. Bogue MA, Philip VM, Walton DO, Grubb SC, Dunn MH, Kolishovski G, et al. Mouse phenome database: a data repository and analysis suite for curated primary mouse phenotype data. *Nucleic Acids Res*. (2020) 48:D716–23. doi: 10.1093/nar/gkz1032
45. Keane TM, Goodstadt L, Danecek P, White MA, Wong K, Yalcin B, et al. Mouse genomic variation and its effect on phenotypes and gene regulation. *Nature*. (2011) 477:289–94. doi: 10.1038/nature10413
46. Kutlu MG, Ortega LA, Gould TJ. Strain-dependent performance in nicotine-induced conditioned place preference. *Behav Neurosci*. (2015) 129:37–41. doi: 10.1037/bne0000029
47. Palesch YY. Some common misperceptions about P values. *Stroke*. (2014) 45:e244–6. doi: 10.1161/STROKEAHA.114.006138
48. Nachmansohn DA, Manchado AL. The formation of acetylcholine. A new enzyme: "choline acetylase". *J Neurophysiol*. (1943) 6:397–403. doi: 10.1152/jn.1943.6.5.397
49. Oda Y. Choline acetyltransferase: the structure, distribution and pathologic changes in the central nervous system. *Pathol Int*. (1999) 49:921–37. doi: 10.1046/j.1440-1827.1999.00977.x
50. Lansdell SJ, Gee VJ, Harkness PC, Doward AI, Baker ER, Gibb AJ, et al. RIC-3 enhances functional expression of multiple nicotinic acetylcholine receptor subtypes in mammalian cells. *Mol Pharmacol*. (2005) 68:1431–8. doi: 10.1124/mol.105.017459
51. Millar NS. RIC-3: a nicotinic acetylcholine receptor chaperone. *Br J Pharmacol*. (2008) 153 (Suppl. 1):S177–83. doi: 10.1038/sj.bjp.0707661
52. Darvesh S, Hopkins DA, Geula C. Neurobiology of butyrylcholinesterase. *Nat Rev Neurosci*. (2003) 4:131–8. doi: 10.1038/nrn1035
53. Marubio LM, Paylor R. Impaired passive avoidance learning in mice lacking central neuronal nicotinic acetylcholine receptors. *Neuroscience*. (2004) 129:575–82. doi: 10.1016/j.neuroscience.2004.09.003
54. Nie T, Abel T. Fear conditioning in inbred mouse strains: an analysis of the time course of memory. *Behav Neurosci*. (2001) 115:951–6. doi: 10.1037/0735-7044.115.4.951
55. March A, Borchelt D, Golde T, Janus C. Differences in memory development among C57BL/6NcrJ, 129S2/SvPasCrl, and FVB/NCrJ mice after delay and trace fear conditioning. *Comp Med*. (2014) 64:4–12.
56. Brown RE, Wong AA. The influence of visual ability on learning and memory performance in 13 strains of mice. *Learn Mem*. (2007) 14:134–44. doi: 10.1101/lm.473907
57. Balogh SA, Wehner JM. Inbred mouse strain differences in the establishment of long-term fear memory. *Behav Brain Res*. (2003) 140:97–106. doi: 10.1016/S0166-4328(02)00279-6
58. Keum S, Park J, Kim A, Park J, Kim KK, Jeong J, et al. Variability in empathic fear response among 11 inbred strains of mice. *Genes Brain Behav*. (2016) 15:231–42. doi: 10.1111/gbb.12278
59. Mineur YS, Crusio WE. Behavioral and neuroanatomical characterization of FVB/N inbred mice. *Brain Res Bull*. (2002) 57:41–7. doi: 10.1016/S0304-7230(01)00635-9
60. Macpherson P, McGaffigan R, Wahlsten D, Nguyen PV. Impaired fear memory, altered object memory and modified hippocampal synaptic plasticity in split-brain mice. *Brain Res*. (2008) 1210:179–88. doi: 10.1016/j.brainres.2008.03.008
61. Szklarczyk K, Korostynski M, Cieslak PE, Wawrzczak-Bargiela A, Przewlocki R. Opioid-dependent regulation of high and low fear responses in two inbred mouse strains. *Behav Brain Res*. (2015) 292:95–101. doi: 10.1016/j.bbr.2015.06.001
62. Van Wyk M, Schneider S, Kleinlogel S. Variable phenotypic expressivity in inbred retinal degeneration mouse lines: a comparative study of C3H/HeOu and FVB/N rd1 mice. *Mol Vis*. (2015) 21:811–27.
63. Wilson MA, Fadel JR. Cholinergic regulation of fear learning and extinction. *J Neurosci Res*. (2017) 95:836–52. doi: 10.1002/jnr.23840
64. Yang M, Abrams DN, Zhang JY, Weber MD, Katz AM, Clarke AM, et al. Low sociability in BTBR T+tf/J mice is independent of partner strain. *Physiol Behav*. (2012) 107:649–62. doi: 10.1016/j.physbeh.2011.12.025
65. Mercier F, Kwon YC, Douet V. Hippocampus/amygdala alterations, loss of heparan sulfates, fractones and ventricle wall reduction in adult BTBR

- T+ tf/J mice, animal model for autism. *Neurosci Lett.* (2012) 506:208–13. doi: 10.1016/j.neulet.2011.11.007
66. Dong H, Csernansky CA, Martin MV, Bertchume A, Vallera D, Csernansky JG. Acetylcholinesterase inhibitors ameliorate behavioral deficits in the Tg2576 mouse model of Alzheimer's disease. *Psychopharmacology.* (2005) 181:145–52.
  67. Csernansky JG, Martin M, Shah R, Bertchume A, Colvin J, Dong H. Cholinesterase inhibitors ameliorate behavioral deficits induced by MK-801 in mice. *Neuropsychopharmacology.* (2005) 30:2135–43. doi: 10.1038/sj.npp.1300761
  68. Wilkinson DS, Gould TJ. The effects of galantamine on nicotine withdrawal-induced deficits in contextual fear conditioning in C57BL/6 mice. *Behav Brain Res.* (2011) 223:53–7. doi: 10.1016/j.bbr.2011.04.010
  69. Poole RL, Connor DA, Gould TJ. Donepezil reverses nicotine withdrawal-induced deficits in contextual fear conditioning in C57BL/6J mice. *Behav Neurosci.* (2014) 128:588–93. doi: 10.1037/bne0000003
  70. Francis PT, Palmer AM, Snape M, Wilcock GK. The cholinergic hypothesis of Alzheimer's disease: a review of progress. *J Neurol Neurosurg Psychiatry.* (1999) 66:137–47. doi: 10.1136/jnnp.66.2.137
  71. Nakagawasai O. Behavioral and neurochemical alterations following thiamine deficiency in rodents: relationship to functions of cholinergic neurons. *Yakugaku Zasshi.* (2005) 125:549–54. doi: 10.1248/yakushi.125.549
  72. Moser MB, Moser EI, Forrest E, Andersen P, Morris RG. Spatial learning with a minislab in the dorsal hippocampus. *Proc Natl Acad Sci USA.* (1995) 92:9697–701. doi: 10.1073/pnas.92.21.9697
  73. Pothuizen HH, Zhang WN, Jongen-Relo AL, Feldon J, Yee BK. Dissociation of function between the dorsal and the ventral hippocampus in spatial learning abilities of the rat: a within-subject, within-task comparison of reference and working spatial memory. *Eur J Neurosci.* (2004) 19:705–12. doi: 10.1111/j.0953-816X.2004.03170.x
  74. Kjelstrup KG, Tuvnes FA, Steffenach HA, Murison R, Moser EI, Moser MB. Reduced fear expression after lesions of the ventral hippocampus. *Proc Natl Acad Sci USA.* (2002) 99:10825–30. doi: 10.1073/pnas.152112399
  75. Sierra-Mercado D, Padilla-Coreano N, Quirk GJ. Dissociable roles of prefrontal and infralimbic cortices, ventral hippocampus, and basolateral amygdala in the expression and extinction of conditioned fear. *Neuropsychopharmacology.* (2011) 36:529–38. doi: 10.1038/npp.2010.184
  76. Giacomini AC, Bueno BW, Marcon L, Scolari N, Genario R, Demin KA, et al. An acetylcholinesterase inhibitor, donepezil, increases anxiety and cortisol levels in adult zebrafish. *J Psychopharmacol.* (2020) 34:1449–56. doi: 10.1177/0269881120944155
  77. Jiang L, Kundu S, Lederman JD, Lopez-Hernandez GY, Ballinger EC, Wang S, et al. Cholinergic signaling controls conditioned fear behaviors and enhances plasticity of cortical-amygdala circuits. *Neuron.* (2016) 90:1057–70. doi: 10.1016/j.neuron.2016.04.028

**Conflict of Interest:** The authors declare that the research was conducted in the absence of any commercial or financial relationships that could be construed as a potential conflict of interest.

**Publisher's Note:** All claims expressed in this article are solely those of the authors and do not necessarily represent those of their affiliated organizations, or those of the publisher, the editors and the reviewers. Any product that may be evaluated in this article, or claim that may be made by its manufacturer, is not guaranteed or endorsed by the publisher.

Copyright © 2021 Mooney-Leber, Zeid, Garcia-Trevizo, Seemiller, Bogue, Grubb, Peltz and Gould. This is an open-access article distributed under the terms of the Creative Commons Attribution License (CC BY). The use, distribution or reproduction in other forums is permitted, provided the original author(s) and the copyright owner(s) are credited and that the original publication in this journal is cited, in accordance with accepted academic practice. No use, distribution or reproduction is permitted which does not comply with these terms.



# Genetic Modifiers of Oral Nicotine Consumption in *Chrna5* Null Mutant Mice

Erin Meyers<sup>1†</sup>, Zachary Werner<sup>1†</sup>, David Wichman<sup>1</sup>, Hunter L. Mathews<sup>1</sup>, Richard A. Radcliffe<sup>2</sup>, Joseph H. Nadeau<sup>3</sup> and Jerry A. Stitzel<sup>1,4\*</sup>

<sup>1</sup> Institute for Behavioral Genetics, University of Colorado Boulder, Boulder, CO, United States, <sup>2</sup> Skaggs School of Pharmacy and Pharmaceutical Sciences, University of Colorado Anschutz Medical Campus, Aurora, CO, United States, <sup>3</sup> Maine Medical Center Research Institute, Scarborough, ME, United States, <sup>4</sup> Department of Integrative Physiology, University of Colorado Boulder, Boulder, CO, United States

## OPEN ACCESS

### Edited by:

Gary T. Hardiman,  
Queen's University Belfast,  
United Kingdom

### Reviewed by:

Maochun Wang,  
The Affiliated Hospital of Nanjing  
University Medical School, China  
Nicole Hawkins,  
Northwestern Medicine, United States

### \*Correspondence:

Jerry A. Stitzel  
Jerry.Stitzel@colorado.edu

<sup>†</sup>These authors have contributed  
equally to this work

### Specialty section:

This article was submitted to  
Psychopharmacology,  
a section of the journal  
Frontiers in Psychiatry

**Received:** 09 September 2021

**Accepted:** 07 October 2021

**Published:** 04 November 2021

### Citation:

Meyers E, Werner Z, Wichman D,  
Mathews HL, Radcliffe RA,  
Nadeau JH and Stitzel JA (2021)  
Genetic Modifiers of Oral Nicotine  
Consumption in *Chrna5* Null Mutant  
Mice. *Front. Psychiatry* 12:773400.  
doi: 10.3389/fpsy.2021.773400

The gene *CHRNA5* is strongly associated with the level of nicotine consumption in humans and manipulation of the expression or function of *Chrna5* similarly alters nicotine consumption in rodents. In both humans and rodents, reduced or complete loss of function of *Chrna5* leads to increased nicotine consumption. However, the mechanism through which decreased function of *Chrna5* increases nicotine intake is not well-understood. Toward a better understanding of how loss of function of *Chrna5* increases nicotine consumption, we have initiated efforts to identify genetic modifiers of *Chrna5* deletion-dependent oral nicotine consumption in mice. For this, we introgressed the *Chrna5* knockout (KO) mutation onto a panel of C57BL/6J-Chr#<sup>A/J</sup>/NAJ chromosome substitution strains (CSS) and measured oral nicotine consumption in 18 CSS and C57BL/6 (B6) mice homozygous for the *Chrna5* KO allele as well as their *Chrna5* wild type littermates. As expected, nicotine consumption was significantly increased in *Chrna5* KO mice relative to *Chrna5* wildtype mice on a B6 background. Among the CSS homozygous for the *Chrna5* KO allele, several exhibited altered nicotine consumption relative to B6 *Chrna5* KO mice. Sex-independent modifiers were detected in CSS possessing A/J chromosomes 5 and 11 and a male-specific modifier was found on chromosome 15. In all cases nicotine consumption was reduced in the CSS *Chrna5* KO mice relative to B6 *Chrna5* KO mice and consumption in the CSS KO mice was indistinguishable from their wild type littermates. Nicotine consumption was also reduced in both *Chrna5* KO and wildtype CSS mice possessing A/J chromosome 1 and increased in both KO and wild type chromosome 17 CSS relative to KO and wild type B6 mice. These results demonstrate the presence of several genetic modifiers of nicotine consumption in *Chrna5* KO mice as well as identify loci that may affect nicotine consumption independent of *Chrna5* genotype. Identification of the genes that underlie the altered nicotine consumption may provide novel insight into the mechanism through which *Chrna5* deletion increases nicotine consumption and, more generally, a better appreciation of the neurobiology of nicotine intake.

**Keywords:** chromosome substitution strains, two-bottle choice, nicotinic acetylcholine receptor, mapping, knockout

## INTRODUCTION

It has become evident that nicotinic acetylcholine receptors (nAChRs) that contain the  $\alpha 5$  subunit play a critical role in the risk for nicotine dependence. Human studies repeatedly have found an association between genetic variants in *CHRNA5*, the gene that codes for the nAChR  $\alpha 5$  subunit, nicotine dependence and other nicotine dependence relevant phenotypes (1–7). In fact, a recent genome-wide meta-analysis reported that a missense (amino acid changing) SNP in *CHRNA5* (rs16969968) exhibited the strongest association with cigarettes per day of all tested SNPs ( $P = 1.2 \times 10^{-278}$ ) (7).

Studies in rodents further support the role of *Chrna5* in nicotine-related behaviors. For example, a few early studies demonstrated that *Chrna5* played a role in sensitivity to the acute effects on nicotine in mice (8, 9). More recent studies using rodent models have provided further insight into the role of *Chrna5* in nicotine dependence. For example, Fowler et al. (10) found that *Chrna5* knockout (KO) mice, unlike wildtype controls, did not reduce their responding for i.v. nicotine self-administration as the unit dose increased. At the highest nicotine dose tested, *Chrna5* KO mice self-administered five times more nicotine than did their wildtype controls. Similarly, Jackson et al. (11) reported that *Chrna5* KO mice exhibited conditioned place preference at higher doses of nicotine than did wildtype controls and Wilking and Stitzel (12) as well as Bagdas et al. (13) showed that *Chrna5* KO mice consume more nicotine via oral administration, especially at higher nicotine concentrations, relative to wildtype littermates.

It is important to note that the non-synonymous mutation in *CHRNA5* that is highly associated with increased risk for nicotine use, including nicotine consumption, in humans leads to a reduction in function of  $\alpha 5$ -containing nAChRs (3, 14–17). In other words, reduced function of  $\alpha 5$ -containing nAChRs is associated with various measures of nicotine use in humans, including increased nicotine consumption, and increased nicotine self-administration and reward in rodents. The sum of these studies suggests that understanding the molecular mechanism through which reduced/loss of function of *Chrna5* leads to increased nicotine consumption may lead to a better understanding of the neurobiology of nicotine use.

One approach that can be used to gain insight into the mechanism through which loss of function of *Chrna5* increases nicotine consumption is to identify genetic modifiers of the increased nicotine consumption caused by *Chrna5* deletion in mice. In essence, a modifier gene is a gene that has one or more alleles that suppresses, enhances or in some other way alters the outcome of an allele or alleles of another gene known to have a phenotypic effect (in this case *Chrna5* deletion increasing nicotine consumption) often without having a measurable effect on the phenotype itself (18, 19). Presumably, modifier genes work by altering a molecular process that is essential for producing the phenotype caused by the allele of the target gene. As a result, the identification of modifier genes can provide novel insight into the underlying molecular processes important for producing the target gene-dependent phenotype. Although there are many approaches to identify genetic modifiers, we utilized

a panel of chromosome substitution strains (CSS) to provide evidence for the existence of modifiers of *Chrna5* KO-dependent nicotine consumption. Chromosome substitution strains (CSS) are a panel of strains that share a common genetic background but differ from one another for a single whole chromosome that comes from a donor strain. A full panel of mouse CSS consists of twenty-two strains, one strain for each of the 19 donor strain autosomes, one each for the donor strain sex chromosomes and one strain harboring the mitochondrial genome from the donor strain [for a review of CSS see (20, 21)]. By parsing the donor strain genome into single chromosomes on the host genome background, CSS have proven to be a very powerful tool for identifying and mapping quantitative trait loci (QTL) (22).

To utilize the CSS to identify chromosomes that harbor modifiers that alter the effect of *Chrna5* deletion on nicotine consumption, we bred the *Chrna5* KO allele into the panel of C57BL/6J-Chr#<sup>A/J</sup>/NaJ CSS (23). For this CSS panel, the host background strain is C57BL/6J (B6), an inbred strain that consumes the most nicotine relative to other tested strains, and the donor strain is A/J, a strain that is amongst the lowest nicotine consuming strains (24, 25). Following introgression of the *Chrna5* KO allele onto the panel of C57BL/6J-Chr#<sup>A/J</sup>/NaJ CSS, oral nicotine consumption was measured in each CSS and the B6 reference strain. Both wildtype and *Chrna5* KO mice from each CSS and B6 were tested in order to identify A/J chromosomes possessing modifiers of *Chrna5* KO-dependent an independent nicotine consumption.

## MATERIALS AND METHODS

### Animals

#### Housing Conditions

All housing and experimental conditions for the mice utilized in this study were approved by the Institutional Animal Care and Utilization Committee (IACUC) at the University of Colorado Boulder and were compliant with the guidelines for animal care and use mandated by the NIH and the Guide for the Care and Use of Laboratory Animals (8th Ed.). Mice were maintained on a standard 12 h light/dark cycle (lights on at 07:00), and food (Envigo Teklad 2914 irradiated rodent diet, Harlan, Madison, WI) and water were available *ad libitum*.

#### Generation of CSS<sup>Chrna5KO</sup> Strains

Chromosome substitution strains C57BL/6J-Chr#<sup>A/J</sup>/NaJ (20, 23), hereafter referred to as CSS, for all chromosomes except Y and the mitochondrial genome, were purchased from the Jackson Laboratory (JAX, Bar Harbor, Maine) and imported to the University of Colorado Boulder. The JAX strain IDs for the CSS are continuous from #004379 to #004398. *Chrna5* null mutant mice were originally obtained from Dr. Mariella de Biasi (9) (MGI:3040917) and have been maintained on a C57BL/6J (B6) background at the University of Colorado Boulder for over 20 years. To minimize genetic drift for mice in our colony that are maintained on a B6 background, new JAX C57BL/6J mice (strain #000664) have been introduced into the University of Colorado Boulder vivarium every 2–3 years. The *Chrna5* null mutation was introgressed into each of the CSS strains using a multi-step

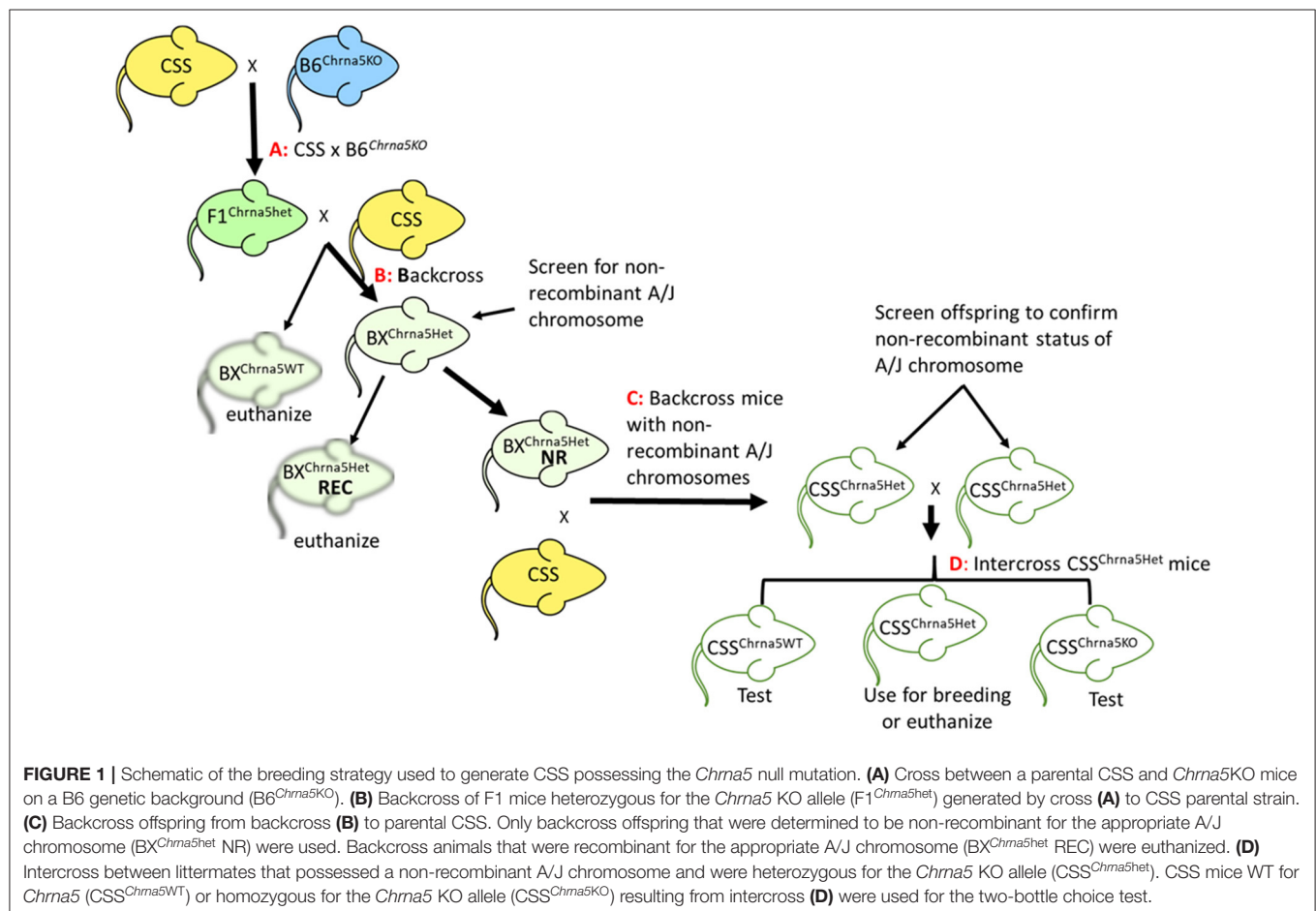
process (**Figure 1**). Initially, each CSS was crossed to B6<sup>Chrna5KO</sup> mice. These mice were then backcrossed to the appropriate parental CSS strain. Offspring of this backcross that were heterozygous for the *Chrna5* null mutation were then screened for the strain-specific non-recombinant A/J chromosome using a series of SNP alleles (see **Supplementary Table 1** for all SNPs used for screening). SNP genotyping was performed by CD Genomics (Shirley NY). Of note, screening the CSS parental strains (prior to any backcrossing) identified 10 SNPs that were homozygous for a B6 allele suggesting incomplete introgression of the A/J chromosome. Six of these SNPs were located near the centromere or telomere of the introgressed chromosome indicating some residual B6 chromosome appears to be present on a few A/J chromosomes (1, 11, 15, 16, 17, and X). Four of these centromeric/telomeric SNPs are in regions previously reported to exhibit incomplete introgression of the A/J chromosome (26). Of the four non-centromeric, non-telomeric SNPs, two have conflicting genotype information and the remaining two SNPs have not been evaluated in more than a handful of strains. Therefore, any interpretation from these SNPs should be done with caution.

Following SNP screening, a minimum of five mice per CSS that were verified as possessing a non-recombinant A/J chromosome and heterozygous for the *Chrna5* null mutation

were then backcrossed again to the parental CSS strain and offspring were again genotyped to verify the non-recombinant status of the A/J chromosome. Offspring of this cross that were heterozygous for the *Chrna5* null mutation were then intercrossed to produce wildtype (WT), heterozygous and homozygous mutant mice. Initial litters of these mice were also screened to verify non-recombinant status of the appropriate A/J chromosome. Only WT and homozygous mutant mice (CSS<sup>#Chrna5KO</sup>) were used for phenotypic assessments. Of the 20 CSS, CSS4, and CSS13 did not breed well so insufficient animals were produced for testing. In addition, *Chrna5* is located on chromosome 9 and we were not able to introgress the region of chromosome 9 centromeric to *Chrna5* into a CSS. Therefore, chromosome 9 from the CSS9<sup>Chrna5KO</sup> line only has been introgressed for the A/J chromosome telomeric to *Chrna5*.

## Two-Bottle Choice Test (2BCT)

Both female and male WT and null mutant mice were tested. The mice were tested between 3 and 6 months of age. Two weeks prior to starting the 2BCT, mice were moved from ventilated cage racks and housed in standard static cages. This 2-week acclimation period was necessary for the mice to adjust to using water bottles with sipper tubes since their water source in the ventilated cages was a hydropac (Lab Products LLC, Seaford, DE).



Preliminary experiments indicated that without this acclimation period to adjust to sipper tubes, 2BCT results were inconsistent. Following the 2-week acclimation period, mice were individually housed and provided 2 glass tubes (PYREX™ 150 mm reusable Borosilicate Glass Tubes, Thermo-Fisher) filled with tap water and fitted with standard ball bearing-free sipper tubes. After 4 days, the tubes were replaced with one tube containing water and the other containing water supplemented with 100 µg/ml nicotine free base (Sigma Aldrich, St. Louis, MO). Four days later, the nicotine concentration was increased to 200 µg/ml and 4 days after that, the nicotine concentration was increased to 300 µg/ml. After an additional 4 days, the experiment was terminated and the animals were euthanized. Throughout the experiment, bottles were rotated daily to minimize any side preference shown by the mice and mice were weighed at the beginning and end of each 4-day period. Fresh tubes and solutions were used for each 4-day testing period. To estimate fluid consumption, tubes were weighed at the beginning and end of each 4-day period or more frequently if the fluid levels needed to be replenished before the end of any given test period. Two cages with tubes but no mice were used to estimate fluid loss due to evaporation, tube rotation and cage handling. The average fluid loss from these “dummy” cages was subtracted from the fluid amount measured from the experimental cages to correct for non-specific fluid loss.

### Data Analysis

All statistical analyses were performed in SPSS version 27 or Graphpad Prism version 9. Because a mixed model ANOVA analysis detected main effects of both strain and sex on total fluid consumed and average weight across each of the 4-day consumption trials, the measure that was used to assess nicotine consumption was µg of nicotine consumed per ml of total fluid consumed (µg/ml). The µg/ml measure of nicotine consumption eliminates any bias caused by differences in fluid consumption between strain or sex by normalizing nicotine intake to per ml of fluid consumed and also eliminates weight as a factor in the intake calculation. For analyses involving repeated measures, a mixed model ANOVA was utilized that included nicotine concentration as a within subject factor and *Chrna5* genotype, sex and strain as between subject factors. For non-repeated measures, a multi-factorial General Linear Model was used. For both types of analysis, initial analyses for the main effects of sex and strain were performed. Because main effects of sex and strain were observed for all measures, each strain was assessed for sex differences and if sex differences were detected, *Chrna5* genotype was analyzed separately by sex. When no effect of sex was detected for a strain, *Chrna5* genotype analyses were collapsed on sex.

Within-*Chrna5* genotype analyses also were performed separately in *Chrna5* WT and *Chrna5* null mutant mice to assess whether nicotine consumption differed between each CSS strain and the relevant reference B6 strain (B6 WT for CSS WT and B6<sup>*Chrna5KO*</sup> for CSS<sup>*Chrna5KO*</sup>). Total µg/ml of nicotine consumed was analyzed via a multi-factorial ANOVA of sex and strain. Welch's ANOVA was used for all subsequent one-way analyses. For those strains in which a main effect of sex was observed, data were assessed and reported separately by sex, otherwise

analyses were collapsed on sex. A false discovery rate (FDR) (27) of 0.05 was used to identify CSS that significantly differed from the relevant B6 reference strain.

## RESULTS

In order to screen for potential genetic modifiers that alter the effect of *Chrna5* deletion on oral nicotine intake, the *Chrna5* null mutation was introgressed onto a panel of 20 B6 x A/J chromosome substitution strains (CSS) (20, 23) as described in the methods. These *Chrna5* null mutant-harboring strains are designated as CSS<sup>*Chrna5KO*</sup>. Due to poor breeding, two of the CSS, CSS4 and CSS13, were excluded from the study.

Because the most common measure used to assess oral nicotine intake is dose and dose is dependent upon the amount of fluid intake as well as the weight of the mice, the CSS panel was assessed for whether there was a main effect of strain on either fluid intake or animal body weight across the study. Results indicated main effects of strain on both fluid consumption [ $F_{(18, 919)} = 24.58, P = 2.58 \times 10^{-66}$ ] and body weight [ $F_{(18, 919)} = 21.75, P = 2.59 \times 10^{-61}$ ], respectively. Therefore, the main measure we used to assess nicotine consumption was µg of nicotine consumed per ml of total fluid drank (µg/ml) which should minimize any confound caused by strain-dependent differences in total fluid intake and weight.

To confirm that *Chrna5* genotype impacts nicotine consumption as previously reported (12, 13), female and male B6 background mice that were homozygous for the *Chrna5* null mutation as well as their wildtype (WT) littermates were tested in an ascending two-bottle choice test for oral nicotine consumption at nicotine concentrations 100, 200, and 300 µg/ml. Results (Table 1 and Figures 2A–C) confirmed a main effect of *Chrna5* genotype on nicotine consumption on a B6 background ( $P = 0.003$ ) with *Chrna5* null mutant mice consuming significantly more nicotine than WT mice. There was no main effect of sex and no genotype by sex interaction. Examination of the entire population of tested CSS mice (Table 1 and Figures 2D–F) also indicated a main effect of genotype ( $P = 5.9 \times 10^{-20}$ ) as well as sex ( $P = 1.6 \times 10^{-10}$ ) but no genotype x sex interaction. Consistent with B6 background mice, CSS mice harboring the *Chrna5* null mutation, on average, consuming more nicotine than CSS mice that were WT for *Chrna5*.

After confirming that *Chrna5* genotype impacts nicotine intake in the CSS, it was then determined whether individual strain impacted nicotine consumption and/or the effect of *Chrna5* genotype on consumption. In order to simplify the phenotype, total µg/ml of nicotine consumed across the experiment (the sum of nicotine consumed at 100, 200, and 300 µg/ml) was used for the analysis. For total µg/ml of nicotine consumed, main effects of strain ( $P = 5.02 \times 10^{-35}$ ), genotype ( $P = 1.88 \times 10^{-25}$ ) and sex ( $P = 2.33 \times 10^{-12}$ ) as well as a strain x genotype interaction ( $P = 0.006$ ) were observed (Table 1).

The significant strain x genotype interaction on nicotine intake suggests the possibility of strain-specific modifiers that alter the effect of *Chrna5* deletion on nicotine consumption. Because the main goal of this study is to identify CSS that harbor

**TABLE 1** | Statistics for population comparisons.

Population tested	<i>Chrna5</i> genotype	Sex	Genotype x sex interaction	Strain	Strain x genotype interaction
B6	$F_{(1, 49)} = 9.81$ , $P = 0.003$	$F_{(1, 49)} = 0.792$ , $P = 0.378$	$F_{(1, 49)} = 0.099$ , $P = 0.754$	NA	NA
CSS collapsed on strain	$F_{(1, 900)} = 87.72$ , $P = 5.9 \times 10^{-20}$	$F_{(1, 900)} = 41.85$ , $P = 1.6 \times 10^{-10}$	$F_{(1, 900)} = 0.772$ , $P = 0.380$	NA	NA
CSS by strain	$F_{(1, 832)} = 116.2$ , $P = 1.88 \times 10^{-25}$	$F_{(1, 832)} = 50.71$ , $P = 2.33 \times 10^{-12}$	$F_{(1, 832)} = 0.949$ , $P = 0.330$	$F_{(17, 832)} = 13.82$ , $P = 5.02 \times 10^{-35}$	$F_{(17, 832)} = 2.02$ , $P = 0.006$
B6 vs. CSS <i>Chrna5</i> KO genotype	NA	$F_{(1, 18)} = 24.29$ , $P = 1 \times 10^{-6}$	NA	$F_{(1, 18)} = 8.13$ , $P = 1.1 \times 10^{-18}$	NA
B6 vs. CSS <i>Chrna5</i> WT genotype	NA	$F_{(1, 18)} = 29.22$ , $P = 1.1 \times 10^{-7}$	NA	$F_{(1, 18)} = 5.93$ , $P = 6.7 \times 10^{-13}$	NA

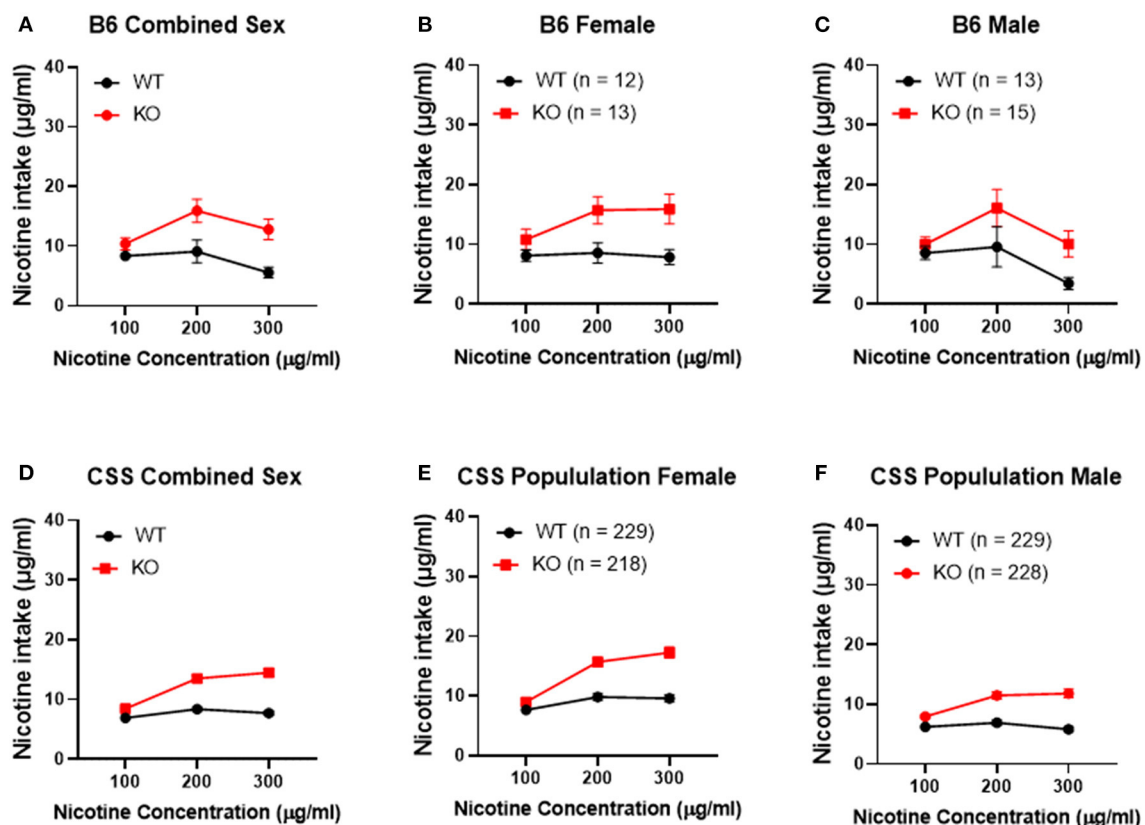
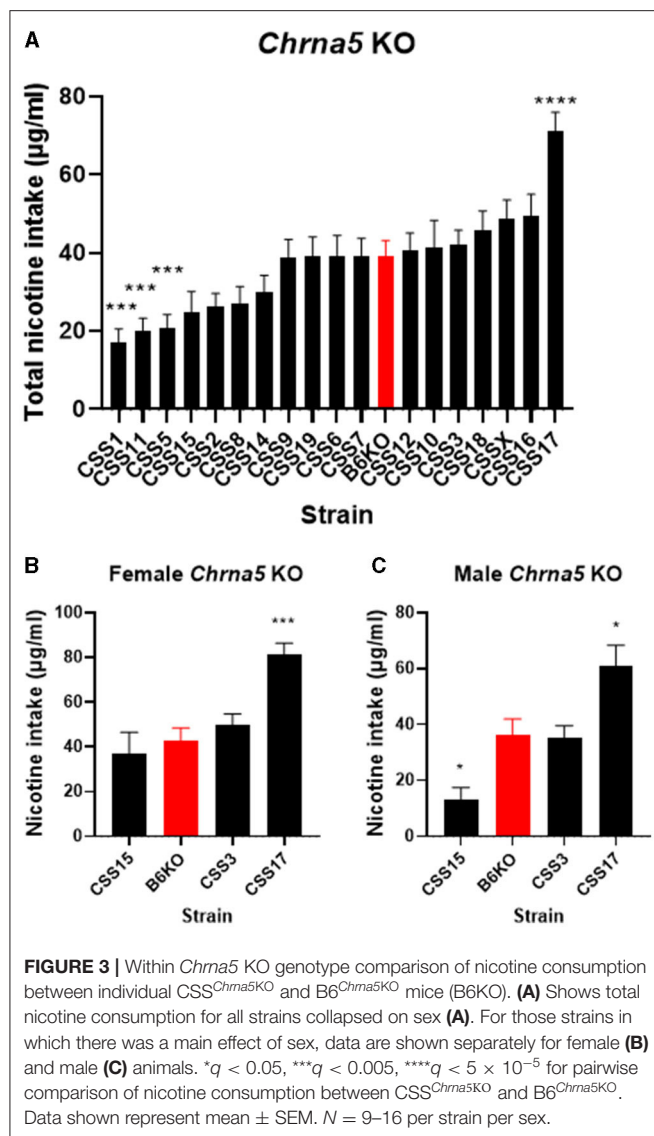


**FIGURE 2** | Effect of *Chrna5* genotype on nicotine consumption in B6 and chromosome substitution strain (CSS) mice. Deletion of *Chrna5* leads to increased nicotine consumption in B6 background mice ( $P = 0.003$ ). Although no main effect of sex was observed in B6 mice, combined sex (A) as well as data for each sex [female (B) and male (C)] are shown for comparison. For the entire population of CSS mice, there is a main effect of *Chrna5* genotype as well as a main effect of sex. The impact of *Chrna5* genotype collapsed on sex (D) and in female CSS (E) ( $P = 1.76 \times 10^{-10}$ ) and male CSS (F) ( $P = 3.43 \times 10^{-11}$ ) is shown. Data represent mean  $\pm$  SEM.

modifiers of the effect of *Chrna5* deletion on nicotine intake, the level of nicotine consumption in each CSS homozygous for the *Chrna5* null mutation (CSS<sup>*Chrna5*KO</sup>) was compared to B6 mice homozygous for the null mutation (B6<sup>*Chrna5*KO</sup>) in a within genotype analysis (Table 1 and Figure 3). Initial analysis indicated main effects of strain ( $P = 1.1 \times 10^{-18}$ ) and sex ( $P = 1 \times 10^{-6}$ ). Due to the main effect of sex, the CSS<sup>*Chrna5*KO</sup>

strains were individually assessed for the effect of sex on nicotine intake (Table 2). Of the 18 CSS<sup>*Chrna5*KO</sup> strains, only three, CSS3<sup>*Chrna5*KO</sup>, CSS15<sup>*Chrna5*KO</sup> and CSS17<sup>*Chrna5*KO</sup>, exhibited sex-dependent differences in nicotine intake. Therefore, these three strains were assessed separately by sex while the remaining strains were collapsed on sex for analysis. Among the CSS<sup>*Chrna5*KO</sup> with no main effect of sex, pairwise comparisons between



B6<sup>Chrna5KO</sup> mice and each CSS<sup>Chrna5KO</sup> strain using an FDR = 0.05 indicated that CSS1<sup>Chrna5KO</sup> ( $q < 0.005$ ), CSS5<sup>Chrna5KO</sup> ( $q < 0.005$ ), and CSS11<sup>Chrna5KO</sup> ( $q < 0.005$ ) consumed less nicotine than did B6<sup>Chrna5KO</sup> mice (Figure 3A). Due to the discovery nature of this study, the FDR threshold was raised to 0.1 to identify suggestive differences. However, no additional strains were detected with this elevated threshold. For the strains with a main effect of sex, nicotine consumption in CSS3<sup>Chrna5KO</sup> mice did not differ from B6<sup>Chrna5KO</sup> mice for either sex while nicotine consumption in CSS15<sup>Chrna5KO</sup> mice was reduced compared to B6<sup>Chrna5KO</sup> in males but not females (female  $q > 0.05$ ; male  $q < 0.05$ ) and increased relative to B6<sup>Chrna5KO</sup> for both sexes in CSS17<sup>Chrna5KO</sup> mice (female  $q < 0.005$ ; male  $q < 0.05$ ) (Figures 3B,C). Increasing the FDR to 0.1 did not identify any additional strains with suggestive sex-dependent effects.

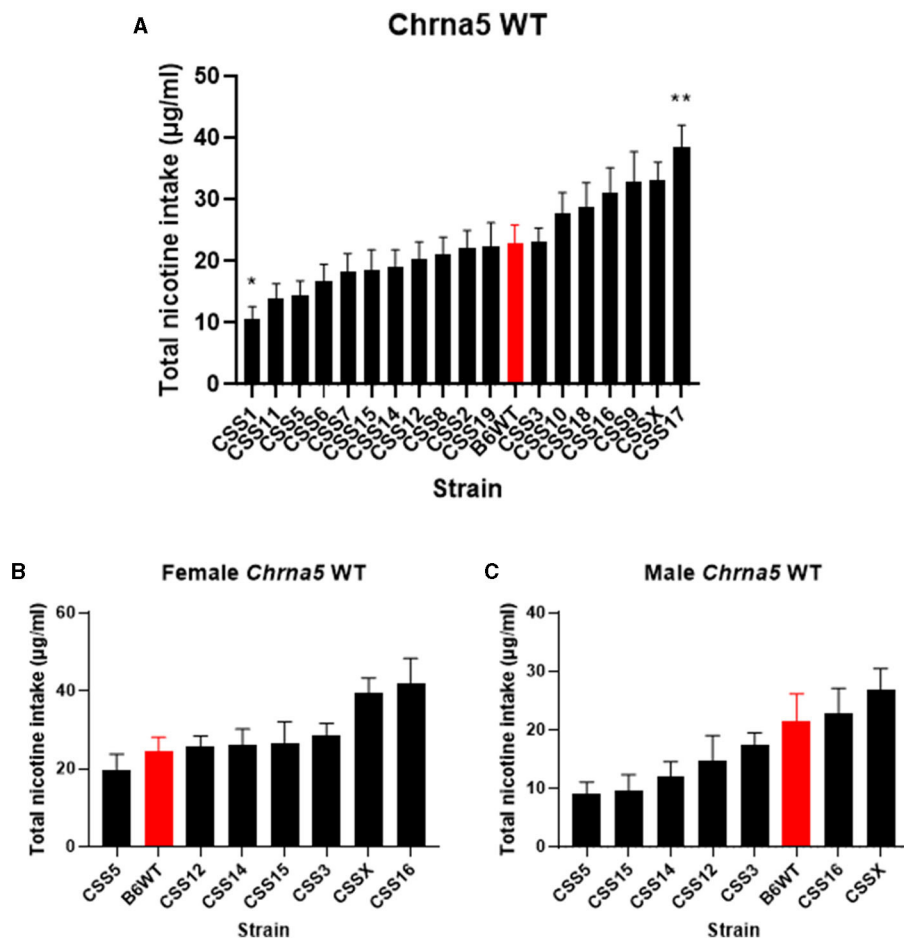
The effect of the individual CSS on nicotine intake in mice homozygous for the *Chrna5* null mutation could be specific to

**TABLE 2 |** Within *Chrna5* genotype analysis of sex effects.

Strain	Main effect of sex in <i>Chrna5</i> KO mice	Main effect of sex in <i>Chrna5</i> WT mice
B6KO	$F_{(1, 28)} = 0.566, P = 0.459$	$F_{(1, 23)} = 0.263, P = 0.613$
CSS1	$F_{(1, 22)} = 2.37, P = 0.138$	$F_{(1, 22)} = 3.85, P = 0.062$
CSS2	$F_{(1, 26)} = 0.584, P = 0.452$	$F_{(1, 22)} = 0.903, P = 0.352$
CSS3	$F_{(1, 23)} = 5.39, P = 0.030$	$F_{(1, 21)} = 8.32, P = 0.009$
CSS5	$F_{(1, 24)} = 1.96, P = 0.175$	$F_{(1, 24)} = 5.96, P = 0.023$
CSS6	$F_{(1, 22)} = 2.94, P = 0.100$	$F_{(1, 24)} = 0.003, P = 0.955$
CSS7	$F_{(1, 22)} = 2.18, P = 0.289$	$F_{(1, 24)} = 0.141, P = 0.711$
CSS8	$F_{(1, 23)} = 1.27, P = 0.271$	$F_{(1, 23)} = 0.646, P = 0.430$
CSS9	$F_{(1, 22)} = 0.015, P = 0.903$	$F_{(1, 22)} = 3.08, P = 0.093$
CSS10	$F_{(1, 19)} = 1.54, P = 0.230$	$F_{(1, 24)} = 0.477, P = 0.496$
CSS11	$F_{(1, 22)} = 0.018, P = 0.893$	$F_{(1, 22)} = 2.99, P = 0.098$
CSS12	$F_{(1, 21)} = 0.608, P = 0.444$	$F_{(1, 23)} = 4.6, P = 0.043$
CSS14	$F_{(1, 22)} = 3.36, P = 0.08$	$F_{(1, 22)} = 8.42, P = 0.008$
CSS15	$F_{(1, 29)} = 5.24, P = 0.030$	$F_{(1, 29)} = 7.81, P = 0.009$
CSS16	$F_{(1, 25)} = 1.31, P = 0.263$	$F_{(1, 28)} = 6.62, P = 0.016$
CSS17	$F_{(1, 22)} = 5.40, P = 0.030$	$F_{(1, 26)} = 0.666, P = 0.442$
CSS18	$F_{(1, 22)} = 0.554, P = 0.465$	$F_{(1, 22)} = 0.462, P = 0.504$
CSS19	$F_{(1, 22)} = 2.38, P = 0.137$	$F_{(1, 22)} = 2.78, P = 0.110$
CSSX	$F_{(1, 22)} = 1.39, P = 0.252$	$F_{(1, 22)} = 6.15, P = 0.021$

the *Chrna5* deletion or could be a main effect of the CSS on nicotine consumption (i.e., independent of *Chrna5* genotype). To establish whether the effect of strain on nicotine consumption was specific to mice possessing the *Chrna5* null mutation or a general effect on nicotine intake, nicotine consumption was assessed in all of the CSS strains possessing the WT allele of *Chrna5* and compared to B6 WT mice (Table 1 and Figure 4). This analysis identified main effects of strain ( $P = 6.7 \times 10^{-13}$ ) and sex ( $P = 1.1 \times 10^{-7}$ ). Again, due to the main effect of sex, individual CSS strains were evaluated for significant sex effects (Table 2). Results indicated that WT CSS3, CSS5, CSS12, CSS14, CSS15, CSS16, and CSSX exhibited sex-dependent differences in nicotine intake and, therefore, were analyzed by individual sex while the remaining strains were collapsed on sex. For those strains collapsed on sex, CSS1 WT ( $q < 0.05$ ) consumed less nicotine than did B6 WT mice while CSS17 WT ( $q < 0.05$ ) drank more nicotine than did B6 WT mice (Figure 4A). For those CSS in which there was a main effect of sex, none differed from B6 background mice for either sex at either an FDR of 0.05 or 0.1 (Figures 4B,C).

Lastly, CSS were examined individually using a between *Chrna5* genotype analysis for the effect of *Chrna5* genotype and sex on nicotine consumption. This analysis was to determine if the effect of *Chrna5* deletion on nicotine intake was eliminated relative to WT controls for each CSS. As shown in Figure 5 and Table 3, the effect of *Chrna5* deletion on nicotine intake was no longer significant in CSS1, CSS2, CSS5, CSS8, CSS9, CSS11, and CSS15. Three of these strains (CSS1, CSS5, and CSS11) also exhibited a main effect of sex. However, the lack of a significant



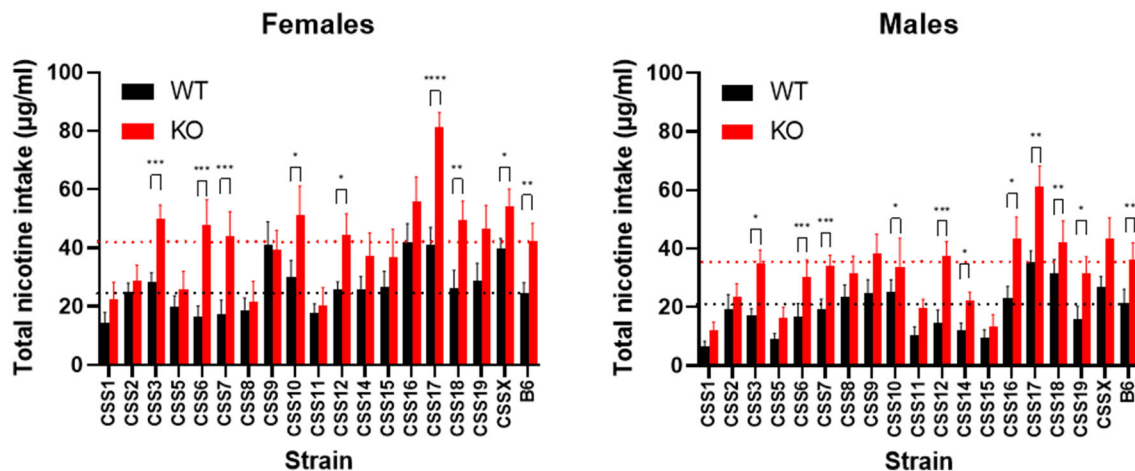


**FIGURE 5 |** Comparison of nicotine consumption between WT and *Chrna5* KO mice for each CSS. Black dotted line indicates mean intake from the B6 WT strain and the red dotted line represents mean nicotine intake from B6 *Chrna5*KO mice. \* $p < 0.05$ , \*\* $p < 0.01$ , \*\*\* $p < 0.005$ , \*\*\*\* $p < 0.001$   $N = 9-17$  per strain per sex. Data represent mean  $\pm$  SEM.

**TABLE 3 |** Effect of *Chrna5* genotype and sex on B6 and individual CSS genetic backgrounds.

CSS	Genotype	Sex
B6	$F_{(1, 49)} = 9.81, P = 0.003$	$F_{(1, 49)} = 0.792, P = 0.378$
CSS1	$F_{(1, 44)} = 2.95, P = 0.093$	$F_{(1, 44)} = 5.43, P = 0.024$ [female: $F_{(1, 22)} = 1.27, P = 0.272$ ; male: $F_{(1, 22)} = 2.59, P = 0.122$ ]
CSS2	$F_{(1, 48)} = 0.824, P = 0.369$	$F_{(1, 48)} = 1.39, P = 0.244$
CSS3	$F_{(1, 44)} = 26.51, P = 1 \times 10^{-6}$	$F_{(1, 44)} = 11.53, P = 0.001$ [female: $F_{(1, 22)} = 14.82, P = 8.7 \times 10^{-4}$ ; male: $F_{(1, 22)} = 11.71, P = 0.002$ ]
CSS5	$F_{(1, 48)} = 2.72, P = 0.106$	$F_{(1, 48)} = 6.24, P = 0.016$ [female: $F_{(1, 23)} = 0.738, P = 0.399$ ; male: $F_{(1, 25)} = 2.95, P = 0.099$ ]
CSS6	$F_{(1, 46)} = 14.66, P = 3.9 \times 10^{-4}$	$F_{(1, 46)} = 2.25, P = 0.140$
CSS7	$F_{(1, 46)} = 15.15, P = 3.2 \times 10^{-4}$	$F_{(1, 46)} = 0.532, P = 0.469$
CSS8	$F_{(1, 46)} = 1.125, P = 0.294$	$F_{(1, 46)} = 1.91, P = 0.173$
CSS9	$F_{(1, 44)} = 0.839, P = 0.365$	$F_{(1, 44)} = 1.75, P = 0.193$
CSS10	$F_{(1, 43)} = 4.09, P = 0.049$	$F_{(1, 43)} = 2.28, P = 0.139$
CSS11	$F_{(1, 44)} = 2.6, P = 0.148$	$F_{(1, 44)} = 1.10, P = 0.299$
CSS12	$F_{(1, 44)} = 17.64, P = 1.3 \times 10^{-4}$	$F_{(1, 44)} = 3.2, P = 0.081$
CSS14	$F_{(1, 44)} = 5.27, P = 0.027$	$F_{(1, 44)} = 9.34, P = 0.004$ [female: $F_{(1, 22)} = 1.7, P = 0.208$ ; male: $F_{(1, 22)} = 7.83, P = 0.01$ ]
CSS15	$F_{(1, 58)} = 1.35, P = 0.25$	$F_{(1, 58)} = 11.54, P = 0.001$ [female: $F_{(1, 29)} = 0.876, P = 0.357$ ; male: $F_{(1, 29)} = 0.556, P = 0.462$ ]
CSS16	$F_{(1, 53)} = 7.19, P = 0.010$	$F_{(1, 53)} = 5.9, P = 0.019$ [female: $F_{(1, 24)} = 1.84, P = 0.187$ ; male: $F_{(1, 29)} = 6.58, P = 0.016$ ]
CSS17	$F_{(1, 48)} = 34.14, P = 4.4 \times 10^{-7}$	$F_{(1, 48)} = 5.36, P = 0.025$ [female: $F_{(1, 25)} = 25.56, P = 3.2 \times 10^{-5}$ ; male: $F_{(1, 23)} = 10.41, P = 0.004$ ]
CSS18	$F_{(1, 44)} = 7.59, P = 0.008$	$F_{(1, 44)} = 0.02, P = 0.887$
CSS19	$F_{(1, 44)} = 7.25, P = 0.01$	$F_{(1, 44)} = 5.0, P = 0.03$ [female: $F_{(1, 22)} = 3.19, P = 0.088$ ; male: $F_{(1, 22)} = 4.59, P = 0.044$ ]
CSSX	$F_{(1, 44)} = 8.47, P = 0.006$	$F_{(1, 44)} = 4.95, P = 0.031$ [female: $F_{(1, 22)} = 4.57, P = 0.044$ ; male: $F_{(1, 22)} = 4.02, P = 0.058$ ]

of networks that can compensate for the genetic alteration of interest (19). Results of the current study indicate that A/J chromosomes 5, 11, and possibly 1 possess sex-independent modifiers of *Chrna5* null mutant-dependent nicotine intake and

A/J chromosome 15 harbors a male-specific modifier. Evidence to support modifiers on CSS5, 11 and 15 (male only) includes the observation that nicotine intake in *CSS5<sup>Chrna5KO</sup>*, *CSS11<sup>Chrna5KO</sup>*, and male *CSS15<sup>Chrna5KO</sup>* mice significantly differs from the

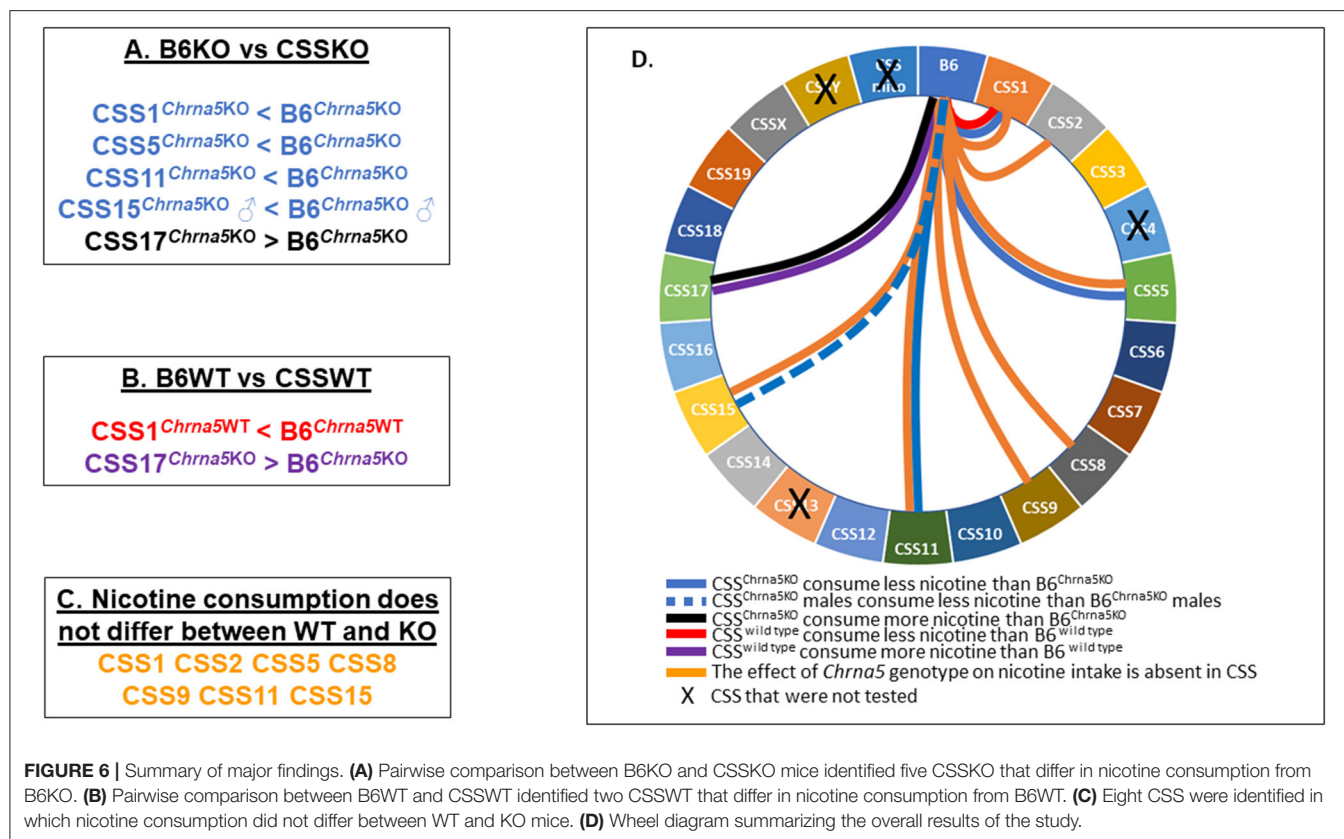


**FIGURE 6 |** Summary of major findings. **(A)** Pairwise comparison between B6KO and CSSKO mice identified five CSSKO that differ in nicotine consumption from B6KO. **(B)** Pairwise comparison between B6WT and CSSWT identified two CSSWT that differ in nicotine consumption from B6WT. **(C)** Eight CSS were identified in which nicotine consumption did not differ between WT and KO mice. **(D)** Wheel diagram summarizing the overall results of the study.

reference B6<sup>Chrna5KO</sup> strain. In all cases, the CSS<sup>Chrna5KO</sup> animals consume less nicotine than B6<sup>Chrna5KO</sup> mice. In addition, mice that possess the WT allele of *Chrna5* in these three strains do not significantly differ from B6 mice harboring the WT allele indicating that the strain effect is specific to the *Chrna5* null allele. Further, the effect of *Chrna5* genotype on nicotine consumption in CSS5, CSS11, and male CSS15 mice is abolished (Table 3) indicating that the modifiers for each of these strains reduces nicotine intake in *Chrna5* null mutant mice to levels indistinguishable from WT mice. To the best of our knowledge, this is the first study to describe the mapping of genetic modifiers for any drug abuse-related trait.

Similar to CSS5<sup>Chrna5KO</sup> and CSS11<sup>Chrna5KO</sup> and male CSS15<sup>Chrna5KO</sup>, CSS1<sup>Chrna5KO</sup> mice consume significantly less nicotine than do B6<sup>Chrna5KO</sup> mice and the effect of *Chrna5* genotype on nicotine intake in CSS1 mice is abolished suggestive of a modifier on A/J chromosome 1. However, CSS1 WT mice also consume significantly less nicotine than do B6 WT mice. These results suggest the possibility that A/J chromosome 1 may possess a combination of alleles, one or more of which affects nicotine consumption in a genotype-independent manner while others act as a modifier in CSS1<sup>Chrna5KO</sup> mice. Alternatively, the same allele or alleles may be responsible for the reduced nicotine intake in both the CSS1<sup>Chrna5KO</sup> and CSS1 WT mice. In this case, the allele or alleles would have a greater effect on nicotine consumption in the CSS1<sup>Chrna5KO</sup> mice relative to the CSS1 WT mice leading to the modifier-like effect. One other possibility is

that there could be a floor effect on nicotine consumption in the CSS1 WT animals preventing a decrease in nicotine consumption similar to that seen in the CSS1<sup>Chrna5KO</sup> mice. Future genetic dissection of chromosome 1 will be required to establish which of these possibilities is/are driving the effect of chromosome 1 on *Chrna5*-dependent and *Chrna5*-independent nicotine intake.

Three additional strains, CSS2, CSS8, and CSS9 show some evidence of possessing modifier alleles although they do not meet all criteria. The main factor that implicates these strains as potential modifier strains is the observation that nicotine consumption did not differ between WT and *Chrna5* null mutant mice in each of these three strains. However, neither the *Chrna5* null mutant or WT animals from these three strains differed significantly from the respective B6 reference control after controlling for an FDR of 0.05 or 0.1 making it somewhat difficult to interpret the modifier status of these three strains. Some support for a chromosome 2 modifier comes from a preliminary study that suggests that functional alleles of *Chrna4*, which differ between B6 and A/J mice (25, 28, 29) and are located on mouse chromosome 2, acts as a modifier of the *Chrna5* null mutation (12). Nonetheless, further studies will be required to determine whether CSS2 as well as CSS8 and CSS9 possess modifier alleles.

Although several A/J chromosomes were identified that possess genetic modifiers that eliminate the increase in nicotine consumption resulting from *Chrna5* deletion, it remains to be determined which gene or genes on each chromosome possess the nicotine consumption-modifying alleles. Once identified,

these alleles should provide new insights into the molecular networks that can reverse the *Chrna5* deletion-dependent increase in nicotine consumption. Such knowledge may lead to a better understanding of the neurobiology of *Chrna5*-dependent nicotine consumption as well as suggest novel therapeutic strategies for treating nicotine dependence in humans.

One CSS that exhibited no evidence of a modifier but had a significant effect on nicotine consumption was CSS17. Both CSS17 WT and CSS17<sup>*Chrna5*KO</sup> mice consumed significantly more nicotine than their respective B6 controls indicating that A/J chromosome 17 possess an allele or alleles that increases nicotine consumption independent of *Chrna5* genotype. In fact, CSS17 WT mice drank as much nicotine as did B6<sup>*Chrna5*KO</sup> mice and CSS17<sup>*Chrna5*KO</sup> mice consumed twice as much nicotine as did B6<sup>*Chrna5*KO</sup> mice. Considering that B6 mice consume the highest level of nicotine among tested inbred strains and A/J mice are amongst the lowest nicotine consuming strains (25), it is somewhat surprising that A/J chromosome 17 harbors an allele or alleles of genes that nearly double the level of nicotine consumption in both the B6 WT and B6<sup>*Chrna5*</sup> null mutant mice.

In the only other study that measured a nicotine response in the C57BL/6J-Chr#<sup>A/J</sup>/NaJ CSS panel, Boyle and Gill (30) assessed the effect of an acute injection of 1.5 mg/kg nicotine on locomotor activity. In this study, CSS17 mice, which showed an increase in locomotor activity following the administration of nicotine, significantly differed from B6 mice which displayed a decrease in activity to the same dose of nicotine. This finding suggests that A/J chromosome 17 either possesses separate alleles of genes that impact the acute effects of nicotine on locomotor activity and oral nicotine consumption independently or raises the possibility that there may be shared alleles on Chromosome 17 that affects both oral nicotine intake and the acute effects of nicotine on locomotion. The latter possibility suggests the potential for genetic overlap between these two nicotine measures. To assess a potential genetic overlap between the acute effects of nicotine on locomotion and oral nicotine intake, a correlational analysis between data extrapolated from Boyle and Gill (30) and data from CSS WT mice in the current study was performed. Comparing locomotor activity following an acute injection of 1.5 mg/kg nicotine to total  $\mu$ g/ml nicotine consumed across all common CSS tested between the two studies gave a non-significant but positive correlation of 0.328 ( $P = 0.183$ ). Removing CSS9 from this analysis due to potential genetic differences from our CSS9 vs. the JAX CSS9 leads to a significant positive correlation (0.560,  $P = 0.019$ ). Using dose (mg/kg/day) as an alternative measure of nicotine consumption in the CSS WT mice led to significant correlations with locomotor activity with (0.512,  $P = 0.03$ ) or without ( $r = 0.666$ ,  $P = 0.003$ ) the inclusion of CSS9. In sum, these correlations are suggestive of a genetic overlap between oral nicotine intake and the acute effects of nicotine on locomotor activity with animals less sensitive to the locomotor depressant effects/more sensitive to the locomotor stimulating effects of nicotine consuming greater amounts of nicotine.

Genetic mapping of oral nicotine consumption in mice also has been reported in one previous study (31). In this study,

which utilized an F2 intercross between B6 and C3H/HeJ mice, no quantitative trait loci (QTL) on chromosome 17 was detected for nicotine intake indicating that the association of chromosome 17 with nicotine consumption in the CSS panel is novel. Whether the association of chromosome 17 with nicotine intake in CSS17 mice and not the B6 and C3H/HeJ F2 intercross is the result of unique variants in A/J relative to C3H/HeJ, due to the distinct genetic structures of the two test populations or a consequence of the different designs of the nicotine consumption assays remains to be determined. Interestingly, a major QTL for nicotine consumption was detected on chromosome 1 in the previously published study. Whether the QTL identified on chromosome 1 in this study encompasses the same alleles that impact nicotine consumption independent of *Chrna5* genotype in CSS1 mice remains to be determined.

In summary, four CSS were identified that harbor apparent modifier alleles that eliminate the effect of *Chrna5* deletion on nicotine consumption and one CSS was identified that possesses an allele or alleles that substantially increases nicotine consumption independent of *Chrna5* genotype. Future studies with the CSS<sup>*Chrna5*KO</sup> and CSS WT mice of interest can take advantage of the unique structure of the CSS (20, 23) to efficiently map the locations of the modifier loci and identify the specific genes/alleles on each of the A/J chromosomes that are responsible for the phenotypic effect on nicotine intake. These results should lead to a better understanding of the neurobiological mechanisms that drive nicotine consumption and potentially lead to the discovery of novel therapeutic targets for treating nicotine dependence.

## LIMITATIONS

At this time, we cannot entirely rule out the possibility that new, unidentified mutations in the B6 background of one or more of the CSS<sup>*Chrna5*KO</sup> mice are responsible for the strain effect on the phenotype instead of the introgressed A/J chromosome. However, this possibility can be readily addressed in future studies by mapping the causal genomic region in a segregating population of CSS<sup>*Chrna5*KO</sup>  $\times$  B6<sup>*Chrna5*KO</sup> mice.

## DATA AVAILABILITY STATEMENT

The original contributions presented in the study are included in the article/**Supplementary Material**, further inquiries can be directed to the corresponding author/s.

## ETHICS STATEMENT

The animal study was reviewed and approved by University of Colorado Boulder Institutional Animal Care and Use Committee.

## AUTHOR CONTRIBUTIONS

EM, ZW, and DW: animal husbandry, behavioral testing, genotyping, data entry, and database management. HM: data analysis and manuscript editing. JN and RR: experimental

design, interpretation and manuscript, and figure editing. JS: experimental conception and design, data analysis, data interpretation, manuscript preparation and editing, and supervision of technical staff. All authors contributed to the article and approved the submitted version.

## FUNDING

This project was provided by NIH NIDA U01043802 (JS, RR, and JN).

## REFERENCES

- Saccone SF, Hinrichs AL, Saccone NL, Chase GA, Konvicka K, Madden PA, et al. Cholinergic nicotinic receptor genes implicated in a nicotine dependence association study targeting 348 candidate genes with 3713 SNPs. *Hum Mol Genet.* (2007) 16:36–49. doi: 10.1093/hmg/ddl438
- Saccone NL, Wang JC, Breslau N, Johnson EO, Hatsukami D, Saccone SF, et al. The CHRNA5-CHRNA3-CHRNA4 nicotinic receptor subunit gene cluster affects risk for nicotine dependence in African-Americans and in European-Americans. *Cancer Res.* (2009) 69:6848–56. doi: 10.1158/0008-5472.CAN-09-0786
- Bierut LJ, Stitzel JA, Wang JC, Hinrichs AL, Grucza RA, Xuei X, et al. Variants in nicotinic receptors and risk for nicotine dependence. *Am J Psychiatry.* (2008) 165:1163–71. doi: 10.1176/appi.ajp.2008.07111711
- Berrettini W, Yuan X, Tozzi F, Song K, Francks C, Chilcoat H, et al. Alpha-5/alpha-3 nicotinic receptor subunit alleles increase risk for heavy smoking. *Mol Psychiatry.* (2008) 13:368–73. doi: 10.1038/sj.mp.4002154
- Thorgeirsson TE, Geller F, Sulem P, Rafnar T, Wiste A, Magnusson KP, et al. A variant associated with nicotine dependence, lung cancer and peripheral arterial disease. *Nature.* (2008) 452:638–42. doi: 10.1038/nature06846
- Hancock DB, Guo Y, Reginsson GW, Gaddis NC, Lutz SM, Sherva R, et al. Genome-wide association study across European and African American ancestries identifies a SNP in DNMT3B contributing to nicotine dependence. *Mol Psychiatry.* (2017) 23:1911–9. doi: 10.1038/mp.2017.193
- Liu M, Jiang Y, Wedow R, Li Y, Brazel DM, Chen F, et al. Association studies of up to 1.2 million individuals yield new insights in the genetic etiology of tobacco and alcohol use. *Nature genetics* In press.
- Stitzel JA, Blanchette JM, Collins AC. Sensitivity to the seizure-inducing effects of nicotine is associated with strain-specific variants of the alpha 5 and alpha 7 nicotinic receptor subunit genes. *J Pharmacol Exp Ther.* (1998) 284:1104–11.
- Salas R, Orr-Urtreger A, Broide RS, Beaudet A, Paylor R, De BM. The nicotinic acetylcholine receptor subunit alpha 5 mediates short-term effects of nicotine *in vivo*. *Mol Pharmacol.* (2003) 63:1059–66. doi: 10.1124/mol.63.5.1059
- Fowler CD, Lu Q, Johnson PM, Marks MJ, Kenny PJ. Habenular alpha5 nicotinic receptor subunit signalling controls nicotine intake. *Nature.* (2011) 471:597–601. doi: 10.1038/nature09797
- Jackson KJ, Marks MJ, Vann RE, Chen X, Gamage TF, Warner JA, et al. Role of alpha5 nicotinic acetylcholine receptors in pharmacological and behavioral effects of nicotine in mice. *J Pharmacol Exp Ther.* (2010) 334:137–46. doi: 10.1124/jpet.110.165738
- Wilking JA, Stitzel JA. Natural genetic variability of the neuronal nicotinic acetylcholine receptor subunit genes in mice: consequences and confounds. *Neuropharmacology.* (2015) 96:205–12. doi: 10.1016/j.neuropharm.2014.11.022
- Bagdas D, Diester CM, Riley J, Carper M, Alkhlaif Y, AlOmari D, et al. Assessing nicotine dependence using an oral nicotine free-choice paradigm in mice. *Neuropharmacology.* (2019) 157:107669. doi: 10.1016/j.neuropharm.2019.107669
- Tammimaki A, Herder P, Li P, Esch C, Laughlin JR, Akk G, et al. Impact of human D398N single nucleotide polymorphism on intracellular calcium response mediated by alpha3beta4alpha5 nicotinic acetylcholine receptors. *Neuropharmacology.* (2012) 63:1002–11. doi: 10.1016/j.neuropharm.2012.07.022
- Kuryatov A, Berrettini W, Lindstrom J. Acetylcholine receptor (AChR) alpha5 subunit variant associated with risk for nicotine dependence and lung cancer reduces (alpha4beta2)alpha5 AChR function. *Mol Pharmacol.* (2011) 79:119–25. doi: 10.1124/mol.110.066357
- George AA, Lucero LM, Damaj MI, Lukas RJ, Chen X, Whiteaker P. Function of human alpha3beta4alpha5 nicotinic acetylcholine receptors is reduced by the alpha5(D398N) variant. *J Biol Chem.* (2012) 287:25151–62. doi: 10.1074/jbc.M112.379339
- Sciacaluga M, Moriconi C, Martinello K, Catalano M, Bermudez I, Stitzel JA, et al. Crucial role of nicotinic alpha5 subunit variants for Ca2+ fluxes in ventral midbrain neurons. *FASEB J.* (2015) 29:3389–98. doi: 10.1096/fj.14-268102
- Nadeau JH. Modifier genes and protective alleles in humans and mice. *Curr Opin Genet Dev.* (2003) 13:290–5. doi: 10.1016/S0959-437X(03)00061-3
- Riordan JD, Nadeau JH. From peas to disease: modifier genes, network resilience, and the genetics of health. *Am J Hum Genet.* (2017) 101:177–91. doi: 10.1016/j.ajhg.2017.06.004
- Nadeau JH, Singer JB, Matin A, Lander ES. Analysing complex genetic traits with chromosome substitution strains. *Nat Genet.* (2000) 24:221–5. doi: 10.1038/73427
- Nadeau JH, Forejt J, Takada T, Shiroishi T. Chromosome substitution strains: gene discovery, functional analysis, and systems studies. *Mamm Genome.* (2012) 23:693–705. doi: 10.1007/s00335-012-9426-y
- Buchner DA, Nadeau JH. Contrasting genetic architectures in different mouse reference populations used for studying complex traits. *Genome Res.* (2015) 25:775–91. doi: 10.1101/gr.187450.114
- Singer JB, Hill AE, Burrage LC, Olszens KR, Song J, Justice M, et al. Genetic dissection of complex traits with chromosome substitution strains of mice. *Science.* (2004) 304:445–8. doi: 10.1126/science.1093139
- Robinson SF, Marks MJ, Collins AC. Inbred mouse strains vary in oral self-selection of nicotine. *Psychopharmacology.* (1996) 124:332–9. doi: 10.1007/BF02247438
- Butt CM, King NM, Hutton SR, Collins AC, Stitzel JA. Modulation of nicotine but not ethanol preference by the mouse Chrna4 A529T polymorphism. *Behav Neurosci.* (2005) 119:26–37. doi: 10.1037/0735-7044.119.1.26
- Simecek P, Forejt J, Williams RW, Shiroishi T, Takada T, Lu L, et al. High-resolution maps of mouse reference populations. *G3.* (2017) 7:3427–34. doi: 10.1534/g3.117.300188
- Benjamini Y, Kreiger AM, Yekutieli D. Adaptive linear step-up procedures that control the false discovery rate. *Biometrika.* (2006) 93:491–507. doi: 10.1093/biomet/93.3.491
- Kim H, Flanagan BA, Qin C, Macdonald RL, Stitzel JA. The mouse Chrna4 A529T polymorphism alters the ratio of high to low affinity alpha 4 beta 2 nAChRs. *Neuropharmacology.* (2003) 45:345–54. doi: 10.1016/S0028-3908(03)00167-9
- Dobelis P, Marks MJ, Whiteaker P, Balogh SA, Collins AC, Stitzel JA. A polymorphism in the mouse neuronal alpha4 nicotinic receptor subunit results in an alteration in receptor function. *Mol Pharmacol.* (2002) 62:334–42. doi: 10.1124/mol.62.2.334

## ACKNOWLEDGMENTS

The authors would like to thank Ms. Brooke Brounstein for her valuable assistance with genotyping.

## SUPPLEMENTARY MATERIAL

The Supplementary Material for this article can be found online at: <https://www.frontiersin.org/articles/10.3389/fpsy.2021.773400/full#supplementary-material>

30. Boyle AE, Gill KJ. Genetic analysis of the psychostimulant effects of nicotine in chromosome substitution strains and F2 crosses derived from A/J and C57BL/6J progenitors. *Mamm Genome*. (2009) 20:34–42. doi: 10.1007/s00335-008-9159-0
31. Li XC, Karadsheh MS, Jenkins PM, Brooks JC, Drapeau JA, Shah MS, et al. Chromosomal loci that influence oral nicotine consumption in C57BL/6J x C3H/HeJ F2 intercross mice. *Genes Brain Behav*. (2007) 6:401–10. doi: 10.1111/j.1601-183X.2006.00266.x

**Conflict of Interest:** The authors declare that the research was conducted in the absence of any commercial or financial relationships that could be construed as a potential conflict of interest.

**Publisher's Note:** All claims expressed in this article are solely those of the authors and do not necessarily represent those of their affiliated organizations, or those of the publisher, the editors and the reviewers. Any product that may be evaluated in this article, or claim that may be made by its manufacturer, is not guaranteed or endorsed by the publisher.

Copyright © 2021 Meyers, Werner, Wichman, Mathews, Radcliffe, Nadeau and Stitzel. This is an open-access article distributed under the terms of the Creative Commons Attribution License (CC BY). The use, distribution or reproduction in other forums is permitted, provided the original author(s) and the copyright owner(s) are credited and that the original publication in this journal is cited, in accordance with accepted academic practice. No use, distribution or reproduction is permitted which does not comply with these terms.



# Neurofilament Light Chain Is a Promising Biomarker in Alcohol Dependence

Yanfei Li<sup>1</sup>, Ranran Duan<sup>1</sup>, Zhe Gong<sup>1</sup>, Lijun Jing<sup>1</sup>, Tian Zhang<sup>2</sup>, Yong Zhang<sup>3</sup> and Yanjie Jia<sup>1\*</sup>

<sup>1</sup> Department of Neurology, First Affiliated Hospital of Zhengzhou University, Zhengzhou, China, <sup>2</sup> Department of Rehabilitation, First Affiliated Hospital of Zhengzhou University, Zhengzhou, China, <sup>3</sup> Department of Magnetic Resonance Imaging, First Affiliated Hospital of Zhengzhou University, Zhengzhou, China

## OPEN ACCESS

### Edited by:

Peter Kalivas,  
Medical University of South Carolina,  
United States

### Reviewed by:

Mauro Ceccanti,  
Sapienza University of Rome, Italy  
Gwang-Won Kim,  
Chonnam National University,  
South Korea

### \*Correspondence:

Yanjie Jia  
jiayanjie1971@zzu.edu.cn

### Specialty section:

This article was submitted to  
Addictive Disorders,  
a section of the journal  
Frontiers in Psychiatry

**Received:** 14 September 2021

**Accepted:** 26 October 2021

**Published:** 18 November 2021

### Citation:

Li Y, Duan R, Gong Z, Jing L, Zhang T,  
Zhang Y and Jia Y (2021)  
Neurofilament Light Chain Is a  
Promising Biomarker in Alcohol  
Dependence.  
Front. Psychiatry 12:754969.  
doi: 10.3389/fpsy.2021.754969

**Background:** Alcohol dependence, a global public health problem, leads to structural and functional damage in the brain. Alcohol dependence patients present complex and varied clinical manifestations and live with general complaints existing in contemporary society, making most people with alcohol dependence hard to identify. Therefore, it is important to find potential biomarkers for the diagnosis and evaluation of alcohol dependence. In the study, we explored potential biomarkers for the diagnosis and monitoring of diseases and evaluated brain structural changes in alcohol dependence patients.

**Methods:** Enzyme-linked immunosorbent assay (ELSA) was employed to detect the expression of serum nucleotide-binding oligomerization domain containing 3 (NLRP3) and single-molecule array (Simoa) assay was used to detect the expression of serum neurofilament light (NfL) in 50 alcohol dependence patients and 50 controls with no drinking history. Alcohol consumption was measured by standard drinks. Neuropsychological assessments, including the Montreal cognitive assessment (MoCA), Pittsburgh sleep quality index (PSQI), generalized anxiety disorder (GAD-7), and patient health questionnaire-9 (PHQ-9), were conducted to evaluate cognitive function and psychological state. The degree of white matter lesions (WMLs) was rated using the Fazekas scale based on magnetic resonance imaging analysis. White matter structure was quantified using the voxel-based morphometry method. The correlations between NLRP3 levels, NfL levels, neuropsychological dysfunction, the degree of WMLs, and white matter volume (WMV) were analyzed in alcohol dependence patients.

**Results:** Serum NLRP3 and NfL levels were higher in the alcohol dependence group. NLRP3 levels were irrelevant to monthly alcohol assumption as well as to the MoCA, PSQI, GAD-7, PHQ-9, and Fazekas scale scores and WMV. NfL levels were positively correlated with the PSQI and PHQ-9 scores as well as the degree of WMLs and negatively correlated with the MoCA scores and WMV. No associations were evident between NfL and monthly alcohol assumption and GAD-7 scores in the alcohol dependence group.

**Conclusion:** This study supports the potential value of serum NfL as a non-invasive biomarker in alcohol dependence. The association with neuropsychological dysfunction

and degree of WMLs has implications to use NfL as a promising biomarker to assess the severity of brain damage as well as the progression and prognosis of alcohol dependence.

**Keywords:** NLRP3, NfL, alcohol dependence, biomarker, white matter lesions, gray matter volume, neuropsychological assessment

## INTRODUCTION

Alcohol dependence is a common global public health problem. Long-term alcohol abuse can result in neuroinflammation, oxidative stress, as well as structural and functional disorders of the brain (1). Structural changes, including myelin disruptions, white matter lesions (WMLs) (2), the atrophy of gray and white matter accompanied by sulcal widening and ventricular enlargement (3), and functional disorders such as cognitive impairment and psychological abnormality are commonly seen in alcohol dependence (4, 5).

A previous study has reported that alcohol dependence is related to increased WMLs. Among middle-aged men, excessive drinking may be associated with both microstructural and macrostructural white matter injury (6). White matter are susceptible to the neurotoxic effects of alcohol caused by thiamine deficiency (7). The Fazekas scale is a widely used scale to evaluate the severity of WMLs in both periventricular (PV) and deep white matter (DWM) areas.

Nucleotide-binding oligomerization domain containing 3 (NLRP3) is one of the extensively studied inflammasomes that acts as a sensor of metabolic stress and plays a vital role in the neuroinflammation and demyelination processes of several neurological diseases. Previous studies have demonstrated that alcohol can activate the NLRP3-inflammasome complex by stimulating the activation of caspase-1 and induction of IL-1 $\beta$  and IL-18 pro-inflammatory cytokines. NLRP3 is increased in the cultured astroglial cells, microglial cells, and cerebral cortex of mice with chronic alcohol treatment (8).

Neurofilaments, which consist of heteropolymers of three subunits named neurofilament light chain (NfL), neurofilament medium chain (NfM), and neurofilament heavy chain (NfH), are important elements of cytoskeletal protein, and they provide structural support for neurons. Following axon damage, neurofilaments are released into the extracellular space, followed by the cerebrospinal fluid (CSF) and blood. Therefore, NfL can be detected in the CSF and plasma or serum after neurological injury, and it is regarded as a potential biomarker of axonal and neuron damage (9, 10). Recent studies have indicated that NfL

expression changes in various neurological diseases, for which it is considered to be a promising marker. It may not only facilitate accurate diagnosis but also predict disease progression and assess treatment responses (11). NfL is associated with the severity of white matter hyperintensities and brain atrophy (12).

Voxel-based morphometry (VBM) is a comprehensive and objective automatic whole-brain analysis method that allows the detection of subtle morphometric differences in the brain structure (13). The atrophy of white matter is commonly seen in alcohol dependence (14). In the present study, we analyzed white matter volume (WMV) in patients with alcohol dependence using VBM.

To explore the potential biomarker for alcohol dependence, we first detected the expression of NLRP3 and NfL in alcohol dependence patients' serum and found that NLRP3 and NfL levels were higher in alcohol dependence patients than in controls. Furthermore, we analyzed the correlations between NLRP3/NfL levels, alcohol consumption, the severity of neuropsychological dysfunction, WMLs, and WMV. We demonstrated the NfL levels were closely correlated with the MoCA scores, PSQI scores, PHQ-9 scores, Fazekas scale scores, and WMV in alcohol dependence patients, which suggests that NfL may act as a biomarker for monitoring disease progression or predicting prognosis in alcohol dependence.

## MATERIALS AND METHODS

### Participants

We enrolled 50 patients with alcohol dependence and 50 age- and sex-matched controls with no drinking history, which were set as the alcohol dependence group and control group, respectively. The diagnosis of alcohol dependence was based on the standards of the fourth edition of the Diagnostic and Statistical Manual of Mental Disorders.

The criteria for the diagnosis of alcohol dependence were as follows (15): tolerance to alcohol, withdrawal syndrome, greater alcohol use than intended, desire to use alcohol and inability to control use, devotion of a large proportion of time to getting and using alcohol, recovering from alcohol use, neglect of social, work, or recreational activities, and continued alcohol use despite physical or psychological problems. Alcohol dependence was designated based on the fulfillment of three or more of the aforementioned criteria within 12 months. The exclusion criteria for both groups were as follows: (1) acute phase of alcohol withdrawal syndrome or Wernicke-Korsakoff syndrome; (2) history of drug abuse or other substance dependence such as cocaine, methamphetamine, marijuana, nicotine, and cigarettes; (3) history of other significant neurological or psychological diseases; (4) history of psychological diseases such as depression

**Abbreviations:** ELSA, enzyme-linked immunosorbent assay; NLRP3, nucleotide-binding oligomerization domain containing 3; Simoa, Single-Molecule Array; NfL, neurofilament light; MoCA, Montreal cognitive assessment; PSQI, Pittsburgh sleep quality index; GAD-7, generalized anxiety disorder; PHQ-9, patient health questionnaire-9; WMLs, white matter lesions; MRI, magnetic resonance imaging; FLAIR, fluid-attenuated inversion recovery; VBM, voxel-based morphometry; NfM, neurofilament medium chain; NfH, neurofilament heavy chain; CSF, cerebrospinal fluid; GMV, gray matter volume; WMV, white matter volume; PV, periventricular; DWM, deep white matter; HIV, human immunodeficiency virus; AIDS, acquired immune deficiency syndrome; FWHM, full width at half maximum; TIV, total intracranial volume; HRP, Horseradish Peroxidase.

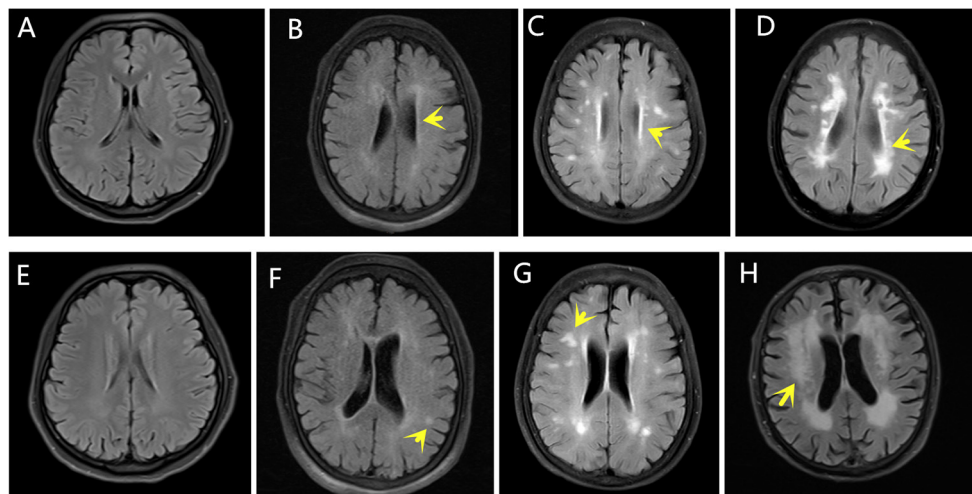


**FIGURE 1 |** Fazekas scores. The yellow arrows indicate WMLs on FLAIR MRI. The PV scores were categorized as follows: (A) 0, (B) 1, (C) 2, (D) 3. The DWM scores were categorized as follows: (E) 0, (F) 1, (G) 2, (H) 3.

and anxiety; (5) history of severe brain trauma or cranial surgery; and (6) medically uncontrolled chronic hypertension and diabetes mellitus, hyperlipidemia chronic obstructive pulmonary disease, and human immunodeficiency virus (HIV)/acquired immune deficiency syndrome (AIDS).

We collected the participants' clinical data, including age, sex, previous history, alcohol use (frequency, quantity, and years of alcohol consumption), MRI results, and neuropsychological assessment outcomes, including the Montreal cognitive assessment (MoCA), Pittsburgh sleep quality index (PSQI), generalized anxiety disorder (GAD-7), and patient health questionnaire-9 (PHQ-9) scores. Alcohol use quantity was measured by standard drinks. A standard drink was defined as 12 oz. beer, 5 oz. wine, or 1.5 oz. liquor. The alcohol dependence scale (ADS) was used to measure the severity of the participant's dependence on alcohol. The study was approved by the Ethics Committee of the First Affiliated Hospital of Zhengzhou University (2018-KY-91). All the participants or their guardians provided written informed consent.

## Magnetic Resonance Imaging Data

MRI scans were performed using a 3.0T scanner (Philips Healthcare, Amsterdam, Netherlands). Sagittal and axial T1-weighted images, T2-weighted images, axial and sagittal fast fluid-attenuated inversion recovery (FLAIR) images, axial diffusion, and apparent diffusion coefficient mapped images were analyzed.

## Fazekas Scale

The degree of WMLs was rated using the Fazekas scale during MRI analysis. PV and DWM demyelination were scored separately using the four-point scale according to the Fazekas scale on the FLAIR MRI data for the axial plane. The PV scores were categorized as follows: 0 (absence of white matter signal abnormalities), 1 (caps or pencil-thin

lining), 2 (smooth halo), or 3 (irregular PV lesions extending into the DWM). The DWM scores were categorized as follows: 0 (absence of white matter signal abnormalities), 1 (punctate foci), 2 (beginning confluent white matter signal abnormalities), or 3 (white matter signal abnormalities in large confluence areas) (16). The Fazekas scale scores were equal to the sum of the PV and DWM scores. The Fazekas scale assessments were completed by an experienced neuroradiologist blinded to the clinical data. **Figure 1** shows the rating of the Fazekas scores in the MRI FLAIR scans for the PV and DWM areas.

## VBM Analysis

Brain T1-weighted images were taken on Siemens Magnetom Skyra 3.0T scanners. T1-weighted images were processed with pipeline steps using the CAT12 toolbox (<http://dbm.neuro.uni-jena.de/cat12/>). All images were checked and processed with the standard setting for all steps, including segmentation into gray and white matter and cerebrospinal fluid, bias correction, normalization into Montreal Neurological Institute space, and non-linear modulation. Then, the images were resampled to a volume image resolution of  $1.5 \times 1.5 \times 1.5 \text{ mm}^3$ . Finally, the images were smoothed with a Gaussian kernel of 6 mm full width at half maximum. The total intracranial volume (TIV) of each participant was also calculated for the next comparative analysis (17, 18).

## Serum Collection

Fresh blood samples were obtained by venipuncture and collected into non-anticoagulant tubes. The serum was obtained by the centrifugation of blood samples at  $200 \times g$  for 20 min at  $4^\circ\text{C}$ . The supernatants were collected in 1.5 ml polypropylene tubes at  $-80^\circ\text{C}$ .

## Enzyme-Linked Immunosorbent Assay

NLRP3 levels were detected using an ELISA kit (CUSABIO). An antibody specific for NLRP3 was pre-coated onto a microplate. Standards and samples were pipetted into the wells and any NLRP3 present was bound by the immobilized antibody. After removing any unbound substances, a biotin-conjugated antibody specific for NLRP3 was added into the wells. After washing, avidin conjugated horseradish peroxidase was added into the wells. Following a wash to remove the unbound avidin-enzyme reagent, a substrate solution was added into the wells and color developed in proportion to the amount of NLRP3 bound in the initial step. The color development was stopped and the intensity of the color was measured.

## Neurofilament Detection

The concentration of NfL was detected using single-molecule array (Simoa; Quanterix, USA), as previously described in detail (19). All the measurements were taken by laboratory technicians blinded to the clinical data.

## Statistical Analysis

Data were presented as mean  $\pm$  standard deviation (SD) if the continuous variables were distributed normally according to the Kolmogorov-Smirnov test. Otherwise, data were presented as median [interquartile range (IQR)]. To analyze the differences, the normally distributed data were compared between the groups using the Student's *t*-test. The categorical data were compared using the chi-square test and abnormal distribution data were compared using the Wilcoxon test. Analysis of covariance was used to evaluate the difference in WMV between the groups and TIV was set as the covariate. The correlation analysis was performed using the Spearman correlation. TIV was set as the covariate and partial correlation analysis was used to evaluate the relationships between NLRP3 levels, NfL levels, and WMV. The differences were considered to be significant when the *P*-values were  $<0.05$ . All the analyses were performed using IBM SPSS Statistics 21. The diagram was generated with GraphPad Prism 5.

## RESULTS

### Clinical Data

We enrolled 50 patients with alcohol dependence and 50 controls. The alcohol dependence group comprised 36 men and 14 women, ranging from 30 to 65 years of age (mean = 48.8 years), and the controls comprised 35 men and 15 women, ranging from 31 to 62 years of age (mean = 48.7 years). The mean years of schooling of the alcohol dependence patients and controls were  $9.4 \pm 3.3$  and  $10.2 \pm 3.2$ , respectively. There were no significant differences in the age, sex, and years of schooling between the alcohol dependence group and controls.

The years of alcohol consumption of the alcohol dependence group ranged from 5 to 50 years. The mean drinking frequency was 4.8 times per week. The drinks/per drinking day were  $6.7 \pm 3.7$ . The drinks/per drinking day were  $7.7 \pm 3.7$  in men and  $4.3 \pm 2.1$  in women ( $P < 0.01$ ). The drinking modalities were almost the same on every drinking day. The median quantity of alcohol consumption was 112.9 standard drinks per month in the

**TABLE 1 |** Clinical data of alcohol dependence patients and controls.

	Alcohol dependence group	Controls	<i>P</i> -value
Male, n (%)	36 (72)	35 (70)	0.826
Age, y, mean $\pm$ SD	48.8 $\pm$ 9.5	48.7 $\pm$ 6.9	0.189
Years of schooling, y, mean $\pm$ SD	9.4 $\pm$ 3.3	10.2 $\pm$ 3.2	0.587
Hypertension, n (%)	9 (18)	7 (14)	0.585
Diabetes mellitus, n (%)	4 (8)	4 (8)	1.000
Hyperlipidemia, n (%)	6 (12)	5 (10)	0.749
MoCA scores, mean $\pm$ SD	23.26 $\pm$ 4.84	27.34 $\pm$ 1.88	0.000*
PSQI scores, median (IQR)	6 (3, 9)	2.00 (1.00, 4.25)	0.000*
GAD-7 scores, median (IQR)	3.00 (0.75, 7.25)	2.00 (1.00, 2.25)	0.048*
PHQ-9 scores, median (IQR)	5 (3, 10)	2.00 (1.00, 4.25)	0.000*
Fazekas scale scores, median (IQR)	2.00 (1.0, 3.25)	1 (0, 2)	0.000*
PV scores, median (IQR)	1 (1, 2)	1 (0, 1)	0.000*
DWM scores, median (IQR)	1 (0, 2)	0.5 (0, 1)	0.006*
<sup>a</sup> WMV (cm <sup>3</sup> ), mean $\pm$ SD	516.94 $\pm$ 45.40	531.51 $\pm$ 42.79	0.102
<sup>b</sup> Adjusted WMV(cm <sup>3</sup> ), mean	512.98	534.73	0.000*

Data are presented as mean  $\pm$  standard deviation, number (percentage), or median (interquartile range).

<sup>a</sup>The actual WMV data without TIV as a covariate.

<sup>b</sup>Covariates appearing in the model are evaluated at the following values: TIV = 1,458.01.

\* $P < 0.05$ .

last year. The ADS scores of the alcohol dependence group were  $16.24 \pm 5.92$ .

The MoCA scores were lower in the alcohol dependence group than in the controls and the PSQI, GAD-7, and PHQ-9 scores were higher in the alcohol dependence group than in the controls. There were statistical differences in the MoCA, PSQI, GAD-7, and PHQ-9 scores between the alcohol dependence group and controls ( $P < 0.05$ ).

The Fazekas scale scores, PV scores, and DWM scores were higher in the alcohol dependence group than in the controls. There were significant differences in the Fazekas scale scores, PV scores, and DWM scores between the alcohol dependence group and controls ( $P < 0.05$ ), which suggest that the WMLs were more severe in the alcohol dependence group than in the controls. WMV was  $516.94 \pm 45.40$  cm<sup>3</sup> in the alcohol dependence group and  $531.51 \pm 42.79$  cm<sup>3</sup> in the controls. After adjustment with the TIV covariate, mean WMV was  $512.98$  cm<sup>3</sup> in the alcohol dependence group and  $534.73$  cm<sup>3</sup> in the controls. The WMV of alcohol dependence patients was significantly less than that of the controls ( $P < 0.05$ , Table 1).

## Expression of Serum NLRP3 and NfL in Alcohol Dependence Patients

The expression levels of serum NLRP3 were 377.72 (367.73, 428.90) pg/ml in the alcohol dependence group and 356.35 (352.68, 361.92) pg/ml in the controls. The expression levels of

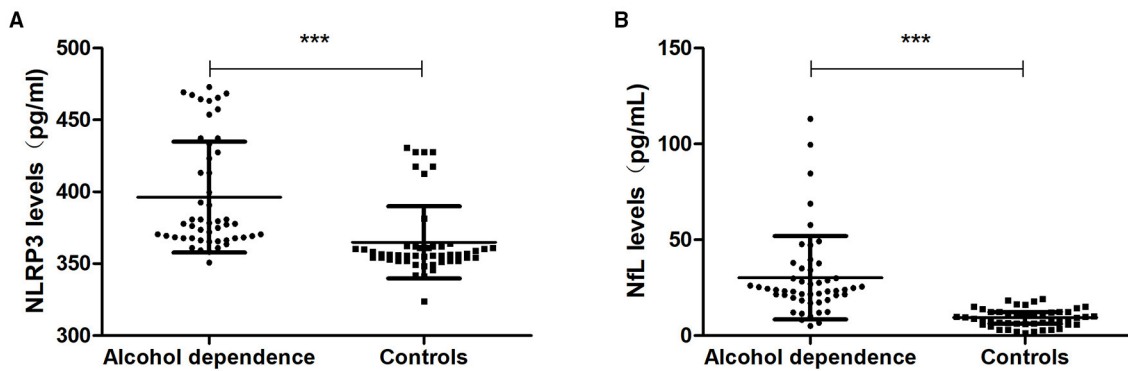


**FIGURE 2 |** NLRP3 and NfL levels in the alcohol dependence group and the controls. **(A)** The NLRP3 levels in the alcohol dependence group were higher than in the controls ( $P < 0.001$ ). **(B)** The NfL levels in the alcohol dependence group were higher than in the controls ( $P < 0.001$ ). \*\*\* $P < 0.001$ .

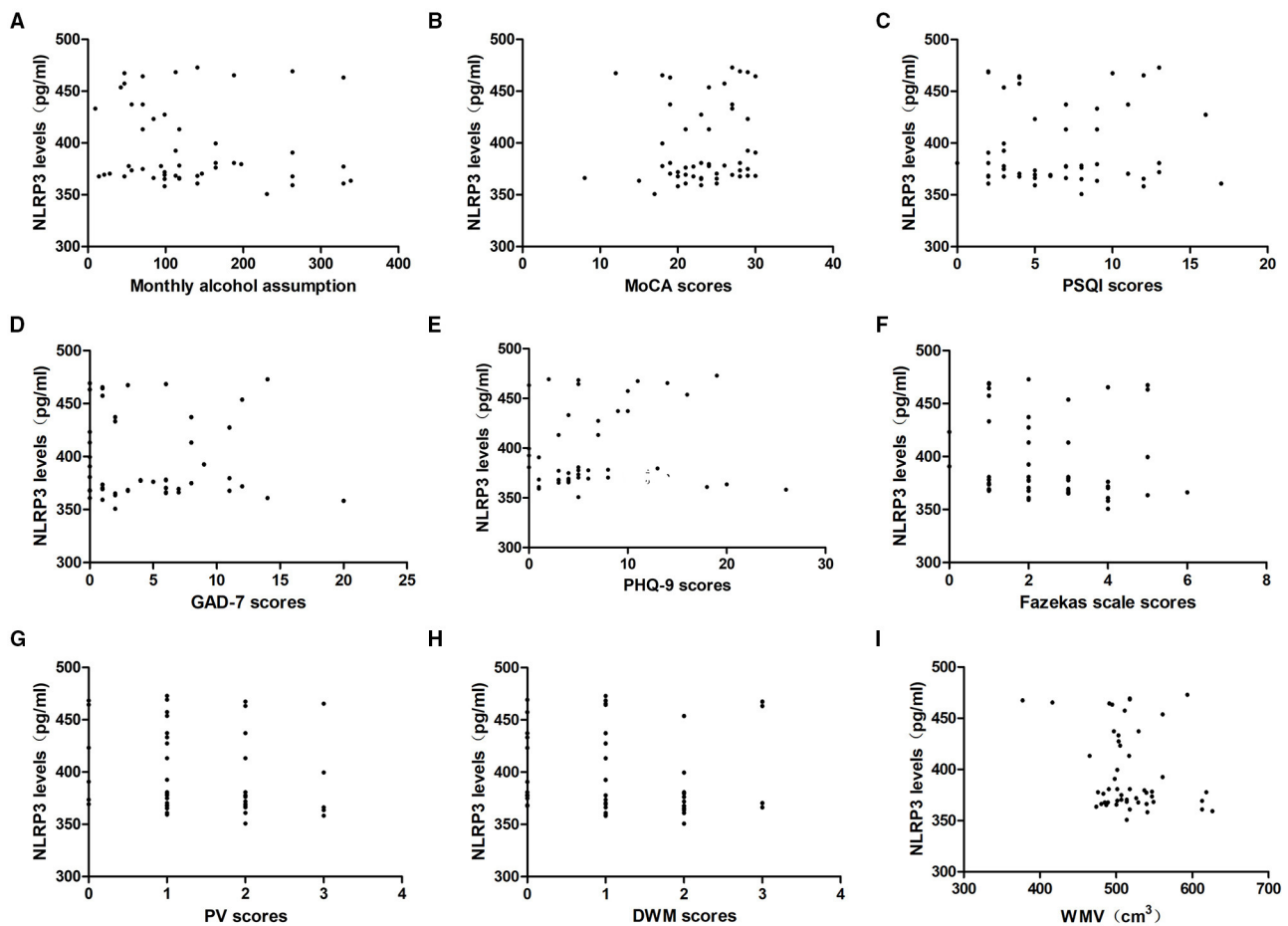


**FIGURE 3 |** Relationship between serum NLRP3 levels and alcohol assumption, neuropsychological function, the severity of WMLs, and WMV in the alcohol dependence group. Correlation of serum NLRP3 levels with **(A)** monthly alcohol consumption, **(B)** MoCA scores, **(C)** PSQI scores, **(D)** GAD-7 scores, **(E)** PHQ-9 scores, **(F)** Fazekas scale scores, **(G)** PV scores and **(H)** DWM scores, **(I)** WMV. NLRP3 levels were irrelevant to monthly alcohol consumption, MoCA scores, PSQI scores, GAD-7 scores, PHQ-9 scores, Fazekas scale scores, PV scores, DWM scores, and WMV in the alcohol dependence group ( $P > 0.05$ ).

serum NLRP3 in the alcohol dependence group were higher than those in the controls ( $P = 0.000$ ) (Figure 2A).

The expression levels of serum NfL were 23.86 (19.39, 34.43) pg/ml in the alcohol dependence group and 9.42 (6.13, 12.25) pg/mL in the controls. The expression levels of serum NfL in the alcohol dependence group were higher than those in the controls ( $P = 0.000$ ) (Figure 2B).

## Relationships Between Serum NLRP3 Levels and Alcohol Consumption, Neuropsychological Function, and Severity of WMLs

To determine whether NLRP3 levels were associated with alcohol assumption, we analyzed the correlation between serum NLRP3 levels and monthly alcohol assumption in the last year. The results indicated that NLRP3 levels were irrelevant to monthly alcohol assumption in the alcohol dependence group ( $P > 0.05$ ).

To explore whether NLRP3 expression could reflect the level of neuropsychological function, we analyzed the correlation between NLRP3 levels and the MoCA, PSQI, GAD-7, and PHQ-9 scores. In the alcohol dependence group, NLRP3 levels were irrelevant to the MoCA, PSQI, GAD-7, and PHQ-9 scores ( $P > 0.05$ ).

MRI images were analyzed and the degree of WMLs was rated using the Fazekas scale. WMV was measured by VBM. In the alcohol dependence group, NLRP3 levels were irrelevant to the Fazekas scale scores, PV scores, DWM scores, and WMV ( $P > 0.05$ , Figure 3).

In the controls, NLRP3 levels were irrelevant to the MoCA, PSQI, GAD-7, and PHQ-9 scores as well as the Fazekas scale scores, PV scores, DWM scores, and WMV ( $P > 0.05$ ).

## Relationships Between Serum NfL Levels and Alcohol Consumption, Neuropsychological Function, and Severity of WMLs

To determine whether NfL levels were associated with alcohol assumption, we analyzed the correlation between serum NfL levels and monthly alcohol assumption in the last year. The results indicated that NfL levels were irrelevant to monthly alcohol assumption ( $P > 0.05$ ).

To explore whether NfL expression could reflect the level of neuropsychological function, we analyzed the correlation between NfL levels and the MoCA, PSQI, GAD-7, and PHQ-9 scores. In the alcohol dependence group, NfL levels were negatively correlated with the MoCA scores ( $r = -0.94$ ,  $P = 0.000$ ) and positively correlated with the PSQI scores ( $r = 0.461$ ,  $P = 0.001$ ) and PHQ-9 scores ( $r = 0.423$ ,  $P = 0.002$ ). However, they were not associated with the GAD-7 scores ( $r = 0.218$ ,  $P = 0.128$ ). The NfL levels were positively correlated with the Fazekas scale scores ( $r = 0.930$ ,  $P = 0.000$ ), PV scores ( $r = 0.815$ ,  $P = 0.000$ ), and DWM scores ( $r = 0.689$ ,  $P = 0.000$ ), but negatively correlated with WMV ( $r = -0.343$ ,  $P = 0.015$ ). When TIV was set as a covariate, the partial correlation analysis indicated that NfL levels were still negatively correlated with WMV ( $r = -0.514$ ,  $P = 0.000$ , Table 2; Figure 4).

**TABLE 2 |** Relevance analysis of serum NfL levels and alcohol assumption, neuropsychological function, the severity of WMLs, and WMV in the alcohol dependence group.

		<i>r</i>	<i>P</i> -value
NfL levels, median (IQR) pg/ml	23.86 (19.39, 34.43)		
Alcohol consumption per month, median (IQR) standard drinks	112.9 (70.5, 170.475)	0.2038	0.1558
MoCA scores, mean $\pm$ SD	23.26 $\pm$ 4.84	-0.94	0.000*
PSQI scores, median (IQR)	6 (3, 9)	0.461	0.001*
GAD-7 scores, median (IQR)	3.00 (0.75, 7.25)	0.218	0.128
PHQ-9 scores, median (IQR)	5 (3, 10)	0.423	0.002*
Fazekas scale scores, median (IQR)	2.00 (1.0, 3.25)	0.930	0.000*
PV scores, median (IQR)	1 (1, 2)	0.815	0.000*
DWM scores, median (IQR)	1 (0, 2)	0.689	0.000*
WMV (cm <sup>3</sup> ), mean $\pm$ SD	516.94 $\pm$ 45.40	-0.343	0.015

Data are presented as mean  $\pm$  standard deviation, or median (interquartile range). The Spearman analysis indicated the relationship between serum NfL levels and alcohol assumption, neuropsychological function, the severity of WMLs, and WMV in the alcohol dependence group.

\* $P < 0.05$ .

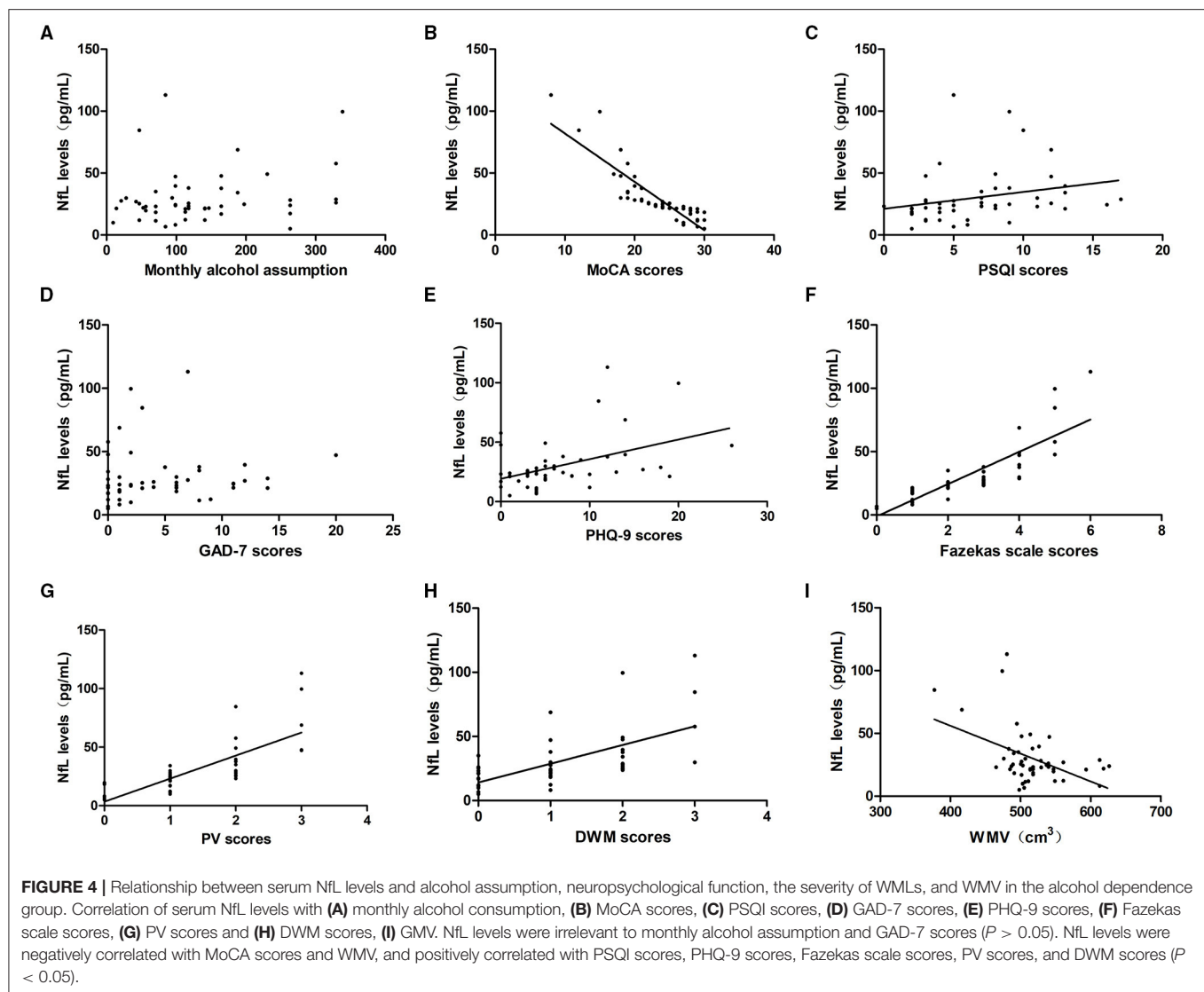
In the control group, NfL levels were irrelevant to the MoCA, PSQI, GAD-7, and PHQ-9 scores as well as the Fazekas scale scores, PV scores, DWM scores, and WMV ( $P > 0.05$ ).

## ROC Curve for NLRP3 and NfL Predicts Alcohol Dependence

ROC curve analysis was used to evaluate the predictive value of NLRP3 and NfL for the diagnosis of alcohol dependence. The areas under the ROC curve were 0.8536 (95% CI = 0.7727–0.9345,  $P < 0.01$ ) for NLRP3 levels and 0.9234 (95% CI = 0.8682–0.9786,  $P < 0.01$ ) for NfL levels (Figure 5). At an NLRP3 cut-off of 364.6 pg/ml, the sensitivity for predicting alcohol dependence was 84% and the specificity was 88%. At an NfL cut-off of 16.65 pg/ml, the sensitivity for predicting alcohol dependence was 84% and the specificity was 94%.

## DISCUSSION

With increasing alcohol consumption, alcohol use disorder has become an intractable and public concern globally. Alcohol use disorder consists of alcohol dependence, alcohol abuse, and dependence or harmful use. Alcohol dependence is characterized by compulsive alcohol consumption or a shift from drinking for pleasure to compulsive alcohol-seeking behavior. Several alcohol dependence patients who drink heavily have cognitive disorders such as mild cognitive impairment, temporary cognitive deficits, and dementia. Prospective studies have indicated that alcohol dependence patients have more than double the risk of later severe memory injury than controls (20, 21). Psychiatric disorders are common in alcohol dependence patients, including depression, anxiety, sleep disturbance, suicide, and the abuse of other drugs and substances. Approximately 40% of patients with alcohol dependence have psychological dysfunction. Alcohol dependence and psychiatric disorders worsen with each other.



Our study evaluated the cognitive and psychological conditions of alcohol dependence patients using the MoCA, PSQI, GAD-7, and PHQ-9 assessments. The results indicated that the MoCA scores in the alcohol dependence group were lower than those in the controls, which showed that enrolled alcohol dependence patients already had cognitive impairments, consistent with alcohol's propensity to cause cognitive injury. The study found that the PSQI, GAD-7, and PHQ-9 scores in the alcohol dependence group were higher than those in the controls, which suggests that alcohol dependence patients tend to have more trouble with sleep and psychiatric disorders than non-alcohol controls.

Previous studies have identified the harmful effects of alcohol dependence on the brain structure, including WMLs and the atrophy of gray and white matter. There is a U-shaped relationship between alcohol dose and WMLs; moderate drinking may be associated with better white matter health, whereas

drinking beyond recommended guidelines may be associated with more white matter damage (7). We assessed the severity of WMLs using the Fazekas scale and found that the Fazekas scale scores were higher in the alcohol dependence group than in the controls, which indicated that WMLs were more severe in alcohol dependence patients than in controls. There was no U-shaped trend between the Fazekas scale scores and alcohol consumption in the alcohol dependence group. We did not see any improvement in WMLs with an increase in alcohol consumption in the alcohol dependence group, perhaps because the enrolled alcohol dependence patients tended to have a history of long-term heavy alcohol use beyond the recommended dose. Previous studies have shown that WMV is significantly smaller in patients with alcohol dependence than in healthy controls (13, 22). In the present study, we also obtained a similar result involving WMV in alcohol dependence patients.

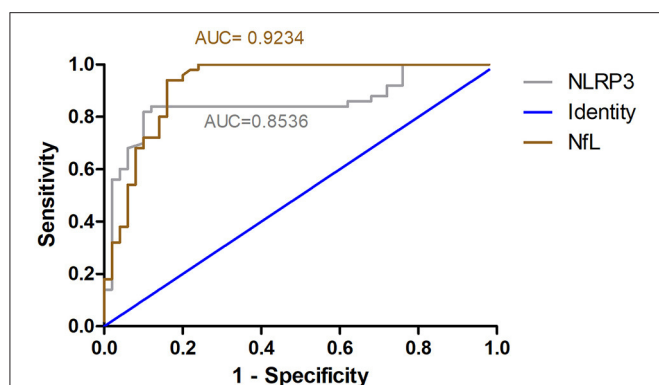


**FIGURE 5 |** ROC curve for NLRP3 and NfL predicts alcohol dependence. ROC curve analysis was used to evaluate the predictive value of NLRP3 and NfL for the diagnosis of alcohol dependence. The areas under the ROC curve were 0.8536 for NLRP3 levels and 0.9234 for NfL levels.

Several alcohol dependence patients are difficult to diagnose initially, since they are likely to have a normal life and family life, go to work regularly, and have general complaints like most healthy people such as depression, anxiety, insomnia, dreaminess, and fatigue. Therefore, we aimed to discover a biomarker for the assessment of the clinical progression and prognosis of alcohol dependence.

The association of NLRP3 has been widely explored in chronic alcoholism. Previous studies have identified alcohol as able to activate the NLRP3-inflammasome complex by stimulating the activation of caspase-1 and induction of IL-1 $\beta$  and IL-18 pro-inflammatory cytokines. An increase in NLRP3 is observed in the cultured astroglial cells, microglial cells, and cerebral cortex of mice with chronic alcohol treatment (8). Thus, we speculated whether NLRP3 changed in the serum of alcohol dependence patients and could act as a biomarker. The study found that NLRP3 levels were higher in the alcohol dependence group than in the controls, but that there were no associations between NLRP3 levels and alcohol consumption, MoCA scores, PSQI scores, GAD-7 scores, PHQ-9 scores, or Fazekas scale scores. This suggests that although NLRP3 was increased in alcohol dependence patients, it may not be a sensitive marker for assessing the severity of brain damage and prognosing alcohol dependence.

NfL is released into the extracellular space, followed by the CSF and blood after axonal damage; therefore, NfL can be detected in the CSF and serum or plasma after neurological injury (23). The pattern of NfL changes is almost identical in the serum and CSF (24). Further, serum/plasma NfL detection is a non-invasive and more direct method than lumbar puncture. In the study, we explored the possibility of NfL as a potential non-invasive and sensitive biomarker for monitoring the progression and prognosis of alcohol dependence. Simoa, a newly developed ultrasensitive immunoassay, is by far the most sensitive platform for detecting the concentration of NfL and it provides a better agreement between the CSF and serum NfL than other

analytical platforms. Therefore, we employed Simoa to detect the expression of serum NfL.

Our study first detected the expression of NfL in alcohol dependence patients and found that the expression levels of serum NfL were increased in alcohol dependence patients than in age- and sex-matched controls. As shown in the scatterplot in the study, there was a negative correlation between the MoCA scores and NfL levels and positive correlations between the PSQI scores, PHQ-9 scores, and NfL levels in alcohol dependence patients. Moreover, we found that NfL levels were positively correlated with the degree of WMLs and negatively with WMV. The Fazekas scale scores were higher and WMV was smaller in the alcohol dependence group than in the controls. The quantitative reports identified that the number of neurons and weight of brain tissue in alcohol dependence patients were decreased. A previous study indicated that NfL levels are related to the progression of brain atrophy and WMLs (25). Further, NfL is generally recognized as a potential biomarker of axonal and neuron damage, which may explain why NfL levels reflect the degree of WMLs and WMV.

Taken together, the expression levels of NfL were speculated to reflect the severity of WMLs and neuropsychological impairment in alcohol dependence. However, the relationship between NfL levels and alcohol dependence requires further validation with additional samples, and longitudinal data on NfL levels in the serum and disease progression are not yet available.

## CONCLUSION

Our study confirmed that the expression of NLRP3 and NfL was higher in alcohol dependence patients than in controls. NfL levels were negatively correlated with the MoCA scores and WMV, and positively correlated with the PSQI scores, PHQ-9 scores, and degree of WMLs, suggesting that the change in the expression of NfL may reflect the progression and prognosis of alcohol dependence.

## DATA AVAILABILITY STATEMENT

The original contributions presented in the study are included in the article/supplementary material, further inquiries can be directed to the corresponding author.

## ETHICS STATEMENT

The study was approved by the Ethics Committee of First Affiliated Hospital of Zhengzhou University (2018-KY-91). The patients/participants provided their written informed consent to participate in this study.

## PERMISSION

The study state that the permission of MoCA scale has been obtained.

## AUTHOR CONTRIBUTIONS

YL: methodology, formal analysis, data curation, writing—original draft, and writing—review and editing. RD: investigation and writing—review and editing. ZG: methodology, investigation, and writing—review and editing. LJ and YZ: data curation. TZ: formal analysis. YJ: conceptualization, methodology, supervision, and funding acquisition. The first draft of the

manuscript was written by YL and all authors agree to be accountable for the content of the work.

## FUNDING

This study was funded by National Key R&D Program of China (2018YFC1314400 and 2018YFC1314403).

## REFERENCES

- Alfonso-Loeches S, Ureña-Peralta J, Morillo-Bargues MJ, Gómez-Pinedo U, Guerri C. Ethanol-Induced TLR4/NLRP3 neuroinflammatory response in microglial cells promotes leukocyte infiltration across the BBB. *Neurochem Res.* (2016) 41:193–209. doi: 10.1007/s11064-015-1760-5
- Fein G, Shimotsu R, Di Sclafani V, Barakos J, Harper C. Increased white matter signal hyperintensities in long-term abstinent alcoholics compared with nonalcoholic controls. *Alcohol Clin Exp Res.* (2009) 33:70–8. doi: 10.1111/j.1530-0277.2008.00812.x
- Charlet K, Rosenthal A, Lohoff FW, Heinz A, Beck A. Imaging resilience and recovery in alcohol dependence. *Addiction.* (2018) 113:1933–50. doi: 10.1111/add.14259
- Magrys SA, Olmstead MC. Alcohol intoxication alters cognitive skills mediated by frontal and temporal brain regions. *Brain Cogn.* (2014) 85:271–6. doi: 10.1016/j.bandc.2013.12.010
- Carvalho AF, Heilig M, Perez A, Probst C, Rehm J. Alcohol use disorders. *Lancet.* (2019) 394:781–92. doi: 10.1016/S0140-6736(19)31775-1
- McEvoy LK, Fennema-Notestine C, Elman JA, Eyler LT, Franz CE, Hagler DJ Jr, et al. Alcohol intake and brain white matter in middle aged men: Microscopic and macroscopic differences. *Neuroimage Clin.* (2018) 18:390–8. doi: 10.1016/j.nicl.2018.02.006
- de la Monte SM, Kril JJ. Human alcohol-related neuropathology. *Acta Neuropathol.* (2014) 127:71–90. doi: 10.1007/s00401-013-1233-3
- Skudric DS, Cruikshank WW, Montgomery PC, Lisak RP, Tse HY. Emerging role of IL-16 in cytokine-mediated regulation of multiple sclerosis. *Cytokine.* (2015) 75:234–48. doi: 10.1016/j.cyt.2015.01.005
- Lin CH, Li CH, Yang KC, Lin FJ, Wu CC, Chieh JJ, et al. Blood NFL: A biomarker for disease severity and progression in Parkinson disease. *Neurology.* (2019) 93:e1104–11. doi: 10.1212/WNL.00000000000008088
- Li QF, Dong Y, Yang L, Xie JJ, Ma Y, Du YC, et al. Neurofilament light chain is a promising serum biomarker in spinocerebellar ataxia type 3. *Mol Neurodegener.* (2019) 14:39. doi: 10.1186/s13024-019-0338-0
- Ng ASL, Tan YJ, Yong ACW, Saffari SE, Lu Z, Ng EY, et al. Utility of plasma Neurofilament light as a diagnostic and prognostic biomarker of the postural instability gait disorder motor subtype in early Parkinson's disease. *Mol Neurodegener.* (2020) 15:33. doi: 10.1186/s13024-020-00385-5
- Kuhle J, Plavina T, Barro C, Disanto G, Sangurdekar D, Singh CM, et al. Neurofilament light levels are associated with long-term outcomes in multiple sclerosis. *Mult Scler.* (2020) 26:1691–9. doi: 10.1177/1352458519885613
- Li J, Wang Y, Xu Z, Liu T, Zang X, Li M, et al. Whole-brain morphometric studies in alcohol addicts by voxel-based morphometry. *Ann Transl Med.* (2019) 7:635. doi: 10.21037/atm.2019.10.90
- Monnig MA, Tonigan JS, Yeo RA, Thoma RJ, McCrady BS. White matter volume in alcohol use disorders: a meta-analysis. *Addict Biol.* (2013) 18:581–92. doi: 10.1111/j.1369-1600.2012.00441.x
- Schuckit MA. Alcohol-use disorders. *Lancet.* (2009) 373:492–501. doi: 10.1016/S0140-6736(09)60009-X
- Rudilosso S, San Román L, Blasco J, Hernández-Pérez M, Urrea X, Chamorro Á. Evaluation of white matter hypodensities on computed tomography in stroke patients using the Fazekas score. *Clin Imaging.* (2017) 46:24–7. doi: 10.1016/j.clinimag.2017.06.011
- Vanneste S, Van De Heyning P, De Ridder D. Tinnitus: a large VBM-EEG correlational study. *PLoS ONE.* (2015) 10:e0115122. doi: 10.1371/journal.pone.0115122
- Bludau S, Bzdok D, Gruber O, Kohn N, Riedl V, Sorg C, et al. Medial prefrontal aberrations in major depressive disorder revealed by cytoarchitectonically informed voxel-based morphometry. *Am J Psychiatry.* (2016) 173:291–8. doi: 10.1176/appi.ajp.2015.15030349
- Rohrer JD, Woollacott IO, Dick KM, Brotherhood E, Gordon E, Fellows A, et al. Serum neurofilament light chain protein is a measure of disease intensity in frontotemporal dementia. *Neurology.* (2016) 87:1329–36. doi: 10.1212/WNL.00000000000003154
- Woods AJ, Porges EC, Bryant VE, Seider T, Gongvatana A, Kahler CW, et al. Current heavy alcohol consumption is associated with greater cognitive impairment in older adults. *Alcohol Clin Exp Res.* (2016) 40:2435–44. doi: 10.1111/acer.13211
- Topiwala A, Ebmeier KP. Effects of drinking on late-life brain and cognition. *Evid Based Ment Health.* (2018) 21:12–5. doi: 10.1136/eb-2017-102820
- Li L, Yu H, Liu Y, Meng YJ, Li XJ, Zhang C, et al. Lower regional grey matter in alcohol use disorders: evidence from a voxel-based meta-analysis. *BMC Psychiatry.* (2021) 21:247. doi: 10.1186/s12888-021-03244-9
- Abu-Rumeileh S, Vacchiano V, Zenesini C, Polischi B, de Pasqua S, Fileccia E, et al. Diagnostic-prognostic value and electrophysiological correlates of CSF biomarkers of neurodegeneration and neuroinflammation in amyotrophic lateral sclerosis. *J Neurol.* (2020) 267:1699–708. doi: 10.1007/s00415-020-09761-z
- Gisslén M, Price RW, Andreasson U, Norgren N, Nilsson S, Hagberg L, et al. Plasma Concentration of the Neurofilament Light Protein (NFL) is a biomarker of CNS injury in HIV infection: a cross-sectional study. *EBioMedicine.* (2015) 3:135–40. doi: 10.1016/j.ebiom.2015.11.036
- Gattringer T, Pinter D, Enzinger C, Seifert-Held T, Kneihsl M, Fandler S, et al. Serum neurofilament light is sensitive to active cerebral small vessel disease. *Neurology.* (2017) 89:2108–14. doi: 10.1212/WNL.00000000000004645

**Conflict of Interest:** The authors declare that the research was conducted in the absence of any commercial or financial relationships that could be construed as a potential conflict of interest.

**Publisher's Note:** All claims expressed in this article are solely those of the authors and do not necessarily represent those of their affiliated organizations, or those of the publisher, the editors and the reviewers. Any product that may be evaluated in this article, or claim that may be made by its manufacturer, is not guaranteed or endorsed by the publisher.

Copyright © 2021 Li, Duan, Gong, Jing, Zhang, Zhang and Jia. This is an open-access article distributed under the terms of the Creative Commons Attribution License (CC BY). The use, distribution or reproduction in other forums is permitted, provided the original author(s) and the copyright owner(s) are credited and that the original publication in this journal is cited, in accordance with accepted academic practice. No use, distribution or reproduction is permitted which does not comply with these terms.



OPEN ACCESS

**Edited by:**

Peter Kalivas,  
Medical University of South Carolina,  
United States

**Reviewed by:**

Matthew Hearing,  
Marquette University, United States

Mark J. Ferris,

Wake Forest School of Medicine,  
United States

Alberto Jose Lopez,

Vanderbilt University, United States

**\*Correspondence:**

Mary Kay Lobo  
mklobo@som.umaryland.edu

**†Present address:**

Megan E. Fox,  
Department of Anesthesiology &  
Perioperative Medicine, Penn State  
College of Medicine, Hershey, PA,  
United States

**Specialty section:**

This article was submitted to  
Addictive Disorders,  
a section of the journal  
Frontiers in Psychiatry

**Received:** 07 July 2021

**Accepted:** 06 October 2021

**Published:** 18 November 2021

**Citation:**

Calarco CA, Fox ME, Van  
Terheyden S, Turner MD, Alipio JB,  
Chandra R and Lobo MK (2021)  
Mitochondria-Related Nuclear Gene  
Expression in the Nucleus Accumbens  
and Blood Mitochondrial Copy  
Number After Developmental Fentanyl  
Exposure in Adolescent Male and  
Female C57BL/6 Mice.  
Front. Psychiatry 12:737389.  
doi: 10.3389/fpsy.2021.737389

# Mitochondria-Related Nuclear Gene Expression in the Nucleus Accumbens and Blood Mitochondrial Copy Number After Developmental Fentanyl Exposure in Adolescent Male and Female C57BL/6 Mice

**Cali A. Calarco, Megan E. Fox<sup>†</sup>, Saskia Van Terheyden, Makeda D. Turner, Jason B. Alipio, Ramesh Chandra and Mary Kay Lobo<sup>\*</sup>**

Department of Anatomy and Neurobiology, University of Maryland School of Medicine, Baltimore, MD, United States

The potency of the synthetic opioid fentanyl and its increased clinical availability has led to the rapid escalation of use in the general population, increased recreational exposure, and subsequently opioid-related overdoses. The wide-spread use of fentanyl has, consequently, increased the incidence of *in utero* exposure to the drug, but the long-term effects of this type of developmental exposure are not yet understood. Opioid use has also been linked to reduced mitochondrial copy number in blood in clinical populations, but the link between this peripheral biomarker and genetic or functional changes in reward-related brain circuitry is still unclear. Additionally, mitochondrial-related gene expression in reward-related brain regions has not been examined in the context of fentanyl exposure, despite the growing literature demonstrating drugs of abuse impact mitochondrial function, which subsequently impacts neuronal signaling. The current study uses exposure to fentanyl via dam access to fentanyl drinking water during gestation and lactation as a model for developmental drug exposure. This perinatal drug-exposure is sufficient to impact mitochondrial copy number in circulating blood leukocytes, as well as mitochondrial-related gene expression in the nucleus accumbens (NAc), a reward-related brain structure, in a sex-dependent manner in adolescent offspring. Specific NAc gene expression is correlated with both blood mitochondrial copy number and with anxiety related behaviors dependent on developmental exposure to fentanyl and sex. These data indicate that developmental fentanyl exposure impacts mitochondrial function in both the brain and body in ways that can impact neuronal signaling and may prime the brain for altered reward-related behavior in adolescence and later into adulthood.

**Keywords:** mitochondria, mitochondrial copy number, developmental drug exposure, fentanyl, nucleus accumbens, gene expression

## INTRODUCTION

Opioid use in the United States has dramatically increased in recent years, with death by opioid overdose reaching epidemic proportions (1, 2). Despite the high potential for opioid misuse and abuse, they remain some of the most effective treatments for pain management available. More recently, the synthetic opioid fentanyl, which is 50–100× more potent than morphine, has become both commonly prescribed and commonly added to illicit drugs increasing both use in the general population and opioid-related overdose deaths (1, 2). The rise in both use and misuse of opioids seen in the general population has also been observed among pregnant women, increasing both *in utero* exposure to opioids and increasing the occurrence of neonatal opioid withdrawal syndrome (NOWS) (3–6). Previous work in both humans and rodents has shown that developmental exposure to traditional opioids like morphine and heroin can lead to behavioral and developmental differences into adolescence and adulthood, including altered attention, stress responsivity, and learning and memory (7–10). Recently, studies examining the impact of developmental exposure to fentanyl have revealed changes in behavior and somatosensory processing into adolescence and adulthood (11, 12).

In addition to the many neurobiological changes in reward related processing, and cycles of negative affect that are associated with opioid use, escalation of use, and substance use disorders (13–18), opioid exposure is also associated with high degrees of oxidative stress and oxidative damage both centrally and peripherally (19–23). Patients with opioid use disorders show higher levels of oxidative and inflammatory markers in blood serum (24), and are more likely to show markers of metabolic syndrome, indicative of increased risk for mortality due to heart disease or diabetes (25). Multiple pre-clinical studies have shown metabolic disruptions and oxidative damage in brain tissue after morphine or heroin exposure (19, 26). Oxidative damage in the form of increased reactive oxygen species and decreased antioxidant enzyme activity caused by drug use can lead to mitochondrial dysfunction and neurotoxicity as well as other cellular damage (22, 26). Mitochondria specifically both absorb inflammatory and metabolic damage (27–29) and mediate brain function, neuroplasticity, and early life brain development (30–34).

Mitochondrial dynamics and changes therein due to stress, damage or altered energy requirements impact mitochondrial copy number, the ratio of mitochondrial DNA to nuclear DNA, which can be used as a proxy for mitochondrial function (35, 36). While brain tissue is not readily available from patient populations and does not allow for repeated sampling over

the course of development, mitochondrial copy number in blood leukocytes is readily accessible in both clinical and pre-clinical samples. Indeed, understanding how peripheral blood-derived mitochondrial DNA copy number is associated with gene expression and mitochondrial function in other tissues is an active and important avenue of investigation (36). With respect to opioid use, mitochondrial copy number is reduced and markers of mitochondrial damage are increased in both human heroin users and rats exposed to chronic morphine (37). In the rats, mitochondrial copy number was also reduced in brain tissue, specifically the hippocampus (37). In cell culture, acute fentanyl and methadone, but not morphine, specifically negatively impact mitochondrial morphology and function (38, 39). It is currently unclear how the changes in mitochondria, accumulating mitochondrial damage, and other behavioral effects of opioid use are related. While mitochondrial function in reward-related brain areas, such as NAc, does regulate anxiety-like behaviors in rodent models (40–42), work on how altered mitochondria function contributes to increases in psychiatric symptoms and mood disorders in individuals with opioid use disorders or opioid exposure (43–45) is still needed.

The relationship between opioid use and mitochondrial function is still actively being explored and the current study sought to determine if developmental exposure to fentanyl causes long-lasting changes in peripheral and central markers of mitochondrial dynamics comparable to those observed after adult opioid use. Further, we sought to understand how peripheral markers of mitochondrial dynamics relate to mitochondrial gene expression in the reward-related brain regions critical for mediating opioid use, escalation of use, and opioid use disorder, specifically the nucleus accumbens (NAc) (46–48). Neuronal morphology and signaling changes in NAc have been shown to be critical for regulating both reward and anxiety- and depression-like behaviors (49, 50). Finally, we examined how both blood mitochondrial copy number and NAc gene expression correlated with behavioral measures of anxiety-like behavior and body weight. In this study we expand on the previously developed model of perinatal fentanyl exposure (11, 12) to explore the effects on blood mitochondrial copy number and expression of mitochondrial-related genes in NAc in adolescent mice. In this pre-clinical model, the perinatal period of mouse development consisting of gestation through weaning roughly corresponds to the full gestational period in humans, due to the developmental differences between species (51, 52). To our knowledge, this is the first study to examine mitochondrial copy number or NAc gene expression after developmental fentanyl exposure and subsequent forced abstinence.

## METHODS

### Animals

All procedures were conducted in accordance with the Guide for the Care and Use of Laboratory Animals and approved by the Institutional Animal Care and Use Committees at the University of Maryland School of Medicine. Male and female C57BL/6J mice were bred to generate developmentally drug-exposed offspring in our facility. After verification of dam pregnancy by copulatory

**Abbreviations:** NAc, Nucleus Accumbens; EPM, elevated plus maze; Cyts, cytochrome C; Park2, parkin; Pink1, PTEN induced kinase 1; Tomm20, translocase of outer mitochondrial membrane 20; Drp1, dynamin-related protein 1; Fis1, mitochondrial fission 1 protein; Mfn1, mitofusin 1; Mfn2, mitofusin 2; Opa1, OPA1 mitochondrial dynamin like GTPase; Egr3, Early Growth Response 3; Nrf1, nuclear respiratory factor 1; Nrf2, erythroid 2 like 2; Pgc1α, peroxisome proliferator-activated receptor gamma coactivator 1-alpha; Poly, DNA Polymerase Subunit Gamma-1; Tfam, mitochondrial transcription factor transcription factor A; Tfbb1, Mitochondrial transcription factor B1.

plug, sires were removed, and water was replaced with fentanyl-containing water or vehicle (see below). Vehicle controls received plain tap water. Water was monitored daily for consumption and replenished as necessary until litters were weaned at P21. After weaning, offspring were housed two to five per cage in single-sex groups, in a temperature- and humidity-controlled vivarium. Food and water were available *ad libitum*, and lights were maintained on a 12-h cycle.

## Drugs

At the time of pregnancy confirmation 10 µg/mL fentanyl citrate (Cayman Chemical; Cat# 22659) in tap water, or plain tap water (vehicle) was administered as the only source of available drinking water. This concentration has been reported previously for use in this developmental exposure model and was selected because mice will readily consume this dose, yet it does not cause motor deficits and is well-below LD50 of fentanyl in mice (11, 12). This dose has previously been shown to induce spontaneous withdrawal signs after weaning, but is not sufficient to disrupt maternal care behavior (11, 12).

## Behavior

After weaning at P21, offspring were left undisturbed until beginning behavioral testing. Each animal underwent an elevated plus maze (EPM) test and splash test, with 24 h separating each test. Twenty-four hours after the final behavioral test on day P35 body weight was measured and tissues were collected. The tissues used for analysis here were obtained from a subset of mice whose developmental exposure to fentanyl and behavioral testing results have been previously published by Alipio et al. (11). Tissue analysis was conducted on all 12 of the male water and male fentanyl mice, while a subset of the female mice were used: 17/22 female water and 17/31 female fentanyl mice. These mice include offspring from 7 different dams receiving water and 10 dams receiving fentanyl. Average litter size was 6 pups for both groups (Mean, SEM - Water: 6.14, 0.553; Fentanyl: 6.4, 0.476). Mice were habituated to the testing room before all behavioral procedures.

To measure anxiety-like behavior, mice were placed in the center of the EPM and were allowed to roam freely for 5 min, as described previously (11, 53, 54). Time spent in the open and closed arms of the maze in addition to the number of times the mouse entered one of the open arms were measured using computer tracking software (TopScan CleverSys, Reston, VA). Open/Closed ratios were calculated by dividing the time spent in the open arms by the time spent in the closed arms.

The splash test was used to measure affective state as has been described previously (11, 54). Mice were placed in an empty glass cylinder and their dorsal coat surface was sprayed three times with a 10% sucrose solution. Five min video recordings were experimenter scored by a blinded experimenter for time spent grooming.

## Tissue Collection

Twenty-four hours following the final behavioral assay, brains were removed, and trunk blood was collected. Blood was collected in a 1.5 mL microcentrifuge tube containing 10 µL EDTA (0.5 M, Invitrogen, Cat#15575) to reduce clotting,

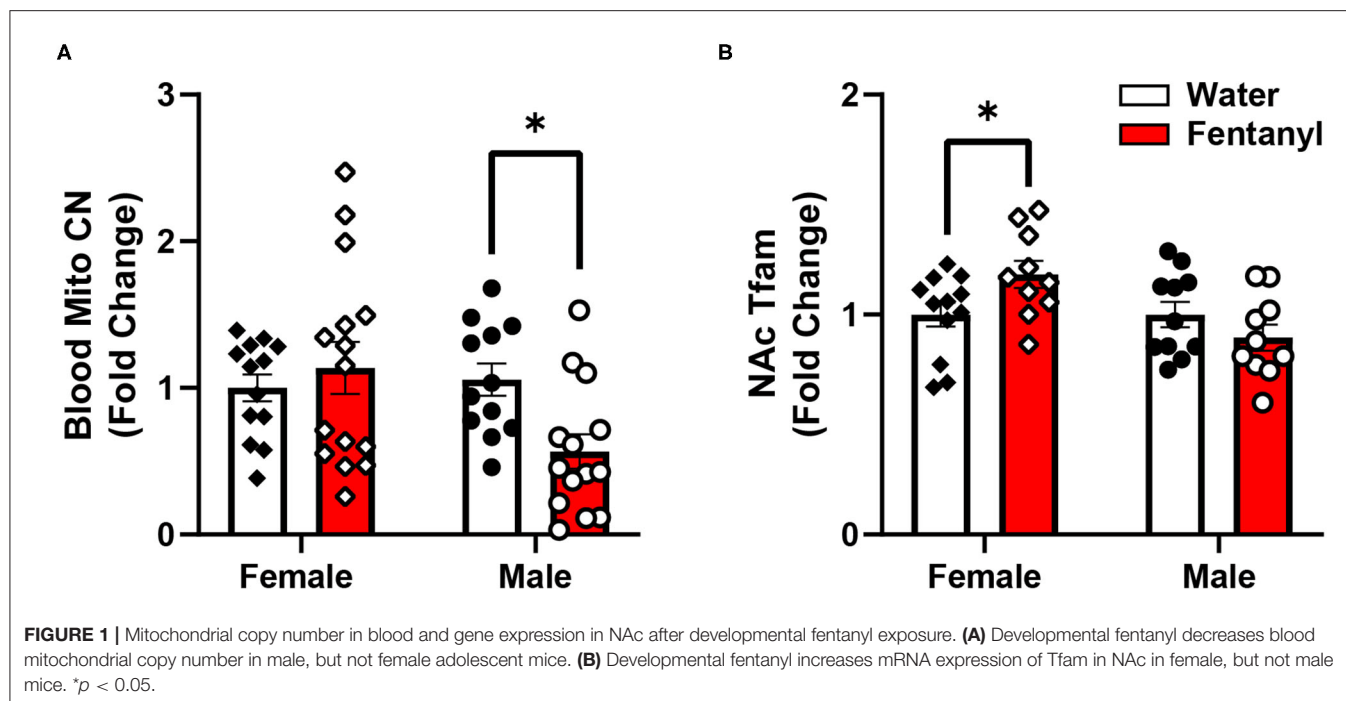
vortexed and stored at  $-80^{\circ}\text{C}$  until further processing. Brains were placed on ice, cut into 1 mm sections using a brain block (Braintree Scientific), and 14-gauge punches surrounding the anterior commissure, encompassing both NAc core and shell, were collected (2 per animal). Tissue punches were stored at  $-80^{\circ}\text{C}$  until further processing.

## DNA Extraction and Analysis

Trunk blood was thawed and homogenized to break up any clots. DNA was extracted from whole blood using a QiaAmp DNA Micro Kit (Qiagen, Germantown, MD; Cat# 56304) following manufacturer instructions. DNA quality and concentration were measured on a Nanodrop (Thermo Scientific), and DNA was diluted to 2 ng/µL for qPCR with PerfeCTa SYBR Green FastMix (Quantabio, Beverly, MA; Cat# 95072). To measure relative mitochondrial copy number, expression of the mitochondrial gene NADH dehydrogenase 1 (*mt-Nd1*) was compared to the nuclear gene glyceraldehyde 3-phosphate dehydrogenase (*Gapdh*) using the  $2^{-\Delta\Delta\text{Ct}}$  method. Forward and reverse primer sets are as follows (F, R; 5'-3'): *Gapdh* AGGTCGGTGTGAACGG ATTTG, TG TAGACCATGTAGTTGAGGTCA; *mt-Nd1* TACA ACCATTTGCAGACGCC, TGTGAGTGATAGGGTAGGTGC. Data was further normalized within sex, such that male animals exposed to fentanyl were compared to male controls and female animals that received fentanyl were compared to female controls.

## RNA Extraction and Analysis

RNA was extracted from NAc tissue punches using Trizol (Invitrogen) and the MicroElute Total RNA Kit (Omega; Cat# R6831) with a DNase step (Qiagen, Germantown, MD; Cat# 79254). RNA quantity and concentration were measured on a Nanodrop (Thermo Scientific), and 400 ng of RNA was used to synthesize complementary DNA using a reverse transcriptase iScript complementary DNA synthesis kit (Bio-Rad, Hercules, CA; Cat# 1708891). Resulting cDNA was diluted to a concentration of 2 ng/µL, which was used to measure relative mRNA expression changes via quantitative PCR with PerfeCTa SYBR Green FastMix (Quantabio, Beverly, MA; Cat# 95072). Sixteen nuclear mitochondrial related genes were tested, and the primer sets are as follows (F, R; 5'-3'): *Cycs* TACATGCT ACCACGGCTCTC, TGAGGTGACATGCCCTATT; *Drp1* GGGCACTTAAATTGGGCTCC, TGTATTCTGTTGGCGT GGAAC; *Egr3* CCGGTGACCATGAGCAGTTT, TAATGGGC TACCGAGTCGCT; *Fis1* GGCTGTCTCCAAGTCCAAATC, GGAGAAAAGGGAAGGCGATG; *Mfn1* TATCGATGCCTT GCGGAGAT, GGCGAATCACAACACTTCCA; *Mfn2* GGAG ACCAACAAGGACTGGA, TGCACAGTGACTTTCAACCG; *Nrf1* AGACCTCTGCTAGATTACCG, CCTGGACTTCAC AAGCACTC; *Nrf2* TCTACTGAAAAGGCGGCTCA, TTGC CATCTCTGGTTTGCTG; *Opa1* CAGCTCAGAAGACCTT GCCA, TCCTTCAACAAGCTGAGGCT; *Park2* GCACCTCA AGCAAGAATGAC, TACAGATGAGTGGGTCAGAGC; *Pgc1α* CGACCATGGTGTGTTCTTG, ATGGCAGCGACTCCAT ACTC; *Pink1* GGGCTACTGTGTCTCTGATGT, CTA CTCCA GCTTGTCCTCTG; *Poly* ACTCCTGGAACAGTTGTGCT, CGTCCATCTACTCAGGACGG; *Tfam* TTTGTTGTGTGT GGGTGCTC, CGAAGGGCCATCCCTGTAT; *Tfb1m* TACG



CCCTTGATAGAGCCCA, TCCTTCGAAACTGAAACGCA; *Tomm20* CTGTGCTCTGGGCACTTAAC, AGGGTGCACACAGGTCTAAT.

All biological samples were run in duplicate, and samples were excluded from analysis if duplicates were not within one CT value. Further, some samples did not yield sufficient RNA to run all genes tested, therefore, these samples were not run for all 16 genes. Quantification of mRNA changes was performed using the  $2^{-\Delta\Delta C_t}$  method, using *Gapdh* and respective male and female control groups to normalize expression as described above.

## Statistics

All statistics were performed using GraphPad Prism version 9.1.2 for Windows (GraphPad Software, San Diego, California USA, www.graphpad.com). Behavioral data for the subset of mice used for tissue analysis were analyzed with two-way ANOVAs with Sidak *post-hoc* tests to compare within sex. Group data was analyzed for outliers using Grubb's-test, and outliers were removed from further analysis (no more than one per group). Relative DNA and RNA concentrations were compared within sex with unpaired *t*-tests when assumptions of equal variance were met and a Welch's corrected *t*-test when this assumption was violated. Data are presented as mean  $\pm$  sem with individual data points overlaid. Simple linear regressions were used for correlations.

## RESULTS

To determine if developmental fentanyl exposure is sufficient to modulate peripheral mitochondria, we measured mitochondrial copy number in blood collected from P35 adolescent mice that had been exposed to fentanyl from conception through weaning.

We did not observe an effect in female mice (Welch's corrected  $t = 0.677$ ,  $df = 20.82$ ,  $p > 0.05$ ), however, blood mitochondrial copy number was significantly reduced in male mice that had received perinatal fentanyl as compared to control male mice (**Figure 1A**:  $t = 3.005$ ,  $df = 24$ ,  $p = 0.0061$ ).

Opioid exposure and withdrawal in adulthood can cause both oxidative stress as well as gene expression changes in multiple brain regions (22, 25, 37, 39). Opioids are also highly addictive drugs with high abuse potential, and as such, readily engage reward-related brain circuitry during drug exposure (48, 55–58). Therefore, we examined the expression of multiple genes related to mitochondrial function in the NAc to determine if the peripheral changes in mitochondria are related to central changes in mitochondrial-related pathways in a reward-related brain region. These data are summarized in **Table 1**.

We examined genes related broadly to multiple facets of mitochondrial function. Genes related to regulating the balance of mitochondrial fission and fusion to maintain mitochondrial number include the fission-related proteins dynamin-related protein 1 (Drp1) and mitochondrial fission 1 protein (Fis1), the fusion-related proteins mitofusin 1 and 2 (Mfn1, Mfn2), and OPA1 mitochondrial dynamin like GTPase (Opa1) (59). Gene expression for these fission and fusion-related proteins was not changed in NAc in either sex by developmental exposure to fentanyl. Genes involved in mitochondrial function, health, stress-resistance, mitophagy, and protein transport including cytochrome C (Cyts), parkin (Park2), PTEN induced kinase 1 (Pink1), and translocase of outer mitochondrial membrane 20 (Tomm20) (60) were also not changed in NAc in either sex after developmental fentanyl exposure.

Finally, we examined expression of genes related to transcription and transcriptional regulation of both nuclear

**TABLE 1 |** Relative gene expression of nuclear mitochondrial related genes in NAc.

Gene	Sex	Control			Fentanyl			Analysis	p-value	Sig
		n	Mean	95% CI	n	Mean	95% CI			
Fission- and fusion-related genes										
Drp1	Female	10	1.00	0.6707–1.329	8	0.8643	0.7428–0.9858	Welch's t-test	0.3798	n.s.
	Male	10	1.00	0.8393–1.161	8	0.8145	0.4416–1.187	t-test	0.2666	n.s.
Fis1	Female	12	1.00	0.820–1.180	11	1.067	0.8969–1.238	t-test	0.556	n.s.
	Male	11	1.00	0.9138–1.086	11	0.8957	0.7357–1.056	t-test	0.2157	n.s.
Mfn1	Female	12	1.00	0.8323–1.168	12	1.032	0.8772–1.187	t-test	0.7603	n.s.
	Male	11	1.00	0.9288–1.07	11	0.9784	0.8127–1.14	Welch's t-test	0.7938	n.s.
Mfn2	Female	12	1.00	0.9157–1.084	12	1.021	0.9245–1.118	t-test	0.7197	n.s.
	Male	12	1.00	0.9372–1.063	10	0.9929	0.8878–1.098	t-test	0.8943	n.s.
Opa1	Female	12	1.00	0.8864–1.114	9	1.022	0.9368–1.108	t-test	0.7443	n.s.
	Male	12	1.00	0.9033–1.097	11	1.076	0.9393–1.213	t-test	0.3194	n.s.
Mitochondrial function, health, stress-resistance, mitophagy, and protein transport										
Cycs	Female	9	1.00	0.7999–1.200	11	0.9385	0.7798–1.097	t-test	0.5868	n.s.
	Male	11	1.00	0.8917–1.108	9	1.735	0.7091–2.760	Welch's t-test	0.1383	n.s.
Park2	Female	10	1.00	0.8322–1.168	12	1.061	0.9342–1.189	t-test	0.5148	n.s.
	Male	11	1.00	0.9005–1.099	9	1.01	0.8131–1.207	t-test	0.916	n.s.
Pink1	Female	10	1.00	0.7716–1.228	12	0.7191	0.8210–1.287	t-test	0.7191	n.s.
	Male	11	1.00	0.8355–1.164	9	0.8873	0.6134–1.161	t-test	0.4136	n.s.
Tomm20	Female	10	1.00	0.8274–1.173	12	1.159	1.012–1.307	t-test	0.1313	n.s.
	Male	11	1.00	0.8941–1.106	9	0.925	0.6860–1.164	Welch's t-test	0.524	n.s.
Nuclear transcription factors and transcriptional co-activators										
Egr3	Female	12	1.00	0.7853–1.215	12	0.9545	0.8528–1.056	Welch's t-test	0.6794	n.s.
	Male	12	1.00	0.8669–1.133	11	1.125	0.8940–1.356	t-test	0.2994	n.s.
Nrf1	Female	11	1.00	0.8882–1.112	12	0.923	0.8101–1.036	t-test	0.2969	n.s.
	Male	11	1.00	0.9055–1.095	11	0.9437	0.7722–1.115	t-test	0.5289	n.s.
Nrf2	Female	12	1.00	0.7022–1.298	12	0.9898	0.7989–1.181	t-test	0.9502	n.s.
	Male	10	1.00	0.8929–1.107	9	1.234	0.4896–1.978	Welch's t-test	0.4934	n.s.
Pgc1α	Female	12	1.00	0.7647–1.235	10	0.9395	0.7330–1.146	t-test	0.6785	n.s.
	Male	10	1.00	0.8878–1.112	8	0.8442	0.4007–1.288	Welch's t-test	0.4451	n.s.
Mitochondrial transcriptase and transcription factors										
Poly	Female	9	1.00	0.9216–1.078	10	1.059	0.8985–1.219	Welch's t-test	0.4693	n.s.
	Male	11	1.00	0.9416–1.058	7	0.99	0.5802–1.400	Welch's t-test	0.9549	n.s.
Tfam	Female	12	1.00	0.8794–1.121	10	1.183	1.043–1.322	t-test	0.0381	*
	Male	11	1.00	0.8720–1.128	10	0.8953	0.7612–1.030	t-test	0.2207	n.s.
Tfb1m	Female	10	1.00	0.88490–1.151	9	0.946	0.8401–1.052	t-test	0.5231	n.s.
	Male	11	1.00	0.9189–1.081	6	1.142	0.6122–1.672	Welch's t-test	0.5254	n.s.

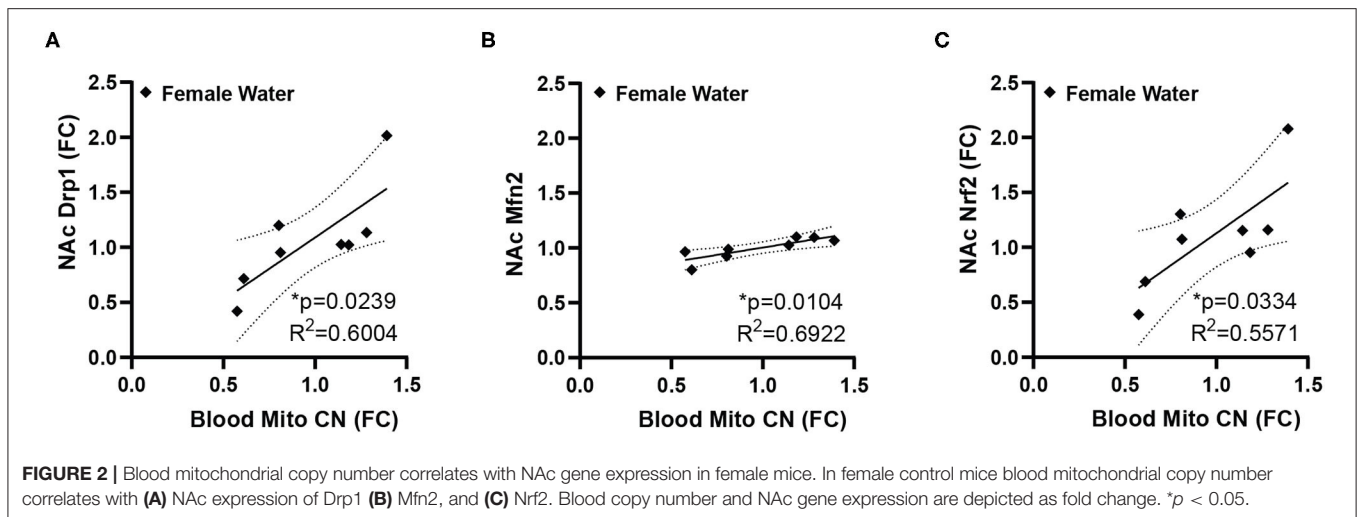
Significant results in bold.

\**p* < 0.05, n.s. = not significant.

and mitochondrial genome genes, broad regulators of overall patterns of gene expression (61, 62). Transcription factors and transcriptional co-activators that regulate nuclear genes related to mitochondrial function including Early Growth Response 3 (*Egr3*), nuclear respiratory factor 1 (*Nrf1*), nuclear factor, erythroid 2 like 2 (*Nrf2*), and peroxisome proliferator-activated receptor gamma coactivator 1-alpha (*Pgc1α*) were not changed in NAc in either sex after developmental fentanyl exposure. DNA Polymerase Subunit Gamma-1 (*Poly*), a mitochondrial DNA polymerase which conducts mitochondrial DNA replication was not altered by developmental fentanyl, however, the mitochondrial transcription factor transcription

factor A (*Tfam*) increased expression in female mice that had been developmentally exposed to fentanyl (**Figure 1B**). *Tfam* expression was not changed in male mice, nor were changes observed in either sex of transcription factor B1, mitochondrial (*Tfb1*). Notably, the change in expression of *Tfam* is double dissociated from the mitochondrial copy number finding in male mice.

While many of the genes examined did not show statistically significant differences, we noticed high degrees of variability in gene expression for many genes, therefore, we decided to explore if this variability in gene expression was related either to peripheral mitochondrial copy number, performance in the



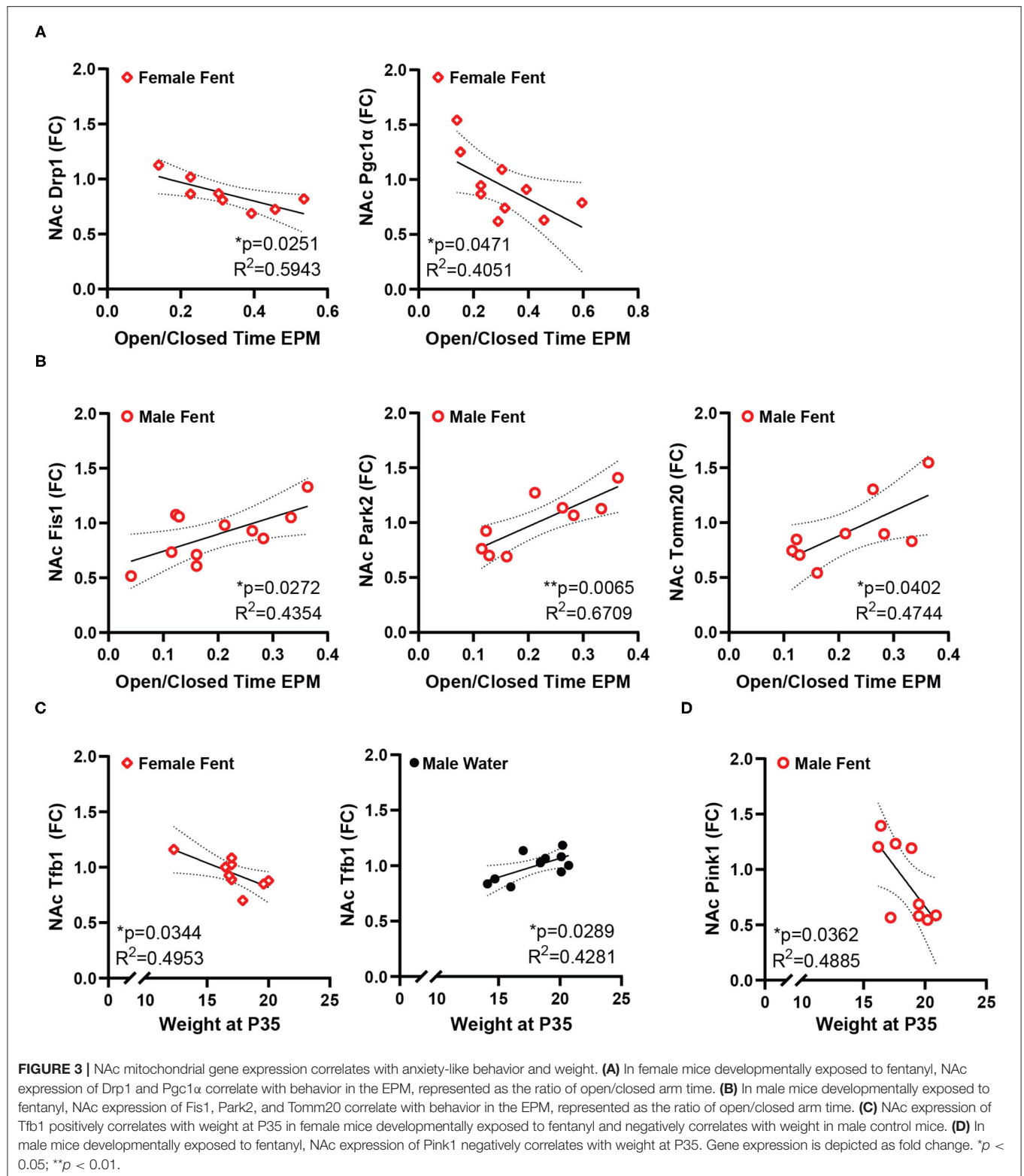
measured behavioral tests, or other factors that may relate to overall metabolic function, specifically body weight at the time of sacrifice. The behavioral data used here represents a subset of the previously published animals (11) used for the molecular analysis. In this subset of animals, male animals showed increased anxiety-like behavior in the EPM, indicated by a reduced ratio of time spent in the open arms of the maze over the time spent in the closed arms, but there was no effect in females (mean ratio, SEM - male control: 0.4081, 0.07036; male fentanyl: 0.1919, 0.02859; female control: 0.3661, 0.0441; female fentanyl: 0.3318, 0.0401) [main effect of drug  $F_{(1,54)} = 7.419$ ,  $p = 0.0087$ ; *post-hoc* male adjusted  $p = 0.0082$ , female adjusted  $p > 0.05$ ]. There was a main effect of sex in the splash test, with females spending more time grooming [ $F_{(1,54)} = 10.48$ ,  $p = 0.0021$ ], however there was no effect of fentanyl or interaction (mean seconds, SEM - male control: 99.01, 5.497; male fentanyl: 81.83, 11.30; female control: 117.2, 4.954; female fentanyl: 112.8, 8.543). Finally, while males weighed more than females [ $F_{(1,54)} = 5.622$ ,  $p = 0.0213$ ], we did not observe an effect of fentanyl on weight at this time point in this cohort (mean grams, SEM - male control: 18.21, 0.6542; male fentanyl: 18.82, 0.4767; female control: 17.2, 0.6829; female fentanyl: 17.11, 0.4271). We performed Pearson correlations on our copy number, gene expression and behavioral data and all correlations are described in **Supplementary Table 1**. Blood mitochondrial copy number showed a significant positive correlation with NAc Drp1, Mfn2, and Nrf1 in female control mice (**Figure 2**) but shows no relationship with NAc gene expression in female mice exposed to fentanyl or male mice of either condition. Specifically, there was no correlation between blood copy number with NAc Tfam expression in female mice, which was significantly increased in fentanyl-exposed mice. While developmental fentanyl does not change blood mitochondrial copy number in female adolescent mice, it does seem to disrupt the correlations with NAc gene expression seen in control mice, possibly indicating an uncoupling of peripheral and central mitochondrial function potentially unique to female mice, or a more complex relationship between NAc gene expression and blood mitochondria copy number in the context of developmental drug exposure.

Conversely, the ratio of time spent in the open/closed arms of the elevated plus maze, an indicator of anxiety-like behavior, showed no correlation with gene expression in control animals, but is correlated with a number of genes in animals that had been exposed to fentanyl (**Figure 3**). In female mice EPM open/closed ratio negatively correlates with both Drp1 and Pgc1 $\alpha$  expression in NAc (**Figure 3A**). In male animals, EPM open/closed ratio positively correlates with NAc expression of Fis1, Park2, and Tomm20 (**Figure 3B**). Time spent grooming in the splash test did not correlate with NAc gene expression for either sex under either drug exposure condition. Body weight positively correlated with NAc Tfmb expression in male control mice, and negatively with Tfmb in female mice exposed to fentanyl (**Figure 3C**). In male mice exposed to fentanyl body weight was negatively correlated with NAc expression of Pink1 (**Figure 3D**).

## DISCUSSION

Opioid exposure is related to increased oxidative damage and mitochondrial damage in adulthood, and many negative impacts of chronic opioid use can be particularly long-lasting if the drug is encountered during development, leading to altered behavior and neurological function (9, 20, 24, 63). Opioid use and opioid use disorders are also associated with an increase in psychiatric mood symptoms as well as mood and anxiety disorders (43, 44). The current study examined how developmental exposure to the synthetic opioid fentanyl altered blood mitochondrial copy number, mitochondrial gene expression, and how these measures related to each other and anxiety-like behaviors in adolescent male and female mice. We showed that developmental exposure to fentanyl reduces blood mitochondrial copy number in male mice and increases NAc expression of Tfam mRNA in female mice. Additionally, mice exposed to fentanyl showed different patterns of correlation between blood mitochondrial copy number, anxiety-like behavior, weight, and NAc gene expression in a sex-dependent manner.

Mitochondria are particularly impacted by oxidative stress both as producers and scavengers of reactive oxygen species, and



in turn are a critical mediator in downstream cellular processing and homeostatic changes in response to such oxidative stress. Mitochondrial DNA is particularly susceptible to oxidative damage compared to nuclear DNA, as it both lacks protective

histone proteins and mitochondria have less robust DNA-repair machinery than nuclei (64). The mitochondrial genome is maintained in a highly dynamic equilibrium, existing in multiple copies per cell, with 1–10 copies per mitochondrion

and multiple mitochondria per cell, depending on cell type (35, 65). Because the mitochondrial genome codes for most of the enzymatic subunits needed for oxidative phosphorylation, mitochondrial copy number can be used as an indicator of mitochondrial biogenesis (35, 66), and changes in mitochondrial copy number may contribute to oxidative stress, inflammation, and mitochondrial dysfunction (67, 68).

Mitochondrial dysfunction has been linked to disorders from diabetes, to cancer, and more recently to stress, psychiatric illnesses and substance use disorders (28, 69–74). Mitochondria copy number is increased in patients with bipolar disorder (75, 76), early childhood maltreatment or adversity (77), and increased in the prefrontal cortex and hippocampus of rats that had undergone cocaine self-administration, but is decreased in human heroin users and mice and rats exposed to chronic heroin (37). Our findings here mimic the decrease in copy number seen in male rodents, despite the developmental exposure and abstinence at the time of tissue collection used here. In the human patients, copy number did partially recover 3 months after initiation of heroin abstinence, although even after 6 months copy number had not fully recover to control levels (37). The clinical population represented female patients, although we did not observe changes in copy number in female mice. Further work will be needed to determine if opioids impact mitochondrial copy number comparably in men and women. Sex differences in substance use, substance use disorders, and successful abstinence have been readily observed for multiple used drugs, including opioids (78–82). A unique feature of the current study is the consistency of gestational fentanyl exposure *in utero* as our sample represents multiple litters consisting of both males and females. Fentanyl dose during the post-natal period was dependent on individual variance in pup milk or water consumption until weaning.

Although a growing number of studies are examining peripheral copy number, fewer studies are relating this measure to changes in other tissues, including the brain. In neurons, mitochondrial quality control and proper functioning impacts many aspects of cellular function related to signaling and circuit function (31). Specifically, in addition to providing the high levels of ATP necessary to maintain electro-chemical gradients, mitochondria buffer both intracellular calcium and reactive oxygen species, influence apoptosis, and have been shown to be critical for dendritic spine formation (31–33). Further, mitochondria and mitochondrial related genes in the NAc specifically have been shown to mediate behavioral responding for cocaine in a mouse model of substance use disorder (34, 83, 84), indicating mitochondrial function in NAc as a specific node for influencing the response to addictive drugs. Of the genes examined in NAc here, only Tfam showed increased expression. Interestingly, Tfam, because it binds to the mitochondrial DNA as a transcription factor, also has been shown to protect mitochondrial DNA from damage due to oxidative stress (61, 85, 86). Thus, it is possible there may be oxidative damage in NAc caused by developmental fentanyl exposure, and the increased expression of Tfam may be neuroprotective in female mice, consistent with their unchanged blood copy number. The sex-specific nature of this effect, and the lack of changes in other

genes of interest may indicate tight regulation of mitochondrial function in NAc through development and during adolescence despite the drug exposure. Future studies should examine more direct measures of mitochondria in NAc, such as copy number. Heroin can reduce mitochondrial copy number in hippocampus indicating drug exposure can influence copy number in brain (37), but copy number can vary independently with brain region, and changes in one area may not predict changes in other connected brain regions (87). Importantly, differences in oxidative damage or gene expression may vary even within the NAc itself, as the NAc core, medial shell, and lateral shell all have previously described variance in regulating reward-related behaviors (88–92). The tissue used in this study included all subregions of the NAc, and future work will be needed to further dissect any unique subregion responses to developmental fentanyl. Mitochondrial morphology in NAc, regulated by many of the genes examined here, is also responsive to both drug exposure (34) and trait-anxiety measures possibly established during development (40). Fentanyl does impact mitochondrial morphology in neuronal-like NG108–15 cells (39), but this has not been demonstrated in any neuronal type *in vivo*. Further, the impact of developmental fentanyl exposure on mitochondria may be cell-type selective; beyond neurons, astrocyte function is altered by opioid exposure (93–95) and it is possible that changes in these glial cells or the immune-related microglia mimic changes seen in peripheral immune cells.

Our data indicate that blood mitochondrial copy number does vary systematically with NAc mitochondrial-related nuclear genes, specifically Drp1, Mfn1, and Nrf1, with higher copy number corresponding to higher gene expression. Drp1 regulates mitochondrial fission, promoting the formation of more mitochondria. In the brain, Drp1 is involved in new dendritic spine formation (33). While opioid exposure is linked to a decrease in dendritic spines, due to internalization of mu opioid receptors (96, 97), the correlation described here is in female mice specifically, which were resistant to both changes in blood copy and changes in EPM anxiety-like behavior, although fentanyl did disrupt the correlation with NAc gene expression. Mfn2 is usually considered a fusion-related protein (98), but it also plays critical role in mediating mitochondrial contact points with the endoplasmic reticulum independent of fusion and its expression in NAc has been linked to anxiety-like behaviors (40). Nrf1, as a nuclear transcription factor, regulates expression of other mitochondrial related genes including those related to mitochondrial respiratory function as well as genes involved in RNA metabolism, DNA damage repair, and ubiquitin-mediated protein degradation (99). While the role of mitochondrial related gene expression and function in NAc with respect to drug exposure is still a relatively new area of investigation, mitochondrial function within reward circuits has already been linked repeatedly to anxiety-like behaviors (41). Specifically, expression of mitochondrial related genes, mitochondria complex I and II function, and mitochondrial respiratory capacity impact both trait anxiety and expressions social dominance (40, 100, 101). Further, increases in ventral tegmental area dopamine input to NAc or D1-dopamine receptor agonism in NAc can increase both mitochondrial respiratory

activity and facilitate social dominance expression in previously identified higher-anxiety rats (102). Both NRF1 and NRF2 regulate mitochondrial function in reward-related brain regions (103, 104), and global NRF2 knockdown is sufficient to decrease open arm time in rats in an EPM (104). NRF1 knockdown did not impact EPM behavior, but did alter expression of other mitochondrial-related proteins in the amygdala, hippocampus and prefrontal cortex (103). Since affect, mood, and anxiety are all impacted by drug use (57, 105–107), including opioid use (43, 44) and withdrawal (108), altered mitochondrial function may be a common underlying mechanism for trait anxiety or altered anxiety-like behavior after exposure to opioids and other drugs. Future work on both the genes of interest identified here and other mitochondrial processes is needed to fully understand their role in regulating behavior after drug exposure.

While these relationships with NAc gene expression exist in control animals, developmental fentanyl presented other relationships with gene expression, which negatively correlated with EPM behavior in female mice and positively in male mice. Both *Drp1* and *Pgc1 $\alpha$* , the genes correlated in female mice, have both been shown in NAc to mediate enhanced behavioral responding to cocaine (34, 83), and here higher expression is related to less time spent in the open arms of the EPM. Conversely, *Fis1*, *Park2*, and *Tomm20* all have functions in mitochondrial degradation pathways (109–112), potentially indicating higher degrees of mitochondrial damage or turn over in male mice after fentanyl which also have reduced blood copy number and significantly reduced open arm time in the EPM (11). Fentanyl also produced negative correlations between body weight and NAc expression of *Pink1* in male mice and with *Tfb1* in female mice. *Pink1* is protective against mitochondrial dysfunction (113), and as a mitochondrial transcription factor *Tfb1* might have the same protective effects for mitochondrial DNA as *Tfam*. Future studies will be needed to further understand the relationship between weight, NAc gene expression, and opioid exposure. While some genes did correlate with behavior, *Tfam* did not, indicating that developmental fentanyl causes dissociable changes in the periphery and in NAc, and each of these tissues independently relate to behavior. Further, the sex differences seen here in both EPM behavior and in gene expression correlations are consistent with previous work showing important sex differences in NAc gene expression in the context of resilience to stress (114) and sex differences in the NAc proteome after exposure to nicotine, a commonly used drug (115).

It is important to note that in this study it is impossible to distinguish if the changes and relationships described here are due to the fentanyl exposure itself or due to the experience of going through withdrawal from the fentanyl after weaning. This regimen of fentanyl exposure is sufficient to induce spontaneous withdrawal signs (12), and it is unclear if the changes in behavior during adolescence are a prolonged result of withdrawal-related plasticity (58), or indicative of shifted baselines in stress reactivity caused by developmental insult (6, 9, 10). It is also possible, that the developmental timing of withdrawal (at weaning rather than at birth) may be significant. As mitochondria in the brain and body have been previously shown to modulate

responses to both acute psychological stress (27), and mediate some of the developmental impacts on the brain of early-life stress (30), it is possible the effects seen here represent the mitochondrial response to opioid withdrawal (116–118). Future studies involving both continuous access to fentanyl and longer periods of abstinence into adulthood will be necessary to resolve this distinction and determine the persistence of these effects.

Taken together, these data indicate developmental fentanyl exposure has similar effects on offspring mitochondrial copy number as adult opioid use potentially including oxidative damage that disturbs mitochondrial function. Changes in the NAc are only one component of the reward circuits that may be impacted by this developmental opioid exposure and future work should examine the impacts on other brain regions, which may show stronger more significant relationships with blood mitochondrial copy number or behavior than those demonstrated here. The relationships with brain gene expression and behavior indicate coordinated responding throughout the body to the developmental insult of fentanyl exposure and future studies should further explore this relationship to better predict health and supplement treatment for infants with prenatal opioid exposure.

## DATA AVAILABILITY STATEMENT

The raw data supporting the conclusions of this article will be made available by the authors, without undue reservation.

## ETHICS STATEMENT

The animal study was reviewed and approved by Institutional Animal Care and Use Committee at the University of Maryland School of Medicine.

## AUTHOR CONTRIBUTIONS

ML, RC, CC, and MF were responsible for study concept and design. JA and MF designed the perinatal exposure paradigm. MF, JA, and MT managed breeding, fentanyl dosing, and behavioral testing. MF, JA, SVT, and CC collected tissues and performed experiments. CC performed data analysis. CC and ML drafted the manuscript. MF provided critical revision of the manuscript for content. All authors critically reviewed content and approved the final version for publication.

## FUNDING

This work was funded by NIH R01DA038613, NIH R01MH106500, T32DK098107, F32DA052966, and K99DA050575.

## SUPPLEMENTARY MATERIAL

The Supplementary Material for this article can be found online at: <https://www.frontiersin.org/articles/10.3389/fpsy.2021.737389/full#supplementary-material>

## REFERENCES

- Florence CS, Zhou C, Luo F, Xu L. The economic burden of prescription opioid overdose, abuse, and dependence in the United States 2013. *Med Care*. (2016) 54:901–6. doi: 10.1097/MLR.0000000000000625
- Ryan SA. Calculating the real costs of the opioid crisis. *Pediatrics*. (2018) 141:18–21. doi: 10.1542/peds.2017-4129
- Honein MA, Boyle C, Redfield RR. Public health surveillance of prenatal opioid exposure in mothers and infants. *Pediatrics*. (2019) 143:e20183801. doi: 10.1542/peds.2018-3801
- Haight SC, Ko JY, Tong VT, Bohm MK, Callaghan WM. Opioid use disorder documented at delivery hospitalization - United States, 1999-2014. *Morb Mortal Wkly Rep*. (2018) 67:845–9. doi: 10.15585/mmwr.mm6731a1
- Whiteman VE, Salemi JL, Mogos ME, Cain MA, Aliyu MH, Salihu HM. Maternal opioid drug use during pregnancy and its impact on perinatal morbidity, mortality, and the costs of medical care in the United States. *J Pregnancy*. (2014) 2014:906723. doi: 10.1155/2014/906723
- Mactier H, Hamilton R. Prenatal opioid exposure - increasing evidence of harm. *Early Hum Dev*. (2020) 150:105188. doi: 10.1016/j.earlhumdev.2020.105188
- Šlamberová R. Drugs in pregnancy: the effects on mother and her progeny. *Physiol Res*. (2012) 61(Suppl. 1):932357. doi: 10.33549/physiolres.932357
- Ross EJ, Graham DL, Money KM, Stanwood GD. Developmental consequences of fetal exposure to drugs: what we know and what we still must learn. *Neuropsychopharmacology*. (2015) 40:61–87. doi: 10.1038/npp.2014.147
- Abu Y, Roy S. Prenatal opioid exposure and vulnerability to future substance use disorders in offspring. *Exp Neurol*. (2021) 339:113621. doi: 10.1016/j.expneurol.2021.113621
- Franks AL, Berry KJ, DeFranco DB. Prenatal drug exposure and neurodevelopmental programming of glucocorticoid signalling. *J Neuroendocrinol*. (2020) 32:1–13. doi: 10.1111/jne.12786
- Alipio JB, Brockett AT, Fox ME, Tennyson SS, DeBettencourt CA, El-Metwally D, et al. Enduring consequences of perinatal fentanyl exposure in mice. *Addict Biol*. (2021) 26:e12895. doi: 10.1111/adb.12895
- Alipio JB, Haga C, Fox ME, Arakawa K, Balaji R, Cramer N, et al. Perinatal fentanyl exposure leads to long-lasting impairments in somatosensory circuit function and behavior. *J Neurosci*. (2021) 41:3400–17. doi: 10.1523/JNEUROSCI.2470-20.2021
- Koob GF. Neurobiological substrates for the dark side of compulsivity in addiction. *Neuropharmacology*. (2009) 56:18–31. doi: 10.1016/j.neuropharm.2008.07.043
- Volkow ND, Koob GF, McLellan AT. Neurobiologic advances from the brain disease model of addiction. *N Engl J Med*. (2016) 374:363–71. doi: 10.1056/NEJMr1511480
- Badiani A, Blein D, Epstein D, Calu D, Shaham Y. Opiate versus psychostimulant addiction: the differences do matter. *Nat Rev Neurosci*. (2008) 12:685–700. doi: 10.1038/nrn3104
- Shaham Y, Erb S, Stewart J. Stress-induced relapse to heroin and cocaine seeking in rats: a review. *Brain Res Rev*. (2000) 33:13–33. doi: 10.1016/S0165-0173(00)00024-2
- Koob GF, Volkow ND. Neurobiology of addiction: a neurocircuitry analysis. *Lancet Psychiatry*. (2016) 3:760–73. doi: 10.1016/S2215-0366(16)00104-8
- Crombag HS, Bossert JM, Koya E, Shaham Y. Context-induced relapse to drug seeking: a review. *Philos Trans R Soc B Biol Sci*. (2008) 363:3233–43. doi: 10.1098/rstb.2008.0090
- Caspani G, Sebok V, Sultana N, Swann JR, Bailey A. Metabolic phenotyping of opioid and psychostimulant addiction: a novel approach for biomarker discovery and biochemical understanding of the disorder. *Br J Pharmacol*. (2021) 1–29. doi: 10.1111/bph.15475
- Zahmatkesh M, Kadkhodae M, Salarian A, Seifi B, Adeli S. Impact of opioids on oxidative status and related signaling pathways: an integrated view. *J Opioid Manag*. (2017) 13:241–51. doi: 10.5055/jom.2017.0392
- Cunha-Oliveira T, Rego A, Oliveira C. Oxidative stress and drugs of abuse: an update. *Mini Rev Org Chem*. (2013) 10:321–34. doi: 10.2174/1570193X113106660026
- Pavlek LR, Dillard J, Rogers LK. The role of oxidative stress in toxicities due to drugs of abuse. *Curr Opin Toxicol*. (2020) 20–21:29–35. doi: 10.1016/j.cotox.2020.04.003
- Katz N, Mazer NA. The impact of opioids on the endocrine system. *Clin J Pain*. (2009) 25:170–5. doi: 10.1097/AJP.0b013e3181850df6
- Salarian A, Kadkhodae M, Zahmatkesh M, Seifi B, Bakhshi E, Akhondzadeh S, et al. Opioid use disorder induces oxidative stress and inflammation: the attenuating effect of methadone maintenance treatment. *Iran J Psychiatry*. (2018) 13:46–54.
- Molavi N, Ghaderi A, Banafshe HR. Short communication: examining metabolic profiles in opioid-dependent patient. *Int J Med Toxicol Forensic Med*. (2020) 10:1–6. doi: 10.32598/ijmtfm.v10i3.28681
- Cunha-Oliveira T, Rego AC, Oliveira CR. Cellular and molecular mechanisms involved in the neurotoxicity of opioid and psychostimulant drugs. *Brain Res Rev*. (2008) 58:192–208. doi: 10.1016/j.brainresrev.2008.03.002
- Picard M, McManus MJ, Gray JD, Nasca C, Moffat C, Kopinski PK, et al. Mitochondrial functions modulate neuroendocrine, metabolic, inflammatory, and transcriptional responses to acute psychological stress. *Proc Natl Acad Sci*. (2015) 112:E6614–23. doi: 10.1073/pnas.1515733112
- Picard M, McEwen BS. Psychological stress and mitochondria: a systematic review. *Psychosom Med*. (2018) 80:141–53. doi: 10.1097/PSY.0000000000000545
- Picard M, McEwen BS, Epel ES, Sandi C. An energetic view of stress: focus on mitochondria. *Front Neuroendocrinol*. (2018) 49:72–85. doi: 10.1016/j.yfrne.2018.01.001
- Hoffmann A, Spengler D. The mitochondrion as potential interface in early-life stress brain programming. *Front Behav Neurosci*. (2018) 12:306. doi: 10.3389/fnbeh.2018.00306
- Rugarli EI, Langer T. Mitochondrial quality control: a matter of life and death for neurons. *EMBO J*. (2012) 31:1336–49. doi: 10.1038/emboj.2012.38
- Li Z, Okamoto K, Hayashi Y, Sheng M. The importance of dendritic mitochondria in the morphogenesis and plasticity of spines and synapses. *Cell*. (2004) 119:873–87. doi: 10.1016/j.cell.2004.11.003
- Divakaruni SS, Van Dyke AM, Chandra R, LeGates TA, Contreras M, Dharmasri PA, et al. Long-term potentiation requires a rapid burst of dendritic mitochondrial fission during induction. *Neuron*. (2018) 100:1–16. doi: 10.1016/j.neuron.2018.09.025
- Chandra R, Engeln M, Schiefer C, Patton MH, Martin JA, Werner CT, et al. Drp1 mitochondrial fission in D1 neurons mediates behavioral and cellular plasticity during early cocaine abstinence. *Neuron*. (2017) 96:1327–41.e6. doi: 10.1016/j.neuron.2017.11.037
- Clay Montier LL, Deng JJ, Bai Y. Number matters: control of mammalian mitochondrial DNA copy number. *J Genet Genomics*. (2009) 36:125–31. doi: 10.1016/S1673-8527(08)60099-5
- Yang SY, Castellani CA, Longchamps RJ, Pillalamarri VK, O'Rourke B, Guallar E, et al. Blood-derived mitochondrial DNA copy number is associated with gene expression across multiple tissues and is predictive for incident neurodegenerative disease. *Genome Res*. (2021) 31:349–58. doi: 10.1101/gr.269381.120
- Feng YM, Jia YF, Su LY, Wang D, Lv L, Xu L, et al. Decreased mitochondrial DNA copy number in the hippocampus and peripheral blood during opiate addiction is mediated by autophagy and can be salvaged by melatonin. *Autophagy*. (2013) 9:1395–406. doi: 10.4161/auto.25468
- Nylander E, Grönbladh A, Zellerroth S, Diwakarla S, Nyberg F, Hallberg M. Growth hormone is protective against acute methadone-induced toxicity by modulating the NMDA receptor complex. *Neuroscience*. (2016) 339:538–47. doi: 10.1016/j.neuroscience.2016.10.019
- Nylander E, Zellerroth S, Nyberg F, Grönbladh A, Hallberg M. The effects of morphine, methadone, and fentanyl on mitochondria: a live cell imaging study. *Brain Res Bull*. (2021) 171:126–34. doi: 10.1016/j.brainresbull.2021.03.009
- Gebara E, Zanoletti O, Ghosal S, Grosse J, Schneider BL, Knott G, et al. Mitofusin-2 in the nucleus accumbens regulates anxiety and depression-like behaviors through mitochondrial and neuronal actions. *Biol Psychiatry*. (2021) 89:1033–44. doi: 10.1016/j.biopsych.2020.12.003

41. Filiou MD, Sandi C. Anxiety and brain mitochondria: a bidirectional crosstalk. *Trends Neurosci.* (2019) 42:573–88. doi: 10.1016/j.tins.2019.07.002
42. Hollis F, van der Kooij MA, Zanoletti O, Lozano L, Cantó C, Sandi C. Mitochondrial function in the brain links anxiety with social subordination. *Proc Natl Acad Sci.* (2015) 112:15486–91. doi: 10.1073/pnas.1512653112
43. Rosoff DB, Smith GD, Lohoff FW. Prescription opioid use and risk for major depressive disorder and anxiety and stress-related disorders: a multivariable mendelian randomization analysis. *JAMA Psychiatry.* (2021) 78:151–60. doi: 10.1001/jamapsychiatry.2020.3554
44. Gros DF, Milanak ME, Brady KT, Back SE. Frequency and severity of comorbid mood and anxiety disorders in prescription opioid dependence. *Am J Addict.* (2013) 22:261–5. doi: 10.1111/j.1521-0391.2012.12008.x
45. Martins SS, Fenton MC, Keyes KM, Blanco C, Zhu H, Storr CL. Mood and anxiety disorders and their association with non-medical prescription opioid use and prescription opioid-use disorder: longitudinal evidence from the National Epidemiologic Study on Alcohol and Related Conditions. *Psychol Med.* (2012) 42:1261–72. doi: 10.1017/S0033291711002145
46. Russo SJ, Dietz DM, Dumitriu D, Malenka RC, Nestler EJ. The addicted synapse: mechanisms of synaptic and structural plasticity in nucleus accumbens. *Trends Neurosci.* (2011) 33:267–76. doi: 10.1016/j.tins.2010.02.002
47. Berridge KC, Kringelbach ML. Pleasure systems in the brain. *Neuron.* (2015) 86:646–64. doi: 10.1016/j.neuron.2015.02.018
48. Volkow ND, Morales M. The brain on drugs: from reward to addiction. *Cell.* (2015) 162:712–25. doi: 10.1016/j.cell.2015.07.046
49. Fox ME, Lobo MK. The molecular and cellular mechanisms of depression: a focus on reward circuitry. *Mol Psychiatry.* (2019) 24:1798–815. doi: 10.1038/s41380-019-0415-3
50. Francis TC, Lobo MK. Emerging role for nucleus accumbens medium spiny neuron subtypes in depression. *Biol Psychiatry.* (2017) 81:645–53. doi: 10.1016/j.biopsych.2016.09.007
51. Clancy B, Darlington RB, Finlay BL. Translating developmental time across mammalian species. *Neuroscience.* (2001) 105:7–17. doi: 10.1016/S0306-4522(01)00171-3
52. Chen VS, Morrison JP, Southwell MF, Foley JF, Bolon B, Elmore SA. Histology atlas of the developing prenatal and postnatal mouse central nervous system, with emphasis on prenatal days E75 to E185. *Toxicol Pathol.* (2017) 45:705–44. doi: 10.1177/019262331728134
53. Pellow S, Chopin P, File SE, Briley M. Validation of open: closed arm entries in an elevated plus-maze as a measure of anxiety in the rat. *J Neurosci Methods.* (1985) 14:149–67. doi: 10.1016/0165-0270(85)90031-7
54. Planchez B, Surget A, Belzung C. Animal models of major depression: drawbacks and challenges. *J Neural Transm.* (2019) 126:1383–408. doi: 10.1007/s00702-019-02084-y
55. Luscher C, Malenka RC. Drug-evoked synaptic plasticity in addiction: from molecular changes to circuit remodeling. *Neuron.* (2011) 69:650–63. doi: 10.1016/j.neuron.2011.01.017
56. Nestler EJ, Luscher C. The molecular basis of drug addiction: linking epigenetic to synaptic and circuit mechanisms. *Neuron.* (2019) 102:48–59. doi: 10.1016/j.neuron.2019.01.016
57. Kenny PJ, Hoyer D, Koob GF. Animal models of addiction and neuropsychiatric disorders and their role in drug discovery: honoring the legacy of Athina Markou. *Biol Psychiatry.* (2018) 83:940–6. doi: 10.1016/j.biopsych.2018.02.009
58. Thompson BL, Oscar-Berman M, Kaplan GB. Opioid-induced structural and functional plasticity of medium-spiny neurons in the nucleus accumbens. *Neurosci Biobehav Rev.* (2021) 120:417–30. doi: 10.1016/j.neubiorev.2020.10.015
59. Yapa NMB, Lisnyak V, Reljic B, Ryan MT. Mitochondrial dynamics in health and disease. *FEBS Lett.* (2021) 595:1184–204. doi: 10.1002/1873-3468.14077
60. Tilokani L, Nagashima S, Paupe V, Prudent J. Mitochondrial dynamics: overview of molecular mechanisms. *Essays Biochem.* (2018) 62:341–60. doi: 10.1042/EBC20170104
61. Kang D, Hamasaki N. Mitochondrial transcription factor A in the maintenance of mitochondrial DNA: overview of its multiple roles. *Ann N Y Acad Sci.* (2005) 1042:101–8. doi: 10.1196/annals.1338.010
62. Ventura-Clapier R, Garnier A, Veksler V. Transcriptional control of mitochondrial biogenesis: the central role of PGC-1 $\alpha$ . *Cardiovasc Res.* (2008) 79:208–17. doi: 10.1093/cvr/cvn098
63. Lee SJ, Bora S, Austin NC, Westerman A, Henderson JMT. Neurodevelopmental outcomes of children born to opioid-dependent mothers: a systematic review and meta-analysis. *Acad Pediatr.* (2020) 20:308–18. doi: 10.1016/j.acap.2019.11.005
64. Yakes FM, Van Houten B. Mitochondrial DNA damage is more extensive and persists longer than nuclear DNA damage in human cells following oxidative stress. *Proc Natl Acad Sci USA.* (1997) 94:514–9. doi: 10.1073/pnas.94.2.514
65. Robin ED, Wong R. Mitochondrial DNA molecules and virtual number of mitochondria per cell in mammalian cells. *J Cell Physiol.* (1988) 136:507–13. doi: 10.1002/jcp.1041360316
66. Phillips NR, Sprouse ML, Roby RK. Simultaneous quantification of mitochondrial DNA copy number and deletion ratio: a multiplex real-time PCR assay. *Sci R.* (2014) 4:3887. doi: 10.1038/srep03887
67. Malik AN, Czajka A. Is mitochondrial DNA content a potential biomarker of mitochondrial dysfunction? *Mitochondrion.* (2013) 13:481–92. doi: 10.1016/j.mito.2012.10.011
68. Zorzano A, Liesa M, Palaci M. Mitochondrial dynamics in mammalian health and disease. *Physiol Rev.* (2009) 89:799–845. doi: 10.1152/physrev.00030.2008
69. Ridout KK, Khan M, Ridout SJ. Adverse childhood experiences run deep: toxic early life stress, telomeres, and mitochondrial DNA copy number, the biological markers of cumulative stress. *BioEssays.* (2018) 40:1–10. doi: 10.1002/bies.201800077
70. Afrifa J, Zhao T, Yu J. Circulating mitochondria DNA, a non-invasive cancer diagnostic biomarker candidate. *Mitochondrion.* (2019) 47:238–43. doi: 10.1016/j.mito.2018.12.003
71. Wang X, Sundquist K, Rastkhani H, Palmér K, Memon AA, Sundquist J. Association of mitochondrial DNA in peripheral blood with depression, anxiety and stress- and adjustment disorders in primary health care patients. *Eur Neuropsychopharmacol.* (2017) 27:751–8. doi: 10.1016/j.euroneuro.2017.06.001
72. Sadakierska-Chudy A, Kotarska A, Frankowska M, Jastrzebska J, Wydra K, Miszkil J, et al. The alterations in mitochondrial DNA copy number and nuclear-encoded mitochondrial genes in rat brain structures after cocaine self-administration. *Mol Neurobiol.* (2017) 54:7460–70. doi: 10.1007/s12035-016-0153-3
73. Silzer T, Barber R, Sun J, Pathak G, Johnson L, O'Bryant S, et al. Circulating mitochondrial DNA: New indices of type 2 diabetes-related cognitive impairment in Mexican Americans. *PLoS ONE.* (2019) 14:e0213527. doi: 10.1371/journal.pone.0213527
74. Lee J-Y, Lee D-C, Im J-A, Lee J-W. Mitochondrial dna copy number in peripheral blood is independently associated with visceral fat accumulation in healthy young adults. *Int J Endocrinol.* (2014) 2014:1–7. doi: 10.1155/2014/586017
75. Wang D, Li Z, Liu W, Zhou J, Ma X, Tang J, et al. Differential mitochondrial DNA copy number in three mood states of bipolar disorder. *BMC Psychiatry.* (2018) 18:1–8. doi: 10.1186/s12888-018-1717-8
76. Yamaki N, Otsuka I, Numata S, Yanagi M, Mouri K, Okazaki S, et al. Mitochondrial DNA copy number of peripheral blood in bipolar disorder: the present study and a meta-analysis. *Psychiatry Res.* (2018) 269:115–7. doi: 10.1016/j.psychres.2018.08.014
77. Tyrka AR, Parade SH, Price LH, Kao HT, Porton B, Philip NS, et al. Alterations of mitochondrial DNA copy number and telomere length with early adversity and psychopathology. *Biol Psychiatry.* (2016) 79:78–86. doi: 10.1016/j.biopsych.2014.12.025
78. Bobzean SAM, DeNobrega AK, Perrotti LI. Sex differences in the neurobiology of drug addiction. *Exp Neurol.* (2014) 259:64–74. doi: 10.1016/j.expneurol.2014.01.022
79. Becker JB, Koob GF. Sex differences in animal models: focus on addiction. *Pharmacol Rev.* (2016) 68:242–63. doi: 10.1124/pr.115.011163
80. Fattore L, Altea S, Fratta W. Sex differences in drug addiction: a review of animal and human studies. *Women's Heal.* (2008) 4:51–65. doi: 10.2217/17455057.4.1.51

81. Lee CWS, Ho IK. Sex differences in opioid analgesia and addiction: interactions among opioid receptors and estrogen receptors. *Mol Pain*. (2013) 9:1–10. doi: 10.1186/1744-8069-9-45
82. Becker JB, Chartoff E. Sex differences in neural mechanisms mediating reward and addiction. *Neuropsychopharmacology*. (2019) 44:166–83. doi: 10.1038/s41386-018-0125-6
83. Chandra R, Engeln M, Francis TC, Konkalmatt P, Patel D, Lobo MK, et al. Role for peroxisome proliferator-activated receptor gamma coactivator-1 $\alpha$  in nucleus accumbens neuron subtypes in cocaine action. *Biol Psychiatry*. (2017) 81:564–72. doi: 10.1016/j.biopsych.2016.10.024
84. Cole S, Chandra R, Harris M, Patel I, Wang T, Kim H, et al. Cocaine-induced neuron subtype mitochondrial dynamics through Egr3 transcriptional regulation. *Mol Brain*. (2021) 14:101. doi: 10.1186/s13041-021-00800-y
85. Xu S, Zhong M, Zhang L, Wang Y, Zhou Z, Hao Y, et al. Overexpression of Tfam protects mitochondria against  $\beta$ -amyloid-induced oxidative damage in SH-SY5Y cells. *FEBS J*. (2009) 276:3800–9. doi: 10.1111/j.1742-4658.2009.07094.x
86. Feng Q, Shao M, Han J, Tang T, Zhang Y, Liu F, et al. a potential oxidative stress biomarker used for monitoring environment pollutants in *Musca domestica*. *Int J Biol Macromol*. (2020) 155:524–34. doi: 10.1016/j.ijbiomac.2020.03.208
87. Fuke S, Kubota-Sakashita M, Kasahara T, Shigeyoshi Y, Kato T. Regional variation in mitochondrial DNA copy number in mouse brain. *Biochim Biophys Acta - Bioenerg*. (2011) 1807:270–4. doi: 10.1016/j.bbabi.2010.11.016
88. Laurent V, Leung B, Maidment N, Balleine BW.  $\mu$ - and  $\delta$ -Opioid-related processes in the accumbens core and shell differentially mediate the influence of reward-guided and stimulus-guided decisions on choice. *J Neurosci*. (2012) 32:1875–83. doi: 10.1523/JNEUROSCI.4688-11.2012
89. Peciña S, Berridge KC. Dopamine or opioid stimulation of nucleus accumbens similarly amplify cue-triggered “wanting” for reward: entire core and medial shell mapped as substrates for PIT enhancement. *Eur J Neurosci*. (2013) 37:1529–40. doi: 10.1111/ejn.12174
90. Di Ciano P, Robbins TW, Everitt BJ. Differential effects of nucleus accumbens core, shell, or dorsal striatal inactivations on the persistence, reacquisition, or reinstatement of responding for a drug-paired conditioned reinforcer. *Neuropsychopharmacology*. (2008) 33:1413–25. doi: 10.1038/sj.npp.1301522
91. Di Chiara G. Nucleus accumbens shell and core dopamine: differential role in behavior and addiction. *Behav Brain Res*. (2002) 137:75–114. doi: 10.1016/S0166-4328(02)00286-3
92. Castro DC, Bruchas MR. A motivational and neuropeptidergic hub: anatomical and functional diversity within the nucleus accumbens shell. *Neuron*. (2019) 102:529–52. doi: 10.1016/j.neuron.2019.03.003
93. Doke M, Pendyala G, Samikkannu T. Psychostimulants and opioids differentially influence the epigenetic modification of histone acetyltransferase and histone deacetylase in astrocytes. *PLoS ONE*. (2021) 16:e0252895. doi: 10.1371/journal.pone.0252895
94. Lacagnina MJ, Rivera PD, Bilbo SD. Glial and neuroimmune mechanisms as critical modulators of drug use and abuse. *Neuropsychopharmacology*. (2017) 42:156–77. doi: 10.1038/npp.2016.121
95. Krueyer A, Chioma VC, Kalivas PW. The opioid-addicted tetrapartite synapse. *Biol Psychiatry*. (2020) 87:34–43. doi: 10.1016/j.biopsych.2019.05.025
96. Miller EC, Zhang L, Dummer BW, Cariveau DR, Loh H, Law PY, et al. Differential modulation of drug-induced structural and functional plasticity of dendritic spines. *Mol Pharmacol*. (2012) 82:333–43. doi: 10.1124/mol.112.078162
97. Liao D, Gringorians OO, Wang W, Wiens K, Loh HH, Law PY. Distinct effects of individual opioids on the morphology of spines depend upon the internalization of mu opioid receptors. *Mol Cell Neurosci*. (2007) 35:456–69. doi: 10.1016/j.mcn.2007.04.007
98. Adebayo M, Singh S, Singh AP, Dasgupta S. Mitochondrial fusion and fission: the fine-tune balance for cellular homeostasis. *FASEB J*. (2021) 35:1–13. doi: 10.1096/fj.202100067R
99. Satoh JI, Kawana N, Yamamoto Y. Pathway analysis of ChIP-seq-based NRF1 target genes suggests a logical hypothesis of their involvement in the pathogenesis of neurodegenerative diseases. *Gene Regul Syst Bio*. (2013) 2013:139–52. doi: 10.4137/GRSB.S13204
100. Beyer F, García-García I, Heinrich M, Schroeter ML, Sacher J, Luck T, et al. Neuroanatomical correlates of food addiction symptoms and body mass index in the general population. *Hum Brain Mapp*. (2019) 40:2747–58. doi: 10.1002/hbm.24557
101. Alonso-Carballo Y, Jorgensen ET, Brown T, Ferrario CR. Functional and structural plasticity contributing to obesity: roles for sex, diet, and individual susceptibility. *Curr Opin Behav Sci*. (2018) 23:160–70. doi: 10.1016/j.cobeha.2018.06.014
102. Van Der Kooij MA, Hollis F, Lozano L, Zalachoras I, Abad S, Zanoletti O, et al. Diazepam actions in the VTA enhance social dominance and mitochondrial function in the nucleus accumbens by activation of dopamine D1 receptors. *Mol Psychiatry*. (2018) 23:569–78. doi: 10.1038/mp.2017.135
103. Khalifeh S, Oryan S, Khodaghohi F, Digaleh H, Shaerzadeh F, Maghsoudi N, et al. Complexity of compensatory effects in Nrf1 knockdown: linking undeveloped anxiety-like behavior to prevented mitochondrial dysfunction and oxidative stress. *Cell Mol Neurobiol*. (2016) 36:553–63. doi: 10.1007/s10571-015-0236-0
104. Khalifeh S, Oryan S, Digaleh H, Shaerzadeh F, Khodaghohi F, Maghsoudi N, et al. Involvement of Nrf2 in development of anxiety-like behavior by linking Bcl2 to oxidative phosphorylation: estimation in rat hippocampus, amygdala, and prefrontal cortex. *J Mol Neurosci*. (2015) 55:492–9. doi: 10.1007/s12031-014-0370-z
105. Haass-Koffler CL, Bartlett SE. Stress and addiction: contribution of the corticotropin releasing factor (CRF) system in neuroplasticity. *Front Mol Neurosci*. (2012) 5:e00091. doi: 10.3389/fnmol.2012.00091
106. Lüthi A, Lüscher C. Pathological circuit function underlying addiction and anxiety disorders. *Nat Neurosci*. (2014) 17:1635–43. doi: 10.1038/nn.3849
107. Kutlu MG, Parikh V, Gould TJ. Nicotine addiction and psychiatric disorders. De Biasi M, editor. *Nicotine Use in Mental Illness and Neurological Disorders*. Amsterdam: Elsevier Inc. (2015). p. 171–208.
108. Koob GF. Neurobiology of opioid addiction: opponent process, hyperkatifeia, and negative reinforcement. *Biol Psychiatry*. (2020) 87:44–53. doi: 10.1016/j.biopsych.2019.05.023
109. Sprenger HG, Langer T. The good and the bad of mitochondrial breakups. *Trends Cell Biol*. (2019) 29:888–900. doi: 10.1016/j.tcb.2019.08.003
110. Yu W, Sun Y, Guo S, Lu B. The PINK1/Parkin pathway regulates mitochondrial dynamics and function in mammalian hippocampal and dopaminergic neurons. *Hum Mol Genet*. (2011) 20:3227–40. doi: 10.1093/hmg/ddr235
111. Wai T, Langer T. Mitochondrial dynamics and metabolic regulation. *Trends Endocrinol Metab*. (2016) 27:105–17. doi: 10.1016/j.tem.2015.12.001
112. Wang L, Qi H, Tang Y, Shen H. Post-translational modifications of key machinery in the control of mitophagy. *Trends Biochem Sci*. (2020) 45:85–75. doi: 10.1016/j.tibs.2019.08.002
113. Narendra DP, Youle RJ. Targeting mitochondrial dysfunction: role for PINK1 and parkin in mitochondrial quality control. *Antioxidants Redox Signal*. (2011) 14:1929–38. doi: 10.1089/ars.2010.3799
114. Hodes GE, Pfau ML, Purushothaman I, Ahn HF, Golden SA, Christoffel DJ, et al. Sex differences in nucleus accumbens transcriptome profiles associated with susceptibility versus resilience to subchronic variable stress. *J Neurosci*. (2015) 35:16362–76. doi: 10.1523/JNEUROSCI.1392-15.2015
115. Lee AM, Mansuri MS, Wilson RS, Lam TT, Nairn AC, Picciotto MR, et al. Sex differences in the ventral tegmental area and nucleus accumbens proteome at baseline and following nicotine exposure. *Front Mol Neurosci*. (2021) 14:657064. doi: 10.3389/fnmol.2021.657064
116. Chartoff EH, Carlezon WAJ. Drug withdrawal conceptualized as a stressor. *Behav Pharmacol*. (2014) 25:473–92. doi: 10.1097/FBP.0000000000000080
117. Neugebauer NM, Einstein EB, Lopez MB, McClure-Begley TD, Mine3 ur YS, Picciotto MR. Morphine dependence and withdrawal induced changes in cholinergic signaling. *Pharmacol Biochem Behav*. (2013) 109:77–83. doi: 10.1016/j.pbb.2013.04.015
118. Kauffling J, Aston-Jones G. Persistent adaptations in afferents to ventral tegmental dopamine neurons after opiate withdrawal.

*J. Neurosci.* (2015) 35:10290–303. doi: 10.1523/JNEUROSCI.0715-15.2015

**Conflict of Interest:** The authors declare that the research was conducted in the absence of any commercial or financial relationships that could be construed as a potential conflict of interest.

**Publisher's Note:** All claims expressed in this article are solely those of the authors and do not necessarily represent those of their affiliated organizations, or those of the publisher, the editors and the reviewers. Any product that may be evaluated in

this article, or claim that may be made by its manufacturer, is not guaranteed or endorsed by the publisher.

Copyright © 2021 Calarco, Fox, Van Terheyden, Turner, Alipio, Chandra and Lobo. This is an open-access article distributed under the terms of the Creative Commons Attribution License (CC BY). The use, distribution or reproduction in other forums is permitted, provided the original author(s) and the copyright owner(s) are credited and that the original publication in this journal is cited, in accordance with accepted academic practice. No use, distribution or reproduction is permitted which does not comply with these terms.



# Network-Based Discovery of Opioid Use Vulnerability in Rats Using the Bayesian Stochastic Block Model

Carter Allen<sup>1†</sup>, Brittany N. Kuhn<sup>2†</sup>, Nazzareno Cannella<sup>3†</sup>, Ayteria D. Crow<sup>2</sup>, Analyse T. Roberts<sup>2</sup>, Veronica Lunerti<sup>3</sup>, Massimo Ubaldi<sup>3</sup>, Gary Hardiman<sup>4</sup>, Leah C. Solberg Woods<sup>5</sup>, Roberto Ciccocioppo<sup>3</sup>, Peter W. Kalivas<sup>2</sup> and Dongjun Chung<sup>1\*</sup>

## OPEN ACCESS

### Edited by:

Wendy J. Lynch,  
University of Virginia, United States

### Reviewed by:

Susan Ferguson,  
University of Washington,  
United States  
Brendan J. Tunstall,  
University of Tennessee Health  
Science Center (UTHSC),  
United States  
Marcello Solinas,  
Institut National de la Santé et de la  
Recherche Médicale (INSERM),  
France

### \*Correspondence:

Dongjun Chung  
chung.911@osu.edu

<sup>†</sup>These authors have contributed  
equally to this work

### Specialty section:

This article was submitted to  
Addictive Disorders,  
a section of the journal  
Frontiers in Psychiatry

**Received:** 23 July 2021

**Accepted:** 29 November 2021

**Published:** 17 December 2021

### Citation:

Allen C, Kuhn BN, Cannella N,  
Crow AD, Roberts AT, Lunerti V,  
Ubaldi M, Hardiman G, Solberg  
Woods LC, Ciccocioppo R,  
Kalivas PW and Chung D (2021)  
Network-Based Discovery of Opioid  
Use Vulnerability in Rats Using the  
Bayesian Stochastic Block Model.  
Front. Psychiatry 12:745468.  
doi: 10.3389/fpsy.2021.745468

<sup>1</sup> Department of Biomedical Informatics, The Ohio State University, Columbus, OH, United States, <sup>2</sup> Department of Neuroscience, Medical University of South Carolina, Charleston, SC, United States, <sup>3</sup> School of Pharmacy, University of Camerino, Camerino, Italy, <sup>4</sup> School of Biological Sciences, Queen's University Belfast, Belfast, United Kingdom, <sup>5</sup> Department of Internal Medicine, Wake Forest University School of Medicine, Winston-Salem, NC, United States

Opioid use disorder is a psychological condition that affects over 200,000 people per year in the U.S., causing the Centers for Disease Control and Prevention to label the crisis as a rapidly spreading public health epidemic. The behavioral relationship between opioid exposure and development of opioid use disorder (OUD) varies greatly between individuals, implying existence of sub-populations with varying degrees of opioid vulnerability. However, effective pre-clinical identification of these sub-populations remains challenging due to the complex multivariate measurements employed in animal models of OUD. In this study, we propose a novel non-linear network-based data analysis workflow that employs seven behavioral traits to identify opioid use sub-populations and assesses contributions of behavioral variables to opioid vulnerability and resiliency. Through this analysis workflow we determined how behavioral variables across heroin taking, refraining and seeking interact with one another to identify potentially heroin resilient and vulnerable behavioral sub-populations. Data were collected from over 400 heterogeneous stock rats in two geographically distinct locations. Rats underwent heroin self-administration training, followed by a progressive ratio and heroin-primed reinstatement test. Next, rats underwent extinction training and a cue-induced reinstatement test. To enter the analysis workflow, we integrated data from different cohorts of rats and removed possible batch effects. We then constructed a rat-rat similarity network based on their behavioral patterns and implemented community detection on this similarity network using a Bayesian degree-corrected stochastic block model to uncover sub-populations of rats with differing levels of opioid vulnerability. We identified three statistically distinct clusters corresponding to distinct behavioral sub-populations, vulnerable, resilient and intermediate for heroin use, refraining and seeking. We implement this analysis workflow as an open source R package, named `m1sbm`.

**Keywords:** clustering, community detection, Bayesian model, opioid use disorder, network analysis, stochastic block model

## INTRODUCTION

Opioid addiction is a chronic neuropsychiatric disorder characterized by compulsive drug taking and relapse, despite efforts to remain abstinent. Opioid use disorder (OUD) has risen substantially in the United States over the past two decades, for both prescription drugs (1), as well as illicit opioids, notably heroin (2). The parallel rise in both prescription and illicit opioid use and abuse are related to one another, as a majority of heroin users report using prescription opioids prior to heroin use (2–4). Death due to an overdose is also positively correlated between these two opioid classes (2), posing an additional obstacle in addressing the current opioid epidemic. Furthermore, heroin use since 2000 has increased in all demographics, regardless of age, sex or socio-economic status (2, 4), suggesting factors independent of these are contributing to the escalation in OUD. This ubiquitous increase in heroin use and dependence across disparate populations highlights the need to assess how individual variation in multiple behavioral traits may be interacting to contribute to an OUD resilient vs. vulnerable phenotype.

OUD remains such a critical social and personal problem in part because we are limited by current animal models that predict neurological pathologies for OUD. Though animal models capturing individual variation in addiction-related behaviors have greatly contributed to our understanding of drug addiction, most focus on one or two behavioral phenotypes, then apply the power of animal experimentation to uncover circuitry and cellular mechanisms for individual phenotypes. While this approach has greatly enhanced our understanding of how brain circuits and cell signaling mechanisms contribute to specific behavioral phenotypes, OUD is a disorder containing many behavioral traits that may contribute differentially to resilience and vulnerability to drug addiction depending on individual genetics and sociology (5–7). Indeed, the DSM-V diagnostic criteria for OUD is neither meeting a single behavioral criterion nor meeting all criteria, but rather a person needs to meet a subcluster of criteria to be considered diagnostic (5). This diagnostic protocol is employed because of individual differences resulting from the presence of one diagnostically positive trait does not necessarily predicting the presence of another trait. In an effort to more accurately portray the multi-trait nature of substance use disorders (SUDs), some studies have created composite scores consisting of a few traits that are generally summed in a linear manner to create an addiction score (8, 9). Here we propose a different approach to analyzing multiple traits and explore a multidimensional data clustering strategy of seven behavioral traits potentially characteristic of heroin use and seeking in 451 outbred rats, examined in two distinct laboratories, one at the Medical University of South Carolina (MUSC) in the USA and the other at the University of Camerino (UCAM) in Italy. This approach allows for non-linear relationships between multiple traits to be simultaneously quantified, resulting in clusters of animals that may correspond to overall resilient and vulnerable subgroups.

Various clustering algorithms are available, including k-means clustering (10), hierarchical clustering (11), and finite mixture

models (12), among others. However, behavioral studies generate complex multivariate measurements which can make clustering difficult using standard algorithms. Recently, network-based clustering approaches have become popular across multiple disciplines due to their flexibility and applicability to high-dimensional data. For example, in high dimensional single cell genomics studies, these algorithms are employed in multiple software packages for identifying latent cell types such as T and B cells (13). In general, these network-based clustering approaches first construct a similarity network based on observations and then implement a community detection algorithm on this similarity network to identify underlying clusters. As a result, these approaches are less affected by violations of underlying assumptions, such as Gaussianity.

In this paper, we adopt the stochastic block model (SBM), which has strong and rigorous theoretical foundation in statistics literature (14, 15). In essence, the SBM allows for identification of latent communities using a probabilistic model that describes interconnectivity between nodes within and between clusters. In this sense, the SBM may be used as a descriptive tool to assess the presence of distinct latent populations in a data set. The biological utility of such populations may then be determined by investigating the distributions of relevant variables (e.g., heroin consumption) across clusters. While we do not seek to propose a predictive model for opioid vulnerability, the sub-populations identified from our approach may be correlated with data from future studies (e.g., genetic studies) to assess the predictive ability of characteristics that define the identified sub-populations.

Due to its probabilistic nature, the SBM has multiple strengths over deterministic approaches. First, it provides a natural framework for deriving uncertainty measures for identified clusters, which are critical to understanding latent community structure, e.g., understanding gradual changes across multiple latent clusters. Second, using goodness-of-fit measures, the SBM helps selection of the number of clusters, which is a long-standing problem in clustering methodology and not straightforward to address in deterministic algorithmic approaches. Finally, the SBM fits naturally into the Bayesian framework, allowing for incorporation of prior expert knowledge to guide the clustering and the ability to make posterior probability statements about all model parameters (15).

## MATERIALS AND METHODS

### Experimental Methods

All experimental procedures were approved by the Institutional Animal Care and Use Committee at MUSC and by the Italian Ministry of Health (approval 1D580.18). Procedures abided by the National Institute of Health Guide for the Care and Use of Laboratory Animals and the Assessment and Accreditation of Laboratory Animals Care, as well as the European Community Council Directive for Care and Use of Laboratory Animals.

A total of 600 heterogeneous stock (HS; originally n/NIH-HS) rats bred at Wake Forest University (currently NMciWFsm:HS; Rat Genome Database number 13673907) were obtained for these studies. Of these rats, 149 were excluded from final analyses due to death following surgery ( $n = 21$ ), death over the course

of training ( $n = 77$ ) or undergoing saline, not heroin, self-administration training ( $n = 51$ ). Final analyses were performed on 451 rats (males,  $n = 238$ ; females,  $n = 213$ ). HS rats were outbred from eight inbred strains and maintained in a way to minimize inbreeding (16), allowing genetic fine-mapping to relatively small intervals (17). Animals were shipped in batches of 40 (20 males and 20 females per site) to either MUSC (USA) or UCAM (Italy) at approximately 5 weeks of age. Upon arrival, animals were pair-housed and left undisturbed in a climate-controlled colony room with a standard 12-h light:dark cycle for 3 weeks prior to the start of testing. Throughout training, rats had *ad libitum* access to food and water. Testing occurred during the dark cycle, between 18:00 and 6:00 h. Heroin hydrochloride supplied by the National Institute on Drug Abuse (Bethesda, MD) dissolved in 0.9% sterile saline was used in these studies.

Following the 3-week acclimation period, rats underwent surgery under isoflurane anesthesia for the implantation of an indwelling jugular catheter. An analgesic (Ketorolac, 2 mg/kg, sc; or Meloxicam, 0.5 mg/kg, sc), and antibiotic (Cefazolin, 0.2 mg/kg, sc; or enrofloxacin, 1 mg/kg, iv), were administered pre-operatively. Rats were given a minimum of 3 days of recovery prior to heroin self-administration training commencing. All testing occurred in standard behavioral testing chambers (MED Associates, St. Albans, VT, USA). Presses on an active lever resulted in presentation of a light and tone cue for 5-s and an infusion of heroin (20  $\mu$ g/kg/100  $\mu$ g infusion over 3 s) on a fixed-ratio 1 schedule of reinforcement. At the start of the infusion, the house light also turned off for 20-s signaling a time-out period during which additional presses on the active lever were recorded but without consequence. Presses on the inactive lever were recorded but without consequence. Sessions lasted for 12 h or until 300 infusions were earned. Self-administration occurred Monday-Friday, with one session off per week, for a total of four sessions/week. Following 12 self-administration sessions rats underwent a progressive ratio test whereby the number of presses  $p(t)$  required to receive an infusion increased exponentially after each infusion  $t = 1, \dots, T$  according to the function  $p(t) = 5e^{0.2t} - 5$  (18). Rats then had three more days of self-administration training to re-establish baseline heroin-taking behavior prior to tests for reinstatement.

At the conclusion of heroin self-administration training, rats underwent a within-session extinction-prime test that lasted for 6 h. The first 4 h were extinction training conditions during which presses on both the active and inactive lever were recorded but without consequence (i.e., active lever presses no longer result in presentation of the light/ tone cues or heroin infusion). With 2 h left in the session, rats were administered an injection of heroin (0.25 mg/mg, sc), and continued testing under extinction conditions. Daily extinction training sessions (2 h) then commenced for 6 consecutive days prior to a test for cue-induced reinstatement. During this test, presses on the active lever resulted in presentation of the light/tone cue and turning off of the house light, but no heroin infusions.

At the conclusion of training, several behavioral measures were selected for clustering analyses to reflect three behaviorally distinct phases of drug addiction: drug-taking (drug reinforced behavior), refraining (drug non-reinforced behavior), and

seeking behaviors (both drug reinforced and non-reinforced). Heroin-taking behaviors include total heroin consumption (total  $\mu$ g/kg heroin consumed across the first 12 self-administration training session), escalation of intake (total heroin consumed the first 3 days of self-administration subtracted from the last 3 days; see **Supplementary Figure 2** for heroin self-administration acquisition curve), and break point achieved during the progressive ratio test. The break point is the total number of active lever presses the rat is willing to perform in order to receive an infusion of heroin. Refraining behavior consisted of active lever presses during the first 2 h of the within-session extinction-prime test (extinction burst) and the last day of extinction training prior to the test for cue-induced reinstatement (extinction day 6). Two extinction training time points were used as to capture refraining behavior immediately after heroin taking, and following several sessions of non-reinforced seeking prior to cue-induced reinstatement. Heroin-seeking behavior is represented by active lever presses during the heroin-prime and cue-induced reinstatement tests. Active lever presses were used for all variables to maintain continuity in measured behavioral output for each behavior.

## Data Pre-processing

### Batch Correction for Multi-Site Samples

To analyze the MUSC and UCAM cohorts simultaneously, we first performed a visual inspection of possible batch effects between the two study sites. Specifically, we began by concatenating the raw data matrices from each site into an integrated data matrix, where rows corresponded to individual rats and columns correspond to behavioral measures, as described in section Experimental Methods. Then, to facilitate visualization, we applied the Uniform Manifold Approximation and Projection (UMAP) (19) algorithm to compute 2-dimensional embeddings for each rat. To correct for the apparent batch effect between study sites, we z-score transformed each behavioral measure *within study site*. This allowed for analysis of each behavioral measurement on a standardized scale, and, in effect, regressed out unwanted site-specific effects. Distributions of raw behavioral measures (i.e., before z-scoring) are shown in **Supplementary Figures 5, 6**.

### Similarity Network Construction

After integrating the behavioral data from each study site as described in section Batch Correction for Multi-Site Samples, we constructed a rat-rat similarity network as follows. First we defined a single parsimonious subset of relevant behavioral measures from the experiments discussed in section Experimental Methods using expert knowledge. Here, the goal was to choose variables that reflected the behavioral propensity of each rat for opioid dependence. Next, we computed the Euclidean distance between each pair of rats using this single parsimonious variable subset. We then formed a rat-rat similarity network, i.e., a collection of nodes and edges, where nodes in the network represent individual rats and edges represent similarities between rats. We placed an edge from each node to its  $R$  closest other nodes based on the rat-rat distance measures. Here, the number of neighbors  $R$  is a tuning parameter that controls the density of

edges in the similarity network. By default, we adopt the widely used heuristic  $R = \sqrt{N}$  (20).

## Stochastic Block Model

To detect communities within the overall rat-rat similarity matrix that might correspond to behaviorally distinct sub-populations, we adopted the Bayesian stochastic block model (SBM), a generative model for network data (15). Let  $\mathbf{A}$  be an  $n \times n$  adjacency matrix encoding the rat-rat similarity network among  $n$  total rats, with  $A_{ij} = 1$  if rat  $i$  shares an edge with rat  $j$  ( $i \neq j$ ), and  $A_{ij} = 0$  otherwise. For a fixed and pre-specified number of communities,  $K$ , the SBM assumes

$$A_{ij} | \mathbf{z}, \Theta \stackrel{\text{ind}}{\sim} \text{Bernoulli}(\theta_{z_i, z_j}) \text{ for } i < j = 1, \dots, n, \quad (1)$$

where  $z_i \in \{1, \dots, K\}$  is a categorical indicator variable that denotes the community membership of rat  $i$ ,  $\mathbf{z} = (z_1, \dots, z_n)$ , and  $\Theta$  is a  $K \times K$  connectivity matrix with elements  $\theta_{rs}$  described in detail below. Equation (1) implies that the probability of an edge occurring between two nodes depends only on the community membership of each node. Thus, all rats belonging to the same sub-population are regarded as *stochastically equivalent*.

While our primary object of inference is the vector of latent community indicators  $\mathbf{z}$ , an advantage of the SBM over other community detection algorithms is its ability to conduct statistical inference on the edge probability parameters  $\theta_{rs}$ , for  $r \leq s = 1, \dots, K$ . By encoding these parameters in a symmetric connectivity matrix  $\Theta$ , we obtain a useful summary of community structure. Here, diagonal elements of  $\Theta$  are within-community edge probabilities, and off-diagonal elements of  $\Theta$  are between-community edge probabilities. In most cases, we expect to find an *assortative* community structure, in which within-community connections are more likely than between-community connections, though the model is capable of detecting *dissortative* community structures as well (21). Thus, in addition to the community labels, the SBM allows us to characterize the global relationships between communities.

Commonly, the SBM as formulated in model (1) is refined to accommodate heterogeneous degree distributions, i.e., *degree correction* (22). Since model (1) assumes that the probability of an edge being place between two nodes only depends on the community membership of the nodes, it is not suitable for networks in which each node may have varying degree, that is, the number of edges connected to it. However, as described in section Similarity Network Construction, our workflow relies on construction of a nearest neighbors network, in which each node, by definition, will have exactly  $R$  edges, thus degree correction is not necessary.

We estimate parameters of the SBM using a fully Bayesian approach by assigning prior distributions to all unknown model parameters. We select conjugate priors to obtain closed-form full conditional distributions of all model parameters, which in turn allows for straightforward Gibbs sampling. First, for the cluster indicators  $z_1, \dots, z_n$ , we assume a conjugate multinomial-Dirichlet prior with  $z_i \stackrel{\text{iid}}{\sim} \text{Categorical}(\boldsymbol{\pi})$  for  $i = 1, \dots, n$ , and  $\boldsymbol{\pi} \sim \text{Dirichlet}(\alpha_1, \dots, \alpha_K)$ , where  $\boldsymbol{\pi} = (\pi_1, \dots, \pi_K)$  control the number of nodes in each community, i.e., the community size. Similarly,

we adopt a conjugate beta-Bernoulli prior for  $\Theta$  by letting  $\theta_{rs} \stackrel{\text{iid}}{\sim} \text{Beta}(\beta_1, \beta_2)$  for  $r < s = 1, \dots, K$ . By default, we opt for weakly informative priors by setting  $\alpha_1 = \alpha_2 = \dots = \alpha_K = 1$  and  $\beta_1 = \beta_2 = 1$  (23).

## Posterior Inference

We implement parameter estimation using Gibbs sampling, as detailed in the **Supplementary Material**. A critical step of our proposed workflow for identifying behavioral sub-populations in rats is the choice of  $K$ , i.e., the number of communities. Since the choice of  $K$  should consider both expert knowledge and evidence from the data, we refrain from proposing a “one size fits all” globally optimal method for choosing of  $K$ . Instead, in section Results we discuss how Bayesian Information Criterion (BIC) (24) can be used in conjunction with biological knowledge to make informed choices for  $K$ .

Label switching is an issue encountered in Markov chain Monte Carlo (MCMC) methods, such as the Gibbs sampler proposed above, wherein the model likelihood is invariant to permutations of a latent categorical variable such as  $\mathbf{z}$ . As a result, we may observe natural permutations of  $\mathbf{z}$  over the course of the MCMC sampling that cause the estimates of all other community-specific parameters to be conflated, thereby jeopardizing the accuracy of model parameter estimates. This problem is exacerbated when communities are not well-separated. Previous works have attempted to address the issue by re-shuffling posterior samples after the sampling has completed (25). However, these post-sampling methods rely on prediction and thereby are fallible to prediction error. To address label switching, we adopt the canonical projection of  $\mathbf{z}$  proposed by (26) in the context of Bayesian SBMs, in which we restrict samples of  $\mathbf{z}$  to the canonical sub-space  $\mathcal{Z} = \{\mathbf{z} : \text{ord}(\mathbf{z}) = (1, \dots, K)\}$ . In other words, we permute  $\mathbf{z}$  at each MCMC iteration such that community 1 appears first in  $\mathbf{z}$ , community 2 appears second in  $\mathbf{z}$ , *et cetera*. Finally, we choose as our final estimate of  $\mathbf{z}$  the maximum *a posteriori* (MAP) estimate of  $\mathbf{z}$  across all post-burn MCMC samples (23).

## Continuous Phenotyping

While the SBM presented thus far assumes that the overall experimental cohort can be decomposed into a fixed number of discrete communities, where each experimental unit (e.g., rat) is assigned to exactly one community, often interest lies in further differentiating members within a community in a more continuous fashion. Indeed, a core benefit of the Bayesian SBM is that the discrete model structure may be augmented using uncertainty measures, i.e., a quantification of our inferred level of confidence in each estimated model parameter. For instance, let  $\hat{\mathbf{z}} = (\hat{z}_1, \dots, \hat{z}_n)$  be the posterior estimate of the true community labeling vector  $\mathbf{z}$  obtained from the MCMC estimation procedure described in the **Supplementary Material**. Letting  $s = 1, \dots, S$  index the post burn-in MCMC iterations, we may quantify the uncertainty in each estimate  $\hat{z}_i$  as

$$u(\hat{z}_i) = 1 - \frac{1}{S} \sum_{s=1}^S I(\hat{z}_i^{(s)} = \hat{z}_i) \quad \text{for } i = 1, \dots, n, \quad (2)$$

where  $\hat{z}_i^{(s)}$  is the estimate of  $z_i$  at MCMC iteration  $s$ , and  $I(\hat{z}_i^{(s)} = \hat{z}_i)$  is the indicator function equal to 1 if  $\hat{z}_i^{(s)} = \hat{z}_i$  and 0 otherwise. In words,  $u(\hat{z}_i)$  represents the proportion of MCMC iterations where the estimate of  $z_i$  was not the posterior MAP estimate  $\hat{z}_i$ . For nodes that share many edges with other nodes within their respective community, i.e., those that are highly typical of their community, the uncertainty measure should be low. Meanwhile, for nodes that share edges with nodes outside of their respective community, the uncertainty measure should be high, as these nodes will likely be assigned to other communities intermittently over the course of the MCMC estimation. In this way, we may augment the cluster labels obtained by the SBM with quantification of our level of confidence in them—a significant advantage over other non-model-based clustering methods.

In addition to uncertainty quantification, we may similarly use the MCMC draws  $\hat{z}^{(1)}, \dots, \hat{z}^{(S)}$  to conduct *continuous phenotyping*, or the ranking of subjects based on their affinity toward a certain phenotype. For example, in our context of assigning rats to vulnerable and resilient phenotypes using the SBM, we may also provide a continuous measure of affinity toward the vulnerable phenotype for each rat that can be used to rank rats within clusters. In this setting, let cluster  $k_v \in \{1, 2, \dots, K\}$  be the cluster annotated as vulnerable for opioid dependence. For each rat  $i = 1, \dots, n$ , we define the continuous phenotype vulnerability score  $v(i)$  as  $\sum_{s=1}^S I(\hat{z}_i^{(s)} = k_v) / S$ , i.e., the proportion of MCMC iterations in which rat  $i$  is assigned to cluster  $k_v$ .

## Software Implementation

For convenient implementation of the workflow proposed throughout section Materials and Methods, we developed “mlsbm,” an efficient and user-friendly R package for the identification of sub-populations in network data (27). The mlsbm package is freely available for download from the Comprehensive R Archive Network (28) (<https://cran.r-project.org/package=mlsbm>). The mlsbm package includes robust documentation to facilitate applications to a variety of clustering tasks.

## Comparison to Alternative Approaches

We sought to assess the performance of the SBM clustering workflow relative to alternative clustering approaches, we applied five popular clustering algorithms, namely the Louvain, walktrap, hierarchical clustering, K-means, and DBSCAN algorithms. The Louvain (29) and walktrap (30) algorithms, like the SBM, are network-based methods that operate on the nearest neighbors network described in section Similarity Network Construction. The Louvain algorithm seeks to maximize the modularity of the graph, a measurement of the strength of clustering structure of a graph relative to randomly generated graphs. The walktrap algorithm uses random walks on the nearest neighbors graph to find the most densely connected sub-graphs, i.e., clusters, within the graph. Hierarchical clustering (11) is a “bottom up” approach that iteratively merges the most similar observations into clusters to form a tree structure that can be used to produce cluster labels for a pre-specified value of  $K$ . K-means (10) and DBSCAN (31) seek to place boundaries around observations in high-dimensional space such that the data points within

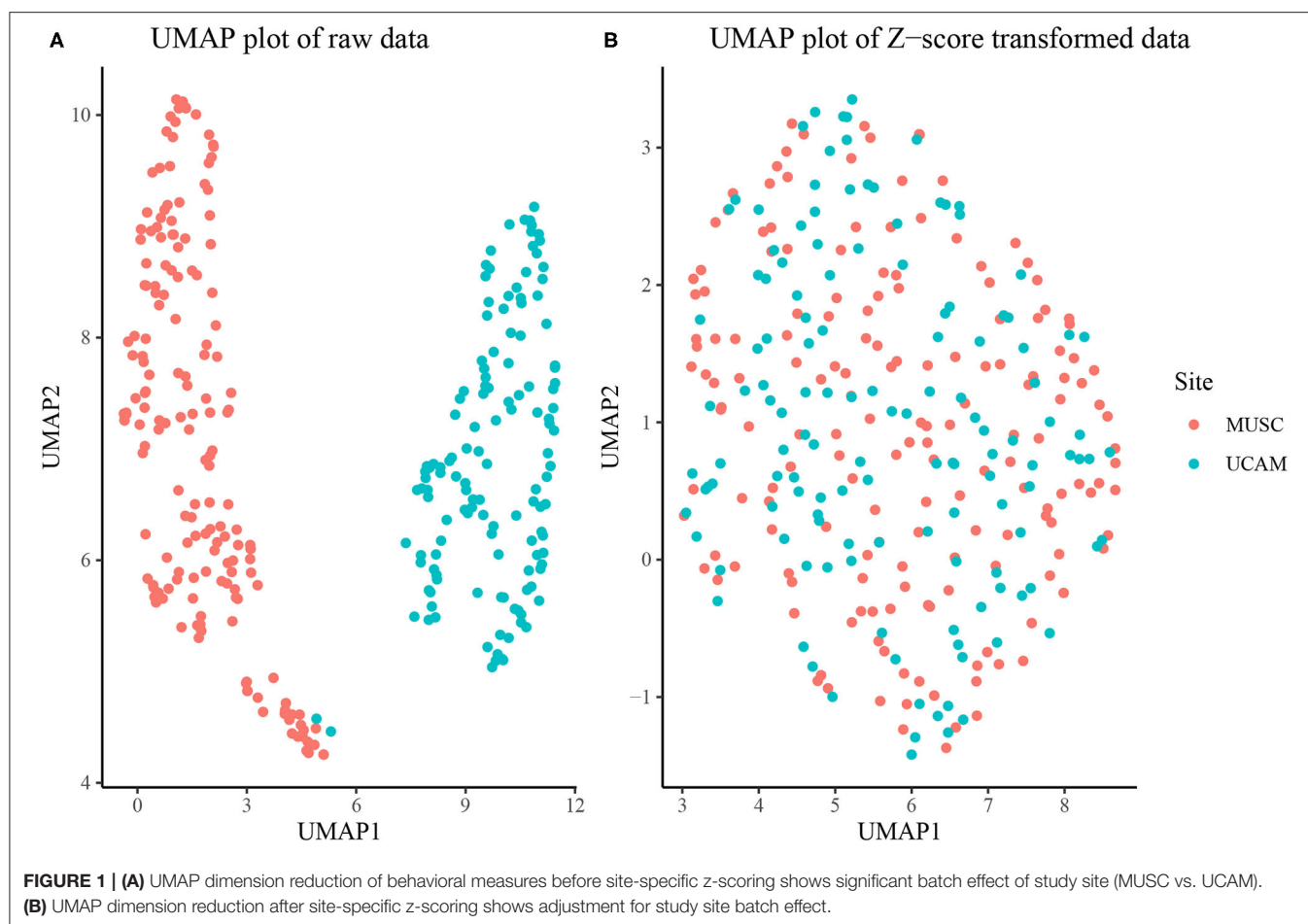
boundaries, i.e., clusters, are more similar than those across boundaries. While these approaches are commonly used, they lack the inferential benefits of the SBM such as the ability to choose  $K$  using model fit criteria and provide uncertainty quantification in addition to cluster labels.

## RESULTS

The overall sample was composed of  $N_m = 238$  males and  $N_f = 213$  females. The MUSC study site contributed 243 rats, while the UCAM study site contributed 208. As seen in **Figure 1A**, the MUSC and UCAM cohorts exhibit clear separation on the 2-dimensional UMAP space, indicating the potential of study site to act as a confounding variable in our analysis, and preventing simultaneous analysis of rats from both cohorts. The site difference is also apparent in **Supplementary Figure 6**, where in spite of substantially overlapping populations, the MUSC site shows higher mean values than the UCAM site in each of the traits quantified, except for escalation, suggesting a location shift batch effect present between study sites. In **Figure 1B**, we present the 2-dimension UMAP embedding of the concatenated z-score transformed data set, in which no distinguishable separation exists between the MUSC and UCAM rats. Hence, the site-specific z-scoring approach detailed in section Batch Correction for Multi-Site Samples was able to effectively remove the site-specific batch effect from the data.

To construct the rat-rat similarity network, we computed the Euclidean distance between each pair of rats using the 7 variables discussed in section Experimental Methods and then formed an adjacency network where each rat was connected to its 21 most similar rats. We applied the SBM clustering analysis described in section Stochastic Block Model to the analysis of  $N = 451$  rats. To choose the most appropriate number of clusters  $K$ , we fit the SBM to the adjacency network for a range of  $K$  from  $K = 2, \dots, 10$ . We ran each model for 10,000 MCMC iterations and discarded the first 1,000 iterations as burn-in, resulting in a total run time of under 4 min for each model using a single 4.7 GHz Intel i7 processor. Using BIC, we found that  $K = 3, 4, 5$  provided approximately equal goodness of fit, with  $K = 2$  or  $K > 5$  provided relatively poor fit (**Figure 2A**). As such, we chose  $K = 3$  to provide the most parsimonious representation of the data and to assess the vulnerable, intermediate, and resilient sub-type hypothesis discussed in section Introduction. An adjacency matrix with rows and columns sorted by inferred cluster indicators from the 3 cluster model is shown in **Figure 2B**. **Figure 2C** shows the SBM estimated cluster labels on UMAP space. In **Table 1**, we present the distribution of two covariates of interest across the three inferred clusters, namely sex and study site. We find a significantly skewed distribution of sex across clusters, with a female bias in cluster 1 and a male bias in cluster 3 (3-sample normal proportion test  $p < 0.0001$ ), while the distribution of study site across inferred clusters is more uniform (3-sample normal proportion test  $p = 0.601$ ).

**Figure 3** shows empirical means and 95%  $z$  confidence intervals for each of the 7 selected behavioral measures across each of the inferred clusters from the SBM. Notably, each cluster appears to show clear separation in most of the behavioral

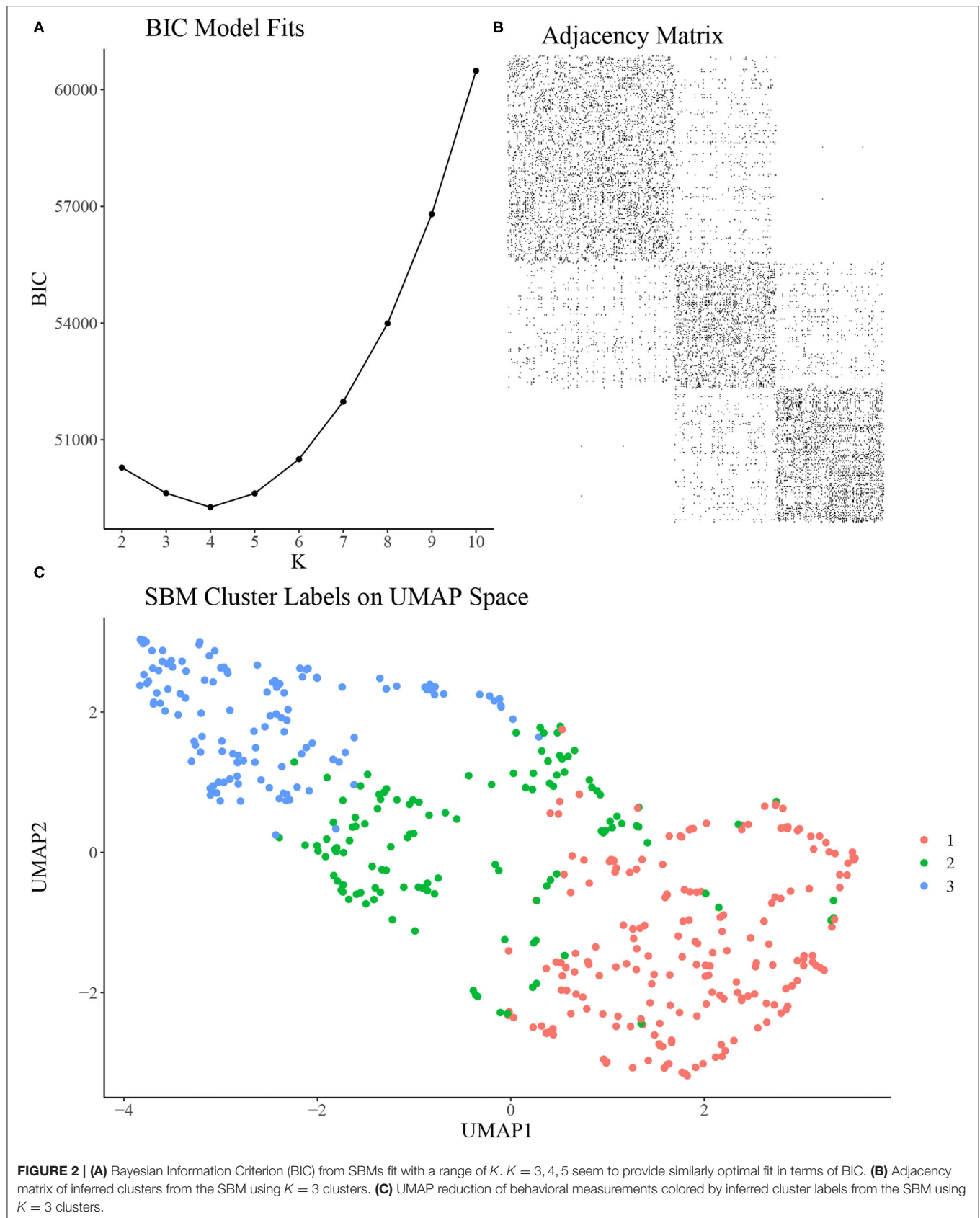


variables. For instance, the total heroin consumption was highest in cluster 1 and lowest in cluster 3, with cluster 2 falling in between clusters 1 and 3, and all 95% confidence intervals not overlapping. Similarly, cluster 1 demonstrated a more rapid escalation of heroin intake relative to clusters 2 and 3. We quantified the difference between clusters by fitting a one-way ANOVA for each of the 7 behavioral measures vs. the SBM cluster indicators. We conducted a global *F*-test for mean differences among groups. *F*-statistics and associated *p*-values are displayed in **Table 2**. Distributions of raw behavioral measures in each cluster are shown in **Supplementary Figure 1**, where the same pattern persists as with standardized variables. We observed qualitatively consistent results in site-specific analyses (**Supplementary Figure 4**). We quantified this observation through use of the adjusted Rand index (ARI) between each site-specific analysis and the integrated analysis, which revealed high correspondence between each site-specific analysis and the integrated analysis (MUSC ARI = 0.43; UCAM ARI = 0.54).

To further investigate the vulnerable, intermediate, and resilient sub-type hypothesis, we leveraged the inferential abilities of the Bayesian SBM to infer the similarity among rats from each cluster. Specifically, by investigating the posterior distribution of the elements of the matrix  $\Theta$ , we may characterize the similarity

among rats within and between each of the three clusters. In **Figure 4**, we show a heatmap of posterior means and 95% Bayesian credible intervals for  $\theta_{11}, \theta_{22}, \theta_{33}, \theta_{12}, \theta_{13}$ , and  $\theta_{23}$ . We found that the estimated values of the within-cluster connectivity parameters  $\theta_{11}, \theta_{22}, \theta_{33}$  were found to be significantly higher than those of the between-cluster parameters  $\theta_{12}, \theta_{13}$ , and  $\theta_{23}$ . In fact, cluster 1, which had the weakest estimated within-cluster connectivity ( $\hat{\theta}_{11} = 0.116$ ), was still over four times more densely connected than the highest between-cluster connection, which was shared between clusters 2 and 3 ( $\hat{\theta}_{23} = 0.025$ ). This is indicative of strong assortative community structure in the rat-rat similarity network, in which rats of the same community are more likely to be correlated in terms of behavioral measurements than rats of differing communities. Further, **Figure 4** shows that clusters 1 and 3 were the most dissimilar, with cluster 2 serving as an intermediate cluster.

In **Figure 5**, we plot results from the uncertainty measure and continuous phenotyping analysis presented in section Continuous Phenotyping. **Figure 5A** plots the cluster assignments on UMAP space, where each point is sized proportionally to its uncertainty measure of cluster assignment (larger points imply higher uncertainty). We label the ID of each rat that featured an uncertainty measure above 0.10, corresponding to rats that spent at least 10% of the post burn-in



MCMC iterations from the  $K = 3$  SBM in a cluster other than the cluster it was assigned to by the MAP estimate  $\hat{z}$ . A number of interesting patterns emerge from this uncertainty analysis. First, we find that rats with higher uncertainty tend to be located near borders between clusters on the UMAP space. Interestingly, rat 101, which was assigned to cluster 2 but is surrounded in UMAP space by rats in cluster 3, featured high uncertainty. Meanwhile, several cluster 2 rats were surrounded by cluster 1 rats in the UMAP space but featured low uncertainty.

**Figure 5B** displays results from the continuous phenotyping analysis, wherein cluster 1 was annotated as the vulnerable cluster (**Figure 3**) and chosen as the phenotype of interest. We computed the vulnerability score of each rat as the proportion of post burn-in MCMC iterations from the SBM that were spent in cluster 1. We labeled the IDs of the most interesting rats:

**TABLE 1** | Distribution of sex and study site across clusters.

Cluster	% Female ( <i>N</i> )	% UCAM ( <i>N</i> )
1: Vulnerable ( <i>N</i> = 200)	58.5 (117)	44.5 (89)
2: Intermediate ( <i>N</i> = 122)	47.5 (58)	50.0 (61)
3: Resilient ( <i>N</i> = 129)	29.5 (38)	45.0 (58)

those with uncertainty measures above 0.10 but vulnerability measures less than 0.90. These rats were located on the border between the intermediate cluster 2 and the vulnerable cluster 1, indicating higher propensity toward opioid dependence than other rats in cluster 2. These results demonstrate the ability of continuous phenotyping to augment the clustering results of the SBM to allow for disambiguation of within-cluster differences between subjects.

**Figure 6** displays results from alternative clustering methods as described in section Comparison to Alternative Approaches.

**TABLE 2** | ANOVA global F-statistics and associated *p*-values for each behavioral measure.

Variable	F-statistic	P-value
Total consumption	283.8	<0.0001
Escalation of intake	220.7	<0.0001
Break point	221.6	<0.0001
Extinction burst	94.78	<0.0001
Extinction day 6	77.12	<0.0001
Prime reinstatement	72.36	<0.0001
Cued reinstatement	200.6	<0.0001

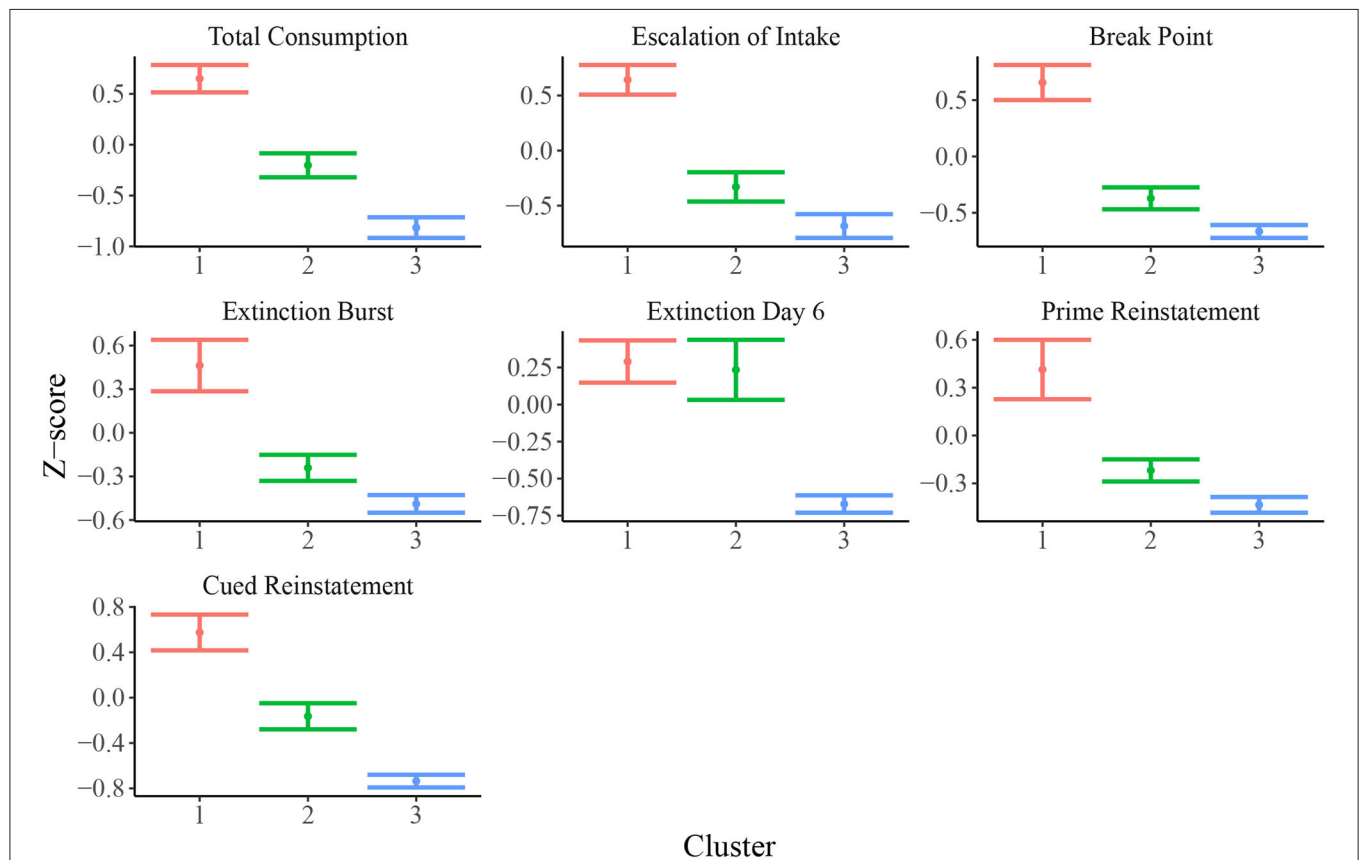


**FIGURE 3** | Means and 95% confidence intervals for relevant behavioral measures (z-scored) in each cluster. Distributions of z-scored behavioral variables indicate evidence for vulnerable (cluster 1; *N* = 200), intermediate (cluster 2; *N* = 122), and resilient (cluster 3; *N* = 129) sub-populations.

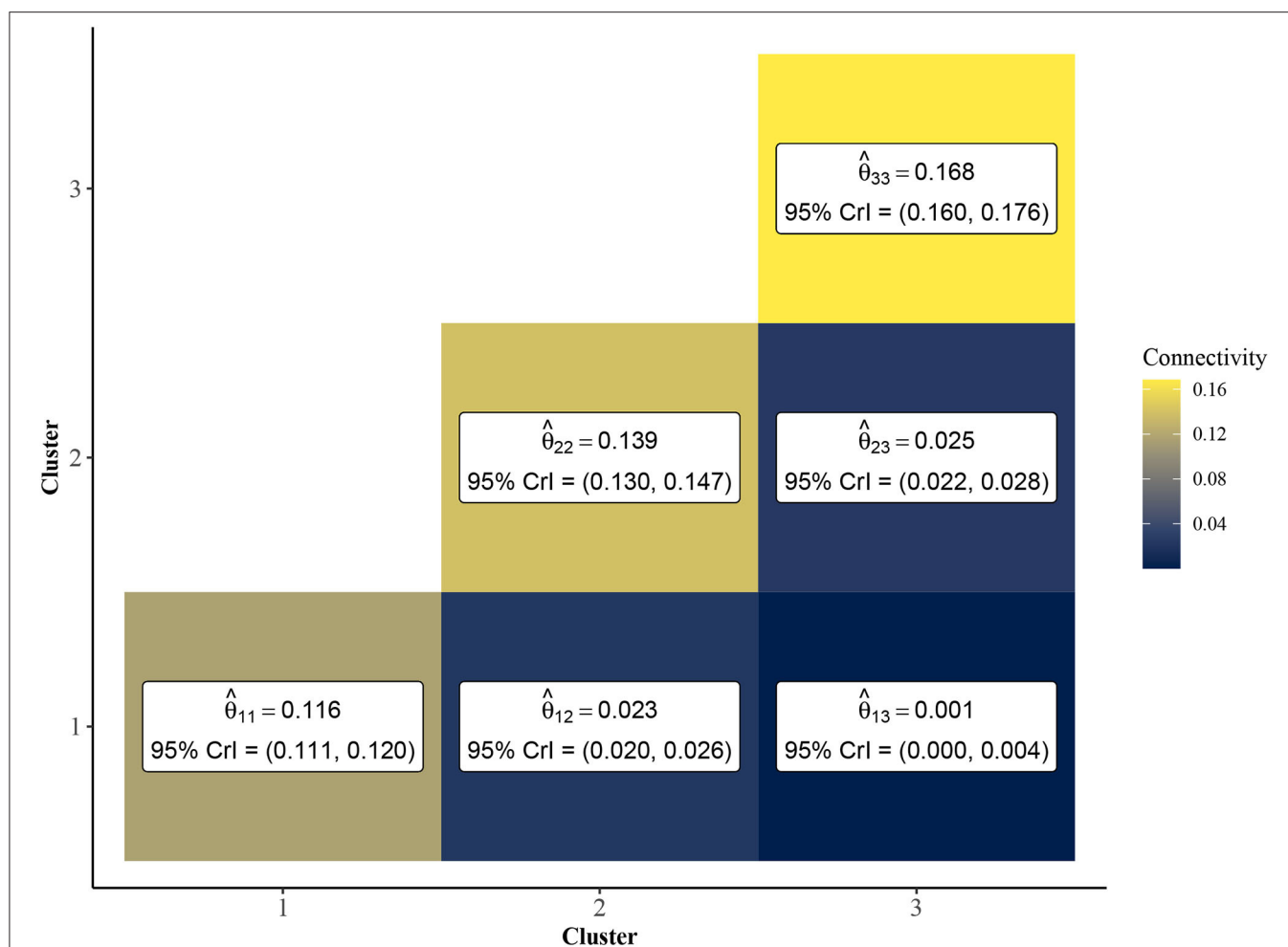
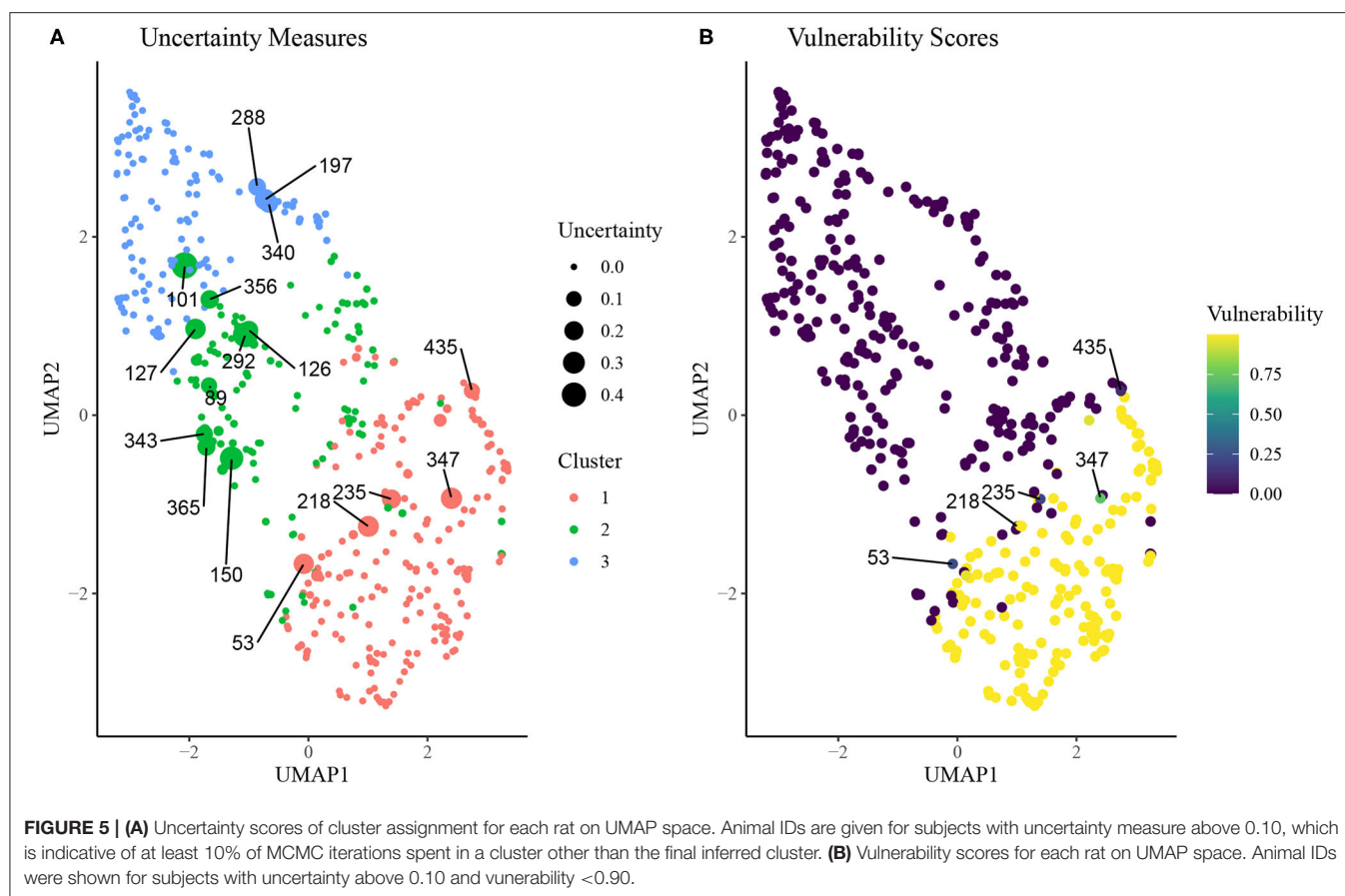


**FIGURE 4 |** Point estimates and 95% credible intervals of cluster connectivity parameters  $\theta$ . The SBM estimates higher values for within-cluster connectivity parameters,  $\theta_{11}$ ,  $\theta_{22}$ , and  $\theta_{33}$ , which is indicative of an assortative community structure. Thus, rats within the same community are expected to have significantly higher similarity than rats of different clusters. Clusters 1 and 3 are most dissimilar as evidenced by lower values of  $\hat{\theta}_{13}$  relative to  $\hat{\theta}_{12}$  and  $\hat{\theta}_{23}$ .

The network-based clustering algorithms such as Louvain and walktrap algorithms tended to produce a larger number of clusters, each smaller in size relative to the SBM. Due to this, the agreement between the results from these methods and those from the SBM is low ( $ARI < 0.30$ ). Both the hierarchical clustering method using squared Ward dissimilarity (32) and the K-means algorithm resulted in moderate agreement with the SBM ( $ARI = 0.343$  and  $0.374$ , respectively), while the DBSCAN algorithm yielded a 4 cluster result using default parameters, two of which were sparsely populated. These results suggest the SBM is best suited to addressing the research question at hand.

In addition to validating the capacity of the SBM to create three sub-populations of rats with high, intermediate and low responding for seven heroin associated behavioral traits, we evaluated how the sub-populations compare in terms of weight, site and cohort differences. **Supplementary Figure 7** shows that between sites proportionally equivalent numbers of rats were assigned to each sub-population between the two testing site,

and when analyzing between cohorts of rats within each site we found that assignment into sub-populations was equivalent across cohorts at the MUSC site, but that differences existed at the UCAM site. Also, because all the behavioral traits involved the same operant response (active lever pressing), we examined whether any traits within each sub-population were correlated using a Pearson's linear correlation statistic. **Supplementary Figure 3** shows the Pearson's coefficient for each trait comparison within each sub-population, which reveals that only Extinction Day 6 and Cued reinstatement were linearly correlated within each cluster. Otherwise, there was no consistent trait correlation across the three sub-populations. The lack of linear relationship between traits within the clusters is also revealed in **Supplementary Figure 8**, which shows the z-scored behavioral responses for all rats in cluster 1 with a selection of rats highlighted for descriptive purposes. Note that rats need not be high responders in all traits to be identified in the cluster 1 sub-population. These differences between clusters and the overall



low levels of linear correlation between traits supports exploring the SBM non-linear clustering approach described here as a means to identify non-linear relationships between multiple traits and thereby identify high (vulnerable) and low (resilient) heroin responding sub-populations. Finally, **Supplementary Figure 9** shows that equivalent weight gains occurred before and after completing the behavioral testing between each sub-cluster.

## DISCUSSION

In this paper, we developed a comprehensive framework for the descriptive analysis of behavioral sub-populations, and applied it to the cohort of 451 outbred rats subject to heroin self-administration exposure. We discovered the presence of batch effects between the two study sites that contributed to this cohort, and we corrected for these effects using study-site specific z-scoring. Seven behavioral measures were chosen to characterize the vulnerability of each rat to forming opioid dependence. Taken together, these measures quantified three important aspects of dependence: drug-taking, refraining and seeking behaviors. Using these measures, we then converted the multidimensional behavioral data into a rat-rat similarity network, which allowed for investigation of distinct communities within the overall network.

We chose the Bayesian stochastic block model, a statistical model for network data, for investigation of behavioral sub-populations within this cohort. We used the model fit criterion BIC to choose a subset of best fitting models in terms of number of communities. Of this best fitting subset, we chose the three cluster model as it offered the best balance between optimizing statistical and biological criteria. Using ANOVA global *F*-tests, we found significant separation between clusters in terms of each of the seven behavioral measures. Additionally, investigation of average trends across clusters in each behavioral measure allowed us to annotate vulnerable, resilient, and intermediate sub-groups with high confidence. Using the community connectivity parameters inferred by the SBM, we described the relative similarity between clusters, with the vulnerable and resilient clusters each displaying similarity to the intermediate cluster but very little similarity to one another.

To augment the discrete community labels obtained from the SBM, we developed an uncertainty measure, which uses samples from the posterior distribution of the cluster labels to estimate our confidence in the inferred community structure. We also implemented continuous phenotyping to investigate heterogeneities within clusters in terms of vulnerability to opioid dependence. We found a subset of intermediate vulnerability animals who featured relatively high affinity toward the vulnerably cluster,

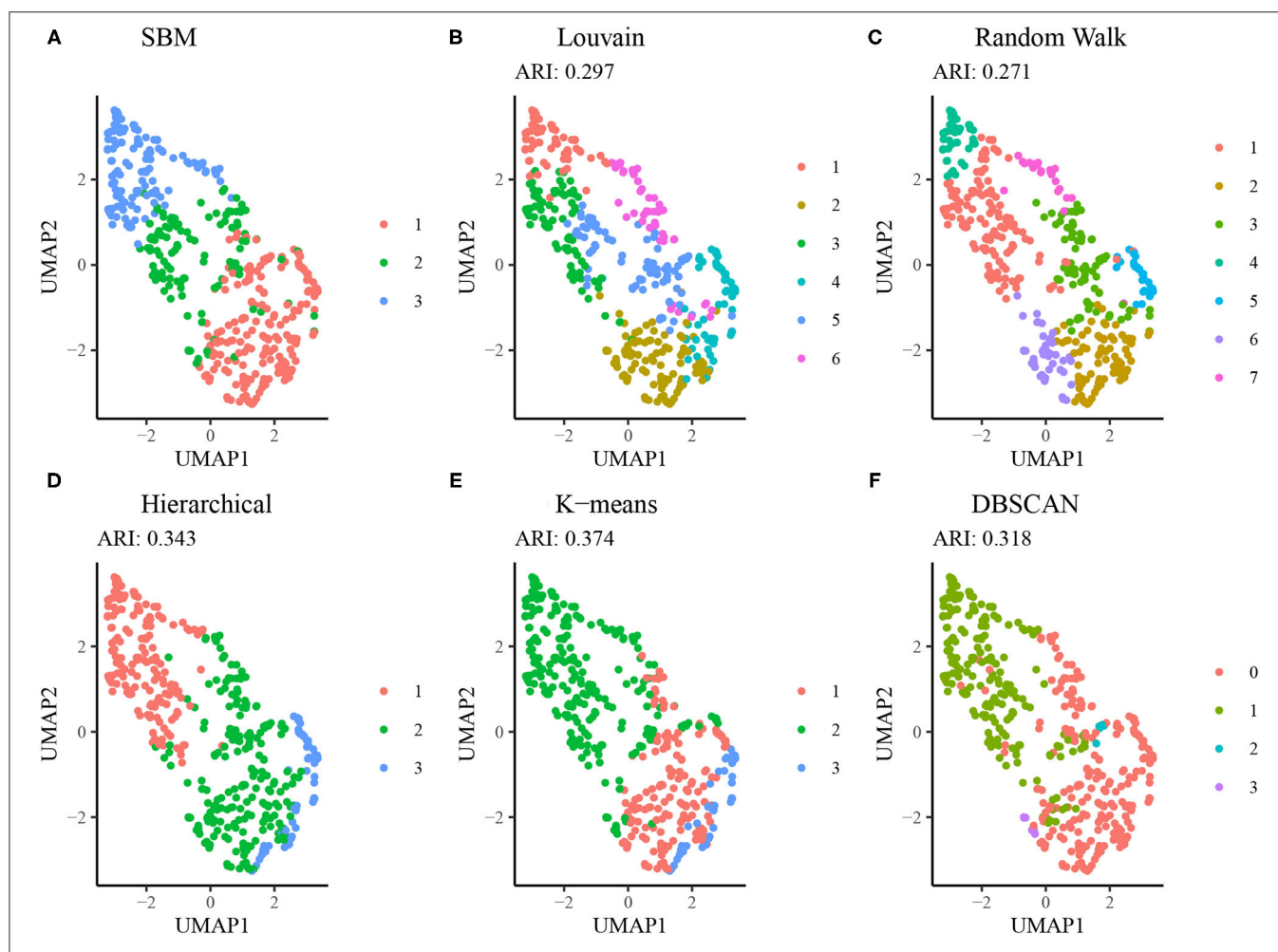


**FIGURE 6 |** Comparison of SBM performance relative to alternative methods. **(A)** Clustering results from the SBM using  $K = 3$ . **(B)** Clustering results from the Louvain algorithm (no tuning parameters available). **(C)** Clustering results from the Walktrap algorithm using random walks of length 4. **(D)** Hierarchical clustering results using a dendrogram cut at  $K = 3$ . **(E)** K-means clustering results using the Hartigan-Wong method and  $K = 3$ . **(F)** DBSCAN clustering results using a radius of 0.8 and minimum neighborhood size of 5.

providing candidate animals for further investigation of the differences between vulnerable and resilient animals. Finally, we developed “mlsbm,” an efficient and robust R package for implementation of our proposed clustering workflow. The mlsbm package is publicly available through CRAN (<https://cran.r-project.org/package=mlsbm>) for use in future behavioral studies.

The SBM analysis identified three behaviorally distinct populations of rats that varied based on their apparent vulnerability to OUD. OUD is a complex and multi-symptomatic disorder, making it imperative to understand how various behaviors over the course of addiction interact with one another to confer vulnerability vs. resiliency. Results indicate that individuals more vulnerable to OUD exhibit higher lever pressing across the behavioral tasks, but largely not in a linear manner (**Supplementary Figure 3**). Thus, in the SBM, it is the non-linear interaction between several variables that ultimately results in differences between clusters. This is illustrated in

**Supplementary Figure 8**, showing how all animals in cluster 1 (vulnerable cluster) vary across the seven traits we used for modeling. Highlighted are examples of three rats each showing a distinct high and low z-score profile depending on the traits. For example, not all rats in the vulnerable cluster had high heroin consumption, although the mean consumption for this cluster was greater than for the other two clusters (**Figure 3**).

Both males and females were used in this study, and we found sex differences in cluster composition with females more represented in Cluster 1, and males in Cluster 3. These data align with what is observed in humans, as females both acquire and maintain higher levels of drug use, and relapse more often, than males across several classes of drugs, including heroin (33). This finding further bolsters the potential translational validity of this model in assessing OUD vulnerability. However, a deeper analysis of translational validity requires future studies where traits determined prior to heroin exposure that predict OUD

vulnerability in humans can be evaluated to determine if they predict which cluster a rat will enter. For example, levels of impulsivity, novelty-induced locomotor behavior and attributing incentive salience to a reward-paired cue have all been shown to predict relapse propensity [for review see (34)]. Moreover, measuring behaviors of drug seeking after obtaining the heroin measures can be used as covariates to further validate cluster allocation by the SBM model. For example, the model would predict that cluster 1 rats would more compulsively seek heroin in the presence of punishment than cluster 3 subpopulations. Also, identifying these three distinct phenotypes using this model allows for further characterization of individual variation in the neurobiological mechanisms and genetic background underlying OUD vulnerability. Finally, we plan to develop an interactive web application using the SBM model to analyze a variety of network-based data sets without the need for programming experience in R, thereby allowing other laboratories to evaluate a variety of network-based data sets for subpopulations of animals and humans that may be more vulnerable or resilient to developing SUDs or other neuropsychiatric disorders.

## DATA AVAILABILITY STATEMENT

The datasets presented in this study can be found in online repositories. The names of the repository/repositories and accession number(s) can be found below: The R package *mlsbm* is publicly available from the Comprehensive R Archive Network (<https://cran.r-project.org/package=mlsbm>). The behavioral data used in this paper are not readily available due to ongoing data collection, which is implemented as part of the ongoing NIH-funded research project. Please contact the corresponding author for any inquiry related to the behavioral data.

## REFERENCES

1. NIH. *Overdose Death Rates*. (2021). Available online at: <https://www.drugabuse.gov/drug-topics/trends-statistics/overdose-death-rates> (accessed June 17, 2021).
2. Jones CM, Logan J, Gladden RM, Bohm MK. Vital signs: demographic and substance use trends among heroin users' United States, 2002–2013. *MMWR Morb Mortal Weekly Rep.* (2015) 64:719.
3. Cicero TJ, Ellis MS, Surratt HL, Kurtz SP. The changing face of heroin use in the United States: a retrospective analysis of the past 50 years. *JAMA Psychiatry.* (2014) 71:821–6. doi: 10.1001/jamapsychiatry.2014.366
4. Compton WM, Jones CM, Baldwin GT. Relationship between nonmedical prescription-opioid use and heroin use. *N Engl J Med.* (2016) 374:154–63. doi: 10.1056/NEJMr1508490
5. APA. *Diagnostic and Statistical Manual of Mental Disorders*. 5th ed. Washington, DC: American Psychiatric Association (2013). doi: 10.1176/appi.books.9780890425596
6. Shmulewitz D, Greene ER, Hasin D. Commonalities and differences across substance use disorders: phenomenological and epidemiological aspects. *Alcohol Clin Exp Res.* (2015) 39:1878–900. doi: 10.1111/acer.12838
7. Venniro M, Banks ML, Heilig M, Epstein DH, Shaham Y. Improving translation of animal models of addiction and relapse by reverse translation. *Nat Rev Neurosci.* (2020) 21:625–43. doi: 10.1038/s41583-020-0378-z
8. Deroche-Gamonet V, Belin D, Piazza PV. Evidence for addiction-like behavior in the rat. *Science.* (2004) 305:1014–7. doi: 10.1126/science.1099020

## ETHICS STATEMENT

All experimental procedures were approved by the Institutional Animal Care and Use Committee at the Medical University of South Carolina and by the Italian Ministry of Health (approval 1D580.18). Procedures abided by the National Institute of Health Guide for the Care and Use of Laboratory Animals and the Assessment and Accreditation of Laboratory Animals Care, as well as the European Community Council Directive for Care and Use of Laboratory Animals.

## AUTHOR CONTRIBUTIONS

Statistical modeling, software development, and data analyses were conducted by CA and DC. The behavioral experiments were designed by NC, BK, MU, LW, GH, RC, and PK. All behavioral experimental procedures were conducted by BK, NC, VL, AC, and AR. This manuscript was written by CA, BK, NC, RC, PK, and DC. All authors contributed to the article and approved the submitted version.

## FUNDING

This work was supported in part by NIH/NIDA grant U01-DA045300, NIH/NIGMS grant R01-GM122078, NIH/NCI grant R21-CA209848, and NIH/NIDA grant T32-DA007288.

## SUPPLEMENTARY MATERIAL

The Supplementary Material for this article can be found online at: <https://www.frontiersin.org/articles/10.3389/fpsy.2021.745468/full#supplementary-material>

9. Venniro M, Zhang M, Caprioli D, Hoots JK, Golden SA, Heins C, et al. Volitional social interaction prevents drug addiction in rat models. *Nat Neurosci.* (2018) 21:1520–9. doi: 10.1038/s41593-018-0246-6
10. Forgey E. Cluster analysis of multivariate data: efficiency vs. interpretability of classification. *Biometrics.* (1965) 21:768–9.
11. McQuitty LL. Similarity analysis by reciprocal pairs for discrete and continuous data. *Educ Psychol Measure.* (1966) 26:825–31. doi: 10.1177/001316446602600402
12. McLachlan GJ, Lee SX, Rathnayake SI. Finite mixture models. *Annu Rev Stat Appl.* (2019) 6:355–78. doi: 10.1146/annurev-statistics-031017-100325
13. Hao Y, Hao S, Andersen-Nissen E, Mauck WM, Zheng S, Butler A, et al. Integrated analysis of multimodal single-cell data. *bioRxiv.* (2020). doi: 10.1101/2020.10.12.335331
14. Holland PW, Laskey KB, Leinhardt S. Stochastic blockmodels: first steps. *Soc Netw.* (1983) 5:109–37. doi: 10.1016/0378-8733(83)90021-7
15. Snijders TA, Nowicki K. Estimation and prediction for stochastic blockmodels for graphs with latent block structure. *J Classif.* (1997) 14:75–100. doi: 10.1007/s003579900004
16. Hansen C, Spuhler K. Development of the National Institutes of Health genetically heterogeneous rat stock. *Alcohol Clin Exp Res.* (1984) 8:477–9. doi: 10.1111/j.1530-0277.1984.tb05706.x
17. Woods LCS, Palmer AA. Using heterogeneous stocks for fine-mapping genetically complex traits. *Rat Genomics.* (2019) 2018:233–47. doi: 10.1007/978-1-4939-9581-3\_11

18. Richardson NR, Roberts DC. Progressive ratio schedules in drug self-administration studies in rats: a method to evaluate reinforcing efficacy. *J Neurosci Methods*. (1996) 66:1–11. doi: 10.1016/0165-0270(95)00153-0
19. McInnes L, Healy J, Melville J. UMAP: uniform manifold approximation and projection for dimension reduction. *arXiv preprint arXiv:1802.03426*. (2018) 66:1–11. doi: 10.21105/joss.00861
20. Stork DG, Duda RO, Hart PE. *Pattern Classification*. 2nd ed. New York, NY: Wiley (2001). p.688.
21. Fortunato S, Hric D. Community detection in networks: a user guide. *Phys Rep*. (2016) 659:1–44. doi: 10.1016/j.physrep.2016.09.002
22. Karrer B, Newman ME. Stochastic blockmodels and community structure in networks. *Phys Rev E*. (2011) 83:016107. doi: 10.1103/PhysRevE.83.016107
23. Gelman A, Carlin JB, Stern HS, Dunson DB, Vehtari A, Rubin DB. *Bayesian Data Analysis*. 3rd ed. Boca raton, FL: CRC Press (2013). doi: 10.1201/b16018
24. Schwarz G. Estimating the dimension of a model. *Ann Stat*. (1978) 6:461–4. doi: 10.1214/aos/1176344136
25. Papastamoulis P. label.switching: an R package for dealing with the label switching problem in MCMC outputs. *J Stat Softw*. (2016) 69:1–24. doi: 10.18637/jss.v069.c01
26. Peng L, Carvalho L. Bayesian degree-corrected stochastic blockmodels for community detection. *Electron J Stat*. (2016) 10:2746–79. doi: 10.1214/16-EJS1163
27. Allen C, Chung D. *mlsbm: Efficient Estimation of Bayesian SBMs & MLSBMs*. (2021). R package version 0.99.2. Available online at: <https://CRAN.R-project.org/package=mlsbm>
28. R Core Team. *R: A Language and Environment for Statistical Computing*. Vienna (2020). Available online at: <https://www.R-project.org/>
29. Blondel VD, Guillaume JL, Lambiotte R, Lefebvre E. Fast unfolding of communities in large networks. *J Stat Mech Theory Exp*. (2008) 2008:P10008. doi: 10.1088/1742-5468/2008/10/P10008
30. Pons P, Latapy M. Computing communities in large networks using random walks. In: *International Symposium on Computer and Information Sciences*. Istanbul: Springer (2005). p. 284–93. doi: 10.1007/11569596\_31
31. EsterM, Kriegl HP, Sander J, Xu X. A density-based algorithm for discovering clusters in large spatial databases with noise. In: *KDD'96: Proceedings of the Second International Conference on Knowledge Discovery and Data Mining*. Portland: AAAI Press (1996). p. 226–31.
32. Murtagh F, Legendre P. Ward's hierarchical agglomerative clustering method: which algorithms implement Ward's criterion? *J Classif*. (2014) 31:274–295. doi: 10.1007/s00357-014-9161-z
33. Becker JB, McClellan ML, Reed BG. Sex differences, gender and addiction. *J Neurosci Res*. (2017) 95:136–47. doi: 10.1002/jnr.23963
34. Kuhn BN, Kalivas PW, Bobadilla AC. Understanding addiction using animal models. *Front Behav Neurosci*. (2019) 13:262. doi: 10.3389/fnbeh.2019.00262

**Conflict of Interest:** The authors declare that the research was conducted in the absence of any commercial or financial relationships that could be construed as a potential conflict of interest.

**Publisher's Note:** All claims expressed in this article are solely those of the authors and do not necessarily represent those of their affiliated organizations, or those of the publisher, the editors and the reviewers. Any product that may be evaluated in this article, or claim that may be made by its manufacturer, is not guaranteed or endorsed by the publisher.

Copyright © 2021 Allen, Kuhn, Cannella, Crow, Roberts, Lunerti, Ubaldi, Hardiman, Solberg Woods, Ciccocioppo, Kalivas and Chung. This is an open-access article distributed under the terms of the Creative Commons Attribution License (CC BY). The use, distribution or reproduction in other forums is permitted, provided the original author(s) and the copyright owner(s) are credited and that the original publication in this journal is cited, in accordance with accepted academic practice. No use, distribution or reproduction is permitted which does not comply with these terms.



## OPEN ACCESS

### Edited by:

Roberto Ciccocioppo,  
University of Camerino, Italy

### Reviewed by:

Anna Brancato,  
University of Palermo, Italy

Harold A. Burgess,  
Eunice Kennedy Shriver National  
Institute of Child Health and Human  
Development (NICHD), United States

### \*Correspondence:

Elisabeth M. Busch-Nentwich  
e.busch-nentwich@qmul.ac.uk  
Caroline H. Brennan  
c.h.brennan@qmul.ac.uk

†These authors have contributed  
equally to this work and share first  
authorship

### \*ORCID:

Aleksandra M. Mech  
orcid.org/0000-0003-0511-6048  
Munise Merteroglu  
orcid.org/0000-0002-9747-2981  
Ian M. Sealy  
orcid.org/0000-0002-2890-6635  
Muy-Teck Teh  
orcid.org/0000-0002-7725-8355  
Richard J. White  
orcid.org/0000-0003-1842-412X  
William Havelange  
orcid.org/0000-0003-1965-5894  
Caroline H. Brennan  
orcid.org/0000-0002-4169-4083  
Elisabeth M. Busch-Nentwich  
orcid.org/0000-0001-6450-744X

### Specialty section:

This article was submitted to  
Addictive Disorders,  
a section of the journal  
Frontiers in Psychiatry

**Received:** 14 October 2021

**Accepted:** 29 November 2021

**Published:** 10 January 2022

### Citation:

Mech AM, Merteroglu M, Sealy IM,  
Teh M-T, White RJ, Havelange W,  
Brennan CH and Busch-Nentwich EM  
(2022) Behavioral and Gene  
Regulatory Responses to  
Developmental Drug Exposures in  
Zebrafish.  
Front. Psychiatry 12:795175.  
doi: 10.3389/fpsy.2021.795175

# Behavioral and Gene Regulatory Responses to Developmental Drug Exposures in Zebrafish

Aleksandra M. Mech<sup>1†</sup>, Munise Merteroglu<sup>2†</sup>, Ian M. Sealy<sup>2†</sup>, Muy-Teck Teh<sup>3†</sup>,  
Richard J. White<sup>2†</sup>, William Havelange<sup>1†</sup>, Caroline H. Brennan<sup>1\*†</sup> and  
Elisabeth M. Busch-Nentwich<sup>1,2\*†</sup>

<sup>1</sup> School of Biological and Behavioural Sciences, Faculty of Science and Engineering, Queen Mary University of London, London, United Kingdom, <sup>2</sup> Department of Medicine, Cambridge Institute of Therapeutic Immunology and Infectious Disease, University of Cambridge, Cambridge, United Kingdom, <sup>3</sup> Centre for Oral Immunobiology and Regenerative Medicine, Institute of Dentistry, Barts and the London School of Medicine and Dentistry, Queen Mary University of London, England, United Kingdom

Developmental consequences of prenatal drug exposure have been reported in many human cohorts and animal studies. The long-lasting impact on the offspring—including motor and cognitive impairments, cranial and cardiac anomalies and increased prevalence of ADHD—is a socioeconomic burden worldwide. Identifying the molecular changes leading to developmental consequences could help ameliorate the deficits and limit the impact. In this study, we have used zebrafish, a well-established behavioral and genetic model with conserved drug response and reward pathways, to identify changes in behavior and cellular pathways in response to developmental exposure to amphetamine, nicotine or oxycodone. In the presence of the drug, exposed animals showed altered behavior, consistent with effects seen in mammalian systems, including impaired locomotion and altered habituation to acoustic startle. Differences in responses seen following acute and chronic exposure suggest adaptation to the presence of the drug. Transcriptomic analysis of exposed larvae revealed differential expression of numerous genes and alterations in many pathways, including those related to cell death, immunity and circadian rhythm regulation. Differential expression of circadian rhythm genes did not correlate with behavioral changes in the larvae, however, two of the circadian genes, *arntl2* and *per2*, were also differentially expressed at later stages of development, suggesting a long-lasting impact of developmental exposures on circadian gene expression. The immediate-early genes, *egr1*, *egr4*, *fosab*, and *junbb*, which are associated with synaptic plasticity, were downregulated by all three drugs and *in situ* hybridization showed that the expression for all four genes was reduced across all neuroanatomical regions, including brain regions implicated in reward processing, addiction and other psychiatric conditions. We anticipate that these early changes in gene expression in response to drug exposure are likely to contribute to the consequences of prenatal exposure and their discovery might pave the way to therapeutic intervention to ameliorate the long-lasting deficits.

**Keywords:** developmental exposure, addiction, zebrafish, nicotine, oxycodone, amphetamine, behavior, RNA-seq

## INTRODUCTION

Despite social awareness campaigns, drug usage amongst pregnant women in the USA remains high, standing at ~17% for nicotine, ~8.5% for alcohol and 5.9% for illicit drugs such as cocaine, methamphetamine, marijuana and prescription-type psychotherapeutics (1). Prenatal drug exposure poses a significant health risk for the developing fetus, either directly by crossing the placenta and acting on molecular targets in the fetus, indirectly through physiological effects on the mother, or a combination of both. The most common effects seen in newborns that have been exposed to drugs of abuse during gestation include growth restriction, decreased weight and cranial and cardiac anomalies (2, 3). However, prenatal drug exposure is also associated with increased vulnerability to psychiatric disease, including addiction (4), schizophrenia (5), autism (6) and ADHD (7), as well as aggression, peer-related problems and learning difficulties (8–11). These findings suggest that drug exposures at developmental stages lead to profound changes that last beyond the exposure period, manifesting both as motor and cognitive impairments and as phenotypes associated with addiction and other psychiatric disorders.

Although the consequences of developmental exposure to drugs of abuse in terms of neural development are not fully understood, a number of studies have shown altered expression of key components of neurotransmitter pathways in regions of the brain associated with behavioral responses and long-term changes in behavior. For example, prenatal methamphetamine exposure in rats showed, among other changes, altered expression of dopamine receptors (Drd3) in the striatum in adulthood (12). Reduced release of dopamine was reported in adult mice following prenatal nicotine exposure (13). Additionally, nicotine exposure has been linked to neuronal loss in striatal and hippocampal regions in adult rats, both of which play a critical role in learning and memory (14, 15). Similarly, alteration in these regions were observed following *in-utero* opioid exposure in humans (16). Widespread neuroapoptosis throughout the developing brain of several species, mechanisms of which are not fully understood, is also reported following prenatal drug exposures (17). Recent evidence from rodent studies suggests that prenatal and postnatal drug exposures lead to changes in gene expression as a result of altered DNA methylation (18, 19). More details on the effect of developmental exposure on development can be found in recent reviews: (20–22).

In this study, we have used zebrafish to investigate the changes in gene expression following developmental exposure to three commonly abused drugs to gain insight into alterations in biological pathways that may contribute to changes in behavior in later life. The zebrafish, a well-established behavioral and genetic model with conserved drug response and reward pathways (23, 24), has rapid *ex utero* embryogenesis which allows non-invasive drug treatments at early embryonic stages. We exposed developing zebrafish to three drugs that are commonly abused by women of reproductive age: amphetamine, oxycodone and nicotine (25). We have chosen drugs with different modes of action—two stimulants, amphetamine and nicotine, and an

opioid, oxycodone—in order to investigate both overlapping and drug class specific changes in gene expression.

Amphetamine is a dopamine (DA) transporter (DAT) inhibitor that prevents presynaptic reuptake of DA and therefore increases the concentration of dopamine and noradrenaline at the synapse, leading to a psychostimulant response (26). Nicotine is a strong alkaloid whose main mechanism of action in the human body is through binding to nicotinic acetylcholine receptors (nAChRs). Consumed nicotine stimulates nAChRs in the central nervous system (CNS) which, in the developed brain, causes a release of dopamine and also glutamate, serotonin, acetylcholine and  $\gamma$ -aminobutyric acid (GABA) (27).

Oxycodone acts by attaching to  $\mu$ -opioid receptors on the surface of neurons. In adults, activation of the  $\mu$ -opioid receptors sends a signal through the ventral tegmental area (VTA) that causes the release of dopamine in the NAc and gives a feeling of pleasure to the user (28). Oxycodone is widely used as a pain relief medication in post-operative, chronic and cancer-related pain management (29). Despite having many beneficial effects it is also one of the most addictive prescription drugs on the market. Currently, the USA has an opioid epidemic with overdose death rates increasing at alarming rates. Therefore, understanding the potential consequences of developmental oxycodone exposure is crucial to ameliorating the impact of this crisis on future generations (30).

We exposed developing zebrafish to amphetamine, nicotine or oxycodone from 1 to 5 days post fertilization (dpf), the period during which all major organ systems develop and begin functioning (31). In the presence of drugs, developmentally exposed larvae showed changes in locomotion and habituation to acoustic startle, consistent with the effects of these drugs in mammalian systems. We show that developmental exposure induces differential expression of numerous genes and alterations in many pathways, including those involved in development, cell death regulation, circadian rhythm, innate immunity and synaptic plasticity.

## MATERIALS AND METHODS

### Zebrafish Husbandry

All *in vivo* experimental work was carried out following consultation of the ARRIVE guidelines (NC3Rs, UK). Zebrafish were maintained in accordance with UK Home Office regulations, UK Animals (Scientific Procedures) Act 1986. All animal work was reviewed by the Animal Welfare and Ethical Review Body at the University of Cambridge (project license P597E5E82) and by the Animal Care and Use ethics committee at Queen Mary University of London (project license P6D11FBCD).

Fish were housed in a recirculating system (Tecniplast, UK) on a 14:10 light:dark cycle. The housing and testing rooms were maintained at ~25–28°C. Fish were maintained in aquarium-treated water and fed twice daily with flake food (ZM-400, Zebrafish Management Ltd, Winchester, United Kingdom) and once daily with live artemia (*Artemia salina*). All zebrafish used in this study originated from a Tupfel long fin (TLF) wild-type

(WT) background line. All animals were selected at random from groups of conspecifics for testing.

At the time of mating, breeding males and females were separated overnight before letting them spawn naturally in the morning to allow for synchronization of developmental stages. Eggs were incubated in groups of no more than 50 per Petri dish at 28°C until 5 days post fertilization (dpf). Then, larvae were transferred to the recirculating system and fed twice daily with commercial fry food (ZM-75, ZM-100, Zebrafish Management Ltd, Winchester, United Kingdom) and live paramecia/brine shrimp, depending on their age.

## Drug Exposure

For developmental drug exposure, wild-type TLF strain prim-5 stage embryos (24 h post fertilization) were divided into three treatment groups and a control group and exposed until 5 dpf. Drug solutions were prepared in egg water to final concentrations of 25  $\mu$ M amphetamine (Sigma-Aldrich, Cat. No. A5880), 5  $\mu$ M nicotine (Sigma-Aldrich, Cat. No. N1019) and 1.14  $\mu$ M oxycodone (Sigma-Aldrich, Cat. No. O1378). Drug concentrations were based on those found to induce maximal conditioned place preference in adults (32). We aimed to model consistent human consumption during pregnancy. The concentrations present in the fish water were higher than those reported to be present in the human fetal blood during pregnancy (33, 34). However, as the pharmacokinetics of the compounds is not known in fish, we selected concentrations that have been previously shown to have a relevant physiological effect in zebrafish when administered via the tank water. Even though the magnitude of any changes in gene expression may differ, we predict that the direction of the changes remains the same. Although oxycodone and amphetamine are stable in water for at least 24 h (35, 36), there is contrasting evidence for the rate of decline in nicotine concentration over time with some evidence suggesting a rapid decline over a 48-h period (personal communication, Sala) and others pointing at decline over a 10 day period (37). To account for potential degradation and for consistency in handling across treatments, we therefore refreshed all solutions every 48 h. At 5 dpf, either solutions were refreshed and larvae taken for behavioral or RNAseq analysis, or larvae were transferred to fresh Petri dishes in the absence of drug and reared.

For acute drug exposure, wild-type TLF larvae were raised in egg water until 5 dpf. An hour before the start of the behavioral experiments water was removed and replaced with freshly made drug solutions of 25  $\mu$ M amphetamine, 5  $\mu$ M nicotine and 1.14  $\mu$ M oxycodone.

## Behavioral Assays

To ensure drug penetration we examined locomotor activity in the presence of the drug and post exposure. We performed two independent larval behavioral assays: forced light-dark assay (FLD) and habituation to acoustic startle. FLD is commonly used as an anxiety measure, based on the assumption that a sudden change of environment from dark to light will increase locomotion through the activation of the hypothalamic-pituitary-interrenal (HPI) axis (38). Habituation to acoustic

startle is a measure of sensorimotor gating, a process that is modulated by dopaminergic signaling (39).

Eggs for all behavioral experiments were collected from multiple adult pairs, pooled and divided across at least three Petri-dishes. Fertile eggs were staged-matched and randomly assigned to treatment groups. Embryos and larvae were carefully monitored for differences in development across dishes. For all experiments, stage-matched larvae were selected from all Petri-dishes, to account for possible batch/dish effects. No morphological or immediate behavioral differences were seen between treatment and control groups in the 5 dpf larvae following developmental drug exposure prior to behavioral analysis. All tested individuals were the same size. Larvae were culled after behavioral experimentation.

### Forced Light-Dark Transition

Experiments were performed between 1 and 6 p.m. Behavior was assessed at 5 dpf in the presence of the drug, or at 6 dpf, in the absence of the drug, 24 h after the end of the exposure. Larvae were individually placed in 96-well plates, pseudo-randomized by drug treatment, and allowed to acclimate for 30 min. After this period, the plate was placed inside a DanioVision Observational Chamber (Noldus Information Technology, Wageningen, The Netherlands). Larval locomotion was recorded during alternating light/dark periods: 10 min in the dark (infrared conditions), which was used as a baseline; 10 min in the light; 10 min in the dark; 1 min in the light; 10 min in the dark. Distance traveled was recorded using Ethovision XT software (Noldus Information Technology, Wageningen, The Netherlands) and data were output in 10 and 1 s time bins for analysis. Larvae were culled after behavioral experimentation.

### Acoustic Startle Habituation

Acoustic startle was performed as described previously (40) with minor modifications. Experiments were performed between 1 and 6 p.m. Behavior was assessed at 5 dpf in the presence of the drug, or at 6 dpf, in the absence of the drug, 24 h after the end of the exposure. Larvae were individually placed in 96-well plates, pseudo-randomized by drug treatment, and allowed to acclimate for 30 min. After this period, the plate was moved to a DanioVision Observational Chamber (Noldus Information Technology, Wageningen, The Netherlands) where, following a 2-min acclimatization period, larval movement was recorded. Following an initial 1 min baseline period, larvae were subjected to 25 sound/vibration stimuli with 2 s inter-stimulus intervals. The distance traveled was recorded using Ethovision XT software (Noldus Information Technology, Wageningen, The Netherlands), and data were output in 1 s time bins.

### Exploratory/Bold Behavior Assay

The exploratory/bold behavior assay was a modified version of a sociability assay performed by Dreosti et al. (41). All experiments were performed between 12 and 7 p.m. with age- and size-matched subject and stimulus fish. Briefly, fish were reared in groups of 50 until 20–22 dpf, a period that can be considered as corresponding to adolescence (puberty) in humans due to the intense growth and transition from sexual immaturity to

maturity that zebrafish undergo within 9–51 dpf (42). Individual fish were then placed in the center of a U-shaped choice chamber. The final third of each arm of the U-shape was separated from the rest of the apparatus by a glass partition. Fish were allowed to explore the apparatus for 30 min. During the next 15 min, three conspecific fish were added to one of the partitioned areas and the time the test fish spent on each side of the apparatus was recorded. Twelve individual fish were tested simultaneously in two DanioVision Observation Chambers (Noldus Information Technology, Wageningen, The Netherlands). Swimming activity and position within the arena were recorded using Ethovision XT software (Noldus Information Technology, Wageningen, The Netherlands) and the data were output in 15-min time bins. To assess social behavior two measures were calculated: Social Preference Index (SPI), as previously described (41), and Correlation Index ( $r$ ), which assesses fish predisposition to socialize: [ $r = \text{SPI}_{\text{ExperimentalPhase}} - \text{SPI}_{\text{AcclimationPeriod}}$ ]. The Correlation Index was also used as a measure of exploratory/bold behavior—bold fish spend more time away from stimuli and therefore values of their Correlation Index are positive. The percentage of individuals with a positive Correlation Index is interpreted as the percentage of fish displaying exploratory/bold behavior.

### Circadian Rhythm

Developmentally exposed larvae were raised in a dark incubator without a 14:10 light:dark cycle. Following the end of exposure, 5 dpf larvae in the absence of the drug were individually placed in a 96-well plate, pseudo-randomized by treatment, and left in the light for 5 h. The plate was then moved to a DanioVision Observational Chamber (Noldus Information Technology, Wageningen, The Netherlands) where fish movement was recorded over 59 h under different light conditions: 3 h light; 54 h dark; 2 h light. Distance traveled by larvae during the assay was recorded using Ethovision XT software (Noldus Information Technology, Wageningen, The Netherlands) and the data were output in 1-min time bins for analysis. Periodicity was assessed using the R package *DiscoRhythm* (43).

### Response to Dusk/Dawn

Developmentally exposed larvae were raised in a dark incubator without a 14:10 light:dark cycle. Following the end of exposure, 5 dpf larvae in the absence of the drug were individually placed in a 96-well plate, pseudo-randomized by treatment, and allowed to acclimate in the light for 30 min. The plate was then moved to a DanioVision Observational Chamber (Noldus Information Technology, Wageningen, The Netherlands) where fish movement was recorded over 16.5 h under different light conditions: 3 h light; 46 min gradual dusk; 10 h dark; 46 min gradual dawn; 2 h light. During gradual dusk, light intensity was decreased by 5% every 2 min until 5% intensity was reached and then every 2 min by 1% until the light went off. During gradual dawn, light intensity was increased every 2 min by 1% until 5% intensity was reached and then by 5% until 100% intensity was reached. Distance traveled by larvae during the assay was recorded using Ethovision XT software (Noldus Information

Technology, Wageningen, The Netherlands) and the data were output in 1-min time bins for analysis.

### Data Analysis

For analysis and visualization of behavioral data R version 4.0.5 (44) and RStudio version 1.4.1106 (45) were used. Data analysis was performed as previously described (40, 46) with slight changes. For FLD, four subsets of the data were created and analyzed separately: baseline, light and dark periods and startle response. All the periods were fitted to a linear mixed model with the mean distance traveled as a response variable, condition as a fixed effect and fish ID as a random effect. During alternating light and dark periods larvae movement increases in light over time. To explore this behavior, linear models of light periods were fitted using distance traveled as a response variable, the interaction between condition and time as an independent variable and fish ID as a random effect. The  $\beta$  coefficient in light period models represents the increase in distance traveled over time and can be interpreted as the larval “recovery rate.” To explore anxiety-related responses to light, startle response was calculated as the distance moved during the first 20 s following light transition divided by the mean distance moved during the 1-min light event. The duration of the startle response was taken as 20 s following the transition from light to dark, as after this time all conditions started to recover from the initial startle response. Distance moved during the 1-min light period and startle response was calculated separately for each fish to account for differences in locomotion. This proportion was analyzed using the R package “betareg” (47), with the proportion of startle response as a response variable and condition as an explanatory variable.

For the response to acoustic startle, the data were divided into two parts—baseline period and response to startle stimuli. The baseline period was analyzed as described above. The response to startle stimuli was analyzed by implementing two approaches. For both, each stimulus (tap) event was defined as a two second event. In the first approach, the slope of habituation to startle stimuli was calculated by fitting a linear mixed model using distance traveled as a response variable, the interaction between condition and tap event as an independent variable and fish ID as a random effect. Then, significant fixed effects were identified using a chi-squared test and, when significant differences were established, *post-hoc* Tukey tests were used to further characterize the effects. In the second approach, a response/non-response status was defined for each fish. The threshold for response status was defined as the mean distance moved per second during the basal period plus two standard deviations (SD) of the mean. As there were significant differences in basal locomotion, thresholds were calculated separately for each condition. For each tap event, each fish was assigned as being a “responder” if it moved more than the threshold during the tap event or as a “non-responder” if it did not. Beta regression was modeled with the percentage of fish responding to a stimulus as a response variable and the interaction between tap event number and condition as an explanatory variable. Then, likelihood ratio tests for nested regression models were performed to assess if the interaction

between the tap event number and condition was a significant predictor of individual responsiveness.

Linear mixed models were calculated using the R package lme4 (48) and significant fixed effects were identified using a chi-squared test. To further characterize the effects, where significant differences were established, *post hoc* Tukey tests were conducted using the R package “multcomp” (49).

## RNA-Seq Sample Collection and Preparation

At the end of the exposure period (1–5 dpf), larvae were collected as six pools of seven embryos per condition for RNA extraction to minimize any differences due to biological variance. A previously described protocol for single embryo RNA extraction (50) was optimized for use with pools of zebrafish larvae. Samples were lysed in 110  $\mu$ l RLT buffer (Qiagen) containing 1.1  $\mu$ l of 14.3 M  $\beta$ -mercaptoethanol (Sigma). The lysate was allowed to bind to 450  $\mu$ l of Agencourt AMPure XP beads (Beckman Coulter) for 15 min. The tubes were left on a magnet (Invitrogen) until the solutions cleared and the supernatant was removed without disturbing the beads. Whilst still on the magnet, beads were washed three times with 70% ethanol and allowed to dry for 20 min. Total nucleic acid was eluted from the beads following the manufacturer's instructions and treated with DNase I (NEB, Catalog number M0303L). RNA was quantified using a NanoDrop (Thermo Scientific NanoDrop One Microvolume UV-Vis Spectrophotometer), RNA integrity numbers were checked using a Bioanalyzer (2100 Bioanalyzer System) and sequencing libraries were made using the Illumina TruSeq Stranded mRNA Sample Prep Kit.

## RNA Sequencing and Analysis

Libraries were pooled and sequenced on one lane of NovaSeq SP PE50 in 54 Gbp single-end mode (between 16 and 24 million reads per sample). RNA-seq data have been deposited in the ArrayExpress database at EMBL-EBI ([www.ebi.ac.uk/arrayexpress](http://www.ebi.ac.uk/arrayexpress)) under accession number E-MTAB-11086. Sequencing data were assessed using FastQC and aligned to the GRCz11 reference genome using STAR (51). Two samples were excluded from data analysis after QC and visual inspection of a Principal Component Analysis: one control sample had a poor RNA integrity number and was degraded and one nicotine sample did not cluster with the rest of the samples.

Read counts per gene were generated by STAR and used as input for differential expression analysis using the R package DESeq2 (52). The following model was used for DESeq2: ~Treatment, modeling counts as a function of the drug treatment. Genes with an adjusted *p*-value of <0.05 were considered to be differentially expressed. Gene sets were analyzed for GO enrichment using topGO.

For analysis of gene expression changes and visualization of data, R version 4.0.5 (44) and RStudio version 1.4.1106 (45) were used. The following packages were utilized: tidyverse (53) for data manipulation; DESeq2 (52), ggfortify (54) and ggplot2 (55) for principal component analysis (PCA); GOplot (56) and VennDiagram (57) for analysis of overlapping gene expression

changes; pheatmap (58) for generating heatmaps; ggplot2 and ggrepel (59) for other plots, including the volcano plots.

## Whole-Mount mRNA *in situ* Hybridization

DIG-labeled RNA probes were generated from cDNA libraries (SuperScriptR IV Reverse Transcriptase, Invitrogen) covering stages of development where genes of interest are expressed. PCR was performed with site-specific primers containing a flanking T7 promoter sequence to produce DNA templates. Then, DIG-labeled RNA probes were generated by enabling *in vitro* transcription using T7 RNA polymerase (Roche). Oligonucleotide sequences for the primers can be found in **Supplementary Table 1**.

Larvae were fixed in 4% PFA (in PBS) at 4°C overnight and progressively dehydrated in ascending concentrations of ethanol (25, 50, 75, and 100%) before being kept in 100% methanol at –20°C until needed. We optimized previously described ISH protocols in zebrafish (60, 61) for 5 dpf larvae and for transcripts of interest. Larvae were incubated for 1 h at room temperature in ethanol/xylol solution (1:1 vol/vol) and then progressively rehydrated in descending concentrations of ethanol (90, 75, 50, 25% and then H<sub>2</sub>O). Eighty percentage acetone treatment at –20°C for 30 min was used for permeabilization followed by bleaching for 1 h in 6% H<sub>2</sub>O<sub>2</sub>. Pre-hybridization was performed at 65°C for 4 h, followed by extended hybridization of approximately 60 h in 50–100 ng/ml of probe at 65°C. Following hybridization, washed larvae were incubated in blocking solution (10% sheep serum diluted in TBST, TBS containing 0.1% Tween20) for 4 h at room temperature and then in alkaline phosphatase anti-DIG antibody (1:2,000) at 4°C overnight.

To remove non-specifically bound antibodies, extended periods of washings (two overnights in TBST) were performed and the larvae were stained using 1 ml of BM Purple. The reaction was stopped when the desired intensity was reached by washing the larvae in PBST (PBS containing 0.1% Tween20) and then in ascending concentrations of ethanol (25, 50, and 70%) to increase contrast. A camera set up on a dissecting microscope (Leica MZ9.5 Stereozoom) with a white background and white-light illumination from the top was used for imaging.

## Quantitative Real Time PCR

Following the end of drug exposure (1–5 dpf), larvae were raised in freshwater in the absence of a drug until 7 or 21 dpf. Samples for qPCR analysis were collected as 10 pools of 5 larvae (at 7 dpf), or 10 pools of 3 heads (at 21 dpf) for each treatment. Samples were kept in RNAlater (Thermo Scientific) until use. RNA was extracted using TRIzol reagent following the protocol provided by the manufacturer and described previously (62). RNA yield and quality were determined using a Thermo NanoDrop 2000 (ThermoFisher). Following the treatment of RNA extracts with DNase I (New England Biolabs), the cDNA libraries were created using the ProtoScript II First Strand cDNA Synthesis Kit (New England Biolabs) as suggested by the manufacturer and described previously (62). Gene expression levels were quantified using the LightCycler 480 qPCR system (Roche) based on our previously published MIQE-compliant (63) protocols (64, 65). mRNA expression levels were checked for

six circadian rhythm associated genes that were differentially expressed in RNA-seq analysis: *cry1a*, *per2*, *per1a*, *cry3b*, *cry5*, and *arntl2*. Reference housekeeping genes  *$\beta$ -actin* and *18s* were chosen based on previous studies (66). Primer sequences for the genes can be found in **Supplementary Table 2**.

## RESULTS

### Forced Light/Dark Transition: Drug Exposure Affects Larval Locomotion

First, we assessed locomotion and anxiety-like behavior in control- and drug-exposed larvae using a forced light-dark (FLD) transition assay consisting of 10 min in the dark (baseline period) followed by 10 min light and 10 min in the dark. At 5 dpf in the presence of the drug, exposure to 25  $\mu$ M amphetamine and 5  $\mu$ M nicotine resulted in significant changes in basal locomotion when compared to controls ( $p < 0.001$ ;  $p = 0.0396$ , respectively) such that treated fish moved less. No significant changes were observed for oxycodone-exposed fish in the baseline period. These changes in locomotion were prevalent for amphetamine- and nicotine-treated fish throughout the duration of the assay (light period:  $p < 0.001$ ;  $p < 0.001$ ; dark period:  $p < 0.001$ ;  $p = 0.0031$ , respectively). Additionally, oxycodone-treated fish moved less than controls during the 10 min light period ( $p = 0.0033$ ).

In response to the transition from dark to light, unexposed control fish displayed an initial period of freezing/reduced movement that gradually increased toward baseline levels over the 10 min period in the light. We assessed these changes in locomotion during the light period measured as the slope from min 10 to 20. There were significant differences in the rate of recovery during the light period, where nicotine-treated fish showed slower recovery than untreated fish ( $F = 6.70e-06$ ,  $p = 0.0002$ ).

We also assessed anxiety-like behavior in response to a short 1 min exposure to light followed by 5 min in the dark. Here, on transition from light to dark, unexposed fish exhibited an initial startle response seen as a rapid increase in movement that gradually decreased in darkness. The startle response of both amphetamine- and nicotine-treated fish was significantly smaller than controls ( $p = 0.0004$ ;  $p = 0.0190$ , respectively). We assessed movement and slope of recovery during the 5 min dark period following 1 min light exposure, in accordance with previously published protocols (38). There was a significant difference in distance moved, where amphetamine-treated fish moved less than controls ( $p < 0.001$ ). Although oxycodone-treated fish showed reduced locomotion, this did not reach significance ( $p = 0.0697$ ). We observed differences in the rate of recovery during this time, such that all treated fish recovered more quickly than controls (amphetamine-treated:  $F = -2.96e-05$ ,  $p < 0.0001$ ; nicotine-treated:  $F = -2.00e-05$ ,  $p < 0.0001$ ; oxycodone-treated:  $F = -1.15e-05$ ,  $p = 0.0189$ ) (**Figures 1A,B**).

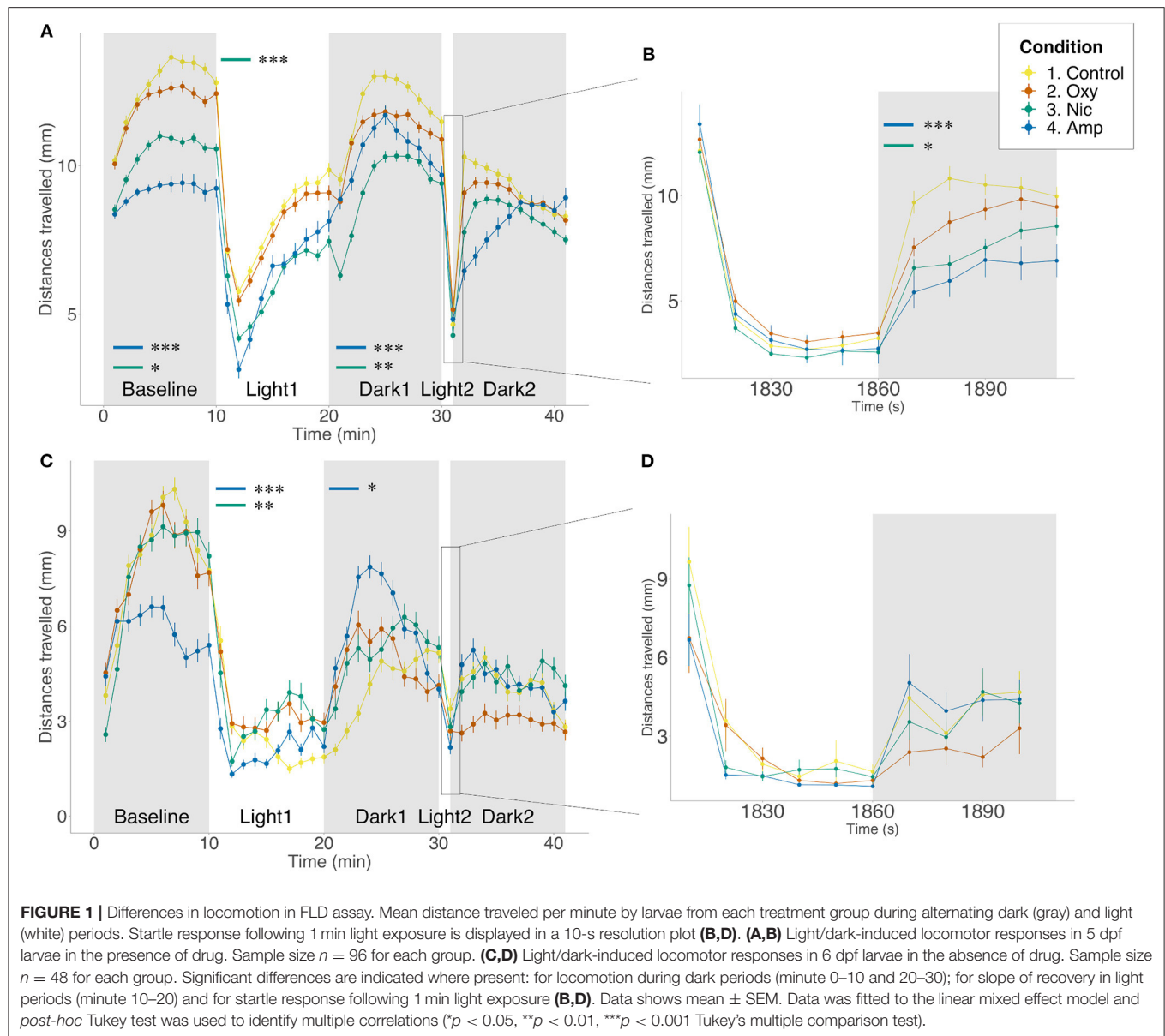
We repeated the FLD assays at 6 dpf, 24 h after the end of exposure. We found no significant differences between the conditions in basal locomotion or in the light period. During the light period, amphetamine- and nicotine-treated fish showed faster rates of recovery than untreated fish ( $F = -1.20e-06$ ,  $p$

$< 0.0001$ ;  $F = -5.97e-07$ ,  $p = 0.0014$ , respectively). There was a significant difference in locomotion during the dark period, where amphetamine-treated fish moved more than controls ( $p = 0.0168$ ). There were no significant differences in behavior following the short exposure to light, either in startle response or the following recovery (**Figures 1C,D**).

Additionally, to determine whether 1–5 dpf drug exposure may have affected the development of pathways involved in the control of behavior, we compared FLD responses in the presence of the drugs following developmental exposure with responses following acute (60 min) drug exposure prior to, and during, the assay. Qualitatively similar results were seen for the majority of measures (see **Supplementary Table 3; Supplementary Figure 1**). However, acute exposure to oxycodone significantly reduced basal locomotion compared to both control ( $p = 0.0025$ ) and larvae developmentally exposed to oxycodone ( $p = 0.0033$ ). Differences in movement between acute and developmental exposure were persistent in light and dark periods ( $p < 0.0001$ ,  $p = 0.0421$ , respectively). However, there was no difference in locomotion between either acutely or developmentally oxycodone-treated larvae and controls in light and dark periods. Similarly to oxycodone-treated fish, although both acute and developmental exposure to amphetamine significantly reduced basal locomotion relative to control ( $p < 0.0001$  for both), significantly greater reduction in locomotion was seen following acute rather than developmental exposure ( $p = 0.0468$ ). Differences in movement compared to controls were persistent in light and dark periods for acute exposure ( $p < 0.0001$ ,  $p = 0.0053$ , respectively) but only in the light period for developmental exposure ( $p = 0.0278$ ). No differences in locomotion were observed for nicotine-treated fish at any stage of the assay.

All treated groups showed faster than control rates of recovery during the light period ( $p < 0.0001$  for all). There was also an effect of length of exposure, where oxycodone developmentally exposed fish recovered more slowly than acutely exposed larvae ( $p = 0.0513$ ), but the opposite could be seen following nicotine exposure, where developmentally exposed larvae recovered more quickly ( $p = 0.0468$ ).

There was no significant difference in startle response magnitude following 1 min light exposure for any treated fish. However, in the dark period following short light exposure, fish acutely exposed to oxycodone ( $p = 0.0125$ ), and acutely and developmentally exposed to amphetamine, move significantly less than controls ( $p < 0.0001$ ,  $p = 0.0309$ , respectively). Acute oxycodone treatment results in a decrease in movement compared to developmental oxycodone exposure ( $p = 0.0031$ ). Additionally, when looking at rate of recovery during the dark period, amphetamine-treated groups recover significantly faster than controls (acute:  $p = 0.0246$ ; developmental:  $p < 0.0001$ ), in contrast to fish acutely exposed to nicotine, which recover more slowly than controls ( $p = 0.0008$ ). Developmental exposure to these two drugs leads to significantly faster recovery when compared to acute exposure (amphetamine:  $p = 0.0001$ ; nicotine:  $p < 0.0001$ ). There was no difference in recovery of oxycodone-treated animals (**Supplementary Figure 1**).



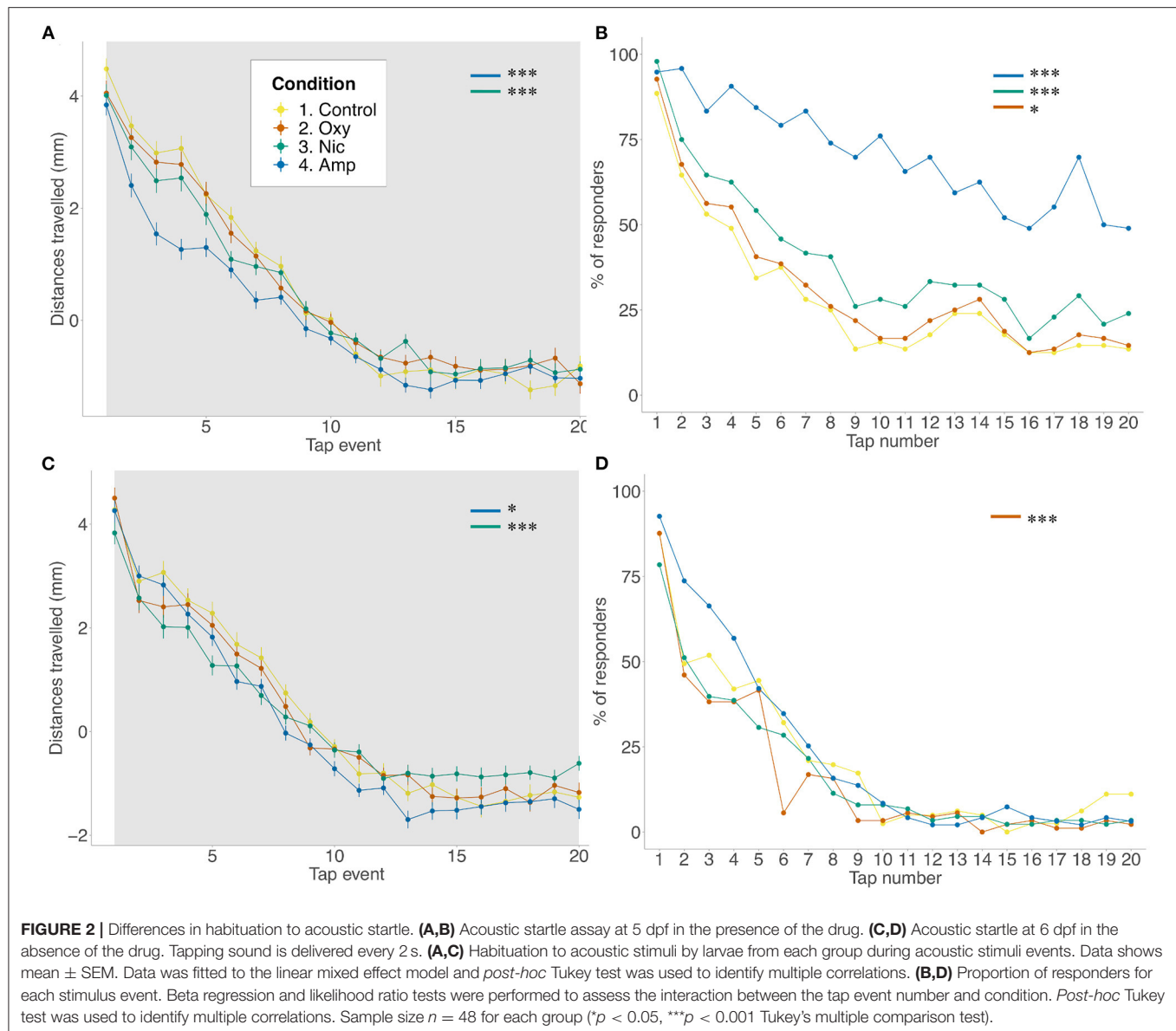
## Drug Exposure Affects Habituation to Acoustic Startle

As response to acoustic startle is also used as a measure of anxiety (67) and habituation to acoustic startle is sensitive to modulation by drugs of abuse, including nicotine, amphetamine and opioids, we assessed the impact of developmental exposure on acoustic startle in larval fish.

As seen for FLD, there was a reduction in distance traveled in the basal period for amphetamine- and nicotine-treated fish ( $p < 0.001$ ;  $p < 0.001$ , respectively) compared to controls, but not for oxycodone-treated fish. The same changes were seen across tap stimuli (amphetamine:  $p < 0.001$ ; nicotine:  $p < 0.001$ ) There was a significant effect of treatment on rates of habituation as assessed by distance traveled such that amphetamine and nicotine fish habituated more slowly than controls ( $F = 0.042538$ ,  $p < 0.0001$ ;

$F = 0.018232$ ,  $p < 0.0001$ , respectively) (**Figure 2A**). A similar effect of treatment was seen when looking at the proportion of responders analysis. Due to observed differences in locomotion, for the number of responders analysis, habituation to the acoustic stimuli was quantified as the proportion of fish moving more than  $2 \times \text{SD}$  above the mean, condition-specific, baseline threshold values. Using the proportion of responders criteria, 88% of control animals responded to the first tap and 13% to the last in line with the habituation response paradigm (40). Treated animals showed significantly reduced habituation such that more treated individuals than control individuals responded to the last tap stimuli (amphetamine- and nicotine-treated fish:  $p < 0.001$ ; oxycodone-treated fish:  $p = 0.0163$ ) (**Figure 2B**).

At 6 dpf, following 24 h of withdrawal, there was a significant effect of treatment on movement during the baseline period



such that amphetamine-, nicotine- and oxycodone-treated fish moved less than controls (amphetamine-treated fish:  $p = 0.0083$ ; nicotine- and oxycodone-treated fish:  $p < 0.001$ ) (**Figure 2C**). However, during the tap events only nicotine treatment resulted in decreased locomotion ( $p = 0.0081$ ). Following exposure to acoustic stimuli, there was a significant effect of condition on rates of habituation such that amphetamine and nicotine fish habituated faster than controls ( $F = -0.012488$ ,  $p = 0.0179$ ;  $F = -0.029279$ ,  $p < 0.0001$ , respectively). There was also a significant effect of condition on proportion of responders for oxycodone-treated fish ( $F = 0.0480$ ,  $p = 0.0002$ ), where exposed larvae habituated faster than unexposed fish (**Figure 2D**).

## Developmentally Exposed Fish Display Less Exploratory/Bold Behavior

Next, we tested whether drug exposure affected social and exploratory/bold behavior using an established sociability assay (41), as these endophenotypes are associated with psychiatric disorders (1).

There were no differences in time spent with conspecifics between exposed and unexposed fish (**Supplementary Figure 2**). There was a non-significant trend for a reduction in the number of exploratory/bold individuals following developmental exposure to drugs ( $p = 0.0846$ ). Control fish had the highest percentage of exploratory/bold individuals at 59.72%,

with 46.48% for amphetamine, 50% for nicotine and 51.39% for oxycodone.

Taken together our behavioral experiments show a clear effect of drug exposure on behavior which are consistent with mammalian systems. Our results show evidence of possible adaptation to the presence of the drug: we see differences in response following acute vs. chronic drug exposure as well as following acute withdrawal.

## RNA Sequencing Shows Common and Drug-Specific Changes in Gene Expression in Response to Developmental Exposures

To investigate the changes in transcriptional profiles and biological pathways of drug-treated larvae, we performed RNA-seq on wild-type zebrafish larvae exposed to 5  $\mu$ M nicotine, 1.14  $\mu$ M oxycodone and 25  $\mu$ M amphetamine from 1 to 5 dpf, along with unexposed controls (Figure 3A). Principal component analysis (PCA) showed, as expected, that the samples that passed all quality control checks cluster according to the treatment (Figure 3B).

Differential gene expression analysis was carried out with an adjusted *p*-value threshold of 0.05. Developmental exposure to amphetamine, oxycodone and nicotine caused differential expression of 381, 341, and 394 genes, respectively (Figure 3C). The distribution of differentially expressed genes (DEGs) for each drug treatment is shown in Figures 3D–F.

Thirty five genes are differentially expressed across all three treatments; seven of these overlapping DEGs are upregulated and 11 are downregulated across all drug treatments, whereas 17 genes are downregulated in amphetamine and oxycodone but upregulated in nicotine treatment (Figures 4A–C). There is a larger overlap of DEGs between amphetamine and oxycodone treatments than between amphetamine and nicotine treatments which is surprising given both amphetamine and nicotine are stimulants and oxycodone is an opioid. Amphetamine and oxycodone treatments share a total of 120 common DEGs, 47 of which are upregulated and 73 of which are downregulated in both sets of treatments (Figure 4A). Amphetamine and oxycodone samples also cluster together in the PCA (Figure 3B), suggesting their expression profiles are more similar to each other than to nicotine.

Among the common DEGs in response to all developmental drug exposures are genes involved in development, regulation of the circadian rhythm and the immune response. The hypoxia inducible factor, *hif1a* (orthologous to mammalian HIF3A), which is reported to play key roles in developmental morphogenesis (68), is upregulated across all three drug exposures. Two central circadian clock genes, *per2*, period circadian clock 2, and *cry1a*, cryptochrome circadian regulator 1a, are also upregulated across all treatments, suggesting an alteration to the regulation of circadian rhythm.

A set of brain-expressed genes including *fosab* and *junbb* (orthologous to mammalian c-FOS and JUNB), which are implicated in addiction (69, 70), and *npas4a* (orthologous to mammalian NPAS4), which is implicated in reward learning and memory processes in rodents (71), are also downregulated by

all three drugs. In addition, early growth response genes *egr1* and *egr4* (EGR1 and EGR4 in mammals), which are involved in numerous biological processes including eye morphogenesis (72), brain development (73) and circadian regulation of gene expression (74), show downregulation across all drug exposures.

Among the group of DEGs which are downregulated in amphetamine and oxycodone but upregulated in nicotine treatment are immune function and metabolism-related genes. For example, *ccl20a.3* (orthologous to mammalian CCL20), which is involved in immune response and leukocyte chemotaxis, is downregulated in amphetamine and oxycodone but upregulated in nicotine treatment. Likewise, *noxo1a*, NADPH oxidase organizer 1a (orthologous to mammalian NOXO1), and *nos2*, nitric oxide synthase 2a (orthologous to mammalian NOS2), show the same trend in differential expression.

## Gene Ontology Term Enrichment: Enrichment for Both Overlapping and Distinct Biological Processes

In order to identify the biological pathways that are affected by developmental drug exposures, we analyzed enriched Gene Ontology (GO) biological process terms in differentially expressed gene lists. As expected, this analysis revealed enrichment of both common and drug-specific biological processes, suggesting an overlap of pathways that are affected across treatments as well as drug-specific changes in cellular pathways. A summary of enriched GO biological process terms can be found in Figure 5A, which is split into those enriched by upregulated genes and downregulated genes in Figure 5B.

Across all developmental drug exposures, there is an enrichment for terms related to development of anatomical structures, such as the notochord (GO:0030903), retina (GO:0060041) and the lymphatic vessels (GO:0001945) (Figures 5A,B). These enrichments are driven by differential expression of genes involved in development and morphogenesis, such as *egr1*.

Multiple genes involved in the regulation of circadian rhythm are differentially expressed across all three drug exposures. Accordingly, there is an enrichment of GO terms related to the regulation of circadian rhythm (GO:0007623, GO:0042752, and GO:0032922) in amphetamine and oxycodone treatments. Two central circadian clock genes, *per2* and *cry1a*, are significantly upregulated across all three conditions and contribute to the enrichments of circadian terms in amphetamine and oxycodone treatments.

Enrichment of GO terms related to hypoxia (GO:0036293 and GO:0001666) are prominent in oxycodone and nicotine exposures. The hypoxia-inducible factor, *hif1a* (orthologous to mammalian HIF3A), which is reported to play important roles in developmental morphogenesis (68), is upregulated across all conditions and contributed to the enrichments in oxycodone and nicotine treatments.

Across all drug treatments, genes involved in cell death show differential expression and GO terms related to neuron death and apoptosis are enriched in amphetamine and oxycodone treatments (including GO:0070997, GO:0051402, GO:0043066 in

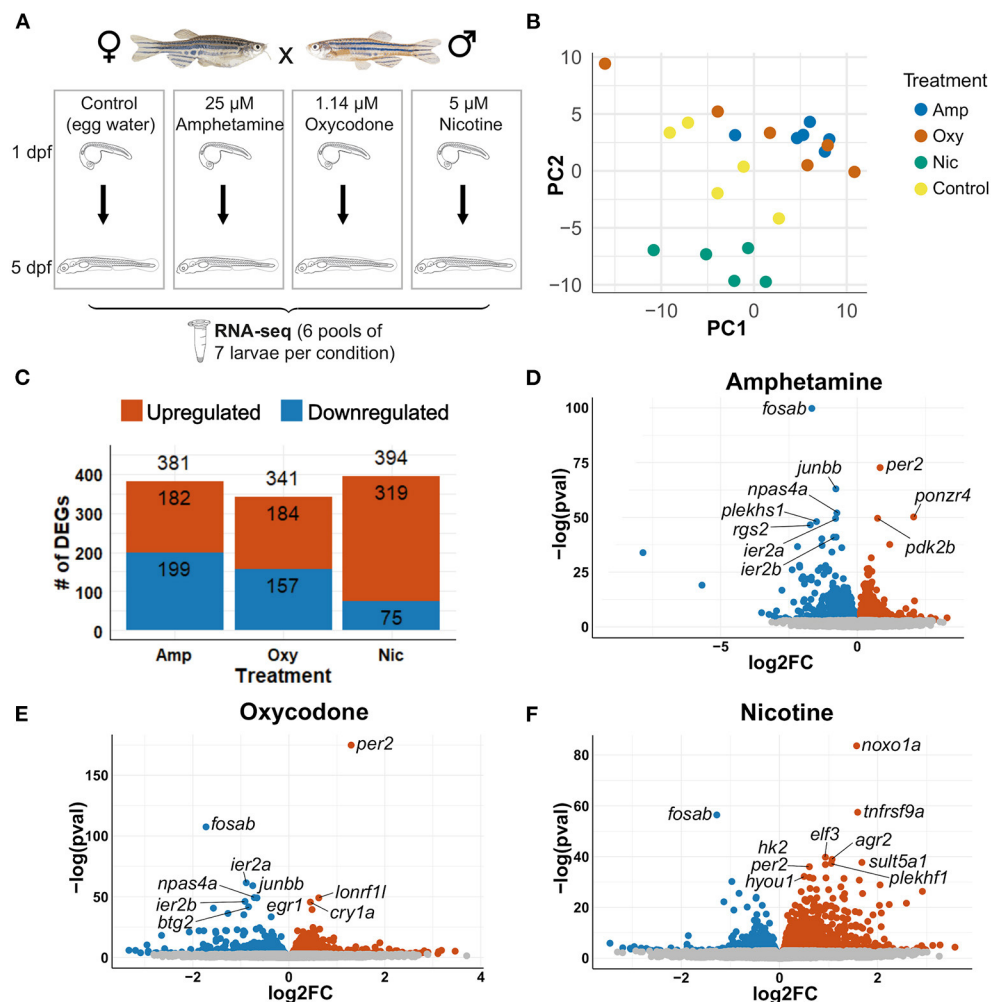


**FIGURE 3 |** Differential gene expression analysis. **(A)** Schematic of the experimental design. Zebrafish were exposed to nicotine, oxycodone and amphetamine or left untreated from 1 to 5 dpf before being collected in six pools of seven larvae per condition for RNA-seq. **(B)** PCA of samples that passed all quality control checks. Samples from each condition group together. Amphetamine and oxycodone samples are clustered more closely (and so have more similar expression profiles) than nicotine samples. **(C)** Bar chart showing the number of differentially expressed genes (DEGs) in each drug treatment. Upregulated genes are shown in red and downregulated genes are in blue. **(D–F)** Volcano plots showing the distribution of DEGs. Genes that are not significant (adjusted  $p$ -value  $\geq 0.05$ ) are in gray, significant genes (adjusted  $p$ -value  $< 0.05$ ) are in red if upregulated and in blue if downregulated. The top 10 DEGs by  $p$ -value are labeled in each plot.

amphetamine and GO:0006915 and GO:0008219 in oxycodone). In amphetamine and oxycodone exposures, genes involved in the regulation of apoptosis (*pycard* and *card14* in amphetamine and *pdc4b* and *niban2a* in oxycodone) are differentially expressed and drive these enrichments. Even though cell death terms are not enriched, there is a significant change in the expression level of caspases in nicotine treatments; the genes *casp3b*, *casp8*, *casp1*, and *casp9* (orthologous to mammalian caspases 3, 8, 1, and 9, respectively) are upregulated in nicotine treatments, suggesting an activation of both intrinsic and extrinsic apoptosis pathways.

Reflecting the larger overlap of differential gene expression between amphetamine and oxycodone exposures, there are some terms which are enriched in amphetamine and oxycodone, but not in nicotine treatments. For example, the term “response to

toxic substance” (GO:0009636) is enriched in amphetamine and oxycodone but not in nicotine.

It is noteworthy that some terms that are enriched across all conditions are not driven by the same changes in gene expression. For example, the term “inflammatory response” (GO:0006954) is enriched across all treatments. However, inflammatory genes driving this enrichment are downregulated in amphetamine and oxycodone treatments but upregulated in nicotine treatments (Figure 5B).

Enrichment of some GO terms are drug specific. For example, there is an enrichment for morphogenesis-related terms among upregulated genes in oxycodone treatments (Figure 5B), such as bone morphogenesis (GO:0060349), cartilage morphogenesis (GO:0060536) and chondrocyte differentiation (GO:0002062).

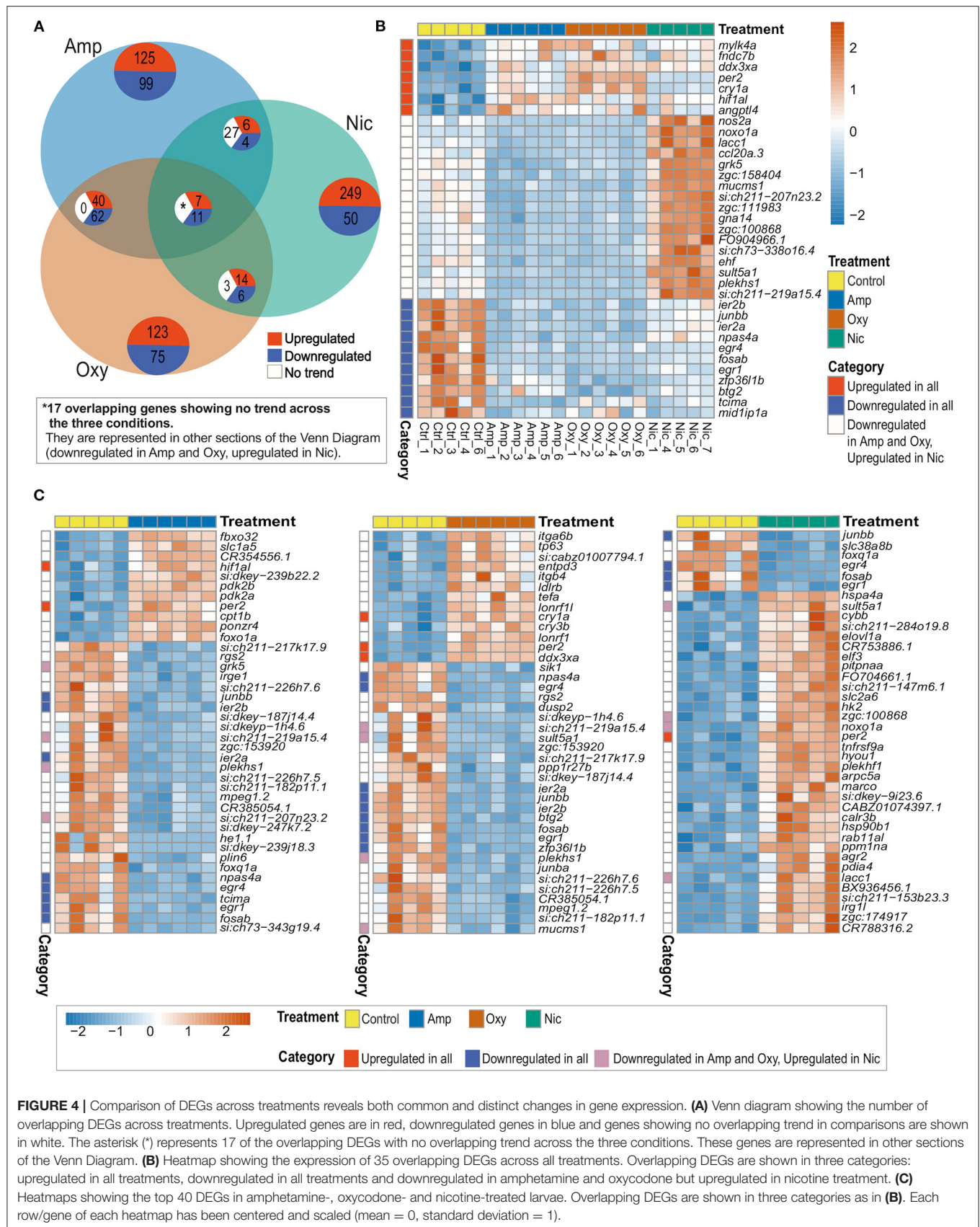




**FIGURE 5 |** Gene Ontology (GO) term enrichment analysis shows enrichment of both common and distinct biological process terms across treatments. **(A)** Bubble plot of the GO BP enrichment results across the three drug treatments. Individual enriched BP terms were aggregated to a parent term. For example, regulation of (Continued)

**FIGURE 5 |** circadian rhythm (GO:0042752), circadian rhythm (GO:0007623) and circadian behavior (GO:0048512) are all aggregated to the parent term circadian regulation of gene expression. The size of each circle represents the number of individual terms enriched for each parent term and they are colored by the smallest of the  $p$ -values ( $-\log_{10}$  scale). **(B)** Bar charts showing top 40 upregulated terms and top 40 downregulated terms (by  $p$ -value) for each drug treatment. Individual enriched BP terms were aggregated to a representative term and colored by the smallest of the  $p$ -values ( $-\log_{10}$  scale) as in **(A)**.

## Developmental Drug Exposures Affect Expression of Innate Immune Genes

Developmental exposures to all three drugs led to differential expression of multiple genes involved in the regulation of the immune system. Accordingly, GO term enrichment analysis shows enrichment of inflammation and immunity-related terms across all treatments. The term “inflammatory response” (GO:0006954) is enriched across all exposures (Figure 5B).

Drugs of abuse, including stimulants such as methamphetamine and cocaine, and opioids such as morphine, are reported to have immunomodulatory effects and increase susceptibility to infectious diseases (75–78). Our transcriptomic analysis showed a downregulation of genes involved in immune response and inflammation in amphetamine and oxycodone treatments. The genes *ccl20b* and *ccl20a.3* (both orthologous to mammalian CCL20) and *nos2a* (orthologous to mammalian NOS2) are significantly downregulated in both sets of treatments, leading to enrichment of the term “inflammatory response” (GO:0006954). The gene *irg1l* (orthologous to mammalian ACOD1) is also among the downregulated genes driving this enrichment in amphetamine. Several other genes, including *tnfsf10* and *cd180*, are also downregulated in amphetamine treatments and collectively lead to enrichment of the term “immune system process” (GO:0002376).

In contrast, pro-inflammatory immune genes such as *il1b*, *il6st*, *nos2a*, and *noxo1a* (orthologous to mammalian IL1B, IL6ST, NOS2, and NOXO1) are upregulated in nicotine treatments, suggesting an activation of the immune response. Accordingly, several terms including inflammatory response, activation of the immune response and defense response (GO:0006954, GO:0002253 and GO:0006952, respectively) are enriched by upregulated immune genes in nicotine treatments.

## Developmental Drug Exposures Lead to Region-Specific Differential Expression of Immediate-Early Genes

Our transcriptomic analysis shows that the IEGs *fosab*, *junbb*, *egr1* and *egr4* (orthologous to mammalian c-FOS, JUNB, EGR1 and EGR4, respectively) are significantly downregulated in response to developmental drug exposures (Figure 6A). These genes are associated with synaptic plasticity and they are implicated in brain development (73), memory consolidation (80), neurodegenerative diseases, addiction and other psychiatric disorders (81). Therefore, we were interested in investigating drug-induced changes to the spatial expression pattern of *fosab*, *junbb*, *egr1*, and *egr4* in zebrafish using whole-mount mRNA ISH staining.

We found that all four genes have overlapping expression patterns and are expressed in the forebrain (both telencephalic and diencephalic areas), in the midbrain (tectum and

tegmentum) and the hindbrain of untreated 5 dpf larvae (Figure 6B). The genes *egr1* and *egr4* are also expressed in the torus semicircularis of the midbrain and the retina is stained for *egr4*, *fosab* and *junbb* transcripts.

Reflecting the downregulation of transcripts seen in RNA-seq (Figure 6A), mRNA hybridization and staining intensity for all four transcripts is reduced across all neuroanatomical regions (Figure 6C; Supplementary Figure 3). Among other regions, we found a reduction in the expression of all four genes in the habenulae and the tegmentum, which are implicated in reward processing, addiction (82) and dementia (83), as well as the optic tectum. In particular, we found that the expression of *fosab* and *junbb* is diminished in the olfactory bulbs, a key area implicated in alcohol preference (84, 85), depression (86) and schizophrenia (87).

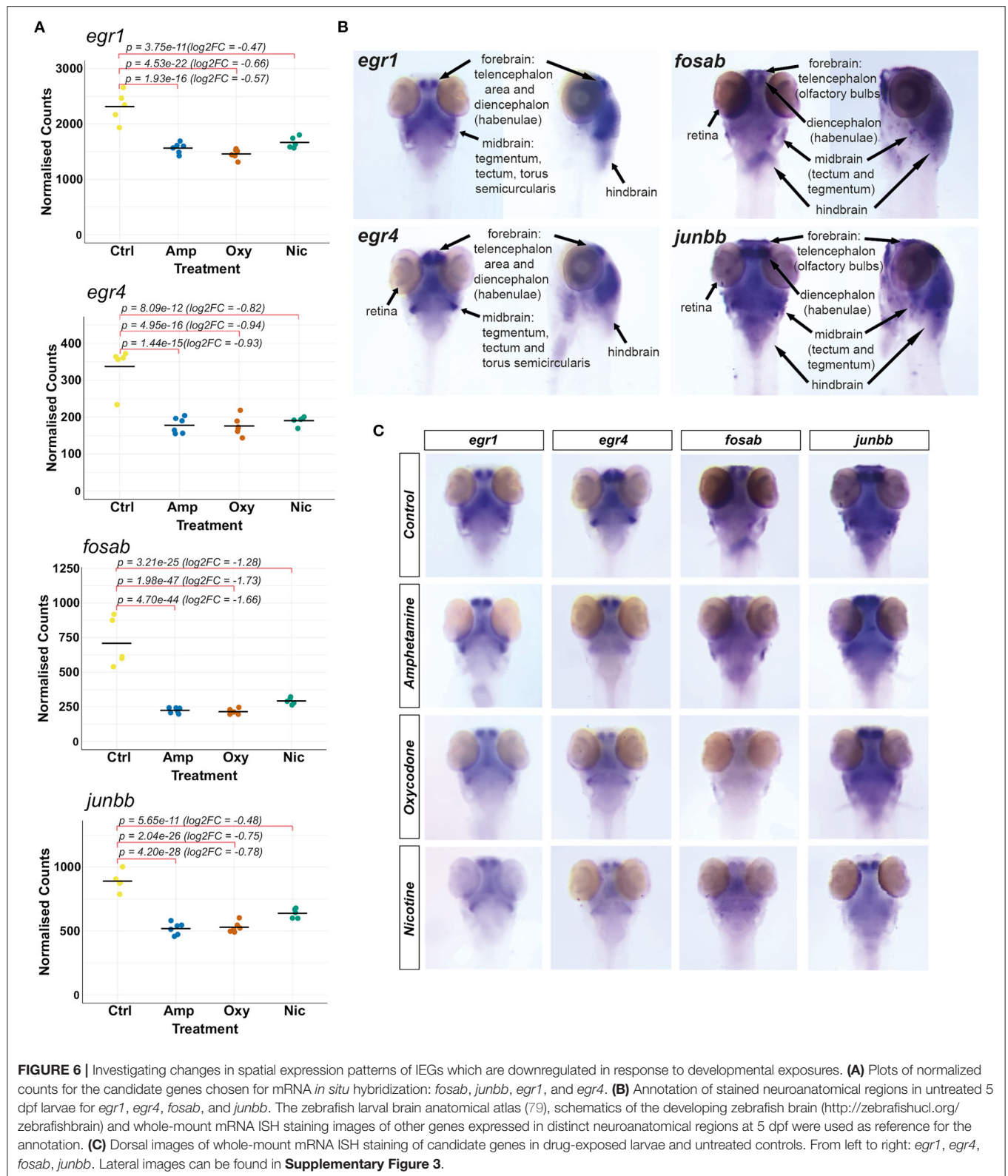
## Developmental Drug Exposures Lead to Differential Expression of Genes Involved in the Regulation of the Circadian Rhythm

Substance use has been reported to alter the circadian rhythm (88), which predisposes individuals to a variety of psychiatric conditions including depression (89, 90), bipolar disorder (91) and addiction (92–97). We found that developmental exposures to all three drugs led to differential expression of multiple genes involved in the regulation of circadian rhythm and related GO terms are enriched in amphetamine and oxycodone treatments (including GO:0007623, GO:0042752, and GO:0032922).

A total of eight genes involved in the regulation of circadian rhythm were differentially expressed, some of which are common whilst others are drug-specific (Figure 7A). Two central circadian clock regulators, *per2* and *cry1a*, are significantly upregulated (Figure 7B) while *egr1* and *egr4*, which are implicated in regulating some components of the circadian clock (74), are significantly downregulated across all treatments, suggesting an overlapping mechanism of circadian disruption. Significant downregulation of *per1a* and upregulation of *cry5* is specific to oxycodone exposures, while *cry3b* and *arntl2* are upregulated both in amphetamine and oxycodone but not in nicotine exposures.

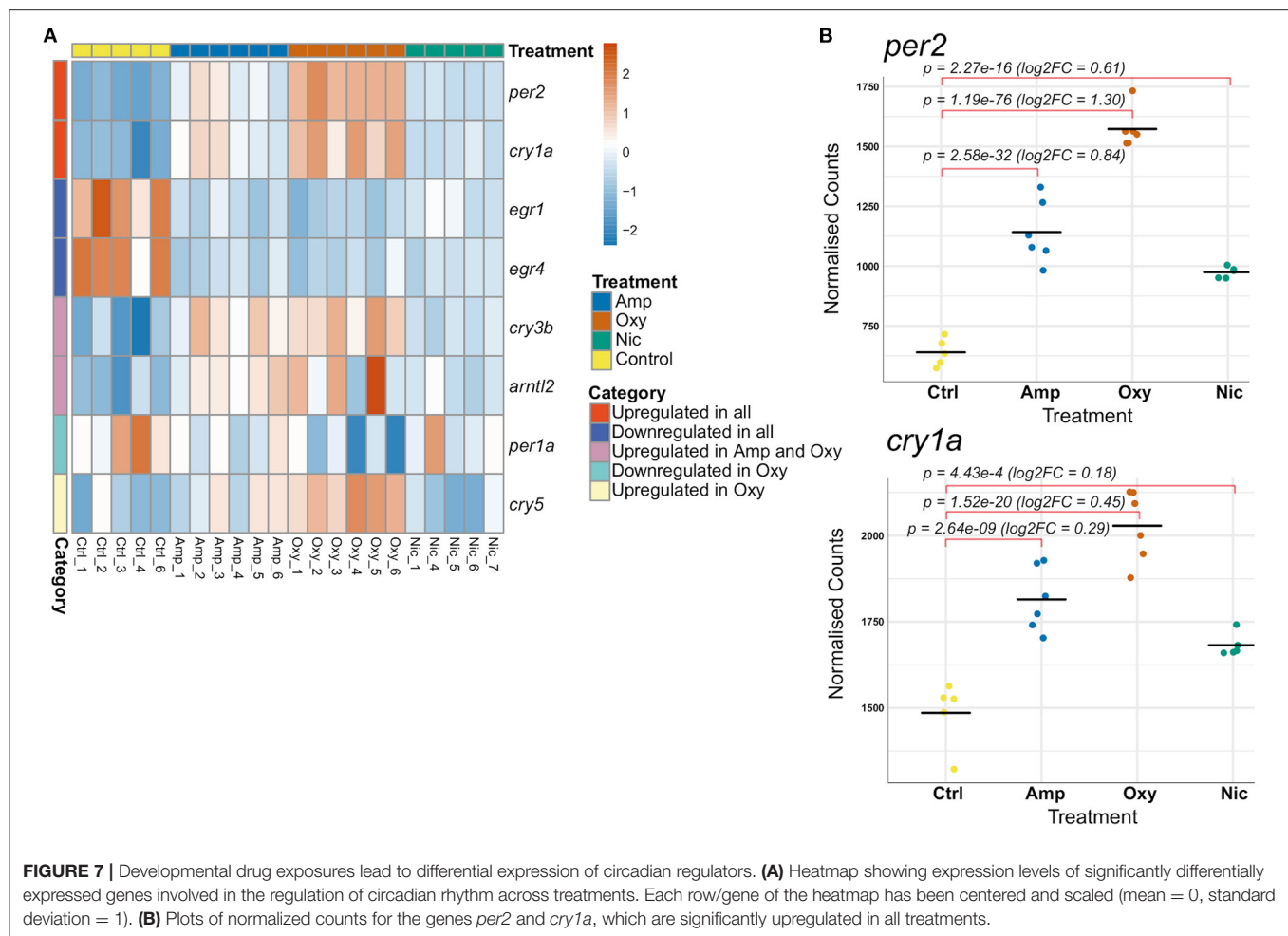
## Changes in Gene Expression Do Not Correlate With Changes in Circadian Rhythm

As RNA-seq analysis showed significant expression differences in genes involved in the circadian cycle, we decided to perform two behavioral assays to determine if changes in expression correlate with changes in behavior in the larvae. First, we looked for differences in the free running period in the dark. At 5–7 dpf, during 54 h in darkness, all groups of developmentally exposed fish moved significantly less than controls (amphetamine:  $p <$



0.001; nicotine:  $p = 0.00201$ ; oxycodone:  $p = 0.00105$ ), however no differences in periodicity were observed between exposed fish and controls (**Supplementary Figure 4**).

Additionally, we assessed responses to dusk and dawn in an assay with gradually changing light and dark periods. Nicotine- and amphetamine-treated fish moved significantly less in the 2-h



light period before dusk ( $p < 0.001$ ;  $p = 0.0022$ , respectively). Similar differences were observed in the 2-h dark period preceding the dawn, when all treated groups showed decreased locomotion compared to controls (amphetamine:  $p < 0.001$ ; nicotine:  $p = 0.0306$ ; oxycodone:  $p = 0.0054$ ). Next, we looked at locomotion and the slope of response during the 46 min of gradual dusk and dawn. All groups of treated fish moved less than untreated fish ( $p < 0.001$  for all) during the dusk period. However, the rate of recovery was significantly slower for only amphetamine-treated fish ( $F = 2.26e-05$ ,  $p < 0.001$ ). During dawn, fish exposed to amphetamine showed significantly reduced locomotion compared to controls ( $p < 0.001$ ) and nicotine-treated fish showed a significantly reduced rate of change of response to increasing light compared to controls ( $F = 8.77e-05$ ,  $p < 0.001$ ) (Supplementary Figure 5). No other comparisons were significant.

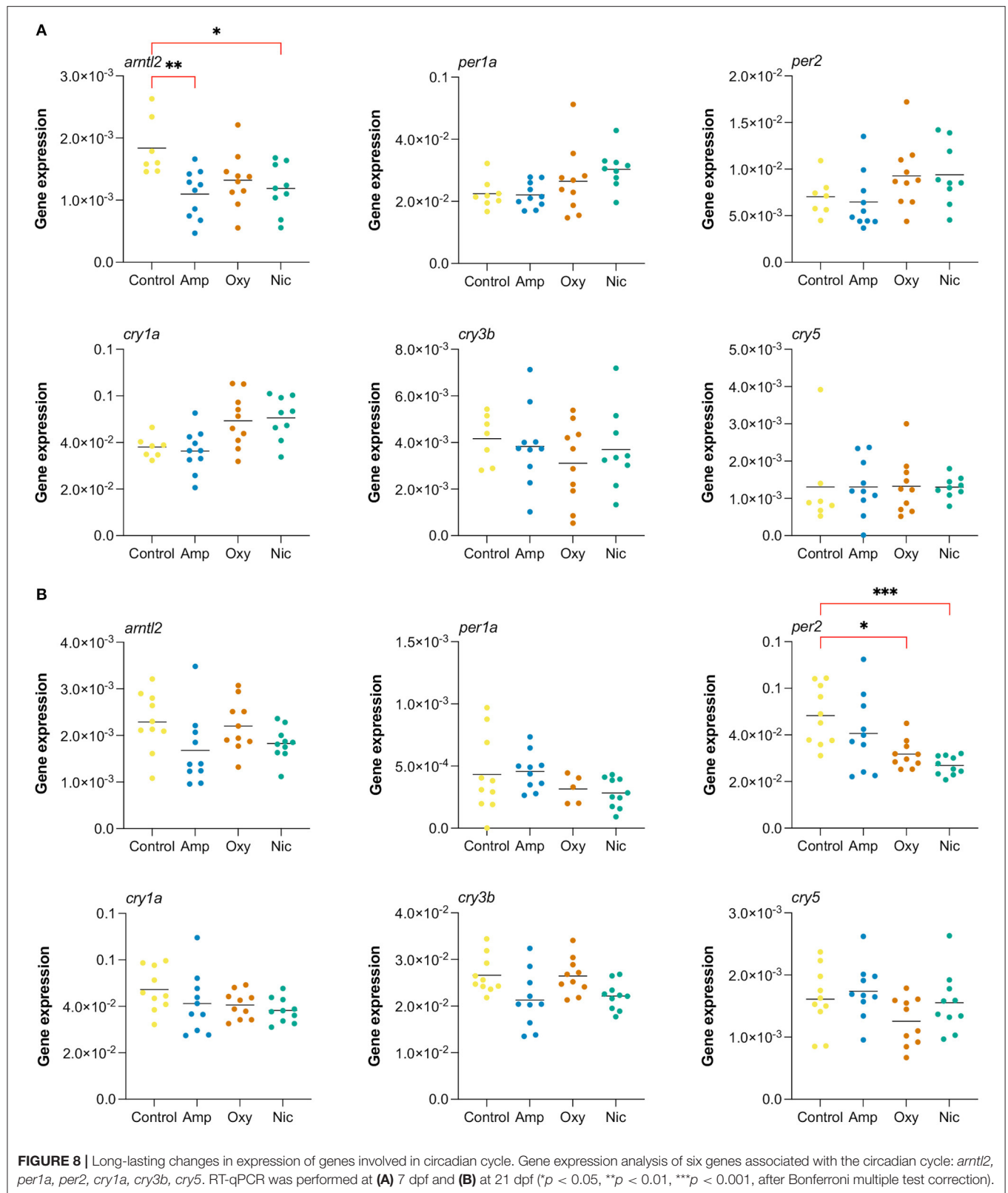
## RT-qPCR Shows a Long-Lasting Impact in Gene Expression of Circadian Rhythm Regulators

Alterations in the circadian rhythm are reported to predispose individuals to addiction and other psychiatric conditions (89–97) and are associated with relapse in recovering addicts (98, 99).

Therefore, we were interested in investigating the persistence of changes in expression of circadian rhythm genes following cessation of substance exposure.

In order to investigate changes in gene expression at later stages of development, we raised developmentally exposed larvae to 7 and 21 dpf stages in the absence of drugs and collected samples for RT-qPCR. We performed RT-qPCR on six circadian rhythm genes that were found to be differentially expressed at 5 dpf, both common, like *cry1a* and *per2*, and drug-specific, like *arntl2*, *per1a*, *cry3b*, and *cry5* (Figure 8).

We found that the gene *arntl2* was differentially expressed at 7 dpf, 2 days after cessation of exposure, in amphetamine- and nicotine-exposed fish. In contrast to the upregulation seen in RNA-seq at day 5, we found a downregulation of *arntl2* at 7 dpf in amphetamine- and nicotine-exposed fish which did not persist at 21 dpf. There were no differences in the expression of *arntl2* in oxycodone-treated fish at either time point. Additionally, we found that the gene *per2* is not differentially expressed at 7 dpf but is downregulated for nicotine- and oxycodone-treated fish at 21 dpf (contrary to the upregulation at 5 dpf), suggesting a long-term impact of developmental drug exposures on the expression of circadian rhythm genes.



## DISCUSSION

We modeled consistent drug usage during pregnancy by exposing wild-type zebrafish larvae to 25  $\mu$ M amphetamine, 5  $\mu$ M nicotine or 1.14  $\mu$ M oxycodone. To be sure drug exposure paradigms were sufficient to cause physiological effects we assessed the impact of drug exposure on larval behavior. We found differences in locomotion, response to FLD transition, and habituation to acoustic startle consistent with the published effects of these drugs in mammalian systems. Following a 5-day exposure, in the presence of the drugs we saw decreases in basal locomotion in FLD and acoustic startle assays for amphetamine- and nicotine-treated fish. In the FLD, all treated groups showed faster recovery in the light, and fish exposed to nicotine or amphetamine, but not to oxycodone, showed smaller startle responses. Additionally, we observed decreased rates of habituation to acoustic startle for all treated groups. These differences were not preserved upon withdrawal of the drug.

Transcriptional profiling of developmentally exposed larvae led to differential expression of over 300 genes for each drug exposure, with 35 shared DEGs across the three drugs, suggesting some commonality in the affected pathways, as well as drug-specific changes in gene expression. Accordingly, Gene Ontology (GO) term enrichment analysis revealed enrichment of common as well as drug-specific biological processes. Among the enriched biological process terms are ones related to development of anatomical structures, innate immunity, regulation of the circadian rhythm and cell death, reflecting the differential expression of multiple genes involved in these processes.

### Drug Exposure Led to Changes in Behavior Consistent With Responses in Mammalian Systems

We assessed the behavior of developmentally exposed fish in the presence of drugs and following a 24-h withdrawal period for evidence of conserved responses to drug exposure. We predicted that drug exposure in larval zebrafish will lead to changes in locomotion and behavior consistent with the effect of the drug in mammalian systems.

In the presence of a drug and following exposure from days 1 to 5 of development, as well as following 1 h of acute exposure, locomotion was decreased in amphetamine-treated fish. Although these results are in contrast with the increased locomotor effect of low dose amphetamine in adult rodents following chronic exposure and in the presence of the drug (100), amphetamine has a dose-dependent effect on locomotion such that low doses cause increased locomotion, and high doses a shift from increased locomotion to stereotypic behavior (101), suggesting that our selected concentration was in the high range for larval zebrafish. Similarly, 1–5 day exposure to nicotine led to a reduction in locomotion that may be explained by desensitization of nicotinic receptors (102) or, possibly, by disruption of motor neuron development; exposure to 15  $\mu$ M nicotine from 1 to 5 dpf was found to delay development of secondary motor neurons in zebrafish previously (103).

Although zebrafish larvae do not show the full complexity of behavior of adult animals, the FLD transition assay has been frequently used to assess anxiety-like behavior in both zebrafish and rodents (104, 105). We assessed effects of the presence of the drugs on FLD using 3 different measures: by looking at the slope of recovery during a 10-min light period; magnitude of the startle response following a short light exposure; and by rate of change in locomotion (slope) in the dark following a short light exposure. We found that nicotine-exposed animals recover more slowly over the 10-min light period, amphetamine- and nicotine-treated animals show a smaller startle response on light/dark transition following a short light exposure, and all exposed groups showed a decreased rate of recovery following a short 1-min light exposure. Although the magnitude of the “startle response” on light to dark transition is commonly used as a measure of anxiety-like behavior (38) where a reduction in distance traveled is taken as indicative of a reduced anxiety-like response, differences in baseline locomotion preclude this interpretation here. A reduced rate of change in locomotion following forced light transition is consistent with reduced rates of recovery that have been interpreted as increased anxiety-like behavior (46), and would be consistent with mammalian studies (106, 107), but again, differences in basal locomotion makes it difficult to draw conclusions here.

On withdrawal of each drug, no differences in basal locomotion were observed. For analysis of anxiety-related behavior, despite what looks like clear qualitative differences, no consistent differences in behavior were observed. However, we observed a lot of variability in all treatment groups which may reflect increased freezing and darting, an indicator of increased anxiety-like behavior in zebrafish (108, 109). Increased intra-condition variability could also explain the lack of significant differences in startle response. Adult studies have shown altered anxiety-like behavior upon exposure and withdrawal of drugs of abuse including ethanol and nicotine in fish as in mammals (110, 111). Developmental exposure and withdrawal from amphetamine, nicotine or opioids result in increased anxiety at later life stages in human and rodent studies (112–117). However, these studies looked at behavior at adult stages following exposure to drugs throughout the entire period of *in utero* development. As we did not examine behavior at adult stages, we are unable to directly relate our findings to previous data. Further, it is not clear how a 1–5 dpf exposure period relates to human gestation. Thus, differences in the exposure period may contribute to observed differences in response.

Although behavioral responses after 24 h of withdrawal following developmental exposures were not as marked as seen following exposure in adult zebrafish, behavioral responses in the presence of each drug following a 5-day exposure were significantly different from the response in the presence of acute drug exposure. Responses were qualitatively similar in that all acutely and developmentally exposed groups showed a faster rate of recovery in the light and no difference in startle response, and both amphetamine-treated groups showed faster recovery in the dark. However, acute exposure led to a significantly greater reduction for nicotine-treated fish in recovery to light and for amphetamine- and nicotine-treated fish in recovery to dark. A

significantly greater rate of recovery to light was observed for oxycodone acutely treated fish compared to developmentally exposed fish. Chronic exposure to a neurotransmitter is frequently associated with reduced sensitivity to subsequent exposures (118) as a result of desensitization, proteolytic cleavage or receptor downregulation. Thus, the observed differences in the effect of acute (1 h) vs. chronic (1–5 dpf) exposure to these drugs of abuse provide evidence of adaptation to the presence of drugs.

We used habituation to acoustic startle to assess sensorimotor gating, a behavior predictive of vulnerability to psychiatric disorders such as schizophrenia and addiction and sensitive to modulation by dopaminergic signaling, in drug-exposed and control larvae (40, 119). Consistent with effects on dopaminergic signaling and acoustic startle in mammalian systems (120, 121), all treated groups habituated more slowly in response to acoustic startle stimuli in the presence of the drug. On withdrawal, larvae that had been exposed to nicotine or oxycodone had increased rates of habituation. This is in contrast to previous rodent studies which reported impaired sensorimotor gating in juveniles following *in utero* exposure to nicotine (122, 123), although different periods of exposure and time points of assessment must be noted. Increased rates of habituation are seen in dopamine receptor D2/D3 loss of function mice (124) and following D2/D3 receptor blockade in both humans and zebrafish (40, 125). Therefore, the increased rates of habituation on drug withdrawal seen here are consistent with reduced D2/D3 signaling, suggesting an effect of drug exposure on development of these pathways.

Thus, we see clear behavioral effects in the presence of the drugs consistent with the known effects of these drugs in mammalian systems. Further, we see significant differences between acute and chronic exposure and on acute withdrawal, suggesting adaptation to the presence of the drugs. It is possible that altered exposure paradigms would impact behavioral outcomes but it is difficult to predict the direction of the effect. For example, other studies of centrally active drugs suggest an intermittent exposure regime increases adaptation (126). However, in line with previous studies in zebrafish (127–129) the behavioral studies provide evidence of conserved physiological effects of drug exposure, supporting the use of this model to examine adaptive effects on gene expression.

To explore the basis of this potential adaptation and subsequent possible long-lasting changes in behavior, we conducted differential gene expression analysis at 5 dpf and examined social behavior at 21 dpf. Altered sociability is associated with a range of psychiatric disorders and has been shown to be correlated with *in utero* drug exposure (1, 130). Here, we did not observe any differences in social behavior in treated vs. untreated animals at the 3-week time point, in contrast to previous evidence from rat studies (131). However, time spent near or away from the stimuli fish in a sociability assay is not only a measure of sociability and can also be considered as an exhibition of exploratory/bold behavior. More adventurous and less scared individuals may be more keen to explore the whole arena of the tank and more willing to leave the “safety” of conspecifics. Although fewer developmentally exposed fish explored the arena away from

conspecifics, possibly suggesting increased anxiety, this did not reach significance.

## Developmental Drug Exposures Lead to Differential Expression of Innate Immune Genes in the Larvae, Which Might Have Behavioral Consequences

Drug abuse is reported to have immunomodulatory effects and increase susceptibility to infectious diseases in adults via a range of mechanisms including modification of protective defenses and proinflammatory responses (75–78, 132–134). Even though the effects of drug exposure during development are different from those in adults, as both the CNS and the immune system are still developing, studies have shown increased hospitalization due to infections in the first year of life for amphetamine-exposed children (8). Our transcriptomic analysis shows that developmental exposure to amphetamine and oxycodone downregulates the expression of inflammatory genes such as *ccl20b*, *ccl20a.3*, and *nos2a*, which may manifest as increased susceptibility to infections in early life. In contrast, several pro-inflammatory genes are upregulated in nicotine treatments, contrary to the anti-inflammatory effect of nicotine seen in adults (135), which might reflect an activation of the neuroimmune system in the brain, associated with addiction and other psychiatric disorders (136, 137).

Neuroinflammation, triggered by drug/alcohol abuse, stress or infections, is characterized by the induction of inflammatory NF- $\kappa$ B and subsequent upregulation of proinflammatory genes, such as IL1B, IL6, TNFA, iNOS, and NOX (136, 137). Studies in humans and mouse models have shown direct links between induction of innate immune genes in the brain and increased susceptibility to attention deficits, addiction and other psychiatric disorders (138–140). Human genetic association studies and post-mortem studies of addicted brains further strengthen the link between addiction and neuroinflammation (141–143). Our transcriptomic analysis shows that pro-inflammatory genes commonly associated with neuroinflammation (*nfkbi*, *il1b*, *il6*, *nos2a*, and *noxa1a*) are upregulated in nicotine exposure, which might play a role in attention deficits (4, 8–11) and increased susceptibility to addiction (4) in substance-exposed children.

It is noteworthy that the innate immune system is influenced by the circadian clock and that, in zebrafish, lack of *per2*, which is upregulated in our RNA-seq data, is shown to dampen the innate immune response (144). Upregulation of *per2* might influence the expression of innate immune genes and explain the activation of the inflammatory response seen in nicotine exposure. However, the opposite effect is seen for amphetamine and oxycodone, which also show upregulation of *per2*.

Overall, differential expression of immune genes in response to developmental exposures might influence susceptibility to infectious diseases and also contribute to attention deficits and behavioral dysfunction due to neuroinflammation. However, the impact needs further mechanistic investigation, for example, by using transgenic zebrafish lines to study localization of and quantify immune cells and behavioral assays to investigate prevalence of attention deficits.

## Developmental Drug Exposures Lead to Region-Specific Differential Expression of Immediate Early Genes

The IEGs *fosab*, *junbb*, *egr1*, and *egr4*, which are regulators of synaptic plasticity, are significantly downregulated in response to developmental drug exposures. These genes are implicated in addiction, psychiatric disorders and neurodegenerative diseases (81).

Fos and Jun family proteins (including *fosab* and *junbb*) are well-studied in the context of learning, memory and addiction (69, 70, 145). *Egr1* has also been shown to be critical for memory consolidation and is downregulated in stress-mediated disorders (146). In fact, reduced mRNA levels of *Egr1* are used as a measure of depressive phenotypes (146, 147). Its homolog *Egr4* has not been studied in the context of reward processing, but it shows differential expression in addiction, depressive disorders and neurodegenerative diseases (81).

Whole-mount mRNA ISH staining showed that, at 5 dpf, all four genes have overlapping expression patterns and are expressed in the forebrain, midbrain and the hindbrain. *egr1* and *egr4* are also expressed in the torus semicircularis of the midbrain and *egr4*, *fosab* and *junbb* in the retina. We found a reduction in expression of these genes across all neuroanatomical regions, including brain regions associated with addiction and other psychiatric disorders, which might impact synaptogenesis in these brain regions during development.

All four genes are downregulated in the habenular nuclei of the diencephalon, a region that regulates dopamine levels by GABAergic inhibition of dopaminergic cells in the VTA. ISH staining shows a possible reduction in the size of habenulae, as seen in dementia patients (83) who display abnormal reward behaviors. However, better quantitative methods are needed to estimate habenular size.

The tegmental area of the midbrain, important for relaying inhibitory signals to the thalamus and basal nuclei to prevent unwanted body movements, also shows a downregulation of these genes in response to developmental exposures. Reduced activity in this region might interfere with these inhibitory signals and manifest as symptoms of withdrawal, including tremors and poorly controlled movements seen in substance-exposed newborns, particularly with opioids (148).

Similarly, the optic tectum of the midbrain (superior colliculus in mammals) shows a downregulation of all four genes and the torus semicircularis in the midbrain shows a downregulation of *egr1* and *egr4*. These regions are both important for receiving and processing sensory information and the tectum is also critical for regulating motor outputs such as control and orientation of gaze movements important for attention. Slower rates of information processing and lack of habituation to auditory stimuli is reported in cocaine-exposed newborns (149) and developmentally cocaine-exposed zebrafish have shown altered habituation to visual stimuli and attention (150). Thus, downregulation of IEGs in these regions might underlie reduced synaptogenesis and lead to deficits in information processing and attention reported in substance-exposed children (7, 11).

Strikingly, we found that the expression of *junbb* and *fosab* is diminished in the olfactory bulbs of the telencephalon in drug-exposed larvae. The olfactory bulbs are implicated in psychiatric diseases, for example, their volume is reduced in schizophrenia patients (87). Rats with olfactory bulbectomy are used as a model for depression studies (86) and animal studies have shown a clear impact of alcohol and drug exposures on neuronal circuitries in the olfactory bulbs (84, 85). Further studies are needed to investigate the effect of developmental exposure on the olfactory bulbs, but this has potential implications for reward processing and depression states.

Early intervention to restore the expression of these IEGs could potentially reduce the impact of prenatal drug exposures and the manifestation of associated phenotypes. However, further work is needed for mechanistic characterization of gene function. Zebrafish knockout models and a combination of phenotyping methods, including brain imaging, behavioral assays and RNA sequencing, can be exploited for mechanistic studies.

## Developmental Drug Exposures Induce Differential Expression of Circadian Genes, Some of Which Show Differential Expression at Later Stages

Developmental exposure to amphetamine, oxycodone and nicotine led to differential expression of genes involved in the regulation of circadian rhythm. Alterations in circadian rhythms are implicated in many psychiatric conditions including depression (89, 90), bipolar disorder (91) and addiction (92–97). Therefore, we investigated the behavioral consequences in the larvae and the persistence of expression changes after cessation of drug exposure.

Circadian rhythms are ~24-h, autoregulatory, daily rhythms that regulate the expression of numerous genes involved in a wide range of biological processes, including the dopaminergic and the immune systems. Monoamine oxidase A, which is required for breakdown of dopamine, is the transcriptional target of circadian clock components CLOCK/BMAL1 and PER2 (151), and CLOCK is also shown to inhibit the transcription of tyrosine hydroxylase, the enzyme required for dopamine synthesis (152). In zebrafish, *per2*<sup>-/-</sup> has also been shown to dampen the innate immune response to LPS (144).

Circadian rhythms can be altered by many factors, including environmental stimuli, genetics and molecular intervention. Given the role of circadian genes in regulating the reward circuitry, these alterations predispose individuals to a variety of psychiatric conditions. Sleep impairments are associated with increased nicotine (95), alcohol and drug consumption (96, 97) and mood disorders (90). A direct impact of circadian genes in periodicity is observed in *per2* knockout zebrafish, which show reduced locomotion under induced light-dark conditions, a 2-h phase delay and lengthened periodicity (153). Similarly, molecular intervention to the clock by drug abuse also alters the circadian rhythm and leads to increased susceptibility to addiction. Daily dopamine agonist injections in mice were reported to entrain the circadian rhythm, which persisted during

withdrawal (154). Thus, alterations in sleep cycles following drug abuse, which are associated with relapse following cessation of drug abuse, might be due to persistent changes in the circadian rhythm (98, 99).

We studied the impact of differentially expressed circadian genes on periodicity and phase-shifts (equivalent to sleep/wakefulness cycles in mammals) in developmentally drug-exposed larvae to assess potential shifts in circadian cycles. However, we found that expression changes in circadian rhythm genes do not correlate with changes in periodicity and phase-shifts. As period genes have been linked to altered responses to dusk/dawn in knockout mice (155), we also assessed responsiveness to gradually changing light conditions in exposed larvae. Even though we found a decrease in the rate of response to dusk for amphetamine-treated fish and to dawn for nicotine-treated fish, these results were strongly confounded by significant differences in locomotion and cannot be used to draw conclusions.

Although we saw no clear correlation with behavioral responses in the larvae, besides potentially influencing many circadian-regulated pathways during development, persistent changes in gene expression after cessation of exposure might have long-term effects and predispose individuals to addiction. We investigated such changes in circadian rhythm genes in developmentally exposed fish at 7 and 21 dpf and found long lasting changes in circadian gene expression, which were contrary to the expression changes seen at 5 dpf.

Overall, developmental exposures induce differential expression of circadian rhythm genes, some of which are still seen at later stages of development. Even though this does not correlate with behavioral changes in the larvae, differential expression of these genes might interfere with other circadian-regulated biological pathways during development, such as functioning of the reward and immune systems. It is important to note that differential expression of circadian rhythm genes is reported in other zebrafish RNA-seq experiments (156) and so could be a stress response rather than a drug-evoked response. Glucocorticoid release following stress is also found to induce *Per2* expression and cause circadian phase delay (157).

## CONCLUSIONS

To conclude, exposure of larval zebrafish to amphetamine, oxycodone and nicotine led to changes in behavior consistent with mammalian systems. Exposure during the period of major organ system development affected locomotion and habituation. However, these differences were most prevalent in the presence of the drug. Differences in acute and developmental effects of the drug are an indicator of adaptation to the presence of the drug.

Whole organism RNA-seq on drug-exposed larvae revealed differential expression of numerous genes and alterations in many pathways, including those related to innate immunity, immunosuppression, neuroinflammation and circadian rhythms, the latter of which were shown to persist after developmental exposure but did not correlate with behavioral changes. Immediate early genes associated with synaptic plasticity were

downregulated across all treatments and this was confirmed to occur, among others, in brain regions implicated in reward processing and addiction by *in situ* hybridization. Differential expression of highly localized transcripts is not always picked up by whole organism RNA-seq if the change is constrained to a small group of cells. This might explain the absence of components of neurotransmitter pathways, which have been shown to be differentially expressed in other studies and might explain the possible adaptation to the presence of drugs we observed. However, we anticipate that these early changes in gene expression in the larvae in response to drug exposures are likely to contribute to the consequences of prenatal exposure and their discovery might pave the way to therapeutic intervention to ameliorate the long-lasting deficits.

## DATA AVAILABILITY STATEMENT

The datasets presented in this study can be found in online repositories. The names of the repository/repositories and accession number(s) can be found in the article/**Supplementary Material**.

## ETHICS STATEMENT

The animal study was reviewed and approved by the Animal Welfare and Ethical Review Body at the University of Cambridge (project license P597E5E82) and by Animal Care and Use Ethics Committee at Queen Mary University of London (project license P6D11FBCD and PP9581087).

## AUTHOR CONTRIBUTIONS

AM and MM conducted experiments, analyzed and interpreted data, and wrote the manuscript. WH conducted experiments. M-TT conducted experiments and analyzed data. IS and RW analyzed and interpreted data. EB-N secured funding and directed and interpreted the gene expression analysis. CB conceived and oversaw the study, interpreted data, and secured funding. All authors contributed to the article and approved the submitted version.

## FUNDING

This work was funded by the National Institute of Health (NIH U01 DA044400-03, AM, MM, IS, WH, EB-N, and CB).

## ACKNOWLEDGMENTS

We thank Dr. Sofia Anagianni for her assistance with troubleshooting the protocols and valuable insight. We thank Luca Galantini and Daniel Holly for fish facility maintenance.

## SUPPLEMENTARY MATERIAL

The Supplementary Material for this article can be found online at: <https://www.frontiersin.org/articles/10.3389/fpsy.2021.795175/full#supplementary-material>

## REFERENCES

- Ross EJ, Graham DL, Money KM, Stanwood GD. Developmental consequences of fetal exposure to drugs: what we know and what we still must learn. *Neuropsychopharmacology*. (2015) 40:61. doi: 10.1038/npp.2014.147
- Oei JL, Kingsbury A, Dhawan A, Burns L, Feller JM, Clews S, et al. Amphetamines, the pregnant woman and her children: a review. *J Perinatol*. (2012) 32:737–47. doi: 10.1038/jp.2012.59
- Smith LM, LaGasse LL, Derauf C, Grant P, Shah R, Arria A, et al. The infant development, environment, and lifestyle study: effects of prenatal methamphetamine exposure, polydrug exposure, and poverty on intrauterine growth. *Pediatrics*. (2006) 118:1149–56. doi: 10.1542/peds.2005-2564
- Dodge NC, Jacobson JL, Jacobson SW. Effects of fetal substance exposure on offspring substance use. *Pediatr Clin North Am*. (2019) 66:1149–61. doi: 10.1016/j.pcl.2019.08.010
- Niemelä S, Sourander A, Surcel H-M, Hinkka-Yli-Salomäki S, McKeague IW, Cheslack-Postava K, et al. Prenatal nicotine exposure and risk of schizophrenia among offspring in a national birth cohort. *Am J Psychiatry*. (2016) 173:799–806. doi: 10.1176/appi.ajp.2016.15.060800
- Bastaki KN, Alwan S, Zahir FR. Maternal prenatal exposures in pregnancy and autism spectrum disorder: an insight into the epigenetics of drugs and diet as key environmental influences. *Adv Neurobiol*. (2020) 24:143–62. doi: 10.1007/978-3-030-30402-7\_5
- Ornoy A, Segal J, Bar-Hamburger R, Greenbaum C. Developmental outcome of school-age children born to mothers with heroin dependency: importance of environmental factors. *Dev Med Child Neurol*. (2001) 43:668–75. doi: 10.1017/S0012162201001219
- Eriksson M, Zetterström R. Amphetamine addiction during pregnancy: 10-year follow-up. *Acta Paediatr*. (1994) 83:27–31. doi: 10.1111/j.1651-2227.1994.tb13380.x
- Eriksson M, Jonsson B, Stenroth G, Zetterström R. Amphetamine abuse during pregnancy: environmental factors and outcome after 14–15 years. *Scand J Public Health*. (2000) 28:154–7. doi: 10.1177/140349480002800212
- Hunt RW, Tzioumi D, Collins E, Jeffery HE. Adverse neurodevelopmental outcome of infants exposed to opiate *in-utero*. *Early Hum Dev*. (2008) 84:29–35. doi: 10.1016/j.earlhumdev.2007.01.013
- Levine TP, Liu J, Das A, Lester B, Lagasse L, Shankaran S, et al. Effects of prenatal cocaine exposure on special education in school-aged children. *Pediatrics*. (2008) 122:e83–91. doi: 10.1542/peds.2007-2826
- Zoubková H, Tomášková A, Nohejlová K, Cerná M, Šlamberová R. Prenatal exposure to methamphetamine: up-regulation of brain receptor genes. *Front Neurosci*. (2019) 13:771. doi: 10.3389/fnins.2019.00771
- Alkam T, Mamiya T, Kimura N, Yoshida A, Kihara D, Tsunoda Y, et al. Prenatal nicotine exposure decreases the release of dopamine in the medial frontal cortex and induces atomoxetine-responsive neurobehavioral deficits in mice. *Psychopharmacology*. (2017) 234:1853–69. doi: 10.1007/s00213-017-4591-z
- Chen WJA, King KA, Lee RE, Sedtal CS, Smith AM. Effects of nicotine exposure during prenatal or perinatal period on cell numbers in adult rat hippocampus and cerebellum: a stereology study. *Life Sci*. (2006) 79:2221–7. doi: 10.1016/j.lfs.2006.07.019
- Levin ED, Hall BJ, Rezvani AH. Heterogeneity across brain regions and neurotransmitter interactions with nicotinic effects on memory function. *Curr Top Behav Neurosci*. (2015) 23:87–101. doi: 10.1007/978-3-319-13665-3\_4
- Levine TA, Woodward LJ. Early inhibitory control and working memory abilities of children prenatally exposed to methadone. *Early Hum Dev*. (2018) 116:68–75. doi: 10.1016/j.earlhumdev.2017.11.010
- Creeley CE, Olney JW. Drug-induced apoptosis: mechanism by which alcohol and many other drugs can disrupt brain development. *Brain Sci*. (2013) 3:1153–81. doi: 10.3390/brainsci3031153
- Chater-Diehl EJ, Laufer BI, Castellani CA, Alberly BL, Singh SM. Alteration of gene expression, DNA methylation, and histone methylation in free radical scavenging networks in adult mouse hippocampus following fetal alcohol exposure. *PLoS ONE*. (2016) 11:e0154836. doi: 10.1371/journal.pone.0154836
- Sadri-Vakili G. Cocaine triggers epigenetic alterations in the corticostriatal circuit. *Brain Res*. (2015) 1628:50. doi: 10.1016/j.brainres.2014.09.069
- Brancato A, Cannizzaro C. Mothering under the influence: How perinatal drugs of abuse alter the mother-infant interaction. *Rev Neurosci*. (2018) 29:283–94. doi: 10.1515/revneuro-2017-0052
- Little B, Sud N, Nobile Z, Bhattacharya D. Teratogenic effects of maternal drug abuse on developing brain and underlying neurotransmitter mechanisms. *Neurotoxicology*. (2021) 86:172–9. doi: 10.1016/j.neuro.2021.08.007
- Pawluski JL, Swain JE, Lonstein JS. Neurobiology of peripartum mental illness. *Handb Clin Neurol*. (2021) 182:63–82. doi: 10.1016/B978-0-12-819973-2.00005-8
- Norton W, Bally-Cuif L. Adult zebrafish as a model organism for behavioural genetics. *BMC Neurosci*. (2010) 11:90. doi: 10.1186/1471-2202-11-90
- Wolman M, Granato M. Behavioral genetics in larval zebrafish: learning from the young. *Dev Neurobiol*. (2012) 72:366–72. doi: 10.1002/dneu.20872
- McHugh RK, Wigderson S, Greenfield SF. Epidemiology of substance use in reproductive-age women. *Obstet Gynecol Clin North Am*. (2014) 41:177–89. doi: 10.1016/j.jogc.2014.02.001
- Boudanova E, Navaroli DM, Melikian HE. Amphetamine-induced decreases in dopamine transporter surface expression are protein kinase C-independent. *Neuropharmacology*. (2008) 54:605–12. doi: 10.1016/j.neuropharm.2007.11.007
- Benowitz NL. Pharmacology of nicotine: addiction, smoking-induced disease, and therapeutics. *Annu Rev Pharmacol Toxicol*. (2009) 49:57–71. doi: 10.1146/annurev.pharmtox.48.113006.094742
- Kosten T. R., and George T. P. (2002). The neurobiology of opioid dependence: implications for treatment. *Sci Pract Perspect*. 1, 13–20. doi: 10.1151/spp021113
- Kalso E. Oxycodone. *J Pain Symptom Manage*. (2005) 29:47–56. doi: 10.1016/j.jpainsymman.2005.01.010
- Hodder SL, Feinberg J, Strathdee SA, Shoptaw S, Altice FL, Ortenzio L, et al. The opioid crisis and HIV in the USA: deadly synergies. *Lancet*. (2021) 397:1139–50. doi: 10.1016/S0140-6736(21)00391-3
- Veldman MB, Lin S. Zebrafish as a developmental model organism for pediatric research. *Pediatr Res*. (2008) 64:470–6. doi: 10.1203/PDR.0b013e318186e609
- Brock AJ, Goody SMG, Mead AN, Sudwarta A, Parker MO, Brennan CH. Assessing the value of the zebrafish conditioned place preference model for predicting human abuse potential. *J Pharmacol Exp Ther*. (2017) 363:66–79. doi: 10.1124/jpet.117.242628
- Luck W, Nau H, Hansen R, Steldinger R. Extent of nicotine and cotinine transfer to the human fetus, placenta and amniotic fluid of smoking mothers. *Dev Pharmacol Ther*. (1985) 8:384–95. doi: 10.1159/000457063
- Stewart JT, Meeker JE. Fetal and infant deaths associated with maternal methamphetamine abuse. *J Anal Toxicol*. (1997) 21:515–7. doi: 10.1093/jat/21.6.515
- Turnbull K, Bielech M, Walker SE, Law S. Stability of oxycodone hydrochloride for injection in dextrose and saline solutions. *Can J Hosp Pharm*. (2002) 55:272–7. doi: 10.4212/CJHP.V55I4.603
- van Nuijs ALN, Abdellati K, Bervoets L, Blust R, Jorens PG, Neels H, et al. The stability of illicit drugs and metabolites in wastewater, an important issue for sewage epidemiology? *J Hazard Mater*. (2012) 239:40:19–23. doi: 10.1016/j.jhazmat.2012.04.030
- Matta SG, Balfour DJ, Benowitz NL, Boyd RT, Buccafusco JJ, Caggiula AR, et al. Guidelines on nicotine dose selection for *in vivo* research. *Psychopharmacology*. (2006) 190:269–319. doi: 10.1007/s00213-006-0441-0
- Lee HB, Schwab TL, Sigafos AN, Gauerke JL, Krug RGII, Serres MR, et al. Novel zebrafish behavioral assay to identify modifiers of the rapid, nongenomic stress response. *Genes Brain Behav*. (2019) 18:e12549. doi: 10.1111/gbb.12549
- Vuillermot S, Feldon J, Meyer U. Relationship between sensorimotor gating deficits and dopaminergic neuroanatomy in Nurr1-deficient mice. *Exp Neurol*. (2011) 232:22–32. doi: 10.1016/j.expneurol.2011.07.008

40. García-González J, Brock AJ, Parker MO, Riley RJ, Joliffe D, Sudworts A, et al. Identification of slit3 as a locus affecting nicotine preference in zebrafish and human smoking behaviour. *Elife*. (2020) 9:1–33. doi: 10.7554/eLife.51295
41. Dreosti E, Lopes G, Kampff AR, Wilson SW. Development of social behavior in young zebrafish. *Front Neural Circuits*. (2015) 9:39. doi: 10.3389/fncir.2015.00039
42. Gómez-Requeni P, Conceição LEC, Jordal AEO, Ronnestad I. A reference growth curve for nutritional experiments in zebrafish (*Danio rerio*) and changes in whole body proteome during development. *Fish Physiol Biochem*. (2010) 36:1199–215. doi: 10.1007/s10695-010-9400-0
43. Carlucci M, Kriščiunas A, Li H, Gibas P, Koncevičius K, Petronis A, et al. DiscoRhythm: an easy-to-use web application and R package for discovering rhythmicity. *Bioinformatics*. (2019) btz834. doi: 10.1093/bioinformatics/btz834
44. R Core Team. *R: A Language and Environment for Statistical Computing*. (2021). Available online at: <https://www.R-project.org/> (accessed October 10, 2021).
45. RStudio Team. *RStudio: Integrated Development for R*. (2020). Available online at: <http://www.rstudio.com/> (accessed October 10, 2021).
46. García-González J, Quadros B, de Havelange W, Brock AJ, Brennan CH. Behavioral effects of developmental exposure to JWH-018 in wild-type and disrupted in schizophrenia 1 (disc1) mutant zebrafish. *Biomolecules*. (2021) 11:319. doi: 10.3390/biom11020319
47. Cribari-Neto F, Zeileis A. Beta regression in R. *J Stat Softw*. (2010) 34:1–24. doi: 10.18637/jss.v034.i02
48. Bates D, Mächler M, Bolker B, Walker S. Fitting linear mixed-effects models using lme4. *J Stat Softw*. (2015) 67:1–48. doi: 10.18637/jss.v067.i01
49. Hothorn T, Bretz F, Westfall P. Simultaneous inference in general parametric models. *Biom J*. (2008) 50:346–63. doi: 10.1002/bimj.200810425
50. White RJ, Collins JE, Sealy IM, Wali N, Dooley CM, Digby Z, et al. A high-resolution mRNA expression time course of embryonic development in zebrafish. *Elife*. (2017) 6:e30860. doi: 10.7554/eLife.30860
51. Dobin A, Davis CA, Schlesinger F, Drenkow J, Zaleski C, Jha S, et al. STAR: Ultrafast universal RNA-seq aligner. *Bioinformatics*. (2013) 29:15–21. doi: 10.1093/bioinformatics/bts635
52. Love MI, Huber W, Anders S. Moderated estimation of fold change and dispersion for RNA-seq data with DESeq2. *Genome Biol*. (2014) 15:550. doi: 10.1186/s13059-014-0550-8
53. Wickham H, Averick M, Bryan J, Chang W, McGowan LD, François R, et al. Welcome to the tidyverse. *J Open Source Softw*. (2019) 4:1686. doi: 10.21105/joss.01686
54. Tang Y, Horikoshi M, Li W. ggfortify: unified interface to visualize statistical results of popular R packages. *R J*. (2016) 8:474. doi: 10.32614/RJ-2016-060
55. Wickham H. *ggplot2: Elegant Graphics for Data Analysis*. New York, NY: Springer-Verlag (Use R!) (2016).
56. Walter W, Sánchez-Cabo F, Ricote M. GOpplot: an R package for visually combining expression data with functional analysis. *Bioinformatics*. (2015) 31:2912–4. doi: 10.1093/bioinformatics/btv300
57. Chen H. *VennDiagram: Generate High-Resolution Venn and Euler Plots*. (2018). Available online at: <https://CRAN.R-project.org/package=VennDiagram> (accessed October 10, 2021).
58. Kolde R. *pheatmap: Pretty Heatmaps*. (2019). Available online at: <https://CRAN.R-project.org/package=pheatmap> (accessed June 28, 2021).
59. Slowikowski K, Schep A, Hughes S, Dang TK, Lukauskas S, Irsson J-O, et al. *ggrepel: Automatically Position Non-Overlapping Text Labels with 'ggplot2' (0.9.1) [Computer software]*. (2021). Available online at: <https://CRAN.R-project.org/package=ggrepel> (accessed October 10, 2021).
60. Thisse C, Thisse B. High-resolution in situ hybridization to whole-mount zebrafish embryos. *Nat Protoc*. (2008) 3:59–69. doi: 10.1038/nprot.2007.514
61. Vauti F, Stegemann LA, Vögele V, Köster RW. All-age whole mount in situ hybridization to reveal larval and juvenile expression patterns in zebrafish. *PLoS ONE*. (2020) 15:e0237167. doi: 10.1371/journal.pone.0237167
62. Ponzoni L, Teh MT, Torres-Perez JV, Brennan CH, Braida D, Sala M. Increased response to 3,4-Methylenedioxymethamphetamine (MDMA) reward and altered gene expression in zebrafish during short- and long-term nicotine withdrawal. *Mol Neurobiol*. (2020) 58:1650–63. doi: 10.1007/s12035-020-02225-5
63. Bustin SA, Benes V, Garson JA, Hellemans J, Huggett J, Kubista M, et al. The MIQE guidelines: minimum information for publication of quantitative real-time PCR experiments. *Clin Chem*. (2009) 55:611–22. doi: 10.1373/clinchem.2008.112797
64. Teh M-T, Gemenetzidis E, Chaplin T, Young BD, Philpott MP. Upregulation of FOXM1 induces genomic instability in human epidermal keratinocytes. *Mol Cancer*. (2010) 9:45. doi: 10.1186/1476-4598-9-45
65. Teh M-T, Hutchison IL, Costea DE, Neppelberg E, Liavaag PG, Purdie K, et al. Exploiting FOXM1-orchestrated molecular network for early squamous cell carcinoma diagnosis and prognosis. *Int J Cancer*. (2013) 132:2095–106. doi: 10.1002/ijc.27886
66. Parker MO, Evans AM-D, Brock AJ, Combe FJ, Teh M-T, Brennan CH. Moderate alcohol exposure during early brain development increases stimulus-response habits in adulthood. *Addict Biol*. (2016) 21:49–60. doi: 10.1111/adb.12176
67. Ray WJ, Molnar C, Aikins D, Yamasaki A, Newman MG, Castonguay L, et al. Startle response in generalized anxiety disorder. *Depress Anxiety*. (2009) 26:147. doi: 10.1002/da.20479
68. Dunwoodie SL. The role of hypoxia in development of the mammalian embryo. *Dev Cell*. (2009) 17:755–73. doi: 10.1016/j.devcel.2009.11.008
69. Nestler EJ, Barrot M, Self DW.  $\Delta$ FosB: a sustained molecular switch for addiction. *Proc Natl Acad Sci USA*. (2001) 98:11042–6. doi: 10.1073/pnas.191352698
70. Nestler EJ. Transcriptional mechanisms of addiction: role of  $\Delta$ FosB. *Philos Transact R Soc B Biol Sci*. (2008) 363:3245–55. doi: 10.1098/rstb.2008.0067
71. Taniguchi M, Carreira MB, Cooper YA, Bobadilla A-C, Heinsbroek JA, Koike N, et al. HDAC5 and its target gene, Npas4, function in the nucleus accumbens to regulate cocaine-conditioned behaviors. *Neuron*. (2017) 96:130–44.e6. doi: 10.1016/j.neuron.2017.09.015
72. Zhang L, Cho J, Ptak D, Leung YF. The role of *egr1* in early zebrafish retinogenesis. *PLoS ONE*. (2013) 8:e56108. doi: 10.1371/journal.pone.0056108
73. Wells T, Rough K, Carter D. Transcription mapping of embryonic rat brain reveals EGR-1 induction in SOX2+ neural progenitor cells. *Front Mol Neurosci*. (2011) 4:6. doi: 10.3389/fnmol.2011.00006
74. Tao W, Wu J, Zhang Q, Lai S-S, Jiang S, Jiang C, et al. EGR1 regulates hepatic clock gene amplitude by activating Per1 transcription. *Sci Rep*. (2015) 5:15212. doi: 10.1038/srep15212
75. Friedman H, Newton C, Klein TW. Microbial infections, immunomodulation, and drugs of abuse. *Clin Microbiol Rev*. (2003) 16:209–19. doi: 10.1128/CMR.16.2.209-219.2003
76. Friedman H, Pross S, Klein TW. Addictive drugs and their relationship with infectious diseases. *FEMS Immunol Med Microbiol*. (2006) 47:330–42. doi: 10.1111/j.1574-695X.2006.00097.x
77. Irwin MR, Olmos L, Wang M, Valladares EM, Motivala SJ, Fong T, et al. Cocaine dependence and acute cocaine induce decreases of monocyte proinflammatory cytokine expression across the diurnal period: autonomic mechanisms. *J Pharmacol Exp Ther*. (2007) 320:507–15. doi: 10.1124/jpet.106.112797
78. Salamanca SA, Sorrentino EE, Nosanchuk JD, Martinez LR. Impact of methamphetamine on infection and immunity. *Front Neurosci*. (2015) 8:445. doi: 10.3389/fnins.2014.00445
79. Ronneberger O, Liu K, Rath M, Rueß D, Mueller T, Skibbe H, et al. ViBE-Z: A framework for 3D virtual colocalization analysis in zebrafish larval brains. *Nat Methods*. (2012) 9:735–42. doi: 10.1038/nmeth.2076
80. Jones MW, Errington ML, French PJ, Fine A, Bliss TVP, Garel S, et al. A requirement for the immediate early gene Zif268 in the expression of late LTP and long-term memories. *Nat Neurosci*. (2001) 4:289–96. doi: 10.1038/85138
81. Shi L, Wang Y, Li C, Zhang K, Du Q, Zhao M. AddictGene: An integrated knowledge base for differentially expressed genes associated with addictive substance. *Comput Struct Biotechnol J*. (2021) 19:2416–22. doi: 10.1016/j.csbj.2021.04.027
82. Velasquez KM, Molfese DL, Salas R. The role of the habenula in drug addiction. *Front Hum Neurosci*. (2014) 8:174. doi: 10.3389/fnhum.2014.00174
83. Bocchetta M, Gordon E, Marshall CR, Slattery CF, Cardoso MJ, Cash DM, et al. The habenula: an under-recognised area of importance in

- frontotemporal dementia? *J Neurol Neurosurg Psychiatry*. (2016) 87:910–2. doi: 10.1136/jnnp-2015-312067
84. Akers KG, Kushner SA, Leslie AT, Clarke L, van der Kooy D, Lerch JP, et al. Fetal alcohol exposure leads to abnormal olfactory bulb development and impaired odor discrimination in adult mice. *Mol Brain*. (2011) 4:29. doi: 10.1186/1756-6606-4-29
  85. Youngentob SL, Glendinning JL. Fetal ethanol exposure increases ethanol intake by making it smell and taste better. *Proc Nat Acad Sci USA*. (2009) 106:5359–64. doi: 10.1073/pnas.0809804106
  86. Song C, Leonard BE. The olfactory bulbectomized rat as a model of depression. *Neurosci Biobehav Rev*. (2005) 29:627–47. doi: 10.1016/j.neubiorev.2005.03.010
  87. Turetsky BI, Moberg PJ, Roalf DR, Arnold SE, Gur RE. Decrements in volume of anterior ventromedial temporal lobe and olfactory dysfunction in schizophrenia. *Arch Gen Psychiatry*. (2003) 60:1193–200. doi: 10.1001/archpsyc.60.12.1193
  88. Logan RW, Williams WP, McClung CA. Circadian rhythms and addiction: mechanistic insights and future directions. *Behav Neurosci*. (2014) 128:387–412. doi: 10.1037/a0036268
  89. Utge SJ, Soronen P, Loukola A, Kronholm E, Ollila HM, Pirkola S, et al. Systematic analysis of circadian genes in a population-based sample reveals association of TIMELESS with depression and sleep disturbance. *PLoS ONE*. (2010) 5:e9259. doi: 10.1371/journal.pone.0009259
  90. Levandovski R, Dantas G, Fernandes LC, Caumo W, Torres I, Roenneberg T, et al. Depression scores associate with chronotype and social jetlag in a rural population. *Chronobiol Int*. (2011) 28:771–8. doi: 10.3109/07420528.2011.602445
  91. Mansour HA, Wood J, Logue T, Chowdari KV, Dayal M, Kupfer DJ, et al. Association study of eight circadian genes with bipolar I disorder, schizoaffective disorder and schizophrenia. *Genes Brain Behav*. (2006) 5:150–7. doi: 10.1111/j.1601-183X.2005.00147.x
  92. Spanagel R, Pendyala G, Abarca C, Zghoul T, Sanchis-Segura C, Magnone MC, et al. The clock gene *Per2* influences the glutamatergic system and modulates alcohol consumption. *Nat Med*. (2005) 11:35–42. doi: 10.1038/nm1163
  93. Kirkpatrick MG, Haney M, Vosburg SK, Comer SD, Foltin RW, Hart CL. Methamphetamine self-administration by humans subjected to abrupt shift and sleep schedule changes. *Psychopharmacology*. (2009) 203:771–80. doi: 10.1007/s00213-008-1423-1
  94. Shumay E, Fowler JS, Wang G-J, Logan J, Alia-Klein N, Goldstein RZ, et al. Repeat variation in the human *PER2* gene as a new genetic marker associated with cocaine addiction and brain dopamine D2 receptor availability. *Transl Psychiatry*. (2012) 2:e86. doi: 10.1038/tp.2012.11
  95. Broms U, Kaprio J, Hublin C, Partinen M, Madden PAF, Koskenvuo M. Evening types are more often current smokers and nicotine dependent - A study of Finnish adult twins. *Addiction*. (2011) 106:170–7. doi: 10.1111/j.1360-0443.2010.03112.x
  96. Adan A. Chronotype and personality factors in the daily consumption of alcohol and psychostimulants. *Addiction*. (1994) 89:455–62. doi: 10.1111/j.1360-0443.1994.tb00926.x
  97. Fisk JE, Montgomery C. Sleep impairment in ecstasy/polydrug and cannabis-only users. *Am J Addict*. (2009) 18:430–7. doi: 10.3109/10550490903077762
  98. Jones EM, Knutson D, Haines D. Common problems in patients recovering from chemical dependency. *Am Fam Physician*. (2003) 68:1971–8.
  99. Falcón E, McClung CA. A role for the circadian genes in drug addiction. *Neuropharmacology*. (2009) 56(Suppl. 1):91–6. doi: 10.1016/j.neuropharm.2008.06.054
  100. Fugariu V, Zack MH, Nobrega JN, Fletcher PJ, Zeeb FD. Effects of exposure to chronic uncertainty and a sensitizing regimen of amphetamine injections on locomotion, decision-making, and dopamine receptors in rats. *Neuropsychopharmacology*. (2020) 45:811. doi: 10.1038/s41386-020-0599-x
  101. Yates JW, Meij JTA, Sullivan JR, Richtand NM, Yu L. Bimodal effect of amphetamine on motor behaviors in C57BL/6 mice. *Neurosci Lett*. (2007) 427:66. doi: 10.1016/j.neulet.2007.09.011
  102. Quik M, Zhang D, Perez XA, Bordia T. Role for the nicotinic cholinergic system in movement disorders; therapeutic implications. *Pharmacol Ther*. (2014) 144:50. doi: 10.1016/j.pharmthera.2014.05.004
  103. Svoboda KR, Vijayaraghavan S, Tanguay RL. Nicotinic receptors mediate changes in spinal motoneuron development and axonal pathfinding in embryonic zebrafish exposed to nicotine. *J Neurosci*. (2002) 22:10731. doi: 10.1523/JNEUROSCI.22-24-10731.2002
  104. Blaser RE, Peñalosa YM. Stimuli affecting zebrafish (*Danio rerio*) behavior in the light/dark preference test. *Physiol Behav*. (2011) 104:831–7. doi: 10.1016/j.physbeh.2011.07.029
  105. Takao K, Miyakawa T. Light/dark transition test for mice. *J Visual Exp*. (2006) 1:104. doi: 10.3791/104
  106. Cheeta S, Irvine EE, Kenny PJ, File SE. The dorsal raphe nucleus is a crucial structure mediating nicotine's anxiolytic effects and the development of tolerance and withdrawal responses. *Psychopharmacology*. (2001) 155:78–85. doi: 10.1007/s002130100681
  107. Silva R, Kameda S, Carvalho R, Rigo G, Costa K, Taricano I, et al. Effects of amphetamine on the plus-maze discriminative avoidance task in mice. *Psychopharmacology*. (2002) 160:9–18. doi: 10.1007/s00213-001-0948-3
  108. Champagne DL, Hoefnagels CCM, de Kloet RE, Richardson MK. Translating rodent behavioral repertoire to zebrafish (*Danio rerio*): relevance for stress research. *Behav Brain Res*. (2010) 214:332–42. doi: 10.1016/j.bbr.2010.06.001
  109. Egan RJ, Bergner CL, Hart PC, Cachat JM, Canavello PR, Elegante MF, et al. Understanding behavioral and physiological phenotypes of stress and anxiety in zebrafish. *Behav Brain Res*. (2009) 205:38. doi: 10.1016/j.bbr.2009.06.022
  110. Krook JT, Duperreault E, Newton D, Ross MS, Hamilton TJ. Repeated ethanol exposure increases anxiety-like behaviour in zebrafish during withdrawal. *PeerJ*. (2019) 7:e6551. doi: 10.7717/peerj.6551
  111. Ponzoni L, Melzi G, Marabini L, Martini A, Petrillo G, Teh MT, et al. Conservation of mechanisms regulating emotional-like responses on spontaneous nicotine withdrawal in zebrafish and mammals. *Prog Neuropsychopharmacol Biol Psychiatry*. (2021) 111:110334. doi: 10.1016/j.pnpbp.2021.110334
  112. Huang LZ, Liu X, Griffith WH, Winzer-Serhan UH. Chronic neonatal nicotine increases anxiety but does not impair cognition in adult rats. *Behav Neurosci*. (2007) 121:1342–52. doi: 10.1037/0735-7044.121.6.1342
  113. Lawford BR, Young R, Noble EP, Kann B, Ritchie T. The D2 dopamine receptor (*DRD2*) gene is associated with co-morbid depression, anxiety and social dysfunction in untreated veterans with post-traumatic stress disorder. *Eur Psychiatry*. (2006) 21:180–5. doi: 10.1016/j.eurpsy.2005.01.006
  114. Santiago SE, Huffman KJ. Prenatal nicotine exposure increases anxiety and modifies sensorimotor integration behaviors in adult female mice. *Neurosci Res*. (2014) 79:41–51. doi: 10.1016/j.neures.2013.10.006
  115. Steingart RA, Abu-Roumi M, Newman ME, Silverman WF, Slotkin TA, Yanai J. Neurobehavioral damage to cholinergic systems caused by prenatal exposure to heroin or phenobarbital: cellular mechanisms and the reversal of deficits by neural grafts. *Dev Brain Res*. (2000) 122:125–33. doi: 10.1016/S0165-3806(00)00063-8
  116. Steingart RA, Silverman WF, Barron S, Slotkin TA, Awad Y, Yanai J. Neural grafting reverses prenatal drug-induced alterations in hippocampal PKC and related behavioral deficits. *Dev Brain Res*. (2000) 125:9–19. doi: 10.1016/S0165-3806(00)00123-1
  117. Thompson BL, Levitt P, Stanwood GD. Prenatal exposure to drugs: effects on brain development and implications for policy and education. *Nat Rev Neurosci*. (2009) 10:303. doi: 10.1038/nrn2598
  118. Tsai SJ. Dopamine receptor downregulation: an alternative strategy for schizophrenia treatment. *Med Hypotheses*. (2004) 63:1047–50. doi: 10.1016/j.mehy.2004.04.012
  119. Burgess HA, Granato M. Sensorimotor gating in larval zebrafish. *J Neurosci*. (2007) 27:4984–94. doi: 10.1523/JNEUROSCI.0615-07.2007
  120. Mirza NR, Misra A, Bright JL. Different outcomes after acute and chronic treatment with nicotine in pre-pulse inhibition in Lister hooded rats. *Eur J Pharmacol*. (2000) 407:73–81. doi: 10.1016/S0014-2999(00)00658-0
  121. Swerdlow NR, Caine SB, Geyer MA. Opiate-dopamine interactions in the neural substrates of acoustics startle gating in the rat. *Prog Neuropsychopharmacol Biol Psychiatry*. (1991) 15:415–26. doi: 10.1016/0278-5846(91)90072-9
  122. Mactutus CF, Harrod SB, Hord LL, Moran LM, Booze RM. Prenatal IV cocaine: alterations in auditory information processing. *Front Psychiatry*. (2011) 2:38. doi: 10.3389/fpsy.2011.00038
  123. Sun W, Hansen A, Zhang L, Lu J, Stolzberg D, Kraus KS. Neonatal nicotine exposure impairs development of auditory temporal processing. *Hear Res*. (2008) 245:58. doi: 10.1016/j.heares.2008.08.009

124. Halberstadt AL, Geyer MA. Habituation and sensitization of acoustic startle: opposite influences of dopamine D1 and D2-family receptors. *Neurobiol Learn Mem.* (2009) 92:243. doi: 10.1016/j.nlm.2008.05.015
125. Quednow BB, Wagner M, Westheide J, Beckmann K, Bliesener N, Maier W, et al. Sensorimotor gating and habituation of the startle response in schizophrenic patients randomly treated with amisulpride or olanzapine. *Biol Psychiatry.* (2006) 59:536–45. doi: 10.1016/j.biopsych.2005.07.012
126. Kily LJM, Cowe YCM, Hussain O, Patel S, McElwaine S, Cotter FE, et al. Gene expression changes in a zebrafish model of drug dependency suggest conservation of neuro-adaptation pathways. *J Exp Biol.* (2008) 211 (Pt 10):1623–34. doi: 10.1242/jeb.014399
127. Cleal M, Fontana BD, Parker MO. The cognitive and behavioral effects of D-amphetamine and nicotine sensitization in adult zebrafish. *Psychopharmacology.* (2021) 1:1–10. doi: 10.1007/s00213-021-05844-5
128. Kirla KT, Erhart C, Groh KJ, Stadnicka-Michalak J, Eggen RIL, Schirmer K, et al. Zebrafish early life stages as alternative model to study 'designer drugs': concordance with mammals in response to opioids. *Toxicol Appl Pharmacol.* (2021) 419:115483. doi: 10.1016/j.taap.2021.115483
129. Klee EW, Ebbert JO, Schneider H, Hurt RD, Ekker SC. Zebrafish for the study of the biological effects of nicotine. *Nicot Tobacco Res.* (2011) 13:301–12. doi: 10.1093/ntr/ntr010
130. Maughan B, Taylor A, Caspi A, Moffitt TE. Prenatal smoking and early childhood conduct problems: testing genetic and environmental explanations of the association. *Arch Gen Psychiatry.* (2004) 61:836–43. doi: 10.1001/archpsyc.61.8.836
131. Niesink RJM, van Buren-Van Duinkerken L, van Ree JM. Social behavior of juvenile rats after *in utero* exposure to morphine: dose-time-effect relationship. *Neuropharmacology.* (1999) 38:1207–23. doi: 10.1016/S0028-3908(99)00050-7
132. Tallóczy Z, Martinez J, Joset D, Ray Y, Gácsér A, Toussi S, et al. Methamphetamine inhibits antigen processing, presentation, and phagocytosis. *PLoS Pathog.* (2008) 4:e28. doi: 10.1371/annotation/bd02ad26-a081-4c61-88c2-ebda285b8bca
133. Harms R, Morsey B, Boyer CW, Fox HS, Sarvetnick N. Methamphetamine administration targets multiple immune subsets and induces phenotypic alterations suggestive of immunosuppression. *PLoS ONE.* (2012) 7:e49897. doi: 10.1371/journal.pone.0049897
134. Coutinho AE, Chapman KE. The anti-inflammatory and immunosuppressive effects of glucocorticoids, recent developments and mechanistic insights. *Mol Cell Endocrinol.* (2011) 335:2–13. doi: 10.1016/j.mce.2010.04.005
135. Piao W-H, Campagnolo D, Dayao C, Lukas RJ, Wu J, Shi F-D. Nicotine and inflammatory neurological disorders. *Acta Pharmacol Sin.* (2009) 30:715–22. doi: 10.1038/aps.2009.67
136. Crews FT, Zou J, Qin L. Induction of innate immune genes in brain create the neurobiology of addiction. *Brain Behav Immun.* (2011) 1(25 Suppl.):S4–12. doi: 10.1016/j.bbi.2011.03.003
137. Crews FT. Immune function genes, genetics, and the neurobiology of addiction. *Alcohol Res Current Rev.* (2012) 34:355–61.
138. Zou JY, Crews FT. TNF alpha potentiates glutamate neurotoxicity by inhibiting glutamate uptake in organotypic brain slice cultures: neuroprotection by NF kappa B inhibition. *Brain Res.* (2005) 1034:11–24. doi: 10.1016/j.brainres.2004.11.014
139. Mulligan MK, Ponomarev I, Hitzemann RJ, Belknap JK, Tabakoff B, Harris RA, et al. Toward understanding the genetics of alcohol drinking through transcriptome meta-analysis. *Proc Natl Acad Sci USA.* (2006) 103:6368–73. doi: 10.1073/pnas.0510188103
140. Eisenberger NI, Berkman ET, Inagaki TK, Rameson LT, Mashal NM, Irwin MR. Inflammation-induced anhedonia: endotoxin reduces ventral striatum responses to reward. *Biol Psychiatry.* (2010) 68:748–54. doi: 10.1016/j.biopsych.2010.06.010
141. Edenberg HJ, Xuei X, Wetherill LF, Bierut L, Bucholz K, Dick DM, et al. Association of NFKB1, which encodes a subunit of the transcription factor NF-kappaB, with alcohol dependence. *Hum Mol Genet.* (2008) 17:963–70. doi: 10.1093/hmg/ddm368
142. Saiz PA, Garcia-Portilla MP, Florez G, Corcoran P, Arango C, Morales B, et al. Polymorphisms of the IL-1 gene complex are associated with alcohol dependence in Spanish Caucasians: data from an association study. *Alcohol Clin Exp Res.* (2009) 33:2147–53. doi: 10.1111/j.1530-0277.2009.01058.x
143. Ökvist A, Johansson S, Kuzmin A, Bazov I, Merino-Martinez R, Ponomarev I, et al. Neuroadaptations in human chronic alcoholics: dysregulation of the NF-κB system. *PLoS ONE.* (2007) 2:e930. doi: 10.1371/journal.pone.0000930
144. Du LY, Darroch H, Keerthisinghe P, Ashimbayeva E, Astin JW, Crosier KE, et al. The innate immune cell response to bacterial infection in larval zebrafish is light-regulated. *Sci Rep.* (2017) 7:12657. doi: 10.1038/s41598-017-12842-1
145. Renthall W, Carle TL, Maze I, Covington HE, Truong H-T, Alibhai I, et al. Delta FosB mediates epigenetic desensitization of the c-fos gene after chronic amphetamine exposure. *J Neurosci.* (2008) 28:7344–9. doi: 10.1523/JNEUROSCI.1043-08.2008
146. Duclot F, Kabbaj M. The role of early growth response 1 (EGR1) in brain plasticity and neuropsychiatric disorders. *Front Behav Neurosci.* (2017) 11:35. doi: 10.3389/fnbeh.2017.00035
147. Covington HE, Lobo MK, Maze I, Vialou V, Hyman JM, Zaman S, et al. Antidepressant effect of optogenetic stimulation of the medial prefrontal cortex. *J Neurosci.* (2010) 30:16082–90. doi: 10.1523/JNEUROSCI.1731-10.2010
148. Jansson LM, Patrick SW. Neonatal abstinence syndrome. *Pediatr Clin North Am.* (2019) 66:353–67. doi: 10.1016/j.pcl.2018.12.006
149. Potter SM, Zelazo PR, Stack DM, Papageorgiou AN. Adverse effects of fetal cocaine exposure on neonatal auditory information processing. *Pediatrics.* (2000) 105:e40. doi: 10.1542/peds.105.3.e40
150. Riley E, Kopotiyenko K, Zhdanova I. Prenatal and acute cocaine exposure affects neural responses and habituation to visual stimuli. *Front Neural Circuits.* (2015) 9:41. doi: 10.3389/fncir.2015.00041
151. Hampf G, Ripberger JA, Houben T, Schmutz I, Blex C, Perreault-Lenz S, et al. Regulation of monoamine oxidase A by circadian-clock components implies clock influence on mood. *Curr Biol.* (2008) 18:678–83. doi: 10.1016/j.cub.2008.04.012
152. McClung CA, Sidiropoulou K, Vitaterna M, Takahashi JS, White FJ, Cooper DC, et al. Regulation of dopaminergic transmission and cocaine reward by the Clock gene. *Proc Nat Acad Sci USA.* (2005) 102:9377–81. doi: 10.1073/pnas.0503584102
153. Wang M, Zhong Z, Zhong Y, Zhang W, Wang H. The zebrafish period2 protein positively regulates the circadian clock through mediation of retinoic acid receptor (RAR)-related orphan receptor α (Rora). *J Biol Chem.* (2015) 290:4367–82. doi: 10.1074/jbc.M114.605022
154. Gallardo CM, Darvas M, Oviatt M, Chang CH, Michalik M, Huddy TE, et al. Dopamine receptor 1 neurons in the dorsal striatum regulate food anticipatory circadian activity rhythms in mice. *Elife.* (2014) 3:e03781. doi: 10.7554/eLife.03781.023
155. Steinlechner S, Jacobmeier B, Scherbarth F, Dernbach H, Kruse F, Albrecht U. Robust circadian rhythmicity of Per1 and Per2 mutant mice in constant light, and dynamics of Per1 and Per2 gene expression under long and short. *Photoperiods.* (2016) 17:202–9. doi: 10.1177/074873040201700303
156. Tuschl K, White RJ, Valdivia LE, Niklaus S, Bianco IH, Sealy IM, et al. Loss of slc39a14 causes simultaneous manganese deficiency and hypersensitivity in zebrafish. *bioRxiv.* (2020). doi: 10.1101/2020.01.31.921130
157. Cheon S, Park N, Cho S, Kim K. Glucocorticoid-mediated Period2 induction delays the phase of circadian rhythm. *Nucleic Acids Res.* (2013) 41:6161–74. doi: 10.1093/nar/gkt307

**Conflict of Interest:** The authors declare that the research was conducted in the absence of any commercial or financial relationships that could be construed as a potential conflict of interest.

**Publisher's Note:** All claims expressed in this article are solely those of the authors and do not necessarily represent those of their affiliated organizations, or those of the publisher, the editors and the reviewers. Any product that may be evaluated in this article, or claim that may be made by its manufacturer, is not guaranteed or endorsed by the publisher.

Copyright © 2022 Mech, Merteroglu, Sealy, Teh, White, Havelange, Brennan and Busch-Nentwich. This is an open-access article distributed under the terms of the Creative Commons Attribution License (CC BY). The use, distribution or reproduction in other forums is permitted, provided the original author(s) and the copyright owner(s) are credited and that the original publication in this journal is cited, in accordance with accepted academic practice. No use, distribution or reproduction is permitted which does not comply with these terms.



# What Have We Learned (or Expect to) From Analysis of Murine Genetic Models Related to Substance Use Disorders?

Gary Peltz\* and Yalun Tan

Department of Anesthesia, Pain and Perioperative Medicine, Stanford University School of Medicine, Stanford, CA, United States

## OPEN ACCESS

### Edited by:

Roberto Ciccocioppo,  
University of Camerino, Italy

### Reviewed by:

Candice Contet,  
The Scripps Research Institute,  
United States  
Sade Monique Spencer,  
University of Minnesota Twin Cities,  
United States

### \*Correspondence:

Gary Peltz  
gpeltz@stanford.edu

### Specialty section:

This article was submitted to  
Addictive Disorders,  
a section of the journal  
Frontiers in Psychiatry

**Received:** 12 October 2021

**Accepted:** 09 December 2021

**Published:** 12 January 2022

### Citation:

Peltz G and Tan Y (2022) What Have  
We Learned (or Expect to) From  
Analysis of Murine Genetic Models  
Related to Substance Use Disorders?  
Front. Psychiatry 12:793961.  
doi: 10.3389/fpsy.2021.793961

The tremendous public health problem created by substance use disorders (SUDs) presents a major opportunity for mouse genetics. Inbred mouse strains exhibit substantial and heritable differences in their responses to drugs of abuse (DOA) and in many of the behaviors associated with susceptibility to SUD. Therefore, genetic discoveries emerging from analysis of murine genetic models can provide critically needed insight into the neurobiological effects of DOA, and they can reveal how genetic factors affect susceptibility drug addiction. There are already indications, emerging from our prior analyses of murine genetic models of responses related to SUDs that mouse genetic models of SUD can provide actionable information, which can lead to new approaches for alleviating SUDs. Lastly, we consider the features of murine genetic models that enable causative genetic factors to be successfully identified; and the methodologies that facilitate genetic discovery.

**Keywords:** mouse genetic models, substance use disorder, neurobiologic basis, computational genetics, opiate addiction

## WHY STUDY MURINE GENETIC MODELS OF SUD?

We believe that the relationship between murine models and human diseases (or biomedical traits) resembles that between a small Cessna airplane and a large 787 jet plane. You can learn most of what you need to know about the fundamental principles of aviation by studying the Cessna, but this will not enable you to pilot the 787. The 787 has many more capabilities, much more complex and computer-controlled systems, and multiple redundancies that are essential for its function than are contained within a Cessna. Nevertheless, you wouldn't be able to pilot a 787 without knowing the aviation principals that are learned by studying the Cessna. Similarly, studying the mouse has revealed the basic principles underlying many areas of human physiology and pathobiology. Within the neurobiology realm, many of the mechanisms and circuits utilized for learning, memory, cognition, and the effects that drugs have on these processes have been uncovered through analysis of mouse models. However, since laboratory mice function within a very limited behavioral domain and lack some of the neural pathways that regulate human behavior, many of the complex factors mediating human psychiatric diseases cannot be understood by analyzing rodent models. The aviation analogy is quite appropriate for SUDs. Rodent models are ideal for understanding DOA neurobiology and for providing information about how drug seeking behaviors are generated; but they provide a very poor substrate for investigating the impact of that

socioeconomic and psychosocial factors have on triggering relapse. This is an important limitation since human drug addiction proceeds through a three-stage cycle whose intensity increases over time, and each stage results from DOA-induced changes in brain circuits (1–3). The first stage (binge/intoxication) is mediated by DOA-induced reward sensations in the brain. The second stage (withdrawal/negative affect) is characterized by an increased threshold for experiencing the reward sensation, and a withdrawal state develops when the DOA cannot be obtained. The third stage (preoccupation-relapse) is characterized by chronic relapse, which is triggered by environmental and emotional cues. Chronic DOA ingestion induces neurochemical changes that lessen the reward sensation that was experienced after DOA ingestion during the initial stage, which increases the stress and compulsivity associated with chronic drug addiction (2, 3). Mouse models are ideal for analyzing the first two stages of the addiction cycle, which are mediated by neurobiological changes that develop after acute (1st stage) or repeated (2nd stage) exposure to a DOA. In contrast, mice provide a less optimal model for analyzing 3rd stage phenomena, which involves responses to environmental triggers and far more complex DOA-induced changes that impact a wider range of neural circuits. Most current research and treatment efforts focus on the later stages of drug addiction (3), which are associated with drug craving and relapse in individuals with SUD of long duration. It could be more productive to increase the research effort devoted to developing prevention strategies, which target the early stage of drug addiction (4). To do this, we must develop a deeper understanding of DOA-induced changes at the synaptic level. In other words, to fly the jet plane (i.e., develop effective prevention or treatment methods for SUDs) we must use murine genetic models of SUD to understand the underlying principles of aviation (i.e., the mechanisms mediating SUDs).

Here, we examine what we have learned from our prior analyses of murine genetic models of responses related to SUD. First, we discuss a murine genetic model of a drug-induced toxicity to indicate the different types of genetic factors that can be identified. We then review the genetic factors identified from our prior analyses of murine genetic models of opiate responses. Lastly, we consider the features of murine models that enable causative genetic factors to be successfully identified; and the methodologies that can facilitate genetic discovery.

## AN ILLUSTRATIVE EXAMPLE

Analysis of a murine genetic model of a drug-induced (haloperidol) CNS toxicity illustrates the potential outcomes that could emerge when evaluating murine genetic models of SUD because drug addiction (in many ways) is a toxicity

caused by DOAs. Although haloperidol is an effective anti-psychotic agent, it causes a treatment-limiting side effect in most treated subjects, which is very debilitating Parkinsonian-like extrapyramidal symptoms. When we began our studies of haloperidol induced toxicity (HIT), genetic susceptibility factors for this toxicity were completely unknown. Therefore, we analyzed a murine genetic model of HIT where the inbred strains exhibited very large and reproducible differences in susceptibility to HIT. Our analysis revealed that susceptibility was quantitatively determined by two distinct genetic loci: one encoded a pharmacokinetic factor and the other a pharmacodynamic factor. The pharmacokinetic factor was allelic variation within a murine ABC-drug efflux transporter (*Abcb5*) that caused susceptible strains to have higher brain haloperidol levels; and a genetic association study in a haloperidol-treated human cohort identified human *ABCB5* alleles as susceptibility determinants for HIT (5). The pharmacodynamic susceptibility factor was allelic variation within pantetheinase genes (*Vnn1*, *Vnn3*) that impaired the biosynthesis of a protective metabolite (cysteamine) (6). While discovery of the murine pharmacokinetic factor led to the identification of a pharmacogenetic susceptibility factor for human HIT (5); characterization of the murine pharmacodynamic factor led to a potential new treatment (co-administration of a cysteamine metabolite) that could completely prevent haloperidol's treatment-limiting toxicity (6). Thus, analysis of a murine model generated information that produced a potential new method for preventing this toxicity.

## MURINE SUD MODELS

Like haloperidol, murine opiate response models hold great promise for genetic discovery. The inbred strains exhibit very large and heritable differences in their responses to opiates, which include the development of opioid analgesia, tolerance, dependence, and hyperalgesia (7–10). We provide a brief description of several rodent SUD models here, but more detailed information can be obtained from recent reviews covering rodent models for CPP (11), opioid (12, 13) and cocaine relapse (14), and opioid abstinence (15). The genetic models of SUD discussed here are ones where various responses are measured after DOAs are administered to panels of inbred mouse strains. For example, physical dependence is a key measure of addiction that is modeled by the jumping behavior that is displayed by opiate-dependent mice after administration of a potent opioid receptor antagonist (naloxone). This response is a highly heritable trait among inbred mouse strains (16) that is independent of differences in the method or duration of opiate administration (17, 18) (**Figure 1**). Of importance, naloxone-precipitated opiate withdrawal (NPOW) has also been used to quantify opioid dependence in human volunteers (19). In addition to their analgesic action, opioids also induce a paradoxical hypersensitivity to painful stimuli during opioid withdrawal (opiate-induced hyperalgesia, OIH); and there are large and heritable differences in the extent of OIH that develops among the inbred strains (7, 20). Drug seeking behavior is observed when abstaining addicts are confronted

**Abbreviations:** CSA, cocaine self-administration; DOA, drugs of abuse; GWAS, genome wide association study; HBCGM, haplotype based computational genetic mapping; HIT, haloperidol induced toxicity; mCPP, morphine-induced conditioned place preference; NPOW, naloxone precipitated opiate withdrawal; NAC, nucleus accumbens; SUD, substance use disorder; VTA, ventral tegmental area.

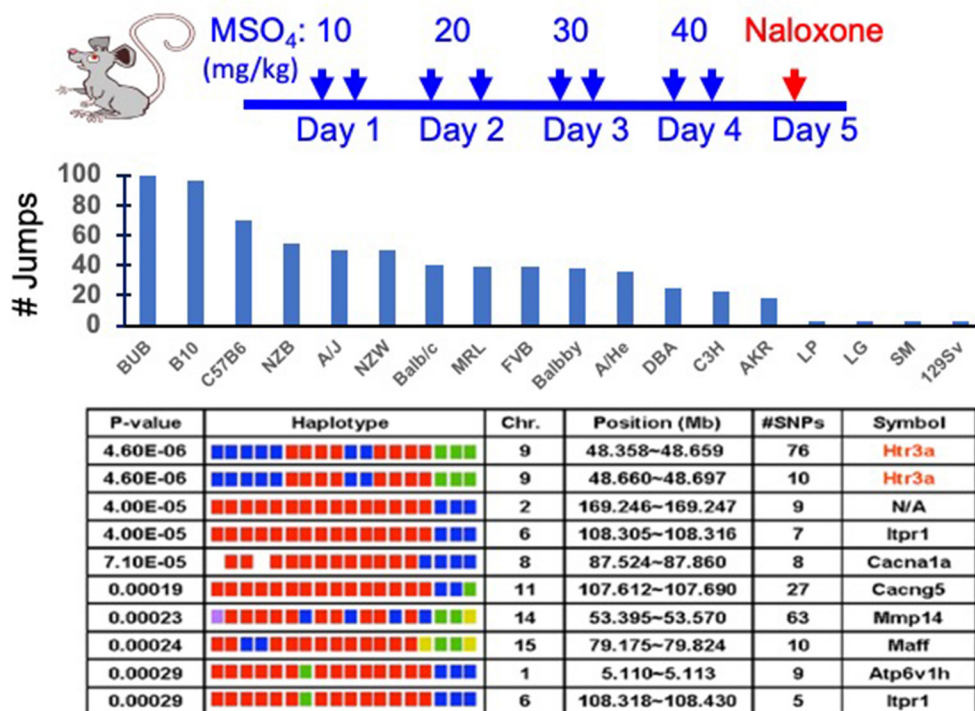


**FIGURE 1 |** Analysis of a murine genetic model of naloxone precipitated opiate withdrawal (NPOW). **(Top)** Eighteen strains (eight mice per strain) were treated for four days with morphine to establish physical dependence. On the 5th day, the number of jumps made during the 15-min period after naloxone injection was measured to indicate the degree of opioid dependence. **(Middle)** The data represent the mean number of jumps for each indicated strain. **(Bottom)** The NPOW data (mean number of jumps for each strain) was analyzed by haplotype based computational genetic mapping. The 10 most strongly correlated haplotype blocks are shown. For each block, the chromosomal location, number of SNPs within a block and its gene symbol are listed. For each gene, the haplotypes are represented by a colored block, and the blocks are presented in the same rank order as the phenotypic data. Strains sharing the same haplotype have the same-colored block. The calculated *p*-value measures the probability that the strain groupings within a block would have the same degree of association with the phenotypic data by random chance. The genetic effect indicates the fraction of the inter-strain variance that is potentially attributable to the haplotype.

with environmental stimuli associated with their drug-taking behavior. Some features of the behavior of human opiate addicts can be modeled in mice using the morphine-induced conditioned place preference (mCPP) test (21–24). In the mCPP paradigm, morphine administration is paired with a particular spatial environment, and then a mouse's preference for this environment is measured to evaluate the rewarding properties of morphine. The OIH, NPOW and mCPP models measure phenomena in mice that are associated with the 2nd stage of the addiction cycle. OIH and withdrawal symptoms can serve as driving forces that promote relapse or escalation of drug intake. As such, the genetic factors identified from analysis of these models are ones that influence susceptibility to an SUD. Behavioral sensitization paradigms, which measure an increase in drug-induced behavior that gradually develops after a period of repeated DOA exposure, can also be used to study cross-sensitization amongst different DOA. Cross-sensitization studies using behavioral sensitization paradigms has identified the neural mechanisms and pathways that are shared by different types of DOA (25, 26). However, since these models are based on non-contingent (i.e., experimenter-initiated) drug administration, they lack face validity, which is the degree to which the model measures what it claims to. This aspect

of addiction could be better studied using contingent models that assess the motivation for drug-taking or the reinstatement of drug-seeking behaviors (27).

Inbred strains also exhibit substantial and heritable differences in their cocaine responses, which include the extent of cocaine-induced locomotor activation (28, 29), cocaine self-administration (CSA) (30–33); and SUD risk-related behaviors that include impulsivity, and sensitivity to drug reward (33). Of the various addiction-related phenotypes studied in mice, the gold standard is operant self-administration (34, 35), where the subjects voluntarily and actively seek and consume drugs with rewarding properties. Rodents, like humans, experience the rewarding effects of a DOA, and they will engage in behaviors to procure them. To measure CSA, mice are fitted with an indwelling jugular catheter and placed in an operant conditioning box where they must depress a lever to trigger cocaine infusions. The rate of CSA reflects the reinforcing potential of cocaine (36). The substantial differences in CSA among the inbred strains (30–33) reflects their different propensities to abuse cocaine (37–39). There are obvious benefits from using a contingent model like CSA, since it more accurately recapitulates the drug-taking and drug-seeking behaviors of

humans. The motivation (the reinforcing properties of the drug reward) as well as the specificity (drug vs. alternative reward) for drug-taking behaviors can also be evaluated in addition to measuring the quantity and frequency of drug administration (27, 40, 41). Thus, just as in the human population, inbred mouse strains exhibit substantial differences in their DOA responses; and characterization of the genetic basis for these differences will help us to understand the neurobiological effects of DOA and will enable us to understand how they generate addiction-related behaviors.

## LESSONS LEARNED FROM CHARACTERIZING MURINE OPIATE RESPONSE FACTORS

As with HIT, multiple studies indicate that differences in the various types of opiate responses exhibited by inbred strains are determined by genetic factors that alter opiate pharmacokinetics and by pharmacodynamic factors that alter the host response to opiates. When a murine genetic model of opioid-induced hyperalgesia (OIH) was analyzed, we discovered that genetic variation within the *P-glycoprotein transporter* (*Abcb1b*) contributed to inter-strain differences in this opiate response (8). Analysis of the effect of pharmacologic inhibitors and of *Abcb1a/1b* knockout mice confirmed that P-glycoprotein function modulates narcotic-induced pain sensitization, as well as the tolerance and physical dependence that develops during opiate treatment. The brain morphine level correlated with the extent of OIH, which indicated a murine pharmacokinetic factor influenced multiple opiate pharmacodynamic responses by altering brain opiate levels. While pharmacokinetic factors are important, characterization of genetic factors affecting opiate pharmacodynamic responses are more likely to generate new approaches for preventing opiate addiction. For example, we analyzed another murine genetic model for OIH and identified the beta-2 adrenergic receptor (*Adrb2*) as a genetic locus contributing to the inter-strain response difference. This response was markedly diminished in *Adrb2* knockout mice and was reversed by administration of a commonly used *Adrb2* antagonist, which suggested a novel strategy for reducing OIH (7). We also found that genetic variation within genes encoding the *Netrin-1 receptor* (*Dcc*) (42) and *multi-PDZ-domain protein* (*Mpdz* that encodes MUPP1) (20) also contributed to inter-strain differences in the extent of tolerance, dependence and OIH that develops after repeated opiate exposure.

The latter two genetic findings indicate that opiate-induced changes at the synaptic level influence opiate responses. For example, *dcc* encodes a receptor for an axonal guidance protein (netrin-1) that plays a role in synaptic plasticity in the adult brain (43–46); and *dcc* itself plays a role in axonal differentiation and synaptogenesis in the developing brain (44, 46–48). Similarly, MUPP1 expression is localized to CNS synapses (49). Genetic variation within *Mpdz* has been associated with alcohol and sedative dependence in both mice and humans, which suggest that it may regulate responses to multiple DOA (50–52).

MUPP1 may enhance the efficiency of neuronal signaling by bringing key intracellular signaling molecules into proximity with cell surface receptors (NMDA receptor) at the post-synaptic membrane (53). By this mechanism, NMDA receptor activation can trigger a MUPP1-facilitated cascade that leads to membrane insertion of AMPA receptor/channels, and persistent facilitation of glutamate signaling. This pathway may contribute to long-term potentiation (LTP) or alternative forms of enhanced AMPA receptor mediated activity (54). Pharmacological blockade of NMDA receptors and genetic deletion of NMDA receptor subunits has been shown to limit tolerance and OIH in mice and rats (55, 56); and the NR2B subunits of NMDA receptors mediate opiate tolerance (57, 58). The *dcc* and *Mpdz* findings also demonstrate that even when an identified causative genetic factor is not a pharmaceutical target, interacting proteins or proteins within an effected pathway may provide new therapeutic targets for SUD.

## TRANSLATION OF A MOUSE GENETIC DISCOVERY

Our most impactful discovery to date emerged from analysis of a murine genetic model that measured the naloxone-precipitated opiate withdrawal (NPOW) response after 4 days of morphine administration in 18 inbred strains (9). Allelic variation within the *Htr3a* gene encoding the 5HT<sub>3A</sub>R was most highly correlated with the severity of the NPOW response (**Figure 1**). Consistent with this result, *Htr3a* mRNA and protein expression was significantly reduced in a strain-specific manner after morphine administration. Moreover, administration of a selective 5HT<sub>3A</sub>R antagonist (ondansetron) reduced NPOW [and opioid-induced hyperalgesia (OIH)] in a dose-dependent fashion; and ondansetron co-administration with morphine impaired the mCPP response, which indicated that ondansetron eliminated the reinforcing effects of morphine (9). Thus, ondansetron also shows promise for preventing opiate dependence. The murine finding was tested in humans by measuring the effect of ondansetron on experimentally induced NPOW in healthy male volunteers. Ondansetron pre-treatment caused a 76% decrease ( $p = 0.03$ ) in the NPOW in the volunteers, and it decreased all 11 of the measured manifestations of opiate withdrawal. *Since the ondansetron effect observed in mice translated to humans, it is likely of fundamental importance.* In a separate study (59), we demonstrated that another 5HT<sub>3A</sub>R antagonist (palonosetron) also prevented NPOW symptoms in normal human subjects and that a pretreatment that combined palonosetron with a commonly used antihistamine (hydroxyzine) caused a 95% reduction ( $p = 0.014$ ) in withdrawal manifestations. The effect of the combination pretreatment was significant even when compared with that of palonosetron alone ( $p = 0.012$ ) (59). *These results demonstrated that a 5HT<sub>3A</sub>R antagonist can be combined with another agent to further reduce opioid withdrawal severity.* Ondansetron is a widely used medication with a well-established safety record. After characterizing its pharmacokinetic properties in pregnant

women and in their neonates (60), we are now performing a placebo-controlled clinical trial investigating whether a brief period of ondansetron treatment can prevent the development of opiate withdrawal symptoms in infants with prenatal opioid exposure (61, 62). This study, which has involved seven medical centers, currently represents the only attempt to develop a preventative treatment for a severe condition that affects the infants of mothers with SUD.

## GENETIC ANALYSIS METHODS

Identification of the genetic factors responsible for DOA response differences among the inbred strains is an essential step for obtaining critically needed information about the neurobiological mechanisms underlying addiction. Only after a genetic factor is identified can the involved pathways be examined, which is required for identifying potential targets for new treatments for SUD. We have found that two inter-related features of a murine genetic model facilitate genetic discovery when genome wide association study (GWAS) methods are used for their analysis. (i) The DOA response must be measured across a large number (preferably  $\geq 15$ ) of inbred strains. When a small number of strains are evaluated, the actual extent of the phenotypic variation present in the mouse population is under-estimated (63, 64). There are >450 available inbred strains (65); and usually only a few strains will exhibit an outlier phenotype for most responses. Unfortunately, the vast majority of murine GWAS performed to date analyze a relatively small number of strains (66). (ii) Since a key factor for successful genetic discovery is when strains that exhibit outlier responses are included in the analysis, the genetic analysis should not begin until after inbred strains that exhibit extreme DOA responses (i.e., top or bottom 10% and are >3-fold above (or below) the mean response of the other strains) have been identified. Preferably, the strain panel should include at least two strains that exhibit an extreme phenotypic response. Other investigators have used one or more of the various recombinant inbred (RI) strain panels for genetic mapping studies, which include: the Hybrid Mouse Diversity Panel (30 founder strains) (67, 68); the Diversity Outbred (69) and Collaborative Cross (70) panels (eight strains); and the BXD RI panel (71) (two strains). While these RI panels have proven to be useful for genetic mapping, they have a limitation. We do not know in advance which strains will exhibit outlier responses to current (or future) DOA that contribute to 21st century addiction-related public health problems, and the strains exhibiting outlier responses may not be among the founder strains for the existing RI panels. To use another disease as an example, Type 2 Diabetes Mellitus (T2DM), and its principal risk factor (obesity) have become a major 21st century public health problem (72); but the TallyHo strain is not among the founder strains used to construct any of the current RI panels. Nevertheless, TallyHo provides a valuable murine model for T2DM and obesity because it spontaneously develops hyperlipidemia, hyperglycemia, insulin resistance, and glucose intolerance (73, 74). A genetic analysis of diabetes-related

traits among the inbred strains would miss important disease-causing genetic variants if the TallyHo strain was not included in the analysis.

While many different methods can be used to analyze GWAS data obtained from inbred strains, we have successfully used haplotype based computational genetic mapping (HBCGM) to identify murine genetic factors underlying 22 biomedical traits (5–9, 18, 20, 42, 64, 75–90). In an HBCGM experiment, a property of interest is measured in a panel of available mouse strains whose genomes have been sequenced; and then genetic factors are computationally predicted by identifying genomic regions (haplotype blocks) where the pattern of within-block genetic variation correlates with the distribution of the phenotypic responses among the strains (63, 64, 75) (**Figure 1**). However, a major barrier to genetic discovery is caused by the fact that HBCGM analyses generate many false positive associations, which appear along with the causative genomic region, for the trait response difference. This can make it difficult to identify the true causative genetic factor for a biomedical trait difference. Because of the ancestral relatedness of the inbred strains, some of the false positives are within genomic regions that are commonly inherited (a property referred to as “population structure”). Statistical methods have been developed to reduce the false discovery rate in GWAS studies by correcting for the population structure that exists that exists in humans (91, 92), plants (93), and mice (94). While these correction methods have substantial utility for analyzing human GWAS results, we have recently shown that population structure correction methods are less useful when analyzing murine GWAS results; and moreover, their use could increase the chance that a true causative genetic factor will be discarded (95). In brief, even though multiple genomic regions have a shared ancestral inheritance, one of them may be responsible for a phenotypic difference. To overcome this problem, we use filtering methods to identify the true causative factor from among the many correlated genomic regions. We have previously identified causative genetic factors from among the many genes with correlated allelic patterns by applying orthogonal criteria (64), which include gene expression, metabolomic (78), or curated biologic data (96), or by examining candidates within previously identified genomic regions (76, 77). This approach can provide results that are superior to that of a typical GWAS, which only uses a single highly stringent criterion to identify candidates. We recently analyzed 8,462 publicly available datasets of biomedical responses (1.52 M individual datapoints) measured in panels of inbred mouse strains. We found that our ability to identify the genetic basis for the biomedical trait differences among the inbred strains was enhanced when structured automated methods were used for filtering the genes output by HBCGM analyses (66). In that study, we selected correlated genes that were expressed in the target organ for the biomedical trait, had high impact SNP alleles, and where the published literature indicated that the gene had a functional relationship with the analyzed trait. Although we are in the early stage of using automated methods for assessing genetic results, we believe that the results from that study (66) provide an early indication of how “*augmented intelligence*” can be used to facilitate genetic discovery. For analysis of mouse

genetic models for SUD, DOA-induced gene expression changes occurring in brain regions, which are known to be important sites for DOA responses (NAc, VTA, mPFC), can be analyzed to facilitate identification of causative genetic factors.

## FUTURE DIRECTIONS

We believe that genetic factors affecting DOA responses will be shared with those impacting learning and memory pathways (97). Multiple lines of evidence indicate that DOA “hijack” the neural circuits used for learning and memory (98–100). An organism’s ability to learn and form memories is mediated by changes within neurons and brain circuits that are produced by changes in neuronal gene expression patterns, which are activated in response to stimuli (101). Synaptic plasticity, which are activity-based changes in synaptic transmission in neuronal networks, is a major component of learning and memory (102). Changes in presynaptic glutamate release as well as postsynaptic ionotropic glutamate receptor expression and subunit composition are associated with DOA-induced changes in neuroplasticity (103). Rapidly occurring changes in synaptic plasticity mediate DOA-induced behavioral effects, and they contribute to the acquisition of instrumental learning. By this mechanism, DOA-induced changes in synaptic plasticity can produce abnormally strong addiction-related memories. The effect of DOA on long-term potentiation (LTP) and long-term depression (LTD) has been well-studied in VTA dopaminergic neurons (104–106). For instance, cocaine exposure increases the AMPA/NMDA receptor ratio, alters GluA2-containing AMPARs, and decreases NMDA receptor functionality in VTA dopaminergic neurons (107–109). Structural plasticity, which is the formation of new

synaptic boutons and dendritic spines, is also observed after DOA exposure (110). Increased dendritic spine density in the NAc and PFC are commonly observed changes in synaptic connections that contribute to the sequela of drug use (111–113). Circuit remodeling also occurs with DOA-induced dopamine-mediated responses. Specifically, DOA act on the mesolimbic dopaminergic pathway, which include the ventral tegmental area (VTA), nucleus accumbens (NAc) and associated limbic regions (114). The medial prefrontal cortex (mPFC), which exerts top-down excitatory glutamatergic control over the NAc and other downstream subcortical regions, might contribute to maladaptive behaviors (115). Different subregions of the mPFC (i.e., dorsal, and ventral infralimbic subregions) can both drive and inhibit drug seeking behaviors depending on the drug history and behavioral context (116). Dysfunction in these regions, such as hypoactivity or selective strengthening of the PFC-striatal pathway, could contribute to compulsion in drug addiction models (116, 117). Therefore, studying DOA-induced effects on synaptic and structural plasticity, as well as characterizing changes in neuronal circuitries, could greatly increase our understanding of DOA responses. Moreover, given the overlap between the neural circuits used for learning and those impacted by DOA, it is likely that there will be some degree of overlap between the genetic factors affecting responses to different types of abused drugs. Hence, it is also important to characterize the impact that genetic factors identified by analysis of mouse genetic models have on responses to different types of DOAs.

In addition to the transcriptional changes associated with neuronal plasticity, chromatin modifications are a major part of learning and memory processes (118–121). Much correlational evidence links changes in histones (predominantly acetylation)

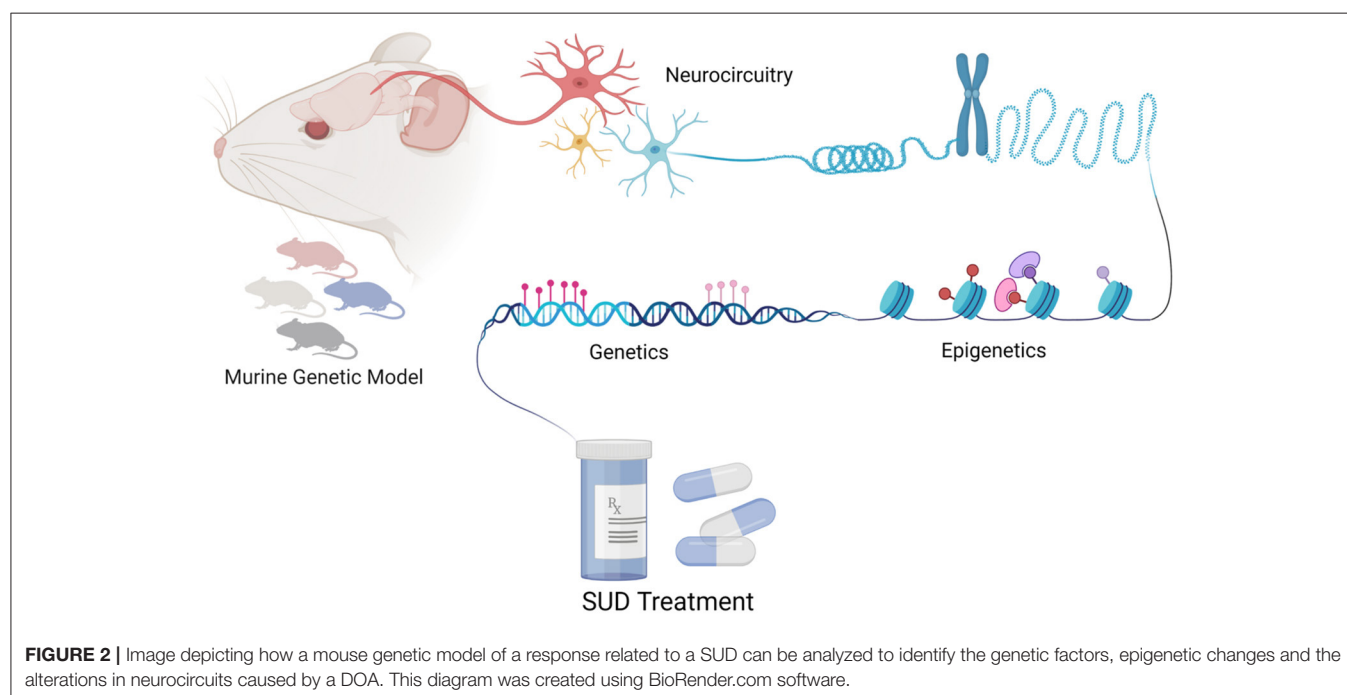


**FIGURE 2 |** Image depicting how a mouse genetic model of a response related to a SUD can be analyzed to identify the genetic factors, epigenetic changes and the alterations in neurocircuits caused by a DOA. This diagram was created using BioRender.com software.

with short and long-term memory generation (121–123). Since the addiction state persists long after the period of DOA ingestion, DOA-induced epigenetic modifications are highly likely to be key contributors to addiction. Hence, DOA-induced chromatin structure changes in specific brain regions should be characterized along with DOA-induced transcriptional changes. The combined characterization of transcriptional and chromatin structure changes in the developing human brain has provided new insight into the mechanisms regulating brain development, and possibly into the pathobiology of psychiatric diseases (124). The methodology for simultaneously characterizing DOA-induced epigenetic and transcriptional changes in brain is now readily available (124). Characterization of DOA-induced chromatin structure changes in specific brain regions will provide the orthogonal information, which will facilitate the identification of genetic factors affecting addiction susceptibility. To do this, chromosomal regions with DOA-induced epigenetic changes can be examined to determine if they overlap with haplotype blocks that contain alleles that correlate with the pattern of DOA responses among the inbred strains. Also, linking genetic and epigenetic mechanisms with changes in synaptic circuit plasticity could lead to a deeper understanding of DOA-induced neuroadaptations (115) (**Figure 2**). For instance, DOA

exposure produces region-specific epigenetic changes, which include an increase in global histone acetylation in the NAc, while this is reduced in the VTA (125, 126). Studying transcriptional and epigenetic changes in specific neuronal subpopulations is also important for understanding neural mechanisms and identifying novel therapeutic targets for prevention of addiction (127, 128). Thus, we believe that murine genetic models can be used to simultaneously characterize DOA-induced epigenetic and transcriptional changes, and for identifying genetic factors that alter DOA responses. Thus, murine models can provide the critically needed information that is required for successfully landing the airplanes whose flight path has been adversely affected by SUDs.

## AUTHOR CONTRIBUTIONS

All authors listed have made a substantial, direct, and intellectual contribution to the work and approved it for publication.

## FUNDING

This work was supported by a NIH/NIDA award (5U01DA04439902) to GP.

## REFERENCES

- Koob GF, Ahmed SH, Boutrel B, Chen SA, Kenny PJ, Markou A, et al. Neurobiological mechanisms in the transition from drug use to drug dependence. *Neurosci Biobehav Rev.* (2004) 27:739–49. doi: 10.1016/j.neubiorev.2003.11.007
- Koob GF. Negative reinforcement in drug addiction: the darkness within. *Curr Opin Neurobiol.* (2013) 23:559–63. doi: 10.1016/j.conb.2013.03.011
- Koob GF, Volkow ND. Neurobiology of addiction: a neurocircuitry analysis. *Lancet Psychiatry.* (2016) 3:760–73. doi: 10.1016/S2215-0366(16)00104-8
- Peltz G, Sudhof TC. The neurobiology of opioid addiction and the potential for prevention strategies. *JAMA.* (2018) 319:2071–2. doi: 10.1001/jama.2018.3394
- Zheng M, Zhang H, Dill DL, Clark JD, Tu S, Yablonovitch AL, et al. The role of Abcb5 alleles in susceptibility to haloperidol-induced toxicity in mice and humans *PLoS Med.* (2015) 12:e1001782. doi: 10.1371/journal.pmed.1001782
- Zhang H, Zheng M, Wu M, Xu D, Nishimura T, Nishimura Y, et al. A Pharmacogenetic Discovery: Cystamine Protects against Haloperidol-Induced Toxicity and Ischemic Brain Injury. *Genetics.* (2016) 203:599–609. doi: 10.1534/genetics.115.184648
- Liang D, Liao G, Wang J, Usuka J, Guo YY, Peltz G, et al. A genetic analysis of opioid-induced hyperalgesia in mice *Anesthesiology.* (2006) 104:1054–62. doi: 10.1097/00000542-200605000-00023
- Liang DY, Liao G, Lighthall G, Peltz G, Clark JD. Genetic variants of the P-glycoprotein gene abcb1b modulate opioid-induced hyperalgesia, tolerance and dependence. *Pharmacogenet Genomics.* (2006) 16:825–35. doi: 10.1097/01.fpc.0000236321.94271.f8
- Chu LF, Liang D-Y, Li X, Sahbaie P, D'arcy N, Liao G, et al. From mouse to man: the 5-HT<sub>3</sub> receptor modulates physical dependence on opioid narcotics. *Pharmacogenet. Genomics.* (2009) 19, 193–205. doi: 10.1097/FPC.0b013e328322e73d
- Liang DY, Li X, Clark JD. 5-hydroxytryptamine type 3 receptor modulates opioid-induced hyperalgesia and tolerance in mice. *Anesthesiology.* (2011) 114:1180–9. doi: 10.1097/ALN.0b013e32820efb19
- Mckendrick G, Graziane NM. Drug-induced conditioned place preference and its practical use in substance use disorder research. *Front Behav Neurosci.* (2020) 14:582147. doi: 10.3389/fnbeh.2020.582147
- Golden SA, Jin M, Shaham Y. Animal models of (or for) aggression reward, addiction, and relapse: behavior and circuits. *J Neurosci.* (2019) 39:3996–4008. doi: 10.1523/JNEUROSCI.0151-19.2019
- Reiner DJ, Fredriksson I, Lofaro OM, Bossert JM, Shaham Y. Relapse to opioid seeking in rat models: behavior, pharmacology and circuits. *Neuropsychopharmacology.* (2019) 44:465–77. doi: 10.1038/s41386-018-0234-2
- Farrell MR, Schoch H, Mahler SV. Modeling cocaine relapse in rodents: behavioral considerations and circuit mechanisms. *Prog Neuropsychopharmacol Biol Psychiatry.* (2018) 87:33–47. doi: 10.1016/j.pnpbp.2018.01.002
- Welsch L, Bailly J, Darcq E, Kieffer BL. The negative affect of protracted opioid abstinence: progress and perspectives from rodent models. *Biol Psychiatry.* (2020) 87:54–63. doi: 10.1016/j.biopsych.2019.07.027
- Kest B, Palmese CA, Juni A, Chesler EJ, Mogil JS. Mapping of a quantitative trait locus for morphine withdrawal severity. *Mamm Genome.* (2004) 15:610–7. doi: 10.1007/s00335-004-2367-3
- Kest B, Hopkins E, Palmese CA, Adler M, Mogil JS. Genetic variation in morphine analgesic tolerance: a survey of 11 inbred mouse strains. *Pharmacol Biochem Behav.* (2002) 73:821–8. doi: 10.1016/S0091-3057(02)00908-5
- Liang DY, Guo T, Liao G, Kingery WS, Peltz G, Clark JD. Chronic pain and genetic background interact and influence opioid analgesia, tolerance, and physical dependence. *Pain.* (2006) 121:232–40. doi: 10.1016/j.pain.2005.12.026
- Bickel WK, Stitzer ML, Wazlavak BE, Liebson IA. Naloxone-precipitated withdrawal in humans after acute morphine administration. *NIDA Res Monogr.* (1986) 67:349–54.
- Donaldson R, Sun Y, Liang D-Y, Zheng M, Sahbaie P, Dill DL, et al. The multiple PDZ domain protein Mpdz/MUPP1 regulates opioid tolerance and opioid-induced hyperalgesia. *BMC Genomics.* (2016) 17. doi: 10.1186/s12864-016-2634-1
- Bardo MT, Rowlett JK, Harris MJ. Conditioned place preference using opiate and stimulant drugs: a meta-analysis. *Neurosci Biobehav Rev.* (1995) 19:39–51. doi: 10.1016/0149-7634(94)00021-R
- Tzschentke TM. Measuring reward with the conditioned place preference paradigm: a comprehensive review of drug effects,

- recent progress and new issues. *Prog Neurobiol.* (1998) 56:613–72. doi: 10.1016/S0304-0082(98)00060-4
23. Tzschentke TM. Measuring reward with the conditioned place preference (CPP) paradigm: update of the last decade. *Addict Biol.* (2007) 12:227–462. doi: 10.1111/j.1369-1600.2007.00070.x
  24. Aguilar MA, Rodriguez-Arias M, Minarro J. Neurobiological mechanisms of the reinstatement of drug-conditioned place preference. *Brain Res Rev.* (2009) 59:253–77. doi: 10.1016/j.brainresrev.2008.08.002
  25. Vanderschuren LJ, Tjon GH, Nestby P, Mulder AH, Schoffelmeier AN, De Vries TJ. Morphine-induced long-term sensitization to the locomotor effects of morphine and amphetamine depends on the temporal pattern of the pretreatment regimen. *Psychopharmacology (Berl).* (1997) 131:115–22. doi: 10.1007/s002130050273
  26. Vanderschuren LJ, Schmidt ED, De Vries TJ, Van Moorsel CA, Tilders FJ, Schoffelmeier AN. A single exposure to amphetamine is sufficient to induce long-term behavioral, neuroendocrine, and neurochemical sensitization in rats. *J Neurosci.* (1999) 19:9579–86. doi: 10.1523/JNEUROSCI.19-21-09579.1999
  27. Kuhn BN, Kalivas PW, Bobadilla AC. Understanding addiction using animal models. *Front Behav Neurosci.* (2019) 13:262. doi: 10.3389/fnbeh.2019.00262
  28. Eisener-Dorman AF, Grabowski-Boase L, Tarantino LM. Cocaine locomotor activation, sensitization and place preference in six inbred strains of mice. *Behav Brain Funct.* (2011) 7:29. doi: 10.1186/1744-9081-7-29
  29. Wiltshire T, Ervin RB, Duan H, Bogue MA, Zamboni WC, Cook S, et al. Initial locomotor sensitivity to cocaine varies widely among inbred mouse strains. *Genes Brain Behav.* (2015) 14:271–80. doi: 10.1111/gbb.12209
  30. Cervantes MC, Laughlin RE, Jentsch JD. Cocaine self-administration behavior in inbred mouse lines segregating different capacities for inhibitory control. *Psychopharmacology (Berl).* (2013) 229:515–25. doi: 10.1007/s00213-013-3135-4
  31. Roberts AJ, Casal L, Huitron-Resendiz S, Thompson T, Tarantino LM. Intravenous cocaine self-administration in a panel of inbred mouse strains differing in acute locomotor sensitivity to cocaine. *Psychopharmacology (Berl).* (2018) 235:1179–89. doi: 10.1007/s00213-018-4834-7
  32. Bagley JR, Khan AH, Smith DJ, Jentsch JD. Extreme phenotypic diversity in operant responding for an intravenous cocaine or saline infusion in the hybrid mouse diversity panel. *BioRxiv [Preprint]*. (2021). Available Online at: <https://www.biorxiv.org/content/10.1101/2021.02.03.429584v1>
  33. Bailey LS, Bagley JR, Dodd R, Olson A, Bolduc M, Philip VM, et al. Heritable variation in locomotion, reward sensitivity and impulsive behaviors in a genetically diverse inbred mouse panel. *BioRxiv [Preprint]*. (2021). doi: 10.1111/gbb.12773
  34. Weeks JR, Collins RJ. Factors affecting voluntary morphine intake in self-maintained addicted rats. *Psychopharmacologia.* (1964) 6:267–79. doi: 10.1007/BF00413156
  35. Collins RJ, Weeks JR, Cooper MM, Good PI, Russell RR. Prediction of abuse liability of drugs using IV self-administration by rats. *Psychopharmacology (Berl).* (1984) 82:6–13. doi: 10.1007/BF00426372
  36. Woolverton WL. Determinants of cocaine self-administration by laboratory animals. *Ciba Found Symp.* (1992) 166:149–161; discussion 161–144. doi: 10.1002/9780470514245.ch9
  37. Jentsch JD, Taylor JR. Impulsivity resulting from frontostriatal dysfunction in drug abuse: implications for the control of behavior by reward-related stimuli. *Psychopharmacology (Berl).* (1999) 146:373–90. doi: 10.1007/PL00005483
  38. de Wit H, Phillips TJ. Do initial responses to drugs predict future use or abuse? *Neurosci Biobehav Rev.* (2012) 36:1565–76. doi: 10.1016/j.neubiorev.2012.04.005
  39. Piazza PV, Deroche-Gamonet V. A multistep general theory of transition to addiction. *Psychopharmacology (Berl).* (2013) 229:387–413. doi: 10.1007/s00213-013-3224-4
  40. Richardson NR, Roberts DC. Progressive ratio schedules in drug self-administration studies in rats: a method to evaluate reinforcing efficacy. *J Neurosci Methods.* (1996) 66:1–11. doi: 10.1016/0165-0270(95)00153-0
  41. Venniro M, Zhang M, Caprioli D, Hoots JK, Golden SA, Heins C, et al. Volitional social interaction prevents drug addiction in rat models. *Nat Neurosci.* (2018) 21:1520–9. doi: 10.1038/s41593-018-0246-6
  42. Liang DY, Zheng M, Sun Y, Sahbaie P, Low SA, Peltz G, et al. The Netrin-1 receptor DCC is a regulator of maladaptive responses to chronic morphine administration. *BMC Genomics.* (2014) 15:345. doi: 10.1186/1471-2164-15-345
  43. Bradford D, Cole SJ, Cooper HM. Netrin-1: diversity in development. *Int J Biochem Cell Biol.* (2009) 41:487–93. doi: 10.1016/j.biocel.2008.03.014
  44. Rajasekharan S, Kennedy TE. The netrin protein family. *Genome Biol.* (2009) 10:239. doi: 10.1186/gb-2009-10-9-239
  45. Yetnikoff L, Eng C, Benning S, Flores C. Netrin-1 receptor in the ventral tegmental area is required for sensitization to amphetamine. *Eur J Neurosci.* (2010) 31:1292–302. doi: 10.1111/j.1460-9568.2010.07163.x
  46. Horn KE, Glasgow SD, Gobert D, Bull SJ, Luk T, Girgis J, et al. DCC expression by neurons regulates synaptic plasticity in the adult brain. *Cell Rep.* (2013) 3:173–85. doi: 10.1016/j.celrep.2012.12.005
  47. Manitt C, Mimeo A, Eng C, Pokinko M, Stroth T, Cooper HM, et al. The netrin receptor DCC is required in the pubertal organization of mesocortical dopamine circuitry. *J Neurosci.* (2011) 31:8381–94. doi: 10.1523/JNEUROSCI.0606-11.2011
  48. Goldman JS, Ashour MA, Magdesian MH, Tritsch NX, Harris SN, Christofi N, et al. Netrin-1 promotes excitatory synaptogenesis between cortical neurons by initiating synapse assembly. *J Neurosci.* (2013) 33:17278–89. doi: 10.1523/JNEUROSCI.1085-13.2013
  49. Sitek B, Poschmann G, Schmidtko K, Ullmer C, Maskri L, Andriske M, et al. Expression of MUPP1 protein in mouse brain. *Brain Res.* (2003) 970:178–87. doi: 10.1016/S0006-8993(03)02338-2
  50. Shirley RL, Walter NA, Reilly MT, Fehr C, Buck KJ. Mpdz is a quantitative trait gene for drug withdrawal seizures. *Nat Neurosci.* (2004) 7:699–700. doi: 10.1038/nn1271
  51. Karpayak VM, Kim JH, Biernacka JM, Wieben ED, Mrazek DA, Black JL, et al. Sequence variations of the human MPDZ gene and association with alcoholism in subjects with European ancestry. *Alcohol Clin Exp Res.* (2009) 33:712–21. doi: 10.1111/j.1530-0277.2008.00888.x
  52. Ehlers CL, Walter NA, Dick DM, Buck KJ, Crabbe JC. A comparison of selected quantitative trait loci associated with alcohol use phenotypes in humans and mouse models. *Addict Biol.* (2010) 15:185–99. doi: 10.1111/j.1369-1600.2009.00195.x
  53. Krapivinsky G, Medina I, Krapivinsky L, Gapon S, Clapham DE. SynGAP-MUPP1-CaMKII synaptic complexes regulate p38 MAP kinase activity and NMDA receptor-dependent synaptic AMPA receptor potentiation. *Neuron.* (2004) 43:563–74. doi: 10.1016/j.neuron.2004.08.003
  54. Rama S, Krapivinsky G, Clapham DE, Medina I. The MUPP1-SynGAPalpha protein complex does not mediate activity-induced LTP. *Mol Cell Neurosci.* (2008) 38:183–8. doi: 10.1016/j.mcn.2008.02.007
  55. Miyamoto Y, Yamada K, Nagai T, Mori H, Mishina M, Furukawa H, et al. Behavioural adaptations to addictive drugs in mice lacking the NMDA receptor epsilon1 subunit. *Eur J Neurosci.* (2004) 19:151–8. doi: 10.1111/j.1460-9568.2004.03086.x
  56. Inturrisi CE. The role of N-methyl-D-aspartate (NMDA) receptors in pain and morphine tolerance. *Minerva Anestesiol.* (2005) 71:401–3.
  57. Ko SW, Wu LJ, Shum F, Quan J, Zhuo M. Cingulate NMDA NR2B receptors contribute to morphine-induced analgesic tolerance. *Mol Brain.* (2008) 1:2. doi: 10.1186/1756-6606-1-2
  58. Liaw WJ, Zhu XG, Yaster M, Johns RA, Gauda EB, Tao YX. Distinct expression of synaptic NR2A and NR2B in the central nervous system and impaired morphine tolerance and physical dependence in mice deficient in postsynaptic density-93 protein. *Mol Pain.* (2008) 4:45. doi: 10.1186/1744-8069-4-45
  59. Erlendson MJ, D'arcy N, Enciso EM, Yu JJ, Rincon-Cruz L, Peltz G., et al. Palonosetron and hydroxyzine pre-treatment reduces the objective signs of experimentally-induced acute opioid withdrawal in humans: a double-blinded, randomized, placebo-controlled crossover study. *Am J Drug Alcohol Abuse.* (2017) 43:78–86. doi: 10.1080/00952990.2016.1210614
  60. Elkomy M, Sultan P, Carvalho B, Peltz G, Wu M, Clavijo C, et al. Ondansetron pharmacokinetics in pregnant women and neonates: towards a new treatment for neonatal abstinence syndrome. *Clin Pharmacol Ther.* (2015) 97:167–76. doi: 10.1002/cpt.5
  61. Maas U, Kattner E, Weingart-Jesse B, Schafer A, Obladen M. Infrequent neonatal opiate withdrawal following maternal methadone

- detoxification during pregnancy. *J Perinat Med.* (1990) 18:111–8. doi: 10.1515/jpme.1990.18.2.111
62. American Academy of Pediatrics Committee on Drugs. Neonatal drug withdrawal. *Pediatrics.* (1998) 101:1079–86. doi: 10.1542/peds.101.6.1079
  63. Wang J, Liao G, Usuka J, Peltz G. Computational genetics: from mouse to man? *Trends in Genetics.* (2005) 21:526–32. doi: 10.1016/j.tig.2005.06.010
  64. Zheng M, Dill D, Peltz G. A better prognosis for genetic association studies in mice. *Trends Genet.* (2012) 28:62–9. doi: 10.1016/j.tig.2011.10.006
  65. Beck JA, Lloyd S, Hafezparast M, Lennon-Pierce M, Eppig JT, Festing MF, et al. Genealogies of mouse inbred strains. *Nat Genet.* (2000) 24:23–5. doi: 10.1038/71641
  66. Arslan A, Guan Y, Chen X, Donaldson R, Zhu W, Ford M, et al. High throughput computational mouse genetic analysis. *BioRxiv.* (2020). doi: 10.1101/2020.09.01.278465
  67. Tewhey R, Bansal V, Torkamani A, Topol EJ, Schork NJ. The importance of phase information for human genomics. *Nat Rev Genet.* (2011) 12:215–23. doi: 10.1038/nrg2950
  68. Ghazalpour A, Rau CD, Farber CR, Bennett BJ, Orozco LD, Van Nas A, et al. Hybrid mouse diversity panel: a panel of inbred mouse strains suitable for analysis of complex genetic traits. *Mamm Genome.* (2012) 23:680–92. doi: 10.1007/s00335-012-9411-5
  69. Chick JM, Munger SC, Simecek P, Huttlin EL, Choi K, Gatti DM, et al. Defining the consequences of genetic variation on a proteome-wide scale. *Nature.* (2016) 534:500–5. doi: 10.1038/nature18270
  70. Chesler EJ, Miller DR, Branstetter LR, Galloway LD, Jackson BL, Philip VM, et al. The collaborative cross at Oak ridge national laboratory: developing a powerful resource for systems genetics. *Mamm Genome.* (2008) 19:382–9. doi: 10.1007/s00335-008-9135-8
  71. Belknap JK, Crabbe JC. Chromosome mapping of gene loci affecting morphine and amphetamine responses in BXD recombinant inbred mice. *Ann N Y Acad Sci.* (1992) 654:311–23. doi: 10.1111/j.1749-6632.1992.tb25977.x
  72. Centers for Disease Control and Prevention (2020). *National Diabetes Statistics Report, 2020*. Atlanta, GA (2020). Available online at: [https://www.cdc.gov/diabetes/data/statistics-report/index.html?CDC\\_AA\\_refVal=https%3A%2F%2F](https://www.cdc.gov/diabetes/data/statistics-report/index.html?CDC_AA_refVal=https%3A%2F%2F) (accessed August 28, 2020).
  73. Kim JH, Saxton AM. The TALLYHO mouse as a model of human type 2 diabetes. *Methods Mol Biol.* (2012) 933:75–87. doi: 10.1007/978-1-62703-068-7\_6
  74. Kim JH, Sen S, Avery CS, Simpson E, Chandler P, Nishina PM, et al. Genetic analysis of a new mouse model for non-insulin-dependent diabetes. *Genomics.* (2001) 74:273–86. doi: 10.1006/geno.2001.6569
  75. Liao G, Wang J, Guo J, Allard J, Chang J, Nguyen A, et al. *In Silico* genetics: identification of a novel functional element regulating H2-Ea gene expression. *Science.* (2004) 306:690–5. doi: 10.1126/science.1100636
  76. Smith SB, Marker CL, Perry C, Liao G, Sotocinal SG, Austin JS, et al. Quantitative trait locus and computational mapping identifies Kcnj9 (GIRK3) as a candidate gene affecting analgesia from multiple drug classes. *Pharmacogenet Genomics.* (2008) 18:231–41. doi: 10.1097/FPC.0b013e3282f55ab2
  77. LaCroix-Fralish ML, Mo G, Smith SB, Sotocinal SG, Ritchie JG, Austin JS, et al. The  $\beta 3$  Subunit of the Na<sup>+</sup>,K<sup>+</sup>-ATPase affects pain sensitivity. *Pain.* (2009) 144:294–302. doi: 10.1016/j.pain.2009.04.028
  78. Liu H-H, Lu P, Guo Y, Farrell E, Zhang X, Zheng M, et al. An integrative genomic analysis identifies bhmt2 as a diet-dependent genetic factor protecting against acetaminophen-induced liver toxicity *Genome Res.* (2010) 20:28–35. doi: 10.1101/gr.097212.109
  79. Liu HH, Hu Y, Zheng M, Suhoski MM, Engleman EG, Dill DL, et al. Cd14 SNPs regulate the innate immune response. *Mol Immunol.* (2012) 51:112–27.
  80. Grupe A, Germer S, Usuka J, Aud D, Belknap JK, Klein RF, et al. *In silico* mapping of complex disease-related traits in mice. *Science.* (2001) 92: 1915–8. doi: 10.1126/science.1058889
  81. Rozzo SJ, Allard J, Choubey D, Vyse T, Izui S, Peltz G, et al. Evidence for an interferon-inducible gene, Ifi202, in the susceptibility to systemic lupus. *Immunity.* (2001) 15:435–43. doi: 10.1016/s1074-7613(01)00196-0
  82. Guo YY, Weller PF, Farrell E, Cheung P, Fitch B, Clark D, et al. *In silico* pharmacogenetics: warfarin metabolism. *Nat Biotechnol.* (2006) 24:531–6. doi: 10.1038/nbt1195
  83. Guo YY, Liu P, Zhang X, Weller PM, Wang J, Liao G, et al. *In vitro* and *in silico* pharmacogenetic analysis in mice. *Proc Natl Acad Sci USA.* (2007) 104:17735–40. doi: 10.1073/pnas.0700724104
  84. Zaas AK, Liao G, Chein J, Usuka J, Weinberg C, Shore D, et al. Plasminogen alleles influence susceptibility to invasive aspergillosis. *PLoS genetic.* (2008) 4:e1000101. doi: 10.1371/journal.pgen.1000101
  85. Tregoning JS, Yamaguchi Y, Wang B, Mihm D, Harker JA, Bushell ESC, et al. Genetic susceptibility to the delayed sequelae of RSV infection is MHC-dependent, but modified by other genetic loci. *J Immunol.* (2010) 185:5384–91. doi: 10.4049/jimmunol.1001594
  86. Hu Y, Liang D, Li X, Liu H-H, Zhang X, Zheng M, et al. The role of IL-1 in wound biology part I: murine *in silico* and *in vitro* experimental analysis. *Anesth Analg.* (2010) 111: 1525–33. doi: 10.1213/ANE.0b013e3181f5ef5a
  87. Hu Y, Liang D, Li X, Liu H-H, Zhang X, Zheng M, et al. The role of IL-1 in wound biology part II: *in vivo* and human translational studies. *Anesth Analg.* (2010) 111:1534–42. doi: 10.1213/ANE.0b013e3181f691eb
  88. Peltz G, Zaas AK, Zheng M, Solis NV, Zhang MX, Liu H-H, et al. Next-generation computational genetic analysis: multiple complement alleles control survival after candida albicans infection. *Infect Immun.* (2011) 79:4472–9. doi: 10.1128/IAI.05666-11
  89. Sorge RE, Trang T, Dorfman R, Smith SB, Beggs S, Ritchie J, et al. Genetically determined P2X7 receptor pore formation regulates variability in chronic pain sensitivity. *Nat Med.* (2012) 18:595–9. doi: 10.1038/nm.2710
  90. Ren M, Kazemian M, Zheng M, He J, Li P, Oh J, et al. Transcription factor p73 regulates Th1 differentiation. *Nat Commun.* (2020) 11:1475. doi: 10.1038/s41467-020-15172-5
  91. Reich DE, Goldstein DB. Detecting association in a case-control study while correcting for population stratification. *Genet Epidemiol.* (2001) 20:4–16.
  92. Yu J, Pressoir G, Briggs WH, Vroh Bi I, Yamasaki M, Doebley JE, et al. A unified mixed-model method for association mapping that accounts for multiple levels of relatedness. *Nat Genet.* (2006) 38:203–8. doi: 10.1038/ng1702
  93. Zhao K, Aranzana MJ, Kim S, Lister C, Shindo C, Tang C, et al. An arabidopsis example of association mapping in structured samples. *PLoS Genet.* (2007) 3:e4. doi: 10.1371/journal.pgen.0030004
  94. Kang HM, Zaitlen NA, Wade CM, Kirby A, Heckerman D, Daly MJ, et al. Efficient control of population structure in model organism association mapping. *Genetics.* (2008) 178:1709–23. doi: 10.1534/genetics.107.080101
  95. Wang M, Fang Z, Yoo B, Bejerano G, Peltz G. The effect of population structure on murine genome-wide association studies. *Front Genet.* (2021) 12:745361. doi: 10.3389/fgene.2021.745361
  96. Zhang X, Liu H-H, Weller P, Tao W, Wang J, Liao G, et al. *In silico* and *in vitro* pharmacogenetics: aldehyde oxidase rapidly metabolizes a p38 kinase inhibitor. *Pharmacogenomics J.* (2011) 11:15–24. doi: 10.1038/tpj.2010.8
  97. Nestler EJ. Cellular basis of memory for addiction. *Dialogues Clin Neurosci.* (2013) 15:431–43. doi: 10.31887/DCNS.2013.15.4/enestler
  98. Nestler EJ. Molecular basis of long-term plasticity underlying addiction. *Nat Rev Neurosci.* (2001) 2:119–28. doi: 10.1038/35053570
  99. Nestler EJ. Is there a common molecular pathway for addiction? *Nat Neurosci.* (2005) 8:1445–9. doi: 10.1038/nn1578
  100. Russo SJ, Dietz DM, Dumitriu D, Morrison JH, Malenka RC, Nestler EJ. The addicted synapse: mechanisms of synaptic and structural plasticity in nucleus accumbens. *Trends Neurosci.* (2010) 33:267–76. doi: 10.1016/j.tins.2010.02.002
  101. Guzman-Karlsson MC, Meadows JP, Gavin CF, Hablitz JJ, Sweatt JD. Transcriptional and epigenetic regulation of Hebbian and non-Hebbian plasticity. *Neuropharmacology.* (2014) 80:3–17. doi: 10.1016/j.neuropharm.2014.01.001
  102. Citri A, Malenka RC. Synaptic plasticity: multiple forms, functions, and mechanisms. *Neuropsychopharmacology.* (2008) 33:18–41. doi: 10.1038/sj.npp.1301559
  103. Volkow ND, Michaelides M, Baler R. the neuroscience of drug reward and addiction. *Physiol Rev.* (2019) 99:2115–40. doi: 10.1152/physrev.00014.2018

104. Thomas MJ, Malenka RC, Bonci A. Modulation of long-term depression by dopamine in the mesolimbic system. *J Neurosci.* (2000) 20:5581–6. doi: 10.1523/JNEUROSCI.20-15-05581.2000
105. Jones S, Bonci A. Synaptic plasticity and drug addiction. *Curr Opin Pharmacol.* (2005) 5:20–5. doi: 10.1016/j.coph.2004.08.011
106. Liu QS, Pu L, Poo MM. Repeated cocaine exposure *in vivo* facilitates LTP induction in midbrain dopamine neurons. *Nature.* (2005) 437:1027–31. doi: 10.1038/nature04050
107. Bellone C, Luscher C. Cocaine triggered AMPA receptor redistribution is reversed *in vivo* by mGluR-dependent long-term depression. *Nat Neurosci.* (2006) 9:636–41. doi: 10.1038/nn1682
108. Mameli M, Balland B, Lujan R, Luscher C. Rapid synthesis and synaptic insertion of GluR2 for mGluR-LTD in the ventral tegmental area. *Science.* (2007) 317:530–3. doi: 10.1126/science.1142365
109. Cheron J, Kerchoue d'Exaerde A. Drug addiction: from bench to bedside. *Transl Psychiatry.* (2021) 11:424. doi: 10.1038/s41398-021-01542-0
110. Solinas M, Belujon P, Fernagut PO, Jaber M, Thiriet N. Dopamine and addiction: what have we learned from 40 years of research. *J Neural Transm (Vienna).* (2019) 126:481–516. doi: 10.1007/s00702-018-1957-2
111. Robinson TE, Kolb B. Structural plasticity associated with exposure to drugs of abuse. *Neuropharmacology.* (2004) 47(Suppl 1):33–46. doi: 10.1016/j.neuropharm.2004.06.025
112. Lee KW, Kim Y, Kim AM, Helmin K, Nairn AC, Greengard P. Cocaine-induced dendritic spine formation in D1 and D2 dopamine receptor-containing medium spiny neurons in nucleus accumbens. *Proc Natl Acad Sci U S A.* (2006) 103:3399–404. doi: 10.1073/pnas.0511244103
113. Dos Santos M, Cahill EN, Bo GD, Vanhoutte P, Caboche J, Giros B, et al. Cocaine increases dopaminergic connectivity in the nucleus accumbens. *Brain Struct Funct.* (2018) 223:913–23. doi: 10.1007/s00429-017-1532-x
114. Kauer JA, Malenka RC. Synaptic plasticity and addiction. *Nat Rev Neurosci.* (2007) 8:844–58. doi: 10.1038/nrn2234
115. Nestler EJ, Luscher C. The molecular basis of drug addiction: linking epigenetic to synaptic and circuit mechanisms. *Neuron.* (2019) 102:48–59. doi: 10.1016/j.neuron.2019.01.016
116. Moorman DE, James MH, McGlinchey EM, Aston-Jones G. Differential roles of medial prefrontal subregions in the regulation of drug seeking. *Brain Res.* (2015) 1628:130–46. doi: 10.1016/j.brainres.2014.12.024
117. Pascoli V, Hiver A, Van Zessen R, Loureiro M, Achargui R, Harada M, et al. Stochastic synaptic plasticity underlying compulsion in a model of addiction. *Nature.* (2018) 564:366–71. doi: 10.1038/s41586-018-0789-4
118. Rudenko A, Dawlaty MM, Seo J, Cheng AW, Meng J, Le T, et al. Tet1 is critical for neuronal activity-regulated gene expression and memory extinction. *Neuron.* (2013) 79:1109–22. doi: 10.1016/j.neuron.2013.08.003
119. Sweatt JD. The emerging field of neuroepigenetics. *Neuron.* (2013) 80:624–32. doi: 10.1016/j.neuron.2013.10.023
120. Zovkic IB, Guzman-Karlsson MC, Sweatt JD. Epigenetic regulation of memory formation and maintenance. *Learn Mem.* (2013) 20:61–74. doi: 10.1101/lm.026575.112
121. Lopez-Atalaya JP, Barco A. Can changes in histone acetylation contribute to memory formation? *Trends Genet.* (2014) 30:529–39. doi: 10.1016/j.tig.2014.09.003
122. Gupta S, Kim SY, Artis S, Molfese DL, Schumacher A, Sweatt JD, et al. Histone methylation regulates memory formation. *J Neurosci.* (2010) 30:3589–99. doi: 10.1523/JNEUROSCI.3732-09.2010
123. Halder R, Hennion M, Vidal RO, Shomroni O, Rahman RU, Rajput A, et al. DNA methylation changes in plasticity genes accompany the formation and maintenance of memory. *Nat Neurosci.* (2016) 19:102–10. doi: 10.1038/nn.4194
124. Trevino AE, Muller F, Andersen J, Sundaram L, Kathiria A, Shcherbina A, et al. Chromatin and gene-regulatory dynamics of the developing human cerebral cortex at single-cell resolution. *Cell.* (2021) 184:5053–69.e5023. doi: 10.1016/j.cell.2021.07.039
125. Martin TA, Jayanthi S, McCoy MT, Brannock C, Ladenheim B, Garrett T, et al. Methamphetamine causes differential alterations in gene expression and patterns of histone acetylation/hypoacetylation in the rat nucleus accumbens. *PLoS ONE.* (2012) 7:e34236. doi: 10.1371/journal.pone.0034236
126. Arora DS, Nimitvilai S, Teppen TL, Mcelvain MA, Sakharkar AJ, You C, et al. Hyposensitivity to gamma-aminobutyric acid in the ventral tegmental area during alcohol withdrawal: reversal by histone deacetylase inhibitors. *Neuropsychopharmacology.* (2013) 38:1674–84. doi: 10.1038/npp.2013.65
127. Mews P, Calipari ES. Cross-talk between the epigenome and neural circuits in drug addiction. *Prog Brain Res.* (2017) 235:19–63. doi: 10.1016/bs.pbr.2017.08.012
128. Salery M, Trifilieff P, Caboche J, Vanhoutte P. From signaling molecules to circuits and behaviors: cell-type-specific adaptations to psychostimulant exposure in the striatum. *Biol Psychiatry.* (2020) 87:944–53. doi: 10.1016/j.biopsych.2019.11.001

**Conflict of Interest:** The authors declare that the research was conducted in the absence of any commercial or financial relationships that could be construed as a potential conflict of interest.

**Publisher's Note:** All claims expressed in this article are solely those of the authors and do not necessarily represent those of their affiliated organizations, or those of the publisher, the editors and the reviewers. Any product that may be evaluated in this article, or claim that may be made by its manufacturer, is not guaranteed or endorsed by the publisher.

Copyright © 2022 Peltz and Tan. This is an open-access article distributed under the terms of the Creative Commons Attribution License (CC BY). The use, distribution or reproduction in other forums is permitted, provided the original author(s) and the copyright owner(s) are credited and that the original publication in this journal is cited, in accordance with accepted academic practice. No use, distribution or reproduction is permitted which does not comply with these terms.



# Ankk1 Loss of Function Disrupts Dopaminergic Pathways in Zebrafish

Adele Leggieri<sup>1†</sup>, Judit García-González<sup>2†</sup>, Jose V. Torres-Perez<sup>3</sup>, William Havelange<sup>1</sup>, Saeedeh Hosseinian<sup>1</sup>, Aleksandra M. Mech<sup>1</sup>, Marcus Keatinge<sup>4</sup>, Elisabeth M. Busch-Nentwich<sup>1,5</sup> and Caroline H. Brennan<sup>1\*</sup>

<sup>1</sup> School of Biological and Behavioural Sciences, Queen Mary University of London, London, United Kingdom, <sup>2</sup> Department of Genetics and Genomic Sciences, Icahn School of Medicine at Mount Sinai, New York, NY, United States, <sup>3</sup> Department of Brain Sciences, UK Dementia Research Institute, Imperial College London, London, United Kingdom, <sup>4</sup> Centre for Discovery Brain Sciences, The University of Edinburgh, Edinburgh, United Kingdom, <sup>5</sup> Department of Medicine, Cambridge Institute of Therapeutic Immunology and Infectious Disease, University of Cambridge, Cambridge, United Kingdom

## OPEN ACCESS

### Edited by:

Roberto Ciccocioppo,  
University of Camerino, Italy

### Reviewed by:

Ross A. McDevitt,  
National Institute on Aging, National  
Institutes of Health (NIH),  
United States  
A. J. Baucum,  
Indiana University–Purdue University  
Indianapolis, United States

### \*Correspondence:

Caroline H. Brennan  
c.h.brennan@qmul.ac.uk

<sup>†</sup> These authors have contributed  
equally to this work

### Specialty section:

This article was submitted to  
Neurogenetics,  
a section of the journal  
Frontiers in Neuroscience

**Received:** 14 October 2021

**Accepted:** 12 January 2022

**Published:** 08 February 2022

### Citation:

Leggieri A, García-González J, Torres-Perez JV, Havelange W, Hosseinian S, Mech AM, Keatinge M, Busch-Nentwich EM and Brennan CH (2022) Ankk1 Loss of Function Disrupts Dopaminergic Pathways in Zebrafish. *Front. Neurosci.* 16:794653. doi: 10.3389/fnins.2022.794653

Ankyrin repeat and kinase domain containing 1 (ANKK1) is a member of the receptor-interacting protein serine/threonine kinase family, known to be involved in cell proliferation, differentiation and activation of transcription factors. Genetic variation within the ANKK1 locus is suggested to play a role in vulnerability to addictions. However, ANKK1 mechanism of action is still poorly understood. It has been suggested that ANKK1 may affect the development and/or functioning of dopaminergic pathways. To test this hypothesis, we generated a CRISPR-Cas9 loss of function *ankk1* zebrafish line causing a 27 bp insertion that disrupts the *ankk1* sequence introducing an early stop codon. We found that *ankk1* transcript levels were significantly lower in *ankk1* mutant (*ankk1*<sup>27ins</sup>) fish compared to their wild type (*ankk1*<sup>+/+</sup>) siblings. In *ankk1*<sup>+/+</sup> adult zebrafish brain, *ankk1* protein was detected in isocortex, hippocampus, basolateral amygdala, mesencephalon, and cerebellum, resembling the mammalian distribution pattern. In contrast, *ankk1* protein was reduced in the brain of *ankk1*<sup>27ins/27ins</sup> fish. Quantitative polymerase chain reaction analysis revealed an increase in expression of *drd2b* mRNA in *ankk1*<sup>27ins</sup> at both larval and adult stages. In *ankk1*<sup>+/+</sup> adult zebrafish brain, *drd2* protein was detected in cerebral cortex, cerebellum, hippocampus, and caudate homolog regions, resembling the pattern in humans. In contrast, *drd2* expression was reduced in cortical regions of *ankk1*<sup>27ins/27ins</sup> being predominantly found in the hindbrain. No differences in the number of cell bodies or axonal projections detected by anti-tyrosine hydroxylase immunostaining on 3 days post fertilization (dpf) larvae were found. Behavioral analysis revealed altered sensitivity to effects of both amisulpride and apomorphine on locomotion and startle habituation, consistent with a broad loss of both pre and post synaptic receptors. *Ankk1*<sup>27ins</sup> mutants showed reduced sensitivity to the effect of the selective dopamine receptor antagonist amisulpride on locomotor responses to acoustic startle and were differentially sensitive to the effects of the non-selective dopamine agonist apomorphine on both

locomotion and habituation. Taken together, our findings strengthen the hypothesis of a functional relationship between *ANKK1* and *DRD2*, supporting a role for *ANKK1* in the maintenance and/or functioning of dopaminergic pathways. Further work is needed to disentangle *ANKK1*'s role at different developmental stages.

**Keywords:** *ANKK1*, *DRD2*, dopaminergic system, addiction, amisulpride, apomorphine

## INTRODUCTION

Addiction or substance use disorder (SUD) is a complex condition characterized by the uncontrolled use of drugs despite harmful and adverse consequences. Although environmental factors such as early life trauma, altered family structure, social pressure, and isolation during childhood increase the risk of developing SUDs (Wong et al., 2013; Baarendse et al., 2014; Koeneke et al., 2020), genetic factors also contribute to the liability of the disorder, with heritability estimates ranging from 40 to 60% (see Prom-Wormley et al., 2017 and Lopez-Leon et al., 2021, for reviews).

The Taq1A polymorphism (rs1800497) is one of the most extensively studied genetic variants in relation to drug addiction (Blum et al., 1990; Noble, 2003; Ponce et al., 2009; Wang et al., 2013) and psychiatric disorders (Neville et al., 2004; Hoenicka et al., 2010). Taq1A is located within exon 8 of the ankyrin repeat and kinase domain containing 1 (*ANKK1*) gene, causing a single nucleotide C(A2)/T(A1) change (Neville et al., 2004) resulting in a glutamate to lysine substitution (Glu713Lys) in the C-terminal ankyrin repeat domain, which might lead to a change in protein function (Völter et al., 2012).

Ankyrin repeat and kinase domain containing 1 is a serine/threonine kinase belonging to the receptor-interacting protein (RIP) family. RIP kinases are important regulators of cell survival, death, and differentiation (Meylan and Tschopp, 2005; Declercq et al., 2009; Zhang et al., 2010; Humphries et al., 2015). *ANKK1* maps to chromosome 11q22-q23 (chr11:11,338,038–113,400,418; GRCh38/hg38) in a 512 kb gene cluster that includes the neural cell adhesion molecule 1 (*NCAM1*), tetratricopeptide repeat domain 12 (*TTC12*) and dopamine receptor 2 (*DRD2*) genes (Neville et al., 2004; Mota et al., 2012). The *NCAM-TTC12-ANKK1-DRD2* (NTAD) cluster is conserved among the vertebrates and has been proposed to be involved in neurogenesis and in the development of dopaminergic pathways (Yi et al., 2007; España-Serrano et al., 2017; Rubio-Solsona et al., 2018; Koeneke et al., 2020). In the adult mouse brain, *ANKK1* protein is expressed in neural stem cells, in post-mitotic

neurons and in migrating neuroblasts (España-Serrano et al., 2017; Koeneke et al., 2020), hinting at a role in neuronal differentiation and migration.

Ankyrin repeat and kinase domain containing 1 may be particularly important for the correct development and regulation of dopaminergic pathways, since *DRD2* protein expression, density and binding is reduced in the striatum of Taq1A A1 allele carriers (Noble, 2003; Neville et al., 2004; Klein et al., 2007; Savitz et al., 2013). It has been suggested that *ANKK1* variants may influence addiction vulnerability by affecting differentiation, migration, and/or connectivity of dopaminergic neurons during development, and by modulating dopaminergic function in the brain during adulthood.

To test the hypothesis that *ANKK1* modulates development and function of the dopaminergic system, we generated a CRISPR-Cas9 loss of function line for *ANKK1* (referred to as *ankk1*<sup>27ins</sup>) using the zebrafish as a model organism. Zebrafish is an established model for developmental genetic studies (see Link and Megason, 2008 and Sakai et al., 2018, for reviews) and show conservation of pathways associated with responses to drugs of abuse (Mathur and Guo, 2010; Clark et al., 2011; Klee et al., 2011, 2012; Stewart et al., 2011; Parker et al., 2013; Bradford et al., 2017). We examined *ankk1* and *drd2* protein expression in the brains of wild type (*ankk1*<sup>+/+</sup>) and mutant (*ankk1*<sup>27ins</sup>) adult fish using immunohistochemistry and quantitative real time polymerase chain reaction (qPCR). We show that *ankk1* and *drd2* proteins are expressed in similar domains in the zebrafish brain as in human. *Ankk1* transcript and protein levels were reduced in the brains of *ankk1* mutants. *Drd2* protein levels were also reduced. In contrast, *drd2b* transcript levels were found to be increased at both larval and adult stages. We observed no differences (*ankk1*<sup>+/+</sup> versus *ankk1*<sup>27ins/27ins</sup>) in the number of cell bodies nor axonal projections when performing anti-tyrosine hydroxylase immunostaining on 3 dpf zebrafish larvae. Behavioral analysis revealed an effect of genotype on baseline locomotion but not on anxiety-like responses. *Ankk1*<sup>27ins</sup> mutants showed reduced sensitivity to the effect of the selective dopamine receptor antagonist amisulpride on locomotor responses to acoustic startle and were differentially sensitive to the effects of the non-selective dopamine agonist apomorphine on both locomotion and habituation.

## MATERIALS AND METHODS

### Animal Maintenance

Wild type Tübingen (TU) strain zebrafish were housed in a recirculating system (Tecniplast, United Kingdom) on a 14 h:10 h light/dark cycle and a constant temperature of 28°C. Fish were

**Abbreviations:** III, oculomotor nerve; Cans, commissura ansulata; D, dorsal telencephalic area; Dc, central zone of D; Dd, dorsal zone of D; Dl, lateral zone of D; DIL, diffuse nucleus of the inferior lobe; Dm, medial zone of D; Dp, posterior zone of D; DV, descending trigeminal root; ECL, external cellular layer of olfactory bulb including mitral cells; GL, glomerular layer of olfactory bulb; Hd, dorsal hypothalamus; ICL, internal cellular layer of olfactory bulb; LLF, lateral longitudinal fascicle; PGZ, periventricular gray zone of the optic tectum; PPa, parvocellular preoptic nucleus, anterior part; TelV, telencephalic ventricle; TeO, optic tectum; Tl, torus longitudinalis; TLa, torus lateralis; TSc, central nucleus of torus semicircularis; TTB, tractus tectobulbaris; Val, lateral division of valvula cerebelli; Vam, medial division of valvula cerebelli; Vas, vascular lacuna of area postrema; Vd, dorsal nucleus of ventral telencephalic area; Vp, posterior nucleus of ventral telencephalic area; Vv, ventral nucleus of ventral telencephalic area.

fed twice daily with ZM-400 fry food (Zebrafish Management Ltd., Winchester, United Kingdom) in the morning, and brine shrimp in the afternoon.

Breeding was set up in the evening, either in sloping breeding tanks (Tecniplast, United Kingdom) or in tanks equipped with a container with marbles to isolate eggs from progenitors. For experiments where the developmental stage of larvae was important, we placed barriers between the fish to keep them isolated in the breeding tank. The following morning, barriers were removed to allow spawning.

Eggs were collected in Petri dishes the following morning, sorted fertile from infertile, and then incubated at 28°C (max 50 eggs/dish). Dishes were checked daily to ensure consistent developmental stage across groups. If reared, larvae were moved to the recirculating system at 5 dpf and fed as stated above.

All procedures were carried out under license in accordance with the Animals (Scientific Procedures) Act, 1986 and under guidance from the Local Animal Welfare and Ethical Review Board at Queen Mary University of London.

## Generation of *Ankk1* Loss of Function Zebrafish Line

Selection of target site and design of guide RNAs (crRNA) was as described previously (Keatinge et al., 2021). The crRNA was designed to target a *Bst*NI restriction enzyme site [CCCTGGATAATCTCCTTAGCAAT (PAM sequence in bold, restriction site underlined)]. 1 nL of a solution containing 62.5 ng/μl crRNA (Sigma-Aldrich/Merck, Darmstadt, Germany), 62.5 ng/μl tracrRNA (TRACRRNA05N, Sigma-Aldrich/Merck, Darmstadt, Germany), and 5 μM Cas9 (NEB M0386M, NEB Ltd., United Kingdom), was injected in one-cell stage zebrafish embryos (wild-type, TU). Around 100 embryos were injected and approximately 50 were raised to identify founders.

Founder carriers were identified by polymerase chain reaction (PCR) from genomic DNA (*ankk1*\_Forward, 5' – TCCAAAATTGGAAGAATGAAGTT – 3'; *ankk1*\_Reverse, 5' – GCAGAAAGTTCATACCCATCG – 3'). Pairs of fish carrying the same mutation were identified and reared over three generations. F<sub>3</sub> heterozygous carriers were then in-crossed to obtain F<sub>4</sub> fish for characterization.

Quantitative real time polymerase chain reaction and immunohistochemistry were used to confirm reduction of *ankk1* mRNA and protein expression.

## RNA Isolation and cDNA Synthesis

Five pools of 16 zebrafish larvae combined according to their genotype (wild type and heterozygous), four pools of 16 zebrafish larvae (homozygous), and 6 whole adult brain (males) for each genotype were collected in RNase free 1.5 mL Eppendorf tubes, water was removed, and samples snap frozen (–80°C) until usage. Total RNA was isolated using TRIzol reagent (Thermo Fisher Scientific, United States) following manufacturer's instructions. Briefly, after homogenization, RNA was isolated by precipitation, rinsed, and resuspended in RNase free water. Total RNA was then quantified using BioDrop (Biochrom Ltd., United Kingdom), and up to 1 μg was reverse

transcribed to cDNA using the ProtoScript II First Strand cDNA Synthesis Kit (NEB Ltd., United Kingdom) following manufacturer's protocol. Resulting cDNA yield and quality were also evaluated using BioDrop (Biochrom Ltd., United Kingdom).

## Quantitative Real-Time PCR

Quantitative real time polymerase chain reaction was performed using the Power SYBR Green PCR Master Mix (Applied Biosystems, Thermo Fisher Scientific, United Kingdom) and in a Bio-Rad 96-well qPCR machine (CFX96 Touch Real-Time PCR Detection System). All reactions were carried out in triplicate. Actin – β 2 (*actb2*), ribosomal protein L13a (*rpl13a*), and eukaryotic translation elongation factor 1 alpha 1 – like 1 (*efl*), were employed as reference genes. Amplification conditions were as follows: 95°C × 5 min, 50 cycles of 95°C × 10 s, 60°C × 12 s, and 72°C × 12 s. *Ankk1* primers were designed downstream of the CRISPR insertion to detect disruption in *ANKK1* mRNA levels as a consequence of the mutation. The qPCR product spans the genomic region chr15: 22,084,486–22,085,215, whereas the CRISPR insertion is located in chr15: 22,078,972 (GRCz10/danRer10 Assembly). Accession numbers, primer sequences and amplification efficiencies for all the reference and target genes can be found in **Supplementary Table 1**.

## Immunohistochemistry on Adult Brain Sections

As *ankk1* transcript level was similarly reduced in both heterozygous and homozygous mutants we compared protein distribution in wild types and homozygous mutants only. Immunohistochemistry was conducted on paraffin embedded zebrafish brains from male wild types and homozygous *ankk1*<sup>27ins/27ins</sup>. Fish were culled by overdose of tricaine prior to head removal. Brains were dissected and fixed in 4% paraformaldehyde (PFA, Sigma, Gillingham, United Kingdom) in 1x phosphate buffered saline (PBS), overnight (ON) at 4°C. Brains were then rinsed in 1x PBS and dehydrated in ascending ethanol series (15 min in each of 30, 50, 70, 80, 90, and 100% ethanol) and embedded in paraffin. Transverse sections of 12 μm thickness were cut using a microtome (Leica, Wetzlar, Germany). To perform immunohistochemistry, slides were de-waxed in xylene (twice, 10 min each), rehydrated in descending ethanol series (2 × 5 min in absolute ethanol, then 90, 80, and 70%, 5 min each), and rinsed in distilled water for 5 min. An antigen retrieval step was performed with citrate buffer solution (0.01 M, pH 6.00): citrate buffer was pre-heated (95–100°C), slides were immersed in the solution, covered with a lid (loosely) and incubated for 30 min. Sections were cooled at room temperature (RT) for 20 min, rinsed in 1x PBS for 5 min and endogenous peroxidase activity was quenched with 3% H<sub>2</sub>O<sub>2</sub>, 20 min at RT. Slides were washed three times in 1x PBS, 5 min each time, and incubated in blocking solution (BS) (10% normal goat serum, and 2 μg/μL bovine serum albumin in 1x PBS) for 30 min in a humid chamber at RT. Slides were subsequently incubated with anti-ankk1 Rabbit pAb (A16178, ABclonal), or anti-drd2 Rabbit pAb (A12930, ABclonal), 1:200 in BS, ON at 4°C. The day after, sections were well washed (5 × 10 min) in

1x PBS, and incubated with ImmPRESS® HRP Goat Anti-Rabbit IgG Polymer Detection Kit (MP-7451-15, Vector), at RT. The immunoreactivity of the cells was visualized using freshly prepared solutions of 3,3'-diaminobenzidine tetrahydrochloride (0.05% in 1x PBS) activated with a solution of 0.03% H<sub>2</sub>O<sub>2</sub>. When the desired staining was obtained, sections were well washed in 1x PBS (3 × 10 min), then 3 × 10 min in distilled water, dehydrated in ascending ethanol series (70, 80, 90, and 100%, 5 min each), cleared in xylene (twice, 5 min each) and mounted with mounting medium.

## Immunohistochemistry on Whole Mount Zebrafish Larvae

As *ankk1* transcript level was similarly reduced in both heterozygous and homozygous mutants we again compared protein distribution in wild type and homozygous mutants only. Fluorescent immunohistochemistry was carried out in 3 dpf larvae from *ankk1*<sup>+/+</sup>, and *ankk1*<sup>27ins/27ins</sup> in-crosses. To prevent skin pigmentation, embryos were incubated in 0.2 mM of 1-phenyl 2-thiourea (PTU) (Sigma, Gillingham, United Kingdom) from 24 h after fertilization. When they reached the desired age (3 dpf), larvae were fixed in 4% PFA (Sigma, Gillingham, United Kingdom) to avoid tissue degradation ON at 4°C. The following day, larvae were rinsed in PBT (1xPBS, 0.05% Tween 20 v/v) supplemented with dimethyl sulfoxide (DMSO, 1% v/v) and Triton X-100 (0.1% v/v), three times 5 min each. After washes, larvae were permeabilized using proteinase K (0.02 µg/µL), for 30 min at 37°C. Larvae were then rinsed again in PBT/DMSO/Triton X-100, three times 5 min each, and incubated in BS supplemented with Tween-20 (0.05% v/v) and sodium azide (0.02% w/v) ON at 4°C. Larvae were subsequently incubated with rabbit polyclonal anti-tyrosine hydroxylase (anti-TH) primary antibody (1:200; Sigma, Gillingham, AB152). The primary antiserum was detected with anti-rabbit Alexa 546-conjugated secondary antibody (1:250, A11010, Thermo Fisher Scientific, Loughborough, United Kingdom). Larvae were cleared in 80% glycerol in 1x PBS and mounted with low melting point agarose in a sandwich of one large coverslip (24 × 60 mm), with medium size coverslips (22 × 22 mm) used as spacers.

## Imaging Acquisition and Processing

For light immunohistochemistry, pictures were acquired by Leica DMRA2 upright epifluorescent microscope with color QIClick camera (Leica, Wetzlar, Germany) and processed with Velocity 6.3.1 software (Quorum Technologies Inc).

Immunofluorescence pictures were acquired with Leica SP5 confocal microscope (Leica, Wetzlar, Germany). Confocal Z stacks were recorded under the same conditions (speed 400 Hz, resolution 2048 × 2048, line average 1 and accumulation 1, frame average 6 and accumulation 1) using diode laser. Areas of interest for quantification were isolated, making sure that for all the individuals the same number of Z stacks (covering the same dorsal/ventral distance) were included. The number of cells and axon peaks were calculated using ImageJ (National Institutes of Health, United States). To calculate the intensity of the axon peak,

a line was drawn from the medulla oblongata interfascicular zone and vagal area to the locus coeruleus. Then the average intensity along the midline was calculated.

Anatomical structures were identified according to the Neuroanatomy of the Zebrafish Brain by Wullimann et al. (1996).

## Behavioral Assays

### Forced Light/Dark Test

Patterns of locomotor activity of 5 dpf mutant and wild type zebrafish larvae were investigated in a forced light dark assay as described previously (Glazer et al., 2018). After an initial 10 min period of dark (baseline), larvae were exposed to two light/dark cycles of 10 min each. Tests were conducted between 9 a.m. and 4 p.m. Larvae were placed in individual wells of a 48-multiwell plate in a volume of 300 µL. To reduce stress due to manipulation, fish were acclimatized for at least 1 h in ambient light before testing. Distances traveled were recorded using EthoVision XT software (Noldus Information Technology, Wageningen, Netherlands). Data were exported in both 1 min and 1 s time bins and analyzed with R programming language (R Core Team, 2020), as previously described (García-González et al., 2021).

### Response and Habituation to Acoustic Startle

We assessed the response and habituation to acoustic startle stimuli in wild type and mutant larvae at 5 dpf in the presence and absence of the dopamine D2/D3 receptor antagonist amisulpride and non-selective dopamine receptor agonist apomorphine. Behavioral assays were conducted between 9 a.m. and 4 p.m. Larvae were placed in individual wells of a 48 multi-well plate. A control (0.05% DMSO) or treatment (0.01 mg/L amisulpride or 0.2 mg/L apomorphine in 0.05% DMSO) dose was added to each well in a final volume of 300 µL. Larvae were acclimatized for 1 h before testing. Then, plates were placed in a DanioVision Observation Chamber containing a dedicated tapping device (Noldus Information Technology, Wageningen, Netherlands). After 5 min of acclimation, larvae were subjected to 20 sound/vibration stimuli over 40 s (2 s intervals between each stimulus). For all experiments, distance traveled was recorded using EthoVision XT software (Noldus Information Technology, Wageningen, Netherlands), and data were outputted in 1 s time bins and analyzed as previously described (García-González et al., 2021).

## Statistical Analysis

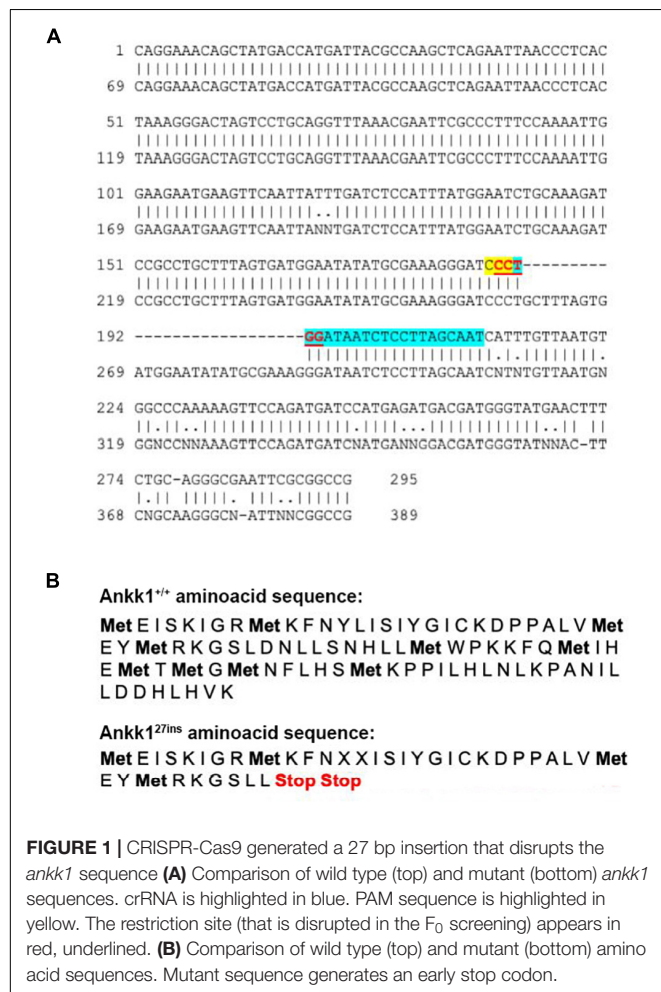
For qPCR, relative mRNA expressions were calculated using a modified version of the Pfaffl method (Pfaffl, 2001) to account for multiple reference genes and slight variation in primer amplification efficiency (Hellems et al., 2007; Evans et al., 2021). Differences in gene expression were assessed using a one-way ANOVA with genotype as independent variables. Data were log 10 transformed to achieve normal distribution for parametric statistical analysis. Log 10 transformed descriptive statistics are presented in **Supplementary Table 2**. We used the R package “emmeans” (R programming language, R Core Team, 2020) to calculate appropriate means and 95% confidence intervals for the contrasts within each gene of interest with a

Dunn-Sidak adjustment (Šidák, 1967). *P*-values were generated and adjusted for multiple comparison using the “pairs” function (Supplementary Table 3).

For behavioral analysis, all data were analyzed with R programming language (R Core Team, 2020). For models where distance moved was a response variable, we fitted data to mixed linear models using the “lme4” package, and where proportion of responders was our response variable, we fitted data to beta regression models using the “betareg” package. In all instances, we used genotype (stimulus number, and drug treatment for acoustic startle assay) as fixed effects, and where permissible we used fish ID and day as random effects. As in García-González et al. (2021), we reported significant fixed effects as Type II Wald  $\chi^2$  from models using the package “car,” *post hoc* Tukey’s tests were also conducted as necessary with the package “emmeans.”

## RESULTS

CRISPR-Cas9 generated a 27 bp insertion that disrupts the *ankk1* sequence introducing an early stop codon. Details are shown in Figure 1.



## Ankk1 Is Reduced at Both mRNA and Protein Levels in *Ankk1<sup>27ins</sup>* Fish

To confirm disruption of *ankk1*, we examined its expression at both mRNA and protein levels.

Transcript levels were significantly lower in *ankk1<sup>27ins</sup>* mutant fish compared to *ankk1<sup>+/+</sup>* [ $F(2,11) = 13.86$ ,  $p = 0.0010$ ] (Figure 2). Within-family comparison showed that *ankk1* expression is significantly downregulated in both *ankk1<sup>+/+</sup>* ( $p = 0.0031$ ) and *ankk1<sup>27ins/27ins</sup>* ( $p = 0.0004$ ) larvae.

Ankk1 immunoreactivity in the brain of *ankk1<sup>27ins/27ins</sup>* versus *ankk1<sup>+/+</sup>* was reduced at adult stage (Figure 3 and Supplementary Figure 1). In *ankk1<sup>+/+</sup>* fish, numerous ankk1 immunoreactive cells were diffusely spread throughout the area dorsalis telencephalic (D) and in the area dorsalis lining the telencephalic ventricle (TelV), in the dorsal nucleus of the TelV (Vd) (Figures 3a,b' and Supplementary Figures 1a–c). Through most of the rostrocaudal extent of the area dorsalis, numerous clustered ankk1 immunoreactive cells were still observed in the areas of the Vd and of the medial zone of the dorsal telencephalic area (Dm) lining the TelV. In contrast, numerous scattered immunoreactive cells were detected centrally in the central zone (Dc) and in the Vd (Figure 3b' and Supplementary Figure 1d). More caudally, in the area ventralis of telencephalon, few ankk1 immunoreactive cells were observed in the post-commissural nucleus (Vp) and in the Dm (Figure 3c' and Supplementary Figures 1e,e').

In *ankk1<sup>+/+</sup>* fish midbrain, few immunoreactive cells were observed in the periventricular gray zone of the optic tectum (PGZ), in the vascular lacuna of area postrema (Vas), and in the lateral longitudinal fascicle (LLF) (Figure 3d' and Supplementary Figures 1g–i).

In *ankk1<sup>+/+</sup>* fish hindbrain, ankk1 immunoreactivity was detected dorsal to the inner arcuate fibers of the secondary octaval population (SO), in the intermediate reticular formation (IMRF),

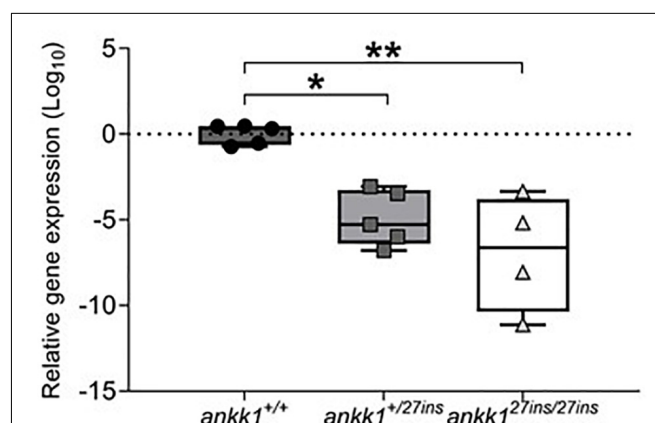
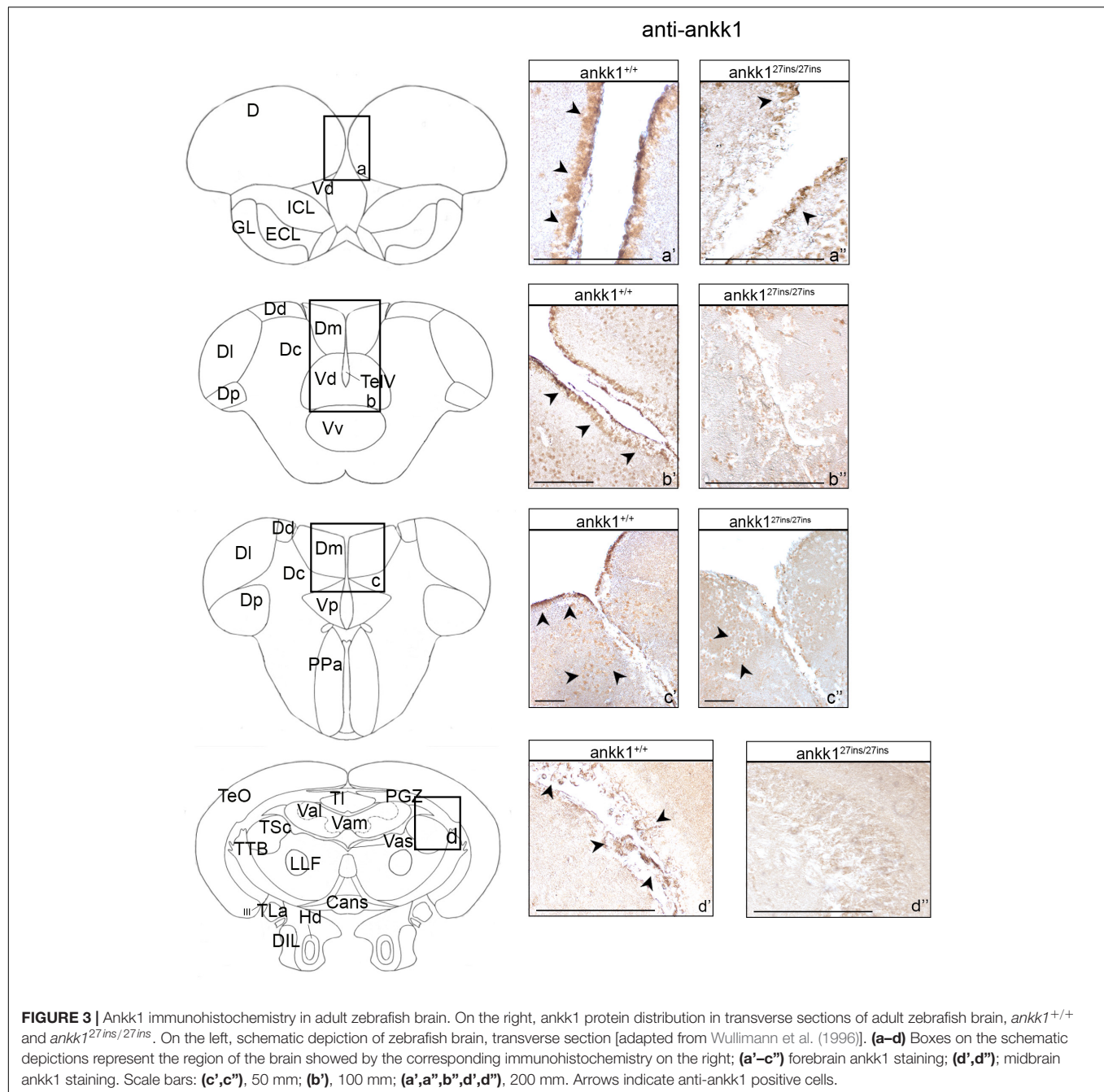


**FIGURE 2 |** Depletion of mRNA transcripts in 5 days post fertilization zebrafish larvae. *ankk1<sup>+/+</sup>* (dark gray), *ankk1<sup>+/27ins</sup>* (gray), and *ankk1<sup>27ins/27ins</sup>* (white). Data shows box and whiskers (5–95 percentile) and single samples (dots, squares, or triangles). Horizontal lines indicate group mean. Legend: \* $p \leq 0.05$ , \*\* $p \leq 0.01$ .



in the inner arcuate fibers (IAF), in the descending trigeminal root (DV), in the magnocellular octaval nucleus (MaON), and in the sensory root of the facial nerve (VIIs). Furthermore, numerous ankk1 immunoreactive cells were detected along the ventral lining of the hindbrain ventricle, in the longitudinally oriented nucleus of the griseum centrale (GC) (Supplementary Figures 1j–l).

When comparing ankk1 immunoreactivity of adult *ankk1*<sup>+/+</sup> versus *ankk1*<sup>27ins/27ins</sup> brains, the staining was reduced in the periventricular forebrain regions (Figures 3a'–c',a''–c'') and absent in the PGZ of the

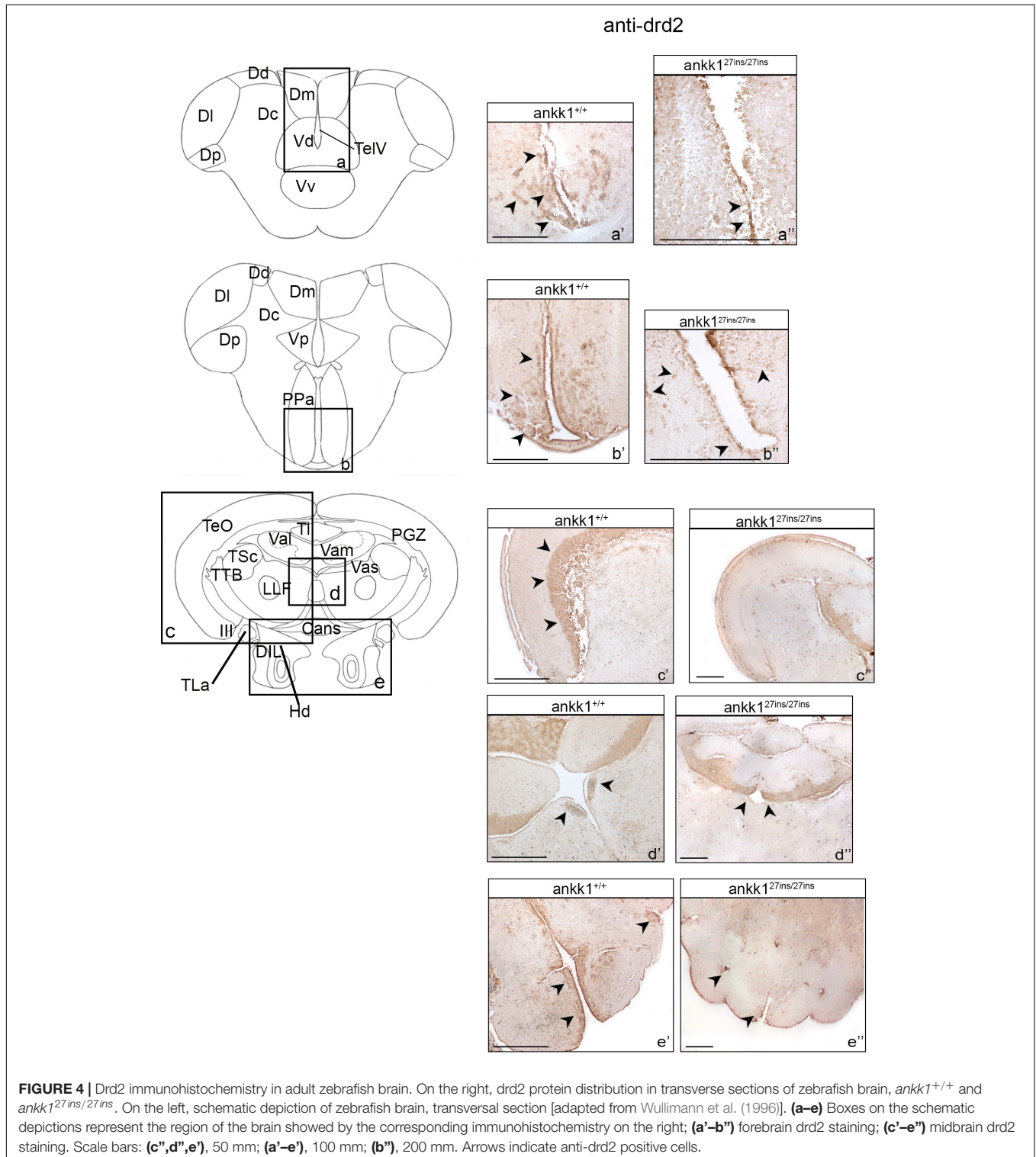
midbrain (Figures 3d',d'') and the hindbrain fibers (Supplementary Figure 4A).

### Ankk1 Loss of Function Alters Drd2 Protein Expression Levels in Adult Zebrafish Brain

As *ankk1* is proposed to regulate *drd2* expression levels, we examined the expression pattern of *drd2* protein in *ankk1*<sup>+/+</sup> adult zebrafish brain and compared it with the expression pattern of *ankk1*<sup>27ins/27ins</sup>.

In *ankk1*<sup>+/+</sup> fish forebrain, numerous drd2 immunoreactive cells clustered in the central area of D (**Figure 4a'** and **Supplementary Figure 2a**). More caudally, drd2 immunoreactive cells were widely diffused in the Vd and ventral nucleus of the ventral telencephalic area (Vv) lining the TelV (**Figure 4b'**

and **Supplementary Figures 2b,c**). A few positive cells were also detected through most of the rostrocaudal extent of the area dorsalis, in the lateral and posterior zones of the dorsal telencephalic areas (respectively Dl and Dp) (**Supplementary Figure 2b**). Clustered drd2 immunoreactive cells were localized



in the central nucleus of the ventral telencephalic area (Vc) and in the lateral olfactory tract (LOT) (Supplementary Figures 2b,c). Furthermore, a high density of drd2 immunoreactive cells was observed in the most ventral region of the Vv (Supplementary Figure 2c). In the periventricular area, numerous cells were found densely packed rostral to the anterior commissure in the Vd (Supplementary Figure 2d). In the diencephalic area, drd2 immunoreactivity was detected in specific areas: ventrally in the preoptic area, specifically in the anterior parvocellular preoptic nucleus (PPa), in the nucleus taeniae (NT) and in the ventral part of the entopeduncular nucleus (Supplementary Figures 2e,f).

In *ankk1*<sup>+/+</sup> fish midbrain, drd2 immunoreactive cells were observed in the entire layer of the PGZ (Supplementary Figure 2g), in the axons perikarya in the layer of torus longitudinalis (TL) (Supplementary Figures 2h,j), in the periventricular region of the lateral and medial divisions of valvula cerebelli (respectively Val and Vas) (Supplementary Figures 2h,j), and in the Vas (Supplementary Figure 2h). A thick layer of drd2 immunoreactive cells was observed in the dorsal zone of the periventricular hypothalamus (Hd) (Supplementary Figure 2i), whereas few positive cells were detected in the diffuse nucleus of the inferior lobe (DIL) (Supplementary Figure 2i).

In *ankk1*<sup>+/+</sup> fish hindbrain, drd2 immunoreactive cells were detected in the entire area of the corpus cerebelli (CCe) (Supplementary Figure 2k).

We observed that drd2 immunoreactivity of adult *ankk1*<sup>27ins/27ins</sup> versus *ankk1*<sup>+/+</sup> was drastically reduced. In *ankk1*<sup>27ins/27ins</sup> caudal forebrain region, drd2 immunoreactivity was detected only in a thin line of cells lining the TelV in the Vv (Figures 4a,a"). In the diencephalic region, a clear reduction in drd2 protein expression was observed in the PPa and in the Vp (Figures 4b,b"). In *ankk1*<sup>27ins/27ins</sup> midbrain, drd2 immunoreactivity was still present in the periventricular Val and Vam regions (Figures 4c,c"), but completely absent in the Vas, PGZ, and in the Hd (Figures 4e,d"). No differences were observed in the hindbrain (Supplementary Figure 4B).

## Ank1 Loss of Function Disrupts Dopaminergic Pathways in Zebrafish Larvae

As *ankk1* has been suggested to play a role in the development of dopaminergic pathways and in the differentiation of dopaminergic neurons, we examined mRNA expression levels of key components of the dopaminergic pathway by qPCR, and tyrosine hydroxylase expression levels by immunohistochemistry.

First, we examined mRNA expression of the components of the dopaminergic pathway *drd2a*, *drd2b*, *drd1*, *drd3*, *drd4a*, *drd4b*, *drd5*, *dat*, and *dbh* in 5 dpf zebrafish larvae (Figure 5). *P*-values, generated and adjusted for multiple comparison using the Dunn-Sidak method (Šidák, 1967), showed upregulation of *drd1* in *ankk1*<sup>+/27ins</sup> fish ( $p = 0.0016$ ); upregulation of *drd2b* in *ankk1*<sup>27ins/27ins</sup> mutants, at both larval ( $p = 0.0128$ ) and adult ( $p = 0.0004$ ) stages; and downregulation of *drd4b* ( $p = 0.0083$ ) and *drd5* ( $p = 0.0299$ ) in *ankk1*<sup>27ins/27ins</sup> mutants.

Next, to test the hypothesis whether *ankk1* possesses an important role in the formation of dopaminergic pathways during development more broadly, we performed fluorescence immunohistochemistry with tyrosine hydroxylase antiserum in 3 dpf zebrafish larvae and examined the number of cell bodies and axonal projections. We observed no significant differences in the number of cell bodies in the diencephalic dopaminergic cluster ( $p > 0.05$ ) between *ankk1*<sup>+/+</sup> and *ankk1*<sup>27ins/27ins</sup>, nor in the axon projections ( $p > 0.05$ ) (Figure 6).

## Ank1<sup>27ins</sup> Zebrafish Larvae Show Behavioral Differences Consistent With Altered Dopaminergic Signaling

As the dopaminergic system plays a key role in stress response and regulation of anxiety levels (de la Mora et al., 2010), we assessed anxiety-like behavior in *ankk1*<sup>+/+</sup> and *ankk1*<sup>27ins</sup> 5 dpf larvae, using a forced light dark transition assay. When the course of the test was examined as a whole (50 min), as well as when distances traveled were examined during light and dark periods separately, only time predicted distance traveled by zebrafish larvae ( $p < 0.0001$ ). No significant differences were observed between genotypes ( $p > 0.05$ ) (Figure 7A). However, when the baseline period (first 10 min of the experiment) was examined separately, distance traveled differed by time [Effect of time:  $\chi^2(1) = 25.14$ ,  $p < 0.0001$ ] and genotype [Effect of genotype:  $\chi^2(2) = 7.33$ ,  $p = 0.025$ ], such that *ankk1*<sup>27ins/27ins</sup> larvae moved significantly less than *ankk1*<sup>+/+</sup> [ $(M_{ankk1^{27ins/27ins}} = 1.09$ ,  $SE = 0.0391)$ ,  $(M_{ankk1^{+/+}} = 1.23$ ,  $SE = 0.0355)$  ( $p = 0.0188$ )].

On transitions from light to dark, all larvae sharply increased their locomotion and then steadily decreased it. On transition from dark to light, a rapid startle response resulting in a brief, sharp increase in locomotion was observed followed by a reduction in movement. The sharp increase in movement was only observable when examined at one second resolution (Figures 7B,C). We observed no significant differences between *ankk1* genotypes during light to dark, nor dark to light transitions ( $p > 0.05$ ).

Another way of assessing the response to light changes is to evaluate the increase in locomotion during the light periods (measured as the slopes from min 10–20 for light period 1, and 30–40 for light period 2), and the decrease of locomotion during the dark periods (measured as the slopes from min 20–30 for dark period 1 and 40–50 for dark period 2). For both the two light and dark periods, despite apparent reduction in rate of recovery in mutant larvae (i.e., lower slopes), there were no significant differences between *ankk1* genotype groups ( $p > 0.05$ ).

To test the impact of *ankk1* loss of function on dopamine regulated behavior associated with addiction vulnerability, we examined habituation to acoustic startle in 5 dpf larvae in the presence and absence of amisulpride and apomorphine. Habituation to acoustic startle is a measure of sensorimotor gating and is sensitive to modulation by dopaminergic agonists and antagonists (Quednow et al., 2006; Burgess and Granato, 2007; Halberstadt and Geyer, 2009; García-González et al., 2020).

In the absence of drugs, larvae showed a habituation response to repeated acoustic startle consistent with previous reports

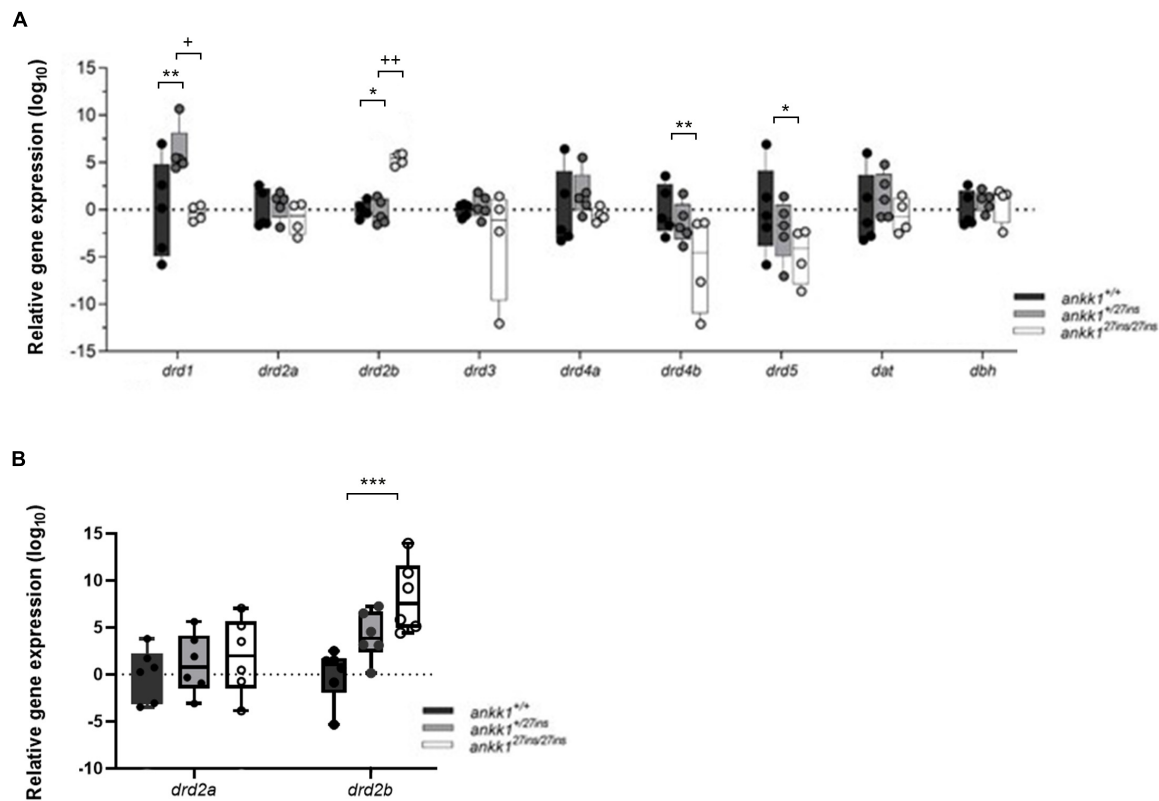


**FIGURE 5 |** Quantification of dopaminergic gene expression. **(A)** Expression levels of *drd2a*, *drd2b*, *drd1*, *drd3*, *drd4a*, *drd4b*, *drd5*, *dat*, and *dbh* in 5 days post fertilization zebrafish larvae ( $ankk1^{+/+}$ ,  $ankk1^{+/27ins}$ , and  $ankk1^{27ins/27ins}$ ) measured by qPCR. Each dot represents a pool of larvae ( $n_{total} = 80$  larvae: 5 samples consisting of 16 larvae for  $ankk1^{+/+}$  and  $ankk1^{+/27ins}$ , and 4 samples consisting of 16 larvae for each sample ( $ankk1^{27ins/27ins}$ ). **(B)** Expression levels of *drd2a* and *drd2b* in adult zebrafish whole brains. Each dot represents a single brain. Data are shown in box-whiskers plot (5–95 percentile). Legend: \* $p < 0.05$  versus  $ankk1^{+/+}$ ; \*\* $p < 0.01$  versus  $ankk1^{+/+}$ ; \*\*\* $p < 0.0001$  versus  $ankk1^{+/+}$ ; + $p < 0.05$  versus corresponding  $ankk1^{+/27ins}$ ; ++ $p < 0.01$  versus corresponding  $ankk1^{+/27ins}$ . Statistics for gene expression data and  $P$  value adjustment are provided in **Supplementary Tables 2, 3**.

(García-González et al., 2020): 73% of wild type animals responded to the first acoustic stimulus, but only 4% responded to the last. We found a significant effect of genotype on distance traveled in the basal portion of the assay (**Figure 8A**) [Effect of genotype:  $\chi^2(2) = 15.8972$ ,  $p < 0.001$ ] whereby  $ankk1^{27ins}$  fish moved significantly less than  $ankk1^{+/+}$  (Tukey's pairwise comparisons:  $ankk1^{+/+}$ - $ankk1^{+/27ins}$   $p = 0.05$ ,  $ankk1^{+/+}$ - $ankk1^{27ins/27ins}$   $p < 0.001$ ).

During the stimulus events we observed a significant effect of stimulus number [Effect of stimulus number:  $\chi^2(19) = 2702.753$ ,  $p < 0.0001$ ], and a significant effect of genotype [Effect of genotype:  $\chi^2(2) = 19.380$ ,  $p < 0.0001$ ], on locomotion whereby  $ankk1^{27ins/27ins}$  fish moved significantly less than  $ankk1^{+/+}$  (Tukey's pairwise comparisons:  $ankk1^{+/+}$ - $ankk1^{27ins/27ins}$   $p < 0.001$ ). There was a genotype by stimulus number interaction [Effect of stimulus number:  $\chi^2(38) = 84.131$ ,  $p < 0.0001$ ] such that  $ankk1^{27ins}$  habituated more slowly.

In the presence of amisulpride we saw no main effect of dose on basal locomotion. However, we detected a two-way interaction [Effect of genotype by dose interaction:  $\chi^2(2) = 13.5008$ ,  $p < 0.01$ ], such that amisulpride exposure increased the distance traveled in  $ankk1^{+/+}$  (Tukey's pairwise comparison:  $ankk1^{+/+}$ -

0.01mg/L -  $ankk1^{+/+}$  control  $p = 0.02$ ), but not in  $ankk1^{+/27ins}$  nor  $ankk1^{27ins/27ins}$  genotypes.

During the stimuli (**Figure 8C**), we found an effect of dose on distance traveled [Effect of dose:  $\chi^2(1) = 40.689$ ,  $p = 0.0001$ ], and a genotype by dose interaction [Effect of genotype by dose interaction:  $\chi^2(2) = 9.036$ ,  $p = 0.01$ ], such that amisulpride exposure increased the distance traveled in  $ankk1^{+/+}$  (Tukey's pairwise comparison:  $ankk1^{+/+}$  0.01mg/L -  $ankk1^{+/+}$  control  $p = 0.02$ ), but not in  $ankk1^{+/27ins}$  nor  $ankk1^{27ins/27ins}$  genotypes. We also found a marginal three-way interaction [Effect of genotype by dose by stimulus number interaction:  $\chi^2(38) = 51.632$ ,  $p = 0.06$ ], such that  $ankk1^{27ins}$  habituate more slowly.

In the presence of apomorphine, we found a significant main effect of dose on basal locomotion [Effect of dose:  $\chi^2(1) = 18.6628$ ,  $p < 0.0001$ ], such that apomorphine treated fish moved less (**Figure 8E**).

During the stimuli (**Figure 8E**) we found a main effect of dose [Effect of dose:  $\chi^2(1) = 30.1613$ ,  $p < 0.0001$ ], where treated fish moved less, and a significant effect of stimulus number [Effect of stimulus number:  $\chi^2(19) = 2165.5652$ ,  $p < 0.0001$ ]. We detected a two-way interaction [Effect of genotype by dose:

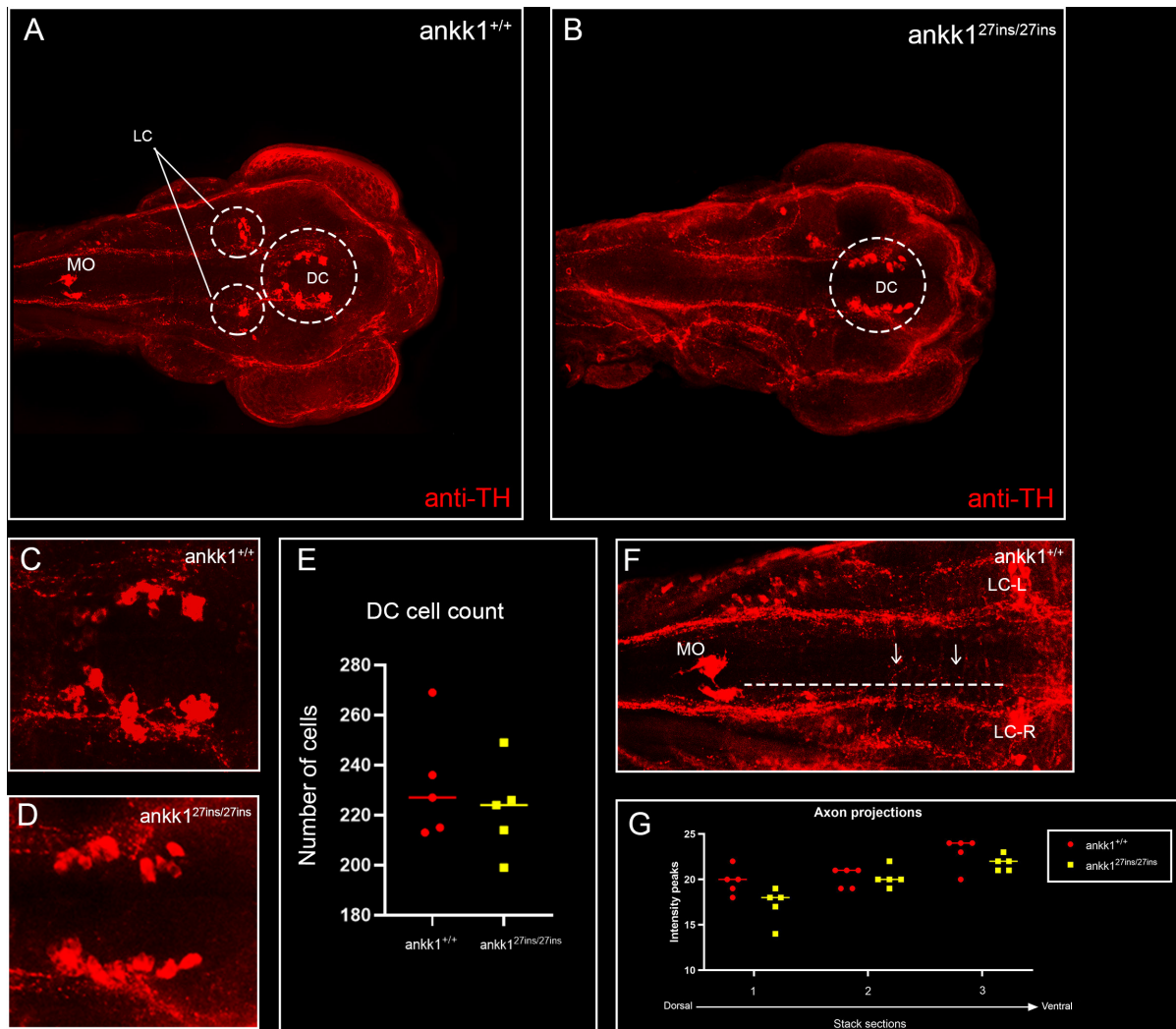


**FIGURE 6 |** Anti-tyrosine hydroxylase (TH) immunolabeling on 3 days post fertilization zebrafish larvae. **(A,C)** *ankk1*<sup>+/+</sup> and **(B,D)** *ankk1*<sup>27ins/27ins</sup>. **(A,B)** Maximum projection dorsal view of whole mount larvae. Circles indicate diencephalic dopaminergic cluster (DC), used for quantification of cell number **(E)**, and locus coeruleus (LC) used as landmark for determining the extent of the medial longitudinal catecholaminergic tract when quantifying the number of anti-TH labeled projections to the midline **(F,G)**. **(C,D)** Representative images of staining of DC used for cell quantification shown in **(E)**. **(F)** Example of sections used for quantification of dopaminergic projections shown in **(G)**. Projections were assessed from posterior to anterior using the LC and anterior extent of the medulla oblongata (MO) as landmarks [(F) dotted line, arrows indicate example of projections], and from dorsal to ventral [(G) stacks 1–3]. *N* = 5 samples × genotype group.

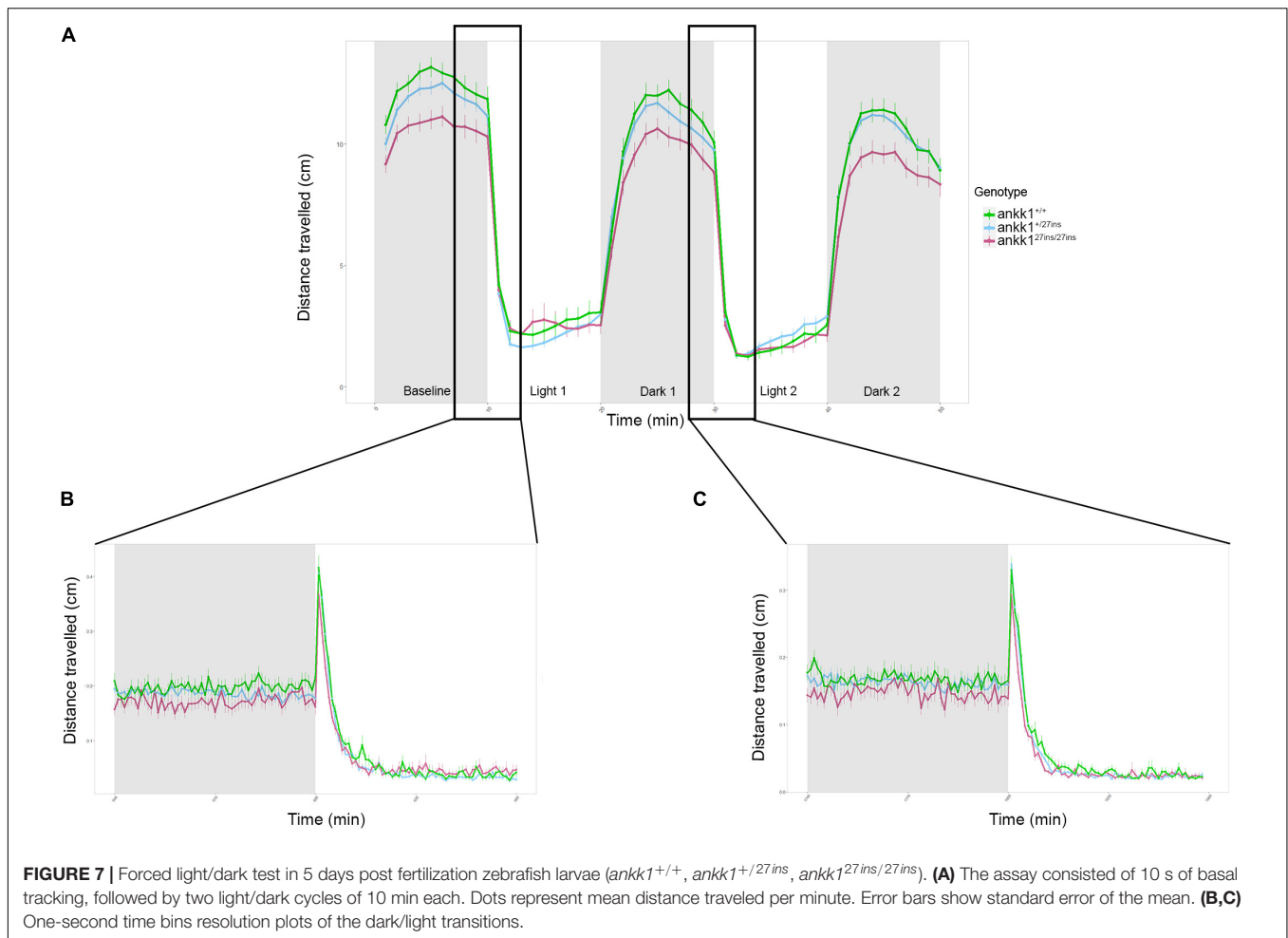
$\chi^2(2) = 37.5713$ ,  $p < 0.0001$ ] and a three-way interaction [Effect of genotype by dose by stimulus number:  $\chi^2(38) = 68.5989$ ,  $p < 0.01$ ] (**Figure 8B**).

Since we discovered significant differences at the genotype and dose levels in basal locomotion, we calculated the proportion of responders to stimulus events using six discrete responder thresholds for each genotype by treatment group (**Figures 8D,F**). In the presence of amisulpride (**Figure 8D**), a lower proportion of *ankk1*<sup>27ins/27ins</sup> fish responded to stimulus events [Effect of genotype:  $\chi^2(2) = 5.1215$ ,  $p < 0.05$  (Tukey's pairwise comparisons: *ankk1*<sup>+/+</sup> - *ankk1*<sup>27ins/27ins</sup>  $p < 0.01$ , *ankk1*<sup>+/+</sup> - *ankk1*<sup>27ins/27ins</sup>  $p < 0.01$ )]. No main effect of dose or genotype by dose interaction was detected. In the presence of apomorphine (**Figure 8F**), a lower proportion of

*ankk1*<sup>27ins</sup> fish responded to stimulus events [Effect of genotype:  $\chi^2(2) = 23.4687$ ,  $p < 0.0001$  (Tukey's pairwise comparisons: *ankk1*<sup>+/+</sup> - *ankk1*<sup>27ins</sup>  $p < 0.0001$ , *ankk1*<sup>+/+</sup> - *ankk1*<sup>27ins/27ins</sup>  $p < 0.0001$ ). We observed a dose by stimulus number interaction [Effect of dose by stimulus number:  $\chi^2(1) = 7.3185$ ,  $p < 0.01$ ], and a genotype by dose interaction [Effect of genotype by dose:  $\chi^2(2) = 19.1113$ ,  $p < 0.0001$ ]; apomorphine reduced *ankk1*<sup>27ins</sup> response to acoustic startle.

## DISCUSSION

In this study, we generated a CRISPR-Cas9 loss of function zebrafish line (*ankk1*<sup>27ins</sup>), to test the hypothesis that *ankk1*



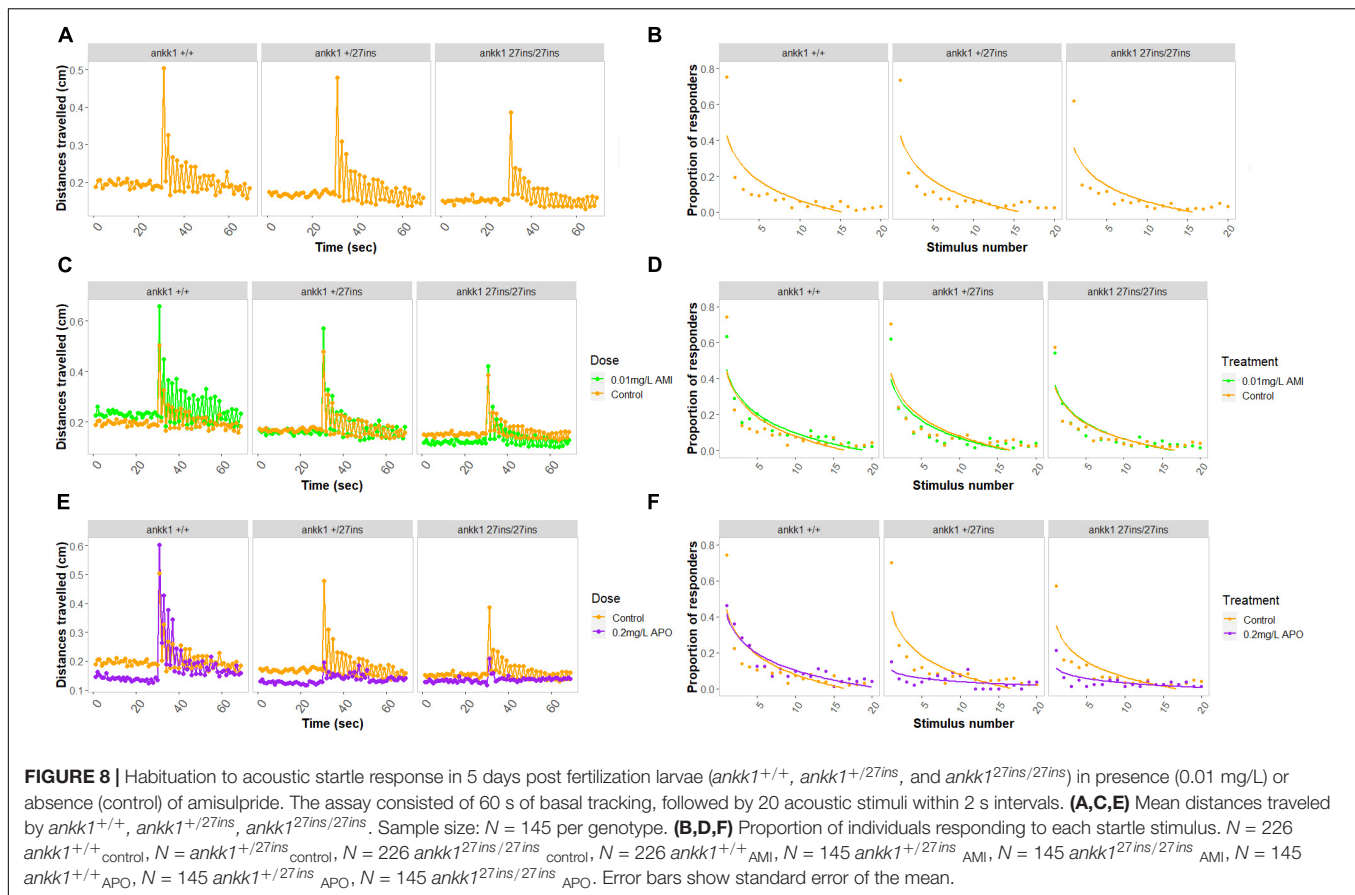
regulates the development and/or functioning of dopaminergic pathways. We confirmed that *ankk1* protein is broadly expressed in regions of the zebrafish brain, and we showed reduction of *ankk1* mRNA and protein expression levels in *ankk1*<sup>27ins</sup> mutants. We found that *drd2b* mRNA was upregulated in *ankk1*<sup>27ins/27ins</sup> whole brain samples at larval and adult stages, but no differences in the number of dopaminergic neurons nor in axon pathfinding were detected in 3 dpf larvae. In contrast, *drd2* protein expression was decreased in cortical regions, and was completely absent in specific midbrain areas of *ankk1*<sup>27ins/27ins</sup> adults. Finally, we reported that *ankk1*<sup>27ins/27ins</sup> larvae had reduced sensitivity to the dopaminergic D2/D3 antagonist amisulpride and were differentially sensitive to the effects of the non-selective dopaminergic agonist apomorphine. Taken together, our results support a role for *ankk1* in the maintenance and/or functioning of zebrafish dopaminergic pathways.

We confirmed *ankk1* loss of function by qPCR experiments. The numerical similarity in *ankk1* mRNA expression between *ankk1*<sup>+/27ins</sup> and *ankk1*<sup>27ins/27ins</sup> is intriguing. This could be due to (i) level of expression at the limit of resolution of our detection, or (ii) we may speculate that an autoregulatory mechanism of *ankk1* expression, such that reduction in active protein seen as a result of heterozygosity, leads to failure to maintain *ankk1*

mRNA expression. However, differences in the expression of the components of the dopaminergic pathway between heterozygotes and homozygotes (e.g., *drd2b*) are not immediately consistent with this latter suggestion. Further experiments are required to address this hypothesis.

As we saw no significant differences between *ankk1*<sup>+/27ins</sup> and *ankk1*<sup>27ins/27ins</sup> in the levels of *ankk1* mRNA expression, we used *ankk1*<sup>27ins/27ins</sup> to assess differences in protein levels in wild type and mutant fish.

We describe the neuroanatomical distribution of *ankk1* protein in the adult zebrafish brain. We detected *ankk1* protein in many forebrain areas of the dorsal, medial, and ventral pallidum, homologous to the mammalian isocortex, hippocampus and basolateral amygdala, respectively (Mueller, 2012; see Cheng et al., 2014 for review), and in the subpallidum, homologous to the basal ganglia (see Cheng et al., 2014 for review). We also found *ankk1* protein expression in the mesencephalon, and in the cerebellum. These results agree with findings in mice where *Ankk1* protein is expressed in the prefrontal cortex, hippocampus, corpus callosum, thalamus, bulb, pons, mesencephalon, encephalic trunk, basal ganglia, cerebellum, and spinal cord (Hoenicka et al., 2010). In contrast, in *ankk1*<sup>27ins/27ins</sup> mutants, *ankk1* protein expression was reduced in the forebrain



and completely absent in the mid- and hindbrain. As the antibody recognizes an epitope before the stop-codon introduced by our mutation (A12930, ABclonal Immunogen Information), the low level of expression detected in the forebrain may reflect (i) incomplete destruction of the mRNA, (ii) non-specific binding or (iii) brain region specific alternative splicing. The use of different antibodies aiming to detect epitopes before and after the stop codon may be useful to interrogate the presence of region-specific splice variants.

In mammals, *ANKK1* has been proposed to modulate development and functioning of dopaminergic signaling pathways (Koenke et al., 2020). Particularly, previous studies showed that the TaqA1 allele is associated with reduced DRD2 density in human striatum (Noble, 2003; Neville et al., 2004; Klein et al., 2007; Savitz et al., 2013). Dopaminergic receptors are well conserved among vertebrates. Due to the whole-genome duplication in teleosts (Glasauer and Neuhauss, 2014), zebrafish possess two *drd2* genes, *drd2a* (Chr15: 22,046,557–22,074,315) and *drd2b* (Chr5: 58,075,301–58,173,627), which show a sequence similarity of 71 and 66%, respectively, with human DRD2 (Boehmler et al., 2004). The antibody employed in our study recognizes an epitope which is common to both proteins. In agreement with previous findings (Noble, 2003; Neville et al., 2004; Klein et al., 2007; Savitz et al., 2013), adult *ankk1*<sup>27ins/27ins</sup> mutant fish showed reduced expression of *drd2* protein in the pallidum and subpallidum. The zebrafish subpallidum

corresponds to the striatum of mammals, which has been shown to be involved in processes such as motor learning (Adrover et al., 2020). We also observed absence of *drd2* protein in the hypothalamus of *ankk1*<sup>27ins/27ins</sup>. In zebrafish, hypothalamic dopaminergic neurons activate premotor circuits involved in swimming and sensorimotor integration (Barrios et al., 2020). These findings may explain the alterations in locomotor effects observed in our behavioral tests.

*Drd2* protein antibody staining in adult mutant fish shows a different trend from *drd2b* mRNA expression at both larval and adult stages, where mutants had a higher *drd2b* gene expression. Such differences may be due to (i) biological processes (such as splicing, translational modifications/regulation, protein complex formation) that affect the relative quantities of mRNA and protein (Guo et al., 2008; Perl et al., 2017), (ii) loss of receptor function/signaling, which is often associated with compensatory increases in gene expression (Perdew et al., 2007), (iii) differences in the detection method.

Interestingly, *ANKK1* and *DRD2* form part of the NTAD genomic cluster in mammals (Yi et al., 2007; España-Serrano et al., 2017; Rubio-Solsona et al., 2018; Koenke et al., 2020) but in zebrafish only *drd2a* (whose mRNA expression was not altered) maps to the NTAD region. It is therefore possible that in zebrafish, *drd2a* (but not *drd2b*) is part of the NTAD functional cluster associated with *ANKK1* function, or that *drd2b* forms part of an interchromosomal NTAD gene cluster (Woods et al., 2005).

In addition to a role in regulation of *drd2* expression, *ankk1* has been proposed to play a role in neurogenesis and cell migration (Mota et al., 2012; España-Serrano et al., 2017; Koenke et al., 2020). To test this hypothesis, we assessed the number of dopaminergic neurons in the diencephalic cluster and axonal projections from the medulla oblongata interfascicular zone and vagal area to the locus coeruleus of 3 dpf larvae but found no differences among *ankk1* genotypes. These findings argue against a role of *ankk1* in dopaminergic neurogenesis. Although our immunohistochemical analysis did not detect differences in axonal projections, our method would not have been sensitive enough to detect subtle changes (e.g., in dendrites and synapses) and it is possible that differences become more apparent at later stages of development.

We therefore conducted behavioral assays to analyze possible disruption of dopaminergic function in 5 dpf larvae using amisulpride and apomorphine, a selective D2/D3 dopamine receptor antagonist (Coulkell et al., 1996) and a non-selective dopamine receptor agonist (Lees, 1993), respectively.

In mammals, dopamine receptors are coupled to G-proteins (see Beaulieu and Gainetdinov, 2011 for review). D1-like receptors (D1 and D5) have an excitatory effect on neurotransmission via activation of Gs proteins, whereas D2-like receptors (D2, D3, and D4) are coupled to Gi/o proteins mediating inhibitory neurotransmission (Beaulieu and Gainetdinov, 2011; Martel and Gatti McArthur, 2020). In rodents, low doses of D2/D3 receptor antagonists decrease locomotion via high affinity presynaptic receptors, whereas high doses increase locomotion via lower affinity postsynaptic receptors (Millan et al., 2004). Although binding affinities of D2/3 receptors in zebrafish are not established, and drugs could be metabolized by zebrafish in a different manner compared to mammals (Achenbach et al., 2018), a biphasic effect of D2/D3 receptor antagonists including amisulpride on locomotion has also been reported (Tran et al., 2015). The findings of Tran et al. (2015) confirm the involvement of both pre- and post-synaptic dopamine receptors in this species. Amisulpride has also been shown to increase habituation to acoustic startle in both humans (Quednow et al., 2006) and zebrafish (García-González et al., 2020).

Apomorphine is a short-acting non-selective dopamine receptor agonist that, similarly to amisulpride, binds to pre- and post-synaptic dopaminergic receptors in a dose-dependent manner (Auffret et al., 2018; Carbone et al., 2019). In mammals, apomorphine at low doses decreases locomotion via presynaptic receptors, whereas at high doses increases locomotion via postsynaptic receptors (Santos et al., 2018). Apomorphine treatment increases startle reactivity with no effect on the rate of habituation (Davis and Aghajanian, 1976; Geyer et al., 1978). In zebrafish it has been reported that apomorphine causes similar effects on locomotor activity as in mammals (Khalili et al., 2021, under review).

The altered sensitivity to effects of both amisulpride and apomorphine on locomotion and startle habituation seen here are consistent with a broad loss of *drd2* as suggested by our immunohistochemistry. Amisulpride increased locomotion and increased habituation in *ankk1*<sup>+/+</sup> but had no

effect in *ankk1*<sup>27ins</sup> suggesting loss of post-synaptic receptors. Apomorphine decreased basal locomotion in both *ankk1*<sup>+/+</sup> and, to a lesser extent, in *ankk1*<sup>27ins</sup> fish, increased locomotion in response to acoustic startle in *ankk1*<sup>+/+</sup> fish, but decreased locomotion in response to acoustic startle in *ankk1*<sup>27ins</sup> fish. The decrease in basal locomotion in *ankk1*<sup>27ins</sup> mutants in the presence of apomorphine suggests action at presynaptic D2 and/or D3 autoreceptors is maintained, albeit possibly reduced. The lack of stimulatory effect in *ankk1*<sup>27ins</sup> mutants suggests disruption of action of apomorphine at post-synaptic sites. As both D1 and D2 receptors modulate the startle response (Halberstadt and Geyer, 2009), loss of a stimulatory effect of apomorphine on startle response may result from disruption of non-*drd2* signaling in *ankk1*<sup>27ins</sup> mutants, possibly as a result of reduced expression of *drd4* or *drd5* as suggested by our qPCR data, or as a secondary effect of loss of *drd2* signaling. The further reduction in response to acoustic startle seen in the presence of apomorphine in mutants might reflect action at residual (pre- or post-synaptic) D2 receptors, or again actions of apomorphine at non-D2 receptors.

Further studies employing more specific dopamine receptor agonists and antagonists in conjunction with analysis of *drd2* binding affinities and additional immunohistochemical analyses are needed to test these hypotheses.

Despite the noticeable difference in size (i.e., smaller cerebral hemispheres) and distinctions that must be considered when establishing translational comparisons [e.g., zebrafish lack the prefrontal cortex, a region involved in high-order functions commonly disrupted in psychiatric disorders (Mueller and Wullmann, 2015)], the general architecture of the key components of the zebrafish central nervous system is highly conserved with that of humans (see Tropepe and Sive, 2003, for review). Here we exemplify how zebrafish can be exploited as a suitable model to study the development and functioning of the vertebrate nervous system, and to interrogate the functional impact of genetic variation relevant for human disease, including psychiatric disease and substance use disorder.

## CONCLUSION

To our knowledge, this is the first study aiming at the characterization, at both behavioral and molecular levels, of a loss of function line for *ankk1* and its effect on the development and functioning of the dopaminergic system. Although an *Ankk1* mouse knockout line has been recently characterized by Powell et al. (2021), their research was focused on obesity and we did not find further studies characterizing this mutation or its effects on the dopaminergic system. Our findings strengthen the hypothesis of a functional relationship between *ANKK1* and *DRD2*, suggesting that *ANKK1* might be involved in the maintenance of *DRD2* in the cell membrane, rather than in the specification of dopaminergic neurons or establishment of dopaminergic neuron circuits. However, further studies must be conducted to address this question, such as conditional knockout of the *ankk1* gene at later developmental stages. Despite

the limitations listed in our discussions, zebrafish represent a powerful model to investigate behaviors and molecular pathways associated with addiction disorders and psychiatric diseases. As the mutation generated is stable, and easy to genotype, this line paves the way to downstream molecular and cellular studies of functionality.

## DATA AVAILABILITY STATEMENT

The original contributions presented in the study are included in the article/**Supplementary Material**, further inquiries can be directed to the corresponding author/s.

## ETHICS STATEMENT

The animal study was reviewed and approved by the Local Animal Welfare and Ethical Review Board at Queen Mary University of London.

## AUTHOR CONTRIBUTIONS

AL conducted the experiments, analyzed the data, and wrote the manuscript. JG-G designed the study, generated the line,

conducted experiments, and analyzed the data. MK helped to design the experiments. JT-P and WH conducted the experiments and analyzed the data. AM and SH conducted the experiments. CB directed the study, designed the experiments, edited the manuscript, and secured funding. EB-N secured funding. All authors contributed to the article and approved the submitted version.

## FUNDING

This work was supported by the NIH grant U01 DA044400-03 (CB and EB-N).

## ACKNOWLEDGMENTS

We sincerely thank Rob Knell for his critical review of statistical methods.

## SUPPLEMENTARY MATERIAL

The Supplementary Material for this article can be found online at: <https://www.frontiersin.org/articles/10.3389/fnins.2022.794653/full#supplementary-material>

## REFERENCES

- Achenbach, J. C., Hill, J., Hui, J. P. M., Morash, M. G., Berrue, F., and Ellis, L. D. (2018). Analysis of the uptake, metabolism, and behavioral effects of cannabinoids on zebrafish larvae. *Zebrafish* 15, 349–360. doi: 10.1089/zeb.2017.1541
- Adrover, M. F., Shin, J. H., Quiroz, C., Ferré, S., Lemos, J. C., and Alvarez, V. A. (2020). Prefrontal Cortex-driven dopamine signals in the striatum show unique spatial and pharmacological properties. *J. Neurosci.* 40, 7510–7522. doi: 10.1523/JNEUROSCI.1327-20.2020
- Auffret, M., Drapier, S., and Vêrin, M. (2018). The many faces of apomorphine: lessons from the past and challenges for the future. *Drugs R D* 18, 91–107. doi: 10.1007/s40268-018-0230-3
- Baarendse, P. J. J., Limpens, J. H. W., and Vanderschuren, L. J. M. J. (2014). Disrupted social development enhances the motivation for cocaine in rats. *Psychopharmacology* 231, 1695–1704. doi: 10.1007/s00213-013-3362-8
- Barrios, J. P., Wang, W.-C., England, R., Reifenberg, E., and Douglass, A. D. (2020). Hypothalamic Dopamine neurons control sensorimotor behavior by modulating brainstem premotor nuclei in zebrafish. *Curr. Biol.* 30, 4606.e–4618.e. doi: 10.1016/j.cub.2020.09.002
- Beaulieu, J.-M., and Gainetdinov, R. R. (2011). The physiology, signaling, and pharmacology of dopamine receptors. *Pharmacol. Rev.* 63, 182–217. doi: 10.1124/pr.110.002642
- Blum, K., Noble, E. P., Sheridan, P. J., Montgomery, A., Ritchie, T., Jagadeeswaran, P., et al. (1990). Allelic association of human dopamine D2 receptor gene in alcoholism. *JAMA* 263, 2055–2060.
- Boehmler, W., Obrecht-Pflumio, S., Canfield, V., Thisse, C., Thisse, B., and Levenson, R. (2004). Evolution and expression of D2 and D3 dopamine receptor genes in zebrafish. *Dev. Dyn.* 230, 481–493. doi: 10.1002/dvdy.20075
- Bradford, Y. M., Toro, S., Ramachandran, S., Ruzicka, L., Howe, D. G., Eagle, A., et al. (2017). Zebrafish models of human disease: gaining insight into human disease at ZFIN. *ILAR J.* 58, 4–16. doi: 10.1093/ilar/ilw040
- Burgess, H. A., and Granato, M. (2007). Sensorimotor gating in larval zebrafish. *J. Neurosci.* 27, 4984–4994. doi: 10.1523/JNEUROSCI.0615-07.2007
- Carbone, F., Djamshidian, A., Seppi, K., and Poewe, W. (2019). Apomorphine for Parkinson's disease: efficacy and safety of current and new formulations. *CNS Drugs* 33, 905–918. doi: 10.1007/s40263-019-00661-z
- Cheng, R.-K., Jesuthasan, S. J., and Penney, T. B. (2014). Zebrafish forebrain and temporal conditioning. *Philosoph. Trans. R. Soc. B* 369:20120462. doi: 10.1098/rstb.2012.0462
- Clark, K. J., Boczek, N. J., and Ekker, S. C. (2011). Stressing zebrafish for behavioral genetics. *Rev. Neurosci.* 22, 49–62. doi: 10.1515/rns.2011.007
- Coukell, A. J., Spencer, C. M., and Benfield, P. (1996). Amisulpride. *CNS Drugs* 6, 237–256. doi: 10.2165/00023210-199606030-00006
- Davis, M., and Aghajanian, G. K. (1976). Effects of apomorphine and haloperidol on the acoustic startle response in rats. *Psychopharmacology* 47, 217–223. doi: 10.1007/BF00427605
- de la Mora, M. P., Gallegos-Cari, A., Arizmendi-García, Y., Marcellino, D., and Fuxe, K. (2010). Role of dopamine receptor mechanisms in the amygdaloid modulation of fear and anxiety: structural and functional analysis. *Prog. Neurobiol.* 90, 198–216. doi: 10.1016/j.pneurobio.2009.10.010
- Declercq, W., Vanden Berghe, T., and Vandenabeele, P. (2009). RIP kinases at the crossroads of cell death and survival. *Cell* 138, 229–232. doi: 10.1016/j.cell.2009.07.006
- España-Serrano, L., Guerra Martín-Palanco, N., Montero-Pedrazuela, A., Pérez-Santamarina, E., Vidal, R., García-Consuegra, I., et al. (2017). The addiction-related protein ank1 is differentially expressed during the cell cycle in neural precursors. *Cerebral. Cortex* 27, 2809–2819. doi: 10.1093/cercor/bhw129
- Evans, J. R., Torres-Pérez, J. V., Miletto Petrazzini, M. E., Riley, R., and Brennan, C. H. (2021). Stress reactivity elicits a tissue-specific reduction in telomere length in aging zebrafish (Danio rerio). *Sci. Rep.* 11:339. doi: 10.1038/s41598-020-79615-1
- García-González, J., Brock, A. J., Parker, M. O., Riley, R. J., Joliffe, D., Sudwats, A., et al. (2020). Identification of slit3 as a locus affecting nicotine preference in zebrafish and human smoking behaviour. *ELife* 9:e51295. doi: 10.7554/eLife.51295
- García-González, J., de Quadros, B., Havelange, W., and Brock, A. J. (2021). Behavioral Effects of Developmental Exposure to JWH-018 in Wild-Type and

- Disrupted in Schizophrenia 1 (disc1) Mutant Zebrafish. *Biomolecules* 11:319. doi: 10.3390/biom11020319
- Geyer, M. A., Petersen, L. R., Rose, G. J., Horwitt, D. D., Light, R. K., Adams, L. M., et al. (1978). The effects of lysergic acid diethylamide and mescaline-derived hallucinogens on sensory-integrative function: tactile startle. *J. Pharmacol. Exp. Ther.* 207, 837–847.
- Glasauer, S. M. K., and Neuhauss, S. C. F. (2014). Whole-genome duplication in teleost fishes and its evolutionary consequences. *Mol. Genet. Genomics* 289, 1045–1060. doi: 10.1007/s00438-014-0889-2
- Glazer, L., Hawkey, A. B., Wells, C. N., Drastal, M., Odamah, K.-A., Behl, M., et al. (2018). Developmental exposure to low concentrations of organophosphate flame retardants causes life-long behavioral alterations in zebrafish. *Toxicol. Sci.* 165, 487–498. doi: 10.1093/toxsci/kfy173
- Guo, Y., Xiao, P., Lei, S., Deng, F., Xiao, G. G., Liu, Y., et al. (2008). How is mRNA expression predictive for protein expression? A correlation study on human circulating monocytes. *Acta Biochimica Et Biophysica Sinica* 40, 426–436. doi: 10.1111/j.1745-7270.2008.00418.x
- Halberstadt, A. L., and Geyer, M. A. (2009). Habituation and sensitization of acoustic startle: opposite influences of dopamine D1 and D2-family receptors. *Neurobiol. Learn. Mem.* 92, 243–248. doi: 10.1016/j.nlm.2008.05.015
- Hellems, J., Mortier, G., De Paepe, A., Speleman, F., and Vandesompele, J. (2007). qBase relative quantification framework and software for management and automated analysis of real-time quantitative PCR data. *Genome Biol.* 8:R19. doi: 10.1186/gb-2007-8-2-r19
- Hoenicka, J., Quiñones-Lombrana, A., España-Serrano, L., Alvira-Botero, X., Kremer, L., Pérez-González, R., et al. (2010). The ANKK1 gene associated with addictions is expressed in astroglial cells and upregulated by apomorphine. *Biol. Psychiatry* 67, 3–11. doi: 10.1016/j.biopsych.2009.08.012
- Humphries, F., Yang, S., Wang, B., and Moynagh, P. N. (2015). RIP kinases: key decision makers in cell death and innate immunity. *Cell Death Diff.* 22, 225–236. doi: 10.1038/cdd.2014.126
- Keatinge, M., Tsarouchas, T. M., Munir, T., Porter, N. J., Larraz, J., Gianni, D., et al. (2021). CRISPR gRNA phenotypic screening in zebrafish reveals pro-regenerative genes in spinal cord injury. *PLoS Genet.* 17:e1009515. doi: 10.1371/journal.pgen.1009515
- Khalili, A., van Wijngaarden, E., Zoidl, G. R., and Rezai, P. (2021). Zebrafish Larvae's Response to Electricity is mediated by dopaminergic agonists and antagonists. *Authorea* 2021:54745545. doi: 10.22541/au.163458135.54745545/v1
- Klee, E. W., Ebbert, J. O., Schneider, H., Hurt, R. D., and Ekker, S. C. (2011). Zebrafish for the Study of the Biological Effects of Nicotine. *Nicot. Tob. Res.* 13, 301–312. doi: 10.1093/ntr/ntr010
- Klee, E. W., Schneider, H., Clark, K. J., Cousin, M. A., Ebbert, J. O., Hooten, W. M., et al. (2012). Zebrafish: a model for the study of addiction genetics. *Hum. Genet.* 131, 977–1008. doi: 10.1007/s00439-011-1128-0
- Klein, T. A., Neumann, J., Reuter, M., Hennig, J., von Cramon, D. Y., and Ullsperger, M. (2007). Genetically determined differences in learning from errors. *Science* 318, 1642–1645. doi: 10.1126/science.1145044
- Koenke, A., Ponce, G., Troya-Balseca, J., Palomo, T., and Hoenicka, J. (2020). Ankyrin Repeat and kinase domain containing 1 gene, and addiction vulnerability. *Internat. J. Mole. Sci.* 21:2516. doi: 10.3390/ijms21072516
- Lees, A. (1993). Dopamine agonists in Parkinson's disease: a look at apomorphine. *Fund. Clin. Pharmacol.* 7, 121–128. doi: 10.1111/j.1472-8206.1993.tb00226.x
- Link, B. A., and Megason, S. G. (2008). "Zebrafish as a Model for Development," in *Sourcebook of Models for Biomedical Research*, ed. P. M. Conn (Totowa: Humana Press), 103–112. doi: 10.1007/978-1-59745-285-4\_13
- Lopez-Leon, S., González-Giraldo, Y., Wegman-Ostrosky, T., and Forero, D. A. (2021). Molecular genetics of substance use disorders: an umbrella review. *Neurosci. Biobehav. Rev.* 124, 358–369. doi: 10.1016/j.neubiorev.2021.01.019
- Martel, J. C., and Gatti McArthur, S. (2020). Dopamine Receptor subtypes, physiology and pharmacology: new ligands and concepts in schizophrenia. *Front. Pharm.* 11:1003. doi: 10.3389/fphar.2020.01003
- Mathur, P., and Guo, S. (2010). Use of zebrafish as a model to understand mechanisms of addiction and complex neurobehavioral phenotypes. *Neurobiol. Dis.* 40, 66–72. doi: 10.1016/j.nbd.2010.05.016
- Meylan, E., and Tschopp, J. (2005). The RIP kinases: crucial integrators of cellular stress. *Trends Biochem. Sci.* 30, 151–159. doi: 10.1016/j.tibs.2005.01.003
- Millan, M. J., Seguin, L., Gobert, A., Cussac, D., and Brocco, M. (2004). The role of dopamine D3 compared with D2 receptors in the control of locomotor activity: a combined behavioural and neurochemical analysis with novel, selective antagonists in rats. *Psychopharmacology* 174, 341–357. doi: 10.1007/s00213-003-1770-x
- Mota, N. R., Araujo-Jnr, E. V., Paixão-Côrtes, V. R., Bortolini, M. C., and Bau, C. H. D. (2012). Linking dopamine neurotransmission and neurogenesis: the evolutionary history of the NTAD (NCAM1-TTC12-ANKK1-DRD2) gene cluster. *Genet. Mole. Biol.* 35(4 (Suppl.)), 912–918. doi: 10.1590/s1415-47572012000600004
- Mueller, T. (2012). What is the Thalamus in Zebrafish? *Front. Neurosci.* 6:64. doi: 10.3389/fnins.2012.00064
- Mueller, T., and Wullmann, M. (2015). *Atlas of Early Zebrafish Brain Development*, 2nd Edn. Amsterdam: Elsevier.
- Neville, M. J., Johnstone, E. C., and Walton, R. T. (2004). Identification and characterization of ANKK1: A novel kinase gene closely linked to DRD2 on chromosome band 11q23.1. *Hum. Mutat.* 23, 540–545. doi: 10.1002/humu.20039
- Noble, E. P. (2003). D2 dopamine receptor gene in psychiatric and neurologic disorders and its phenotypes. *Am. J. Med. Genet.* 116B, 103–125. doi: 10.1002/ajmg.b.10005
- Parker, M., Brock, A., Walton, R., and Brennan, C. (2013). The role of zebrafish (Danio rerio) in dissecting the genetics and neural circuits of executive function. *Front. Neural Circuits* 7:63. doi: 10.3389/fncir.2013.00063
- Perdew, G. H., Vanden Heuvel, J. P., and Peters, J. M. (eds) (2007). *Transcriptional Regulation of Gene Expression. In Regulation of Gene Expression: Molecular Mechanisms*. Totowa, NJ: Humana Press, 49–103. doi: 10.1007/978-1-59745-228-1\_4
- Perl, K., Ushakov, K., Pozniak, Y., Yizhar-Barnea, O., Bhonker, Y., Shivatzki, S., et al. (2017). Reduced changes in protein compared to mRNA levels across non-proliferating tissues. *BMC Genomics* 18:305. doi: 10.1186/s12864-017-3683-9
- Pfaffl, M. W. (2001). A new mathematical model for relative quantification in real-time RT-PCR. *Nucleic Acids Res.* 29:e45.
- Ponce, G., Pérez-González, R., Aragüés, M., Palomo, T., Rodríguez-Jiménez, R., Jiménez-Arriero, M. A., et al. (2009). The ANKK1 kinase gene and psychiatric disorders. *Neurosci. Res.* 16, 50–59. doi: 10.1007/s12640-009-9046-9
- Powell, D. R., Revelli, J.-P., Doree, D. D., DaCosta, C. M., Desai, U., Shadoan, M. K., et al. (2021). High-throughput screening of mouse gene knockouts identifies established and novel high body fat phenotypes. *Diabetes Metab. Syndr. Obes.* 14, 3753–3785. doi: 10.2147/DMSO.S322083
- Prom-Wormley, E. C., Ebejer, J., Dick, D. M., and Bowers, M. S. (2017). The genetic epidemiology of substance use disorder: a review. *Drug Alcohol. Depend.* 180, 241–259. doi: 10.1016/j.drugalcdep.2017.06.040
- Quednow, B. B., Wagner, M., Westheide, J., Beckmann, K., Bliesener, N., Maier, W., et al. (2006). Sensorimotor gating and habituation of the startle response in schizophrenic patients randomly treated with amisulpride or olanzapine. *Biolog. Psychiatry* 59, 536–545. doi: 10.1016/j.biopsych.2005.07.012
- R Core Team (2020). *R: A Language and Environment for Statistical Computing*. Vienna: R Foundation for Statistical Computing.
- Rubio-Solsona, E., Martí, S., Vilchez, J. J., Palau, F., and Hoenicka, J. (2018). ANKK1 is found in myogenic precursors and muscle fibers subtypes with glycolytic metabolism. *PLoS One* 13:e0197254. doi: 10.1371/journal.pone.0197254
- Sakai, C., Ijaz, S., and Hoffman, E. J. (2018). Zebrafish Models of Neurodevelopmental Disorders: Past, Present, and Future. *Front. Mole. Neurosci.* 11:294. doi: 10.3389/fnmol.2018.00294
- Santos, B. G., Carey, R. J., and Carrera, M. P. (2018). Repeated pre-trial and post-trial low and high dose apomorphine treatments induce comparable inhibitory/excitatory sensitization and conditioned drug effects. *Pharm. Biochem. Behav.* 175, 108–115. doi: 10.1016/j.pbb.2018.09.011
- Savitz, J., Hodgkinson, C. A., Martin-Soelch, C., Shen, P.-H., Szczepanik, J., Nugent, A. C., et al. (2013). DRD2/ANKK1 Taq1A polymorphism (rs1800497) has opposing effects on D2/3 receptor binding in healthy controls and patients

- with major depressive disorder. *Internat. J. Neuropsychopharm.* 16, 2095–2101. doi: 10.1017/S146114571300045X
- Šidák, Z. (1967). Rectangular Confidence Regions for the Means of Multivariate Normal Distributions. *J. Am. Stat. Assoc.* 62, 626–633. doi: 10.1080/01621459.1967.10482935
- Stewart, A., Wong, K., Cachat, J., Gaikwad, S., Kyzar, E., Wu, N., et al. (2011). Zebrafish models to study drug abuse-related phenotypes. *Rev. Neurosci.* 22, 95–105. doi: 10.1515/RNS.2011.011
- Tran, S., Nowicki, M., Muraleetharan, A., and Gerlai, R. (2015). Differential effects of dopamine D1 and D 2/3 receptor antagonism on motor responses. *Psychopharmacology* 232, 795–806. doi: 10.1007/s00213-014-3713-0
- Tropepe, V., and Sive, H. L. (2003). Can zebrafish be used as a model to study the neurodevelopmental causes of autism? *Genes Brain Behav.* 2, 268–281. doi: 10.1034/j.1601-183X.2003.00038.x
- Völter, C., Riedel, M., Wöstmann, N., Aichert, D. S., Lobo, S., Costa, A., et al. (2012). Sensorimotor gating and D2 receptor signalling: evidence from a molecular genetic approach. *Internat. J. Neuropsychopharmacol.* 15, 1427–1440. doi: 10.1017/S1461145711001787
- Wang, F., Simen, A., Arias, A., Lu, Q.-W., and Zhang, H. (2013). A large-scale meta-analysis of the association between the ANKK1/DRD2 Taq1A polymorphism and alcohol dependence. *Hum. Genet.* 132, 347–358. doi: 10.1007/s00439-012-1251-6
- Wong, W. C., Ford, K. A., Pagels, N. E., McCutcheon, J. E., and Marinelli, M. (2013). Adolescents Are more vulnerable to cocaine addiction: behavioral and electrophysiological Evidence. *J. Neurosci.* 33, 4913–4922. doi: 10.1523/JNEUROSCI.1371-12.2013
- Woods, I. G., Wilson, C., Friedlander, B., Chang, P., Reyes, D. K., Nix, R., et al. (2005). Postlethwait JH, Talbot WS. The zebrafish gene map defines ancestral vertebrate chromosomes. *Genome Res* 15, 1307–1314. doi: 10.1101/gr.4134305
- Wullimann, M. F., Rupp, B., and Reichert, H. (1996). “Functional anatomy of the zebrafish brain: a comparative evaluation,” in *Neuroanatomy of the Zebrafish Brain: A Topological Atlas*, eds M. F. Wullimann, B. Rupp, and H. Reichert (Basel: Birkhäuser), 89–101. doi: 10.1007/978-3-0348-8979-7\_6
- Yi, G., Sze, S.-H., and Thon, M. R. (2007). Identifying clusters of functionally related genes in genomes. *Bioinformatics* 23, 1053–1060. doi: 10.1093/bioinformatics/btl673
- Zhang, D., Lin, J., and Han, J. (2010). Receptor-interacting protein (RIP) kinase family. *Cell. Mole. Immunol.* 7, 243–249. doi: 10.1038/cmi.2010.10
- Conflict of Interest:** The authors declare that the research was conducted in the absence of any commercial or financial relationships that could be construed as a potential conflict of interest.
- Publisher’s Note:** All claims expressed in this article are solely those of the authors and do not necessarily represent those of their affiliated organizations, or those of the publisher, the editors and the reviewers. Any product that may be evaluated in this article, or claim that may be made by its manufacturer, is not guaranteed or endorsed by the publisher.

Copyright © 2022 Leggieri, García-González, Torres-Perez, Havelange, Hosseinian, Mech, Keatinge, Busch-Nentwich and Brennan. This is an open-access article distributed under the terms of the Creative Commons Attribution License (CC BY). The use, distribution or reproduction in other forums is permitted, provided the original author(s) and the copyright owner(s) are credited and that the original publication in this journal is cited, in accordance with accepted academic practice. No use, distribution or reproduction is permitted which does not comply with these terms.



# Genome-Wide Association Study on Three Behaviors Tested in an Open Field in Heterogeneous Stock Rats Identifies Multiple Loci Implicated in Psychiatric Disorders

Mustafa Hakan Gunturkun<sup>1</sup>, Tengfei Wang<sup>1</sup>, Apurva S. Chitre<sup>2</sup>, Angel Garcia Martinez<sup>1</sup>, Katie Holl<sup>3</sup>, Celine St. Pierre<sup>2</sup>, Hannah Bimschleger<sup>2</sup>, Jianjun Gao<sup>2</sup>, Riyan Cheng<sup>2</sup>, Oksana Polesskaya<sup>2</sup>, Leah C. Solberg Woods<sup>3</sup>, Abraham A. Palmer<sup>2,4</sup> and Hao Chen<sup>1\*</sup>

<sup>1</sup> Department of Pharmacology, Addiction Science and Toxicology, University of Tennessee Health Science Center, Memphis, TN, United States, <sup>2</sup> Department of Psychiatry, University of California, San Diego, La Jolla, CA, United States, <sup>3</sup> Department of Internal Medicine, Wake Forest School of Medicine, Winston Salem, NC, United States, <sup>4</sup> Institute for Genomic Medicine, University of California, San Diego, La Jolla, CA, United States

## OPEN ACCESS

### Edited by:

Peter Kalivas,  
Medical University of South Carolina,  
United States

### Reviewed by:

Massimo Ubaldi,  
University of Camerino, Italy  
Ritchy Hodebourg,  
Medical University of South Carolina,  
United States

### \*Correspondence:

Hao Chen  
hchen@uthsc.edu

### Specialty section:

This article was submitted to  
Addictive Disorders,  
a section of the journal  
Frontiers in Psychiatry

**Received:** 06 October 2021

**Accepted:** 18 January 2022

**Published:** 14 February 2022

### Citation:

Gunturkun MH, Wang T, Chitre AS,  
Garcia Martinez A, Holl K, St. Pierre C,  
Bimschleger H, Gao J, Cheng R,  
Polesskaya O, Solberg Woods LC,  
Palmer AA and Chen H (2022)  
Genome-Wide Association Study on  
Three Behaviors Tested in an Open  
Field in Heterogeneous Stock Rats  
Identifies Multiple Loci Implicated in  
Psychiatric Disorders.  
Front. Psychiatry 13:790566.  
doi: 10.3389/fpsy.2022.790566

Many personality traits are influenced by genetic factors. Rodents models provide an efficient system for analyzing genetic contribution to these traits. Using 1,246 adolescent heterogeneous stock (HS) male and female rats, we conducted a genome-wide association study (GWAS) of behaviors measured in an open field, including locomotion, novel object interaction, and social interaction. We identified 30 genome-wide significant quantitative trait loci (QTL). Using multiple criteria, including the presence of high impact genomic variants and co-localization of cis-eQTL, we identified 17 candidate genes (*Adarb2*, *Ankrd26*, *Cacna1c*, *Cacng4*, *Clock*, *Ctu2*, *Cyp26b1*, *Dnah9*, *Gda*, *Grxcr1*, *Eva1a*, *Fam114a1*, *Kcnj9*, *Mlf2*, *Rab27b*, *Sec11a*, and *Ube2h*) for these traits. Many of these genes have been implicated by human GWAS of various psychiatric or drug abuse related traits. In addition, there are other candidate genes that likely represent novel findings that can be the catalyst for future molecular and genetic insights into human psychiatric diseases. Together, these findings provide strong support for the use of the HS population to study psychiatric disorders.

**Keywords:** GWAS, outbred, anxiety, open field, novelty-seeking, social interaction, heterogeneous stock, rats

## 1. INTRODUCTION

Many personality traits are predictors of vulnerability to addiction (1). For example, individuals with symptoms of anxiety are more likely to be smokers (2, 3), and novelty seeking is positively correlated with both smoking onset (4) and cocaine abuse (5). In addition, the social environment plays a critical role in the development and treatment of addiction (6). Many of these phenomena can be modeled using rodents to unveil their neural, genetic, and molecular mechanisms (7–10).

The open-field test (OFT) is a widely used behavioral test for measuring anxiety-like and exploratory behavior in rodents (11–14). A rodent is typically placed in an open chamber surrounded by tall walls. Video recording of the rodent's locomotor movements is then analyzed. In general, rats spend most of the testing session walking along the wall (i.e., thigmotaxis). Increased

time spent in the center of the area or decreased latency to enter the center are interpreted as indications of lower anxiety. The OFT is widely used to model anxiety and is sensitive to the anxiolytic-like effects of classical benzodiazepines, and 5-HT<sub>1A</sub> receptor agonists (11). The novel object interaction test (NOIT) is usually conducted in an open arena where a novel object is placed in the center. The time spent and distance traveled around the object zone are used as indicators of preference for novelty. Novel object interaction has been considered as an important predictor in addiction-like traits (15, 16) and high novelty preference increases the propensity for addictive drug-seeking behavior (9, 17, 18). There are multiple different methods for conducting social interaction test (SIT) in rats (19–21). In general, an unfamiliar stimulus rat and the rats to be tested are placed in the same arena. While manual scoring of social interaction often allows both rats to be freely moving, experiments using automated video analysis often limit the movement of the stimulus rat. Computer algorithm then extract the time spend and distance traveled by the test rat around the stimulus rat, which reflects the social tendency of the test rat.

The heterogeneous stock (HS) rats were originally derived from interbreeding eight inbred strains (22). An analysis on these founders reported 7.2 million single nucleotide variants (23). This population has been maintained as outbred for more than 90 generations. The chromosomes of individuals in this population represent a genetic mosaic of the founders' haplotypes, with the average distance between recombination events in the centiMorgan range (24). This allows for genetic mapping to only a few million bases (Mb), a much smaller region than what can be identified using traditional F<sub>2</sub> intercross or backcross mapping strategies. Several high-resolution genome-wide association studies (GWAS) (23, 25–27) have been successfully carried out. Here we report the results on associations of genomic loci with measures obtained from OFT, NOIT and SIT. These analyses were based on an expanded data set that contained about twice the sample size of that reported previously (28). These data were collected as part of a larger GWAS on socially acquired nicotine intravenous self-administration, which will be the subject of a separate publication.

## 2. MATERIALS AND METHODS

### 2.1. Animals

The N/NIH heterogeneous stock (HS) rat (RRID:RGD\_2314009), was created at the NIH in 1984 by interbreeding the following eight inbred founder strains: ACI/N, BN/SsN, BUF/N, F344/N, M520/N, MR/N, WKY/N and WN/N (22). The HS rats used in this study were sent from The Medical College of Wisconsin to the University of Tennessee Health Science Center (UTHSC) at 3–6 weeks of age. A total of 16 batches of HS rats were transferred between October 27, 2014 and September 20, 2018. Each batch consisted of 25 males and 25 females that were used as breeders. After a 2-week quarantine period, rats were transferred to a reversed 12 h light-dark cycle (lights off at 9:00 a.m.) housing room. Breeding pairs were assigned according to an algorithm that maximized the genetic diversity of the offspring. Litters were culled to a maximum

of 8 pups to ensure a consistent nutritional environment. Rats were weaned on postnatal day (PND) 21. A radio frequency identification (RFID) chip was inserted subcutaneously into each rat at the time of weaning. Two male and two female rats per litter were used for behavioral studies. Sprague-Dawley (SD) rats (20 for each sex, purchased from Harlan Laboratories, Madison, WI, RRID:RGD\_737903) were used as the stimulus rats in the social interaction test. Teklad Irradiated LM-485 Mouse/Rat Diet and water were provided *ad libitum*. All rats were group-housed with 2–4 same-sex peers throughout the experiments to avoid social isolation. All procedures were conducted in accordance with the NIH Guidelines concerning the Care and Use of Laboratory Animals, as approved by the Institutional Animal Care and Use Committee of the University of Tennessee Health Science Center.

### 2.2. Study Design

All HS rats (626 males and 620 females in total from 16 batches) were adolescents when tests began. Their age was  $31.8 \pm 2.6$  (mean  $\pm$  STD) on the day of the OFT. Adolescent rats were used because the onset of many psychiatric diseases occur during this age (29). Each HS rat was tested in all three behavioral tests, one test per day, in the following sequence: OFT, NOIT, and SIT. All tests were conducted in the dark phase of the light cycle (9 a.m.–4 p.m.) and were conducted in the same open field and recorded using the same video capture system.

### 2.3. Behavioral Testing Procedure

#### 2.3.1. Open Field Test

Two OFT arenas were constructed using black acrylic glass, measuring 100 cm (L)  $\times$  100 cm (W)  $\times$  50 cm (H), which were placed side by side. The floors were covered by wood boards painted with either black or white acrylic paint (ART-Alternatives, ASTM D-4236, Emeryville, CA, USA) to contrast the coat of the animals (i.e., a black board was used for rats with white fur). The test chambers were illuminated by a long-range, 850-nm infrared light (LIR850-70, LDP LLC, Carlstadt, NJ) located 160 cm above the center of the two test chambers. No source of visible light was present during behavioral testing, with the exception of a flat panel monitor (Dell 1908FP). A digital camera (Panasonic WV-BP334) fitted with an 830 nm infrared filter (X-Nite830-M37, LTP LLC, Carlstadt, NJ) and located next to the infrared light source was used to record the behavior of the rats. All rats were released at the same corner of the test chamber, and data were collected for 1 h.

#### 2.3.2. Novel Object Interaction Test

This test was conducted the day after the OFT in the same arena. A cylindrical rat cage constructed using 24 aluminum rods (30 cm in length) spaced 1.7 cm apart was used as the novel object. The bottom and top of the cage (15 cm in diameter) were manufactured using a 3D printer from polylactic acid. The design can be downloaded from <https://github.com/ch42/RatSocialInteractionTest>. The novel object was placed in the center of the arena before testing. The test duration was 20 min and was recorded using the same camera as that used in the OFT.

### 2.3.3. Social Interaction Test

This test was conducted the day after the NOIT. This test compares the preference of a subject rat for a stimulus rat restricted in a cylindrical cage (i.e., the novel object used in the NOIT) against an empty cylindrical cage. The test arena was reduced to  $100\text{cm}(L) \times 60\text{cm}(W) \times 50\text{cm}(H)$  by using a black board placed vertically in the arena. Two cylindrical cages described above were placed  $\sim 30$  cm away from the walls on opposite sides (i.e., similar to the arrangement commonly used in the three-chamber test). A randomly selected stimulus Sprague-Dawley rat of the same sex and similar weight as the HS test rat was placed into one of the cylindrical cages (kept the same throughout the experiment) 5 min before the HS subject rat was placed into the arena. The stimulus and subject rats were never housed together and thus were unfamiliar to each other. No social isolation was conducted on either rat. Each stimulus rat was used no more than once per day. The test duration was 20 min and was recorded using the same camera as that used in the OFT.

### 2.3.4. Analysis of Video Data

Ethovision XT video tracking system (RRID:SCR\_000441, Version 4.0, Noldus Information Technology, The Netherlands) was used to analyze the videos recorded in all behavioral tests. After identifying the arena and calibrating the size of the arena, specific zones in the arena were outlined. For OFT and NOIT, one center zone, which was a circular region with a diameter of 20 cm, was used. For the SIT, one object zone and one social zone, both were circular regions with diameters of 20 cm, corresponding to the two cylindrical cages, respectively, were specified. The extracted data included the total distance traveled in the arena, the duration and the frequency the test rat was present in specific zones, the distance of the subject to the zones, and the latency of the test rat entering the zones. The center of the subject rat was used for all calculations. Phenotypic correlations were determined using the Pearson test.

## 2.4. Pre-processing of Phenotype Data

All phenotype data were stored in the C-GORD (RRID:SCR\_021866) relational database. For genetic analysis, each trait was quantile-normalized separately for males and females; this approach is similar to using sex as a covariate. Other relevant covariates (including age, batch number, and coat color) were identified for each trait, and covariate effects were regressed out if they were significant and if they explained more than 2% of the variance. Residuals were then quantile-normalized again, after which the data for each sex were pooled prior to further analysis. This approach removed mean differences due to sex; further, it did not attempt to model gene-by-sex interactions.

## 2.5. Genotyping and Estimates of Heritability

Genotypes were determined using genotyping-by-sequencing (GBS), as described previously (30). This produced approximately 3.5 million single nucleotide polymorphisms (SNP) with an estimated error rate  $<1\%$ . Variants for X- and Y-chromosomes were not called. We used this set of SNPs for GWAS, genetic correlations, and heritability estimates. We used

GCTA-GREML (31) analysis to estimate proportion of variance attributable to SNPs.

## 2.6. Genetic Mapping

GWAS analysis employed a linear mixed model, as implemented in the software GCTA (32), using a genetic relatedness matrix (GRM) to account for the complex family relationships within the HS population and the Leave One Chromosome Out (LOCO) method to avoid proximal contamination (33, 34). Significance thresholds were calculated using permutation. Because all traits were quantile normalized, we used the same threshold for all traits (35). To identify quantitative trait loci (QTL), we scanned each chromosome to determine if there was at least one SNP that exceeded the permutation-derived threshold of  $-\log_{10}(p) > 5.6$ , which was supported by a second SNP within 0.5 Mb that had a  $p$ -value that was within  $2 - \log_{10}(p)$  units of the most significant SNP.

There could be more than one QTL on the same chromosome for one trait. We resolve the dependency and determine their locations as follows: we used the top SNP from the most significant QTL as a covariate and performed a second GWAS of the chromosome in question. If the resulting GWAS had an additional SNP with a  $p$ -value that exceeded our permutation-derived threshold, it was considered to be a second, independent locus. This process was repeated (including all previously significant SNPs as covariates), until no more QTLs were detected on a given chromosome. Linkage disequilibrium (LD) intervals for the identified QTL were determined by identifying those markers that had a high correlation coefficient with the peak marker ( $r^2 = 0.6$ ).

Genetic fine mapping were conducted using Credible Set analysis (36) and SuSieR (37). The analysis determines the 99% credible set by a Bayesian approach, that is the smallest set of SNPs in a genomic region that were 99% likely, to contain the causal SNPs. SuSieR also uses a Bayesian approach but also quantify uncertainty in which variants should be selected when multiple, highly correlated variants compete with one another.

We used fastENLoc (38) and a LD cutoff-based method to colocalize behavioral and gene expression QTLs. For the LD cutoff-based method, we retained those behavioral and gene expression QTLs where the top SNPs were in strong LD (i.e.,  $r^2 > 0.6$ ). The gene expression data were collected from 88 naive adult HS rats. Five brain regions (prelimbic, infralimbic, and orbitofrontal cortex, lateral habenula, and nucleus accumbens core) were collected for RNA-seq from each rat (39).

## 3. RESULTS

### 3.1. Sex Differences

We found that many of the traits measured in OFT, NOIT, and SIT are different between males and females (Supplementary Table S1). In OFT, with the exception of latency of entering the center zone, all traits have statistically significant sex differences. In addition, four out of six traits in NOIT and seven out of eleven traits in SIT are different between males and females. The range of effect size (Cohen's  $d$ ) for statistically significant differences is (0.14, 0.31). Our genetic analysis quantile-normalized each trait

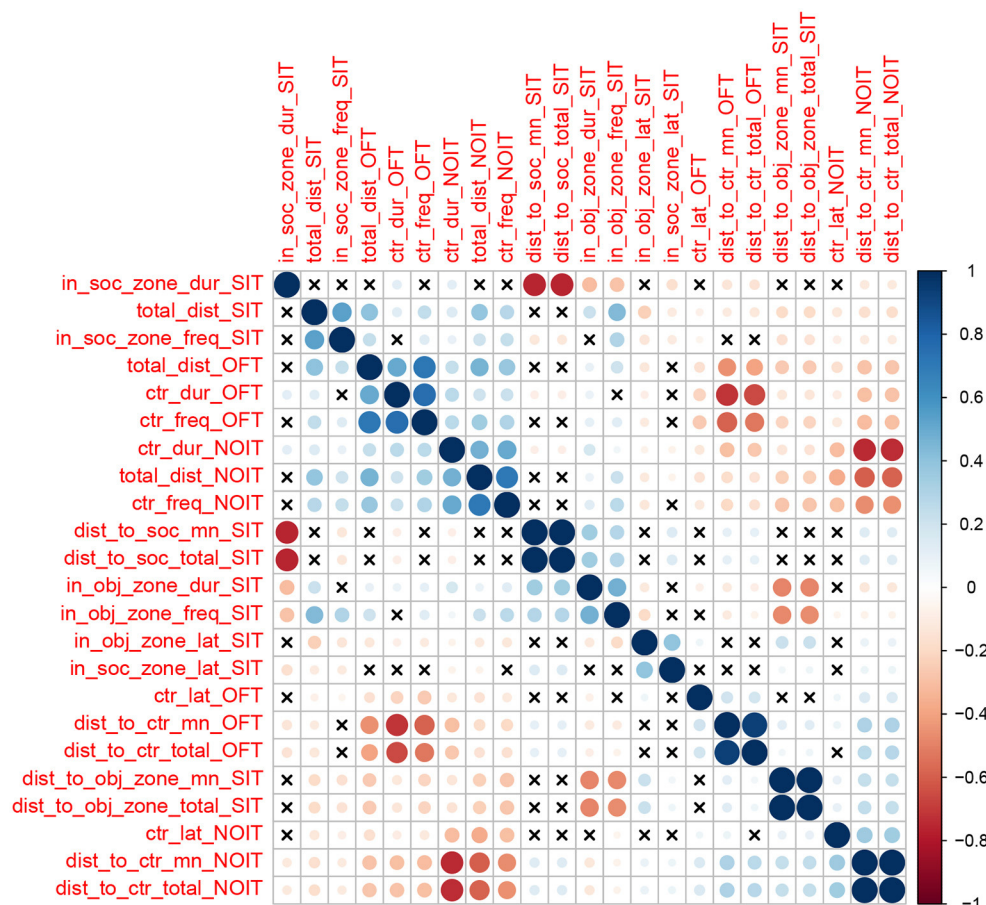


**FIGURE 1 |** Heatmap showing the correlations between behavioral traits. The color scheme represents the direction of the correlation, whereas the intensity of the colors and the size of the circles are proportional to coefficients of the correlation. The cross signs indicate that the correlation of the two traits is not statistically significant ( $p > 0.05$ ).

separately for males and females. This approach removed mean differences due to sex and allowed us to combine males and females in the same analysis to increase the power of GWAS.

### 3.2. Phenotypic Correlations

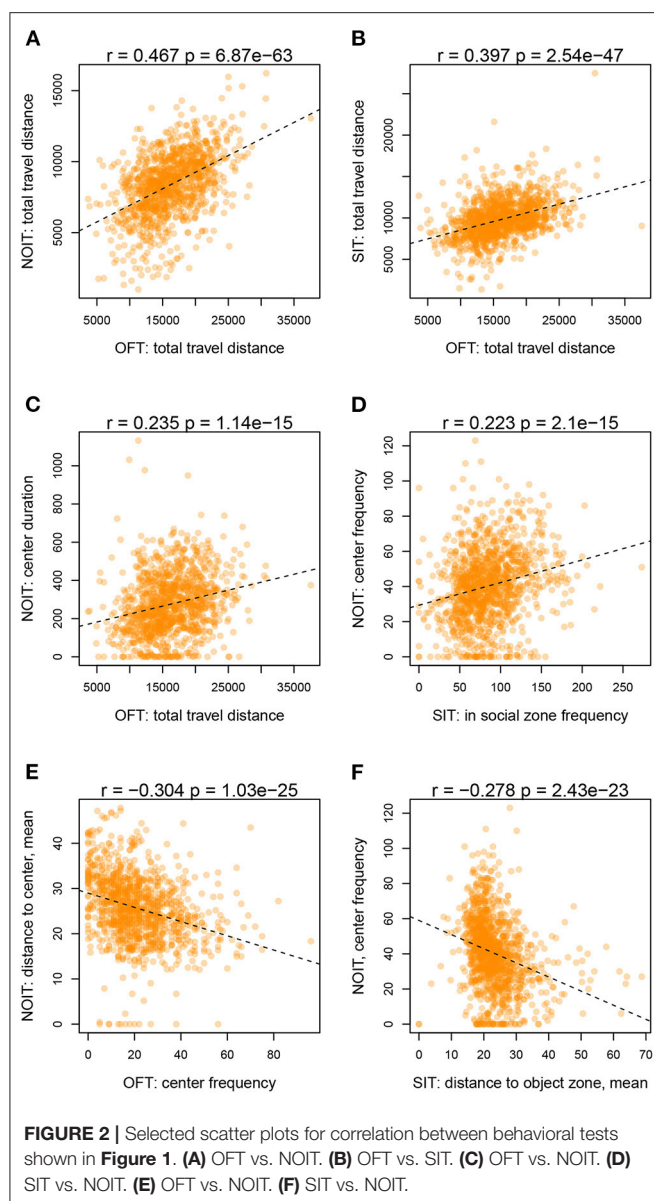
We calculated Pearson correlation between the 23 traits (Figure 1). We found 197 correlations with un-adjusted  $p$ -values  $< 0.05$ . Most of these correlations have relatively low Pearson coefficient (mean is 0.23, median is 0.18). However, due to the large sample size, most of these correlations are highly significant (median  $-\log_{10}(p)$  is 7.8). In general, correlations of traits obtained from the same behavioral test are among the strongest. For example, frequency of visiting the center and duration of staying in the center are positively correlated in OFT ( $r = 0.76$ ), and duration in the social zone and distance to the social zone in the SIT are negatively correlated ( $r = -0.76$ ). Most of these correlations are expected from the definitions of these variables.

Among the correlations of variables derived from two different behavioral tests, correlations for measures of distance traveled are among the highest (range of Pearson  $r$ : 0.39–0.47, e.g., Figures 2A,B). Distance traveled in the OFT is also

correlated with duration of center time in the NOIT (e.g., Figure 2C). Interestingly, the frequencies of visiting the center of the area in the NOIT is correlated with the frequency of visiting the social zone in the SIT (Figure 2D). In contrast, OFT center frequency is negatively correlated with NOIT mean distance to center in NOIT (Figure 2E), and distance to object zone in SIT is negatively correlated with center frequency in NOIT (Figure 2F).

### 3.3. Heritability

SNP heritability estimates ( $h^2$ ) for traits are provided in Table 1. In all the three behavioral tests, total travel distance has the highest heritability. In OFT, all heritability estimates are between 0.28 and 0.38, with the exception of that for latency of entering the center zone ( $h^2 = 0.08$ ). Heritability estimates for variables from the NOIT are slightly lower than that of the OFT; most of them are in the range of 0.21–0.29, with the exception of that for the latency of entering the center zone ( $h^2 = 0.10$ ). Heritability estimates for various measures of the SIT are in the range of 0.10–0.28. Interestingly, heritability estimates for measures on the social zone are consistently greater than those for the object zone.



### 3.4. Identification of Multiple QTLs

In Table 2, we present SNPs that are significantly associated with the phenotypes. The genome-wide statistical significance of the association is determined by  $-\log_{10}P$  values greater than 5.609. For OFT, there are 9 significant loci for 5 traits. We did not find a significant QTL for *Duration in center zone* ( $h^2 = 0.284 \pm 0.045$ ). We identified two loci for *Frequency of entering center zone* and *Total travel distance*, 3 loci for *Total distance to center zone*. We found 4 NOIT traits have significant loci. Among them, *Total distance to center zone* has 3 loci and *Mean distance to center zone* has 2 loci. We did not find any significant loci for *Frequency of entering center zone* ( $h^2 = 0.209 \pm 0.041$ ) and *Latency of entering center zone* ( $h^2 = 0.100 \pm 0.034$ ). For SIT, we identified significant loci for all traits except *Latency of entering object zone* which has heritability of  $h^2 = 0.082 \pm 0.032$ . We

**TABLE 1 |** Heritability of open field (OFT), novel object (NOIT) and social interaction (SIT) tests.

Test	Trait	Heritability $\pm$ SE
OFT	Duration in center zone	$0.284 \pm 0.045$
	Frequency of entering center zone	$0.323 \pm 0.044$
	Latency of entering center zone	$0.083 \pm 0.034$
	Mean distance to center zone	$0.295 \pm 0.043$
	Total distance to center zone	$0.300 \pm 0.043$
	Total travel distance	$0.379 \pm 0.044$
NOIT	Duration in center zone	$0.247 \pm 0.043$
	Frequency of entering center zone	$0.209 \pm 0.041$
	Latency of entering center zone	$0.100 \pm 0.034$
	Mean distance to center zone	$0.249 \pm 0.042$
	Total distance to center zone	$0.221 \pm 0.041$
	Total travel distance	$0.287 \pm 0.044$
SIT	Duration in object zone	$0.161 \pm 0.037$
	Duration in social zone	$0.275 \pm 0.040$
	Frequency of entering object zone	$0.177 \pm 0.036$
	Frequency of entering social zone	$0.215 \pm 0.036$
	Latency of entering object zone	$0.082 \pm 0.032$
	Latency of entering social zone	$0.142 \pm 0.034$
	Mean distance to object zone	$0.165 \pm 0.038$
	Mean distance to social zone	$0.265 \pm 0.041$
	Total distance to object zone	$0.153 \pm 0.037$
	Total distance to social zone	$0.265 \pm 0.041$
	Total travel distance	$0.281 \pm 0.040$

found 2 loci for the traits *Latency of entering social zone*, *Mean distance to social zone*, *Total distance to social zone* and *Total travel distance*. All genome-wide significant loci are shown in Figure 3. Genetic mapping of individual traits are shown as Manhattan plots as Supplementary Figures S1–S23. Regional association plots for representative traits are shown in Figures 4–6 for OFT, NOIT, and SIT, respectively. Other regional association plots are provided as Supplementary Figures S24–S50.

### 3.5. Pleiotropic Loci

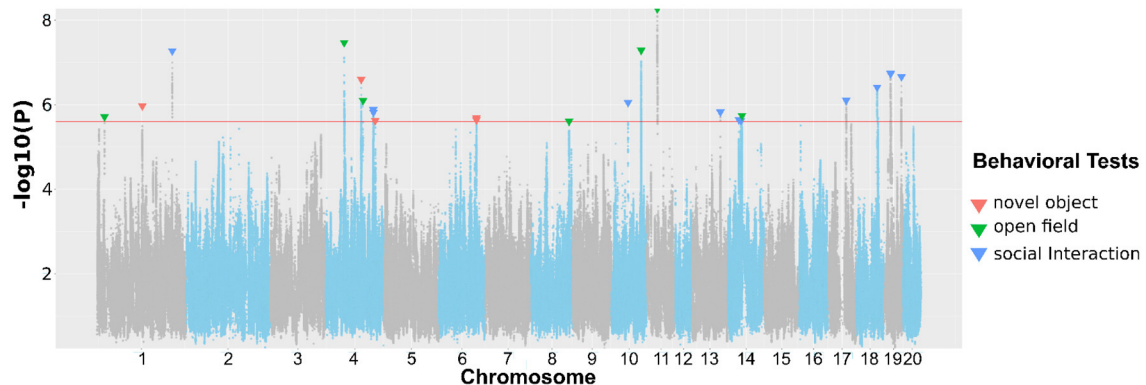
To determine if traits that mapped to the same location are pleiotropic, we considered the minor allele frequency (MAF), and the strain distribution pattern (SDP) of the most significant SNP among the 8 founder strains that were used to create the HS. Using these criteria, we did not observe any pleiotropic loci between the traits analyzed in different tests. However, we did identify pleiotropic loci between the traits of the same behavior test. Most of these traits are highly correlated, as shown in Figure 1. With the exception of three sets of QTL (Supplementary Table S3), all others share the same top SNP (Supplementary Table S2).

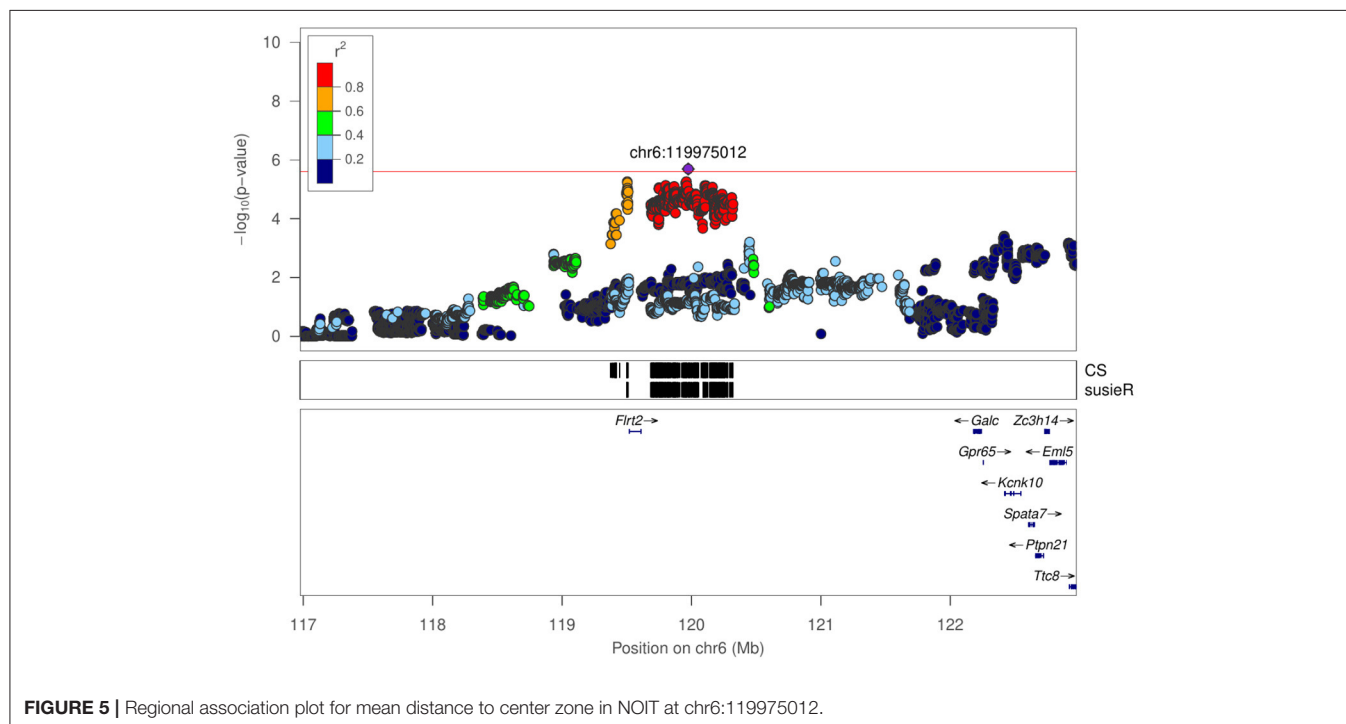
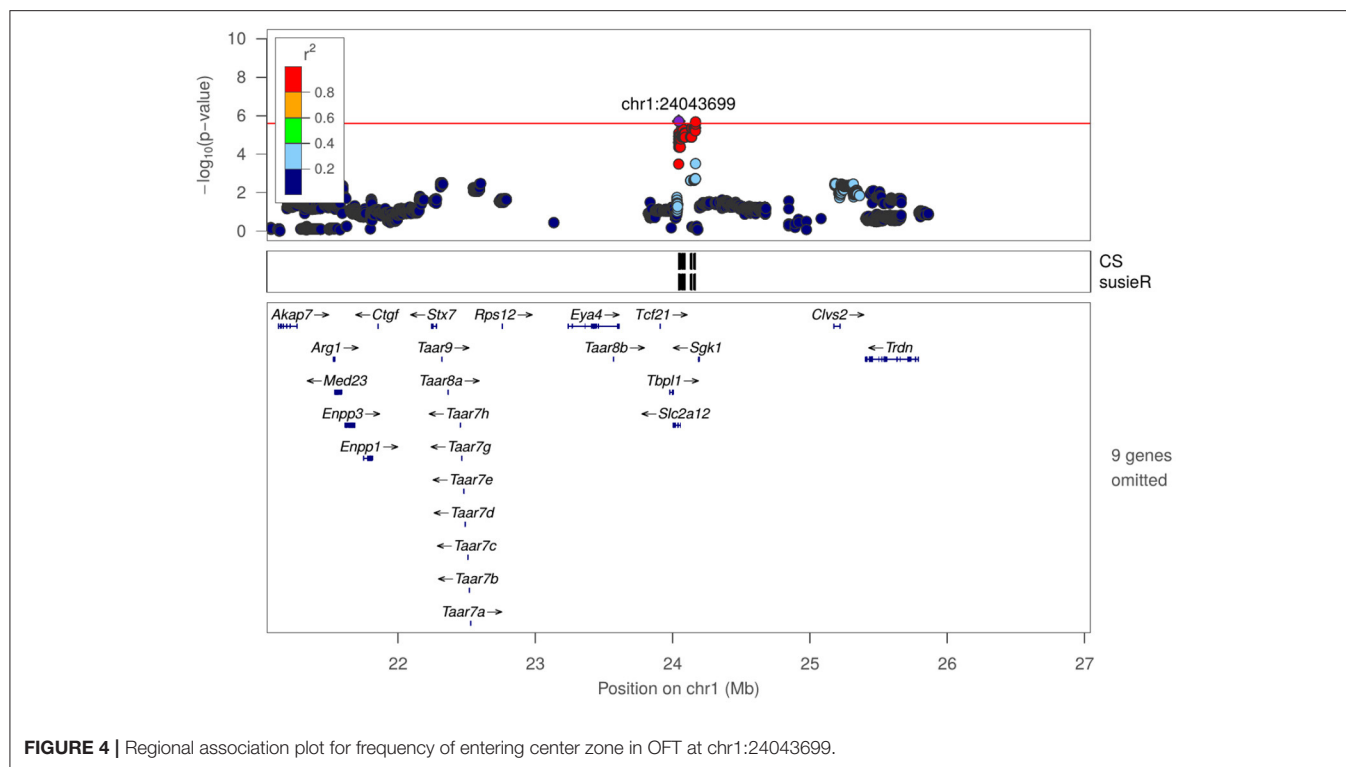
### 3.6. Candidate Gene Identification

The number of genes within the identified QTL ranges from 1 to 127 (mean: 30.1, median: 19, Table 2). There is only one region that contains a single gene: *Adarb2* within chr17:58Mb for latency of entering social zone in SIT. However, it is also

**TABLE 2 |** QTL for open field (OFT), novel object interaction (NOIT), and social interaction (SIT) tests.

Test	Trait	Top SNP	$-\log_{10}P$	Interval size	Number of genes
OFT	Frequency of entering center zone	chr1:24043699	5.714	0.12 Mb	5
	Frequency of entering center zone	chr4:118013062	5.777	2.0 Mb	47
	Latency of entering center zone	chr8:120910798	5.609	1.0 Mb	12
	Mean distance to center zone	chr4:58009499	7.469	2.4 Mb	60
	Total distance to center zone	chr4:58009499	7.254	2.4 Mb	60
	Total distance to center zone	chr4:118013062	6.099	2.0 Mb	47
	Total distance to center zone	chr14:44904830	5.741	2.1 Mb	44
	Total travel distance	chr10:94549701	7.286	4.2 Mb	98
	Total travel distance	chr11:33359859	8.268	0.92 Mb	23
NOIT	Duration in center zone	chr4:112234344	6.028	1.2 Mb	8
	Mean distance to center zone	chr4:112234344	6.598	1.2 Mb	8
	Mean distance to center zone	chr6:119975012	5.692	0.95 Mb	3
	Total distance to center zone	chr1:144080083	5.969	4.1 Mb	109
	Total distance to center zone	chr4:112234344	5.975	1.2 Mb	8
	Total distance to center zone	chr4:156801420	5.622	4.4 Mb	127
	Total travel distance	chr6:120117521	5.640	0.95 Mb	3
	Total travel distance	chr6:120117521	5.640	0.95 Mb	3
SIT	Duration in object zone	chr18:65869186	6.414	3.4 Mb	22
	Duration in social zone	chr4:151128675	5.820	2.9 Mb	34
	Frequency of entering object zone	chr13:90335374	5.827	1.1 Mb	46
	Frequency of entering social zone	chr1:239076581	7.273	0.27 Mb	6
	Latency of entering social zone	chr10:52831274	6.052	0.34 Mb	2
	Latency of entering social zone	chr17:58611795	6.104	0.86 Mb	1
	Mean distance to object zone	chr19:20666789	6.746	1.6 Mb	23
	Mean distance to social zone	chr19:55339863	6.661	0.68 Mb	16
	Mean distance to social zone	chr4:150582701	5.884	1.1 Mb	19
	Total distance to object zone	chr19:20667417	6.619	1.6 Mb	23
	Total distance to social zone	chr19:55339863	6.643	0.68 Mb	16
	Total distance to social zone	chr4:150582701	5.788	1.1 Mb	19
	Total travel distance	chr14:34908176	5.648	0.74 Mb	10
	Total travel distance	chr14:41727329	5.627	0.85 Mb	5

**FIGURE 3 |** Association of approximately 3 million SNPs with behavioral traits measured in OFT, NOIT, or SIT. The red horizontal line denotes the  $p$ -value for reaching genome-wide significance. The downward arrows denote the SNPs with the largest  $-\log_{10}(P)$  for each genome-wide significant association.



possible that the causal allele is a regulatory variant that is located in this interval but regulates a gene outside of the identified interval.

All other loci contained more than one gene. To identify candidate genes, we combined several criteria: (1) located in

the credible set identified by either one of the fine mapping methods. (2) the presence of moderate or high impact variants located within the gene, as predicted by SnpEff (40). We also require these variants are in high LD with the top SNP. We identified 149 coding variants within 30 QTL, 8 of which were

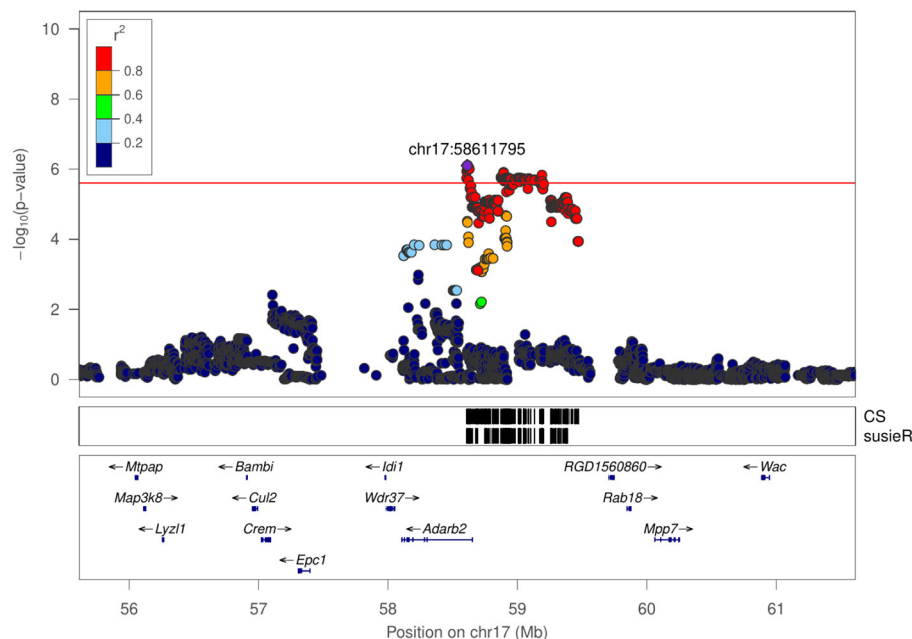


**FIGURE 6 |** Regional association plot for latency of entering social zone in SIT at chr17:58611795.

predicted to have a high impact (**Supplementary Table S4**). (3) the presence of a significant cis-eQTL in one or more of the five brain regions in a dataset containing 88 naive adult HS rats (39), (4) has a human ortholog that has been reported to be associated with psychiatric diseases (including drug abuse). When multiple candidates are present using the above criteria, we remove the gene with very low expression levels across all five regions in the RNA-seq data set (e.g., FPKM < 0.5) and select the candidate with the strongest support for the literature. Combining these criteria with a literature search conducted using GeneCup (41), we identified plausible candidate genes within 17 loci (**Table 3**).

In addition, for total distance to the novel object zone, the QTL region on chr1 (144 Mb, size: 4.1 Mb, **Supplementary Figure S4**) contains 69 gene with human orthologs. We found 14 of these genes have been reported in human GWAS to be associated with psychiatric conditions or addiction with genome-wide significance (*ACAN*, *ADAMTSL3*, *ALPK3*, *CPEB1*, *FES*, *FURIN*, *LINC00933*, *MIR9-3HG*, *MRPL46*, *NMB*, *POLG-DT*, *SEC11A*, *ZNF592*, and *ZSCAN2*, **Supplementary Table S5**). Three additional genes with sub-threshold significance in human GWAS are also included. These genes are all located in a syntenic region on human chromosome 15 (82.5–90.8 Mb). Although based on the criteria described above, *Sec11a* is the best candidate gene (**Table 3**), it is possible that this region contains multiple genes that are associated with the trait.

## 4. DISCUSSION

As part of a GWAS on intravenous nicotine self-administration in adolescent HS rats that we are conducting (28, 81), we collected several behavioral phenotypes related to anxiety,

novelty exploration, and social interaction. We have previously reported that these behavioral traits contribute to the variation in nicotine intake (28). We report here GWAS results of three behavioral traits: OFT, NOIT, and SIT, which were all conducted in the same open field. We identified 30 QTLs for 23 traits. Using a set criteria outlined above, we identified 17 candidate genes.

OFT, NOIT, and SIT are widely used behavioral assays in rodents. With over 1,200 rats, ours represent some of the largest data collected using these assays. Similar to our interim report on this data set (28), we found a large number of correlations with relatively low coefficients (e.g.,  $r < 0.4$ ) but with high statistical significance. It is likely that these correlated traits are controlled by the same behavioral processes and thus are influenced by the same genetic factors. In fact, our genetic analysis did find several pleiotropic sites (**Supplementary Table S3**). Almost all pleiotropic loci are reported for traits measured in the same behavior assay. It is likely that further increasing sample size will provide greater statistical power to detect pleiotropic effect across different behavioral assays.

Many of the candidate genes in this study have been associated with psychiatric or drug abuse traits in humans. For example, we identified *Cyp26b1*, a retinoic acid degrading enzyme, as a candidate gene for the frequency of entering the center zone and total distance to the center zone in OFT; both of which are measures of anxiety-like behaviors (rats with more anxiety-like behavior would enter the center zone less frequently and have smaller distance to the center zone) (11). *Cyp26b1* has been associated with Schizophrenia in several human GWAS (42, 43). Anxiety symptoms are common in schizophrenia patients (82, 83). *Cyp26b1* is expressed in parvalbumin-positive interneurons (84). Most interestingly, knockdown *Cyp26b1* in the nucleus accumbens shell decreased anxiety-like behavior (44).

**TABLE 3 |** Candidate genes.

Test	Trait	Top SNP	Candidate gene	Supporting evidence	Human GWAS	Expression level (FPKM)	Gene function
OFT	Frequency of entering center zone, Total distance to center zone	chr4:118013062	Cyp26b1	Missense variants, cis-eQTL in IL and PL	Schizophrenia (42, 43)	IL 7.29 ± 2.26	Inactivate all-trans retinoic acid (44)
OFT	Total distance to center zone	chr14:44904830	Fam114a1	Missense variants, cis-eQTL in LHb	Alcohol consumption measurement (45)	LHb 3.72 ± 0.77	Also known as Noxp20, neuronal cell development (46)
OFT	Total travel distance	chr10:94549701	Cacng4	cis-eQTL in Acbc	Bipolar disorder and Schizophrenia (47)	Acbc 55.22 ± 4.79	Calcium channel (48)
OFT	Total distance to center zone	chr4:58009499	Ube2h	cis-eQTL in OFC	Unipolar depression, mood disorder (49)	OFC 49.22 ± 2.72	Ubiquination of proteins (50)
NOIT	Duration in center zone, distance to center zone	chr4:112234344	Eva1a	Missense variants, cis-eQTL in PL, IL and OFC		LHb 6.74 ± 1.69	Formation of the autophagosome (51)
NOIT	Total distance to center zone	chr1:144080083	Sec11a	cis-eQTL in PL and IL	Unipolar depression, depressive symptom measurement, response to ketamine, bipolar disorder, schizophrenia (43, 52, 53)	Acbc 33.34 ± 3.73	Metabolism of proteins (54)
NOIT	Total distance to center zone	chr4:156801420	Mlf2	cis-eQTL in PL	Smoking status measurement (55)	Acbc 307.85 ± 40.01	Molecular chaperone in multi-protein complex assembly, signaling transduction, and endocytosis (56).
SIT	Duration in object zone	chr18:65869186	Rab27b	missense variants, cis-eQTL in LHb	Unipolar depression, bipolar disorder (57–59)	Acbc 8.03 ± 2.7	Vesicular fusion and trafficking (60)
SIT	Duration in social zone, distance to social zone	chr4:151128675	Ankrd26	Missense variants	smoking initiation (61)	IL 4.75 ± 1.21	Cell signaling (62)
SIT	Frequency of entering object zone	chr13:90335374	Kcnj9	Missense variants, cis-eQTL in IL, PL and OFC	Alcohol consumption measurement (63)	OFC 65.46 ± 6.64	Adult neurogenesis (64), cocaine addiction (65)
SIT	Frequency of entering object zone	chr1:239076581	Gda	cis-eQTL in IL	General cognitive function (66)	Acbc 84.67 ± 16.92	Cypin, cytoplasmic PSD95 Interactor (67)
SIT	Latency of entering social zone	chr10:52831274	Dnah9	Missense variants	Schizophrenia (68)	LH 3.59 ± 1.33	Component of microtubule (69)
SIT	Latency of entering social zone	chr17:58611795	Adarb2	cis-eQTL in Acbc and LH	Unipolar depression, smoking status measurement, systolic blood pressure (58, 70)	PL 2.22 ± 0.68	Editing of neurotransmitter mRNA (71)
SIT	Distance to social zone	chr19:55339863	Ctu2	Missense variants, cis-eQTL in IL	Autism spectrum disorder symptom (72)	LHb 6.39 ± 1.14	Post-transcriptional modification of tRNAs (73)
SIT	Distance to social zone	chr4:150582701	Cacna1c		Schizophrenia (74), biopolar disorder (75)	PL 6.76 ± 1.49	Calcium channel (76)

(Continued)

TABLE 3 | Continued

Test	Trait	Top SNP	Candidate gene	Supporting evidence	Human GWAS	Expression level (FPKM)	Gene function
SIT	Total travel distance	chr14:34908176	Clock	Missense variants, cis-eQTL in LHb		Acbc 11.15 ± 1.82	Regulate circadian rhythms (77, 78)
SIT	Total travel distance	chr14:41727329	Grxr1	cis-eQTL in Acbc and LHb	Cognitive decline in depression (79)	IL 2.97 ± 1.02	S-glutathionylation of proteins (80)

Acbc, *Accumbens core*; IL, *infralimbic cortex*; LHb, *lateral habenular*; OFC, *orbitofrontal*; PL, *prelimbic cortex*.

Among the candidate genes for NOIT, *Evala* is a candidate gene for the duration stayed in the center zone that contained the novel object. *Evala* is supported by strong cis-eQTL and a missense variant but has no literature support. Thus, further evaluating the role of *Evala* could potentially lead to new mechanisms for novelty seeking-like behavior. *Sec11a*, a candidate gene for total distance in the center zone, is associated with depression and schizophrenia (43, 52, 53). *Mlf2*, a candidate gene for total distance to center zone in NOIT, is associated with smoking in humans (55) and has very high expression levels in the accumbens (Table 3).

For the SIT, we identified *Cacna1c*, encoding the  $Ca_v1.2$  subunit of the L-type  $Ca^{2+}$  channel, as a candidate gene for distance to the social zone, where the stimulus rat resided. *Cacna1c* has been associated with schizophrenia (74) and bipolar disorder (75) in human GWAS. Both schizophrenia and bipolar disorders are associated with impairments in a range of social deficits (85, 86). In animal studies, Sprague-Dawley rats with heterozygotic deletion of the *Cacna1c* gene (homozygotic mutation is lethal) showed many deficits in social behavior. These included reduced levels of ultrasonic vocalizations during rough-and-tumble play, as well as social approach behavior elicited by playback of ultrasonic vocalizations (87, 88). In mice, a knockdown of *Cacna1c* in the nucleus accumbens significantly increased susceptibility to social stress (89). Knocking down of *Cacna1c* in the prefrontal cortex of adult mice also recapitulated many of the social deficits (90). Importantly, some of the behavioral effects of *Cacna1c* appear to interact with genetic background (91).

Among the other candidate genes for the SIT traits, *Rab27b* is involved in the presynaptic mechanism of long-term potentiation (92) as well as myelin biogenesis in oligodendrocytes (93). *Ankrd26* is expressed in the arcuate and ventromedial nuclei and in the ependyma (62). *Kcnj9* is involved in neurite outgrowth (94). *Gda*, also known as Cypin, is located in the postsynaptic density (95). *Ctu2* is involved in post-translational modification of tRNAs (73). *Adarb2* has been associated with home cage activity (96) and unipolar depression (58). The *Clock* gene is involved in the maintenance of locomotor rhythms (97). Mutations of the *CLOCK* gene have been implicated in many psychiatric disorders (98). Although these candidates are well supported by multiple lines of evidence, additional work is needed to confirm their causal relationship to the corresponding behavioral traits.

The total distance to the novel object zone is associated with chr1:144080083 (allele frequency: 0.91,  $-\log_{10}(p) = 5.969$ , size of interval: 4.1 Mb, **Supplementary Figure S34**). This SNP is also associated with the duration rats stayed in the novel object zone, although the  $p$ -value did not reach genome-wide significance ( $-\log P = 4.63$ ). This region contains 69 known genes. Its syntenic region on human Chr15 (82.5–90.8 Mb) is a hotspot for human psychiatric diseases, containing 30 SNPs and 14 genes (*ACAN*, *ADAMTSL3*, *ALPK3*, *CPEB1*, *FES*, *FURIN*, *LINC00933*, *MIR9-3HG*, *MRPL46*, *NMB*, *POLG-DT*, *SEC11A*, *ZNF592*, and *ZSCAN2*) associated with generalized anxiety disorder, schizophrenia, bipolar disorder, obsessive compulsive disorder, attention deficit hyperactivity disorder, autism spectrum disorder, and unipolar depression, smoking

behavior, etc. These results are reported in 21 publications (Supplementary Table S5). Using the criteria described above, we identified *Sec11a* as the best candidate gene (Table 3). However, given the large number of genetic variants reported in human GWAS that are associated with psychiatric conditions within this syntenic region, it is very likely that this region contains multiple genes that are associated with novelty seeking-like behavior.

We include overlapping with human psychiatric GWAS results as part of the criteria in prioritizing candidate genes. It is possible that this approach could introduce bias and prevent us from making novel discoveries. For example, two (*Cyp26b1* and *Cacng4*) of the four candidate genes for OFT have been associated with schizophrenia, rather than anxiety. However, many genetic variants are pleiotropic for multiple psychiatric diseases (99). For example, polygenic risk scores for schizophrenia have been associated with many other psychiatric diseases, such as anxiety disorder (100) or major depressive disorder (101), or cognitive performance (102). Together with other evidence, we believe considering human psychiatric GWAS findings when identifying candidate genes in our study, even when the behavior trait in rats does not map directly to the psychiatric disease, is still valid and will likely increase the translational value of our findings.

The presence of cis-eQTL in the brain is one of the strongest pieces of evidence that we use to prioritize candidate genes. Fourteen of the 17 candidate genes we identified have cis-eQTL. Seven of these genes also contained missense mutations, which further support their biological function related to the phenotype they are associated with. The only candidate gene that is not supported by either cis-eQTL or missense mutation is *Cacna1c*, associated with distance to the social zone. However, the role of *Cacna1c* in social behavior has been well documented in rats and mice (87–90). We also required all candidate genes located in regions confirmed by fine mapping. For example, the *Crhr1* gene, which encodes corticotrophin release hormone receptor 1, is located in the locus for total travel distance in the OFT but is not supported by fine mapping. Despite strong literature support for the role of *Crhr1* in anxiety-like behavior in OFT in rats (103, 104) and mice (105), we nominated a different gene, *Cacng4*, to be the candidate gene for this locus. We anticipate further improvement in the statistical power of eQTL data and the availability of additional functional genomics data, such as 3D chromatin interaction (106, 107), will help us to identify additional candidate genes.

The HS rat population has already been successfully used in genetic mapping studies of physiological or behavioral traits (24, 25, 27). Prior study mapped several anxiety-like traits using zero maze (23). GWAS using HS to study behavioral regulation

(108), response to cocaine cues (109), cocaine (110), nicotine (28, 81), or oxycodone (111) self-administration are underway. Our study adds to the literature 30 QTLs and 17 candidate genes for psychiatric related behavioral traits. Although we prioritized candidate gene selection based on functional genomics evidence, most of the candidate genes we identified have strong literature support for their role in human psychiatric diseases. This suggests that the rest of the candidate genes likely represent novel findings that can be the catalyst for future molecular and genetic insights on psychiatric diseases. In addition, these findings provide strong support for the use of the HS population in study psychiatric disorders.

## DATA AVAILABILITY STATEMENT

The original contributions presented in the study are publicly available. This data can be found through the C-GORD database at doi: 10.48810/P44W2 and through <https://www.genenetwork.org>.

## ETHICS STATEMENT

The animal study was reviewed and approved by University Tennessee Health Science Center IACUC.

## AUTHOR CONTRIBUTIONS

HC and AP designed the study. TW and AG collected the data. AC, OP, and MG analyzed the data. MG, AP, and HC wrote the manuscript. All authors contributed to the article and approved the submitted version.

## FUNDING

This work was supported by the National Institute on Drug Abuse (P50 DA037844).

## ACKNOWLEDGMENTS

The authors thank Wenyan Han, Yanyan Lin, and Pawandeep Kaur for their contributions in collecting some of the behavioral data. We thank the GeneNetwork team for hosting the data.

## SUPPLEMENTARY MATERIAL

The Supplementary Material for this article can be found online at: <https://www.frontiersin.org/articles/10.3389/fpsy.2022.790566/full#supplementary-material>

## REFERENCES

- Hamidullah S, Thorpe H, Frie J, Mccurdy R, Khokhar J. Adolescent substance use and the brain: behavioral, cognitive and neuroimaging correlates. *Front Hum Neurosci.* (2020) 14:298. doi: 10.3389/fnhum.2020.00298
- Garey L, Olofsson H, Garza T, Shepherd J, Smit T, Zvolensky M. The role of anxiety in smoking onset, severity, and cessation-related outcomes: a review of recent literature. *Curr Psychiatry Rep.* (2020) 22:38. doi: 10.1007/s11920-020-01160-5
- DuPont R. Anxiety and addiction: a clinical perspective on comorbidity. *Bull Menninger Clin.* (1995) 59(2 Suppl A):53–72.
- Laucht M, Becker K, El-Faddagh M, Hohm E, Schmidt M. Association of the DRD4 exon III polymorphism with smoking in fifteen-year-olds: a mediating role for novelty seeking? *J Am Acad Child Adolesc*

- Psychiatry*. (2005) 44:477–84. doi: 10.1097/01.chi.0000155980.01792.7f
5. Mahoney J, Thompson-Lake D, Cooper K, Verrico C, Newton T, De La Garza R. A comparison of impulsivity, depressive symptoms, lifetime stress and sensation seeking in healthy controls versus participants with cocaine or methamphetamine use disorders. *J Psychopharmacol*. (2015) 29:50–6. doi: 10.1177/0269881114560182
  6. Truan F. Addiction as a social construction: a postempirical view. *J Psychol*. (1993) 127:489–99. doi: 10.1080/00223980.1993.9914886
  7. Wilking J, Hesterberg K, Nguyen V, Cyboron A, Hua A, Stitzel J. Comparison of nicotine oral consumption and baseline anxiety measures in adolescent and adult C57BL/6J and C3H/1Bg mice. *Behav Brain Res*. (2012) 233:280–7. doi: 10.1016/j.bbr.2012.05.022
  8. Manhães A, Guthierrez M, Filgueiras C, Abreu-Villaça Y. Anxiety-like behavior during nicotine withdrawal predict subsequent nicotine consumption in adolescent C57BL/6 mice. *Behav Brain Res*. (2008) 193:216–24. doi: 10.1016/j.bbr.2008.05.018
  9. Redolat R, Pérez-Martínez A, Carrasco M, Mesa P. Individual differences in novelty-seeking and behavioral responses to nicotine: a review of animal studies. *Curr Drug Abuse Rev*. (2009) 2:230–42. doi: 10.2174/1874473710902030230
  10. Pelloux Y, Giorla E, Montanari C, Baunez C. Social modulation of drug use and drug addiction. *Neuropharmacology*. (2019) 159:107545. doi: 10.1016/j.neuropharm.2019.02.027
  11. Prut L, Belzung C. The open field as a paradigm to measure the effects of drugs on anxiety-like behaviors: a review. *Eur J Pharmacol*. (2003) 463:3–33. doi: 10.1016/S0014-2999(03)01272-X
  12. Kraeuter AK, Guest PC, Sarnyai Z. The open field test for measuring locomotor activity and Anxiety-Like behavior. *Methods Mol. Biol.* (2019) 1916:99–103. doi: 10.1007/978-1-4939-8994-2\_9
  13. Kulesskaya N, Voikar V. Assessment of mouse anxiety-like behavior in the light-dark box and open-field arena: role of equipment and procedure. *Physiol Behav*. (2014) 133:30–8. doi: 10.1016/j.physbeh.2014.05.006
  14. Seibenhener ML, Wooten MC. Use of the open field maze to measure locomotor and anxiety-like behavior in mice. *J Vis Exp*. (2015) 96:e52434. doi: 10.3791/52434
  15. Fligel SB, Waselus M, Clinton SM, Watson SJ, Akil H. Antecedents and consequences of drug abuse in rats selectively bred for high and low response to novelty. *Neuropharmacology*. (2014) 76(Pt B):425–36. doi: 10.1016/j.neuropharm.2013.04.033
  16. Bardo MT, Donohew RL, Harrington NG. Psychobiology of novelty seeking and drug seeking behavior. *Behav Brain Res*. (1996) 77:23–43. doi: 10.1016/0166-4328(95)00203-0
  17. Belin D, Berson N, Balado E, Piazza PV, Deroche-Gamonet V. High-novelty-preference rats are predisposed to compulsive cocaine self-administration. *Neuropsychopharmacology*. (2011) 36:569–79. doi: 10.1038/npp.2010.188
  18. Cain ME, Saucier DA, Bardo MT. Novelty seeking and drug use: contribution of an animal model. *Exp Clin Psychopharmacol*. (2005) 13:367–75. doi: 10.1037/1064-1297.13.4.367
  19. Toth I, Neumann ID. Animal models of social avoidance and social fear. *Cell Tissue Res*. (2013) 354: 107–118. doi: 10.1007/s00441-013-1636-4
  20. File SE, Seth P. A review of 25 years of the social interaction test. *Eur J Pharmacol*. (2003) 463:35–53. doi: 10.1016/S0014-2999(03)01273-1
  21. File S, Cheeta S, Irvine E, Tucci S, Akthar M. Conditioned anxiety to nicotine. *Psychopharmacology (Berl)*. (2002) 164:309–17. doi: 10.1007/s00213-002-1219-7
  22. Hansen C, Spuhler K. Development of the national institutes of health genetically heterogeneous rat stock. *Alcohol Clin Exp Res*. (1984) 8:477–9. doi: 10.1111/j.1530-0277.1984.tb05706.x
  23. Baud A, Hermesen R, Gurjev V, Stridh P, Graham D, McBride M, et al. Combined sequence-based and genetic mapping analysis of complex traits in outbred rats. *Nat Genet*. (2013) 45:767–75. doi: 10.1038/ng.2644
  24. Woods L, Mott R. Heterogeneous stock populations for analysis of complex traits. *Methods Mol Biol*. (2017) 1488:31–44. doi: 10.1007/978-1-4939-6427-7\_2
  25. Solberg Woods L, Palmer A. Using heterogeneous stocks for fine-mapping genetically complex traits. *Methods Mol Biol*. (2019) 2018:233–47. doi: 10.1007/978-1-4939-9581-3\_11
  26. Chitre AS, Polesskaya O, Holl K, Gao J, Cheng R, Bimschleger H, et al. Genome-Wide association study in 3,173 outbred rats identifies multiple loci for body weight, adiposity, and fasting glucose. *Obesity*. (2020) 28:1964–73. doi: 10.1002/oby.22927
  27. Keele G, Prokop J, He H, Holl K, Littrell J, Deal A, et al. Genetic fine-mapping and identification of candidate genes and variants for adiposity traits in outbred rats. *Obesity (Silver Spring)*. (2018) 26:213–22. doi: 10.1002/oby.22075
  28. Wang T, Han W, Chitre A, Polesskaya O, Solberg Woods L, Palmer A, et al. Social and anxiety-like behaviors contribute to nicotine self-administration in adolescent outbred rats. *Sci Rep*. (2018) 8:18069. doi: 10.1038/s41598-018-36263-w
  29. Kessler R, Amminger G, Aguilar-Gaxiola S, Alonso J, Lee S, Ustün T. Age of onset of mental disorders: a review of recent literature. *Curr Opin Psychiatry*. (2007) 20:359–64. doi: 10.1097/YCO.0b013e32816ebc8c
  30. Gileta A, Gao J, Chitre A, Bimschleger H, St Pierre C, Gopalakrishnan S, et al. Adapting genotyping-by-sequencing and variant calling for heterogeneous stock rats. *G3 (Bethesda)*. (2020) 10:2195–205. doi: 10.1534/g3.120.401325
  31. Yang J, Benyamin B, McEvoy B, Gordon S, Henders A, Nyholt D, et al. Common SNPs explain a large proportion of the heritability for human height. *Nat Genet*. (2010) 42:565–9. doi: 10.1038/ng.608
  32. Yang J, Lee S, Goddard M, Visscher P. GCTA: a tool for genome-wide complex trait analysis. *Am J Hum Genet*. (2011) 88:76–82. doi: 10.1016/j.ajhg.2010.11.011
  33. Cheng R, Parker C, Abney M, Palmer A. Practical considerations regarding the use of genotype and pedigree data to model relatedness in the context of genome-wide association studies. *G3 (Bethesda)*. (2013) 3:1861–7. doi: 10.1534/g3.113.007948
  34. Gonzales N, Seo J, Hernandez Cordero A, St Pierre C, Gregory J, Distler M, et al. Genome wide association analysis in a mouse advanced intercross line. *Nat Commun*. (2018) 9:5162. doi: 10.1038/s41467-018-07642-8
  35. Cheng R, Palmer A. A simulation study of permutation, bootstrap, and gene dropping for assessing statistical significance in the case of unequal relatedness. *Genetics*. (2013) 193:1015–8. doi: 10.1534/genetics.112.146332
  36. Maller J, McVean G, Byrnes J, Vukcevic D, Palin K, Su Z, et al. Bayesian refinement of association signals for 14 loci in 3 common diseases. *Nat Genet*. (2012) 44:1294–301. doi: 10.1038/ng.2435
  37. Wang G, Sarkar A, Carbonetto P, Stephens M. A simple new approach to variable selection in regression, with application to genetic fine mapping. *J R Stat Soc B*. (2020) 82:1273–300. doi: 10.1111/rssb.12388
  38. Hukku A, Pividori M, Luca F, Pique-Regi R, Im H, Wen X. Probabilistic colocalization of genetic variants from complex and molecular traits: promise and limitations. *Am J Hum Genet*. (2021) 108:25–35. doi: 10.1016/j.ajhg.2020.11.012
  39. Munro D, Wang T, Chitre AS, Polesskaya O, Saba L, Chen H, et al. Mapping genotype-expression associations in Heterogeneous Stock rat brains to advance behavioral genetics research. In: *Genetics and Epigenetics Cross-Cutting Research Team (GECCRT) Meeting*. (Washington, D.C.), (2021).
  40. Cingolani P, Platts A, Wang IL, Coon M, Nguyen T, Wang L, et al. A program for annotating and predicting the effects of single nucleotide polymorphisms, SnpEff: SNPs in the genome of *Drosophila melanogaster* strain w1118; iso-2; iso-3. *Fly (Austin)*. (2012) 6:80–92. doi: 10.4161/fly.19695
  41. Gunturkun MH, Flashner E, Wang T, Mulligan MK, Williams RW, Prins P, et al. GeneCup: mine PubMed for gene relationships using custom ontology and deep learning. *bioRxiv*. (2021) doi: 10.1101/2020.09.17.297358
  42. Schizophrenia Working Group of the Psychiatric Genomics Consortium. Biological insights from 108 schizophrenia-associated genetic loci. *Nature*. (2014) 511:421–7. doi: 10.1038/nature13595
  43. Goes F, McGrath J, Avramopoulos D, Wolyniec P, Pirooznia M, Ruczinski I, et al. Genome-wide association study of schizophrenia in ashkenazi jews. *Am J Med Genet B Neuropsychiatr Genet*. (2015) 168:649–59. doi: 10.1002/ajmg.b.32349
  44. Zhang Y, Crofton E, Smith T, Koshy S, Li D, Green T. Manipulation of retinoic acid signaling in the nucleus accumbens shell alters rat emotional behavior. *Behav Brain Res*. (2019) 376:112177. doi: 10.1016/j.bbr.2019.112177
  45. Gelernter J, Kranzler H, Sherva R, Almasy L, Koesterer R, Smith A, et al. Genome-wide association study of alcohol dependence: significant

- findings in African- and European-Americans including novel risk loci. *Mol Psychiatry*. (2014) 19:41–9. doi: 10.1038/mp.2013.145
46. Boucquoy M, De Plaen E, Locker M, Poliard A, Mouillet-Richard S, Boon T, et al. Noxp20 and Noxp70, two new markers of early neuronal differentiation, detected in teratocarcinoma-derived neuroectodermic precursor cells. *J Neurochem*. (2006) 99:657–69. doi: 10.1111/j.1471-4159.2006.04093.x
  47. Curtis D, Vine A, McQuillin A, Bass N, Pereira A, Kandaswamy R, et al. Case-case genome-wide association analysis shows markers differentially associated with schizophrenia and bipolar disorder and implicates calcium channel genes. *Psychiatr Genet*. (2011) 21:1–4. doi: 10.1097/YPG.0b013e3283413382
  48. Kious B, Baker C, Bronner-Fraser M, Knecht A. Identification and characterization of a calcium channel gamma subunit expressed in differentiating neurons and myoblasts. *Dev Biol*. (2002) 243:249–59. doi: 10.1006/dbio.2001.0570
  49. Li Q, Tian C, Seabrook G, Drevets W, Narayan V. Analysis of 23andMe antidepressant efficacy survey data: implication of circadian rhythm and neuroplasticity in bupropion response. *Transl Psychiatry*. (2016) 6:e889. doi: 10.1038/tp.2016.171
  50. Vourc'h P, Martin I, Bonnet-Brilhault F, Marouillat S, Barthélémy C, Pierre Müh J, et al. Mutation screening and association study of the UBE2H gene on chromosome 7q32 in autistic disorder. *Psychiatr Genet*. (2003) 13:221–5. doi: 10.1097/00041444-200312000-00005
  51. Hu J, Li G, Qu L, Li N, Liu W, Xia D, et al. TMEM166/EVA1A interacts with ATG16L1 and induces autophagosome formation and cell death. *Cell Death Dis*. (2016) 7:e2323. doi: 10.1038/cddis.2016.230
  52. Guo W, Machado-Vieira R, Mathew S, Murrrough J, Charney D, Grunebaum M, et al. Exploratory genome-wide association analysis of response to ketamine and a polygenic analysis of response to scopolamine in depression. *Transl Psychiatry*. (2018) 8:280. doi: 10.1038/s41398-018-0311-7
  53. Pardiñas A, Holmans P, Pocklington A, Escott-Price V, Ripke S, Carrera N, et al. Common schizophrenia alleles are enriched in mutation-intolerant genes and in regions under strong background selection. *Nat Genet*. (2018) 50:381–9. doi: 10.1038/s41588-018-0059-2
  54. Fine A, Irihimovitch V, Dahan I, Konrad Z, Eichler J. Cloning, expression, and purification of functional Sec11a and Sec11b, type I signal peptidases of the archaeon *Haloferax volcanii*. *J Bacteriol*. (2006) 188:1911–9. doi: 10.1128/JB.188.5.1911-1919.2006
  55. Liu M, Jiang Y, Wedow R, Li Y, Brazel D, Chen F, et al. Association studies of up to 1.2 million individuals yield new insights into the genetic etiology of tobacco and alcohol use. *Nat Genet*. (2019) 51:237–44. doi: 10.1038/s41588-018-0307-5
  56. Yang J, Cao D, Zhang Y, Ou R, Yin Z, Liu Y, et al. The role of phosphorylation of MLF2 at serine 24 in BCR-ABL leukemogenesis. *Cancer Gene Ther*. (2020) 27:98–107. doi: 10.1038/s41417-019-0152-4
  57. Coleman J, Gaspar H, Bryois J, Breen G. The genetics of the mood disorder spectrum: genome-wide association analyses of more than 185,000 cases and 439,000 controls. *Biol Psychiatry*. (2020) 88:169–84. doi: 10.1016/j.biopsych.2019.10.015
  58. Howard D, Adams M, Clarke T, Hafferty J, Gibson J, Shirihi M, et al. Genome-wide meta-analysis of depression identifies 102 independent variants and highlights the importance of the prefrontal brain regions. *Nat Neurosci*. (2019) 22:343–52. doi: 10.1038/s41593-018-0326-7
  59. Wray N, Ripke S, Mattheisen M, Trzaskowski M, Byrne E, Abdellaoui A, et al. Genome-wide association analyses identify 44 risk variants and refine the genetic architecture of major depression. *Nat Genet*. (2018) 50:668–81. doi: 10.1038/s41588-018-0090-3
  60. Chen D, Guo J, Miki T, Tachibana M, Gahl W. Molecular cloning and characterization of rab27a and rab27b, novel human rab proteins shared by melanocytes and platelets. *Biochem Mol Med*. (1997) 60:27–37. doi: 10.1006/bmme.1996.2559
  61. Brazel D, Jiang Y, Hughey J, Turcot V, Zhan X, Gong J, et al. Exome chip meta-analysis fine maps causal variants and elucidates the genetic architecture of rare coding variants in smoking and alcohol use. *Biol Psychiatry*. (2019) 85:946–55. doi: 10.1016/j.biopsych.2018.11.024
  62. Bera T, Liu X, Yamada M, Gavrilova O, Mezey E, Tessarollo L, et al. A model for obesity and gigantism due to disruption of the Ankrd26 gene. *Proc Natl Acad Sci USA*. (2008) 105:270–5. doi: 10.1073/pnas.0710978105
  63. Sanchez-Roige S, Fontanillas P, Elson S, Gray J, de Wit H, Davis L, et al. Genome-wide association study of alcohol use disorder identification test (AUDIT) scores in 20 328 research participants of European ancestry. *Addict Biol*. (2019) 24:121–31. doi: 10.1111/adb.12574
  64. Kempermann G, Chesler E, Lu L, Williams R, Gage F. Natural variation and genetic covariance in adult hippocampal neurogenesis. *Proc Natl Acad Sci USA*. (2006) 103:780–5. doi: 10.1073/pnas.0510291103
  65. Huggett S, Stallings M. Genetic architecture and molecular neuropathology of human cocaine addiction. *J Neurosci*. (2020) 40:5300–13. doi: 10.1523/JNEUROSCI.2879-19.2020
  66. Davies G, Lam M, Harris S, Trampush J, Luciano M, Hill W, et al. Study of 300,486 individuals identifies 148 independent genetic loci influencing general cognitive function. *Nat Commun*. (2018) 9:2098. doi: 10.1038/s41467-018-04362-x
  67. Patel M, Swiatkowski P, Kwon M, Rodriguez A, Campagno K, Firestein B. A novel short isoform of cytosolic PSD-95 Interactor (Cypin) regulates neuronal development. *Mol Neurobiol*. (2018) 55:6269–81. doi: 10.1007/s12035-017-0849-z
  68. Liu L, Gu H, Hou F, Xie X, Li X, Zhu B, et al. Dyslexia associated functional variants in Europeans are not associated with dyslexia in Chinese. *Am J Med Genet B Neuropsychiatr Genet*. (2019) 180:488–95. doi: 10.1002/ajmg.b.32750
  69. Olczak M, Poniatowski L, Kwiatkowska M, Samojlowicz D, Tarka S, Wierzb-Bobrowicz T. Immunolocalization of dynein, dynactin, and kinesin in the cerebral tissue as a possible supplemental diagnostic tool for traumatic brain injury in postmortem examination. *Folia Neuropathol*. (2019) 57:51–62. doi: 10.5114/fn.2019.83831
  70. Sung Y, Winkler T, de Las Fuentes L, Bentley A, Brown M, Kraja A, et al. A large-scale multi-ancestry genome-wide study accounting for smoking behavior identifies multiple significant loci for blood pressure. *Am J Hum Genet*. (2018) 102:375–400. doi: 10.1016/j.ajhg.2018.01.015
  71. Mittaz L, Antonarakis S, Higuchi M, Scott H. Localization of a novel human RNA-editing deaminase (hRED2 or ADARB2) to chromosome 10p15. *Hum Genet*. (1997) 100:398–400. doi: 10.1007/s004390050523
  72. Chaste P, Klei L, Sanders S, Hus V, Murtha M, Lowe J, et al. A genome-wide association study of autism using the simons simplex collection: does reducing phenotypic heterogeneity in autism increase genetic homogeneity? *Biol Psychiatry*. (2015) 77:775–84. doi: 10.1016/j.biopsych.2014.09.017
  73. Erratum. *Hum Mutat*. (2021) 42:219. doi: 10.1002/humu.24157
  74. Liu Y, Wu X, Xia X, Yao J, Wang B. The genome-wide supported CACNA1C gene polymorphisms and the risk of schizophrenia: an updated meta-analysis. *BMC Med Genet*. (2020) 21:159. doi: 10.1186/s12881-020-01084-0
  75. Mosheva M, Serretti A, Stukalin Y, Fabbri C, Hagin M, Horev S, et al. Association between CANCA1C gene rs1034936 polymorphism and alcohol dependence in bipolar disorder. *J Affect Disord*. (2020) 261:181–6. doi: 10.1016/j.jad.2019.10.015
  76. Yamakage M, Namiki A. Calcium channels-basic aspects of their structure, function and gene encoding: anesthetic action on the channels-a review. *Can J Anaesth*. (2002) 49:151–64. doi: 10.1007/BF03020488
  77. Mendoza J. Food intake and addictive-like eating behaviors: time to think about the circadian clock(s). *Neurosci Biobehav Rev*. (2019) 106:122–32. doi: 10.1016/j.neubiorev.2018.07.003
  78. Salaberry N, Mendoza J. Insights into the role of the habenular circadian clock in addiction. *Front Psychiatry*. (2015) 6:179. doi: 10.3389/fpsy.2015.00179
  79. Steffens D, Garrett M, Soldano K, McQuoid D, Ashley-Koch A, Potter G. Genome-wide screen to identify genetic loci associated with cognitive decline in late-life depression. *Int Psychogeriatr*. (2020) 1–9. doi: 10.1017/S1041610220001143
  80. Blanco-Sánchez B, Clément A, Fierro J, Stednitz S, Phillips J, Wegner J, et al. Grxcr1 promotes hair bundle development by destabilizing the physical interaction between harmonin and sans usher syndrome proteins. *Cell Rep*. (2018) 25:1281–91. doi: 10.1016/j.celrep.2018.10.005
  81. Wang T, Han W, Wang B, Jiang Q, Solberg-Woods L, Palmer A, et al. Propensity for social interaction predicts nicotine-reinforced behaviors in outbred rats. *Genes Brain Behav*. (2014) 13:202–12. doi: 10.1111/gbb.12112
  82. Temmingh H, Stein D. Anxiety in patients with schizophrenia: epidemiology and management. *CNS Drugs*. (2015) 29:819–32. doi: 10.1007/s40263-015-0282-7

83. Howells F, Kingdon D, Baldwin D. Current and potential pharmacological and psychosocial interventions for anxiety symptoms and disorders in patients with schizophrenia: structured review. *Hum Psychopharmacol.* (2017) 32. doi: 10.1002/hup.2628
84. Larsen R, Proue A, Scott E, Christiansen M, Nakagawa Y. The thalamus regulates retinoic acid signaling and development of parvalbumin interneurons in postnatal mouse prefrontal cortex. *eNeuro.* 6. doi: 10.1523/ENEURO.0018-19.2019
85. Samamé C. Social cognition throughout the three phases of bipolar disorder: a state-of-the-art overview. *Psychiatry Res.* (2013) 210:1275–86. doi: 10.1016/j.psychres.2013.08.012
86. Green M, Horan W, Lee J. Social cognition in schizophrenia. *Nat Rev Neurosci.* (2015) 16:620–31. doi: 10.1038/nrn4005
87. Kisko T, Braun M, Michels S, Witt S, Rietschel M, Culmsee C, et al. Cacna1c haploinsufficiency leads to pro-social 50-kHz ultrasonic communication deficits in rats. *Dis Model Mech.* (2018) 11. doi: 10.1242/dmm.034116
88. Wöhr M, Kisko T, Schwarting R. Social behavior and ultrasonic vocalizations in a genetic rat model haploinsufficient for the cross-disorder risk gene cacna1c. *Brain Sci.* (2021) 11:724. doi: 10.3390/brainsci11060724
89. Terrillion C, Francis T, Puche A, Lobo M, Gould T. Decreased nucleus accumbens expression of psychiatric disorder risk gene cacna1c promotes susceptibility to social stress. *Int J Neuropsychopharmacol.* (2017) 20:428–33. doi: 10.1093/ijnp/pyw112
90. Kabir Z, Che A, Fischer D, Rice R, Rizzo B, Byrne M, et al. Rescue of impaired sociability and anxiety-like behavior in adult cacna1c-deficient mice by pharmacologically targeting eIF2 $\alpha$ . *Mol Psychiatry.* (2017) 22:1096–109. doi: 10.1038/mp.2017.124
91. Sittig L, Carbonetto P, Engel K, Krauss K, Barrios-Camacho C, Palmer A. Genetic background limits generalizability of genotype-phenotype relationships. *Neuron.* (2016) 91:1253–9. doi: 10.1016/j.neuron.2016.08.013
92. Arias-Hervert E, Xu N, Njus M, Murphy G, Hou Y, Williams J, et al. Actions of Rab27B-GTPase on mammalian central excitatory synaptic transmission. *Physiol Rep.* (2020) 8:e14428. doi: 10.14814/phy2.14428
93. Shen Y, Gu Y, Su W, Zhong J, Jin Z, Gu X, et al. Rab27b is involved in lysosomal exocytosis and proteolipid protein trafficking in oligodendrocytes. *Neurosci Bull.* (2016) 32:331–40. doi: 10.1007/s12264-016-0045-6
94. Kleene R, Cassens C, Bähring R, Theis T, Xiao M, Dityatev A, et al. Functional consequences of the interactions among the neural cell adhesion molecule NCAM, the receptor tyrosine kinase TrkB, and the inwardly rectifying K<sup>+</sup> channel KIR3.3. *J Biol Chem.* (2010) 285:28968–79. doi: 10.1074/jbc.M110.114876
95. Firestein B, Firestein B, Brenman J, Aoki C, Sanchez-Perez A, El-Husseini A, et al. Cypin: a cytosolic regulator of PSD-95 postsynaptic targeting. *Neuron.* (1999) 24:659–72. doi: 10.1016/S0896-6273(00)81120-4
96. Nicod J, Davies R, Cai N, Hassett C, Goodstadt L, Cosgrove C, et al. Genome-wide association of multiple complex traits in outbred mice by ultra-low-coverage sequencing. *Nat Genet.* (2016) 48:912–8. doi: 10.1038/ng.3595
97. Ludin N, Orts-Sebastian A, Cheeseman J, Chong J, Merry A, Cumin D, et al. General anaesthesia shifts the murine circadian clock in a time-dependant fashion. *Clocks Sleep.* (2021) 3:87–97. doi: 10.3390/clockssleep3010006
98. Schuch J, Genro J, Bastos C, Ghisleni G, Tovo-Rodrigues L. The role of CLOCK gene in psychiatric disorders: evidence from human and animal research. *Am J Med Genet B Neuropsychiatr Genet.* (2018) 177:181–98. doi: 10.1002/ajmg.b.32599
99. Smoller J, Andreassen O, Edenberg H, Faraone S, Glatt S, Kendler K. Psychiatric genetics and the structure of psychopathology. *Mol Psychiatry.* (2019) 24:409–20. doi: 10.1038/s41380-017-0010-4
100. Jones H, Stergiakouli E, Tansey K, Hubbard L, Heron J, Cannon M, et al. Phenotypic Manifestation of Genetic Risk for Schizophrenia During Adolescence in the General Population. *JAMA Psychiatry.* (2016) 73:221–8. doi: 10.1001/jamapsychiatry.2015.3058
101. Cross-Disorder Group of the Psychiatric Genomics Consortium. Identification of risk loci with shared effects on five major psychiatric disorders: a genome-wide analysis. *Lancet.* (2013) 381:1371–9. doi: 10.1016/S0140-6736(12)62129-1
102. Hatzimanolis A, Bhatnagar P, Moes A, Wang R, Roussos P, Bitsios P, et al. Common genetic variation and schizophrenia polygenic risk influence neurocognitive performance in young adulthood. *Am J Med Genet B Neuropsychiatr Genet.* (2015) 1688:392–401. doi: 10.1002/ajmg.b.32323
103. Zhu J, Chen Z, Tian J, Meng Z, Ju M, Wu G, et al. miR-34b attenuates trauma-induced anxiety-like behavior by targeting CRHR1. *Int J Mol Med.* (2017) 40:90–100. doi: 10.3892/ijmm.2017.2981
104. Fan J, Wang X, Hao K, Yuan Y, Chen X, Du J. Upregulation of PVN CRHR1 by gestational intermittent hypoxia selectively triggers a male-specific anxiogenic effect in rat offspring. *Horm Behav.* (2013) 63:25–31. doi: 10.1016/j.yhbeh.2012.11.005
105. Wang X, Labermaier C, Holsboer F, Wurst W, Deussing J, Müller M, et al. Early-life stress-induced anxiety-related behavior in adult mice partially requires forebrain corticotropin-releasing hormone receptor 1. *Eur J Neurosci.* (2012) 36:2360–7. doi: 10.1111/j.1460-9568.2012.08148.x
106. Sey N, Hu B, Mah W, Fauni H, McAfee J, Rajarajan P, et al. A computational tool (H-MAGMA) for improved prediction of brain-disorder risk genes by incorporating brain chromatin interaction profiles. *Nat Neurosci.* (2020) 23:583–93. doi: 10.1038/s41593-020-0603-0
107. Watanabe K, Taskesen E, van Bochoven A, Posthuma D. Functional mapping and annotation of genetic associations with FUMA. *Nat Commun.* (2017) 8:1826. doi: 10.1038/s41467-017-01261-5
108. King C, Palmer A, Woods L, Hawk L, Richards J, Meyer P. Premature responding is associated with approach to a food cue in male and female heterogeneous stock rats. *Psychopharmacology (Berl).* (2016) 233:2593–605. doi: 10.1007/s00213-016-4306-x
109. King C, Tripi J, Hughson A, Horvath A, Lamparelli A, Holl K, et al. Sensitivity to food and cocaine cues are independent traits in a large sample of heterogeneous stock rats. *Sci Rep.* (2021) 11:2223. doi: 10.1038/s41598-020-80798-w
110. Sedighim S, Carrette L, Venniro M, Shaham Y, de Guglielmo G, George O. Individual differences in addiction-like behaviors and choice between cocaine versus food in Heterogeneous Stock rats. *Psychopharmacology (Berl).* (2021) 238:3423–33. doi: 10.1101/2021.07.21.453270
111. Carrette L, de Guglielmo G, Kallupi M, Maturin L, Brennan M, Boomhower B, et al. The cocaine and oxycodone biobanks, two repositories from genetically diverse and behaviorally characterized rats for the study of addiction. *eNeuro.* (2021) 8:ENEURO.0033-21.2021. doi: 10.1523/ENEURO.0033-21.2021

**Conflict of Interest:** The authors declare that the research was conducted in the absence of any commercial or financial relationships that could be construed as a potential conflict of interest.

**Publisher's Note:** All claims expressed in this article are solely those of the authors and do not necessarily represent those of their affiliated organizations, or those of the publisher, the editors and the reviewers. Any product that may be evaluated in this article, or claim that may be made by its manufacturer, is not guaranteed or endorsed by the publisher.

Copyright © 2022 Gunturkun, Wang, Chitre, Garcia Martinez, Holl, St. Pierre, Bimschleger, Gao, Cheng, Polesskaya, Solberg Woods, Palmer and Chen. This is an open-access article distributed under the terms of the Creative Commons Attribution License (CC BY). The use, distribution or reproduction in other forums is permitted, provided the original author(s) and the copyright owner(s) are credited and that the original publication in this journal is cited, in accordance with accepted academic practice. No use, distribution or reproduction is permitted which does not comply with these terms.



# Functional Genomic Analysis of Amphetamine Sensitivity in *Drosophila*

Caline S. Karam<sup>1,2\*</sup>, Brenna L. Williams<sup>2</sup>, Irina Morozova<sup>3,4</sup>, Qiaoping Yuan<sup>5</sup>, Rony Panarsky<sup>5</sup>, Yuchao Zhang<sup>1,2</sup>, Colin A. Hodgkinson<sup>5</sup>, David Goldman<sup>5</sup>, Sergey Kalachikov<sup>3,4</sup> and Jonathan A. Javitch<sup>1,2,6\*</sup>

## OPEN ACCESS

### Edited by:

Gary T. Hardiman,  
Queen's University Belfast,  
United Kingdom

### Reviewed by:

Suzanne Underhill,  
National Institutes of Health (NIH),  
United States  
R. Dayne Mayfield,  
University of Texas at Austin,  
United States  
Sammanda Ramamoorthy,  
Virginia Commonwealth University,  
United States

### \*Correspondence:

Caline S. Karam  
cskaram@gmail.com  
Jonathan A. Javitch  
jaj2@columbia.edu

### Specialty section:

This article was submitted to  
Psychopharmacology,  
a section of the journal  
Frontiers in Psychiatry

**Received:** 08 December 2021

**Accepted:** 24 January 2022

**Published:** 18 February 2022

### Citation:

Karam CS, Williams BL, Morozova I,  
Yuan Q, Panarsky R, Zhang Y,  
Hodgkinson CA, Goldman D,  
Kalachikov S and Javitch JA (2022)  
Functional Genomic Analysis of  
Amphetamine Sensitivity in  
*Drosophila*.  
Front. Psychiatry 13:831597.  
doi: 10.3389/fpsy.2022.831597

<sup>1</sup> Department of Psychiatry, Columbia University Vagelos College of Physicians and Surgeons, New York, NY, United States, <sup>2</sup> Division of Molecular Therapeutics, New York State Psychiatric Institute, New York, NY, United States, <sup>3</sup> Center for Genome Technology and Biomolecular Engineering, Columbia University, New York, NY, United States, <sup>4</sup> Department of Chemical Engineering, Columbia University, New York, NY, United States, <sup>5</sup> Laboratory of Neurogenetics, National Institute on Alcohol Abuse and Alcoholism, Bethesda, MD, United States, <sup>6</sup> Department of Molecular Pharmacology and Therapeutics, Columbia University Vagelos College of Physicians and Surgeons, New York, NY, United States

Abuse of psychostimulants, including amphetamines (AMPHs), is a major public health problem with profound psychiatric, medical, and psychosocial complications. The actions of these drugs at the dopamine transporter (DAT) play a critical role in their therapeutic efficacy as well as their liability for abuse and dependence. To date, however, the mechanisms that mediate these actions are not well-understood, and therapeutic interventions for AMPH abuse have been limited. Drug exposure can induce broad changes in gene expression that can contribute to neuroplasticity and effect long-lasting changes in neuronal function. Identifying genes and gene pathways perturbed by drug exposure is essential to our understanding of the molecular basis of drug addiction. In this study, we used *Drosophila* as a model to examine AMPH-induced transcriptional changes that are DAT-dependent, as those would be the most relevant to the stimulatory effects of the drug. Using this approach, we found genes involved in the control of mRNA translation to be significantly upregulated in response to AMPH in a DAT-dependent manner. To further prioritize genes for validation, we explored functional convergence between these genes and genes we identified in a genome-wide association study of AMPH sensitivity using the *Drosophila* Genetic Reference Panel. We validated a number of these genes by showing that they act specifically in dopamine neurons to mediate the behavioral effects of AMPH. Taken together, our data establish *Drosophila* as a powerful model that enables the integration of behavioral, genomic and transcriptomic data, followed by rapid gene validation, to investigate the molecular underpinnings of psychostimulant action.

**Keywords:** *Drosophila*, dopamine transporter, DGRP, transcriptomic (RNA-Seq), amphetamine, psychostimulants, mammalian target of rapamycin (mTOR), S6K (70-kDa ribosomal protein S6 kinase)

## INTRODUCTION

The use of prescribed and illicit amphetamines (AMPHs) has been growing steadily, with an estimated 50 million worldwide users in 2017 (1). These drugs are widely abused, often leading to aggression, psychosis, cardiovascular damage, and a host of other medical and psychosocial complications (2, 3). AMPHs act as substrates for the dopamine transporter (DAT), which mediates the inactivation of released dopamine through reuptake. The actions of AMPHs lead to a dramatic increase of extracellular dopamine *via* non-exocytic efflux of dopamine through DAT-mediated reverse transport (4–7). This dopamine increase is believed to play a major role in the psychostimulatory and rewarding properties of AMPHs (4, 5, 8). To date, however, the mechanisms that mediate the transition from drug use to abuse are not fully understood, and therapeutic interventions for AMPH abuse have been limited and largely ineffective.

Neuroadaptations in response to drugs of abuse have been extensively reported (9–13). Specifically, studies have shown that drug exposure can induce broad changes in gene expression, which can contribute to neuroplasticity and effect long-lasting changes in neuronal function, ultimately leading to the development of drug-seeking behavior (11, 14). Identifying genes and gene pathways perturbed by drug exposure is essential to our understanding of the molecular basis of drug addiction and can help identify novel therapeutic targets and guide the development of novel treatment and prevention measures for substance use disorders.

Studies in humans encounter multiple challenges, including the difficulty of quantifying behavioral phenotypes presented by complex brain disorders, such as addiction, and gene x environment interactions, which can further confound results (15–17). To overcome these challenges, animal models have emerged as critical tools for investigating in a systematic manner the molecular and cellular mechanisms underlying the actions of drugs of abuse (18). Acute stimulation of locomotor behaviors is one of the most widely studied effects of psychostimulants. It has been suggested that acute drug effects in animals may model the initial sensitivity experienced by humans during early drug use. This initial sensitivity varies significantly among individuals (19) and has been associated with continued drug use (20–23). Similarly, in mice, differences in the sensitivity to the locomotor effects of methamphetamines are heritable (24) and, importantly, predict later self-administration (25, 26).

Using a *Drosophila* behavioral assay, we previously showed that flies respond to AMPH by increasing their locomotor activity (27, 28) and decreasing their sleep (27) in a dopamine-dependent manner. Flies that carry a loss-of-function mutation in the gene encoding the *Drosophila* DAT homolog (*dDAT<sup>fmm</sup>*, henceforth referred to as *DAT* mutants) display no detectable DAT in the brain and exhibit heightened activity levels at baseline, consistent with increased levels of extracellular dopamine caused by the impairment of reuptake (27, 29). Critically, our data showed that *DAT* mutant flies failed to increase their activity in response to AMPH (27), consistent with DAT being the principal molecular target for AMPH (4, 5). Taken together, these data demonstrate that we have developed a robust tool to associate molecular

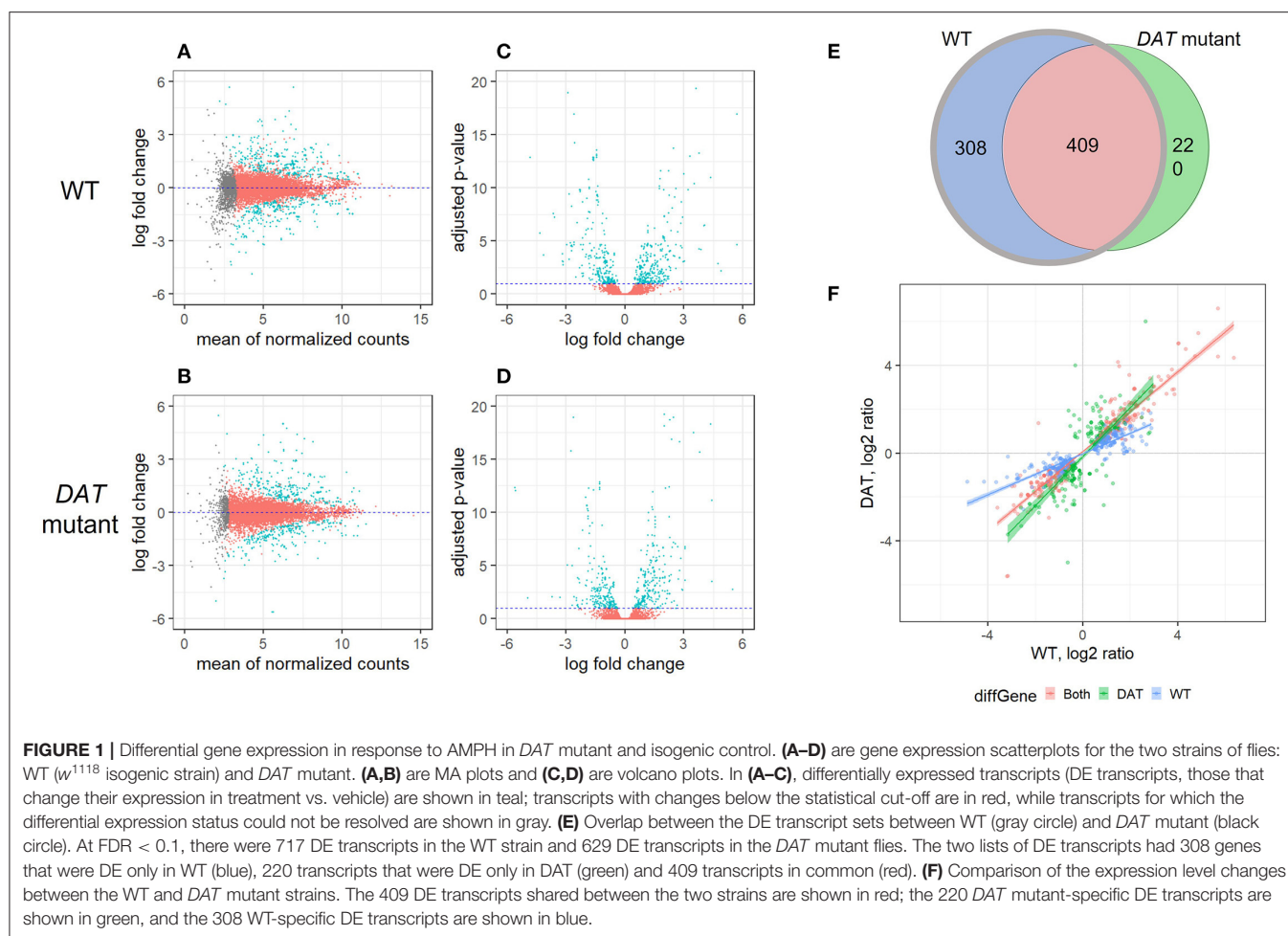
perturbations with the actions of AMPH *in vivo*. In this study, we used this model to examine the transcriptional changes induced by AMPH treatment. Since DAT is essential for the locomotor effects of AMPH (27), we focused our analysis on gene expression changes that were DAT-dependent by comparing the transcriptomes of *DAT* mutant flies to those of control flies, to identify genes that were associated specifically with the actions of AMPH at DAT, as those would be the most relevant to the stimulatory effects of the drug. To further prioritize genes for validation, we explored functional convergence between these genes and genes we identified in a genome-wide association study of AMPH sensitivity using the *Drosophila* Genetic Reference Panel (DGRP) (30). Using this approach, we identified several genes that play a role in modulating mRNA translation and processing. Taking advantage of the tools available in flies for targeted gene manipulation (31, 32), we validated a number of these genes by showing that they act specifically in dopamine neurons to mediate the behavioral effects of AMPH. Taken together, our data establish *Drosophila* as a powerful model that enables the integration of behavioral data, with transcriptomic data and GWAS, followed by rapid gene validation, to investigate the molecular underpinnings of psychostimulant action.

## RESULTS

### Transcriptional Response to AMPH in *Drosophila*

To identify DAT-dependent changes in AMPH-induced gene expression, we performed RNA-seq on *Drosophila* head extracts from isogenic *w<sup>1118</sup>* flies (WT) and flies carrying a loss-of-function mutation in the *Drosophila* *DAT* gene (*DAT* mutant) (29). We used the DEseq2 method (33) to identify gene transcripts that were differentially expressed in either strain in response to AMPH treatment, as compared to exposure to vehicle alone (DE transcripts). We then compared the DE transcripts between the two strains. DEseq2 analysis showed profound transcriptional responses to AMPH in both strains (Figures 1A–D, statistically significant DE transcripts are shown in teal). We identified 717 DE transcripts corresponding to 362 unique genes in WT and 629 DE transcripts corresponding to 332 unique genes in *DAT* mutants (Figure 1, Supplementary Table 1), with approximately the same number of transcripts up and downregulated after the exposure (the MA plots in Figures 1A,B show similar number of transcripts above and below the zero line on the Y-axis).

As we were primarily interested in the DAT-dependent contribution to the transcriptional response to AMPH, we focused our further analysis on genes that no longer respond to AMPH in the absence of DAT, i.e., genes that are differentially expressed in the WT but not in the *DAT* mutant, when comparing the AMPH-treated groups to their respective vehicle controls. These are genes corresponding to the 308 transcripts that constitute the *w<sup>1118</sup>* complement to the *w<sup>1118</sup>/DAT* intersection (shown in blue in Figures 1E,F) we refer to as DAT-dependent. We identified 409 transcripts that are differentially expressed in both strains (Figures 1E,F, red), 408 of which were



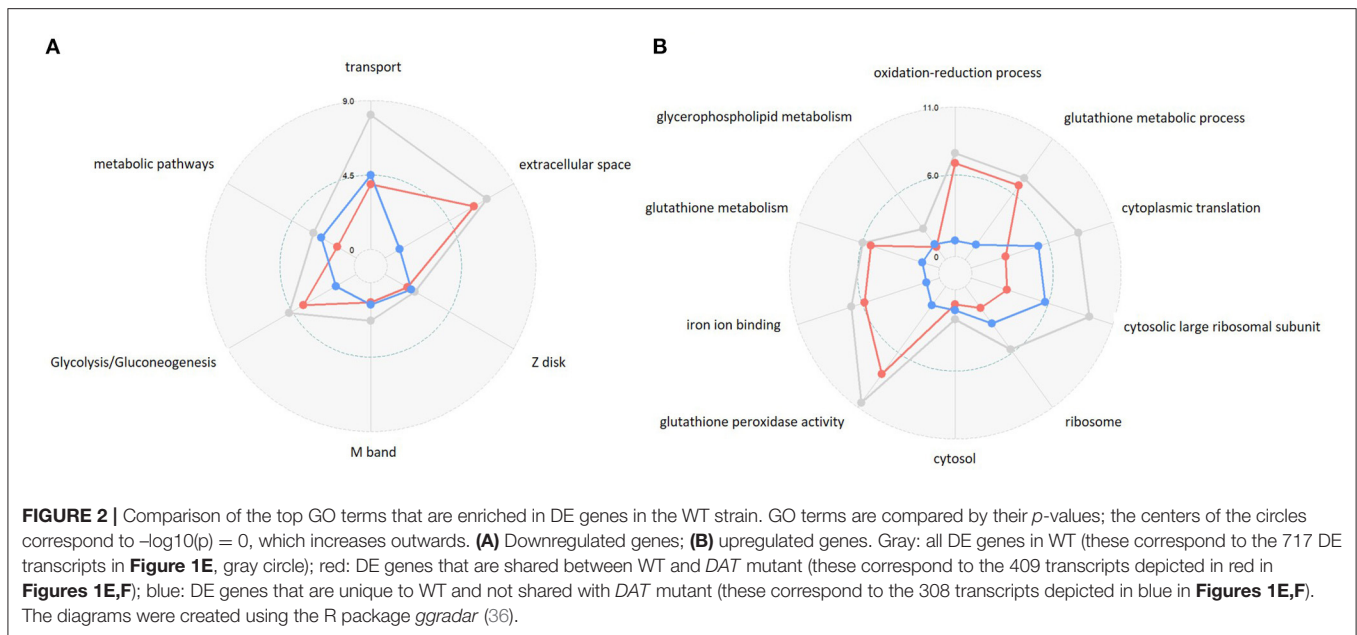
changed in the same direction. Given that the *DAT* mutants do not express a functional DAT, we posit that the expression changes in these 408 shared transcripts (**Figures 1E,F**, red) are due to the effects of AMPH that are not mediated by DAT (DAT-independent), such as the responses to the actions of AMPH at other targets, including other neurotransmitter transporters (34). One gene, *takeout*, changed its expression in the opposite direction in the *DAT* mutant compared to control (**Figure 1F**, upper left quadrant). Lastly, we found 220 transcripts that only respond to AMPH in the *DAT* mutants and not in the controls (**Figures 1E,F**, green). These may reflect compensatory mechanisms that arise in response to the underlying hyperdopaminergic state in *DAT* mutants, such as the activation of other neurotransmitter systems that gain functional significance in the absence of DAT and the presence of AMPH.

### Functional Categories of Genes That Are Differentially Regulated by AMPH in a DAT-Dependent Manner

For functional interpretation of the DAT-dependent transcriptional effects of AMPH, we next compared known functions of the DAT-dependent genes to those

of the DAT-independent genes, separately for upregulated and downregulated genes, to find significant differential functional enrichment [in KEGG pathways and Gene Ontology (GO) Biological Process (BP) categories (35)] (**Supplementary Tables 2, 3**). We found several functional terms that were differentially enriched when the group of DAT-dependent genes was compared with the DAT-independent group (**Figure 2, Supplementary Figure 1**). We also detected a number of common functional themes between these two gene sets, which could reflect the cumulative changes in gene activity in response to AMPH across different parts of the fly brain. Notably, even among the shared functional terms, we found significant differences in the distribution of the *p*-values between the two groups (**Figure 2**, compare blue to red). Taken together, the differential enrichment of the shared terms as well as the significant differences in overall functional themes suggest that the two gene lists, DAT-dependent and DAT-independent, were drawn from functionally distinct sets of genes representing the distinct actions of AMPH in the presence or absence of its primary molecular target.

The functional differences between DAT-dependent and DAT-independent genes were more pronounced among the upregulated genes (**Figure 2**, compare blue to red). Furthermore,

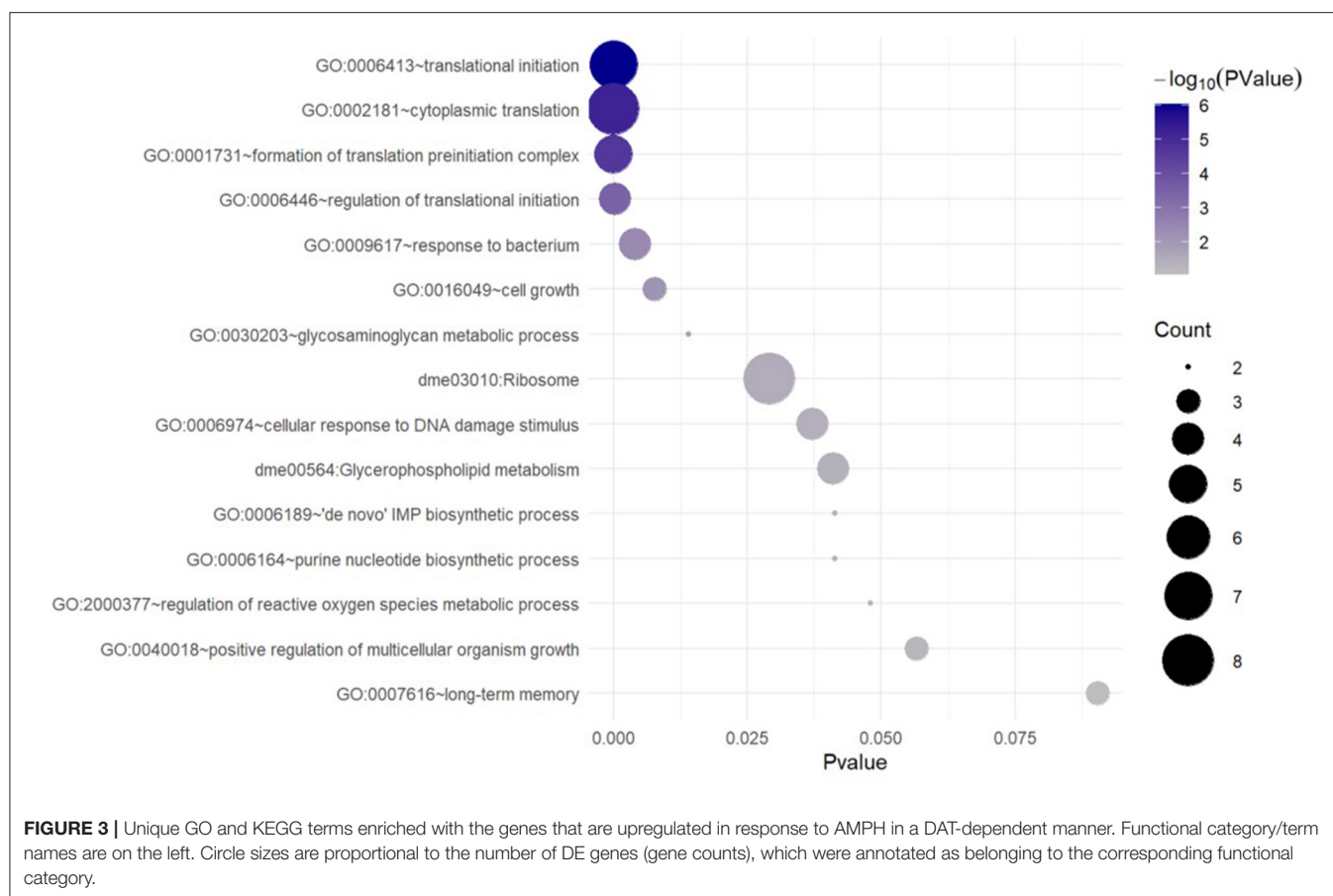


upregulated genes had a higher number of specific differentially enriched functional annotation terms (as opposed to general ones) than downregulated genes, which did not show any particular predominant categories in the enrichment analysis (**Figure 2A**, **Supplementary Figure 1E**). Major functional categories that were predominantly enriched in the *DAT*-independent group, and therefore represented a common response to the drug between WT and *DAT* mutant, included oxidation-reduction process and glutathione metabolism (**Figure 2**, red), consistent with the presence of a general xenobiotic response to drug exposure (37).

To characterize the functions specific to the *DAT*-dependent groups, we subtracted from the WT enrichment list the categories that were predominantly shared between WT and *DAT* mutant [categories that exhibited high significance (low  $p$ -values) in the *DAT*-independent set]. This resulted in a unique subset of terms specific to the genes that are upregulated in response to AMPH treatment in a *DAT*-dependent manner (**Figure 3**). This enrichment analysis showed that the predominant functional theme in the AMPH-induced *DAT*-dependent gene regulation was the activation of *de novo* mRNA translation. Among the upregulated genes were those encoding ribosomal subunits and components of the eukaryotic translation initiation factor 3 complex (eIF3) (**Supplementary Table 3**). We did not find any exclusively neuron-specific processes in this analysis, with the exception of genes encoding proteins that modulate cell-cell adhesion (in the downregulated group) and long-term memory (in the upregulated group); however, neither one of these general categories accumulated enough genes to provide more specific annotation that would allow for a more detailed functional classification (**Supplementary Table 3**).

## Convergent Data From a Genome-Wide Association Study (GWAS) of AMPH Sensitivity

The above transcriptomic analyses comparing AMPH-associated gene regulation in *DAT* mutants and their isogenic control (WT) were performed with the intention to prioritize for validation genes that were regulated only in the presence of AMPH, as we anticipated those to be more relevant to the actions of AMPH at dopaminergic release sites. To further explore the functional relevance of the genes uncovered by this analysis, we mined data collected from an independent GWAS of AMPH-induced hyperactivity we conducted using the DGRP (Williams et al, *GWA uncovers a novel role for Ctr9 in AMPH sensitivity in Drosophila*, not yet published), a collection of inbred, fully sequenced fly lines (30). In addition to 3 SNPs that met the Bonferroni threshold of  $p < 10^{-8}$ , our analyses found 288 SNPs within or near 123 genes associated with the response to AMPH at an empirical threshold of  $p < 10^{-5}$ . Similarly to previous GWA studies performed with the DGRP (38), quantile-quantile plots of observed  $p$ -values against the distribution of expected  $p$ -values demonstrated significant deviation from linearity that supports the enrichment in true positive associations at or above this empirical threshold (Williams et al., *ibid*). Previous efforts by other groups using mutational analyses or targeted RNAi knockdown have validated 60–80% of gene associations that fall into this category (38). We posited that we could identify high-priority genes for further validation by looking for functional convergence between the genes we identified in our GWAS with those identified in the transcriptomic analyses presented above. Indeed, we found associated SNPs within or near several genes encoding ribosomal subunits (*RpL8*, *RpS13*, *RpS23*, and *RpS26*) (39) and *smooth* (*sm*), a heterogeneous nuclear ribonucleoprotein

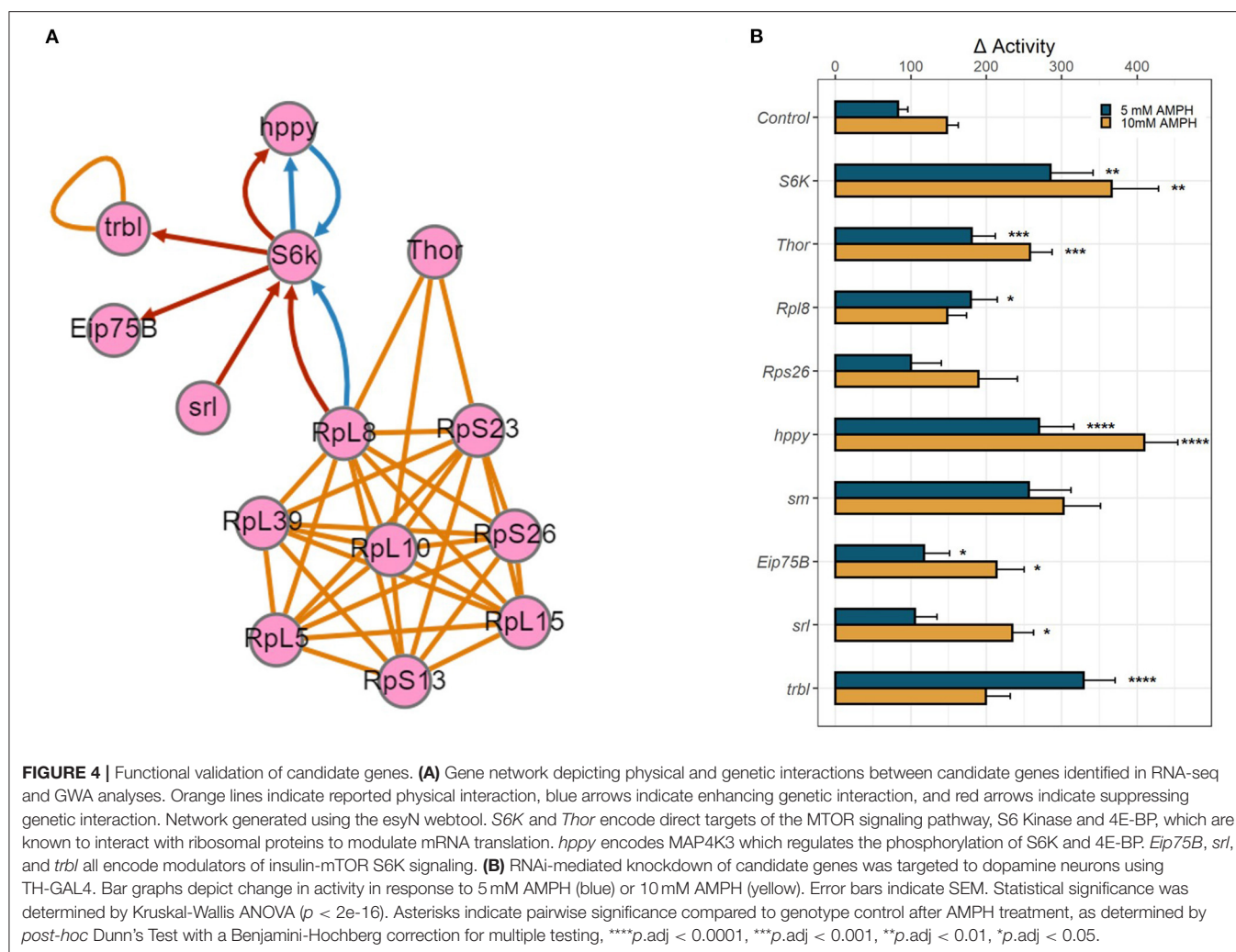


(hnRNP) with a role in mRNA splicing (40), which was also identified in the RNA-seq analysis. Pathway analysis further identified candidate genes from either study that encode proteins essential to the modulation of mRNA translation (**Figure 4A**). We found associated SNPs within or near the gene encoding the ribosomal protein S6 kinase (*S6k*), which promotes protein synthesis by phosphorylating the S6 ribosomal protein, and the gene *happyhour* (*hppy*), which encodes a member of the Ste20 family member (MAP4K3) that has been shown to be required for maximal phosphorylation of S6K and the eukaryotic translation initiation factor 4E binding protein (4E-BP1) (41). Notably, the fly has only one gene encoding a 4E binding protein, *Thor* (42, 43), which was also identified in our transcriptomic analyses above. Other candidate genes from the GWAS include *Eip75b*, the fly homolog of peroxisome proliferator-activated receptor  $\gamma$  (PPAR $\gamma$ ), and *spargel* (*srl*), the homolog of PPAR $\gamma$  coactivator 1 $\alpha$  (PGC-1 $\alpha$ ) (44, 45). PGC-1 $\alpha$  has been previously shown to play a role in insulin-TOR signaling downstream of S6K (44). The RNA-seq analysis also identified *tribbles* (*trbl*), which encodes a Trib kinase previously shown to modulate Akt-mediated insulin signaling through S6K and PPAR $\gamma$  (46).

## Functional Validation of Candidate Genes

We employed targeted RNA interference (RNAi) using the GAL4/UAS system to knock down gene expression

to test the role of the candidate genes identified in our analyses above. We targeted the expression of select RNAi constructs first pan-neuronally, using the elav-GAL4 driver (**Supplementary Figure 2**), and then in a more targeted manner using the dopamine neuron-specific TH-GAL4 driver (**Figure 4B**). Knockdown of several candidate genes, especially ribosomal proteins, was lethal when either GAL4 driver was utilized, precluding us from validating the role of these genes in the behavioral response to AMPH. For those that survived, knockdown of *Rpl8* significantly enhanced the response to 5mM AMPH, whereas knockdown of *Rps26* had no effect. Knockdown of *S6K* led to a dramatic increase in AMPH-induced hyperactivity, using either GAL4 driver and at each AMPH concentration tested, suggesting that the gene plays a critical role in modulating the sensitivity to AMPH in general, and in dopamine neurons in particular (**Figure 4B**, **Supplementary Figure 2**). Similarly, knockdown of *Thor* (4E-BP), *hppy* (MAP43K), *Eip75B* (PPAR $\gamma$ ), *srl* (PGC-1 $\alpha$ ), or *trbl* significantly enhanced the response to AMPH (**Figure 4B**, **Supplementary Figure 2**). These findings suggest a specific role for the S6K signaling pathway in dopamine neurons in modulating the initial sensitivity to AMPH and also point to a potential role for the insulin signaling pathway in regulating this process.



## DISCUSSION

Understanding the genetic and molecular mechanisms underlying behavioral disorders, such as substance use and abuse, is critical for developing targeted therapeutic strategies to treat these disorders. Next-generation sequencing has greatly facilitated transcriptomic and genomic analyses, thereby allowing for unbiased approaches to identifying novel genes and gene pathways that mediate the actions of drugs of abuse. However, the direct functional implication of candidate genes remains challenging, especially in rodent models where *in vivo* gene validation can be costly and laborious. To effectively prioritize genes that modulate AMPH action, we analyzed the convergence of a combination of behavioral, transcriptomic, and genomic datasets, and followed up by high-throughput targeted validation in *Drosophila*.

Given that DAT is the principal molecular target of AMPH (4, 5), we first analyzed the transcriptional response to the psychostimulant in fly brains in the presence or absence of DAT. We focused on genes that are differentially regulated in response to the psychostimulant in a DAT-dependent manner,

as we hypothesize that they are mechanistically linked to the behavioral response to AMPH, which is also DAT-dependent. Using functional enrichment analysis, we found that the major affected process was the upregulation of genes that govern *de novo* mRNA translation. We then examined whether genes that display similar ontology are enriched in an independent GWAS dataset. This approach allowed us to prioritize GWAS hits that met the empirical threshold of  $p < 10^{-5}$  but fell short of meeting the more stringent Bonferroni significance. Consistent with the results of the RNA-seq analysis, we identified several genes encoding ribosomal proteins, in addition to several modulators of mRNA translation. By exploring the functional convergence between transcriptomic and genomic data, we were able to identify genes that confer AMPH sensitivity via mechanisms downstream of the transcriptional response to the drug. The existence of such convergence suggests that the underlying genetic architecture can have a significant impact on signaling pathways triggered by drug exposure. Other functional themes identified by our GWAS include neurodevelopment, cell adhesion, and control of locomotion and sleep, among others (Williams et al., *ibid*).

Taking advantage of the high-throughput gene targeting tools available in *Drosophila*, we validated the role of several of these genes, including the fly homologs of S6K and 4E-BP, which are direct targets of the mammalian Target of Rapamycin in Complex 1 (mTORC1). Remarkably, even though we measured transcripts from whole heads, we were able to identify genes that regulate AMPH sensitivity specifically in dopamine neurons, which represent a tiny fraction of neurons in the central nervous system. We believe that this success in identifying genes that are critical to the dopaminergic response to AMPH was facilitated by our prioritizing DAT-dependent transcriptional changes. The classification of DAT-dependent vs. DAT-independent transcriptional changes is imperfect, given the compensatory changes associated with the mutant and time course of drug action. This is in part supported by our findings that pan-neuronal knockdown of some of the candidate genes leads to an even more enhanced AMPH response compared to dopamine neuron-specific knockdown, suggesting a role for these genes in neurons pre- and/or postsynaptic to dopamine neurons, or in other neuronal circuits altogether. Nonetheless, we believe that this initial prioritization helped focus our subsequent functional analyses and validation to identify gene pathways in dopamine neurons that modulate the response to AMPH's actions at DAT. Future studies will be needed to explore the role of these pathways in other neuronal populations.

In recent years, a wealth of data has implicated the kinase mTORC1 (mammalian/mechanistic Target of Rapamycin in Complex 1) as an essential mediator of protein synthesis (47), including dendritic translation of synaptic proteins (48, 49). In this role, mTORC1 is known to promote neuroadaptations in response to key signaling events, such as those that are induced by drugs of abuse (12, 13, 50). mTORC1 targets S6K and 4E-BP (51), candidate genes we identified that are critical for the initiation and elongation of mRNA translation. Our data further showed that targeted RNAi knockdown of either protein in dopamine neurons dramatically enhanced the response to AMPH. More work needs to be done to explicate the mechanisms underlying the roles of these genes in AMPH sensitivity. It would be particularly interesting to perform cell-specific ribosome profiling (52) in order to delineate the translational network activated in response to AMPH in dopamine neurons, as well as other neuronal subtypes, to begin to understand the link between the observed transcriptional changes and behavioral phenotype.

Previous studies have implicated mTOR signaling in the actions of psychostimulants, but these mostly focused on pharmacological inhibition or genetic knockdown or deletion of *mTORC1* and downstream effectors in adulthood, which attenuated psychostimulant-induced reward and reinforcement behavior (53–58). Notably, our knockdown approach targets candidate genes early during development. Thus, one possible explanation for the different results is that S6K signaling plays a role in the neurodevelopment of dopamine neurons in ways that influences the response to AMPH later in life, and that this role may be distinct from its function in the acute response to AMPH in adulthood. Consistent with this hypothesis, our data also

showed that dopamine neuron-specific knockdown of *srl* (dPGC-1) (44) and its coactivator *Eip75b* (dPPAR $\gamma$ ) (45), transcriptional regulators that act downstream of the insulin/Akt/TOR pathway (44), enhanced the response to AMPH. PGC-1 and PPAR $\gamma$  have been studied as therapeutic targets in Parkinson's disease (59, 60) and have been shown to confer neuroprotective effects in dopamine neurons (61). Interestingly, the Trib kinase encoded by the candidate gene *trbl* has been shown to modulate Akt-mediated insulin signaling through S6K and PPAR $\gamma$  (46). In light of a series of studies implicating insulin as a regulator of dopamine uptake and release (62–64), our data suggest a working model in which insulin signaling in dopamine neurons acts through S6K during neurodevelopment to modulate AMPH sensitivity, possibly by altering the functional expression of DAT, its dopamine reuptake capacity, or its ability to efflux dopamine in response to AMPH. This is also consistent with a study showing that insulin promotes dopamine neuron differentiation through PI3K/Akt/mTOR-dependent S6K signaling in human neural stem cells (65). Further studies will be needed to test this hypothesis, using tools readily available in flies for temporal control of gene knockdown (66), which would enable comparison of the effect of knockdown during development to knockdown in adulthood. It will also be interesting to explore whether the genes identified effect changes in AMPH sensitivity by modulating autophagy, another major cellular process controlled by mTOR (50). Previous studies have shown that inhibition of mTOR induces formation of autophagic vacuoles in presynaptic dopamine terminals, leading to decreased size of axonal profiles, synaptic vesicle numbers, and evoked dopamine release (67). Several studies have also shown that autophagy mediates psychostimulant-induced neurotoxicity (68–70). More recently, a study showed that low, non-toxic levels of cocaine also induce neuronal autophagy *in vitro* and *in vivo*, and that inhibitors of autophagy blunt conditioned place preference in mice (71). Interestingly, cocaine-induced autophagy was also shown to induce DAT degradation in the nucleus accumbens of mice, and it would be interesting to determine if mTOR is linked mechanistically to this process as well (71).

Taken together, our data demonstrate the power of *Drosophila* as a genetic model that facilitates high-throughput behavioral screens, combined with GWAS and whole transcriptome sequencing, to identify, prioritize, and validate candidate genes that can be subsequently evaluated in rodent models of self-administration.

## MATERIALS AND METHODS

### Fly Stocks and Transgenic *Drosophila* Lines

All fly strains were reared on a standard corn meal, yeast, molasses, and agar medium at 25°C and 45–47% humidity under a 12:12 h light:dark cycle. An isogenic *w*<sup>1118</sup> fly strain (Exelixis strain A5001, BL-6326) was used as the control. The *DAT* mutants (*dDAT*<sup>f<sup>mn</sup></sup>) were a gift from Dr. K. Kume (Kumamoto, Japan) (29) and were back-crossed to the *w*<sup>1118</sup> isogenic strain for 7 generations. These mutants have the 5' portion of a roo

transposon inserted into intron 6 of the *dDAT* gene resulting in an in-frame stop codon (29). All RNAi lines were driven by the TH-GAL4 driver (72), a gift from Dr. S. Birman (Paris, France). Transgenic RNAi strains were obtained from Bloomington Stock Center (Stocks: GFP RNAi #9330, Rpl8 RNAi #50610, Rps26 RNAi #33393, S6K RNAi #42572, Thor RNAi #80427, trbl RNAi #60007, hppy RNAi #53884, srl RNAi #33915, Eip75B RNAi #35780, Sm RNAi #64524).

## Behavioral Assay

Flies were aged for 7 days after eclosion, housed in vials containing standard medium, and entrained to a 12:12 h light:dark regime under rearing conditions. Individual aged male flies were then anesthetized briefly with CO<sub>2</sub> and placed in polycarbonate tubes containing food consisting of 1% agar and 3% sucrose delivered in water (vehicle) or AMPH solution (10 mM) (Sigma, A5880). Flies were continuously monitored for movement by four infrared beams evenly distributed across the tube using Trikinetics *Drosophila* Activity Monitors (TriKinetics, Waltham, MA). Locomotor activity was measured by recording infrared beam crossings (activity counts) by individual flies totaled in 2 min bins. All experiments were carried out in a designated behavior room under LD conditions at 25°C and ~45–50% humidity with *ad libitum* access to food (Vehicle or AMPH). Animals that died within the first 12 h of the experiment were excluded from the analysis.

Output files were analyzed in R using the previously published Rethomics framework (73). The mean activity was calculated by binning activity counts over 60 min and averaging across the first night of recording (0–12 h) for each individual animal.

Bar graphs were generated using ggplot2 (36, 74) and represent the change in response to AMPH for each group. Error bars indicate SEM. When the assumption of homogeneity of variance for the data was not met, statistical significance was determined by Kruskal-Wallis ANOVA. Asterisks indicate pairwise significance compared to genotype control after AMPH treatment, as determined by *post-hoc* Dunn's Test with a Benjamini-Hochberg correction for multiple testing, \*\*\*\**p*.adj < 0.0001, \*\*\**p*.adj < 0.001, \*\**p*.adj < 0.01, \**p*.adj < 0.05.

## RNA-Seq

PolyA+ selected libraries were produced from individual whole *Drosophila* brains (4 heads per group). Specifically, total RNA was prepared using the RNAqueous-Micro kit (Ambion) followed by polyA+ mRNA isolation with the Dynabeads mRNA DIRECT Micro kit (Ambion) according to the manufacturer's protocols. Barcoded libraries (Ion XpressRNA) were made using the Ion Total RNA-Seq Kit v2 (Fisher Scientific), PCR-amplified, and quantified with Agilent Bioanalyzer (Agilent). The resulting libraries were pooled and sequenced on the Ion OneTouch 2 System using P1.1.17 chips and Ion HiQ chemistry. Data was collected with Ion Suite (version 4.4.3. 1). Reads were mapped to UCSC dm3 reference genome with tmap-f3 in Torrent Suite (v4.4.3). The raw and processed RNA-Seq data were submitted to

the NCBI Gene Expression Omnibus with the Accession Number GSE196162.

## Differential Gene Expression Analysis

Differential gene expression analysis based on the negative binomial distribution model was performed using the DESeq2 R package (33). In this analysis, we first found the differential expression in each AMPH treatment group (namely, the isogenic *w<sup>1118</sup>* flies (WT) and *DAT* mutant flies) against their respective untreated controls. The differentially expressed genes in each comparison were selected at the adjusted *p*-value (Benjamini and Hochberg) of <0.1, followed by the analysis of similarities between the resulting gene lists.

## Gene Ontology (GO) and Functional Enrichment Analysis

Functional classification of candidate genes was performed using established GO terms and canonical pathways available in the Database for Annotation, Visualization and Integrated Discovery (DAVID) (35). Enrichment in functional GO categories and pathways (from the annotated pathway collections and tools such as KEGG and GO BP terms) was assessed using Fisher's exact and hypergeometric tests available through DAVID. Genetic and physical interactions between candidate genes were identified and graphed using the esyN webtool (which uses the Flybase Gene Report and Flybase Interaction Report to identify functional gene networks) (75), and by mining the literature for functional interaction between mammalian homologs of candidate genes.

## DATA AVAILABILITY STATEMENT

The original contributions presented in the study are publicly available. This data can be found here: <https://www.ncbi.nlm.nih.gov/>, accession: GSE196162.

## AUTHOR CONTRIBUTIONS

CK, SK, CH, DG, and JJ designed the experiments. SK designed data analysis tools for functional enrichment analysis. CK, BW, RP, and YZ performed the experiments. CK, BW, IM, QY, SK, and CH contributed analysis tools and performed data analysis. CK, BW, IM, SK, and JJ discussed the results and interpretation of the data and wrote the manuscript. All authors contributed to the article and approved the submitted version.

## FUNDING

This work was supported by U01 DA042233 (CK, BW, YZ, and JJ), a Seed Grant from the Columbia University Data Science Institute (SK and IM), and the Intramural Research Program of the National Institute on Alcohol Abuse and Alcoholism (RP, QY, CH, and DG).

## ACKNOWLEDGMENTS

We thank Dr. Trudy Mackay, Dr. Robert Anholt, and Dr. Wen Huang for helpful discussion and access to analysis tools, including the DGRP GWAS webtool.

## SUPPLEMENTARY MATERIAL

The Supplementary Material for this article can be found online at: <https://www.frontiersin.org/articles/10.3389/fpsy.2022.831597/full#supplementary-material>

**Supplementary Figure 1** | Prevalent Biological Process categories (GO BP terms) and KEGG pathways (dme term) enriched in genes differentially expressed in WT AMPH response. **(A)** Downregulated genes; **(B)** upregulated genes. All enriched functional annotation terms were selected at the  $p$ -value threshold below 0.05 and sorted in increasing order from left to right in the diagrams; **(C)** terms enriched with downregulated genes, which are also downregulated in the *DAT* mutant; **(D)** terms enriched with upregulated genes, which are also upregulated in the *DAT* mutant strain. These genes are red in **Figures 2A,B**. As before, all enriched functional annotation terms were selected at the  $p$ -value threshold below 0.05 and sorted in increasing order from left to right in the diagrams; **(E)** terms enriched with downregulated genes, which are not differentially expressed in the *DAT* mutant; **(F)** Terms enriched with upregulated genes, which are not differentially expressed in the *DAT* mutant. These genes are blue in **Figures 2A,B**. As before, all enriched functional annotation terms were selected at the  $p$ -value

threshold below 0.05 and sorted in increasing order from left to right in the diagrams.

**Supplementary Figure 2** | RNAi-mediated knockdown of candidate genes was targeted to all neurons using elav-GAL4. Bar graphs depict change in activity in response to 5 mM AMPH (blue) or 10 mM AMPH (yellow). Error bars indicate SEM. Statistical significance was determined by Kruskal-Wallis ANOVA ( $p < 2e-16$ ). Asterisks indicate pairwise significance compared to genotype control after AMPH treatment, as determined by *post-hoc* Dunn's Test with a Benjamini-Hochberg correction for multiple testing, \*\*\*\* $p$ .adj < 0.0001, \*\*\* $p$ .adj < 0.001, \*\* $p$ .adj < 0.01, \* $p$ .adj < 0.05.

**Supplementary Table 1** | List of transcripts differentially expressed in response to AMPH in WT and in *DAT* mutant.

**Supplementary Table 2** | GO terms and functional enrichment analysis for *DAT*-independent genes. **DATindependent** is the list of DE genes common between WT and *DAT* mutant; **up** and **dn** list the FBtr recognized by DAVID for up- and downregulated genes; **upANNO** and **dnANNO** contain all significant annotations ( $p < 0.1$ ) in all functional databases used in DAVID.

**Supplementary Table 3** | GO terms and functional enrichment analysis for *DAT*-dependent genes. **DATdependent** is the list of DE genes unique to WT; **up** and **dn** list the FBtr recognized by DAVID for up- and downregulated genes; **upANNO** and **dnANNO** contain all significant annotations ( $p < 0.1$ ) in all functional databases used in DAVID. Several functionally related categories share common genes, e.g., GO: 0006413~translational initiation; GO: 0001731~formation of translation preinitiation complex; GO: 0005852~eukaryotic translation initiation factor 3 complex. There are no shared genes for unrelated functional categories.

## REFERENCES

- Vearrier D, Greenberg MI, Miller SN, Okaneku JT, Haggerty DA. Methamphetamine: history, pathophysiology, adverse health effects, current trends, and hazards associated with the clandestine manufacture of methamphetamine. *Dis Mon.* (2012) 58:38–89. doi: 10.1016/j.disamonth.2011.09.004
- Heal DJ, Smith SL, Gosden J, Nutt DJ. Amphetamine, past and present—a pharmacological and clinical perspective. *J Psychopharmacol.* (2013) 27:479–96. doi: 10.1177/0269881113482532
- Spiller HA, Hays HL, Aleguas A. Overdose of drugs for attention-deficit hyperactivity disorder: clinical presentation, mechanisms of toxicity, and management. *CNS Drugs.* (2013) 27:531–43. doi: 10.1007/s40263-013-0084-8
- Sulzer D. How addictive drugs disrupt presynaptic dopamine neurotransmission. *Neuron.* (2011) 69:628–49. doi: 10.1016/j.neuron.2011.02.010
- Sulzer D, Sonders MS, Poulsen NW, Galli A. Mechanisms of neurotransmitter release by amphetamines: a review. *Prog Neurobiol.* (2005) 75:406–33. doi: 10.1016/j.pneurobio.2005.04.003
- Reith MEA, Ngegy ME. Molecular mechanisms of amphetamines. *Handb Exp Pharmacol.* (2020) 258:265–97. doi: 10.1007/164\_2019\_251
- Freyberg Z, Sonders MS, Aguilar JJ, Hiranita T, Karam CS, Flores J, et al. Mechanisms of amphetamine action illuminated through optical monitoring of dopamine synaptic vesicles in *Drosophila* brain. *Nat Commun.* (2016) 7:10652. doi: 10.1038/ncomms10652
- Karam CS, Javitch JA. Phosphorylation of the amino terminus of the dopamine transporter: regulatory mechanisms and implications for amphetamine action. *Adv Pharmacol.* (2018) 82:205–34. doi: 10.1016/bs.apha.2017.09.002
- Gipson CD, Kupchik YM, Kalivas PW. Rapid, transient synaptic plasticity in addiction. *Neuropharmacology.* (2014) 76(Pt B):276–86. doi: 10.1016/j.neuropharm.2013.04.032
- Kalivas PW, O'Brien C. Drug addiction as a pathology of staged neuroplasticity. *Neuropsychopharmacology.* (2008) 33:166–80. doi: 10.1038/sj.npp.1301564
- Madsen HB, Brown RM, Lawrence AJ. Neuroplasticity in addiction: cellular and transcriptional perspectives. *Front Mol Neurosci.* (2012) 5:99. doi: 10.3389/fnmol.2012.00099
- Dayas CV, Smith DW, Dunkley PR. An emerging role for the Mammalian target of rapamycin in “pathological” protein translation: relevance to cocaine addiction. *Front Pharmacol.* (2012) 3:13. doi: 10.3389/fphar.2012.00013
- Neasta J, Barak S, Hamida SB, Ron D. mTOR complex 1: a key player in neuroadaptations induced by drugs of abuse. *J Neurochem.* (2014) 130:172–84. doi: 10.1111/jnc.12725
- McClung CA, Nestler EJ. Neuroplasticity mediated by altered gene expression. *Neuropsychopharmacology.* (2008) 33:3–17. doi: 10.1038/sj.npp.1301544
- Agrawal A, Verweij KJH, Gillespie NA, Heath AC, Lessov-Schlaggar CN, Martin NG, et al. The genetics of addiction—a translational perspective. *Transl Psychiatry.* (2012) 2:e140. doi: 10.1038/tp.2012.54
- Kaun KR, Devineni AV, Heberlein U. *Drosophila melanogaster* as a model to study drug addiction. *Hum Genet.* (2012) 131:959–75. doi: 10.1007/s00439-012-1146-6
- Klee EW, Schneider H, Clark KJ, Cousin MA, Ebbert JO, Hooten WM, et al. Zebrafish: a model for the study of addiction genetics. *Hum Genet.* (2012) 131:977–1008. doi: 10.1007/s00439-011-1128-0
- Cates HM, Benca-Bachman CE, de Guglielmo G, Schoenrock SA, Shu C, Kallupi M. National Institute on Drug Abuse genomics consortium white paper: coordinating efforts between human and animal addiction studies. *Genes Brain Behav.* (2019) 18:e12577. doi: 10.1111/gbb.12577
- Hart AB, de Wit H, Palmer AA. Genetic factors modulating the response to stimulant drugs in humans. *Curr Top Behav Neurosci.* (2012) 12:537–77. doi: 10.1007/7854\_2011\_187
- Gabbay FH. Variations in affect following amphetamine and placebo: markers of stimulant drug preference. *Exp Clin Psychopharmacol.* (2003) 11:91–101. doi: 10.1037//1064-1297.11.1.91
- de Wit H, Uhlhuth EH, Johanson CE. Individual differences in the reinforcing and subjective effects of amphetamine and diazepam. *Drug Alcohol Depend.* (1986) 16:341–60. doi: 10.1016/0376-8716(86)90068-2
- Haertzen CA, Kocher TR, Miyasato K. Reinforcements from the first drug experience can predict later drug habits and/or addiction: results with coffee, cigarettes, alcohol, barbiturates, minor and major tranquilizers, stimulants, marijuana, hallucinogens, heroin, opiates and cocaine. *Drug Alcohol Depend.* (1983) 11:147–65. doi: 10.1016/0376-8716(83)90076-5
- Davidson ES, Finch JF, Schenk S. Variability in subjective responses to cocaine: initial experiences of college students. *Addict Behav.* (1993) 18:445–53. doi: 10.1016/0306-4603(93)90062-e

24. Phillips TJ, Kamens HM, Wheeler JM. Behavioral genetic contributions to the study of addiction-related amphetamine effects. *Neurosci Biobehav Rev.* (2008) 32:707–59. doi: 10.1016/j.neubiorev.2007.10.008
25. Kamens HM, Burkhart-Kasch S, McKinnon CS, Li N, Reed C, Phillips TJ. Sensitivity to psychostimulants in mice bred for high and low stimulation to methamphetamine. *Genes Brain Behav.* (2005) 4:110–25. doi: 10.1111/j.1601-183X.2004.00101.x
26. Palmer AA, Verbitsky M, Suresh R, Kamens HM, Reed CL, Li N, et al. Gene expression differences in mice divergently selected for methamphetamine sensitivity. *Mamm Genome.* (2005) 16:291–305. doi: 10.1007/s00335-004-2451-8
27. Karam CS, Williams BL, Jones SK, Javitch JA. The role of the dopamine transporter in the effects of amphetamine on sleep and sleep architecture in *Drosophila*. *Neurochem Res.* (2021) 47. doi: 10.1007/s11064-021-03275-4
28. Pizzo AB, Karam CS, Zhang Y, Yano H, Freyberg RJ, Karam DS, et al. The membrane raft protein Flotillin-1 is essential in dopamine neurons for amphetamine-induced behavior in *Drosophila*. *Mol Psychiatry.* (2013) 18:824–33. doi: 10.1038/mp.2012.82
29. Kume K, Kume S, Park SK, Hirsh J, Jackson FR. Dopamine is a regulator of arousal in the fruit fly. *J Neurosci.* (2005) 25:7377–84. doi: 10.1523/JNEUROSCI.2048-05.2005
30. Mackay TFC, Richards S, Stone EA, Barbadilla A, Ayroles JF, Zhu D, et al. The *Drosophila melanogaster* genetic reference panel. *Nature.* (2012) 482:173–8. doi: 10.1038/nature10811
31. Heigwer F, Port F, Boutros M. RNA interference (RNAi) screening in *Drosophila*. *Genetics.* (2018) 208:853–74. doi: 10.1534/genetics.117.300077
32. Duffy JB. GAL4 system in *Drosophila*: a fly geneticist's Swiss army knife. *Genesis.* (2002) 34:1–15. doi: 10.1002/gene.10150
33. Love MI, Huber W, Anders S. Moderated estimation of fold change and dispersion for RNA-seq data with DESeq2. *Genome Biol.* (2014) 15:550. doi: 10.1186/s13059-014-0550-8
34. Sora I, Li B, Fumushima S, Fukui A, Arime Y, Kasahara Y, et al. Monoamine transporter as a target molecule for psychostimulants. In: Bagetta GM, Corasaniti TT, Sakurada T, Sakurada S, editors. *International Review of Neurobiology*. Elsevier (2009). p. 29–33.
35. Huang DW, Sherman BT, Lempicki RA. Systematic and integrative analysis of large gene lists using DAVID bioinformatics resources. *Nat Protoc.* (2009) 4:44–57. doi: 10.1038/nprot.2008.211
36. Kassambara A. *ggpubr: "ggplot2" Based Publication Ready Plots*. CRAN (2020).
37. Jitcá G, Osz BE, Tero-Vescan A, Vari CE. Psychoactive drugs-from chemical structure to oxidative stress related to dopaminergic neurotransmission. A review. *Antioxidants.* (2021) 10:1–26. doi: 10.3390/antiox10030381
38. Anholt RRH, Mackay TFC. The road less traveled: from genotype to phenotype in flies and humans. *Mamm Genome.* (2018) 29:5–23. doi: 10.1007/s00335-017-9722-7
39. Polymenis M. Ribosomal proteins: mutant phenotypes by the numbers and associated gene expression changes. *Open Biol.* (2020) 10:200114. doi: 10.1098/rsob.200114
40. Piccolo LL, Corona D, Onorati MC. Emerging roles for hnRNPs in post-transcriptional regulation: what can we learn from flies? *Chromosoma.* (2014) 123:515–27. doi: 10.1007/s00412-014-0470-0
41. Bryk B, Hahn K, Cohen SM, Teleman AA. MAP4K3 regulates body size and metabolism in *Drosophila*. *Dev Biol.* (2010) 344:150–7. doi: 10.1016/j.ydbio.2010.04.027
42. Miron M, Lasko P, Sonenberg N. Signaling from Akt to FRAP/TOR targets both 4E-BP and S6K in *Drosophila melanogaster*. *Mol Cell Biol.* (2003) 23:9117–26. doi: 10.1128/MCB.23.24.9117-9126.2003
43. Bernal A, Kimbrell DA. *Drosophila* Thor participates in host immune defense and connects a translational regulator with innate immunity. *Proc Natl Acad Sci USA.* (2000) 97:6019–24. doi: 10.1073/pnas.100391597
44. Mukherjee S, Duttaroy A. Spargel/dPGC-1 is a new downstream effector in the insulin-TOR signaling pathway in *Drosophila*. *Genetics.* (2013) 195:433–41. doi: 10.1534/genetics.113.154583
45. Zipper L, Jassmann D, Burgmer S, Görlich B, Reiff T. Ecdysone steroid hormone remote controls intestinal stem cell fate decisions via the PPAR $\gamma$ -homolog Eip75B in *Drosophila*. *Elife.* (2020) 9:1–27. doi: 10.7554/eLife.55795
46. Weismann D, Erion DM, Ignatova-Todorova I, Nagai Y, Stark R, Hsiao JJ, et al. Knockdown of the gene encoding *Drosophila* tribbles homologue 3 (Trib3) improves insulin sensitivity through peroxisome proliferator-activated receptor- $\gamma$  (PPAR- $\gamma$ ) activation in a rat model of insulin resistance. *Diabetologia.* (2011) 54:935–44. doi: 10.1007/s00125-010-1984-5
47. Ma XM, Blenis J. Molecular mechanisms of mTOR-mediated translational control. *Nat Rev Mol Cell Biol.* (2009) 10:307–18. doi: 10.1038/nrm2672
48. Costa-Mattioli M, Sossin WS, Klann E, Sonenberg N. Translational control of long-lasting synaptic plasticity and memory. *Neuron.* (2009) 61:10–26. doi: 10.1016/j.neuron.2008.10.055
49. Liu-Yesucevitz L, Bassell GJ, Gitler AD, Hart AC, Klann E, Richter JD, et al. Local RNA translation at the synapse and in disease. *J Neurosci.* (2011) 31:16086–93. doi: 10.1523/JNEUROSCI.4105-11.2011
50. Costa-Mattioli M, Monteggia LM. mTOR complexes in neurodevelopmental and neuropsychiatric disorders. *Nat Neurosci.* (2013) 16:1537–43. doi: 10.1038/nn.3546
51. Biever A, Valjent E, Puighermanal E. Ribosomal protein S6 phosphorylation in the nervous system: from regulation to function. *Front Mol Neurosci.* (2015) 8:75. doi: 10.3389/fnmol.2015.00075
52. Ingolia NT. Ribosome profiling: new views of translation, from single codons to genome scale. *Nat Rev Genet.* (2014) 15:205–13. doi: 10.1038/nrg3645
53. Huang S-H, Wu W-R, Lee L-M, Huang P-R, Chen J-C. mTOR signaling in the nucleus accumbens mediates behavioral sensitization to methamphetamine. *Prog Neuropsychopharmacol Biol Psychiatry.* (2018) 86:331–9. doi: 10.1016/j.pnpbp.2018.03.017
54. Ucha M, Roura-Martínez D, Ambrosio E, Higuera-Matas A. The role of the mTOR pathway in models of drug-induced reward and the behavioural constituents of addiction. *J Psychopharmacol.* (2020) 34:1176–99. doi: 10.1177/0269881120944159
55. Liu X, Li Y, Yu L, Vickstrom CR, Liu Q-S. VTA mTOR signaling regulates dopamine dynamics, cocaine-induced synaptic alterations, and reward. *Neuropsychopharmacology.* (2018) 43:1066–77. doi: 10.1038/npp.2017.247
56. Bailey J, Ma D, Szumlanski KK. Rapamycin attenuates the expression of cocaine-induced place preference and behavioral sensitization. *Addict Biol.* (2012) 17:248–58. doi: 10.1111/j.1369-1600.2010.00311.x
57. Wang X, Luo Y, He Y, Li F, Shi H, Xue L, et al. Nucleus accumbens core mammalian target of rapamycin signaling pathway is critical for cue-induced reinstatement of cocaine seeking in rats. *J Neurosci.* (2010) 30:12632–41. doi: 10.1523/JNEUROSCI.1264-10.2010
58. Wu J, McCallum SE, Glick SD, Huang Y. Inhibition of the mammalian target of rapamycin pathway by rapamycin blocks cocaine-induced locomotor sensitization. *Neuroscience.* (2011) 172:104–9. doi: 10.1016/j.neuroscience.2010.10.041
59. Le Foll B, Di Ciano P, Panlilio LV, Goldberg SR, Ciccocioppo R. Peroxisome proliferator-activated receptor (PPAR) agonists as promising new medications for drug addiction: preclinical evidence. *Curr Drug Targets.* (2013) 14:768–76. doi: 10.2174/1389450111314070006
60. Soyak SM, Zara G, Ferger B, Felder TK, Kwik M, Nofziger C, et al. The PPARGC1A locus and CNS-specific PGC-1 $\alpha$  isoforms are associated with Parkinson's disease. *Neurobiol Dis.* (2019) 121:34–46. doi: 10.1016/j.nbd.2018.09.016
61. Lucas EK, Dougherty SE, McMeekin LJ, Trinh AT, Reid CS, Cowell RM. Developmental alterations in motor coordination and medium spiny neuron markers in mice lacking pgc-1 $\alpha$ . *PLoS ONE.* (2012) 7:e42878. doi: 10.1371/journal.pone.0042878
62. Lute BJ, Khoshbouei H, Saunders C, Sen N, Lin RZ, Javitch JA, et al. PI3K signaling supports amphetamine-induced dopamine efflux. *Biochem Biophys Res Commun.* (2008) 372:656–61. doi: 10.1016/j.bbrc.2008.05.091
63. Williams JM, Owens WA, Turner GH, Saunders C, Dipace C, Blakely RD, et al. Hypoinsulinemia regulates amphetamine-induced reverse transport of dopamine. *PLoS Biol.* (2007) 5:e274. doi: 10.1371/journal.pbio.0050274
64. Owens WA, Sevak RJ, Galici R, Chang X, Javors MA, Galli A, et al. Deficits in dopamine clearance and locomotion in hypoinsulinemic rats unmask novel modulation of dopamine transporters by amphetamine. *J Neurochem.* (2005) 94:1402–10. doi: 10.1111/j.1471-4159.2005.03289.x
65. Lee JE, Lim MS, Park JH, Park CH, Koh H, Koh HC. S6K promotes dopaminergic neuronal differentiation through PI3K/Akt/mTOR-dependent signaling

- pathways in human neural stem cells. *Mol Neurobiol.* (2016) 53:3771–82. doi: 10.1007/s12035-015-9325-9
66. Suster ML, Seugnet L, Bate M, Sokolowski MB. Refining GAL4-driven transgene expression in *Drosophila* with a GAL80 enhancer-trap. *Genesis.* (2004) 39:240–5. doi: 10.1002/gene.20051
  67. Hernandez D, Torres CA, Setlik W, Cebrián C, Mosharov EV, Tang G, et al. Regulation of presynaptic neurotransmission by macroautophagy. *Neuron.* (2012) 74:277–84. doi: 10.1016/j.neuron.2012.02.020
  68. Valente MJ, Amaral C, Correia-da-Silva G, Duarte JA, Bastos M de L, Carvalho F, et al. Methylone and MDPV activate autophagy in human dopaminergic SH-SY5Y cells: a new insight into the context of  $\beta$ -keto amphetamines-related neurotoxicity. *Arch Toxicol.* (2017) 91:3663–76. doi: 10.1007/s00204-017-1984-z
  69. Mercer LD, Higgins GC, Lau CL, Lawrence AJ, Beart PM. MDMA-induced neurotoxicity of serotonin neurons involves autophagy and rilmenidine is protective against its pathobiology. *Neurochem Int.* (2017) 105:80–90. doi: 10.1016/j.neuint.2017.01.010
  70. Larsen KE, Fon EA, Hastings TG, Edwards RH, Sulzer D. Methamphetamine-induced degeneration of dopaminergic neurons involves autophagy and upregulation of dopamine synthesis. *J Neurosci.* (2002) 22:8951–60. doi: 10.1523/JNEUROSCI.22-20-08951.200
  71. Harraz MM, Guha P, Kang IG, Semenza ER, Malla AP, Song YJ, et al. Cocaine-induced locomotor stimulation involves autophagic degradation of the dopamine transporter. *Mol Psychiatry.* (2021) 26:370–82. doi: 10.1038/s41380-020-00978-y
  72. Friggi-Grelín F, Coulom H, Meller M, Gomez D, Hirsh J, Birman S. Targeted gene expression in *Drosophila* dopaminergic cells using regulatory sequences from tyrosine hydroxylase. *J Neurobiol.* (2003) 54:618–27. doi: 10.1002/neu.10185
  73. Geissmann Q, Garcia Rodriguez L, Beckwith EJ, Gilestro GF. Rethomics: an R framework to analyse high-throughput behavioural data. *PLoS ONE.* (2019) 14:e0209331. doi: 10.1371/journal.pone.0209331
  74. Wickham H. ggplot2. *WIREs Comp Stat.* (2011) 3:180–5. doi: 10.1002/wics.147
  75. Bean DM, Heimbach J, Ficorella L, Micklem G, Oliver SG, Favrin G. esyN: network building, sharing and publishing. *PLoS ONE.* (2014) 9:e106035. doi: 10.1371/journal.pone.0106035

**Conflict of Interest:** The authors declare that the research was conducted in the absence of any commercial or financial relationships that could be construed as a potential conflict of interest.

**Publisher's Note:** All claims expressed in this article are solely those of the authors and do not necessarily represent those of their affiliated organizations, or those of the publisher, the editors and the reviewers. Any product that may be evaluated in this article, or claim that may be made by its manufacturer, is not guaranteed or endorsed by the publisher.

Copyright © 2022 Karam, Williams, Morozova, Yuan, Panarsky, Zhang, Hodgkinson, Goldman, Kalachikov and Javitch. This is an open-access article distributed under the terms of the Creative Commons Attribution License (CC BY). The use, distribution or reproduction in other forums is permitted, provided the original author(s) and the copyright owner(s) are credited and that the original publication in this journal is cited, in accordance with accepted academic practice. No use, distribution or reproduction is permitted which does not comply with these terms.



# Beyond Genes: Inclusion of Alternative Splicing and Alternative Polyadenylation to Assess the Genetic Architecture of Predisposition to Voluntary Alcohol Consumption in Brain of the HXB/BXH Recombinant Inbred Rat Panel

## OPEN ACCESS

### Edited by:

Hua Lou,  
Case Western Reserve University,  
United States

### Reviewed by:

Xusheng Wang,  
University of North Dakota,  
United States  
R. Dayne Mayfield,  
University of Texas at Austin,  
United States

### \*Correspondence:

Laura M. Saba  
laura.saba@cuanschutz.edu

### Specialty section:

This article was submitted to  
Neurogenomics,  
a section of the journal  
Frontiers in Genetics

**Received:** 23 November 2021

**Accepted:** 10 February 2022

**Published:** 15 March 2022

### Citation:

Lusk R, Hoffman PL, Mahaffey S,  
Rosean S, Smith H, Silhavy J,  
Pravenec M, Tabakoff B and Saba LM  
(2022) Beyond Genes: Inclusion of  
Alternative Splicing and Alternative  
Polyadenylation to Assess the Genetic  
Architecture of Predisposition to  
Voluntary Alcohol Consumption in  
Brain of the HXB/BXH Recombinant  
Inbred Rat Panel.  
Front. Genet. 13:821026.  
doi: 10.3389/fgene.2022.821026

Ryan Lusk<sup>1</sup>, Paula L. Hoffman<sup>2</sup>, Spencer Mahaffey<sup>1</sup>, Samuel Rosean<sup>1</sup>, Harry Smith<sup>1</sup>,  
Jan Silhavy<sup>3</sup>, Michal Pravenec<sup>3</sup>, Boris Tabakoff<sup>1</sup> and Laura M. Saba<sup>1\*</sup>

<sup>1</sup>Department of Pharmaceutical Sciences, University of Colorado Anschutz Medical Campus, Aurora, CO, United States,

<sup>2</sup>Department of Pharmacology, University of Colorado Anschutz Medical Campus, Aurora, CO, United States, <sup>3</sup>Institute of  
Physiology of the Czech Academy of Sciences, Prague, Czechia

Post transcriptional modifications of RNA are powerful mechanisms by which eukaryotes expand their genetic diversity. For instance, researchers estimate that most transcripts in humans undergo alternative splicing and alternative polyadenylation. These splicing events produce distinct RNA molecules, which in turn yield distinct protein isoforms and/or influence RNA stability, translation, nuclear export, and RNA/protein cellular localization. Due to their pervasiveness and impact, we hypothesized that alternative splicing and alternative polyadenylation in brain can contribute to a predisposition for voluntary alcohol consumption. Using the HXB/BXH recombinant inbred rat panel (a subset of the Hybrid Rat Diversity Panel), we generated over one terabyte of brain RNA sequencing data (total RNA) and identified novel splice variants (*via* StringTie) and alternative polyadenylation sites (*via* aptardi) to determine the transcriptional landscape in the brains of these animals. After establishing an analysis pipeline to ascertain high quality transcripts, we quantitated transcripts and integrated genotype data to identify candidate transcript coexpression networks and individual candidate transcripts associated with predisposition to voluntary alcohol consumption in the two-bottle choice paradigm. For genes that were previously associated with this trait (e.g., *Lrap*, *Ift81*, and *P2rx4*) (Saba et al., *Febs. J.*, 282, 3556–3578, Saba et al., *Genes. Brain. Behav.*, 20, e12698), we were able to distinguish between transcript variants to provide further information about the specific isoforms related to the trait. We also identified additional candidate transcripts associated with the trait of voluntary alcohol consumption (i.e., isoforms of *Mapkapk5*, *Aldh1a7*, and *Map3k7*). Consistent with our previous work, our results indicate that transcripts and networks related to inflammation and the immune system in brain can be linked to voluntary alcohol consumption. Overall, we have established a pipeline for including the quantitation of alternative splicing and alternative

polyadenylation variants in the transcriptome in the analysis of the relationship between the transcriptome and complex traits.

**Keywords:** HXB/BXH recombinant inbred panel, voluntary alcohol consumption, transcriptome, weighted gene co expression network analysis, alternative splicing, alternative polyadenylation, RNA-seq—RNA sequencing, isoform

## 1 INTRODUCTION

Post transcriptional phenomena are powerful mechanisms by which eukaryotes expand their genetic diversity. For instance, researchers estimate that 95–100% of multi-exon genes in human can undergo alternative splicing (Pan et al., 2008; Wang et al., 2008; Nilsen and Graveley, 2010). Likewise, an estimated 70% or more mammalian genes have multiple polyadenylation sites (Derti et al., 2012; Hoque et al., 2013) and can therefore express alternative polyadenylation isoforms. Biologically, alternative splicing of exons can lead to diverse functions (Garcia-Blanco et al., 2004) by changing the protein encoded by the mRNA (Kelemen et al., 2013). In contrast, the vast majority of alternative polyadenylation occurs in the 3' untranslated region (3' UTR) (Tian and Manley, 2017) and thus generates identical proteins. However, alternative polyadenylation profoundly impacts the mRNA by modifying its stability, translocation, nuclear export, and cellular localization, as well as the localization of the encoded protein (Yeh and Yong, 2016; Tian and Manley, 2017). Alternative polyadenylation most often exerts its effects through gain or loss of microRNA binding sites in the 3' UTR; more than 50% of conserved microRNA binding sites reside downstream of the most proximal polyadenylation site in mammalian genes (Ren et al., 2020).

Alternative splicing and alternative polyadenylation have increasingly been associated with disease. For example, alternative splicing has been recognized as a genetic modifier of disease phenotype (Garcia-Blanco et al., 2004) and susceptibility to disease (Wang and Cooper, 2007). Notably, alternative splicing has also been shown to impact the phenotypic variation of diseases, or in other words impact quantitative (complex) traits, via changes in the relative expression levels among different mRNA isoforms produced from the same gene (Nissim-Rafinia and Kerem, 2002). One example of the latter is the tau protein; exon 10 of this gene can be included or skipped, and dysregulation of the ratio between these two alternative splicing isoforms can lead to the development of inherited frontotemporal dementia and parkinsonism (Hong et al., 1998; Hutton et al., 1998; Spillantini et al., 1998). Furthermore, several other alternative splicing events have been linked to neurological diseases (Dredge et al., 2001).

Although alternative polyadenylation is a relatively new research area, it too has been associated with biological processes such as the innate antiviral immune response, cancer initiation and prognosis, and development of drug resistance (Ren et al., 2020). Alternative polyadenylation also affects brain function. For instance, the serotonin transporter has two 3' UTR alternative polyadenylation isoforms, the longer of which is implicated in anxiolytic effects (Hartley et al., 2012; Yoon

et al., 2013). The long 3' UTR isoform of the *alpha-synuclein* gene is associated with Parkinson's disease pathology (Rhinn et al., 2012), and a shift to increased usage of the long 3' UTR version of this gene has been shown in response to elevated cytoplasmic dopamine levels and other conditions causing oxidative stress (Miura et al., 2014). Only the long 3' UTR version was found to mediate translational upregulation of the BDNF protein, and modulation of activity-dependent neuronal signaling is thought to predispose individuals to many psychiatric disorders (Lau et al., 2010). Overall, differences in expression of alternative polyadenylation transcripts have been implicated in disease (Yoon et al., 2012) and alternative polyadenylation is increasingly being acknowledged as a risk factor for several complex traits (Manning and Cooper, 2017).

Importantly, these post-transcriptional modifications are dynamic. For example, alternative splicing patterns constantly change under specific physiological conditions (Kelemen et al., 2013) and are modulated according to cell type, developmental stage, sex, or in response to stimuli (Faustino and Cooper, 2003). Additionally, *in vivo* expression of alternative polyadenylation isoforms varies based on a myriad of factors such as tissue, physiological, and disease states (Di Giammartino et al., 2011; Sanfilippo et al., 2017) and displays tissue specificity (Beaudoing and Gautheret, 2001; Zhang et al., 2005). Of note, the brain expresses the greatest mRNA diversity compared to other tissues due to alternative splicing and alternative polyadenylation (MacDonald, 2019), and broad neural 3' UTR lengthening is ubiquitous in the adult mammalian brain (Miura et al., 2014).

However, reference annotation (especially for non-human organisms such as the rat) often lacks annotation of alternative splicing and alternative polyadenylation transcripts. Likewise, reference annotation, in general, represents data pooled from multiple tissues, experiments, etc., and thus may not accurately represent the transcriptome for a given organ or condition.

The objective in our present study was twofold: 1) characterize the alternative splicing and alternative polyadenylation landscape in brain of the HXB/BXH recombinant inbred (RI) rat panel, and 2) identify candidate RNA transcripts associated with the complex trait of voluntary alcohol (i.e., ethanol) consumption using both a network and individual transcript approach to better understand biological mechanisms related to why some animals drink more than others. Throughout this paper, we use the term “transcript” to refer to the sequence of a processed mature RNA and the term “gene” as the DNA locus that codes for a particular transcript or set of transcripts. In this context a single gene can produce many distinct transcripts through alternative splicing and alternative transcription start and stop sites (e.g., alternative polyadenylation).

Alcohol use disorder (AUD) and its endophenotypes, including alcohol consumption [an etiologic essential to the development of AUD (Grant et al., 2009; Dawson and Grant, 2011)], have a noteworthy genetic component (Verhulst et al., 2015). Yet much of the genetic architecture of alcohol related phenotypes remains unclear. Traditionally, scientists investigated the role of alternative splicing and alternative polyadenylation on alcohol related phenotypes by interrogating individual candidate genes. For example, studies on N-methyl-D-aspartate (NMDA) receptor found greater basal expression of a subunit splicing variant in alcohol non-preferring rats compared to alcohol preferring rats in the hippocampus (Winkler et al., 1999). Besides NMDA, alternative splicing of DRD2, GABA<sub>A</sub> receptor, ion channels, voltage-gated Ca<sup>2+</sup> channels, and neurexin-3, among others, have been linked to various alcohol related phenotypes (Sasabe and Ishiura, 2010). Recent advances in next generation sequencing and have allowed researchers to characterize alternative splicing and alternative polyadenylation across the entire transcriptome to increase our understanding of their roles. For instance, alcohol use disorder was associated with global changes in splicing (i.e., alternative splicing and alternative polyadenylation) in human brains and, furthermore, may be controlled by long non-coding RNAs that act as master regulators of splicing (Van Booven et al., 2021). Changes in expression of splice variants were linked to alcohol related associated learning in the brains of fruit flies, and knockdown of spliceosome-associated proteins prevent the formation of alcohol memories (Petrucelli et al., 2020). In addition, significant changes in alternative splicing were observed between alcohol- and control-exposed human fetal cortical samples (Kawasawa et al., 2017).

To accomplish our first goal, we utilized an extensive RNA expression database from whole brain samples of the HXB/BXH RI panel that consisted of over one terabyte of RNA sequencing (RNA-Seq) data. We then applied two computational methods, StringTie (Pertea et al., 2015) and aptardi (Lusk et al., 2021), to characterize *in vivo* expression of alternative splice variants and alternative polyadenylation in the brains of these animals. We furthermore developed a transcriptome reconstruction pipeline that integrates these tools (Pertea et al., 2015; Lusk et al., 2021) and also filters transcripts to eliminate potential false positives yielding high-quality transcriptome information.

To accomplish our second goal, we focused on examining the role of quantitative RNA expression levels as possible mediators of genetic determinants of alcohol consumption. We integrated RNA expression data with phenotypic data to identify candidate coexpression modules and individual candidate transcripts that are associated with a rat's predisposition to voluntarily consume more or less alcohol than other rats, i.e., RNA expression data were obtained from animals which were not tested for alcohol preference and the behavioral data was obtained from genetically identical rats (i.e., rats from the same inbred strain), as done in our prior work (Tabakoff et al., 2009; Saba et al., 2015; Harrall et al., 2016; Pravenec et al., 2018). Particularly, we had previously used whole brain RNA expression data and the identical phenotype of voluntary alcohol consumption to identify candidate gene coexpression modules associated with the

alcohol drinking phenotype (Saba et al., 2015). However, our earlier study utilized expression data obtained from microarrays and analysis was limited to genes and transcripts that were unambiguously probed by the microarray. In the current study, we can quantify all RNA-Seq amenable transcripts expressed in brain and identify specific transcripts associated with the alcohol drinking trait.

## 2 MATERIALS AND METHODS

### 2.1 Animals

The HXB/BXH RI rat panel, a subset of the Hybrid Rat Diversity Panel (HRDP) (Tabakoff et al., 2019), was used in this study. This RI panel consists of 30 inbred strains derived from the congenic Brown Norway strain with polydactyl-luxate syndrome (BN-Lx/Cub) and the Wistar origin spontaneously hypertensive rat strain (SHR/OlaIpcv) using gender reciprocal crossing and more than 80 generations of brother sister mating after the F2 generation (Pravenec et al., 1989). This subset of the HRDP was used because phenotype data is publicly available on alcohol consumption (Tabakoff et al., 2009) and other alcohol-related phenotypes (Lusk et al., 2018).

### 2.2 Voluntary Alcohol Consumption in the HXB/BXH Recombinant Inbred Rat Panel

Voluntary alcohol consumption was measured using a two-bottle choice paradigm in 23 HXB/BXH RI strains and the two progenitor strains of the RI panel. The alcohol consumption phenotype was measured in male rats that were 70–100 days old at the beginning of the study. The two-bottle choice paradigm and voluntary alcohol consumption measurements during week two of the paradigm are described in our previous study (Tabakoff et al., 2009) and constituted the voluntary alcohol consumption phenotype. We have used this phenotype in previous genetics studies (Tabakoff et al., 2009; Vanderlinden et al., 2014; Saba et al., 2015; Saba et al., 2020) and established its heritability ( $R^2 = 0.39$ ) (Tabakoff et al., 2009), making it amenable to genomics studies.

### 2.3 Whole Brain RNA Sequencing

The University of Colorado Anschutz Medical Campus received shipments of brain tissue from male rats (~70–90 days old) stored in liquid nitrogen from Dr. Michal Pravenec at the Institute of Physiology of the Czech Academy of Sciences. These animals were maintained in accordance with the Animal Protection Law of the Czech Republic and were approved by the Ethics Committee of the Institute of Physiology, Czech Academy of Sciences, Prague. A total 90 HXB/BXH brains from individual rats (three each from 30 HXB/BXH RI strains) were received, as well as three brains from the SHR/OlaIpcv progenitor strain (93 brains total). The SHR/OlaIpcv brains were used as loading controls, and technical replicate(s), i.e., multiple sequencing libraries, were generated and assayed in each sequencing batch to assess reproducibility of the RNA-Seq results. Including

these technical replicates in the SHR/OlaIpcv strain, 100 sequencing libraries were generated from 93 rat brains.

Total RNA (>200 nucleotides) was extracted from whole brain using the RNeasy Plus Universal Midi Kit (Qiagen, Valencia, CA, United States) and cleaned using the RNeasy Mini Kit (Qiagen, Valencia, CA, United States). Four  $\mu$ L 1:100 dilution of either ERCC Spike-In Mix 1 or Mix 2 (ThermoFisher Scientific, Wilmington, DE, United States) was added to each RNA sample. The Illumina TruSeq Stranded RNA Sample Preparation kit (Illumina, San Diego, CA, United States) was used to construct sequencing libraries, which includes a ribosomal RNA depletion step that uses the Ribo-Zero rRNA reduction chemistry. Sequencing library quality was evaluated using an Agilent Technologies Bioanalyzer 2100 (Agilent Technologies, Santa Clara, CA, United States). Samples were sequenced in eight batches on an Illumina HiSeq2500 or HiSeq4500 (Illumina, San Diego, CA, United States) in High Output mode to generate  $2 \times 100$  or  $2 \times 150$  paired end reads.

## 2.4 Brain Specific Transcriptome Reconstruction and Quantitation Using Whole Brain RNA Sequencing

Brain-specific transcriptome information for the HXB/BXH RI panel used in this study was generated by incorporating RNA expression data (in the form of short read RNA-Seq), DNA sequence information, and computational methods, namely StringTie (Pertea et al., 2015) and aptardi (Lusk et al., 2021), to annotate expressed alternative splicing and alternative polyadenylation transcripts, respectively. In particular, StringTie utilizes RNA-Seq data to reconstruct the transcriptome and identify expressed transcripts not present in the Ensembl reference annotation. However, StringTie only identifies single polyadenylation sites per transcript, i.e., it cannot identify alternative polyadenylation transcript isoforms (Faustino and Cooper, 2003). In contrast, aptardi is designed to evaluate a set of input transcripts and annotate any alternative polyadenylation sites based on the corresponding RNA-Seq data and surrounding DNA sequence to aid in its identification. Therefore, applying these computational methods enables the characterization of the expressed transcriptome to identify alternative splicing and alternative polyadenylation transcripts not in the Ensembl reference annotation but supported by RNA-Seq expression data specific to the sample(s). The transcriptome was then quantitated at the individual transcript level to enable downstream quantitative analyses for evaluating the role of transcripts in predisposition to voluntary alcohol consumption. An outline of the transcriptome reconstruction and quantitation steps are presented in **Supplementary Figures S1, S2**.

### 2.4.1 Read Processing for Quality

Initially, adapter sequences and low quality base calls were eliminated from raw reads using cutadapt (v.1.9.1) (Martin, 2011). Reads were removed from further analysis if they aligned to rRNA from the RepeatMasker database (Smit et al.,

1996) (accessed through the UCSC Genome Browser; <https://genome.ucsc.edu/>) (Kent et al., 2002). This alignment was done using Bowtie 2 (v.2.3.4.3) (Langmead and Salzberg, 2012).

### 2.4.2 Evaluation of Unannotated Genes and Unannotated Splicing—StringTie Transcriptome Reconstruction

Individual RNA-Seq libraries were aligned to their strain-specific genomes using HISAT2 (v.2.1.0) (Kim et al., 2015), and then alignments from libraries produced from brains of animals of the same strain were concatenated using SAMtools (v.1.9) (Li et al., 2009) *merge* to generate a single genome alignment per strain. Strain-specific genomes were constructed from the Rat Genome Sequencing Consortium (RGSC) Rnor\_6.0/rn6 version of the rat genome (Gibbs et al., 2004) by imputing single nucleotide polymorphism (SNP) information for each strain based on their STAR Consortium genotypes (STAR Consortium, 2008) and DNA sequencing (DNA-Seq) data from male rats of the progenitor strains (Hermesen et al., 2015). StringTie (v.1.3.5) (Pertea et al., 2015) was used to generate *de novo* strain-specific transcriptomes using default settings and included the strain-specific genome alignment and the rat Ensembl reference transcriptome (v.99) (Yates et al., 2020) to guide transcriptome assembly. A combined StringTie transcriptome for the HXB/BXH RI panel was generated using the merge functionality of StringTie by providing all strain-specific transcriptomes and the rat Ensembl reference transcriptome as a guide.

### 2.4.3 Evaluation of 3' Termini—Aptardi Transcriptome Reconstruction

The transcriptome was further processed by aptardi (v.1.0.0) to identify alternative polyadenylation sites, i.e., 3' termini (Lusk et al., 2021). While transcriptome assemblers (e.g., StringTie) that consider expression data can identify study-specific transcripts, they are not designed to identify transcripts that share exon junctions (i.e., splice sites) and only differ at the location of the polyadenylation site (i.e., alternative polyadenylation transcripts). In contrast, aptardi is designed to specifically probe the 3' ends of transcripts in order to identify multiple polyadenylation sites per transcript. The input transcripts for aptardi analysis were provided by the combined StringTie transcriptome. By considering expression data, aptardi can annotate unique expressed polyadenylation sites. The strain-specific BAM files of all HXB/BXH RI strains (but not the SHR/OlaIpcv BAM file) were merged into a single BAM file using SAMtools *merge* to generate the aligned RNA expression data for aptardi. Finally, aptardi leverages DNA sequence indicators of polyadenylation to better predict polyadenylation sites. The rat Rnor\_6.0/rn6 reference genome accessed via the UCSC Genome Browser (Gibbs et al., 2004; Havlak et al., 2004) was used for genomic sequence information. If more than one polyadenylation site in the 3' area of a transcript is identified by aptardi, each transcript/polyadenylation site pair is enumerated as a separate transcript by aptardi. All of the

input transcript/3' terminus pairs are also included in the aptardi output, i.e., aptardi only adds transcript/3' terminus pairs.

#### 2.4.4 Detected Above Background Transcriptome Generation and Quantitation

The strength of aptardi is the identification of active polyadenylation sites within a specific genomic region and it does not currently include computational methodology to identify the correct transcript/3' terminus pair when multiple transcripts have 3' termini in the region and multiple polyadenylation sites are identified in the region. Instead, it enumerates all transcript/3' termini pairs. One way to determine the correct pairing of transcript and 3' terminus in this scenario is to examine the RNA expression levels estimated by RSEM, RNA-Seq by Expectation-Maximization (Li and Dewey, 2011). Correct pairings should have higher expression values than incorrect pairings since RSEM uses an iterative method to "assign" a read to a transcript when the read aligns to multiple transcripts. Therefore, quantitation was used to establish the detected above background (DABG) transcriptome.

Prior to quantitation, libraries with less than 10 million paired end raw reads were removed from all subsequent analyses, resulting in the removal of a single SHR/OlaIpcv library. Also, transcripts not derived from autosomal or sex chromosomes were removed, i.e., transcripts derived from contigs in the current rat genome. Transcripts in the aptardi transcriptome were then quantitated in each of the 90 HXB/BXH RNA-Seq libraries using RSEM (v.1.3.0) (Li and Dewey, 2011). Transcripts with zero estimated read counts in one third or more of these 90 libraries were removed, as well as transcripts that were 200 nucleotides or fewer in length. This high-quality transcriptome was then used to re-quantitate transcripts with RSEM for each of the HXB/BXH libraries as well as the SHR/OlaIpcv libraries. This re-quantitation step was used to allow the reads that originally aligned to a transcript with low expression to be reassigned to a transcript with higher RNA expression levels. Once again, transcripts with zero counts in one third or more of samples were removed to yield the DABG transcriptome and the corresponding estimated read counts for each RNA-Seq library and for each transcript.

Estimated read counts of transcripts in the DABG transcriptome for each RNA-Seq library generated by RSEM were normalized for sequencing depth using upper quartile normalization (Bullard et al., 2010) implemented in the *EDASeq* R package (v.2.22.0) (Risso et al., 2011) followed by a regularized log (rlog) normalization with the *DESeq2* R package (v.1.28.1) (Love et al., 2014). Finally, expression values were adjusted for batch effects using ComBat (Johnson et al., 2007) from *sva* R package (v.3.36.0) (Leek et al., 2012).

## 2.5 Quantitative Trait Loci Analysis

### 2.5.1 Genetic Markers for Quantitative Trait Loci Analyses

Genetic markers were initially procured from publicly available SNP genotype data for the HXB/BXH RI rats originally published by the STAR Consortium (STAR Consortium, 2008). Probes

from the original array were aligned to the Rnor\_6.0/rn6 version of the rat genome using BLAT (Kent, 2002). Markers were further processed into unique strain distribution patterns for QTL analyses as detailed in our previous work (Lusk et al., 2018).

### 2.5.2 Statistical Methods for Quantitative Trait Loci Analyses

Quantitative trait loci (QTL) analysis was performed using marker regression for the behavioral phenotype (pQTL), for module eigengenes (meQTL), and for transcript expression levels (eQTL) to calculate the logarithm of odds (LOD) scores for each SNP as described by Broman and Sen (Broman and Sen, 2009). eQTL and meQTL were only calculated for transcripts/module eigengenes that were associated with alcohol consumption. All empirical genome-wide *p*-values were calculated using 1,000 permutations (Churchill and Doerge, 1994). Both significant (genome-wide *p*-value < 0.05) and suggestive (genome-wide *p*-value < 0.63) (Lander and Kruglyak, 1995) QTL were considered for pQTL analysis (Lander and Kruglyak, 1995; Abiola et al., 2003). For meQTL and eQTL analyses, a stricter genome-wide significant *p*-value of <0.01 was enforced and only the most significant QTL per transcript or module eigengene was considered. The 95% Bayesian credible intervals of significant or suggestive pQTL, significant meQTL, and significant eQTL were estimated as described by Sen and Churchill (Sen and Churchill, 2001) and all QTL analyses and graphics were generated using the R/qtl package (v.1.47-9) (Broman and Sen, 2009). Strain mean voluntary alcohol consumption values were also used for pQTL analysis. Strain mean transcript normalized expression estimates were used for eQTL analyses, and module eigengene values (which were produced from WGCNA using strain mean transcript normalized expression estimates and thus represent strain means) were used for meQTL analysis.

## 2.6 Heritability of Transcripts

Heritability of transcripts in the DABG transcriptome was estimated as the coefficient of determination ( $R^2$ ) from a one-way ANOVA of individual rat expression values using strain as the predictor and transcript normalized expression estimates as the response.

## 2.7 Identification of Candidate Coexpression Networks and Candidate Individual Transcripts Associated With Voluntary Alcohol Consumption

RNA expression data from alcohol naïve rats were used to determine candidate coexpression modules and individual candidate transcripts that are associated with a predisposition to higher or lower levels of voluntary alcohol consumption. Prior to these analyses, additional filtering of the DABG transcriptome was performed to include only transcripts that 1) were the dominant isoforms expressed for a gene (i.e., the three transcripts of a gene with the highest expression based on mean transcripts per million), 2) demonstrated heritability in the HXB/BXH RI panel and thus genetic influence on RNA

expression levels, and 3) could be associated with an Ensembl Gene ID (i.e., shared at least one splice junction with an annotated Ensembl transcript) for annotation purposes. Of the 59,751 transcripts in the DABG transcriptome, 37,453 (63%) were kept after removing transcripts that were not within the top three expressed isoforms for a gene. Eliminating transcripts equal to or below the median heritability across all transcripts (heritability  $\leq 0.478$ ), resulted in 20,442 transcripts. Finally, removing transcripts without an associated Ensembl Gene ID produced a final set of 18,543 transcripts (**Supplementary Figure S3**). The final set of transcripts were derived from 12,609 genes, of which 7,945 (63%), 3,403 (27%), and 1,261 (10%) possessed one, two, or three isoforms, respectively. Of the 18,543 transcripts, 5,427 (29%), 4,932 (27%), and 8,175 (44%) transcripts were identified by aptardi, StringTie, or the Ensembl reference transcriptome, respectively.

### 2.7.1 Weighted Gene Coexpression Network Analysis

The WGCNA R package (v.1.69) (Langfelder and Horvath, 2008) was used to build a transcript coexpression network and to identify coexpression modules within that network from the strain mean normalized expression estimates for individual transcripts. Minimum module size was set to five and the deepSplit parameter was set to four to promote identification of smaller modules, but otherwise default settings were used including a Pearson correlation to determine the initial adjacency matrix. A soft-thresholding index ( $\beta$ ) of seven was chosen to approximate a scale-free topology (Zhang and Horvath, 2005) in an unsigned network (**Supplementary Figure S4**). The module eigengene (first principal component) was used to summarize transcript expression values within a module across strains.

### 2.7.2 Candidate Coexpression Networks and Individual Candidate Transcripts

Multiple criteria similar to those previously established (Lusk et al., 2018) were used to determine candidate modules and individual candidate transcripts; 1) expression of the transcripts/module is correlated with voluntary alcohol consumption (Spearman correlation coefficient  $p$ -value  $< 0.01$ ) (For the module analysis the module eigengene expression values were used for correlation, and for the individual transcripts the strain mean normalized expression estimates were used.), 2) The module eigengene QTL (meQTL; for modules) or expression QTL (eQTL; for individual transcripts) must have genome-wide significance (genome-wide  $p$ -value  $< 0.01$ ), and 3) meQTL or eQTL must overlap the significant (genome-wide  $p$ -value  $< 0.05$ ) or suggestive (genome-wide  $p$ -value  $< 0.63$ ) pQTL where overlap was considered if the SNP with the highest LOD score for the meQTL/eQTL analyses fell within the 95% Bayesian credible interval for the pQTL.

## 2.8 Single Molecule RNA Sequencing (Iso-Seq)

Publicly available single molecule RNA sequencing (Iso-Seq) data from rat brain was used to qualitatively validate splicing and

active polyadenylation sites (SRA Accession ID: PRJNA801761). Briefly, total RNA ( $>200$  bases) was extracted from brain samples from a single male rat from the F344/Stm inbred strain and a single male rat from the LE/Stm inbred strain and cleaned using the RNeasy Plus Universal Midi Kit and RNeasy Mini Kit, respectively (Qiagen, Valencia, CA, United States). RNA was transferred to GeneWiz, Inc. (South Plainfield, NJ, United States) for processing on the PacBio Sequel platform using two SMRT cells per sample. PacBio Iso-Seq SMRTbell library preparation followed the manufacturer's protocol and high and low quality consensus reads (CCS) were transferred to University of Colorado Anschutz Medical Campus for further bioinformatic processing. CCS were aligned to the rat genome (RN6) using minimap2 [v. 2.17 with the flags (-ax splice:hq -uf -secondary = yes -N 15 -K 1G -t 16 -k 12 -w 4); (Li, 2018)]. Alignment files were converted to GTF (gene transfer format) for upload and visualization with the UCSC Genome Browser (<https://genome.ucsc.edu/>; Kent et al., 2002).

## 3 RESULTS

### 3.1 Whole Brain RNA Sequencing

After processing reads for quality, the number of paired end reads in the 90 HXB/BXH RI panel RNA-Seq libraries ranged from 29 million to 199 million (median number of paired end reads per sample = 71 million). The number of paired end reads in each RNA-Seq library, including the SHR/OlaIpcv libraries, is provided in **Supplementary Table S1**.

The median strain-specific genome alignment rate of the 90 HXB/BXH RI panel RNA-Seq libraries was 97% (interquartile range = 96.8–97.5%) and the alignment rate ranged from 79 to 98%. The alignment rate of each RNA-Seq library, including the 10 SHR/OlaIpcv libraries, is provided in **Supplementary Table S2**.

### 3.2 Brain Specific Transcriptome Generation for the HXB/BXH Recombinant Inbred Rat Panel

#### 3.2.1 Comparison of the Number of Isoforms per Gene in the Ensembl, StringTie, Aptardi, and Detected Above Background Transcriptomes

The transcriptome reconstruction pipeline that we have utilized consists of four steps. In the first three steps, novel transcripts are identified within the transcriptome. The fourth and final step eliminates transcripts which do not meet the threshold for detection above background. Of the 40,772 initial rat Ensembl transcripts, only 17,028 (42%) were included in the DABG transcriptome (**Table 1**). In the DABG transcriptome, the majority (40.5%) of transcripts were derived using reconstruction methods implemented in StringTie. There were slightly more aptardi transcripts in the DABG transcriptome than Ensembl transcripts. In summary, 71.5% of the transcripts in the DABG transcriptome were computationally derived and are not in the Rat Ensembl Transcriptome (v.99). By including the computational pipeline for transcriptome reconstruction, the

**TABLE 1 |** Summary of the number genes and transcripts generated/retained at each step in the transcriptome reconstruction pipeline. The percent of total transcripts identified by each source at each step is shown in parenthesis. The rat Ensembl reference transcriptome (v.99) was used as input for StringTie, along with whole brain RNA sequencing data, to characterize alternative splicing in brain of the HXB/BXH recombinant inbred rat panel. RNA sequencing data was likewise used, in conjunction with DNA sequence of the rat reference Rnor\_6.0/m6, to identify brain-specific alternative polyadenylation events in the HXB/BXH recombinant inbred rat panel. Finally, transcripts were filtered based on their expression estimates as determined by RSEM to retain only transcripts with substantial expression in the detected above background (DABG) transcriptome.

Dataset	Transcriptome generation step	Number of genes	Number of transcripts	Transcript:Gene ratio	Number of Ensembl transcripts	Number of StringTie transcripts	Number of aptardi transcripts
Ensembl	Step 1	32,586	40,772	1.25	40,772 (100.0%)	—	—
StringTie	Step 2	33,649	83,920	2.49	40,754 (48.6%)	43,166 (51.4%)	—
Aptardi	Step 3	33,649	155,677	4.63	40,754 (26.2%)	43,166 (27.7%)	71,757 (46.1%)
DABG	Step 4	19,517	59,751	3.06	17,028 (28.5%)	24,219 (40.5%)	18,504 (31.0%)

Transcript:Gene ratio increased from 1.25 to 3.06. Furthermore, 83% of genes in the reference Ensembl transcriptome were annotated as though they produce a single transcript, i.e., genes without documented alternative splicing or alternative polyadenylation isoforms (**Supplementary Figure S5A**). In contrast, only 44% of genes in the DABG transcriptome were found to express a single transcript in brain of the HXB/BXH RI rat population (**Supplementary Figure S5B**).

### 3.2.2 Evaluation of 3'Termini

Since this is one of the first demonstrations of the integration of aptardi into the transcriptome reconstruction pipeline in a dataset of this magnitude, it was important to examine, in detail, the 3' termini of the resulting transcriptome. To examine the performance of this pipeline we 1) compared the number of transcript/3' terminus pairs in the aptardi transcriptome (when all possible pairs are enumerated) to the number of pairs that remained in DABG transcriptome, i.e., could we use read counts to determine the most appropriate transcript/3' terminus pairs, and 2) compared aptardi-identified polyadenylation sites to annotated polyadenylation sites *via* the Ensembl transcriptome or the StringTie reconstruction.

Filtering transcript/3' terminus pairs using our computational pipeline dramatically reduced the number of transcripts with which a 3' terminus was associated. The aptardi analysis identified 71,757 new transcript/3' terminus pairs (i.e., aptardi transcripts). These represent 34,003 unique 3' termini resulting in each unique 3' terminus being associated with approximately two transcripts on average. After filtering to yield the DABG transcriptome, there were 18,504 aptardi transcripts representing 14,388 3' termini (approximately 1.3 aptardi transcripts associated with each 3' terminus).

Within this pipeline, aptardi analyzes the 3' end of all transcripts. Because of this, it is possible for aptardi to identify a 3' terminus in a transcript/3' terminus pair that has been identified using another source (i.e., Ensembl or StringTie). Of the initial 71,757 aptardi transcripts, 19% matched the 3' terminus of an Ensembl or StringTie transcript  $\pm 100$  bases, i.e., the 3' terminus was not novel but had not been paired with that particular transcript before. When the percent of aptardi transcripts that matched the 3' terminus of an Ensembl or

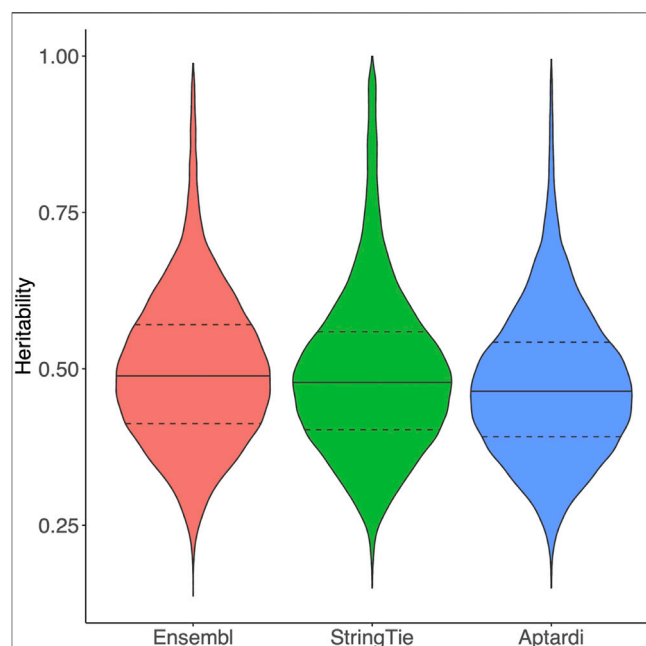


**FIGURE 1 |** Heritability of transcripts in the detected above background transcriptome. Heritability of transcripts derived from the Ensembl reference annotation, StringTie, and aptardi. Heritability was estimated as the coefficient of determination ( $R^2$ ) from a one-way ANOVA of individual rat expression values using strain as the predictor (30 strains total) and transcript normalized expression estimates as the response. The solid horizontal line within each violin plot represents the median heritability for that group of transcripts. The dashed horizontal lines represent the upper quartile and lower quartile heritabilities for that group of transcripts.

StringTie transcript  $\pm 100$  bases was calculated based on the number of aptardi 3' termini rather than the number of aptardi transcripts (i.e., aptardi transcripts with matching 3' termini were only counted once), a similar percentage was observed (21%; **Supplementary Table S3**). Of the 18,504 DABG aptardi transcripts, 16% had a 3' terminus that matched annotation ( $\pm 100$  bases) from the Ensembl reference or StringTie transcriptome (**Supplementary Table S3**). The slight decrease in the number of aptardi 3' termini matching a StringTie or Ensembl 3' terminus in the DABG transcriptome compared to

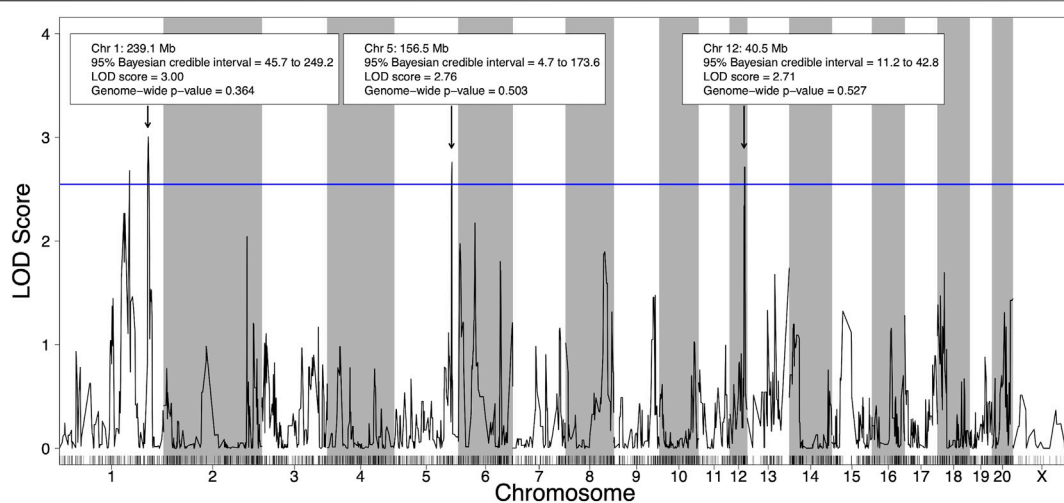


**FIGURE 2 |** Quantitative trait loci (QTL) for voluntary alcohol consumption in the HXB/BXH recombinant inbred panel. Strain means were used in a marker regression to determine phenotypic QTL. The blue line represents the logarithm of the odds (LOD) score threshold for a suggestive QTL (genome-wide  $p$ -value = 0.63). Suggestive QTL are labeled with their location, 95% Bayesian credible interval, LOD score, and genome-wide  $p$ -value. Empirical genome-wide phenotypic QTL  $p$ -values were calculated using 1,000 permutations.

pre-filtering suggests the filtering removes some false positive aptardi transcript/3' terminus pairs in favor of the original StringTie/Ensembl transcript with the given polyadenylation site. At the same time, the relatively high number of overlapping Ensembl/StringTie and aptardi 3' termini in the DABG transcriptome suggests that aptardi annotation of the polyadenylation site for the given transcript is accurate and simply represents a transcript with a similar 3' terminus to another StringTie/Ensembl transcript with a different upstream exon structure.

### 3.2.3 Heritability of Transcripts in the Detected Above Background Transcriptome

Transcripts in the DABG transcriptome identified by Ensembl, StringTie, or aptardi displayed similar heritability to one another (Figure 1).

## 3.3 Voluntary Alcohol Consumption Quantitative Trait Loci

Using the 21 HXB/BXH RI strains with voluntary alcohol consumption data and genotype data (Supplementary Table S4), four suggestive ( $p$ -value < 0.63) pQTL for voluntary alcohol consumption were identified; two on chromosome 1, one on chromosome 5 and one on chromosome 12 (Figure 2). To deduce if the two suggestive peaks on chromosome 1 represented independent QTLs, a second QTL analysis was done that included the maximum peak on chromosome 1 as a covariate (Supplementary Figure S6). Since the second QTL analysis did not include any QTL on chromosome 1, the two peaks on chromosome 1 likely represent regions in linkage disequilibrium and were treated as a single QTL in the remainder of the analysis. Notably, the other pQTL on chromosomes 5 and 12 remained suggestive in

the second QTL analysis, indicating these pQTL are independent of the pQTL on chromosome 1.

## 3.4 Identification of Candidate Coexpression Networks and Candidate Individual Transcripts Associated With Voluntary Alcohol Consumption

### 3.4.1 Candidate Individual Transcripts

Of the 18,534 individual transcripts whose strain mean normalized expression estimates were subjected to correlation analysis with strain mean voluntary alcohol consumption, 64 were significantly ( $p$ -value < 0.01) correlated with voluntary alcohol consumption. Requiring a significant (genome-wide  $p$ -value < 0.01) eQTL, as well as eQTL overlap with a pQTL (using 95% Bayesian credible intervals) resulted in a final set of 11 transcripts (Table 2). One of these transcripts was identified by aptardi, six were identified by StringTie, and four were identified by Ensembl. Seven of the 11 transcripts belonged to genes expressing multiple isoforms. All 11 transcripts possessed local eQTL with the exception of the transcript from the *Map3k7* gene (*MSTRG.23809.1*).

#### 3.4.1.1 *Map3k7*

Two isoforms of *Map3k7* (gene ID = *MSTRG.23809*) were present in the DABG transcriptome (Figure 3A), of which one was from the rat Ensembl reference transcriptome (*ENSRNOT00000007657*) and one was identified by StringTie (*MSTRG.23809.1*). *MSTRG.23809.1*, the transcript associated with alcohol consumption, is located on the plus strand of chromosome 9 (114.02–114.07 Mb), but its eQTL overlapped the voluntary alcohol consumption pQTL on chromosome 5. The transcript structure of *MSTRG.23809.1*

**TABLE 2 |** Individual candidate transcripts in brain for predisposition to voluntary alcohol consumption. Strain mean normalized expression estimates and strain mean voluntary alcohol consumption values were used to determine Spearman's rank correlation coefficients. Strain mean normalized expression estimates were used in a marker regression to determine expression quantitative trait loci (eQTL) and corresponding logarithm of the odds (LOD) scores. Empirical genome-wide expression QTL *p*-values were calculated using 1,000 permutations. Transcripts are ordered by their *p*-value related to correlation with alcohol consumption. The total number of transcripts generated from the same gene in the detected above background transcriptome, and the source(s) identifying the transcripts, is also shown. All transcripts possessed local eQTL with the exception of the transcript from the *Map3k7* gene (*MSTRG.23809.1*).

Transcript ID	Gene symbol(s)	Gene description(s)	Source	Transcript correlation with alcohol consumption (correlation coefficient ( <i>p</i> -value))	Expression QTL LOD score (genome-wide ( <i>p</i> -value))	Expression QTL (chromosome: Position (Mb))	Number of brain transcripts identified in HXB/BXH RI panel	Number of Ensembl/ StringTie/ aptardi transcripts
ENSRNOT00000072618	<i>E2f2</i>	E2F transcription factor	Ensembl	-0.66 (0.0013)	13.88 (<0.001)	5:154.8	1	1/0/0
MSTRG. 1868.13	<i>Tmem9b</i>	Transmembrane protein 9b	StringTie	-0.62 (0.0030)	5.26 (<0.001)	1:173.9	11	0/10/1
MSTRG.1793.4	<i>Trim68</i>	Tripartite motif-containing 68	StringTie	0.61 (0.0031)	13.06 (<0.001)	1:167.2	4	3/1/0
ENSRNOT00000075003	<i>Tmem159</i>	Transmembrane protein 159	Ensembl	-0.60 (0.0038)	9.33 (<0.001)	1:189.2	1	1/0/0
MSTRG.23809.1	<i>Map3k7</i>	Mitogen activated protein kinase kinase 7	StringTie	0.60 (0.0041)	5.92 (0.004)	5:46.8	2	1/1/0
ENSRNOT00000090867	<i>Oas3</i>	2'-5'-oligoadenylate synthase 3	Ensembl	0.60 (0.0043)	9.29 (<0.001)	12:40.5	1	1/0/0
ENSRNOT00000024093.1	<i>Aldh1a7</i>	Aldehyde dehydrogenase, cytosolic 1	aptardi	-0.59 (0.0051)	14.28 (<0.001)	1:237.6	1	0/0/1
ENSRNOT00000001752	<i>P2rx4</i>	Purinergic receptor P2X 4	Ensembl	-0.58 (0.0059)	9.81 (<0.001)	12:39.1	2	1/1/0
MSTRG. 1874.1	<i>Tmem41b</i>	Transmembrane protein 41B	StringTie	0.57 (0.0068)	9.37 (<0.001)	1:173.9	3	1/2/0
MSTRG. 2084.2	<i>Lat, Spns1, Nfatc2ip</i>	Linker for activation of T-cells family member 1, Protein spinster homolog 1, NFATC2-interacting protein	StringTie	0.56 (0.0089)	7.65 (<0.001)	1:197.0	7	1/6/0
MSTRG.1526.1	<i>Pex11a</i>	Peroxisomal membrane protein 11A	StringTie	0.55 (0.0093)	11.02 (<0.001)	1:141.0	2	1/1/0

represents an exon skipping isoform of *ENSRNOT0000007657*; specifically, it lacks exon 12 (Figure 3B). No transcripts for *Map3k7* were detected in the single molecule RNA sequencing. Across the 63 individual rat RNA-Seq libraries (21 HXB/BXH RI strains) with voluntary alcohol consumption data, the mean transcripts per million transcripts (TPM) of *MSTRG.23809.1* and *ENSRNOT0000007657* was 0.95 and 1.30, respectively.

We note that a transcript with a nearly identical transcript sequence as *MSTRG.23809.1* was identified *de novo* by StringTie (*MSTRG.17584.2*) on the plus strand of chromosome 5 (47.19–47.24 Mb), which overlaps the voluntary alcohol consumption pQTL. The two transcripts only differed in the lengths of their untranslated regions (less than 10 nucleotides in the 5' UTR and approximately 200

nucleotides in the 3' UTR). In fact, the two transcripts have identical nucleotide sequences in the largest open reading frame of each transcript. When the transcript sequences were aligned to the genome, both transcripts align perfectly to both genomic regions. While the gene of *MSTRG.17584.2* (*LOC100910771*) is annotated as *Map3k7-like* in both Ensembl v.99 and the latest release (v.104), the Rat Genome Database has since retired the *Map3k7-like* annotation in favor of *Map3k7*. Therefore, there are multiple locations of this gene/transcript currently annotated in rat according to the Rat Genome Database. The two transcripts are highly negatively correlated (Spearman's rank correlation coefficient = -0.835), and both transcripts' strain mean normalized expression estimates have a similar (absolute) Spearman's rank correlation coefficient to strain mean

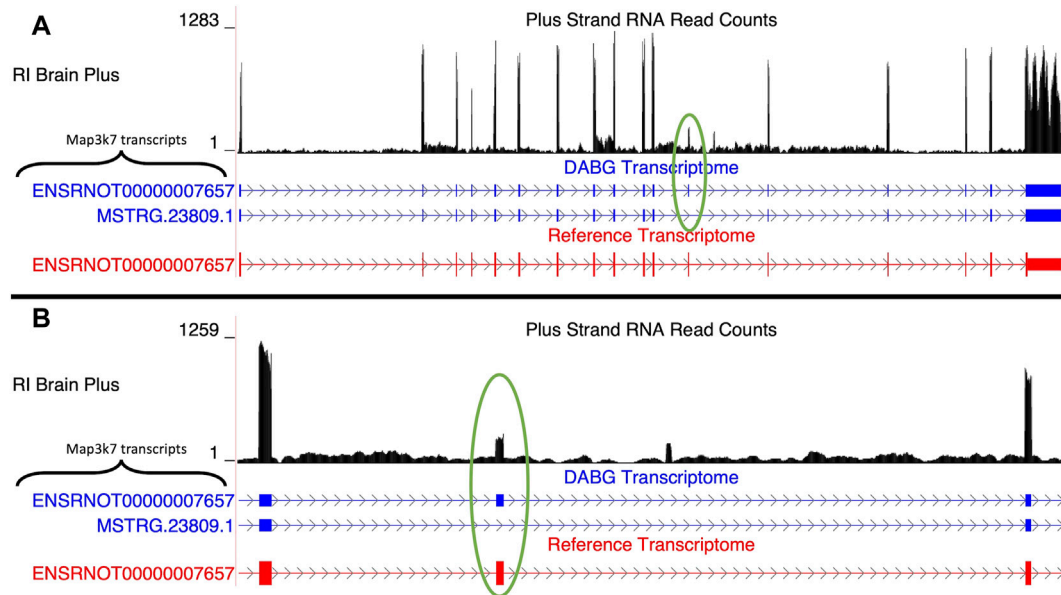


**FIGURE 3 |** Isoforms of the *Map3k7* gene. **(A)** Blue transcripts represent those identified in the detected above background (DABG) transcriptome, and the red transcript represents the transcript present in the Ensembl reference annotation. *ENSRNOT0000007657* is annotated in the Ensembl reference transcriptome and retained in the DABG transcriptome. *MSTRG.23809.1* represents a novel isoform identified by StringTie. *MSTRG.23809.1* represents an isoform with exon 12 skipped compared to *ENSRNOT0000007657* (circled in green). **(B)** Detailed view of the exon 12 region. The RNA sequencing reads on the positive strand (black plot) represent a 10% randomly sampled subset from the HXB/BXH recombinant inbred rat panel RNA sequencing data in brain. This image was generated using the UCSC Genome Browser (Kent et al., 2002).

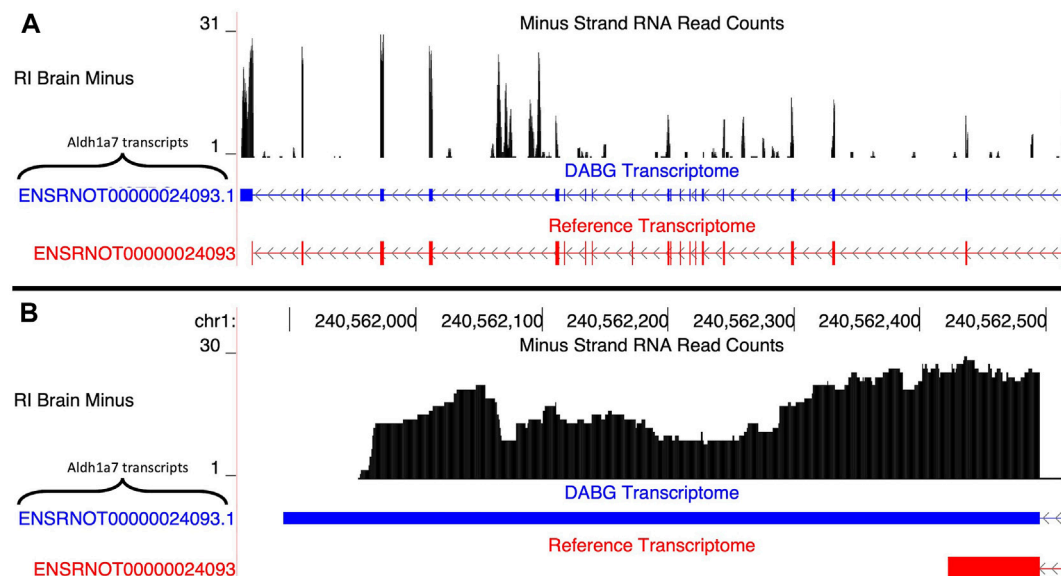
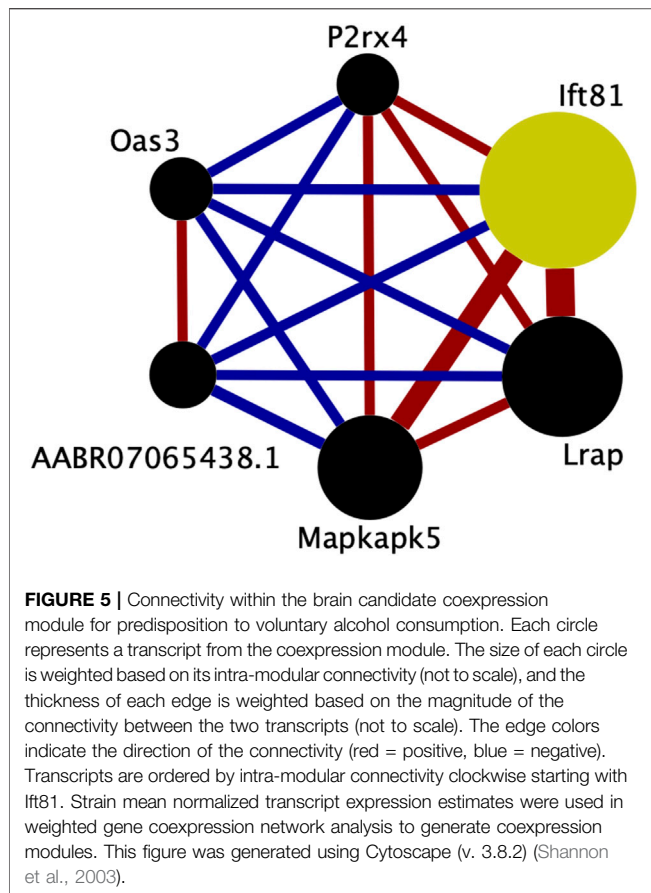


**FIGURE 4 |** Isoforms of the *Aldh1a7* gene. **(A)** The blue transcript represents those identified in the detected above background (DABG) transcriptome, and the red transcript represents the transcript present in Ensembl reference annotation. *ENSRNOT00000024093* is annotated in the Ensembl reference transcriptome but was filtered out of the DABG transcriptome. *ENSRNOT00000024093.1* represents a novel isoform identified by aptardi. **(B)** Detailed view of the 3' region comparing aptardi annotation (*ENSRNOT00000024093.1*) to Ensembl reference annotation (*ENSRNOT00000024093*). *ENSRNOT00000024093* and *ENSRNOT00000024093.1* differ only in the length of their 3' most exon. The RNA sequencing reads on the negative strand (black plot) represent a 10% randomly sampled subset from the HXB/BXH recombinant inbred rat panel RNA sequencing data in brain. This image was generated using the UCSC Genome Browser (Kent, 2002).



voluntary alcohol consumption (*MSTRG.23809.1* = 0.599; *MSTRG.17584.2* = -0.509), but the slightly weaker correlation of *MSTRG.17584.2* caused it to be removed as a candidate transcript based on correlation *p*-value (*p*-value = 0.018). Yet its eQTL (chromosome 5, position = 46.8 Mb, 95% Bayesian credible = 46.8–46.8 Mb) overlapped the alcohol pQTL on chromosome 5, thus meeting this criterion for candidacy and, with respect to the eQTL peak, the LOD score and corresponding genome-wide *p*-value were more significant for *MSTRG.17584.2* (LOD = 8.72, *p*-value < 0.001) than *MSTRG.23809.1* (LOD = 5.92, *p*-value = 0.004). Also of note, the eQTL for *MSTRG.17584.2* overlaps its genomic position (i.e., is a local eQTL), whereas *MSTRG.17584.2* possesses a distal eQTL. According to our quantitation, *MSTRG.17584.2* is the dominant transcript (mean TPM = 2.84 vs 0.95).

#### 3.4.1.2 *Aldh1a7*

A single transcript of *Aldh1a7*, *ENSRNOT00000024093.1*, was present in the DABG transcriptome (Figure 4A). The Ensembl version of this transcript, *ENSRNOT00000024093*, was removed during filtering and thus not present in the DABG transcriptome. The Ensembl transcript was removed after the first quantitation step that generated the high-quality transcriptome from the aptardi transcriptome (i.e., it was removed because it had estimated read counts

of zero in one third or more of the 90 HXB/BXH RI panel libraries). *ENSRNOT00000024093.1* shares exon junctions with *ENSRNOT00000024093* (Figure 4A) but possesses a unique 3' terminus on the negative strand of chromosome 1 compared to Ensembl (*ENSRNOT00000024093.1* 3' end = 240,561,896; *ENSRNOT00000024093* 3' end = 240,562,423; Figure 4B). No *Aldh1a7* transcripts were detected in the single molecule RNA sequencing.

#### 3.4.2 Candidate Modules From Weighted Gene Coexpression Network Analysis

A total of 30 HXB/BXH RI strains with expression data (Supplementary Table S4) were used to generate transcript coexpression modules using strain means of transcript normalized expression estimates. WGCNA identified 215 modules along with 137 transcripts (out of the 18,543) that were not assigned a module. The median module size was 10 transcripts (Supplementary Figure S7). Module eigengenes captured much of the within-module transcript expression variability (interquartile range: 60–72%). In addition, when a gene had multiple isoforms included in the WGCNA, most often (54% of genes) isoforms generated from the same gene were assigned to different modules (Supplementary Figure S8).

Of the 215 modules, the module eigengene of a single module—blue1—was the only module significantly associated with voluntary alcohol consumption (correlation coefficient = -0.62, *p*-value = 0.0026). A significant meQTL for the blue1 module was identified on chromosome 12 (LOD score = 16.83, genome-wide *p*-value < 0.0001). Furthermore, the location of the meQTL (chromosome 12, position = 39.1 Mb, 95% Bayesian credible = 39.1–40.5 Mb) overlapped the suggestive pQTL on chromosome 12 (chromosome 12, position = 40.5 Mb, 95% Bayesian credible = 11.2–42.8 Mb) thereby satisfying all the requirements for candidacy. The module eigengene explained 75% of the within-module expression variability.

The transcripts comprising the blue1 module are shown in Figure 5 and listed in Table 3. One transcript was identified by aptardi (*Ifl81*), three were identified by StringTie (*Lrap*, *Mapkapk5*, *AABR07065438.1*) and two were in the original Ensembl annotation (*P2rx4* and *Oas3*). Most of these transcripts reside near the physical location of the meQTL and pQTL. The expression of all individual transcripts in the blue1 module displayed correlation with voluntary alcohol consumption (*p*-value < 0.05). Three of the six transcripts were associated with genes that had more than one transcript (*Mapkapk5*, *P2rx4*, and *Ifl81*) in the DABG transcriptome, although not all of these transcripts were included in WGCNA after applying the computational pipeline that removes lowly expressed transcripts. The genes of three transcripts (*Lrap*, *P2rx4* and *Ifl81*) were also identified in our previous candidate module (Saba et al., 2015) using microarray data (vs. RNA-Seq data here).

##### 3.4.2.1 *P2rx4*

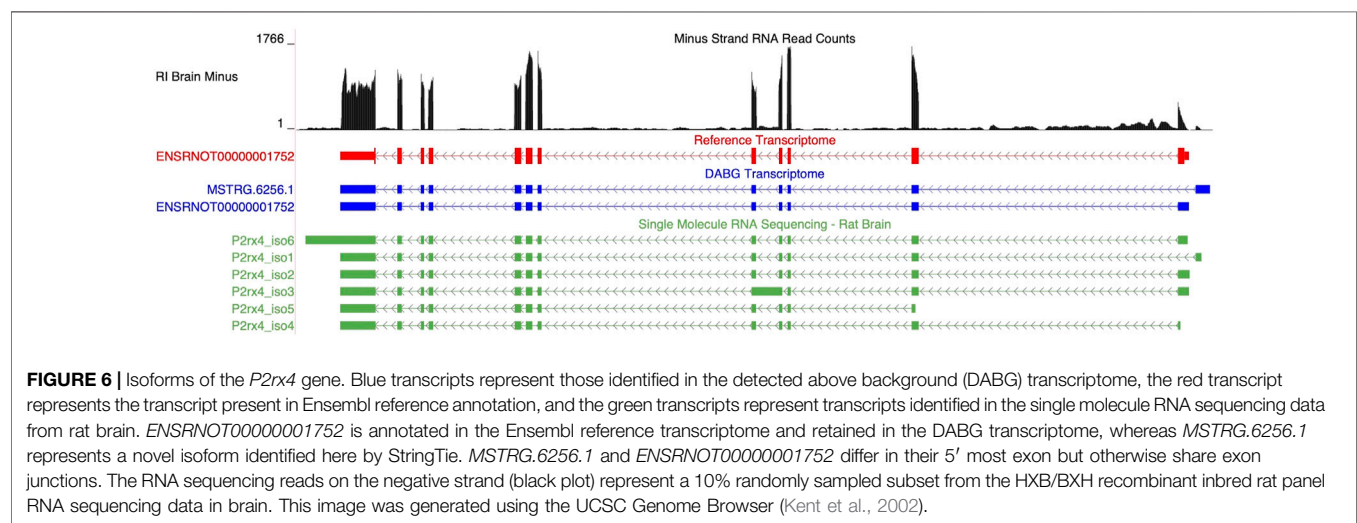
Two isoforms of *P2rx4* (gene ID = *MSTRG.6256*) were identified in the DABG transcriptome: *ENSRNOT0000001752*, which was annotated in the Ensembl transcriptome and included in the candidate module, and *MSTRG.6256.1*, which was annotated by

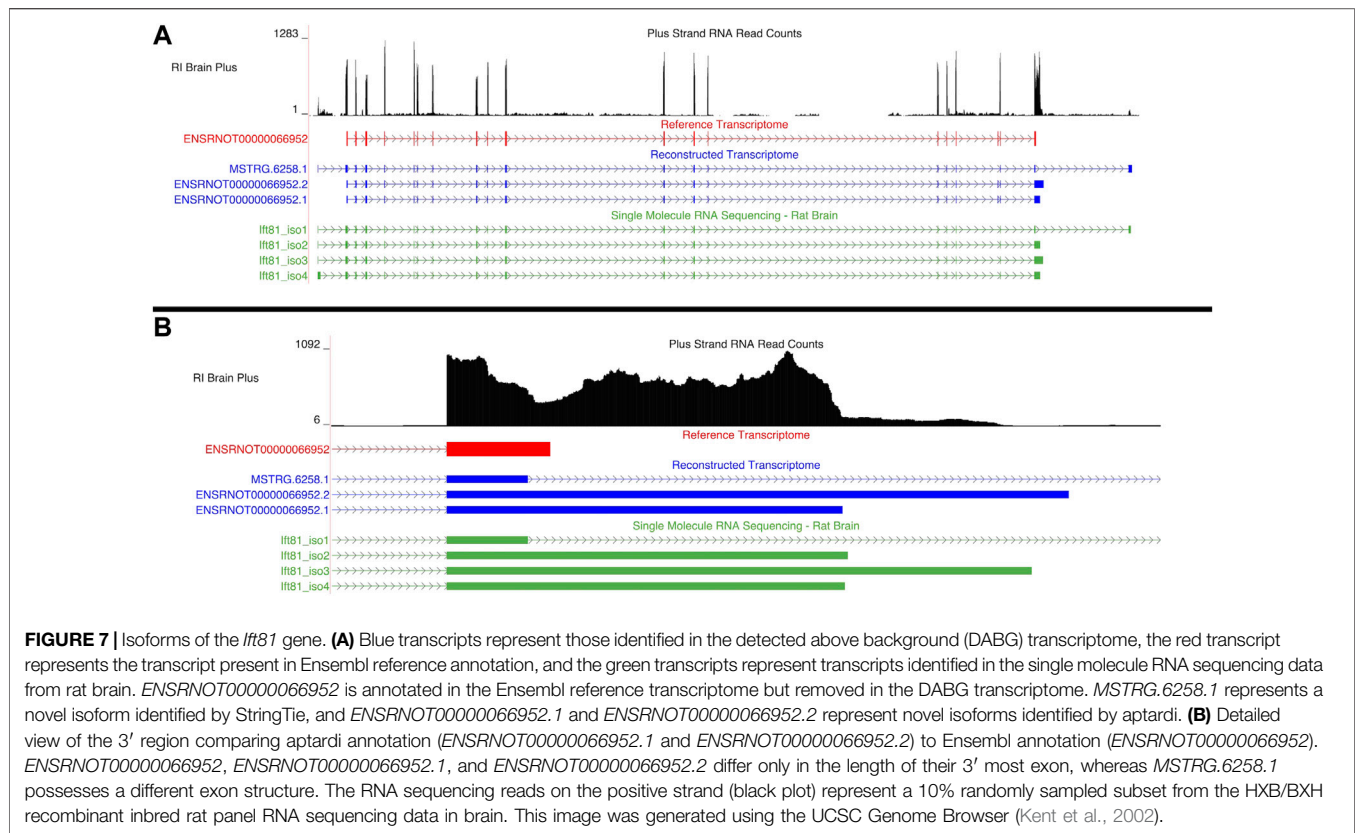
**TABLE 3 |** Transcripts in the brain candidate coexpression module for predisposition to voluntary alcohol consumption. Transcripts are ordered by intra-modular connectivity, and the source that identified the transcript is shown. The total number of transcripts with the same gene ID as the individual candidate transcript (i.e., isoforms of the same gene) in the detected above background transcriptome, and the source(s) identifying the transcripts, is also shown. Strain mean normalized expression estimates and strain mean voluntary alcohol consumption values were used to determine Spearman's rank correlation coefficients.

Transcript ID	Gene symbol	Gene description	Source	Chromosome: Start position-end position (Mb) (strand)	Intra-modular connectivity	Transcript correlation with alcohol consumption (correlation coefficient (p-value))	Number of transcripts identified in HXB/BXH RI panel	Number of ensembl/ StringTie/ aptardi transcripts
ENSRNOT00000066952.1	Itf81	Intraflagellar transport 81	aptardi	12: 39.42–39.51 (+)	1.22	−0.44 (0.0487)	3	0/1/2
MSTRG.6250.1	Lrap	Locus regulating alcohol preference	StringTie	12: 39.01–39.02 (−)	1.14	−0.45 (0.0417)	1	0/1/0
MSTRG.6281.1	Mapkapk5	MAPK activated protein kinase 5	StringTie	12: 40.51–40.53 (+)	1.10	−0.49 (0.0238)	3	2/1/0
MSTRG.19929.1	AABR07065438.1	Ribosomal protein L6, pseudo 1	StringTie	6: 128.74–128.74 (+)	1.01	0.51 (0.0191)	1	0/1/0
ENSRNOT00000090867	Oas3	2'-5'-oligoadenylate synthetase 3	Ensembl	12: 41.32–41.34 (+)	1.01	0.60 (0.0043)	1	1/0/0
ENSRNOT00000001752	P2rx4	Purinergic receptor P2X 4	Ensembl	12: 39.31–39.33 (−)	1.00	−0.58 (0.0059)	2	1/1/0

StringTie (**Figure 6**). The Ensembl and StringTie transcripts differ at their 5' exon but otherwise share identical transcript structure. Both were included in WGCNA but belonged to different coexpression networks. Six isoforms of *P2rx4* were identified in the single molecule RNA sequencing. The isoform labeled P2rx4\_iso2 in **Figure 6** matches *ENSRNOT00000001752* while P2rx4\_iso1 validates the novel splice variant identified by StringTie.

*ENSRNOT00000001752* was also identified as a candidate transcript (**Table 2**). While the strain mean normalized expression estimates of *ENSRNOT00000001752* were negatively correlated with strain mean voluntary alcohol consumption (Spearman's rank correlation = −0.579, *p*-value = 0.0051), *MSTRG.6256.1* was not significantly associated with alcohol consumption (Spearman's rank correlation = 0.166, *p*-value =





0.471). *ENSRNOT00000001752* was the dominant isoform in the 63 individual rat RNA-Seq libraries (21 HXB/BXH RI strains) with voluntary alcohol consumption data (*ENSRNOT00000001752* mean TPM = 6.143; *MSTRG.6256.1* mean TPM = 0.254).

#### 3.4.2.2 *Ift81*

An aptardi isoform of *Ift81*, *ENSRNOT00000066952.1*, was the hub transcript, (i.e., the transcript with the highest intra-modular connectivity within the blue1 module). Two additional isoforms of this gene were annotated in the DABG transcriptome: *ENSRNOT00000066952.2*, which was annotated by aptardi, and *MSTRG.6258.1*, which was identified by StringTie (Figure 7A). The Ensembl annotation of *Ift81*, *ENSRNOT00000066952*, was not present in the DABG transcriptome. Like *Aldh1a7*, the Ensembl transcript for *Ift81* was removed after the first quantitation step that generated the high-quality transcriptome (i.e., it was removed because it had zero estimated read counts in one third or more of the 90 HXB/BXH RI panel libraries). Both aptardi transcripts only differ in their 3' base position (on the plus strand of chromosome 12) compared to the Ensembl transcript (*ENSRNOT00000066952* 3' end = 39,506,890; *ENSRNOT00000066952.1* 3' end = 39,507,407; *ENSRNOT00000066952.2* 3' end = 39,507,807; Figure 7B). In contrast, the transcript identified by StringTie, *MSTRG.6258.1*, possesses unique exon structure (Figure 7A). The unique exon structure of *MSTRG.6258.1* was validated using the single molecule RNA sequencing

(*Ift81\_iso1* in Figure 7A). The alternative 3' ends were also validated in the single molecule RNA sequencing. The 3' ends of *Ift81\_iso2* and *Ift81\_iso4* were less than 10 basepairs from the 3' end of *ENSRNOT00000066952.1* and the 3' end of *Ift81\_iso3* 66 basepairs shorter than the 3' end of *ENSRNOT00000066952.2*.

The isoform assigned to the blue1 module (*ENSRNOT00000066952.1*) was the only individual isoform of this gene significantly associated with voluntary alcohol consumption (*ENSRNOT00000066952.1*: correlation = -0.44, *p*-value = 0.049; *ENSRNOT00000066952.2*: correlation = -0.33, *p*-value = 0.14, *MSTRG.6258.1*: correlation = -0.15, *p*-value = 0.52). Across the 63 RNA-Seq samples of the 21 HXB/BXH RI strains with voluntary alcohol consumption data, the mean TPM was 0.68, 2.35, and 2.67 for *ENSRNOT00000066952.2*, *ENSRNOT00000066952.1*, and *MSTRG.6258.1*, respectively. Only *ENSRNOT00000066952.1*, and *MSTRG.6258.1* were subjected to WGCNA due to the computational pipeline that filtered lowly expressed transcripts prior to WGCNA.

#### 3.4.2.3 *Mapkapk5*

The DABG transcriptome contained three isoforms for the *Mapkapk5* gene (gene ID = *MSTRG.6281*), two of which were annotated by Ensembl (*ENSRNOT00000065314*, *ENSRNOT00000001817*) and one that was identified by StringTie (*MSTRG.6281.1*). The StringTie transcript represents the transcript in the candidate module; both

Ensembl transcripts were removed during the DABG transcriptome generation process due to heritability values below the median, and thus these transcripts were not subjected to WGCNA. *MSTRG.6281.1* shares similar exons to the longer Ensembl isoform *ENSRNOT00000001817* but with a noticeably longer 3' terminal exon and an additional, long 5' exon (Supplementary Figure S9). The alternative 3' terminal exon was not observed in the single molecule RNA sequencing data. The mean TPM values across the 63 RNA-Seq samples of the 21 HXB/BXH RI strains with voluntary alcohol consumption data were 1.29, 1.46, and 8.25 for *ENSRNOT000000065314*, *MSTRG.6281.1*, and *ENSRNOT00000001817*, respectively. The strain mean normalized expression estimates of *MSTRG.6281.1* displayed the greatest individual association with voluntary alcohol consumption (correlation = -0.49,  $p$ -value = 0.024) compared to the Ensembl transcripts (*ENSRNOT000000065314*: correlation = 0.17,  $p$ -value = 0.46, *ENSRNOT00000001817*: correlation = 0.39,  $p$ -value = 0.081).

## 4 DISCUSSION

### 4.1 Characterization of the Brain Specific Transcriptome in the HXB/BXH Recombinant Inbred Rat Panel

A major goal of this work was to annotate the brain specific transcriptome in the HXB/BXH recombinant inbred rat panel by applying computational methods—namely StringTie and aptardi—that incorporate expression data (in the form of RNA-Seq). By including expression data, we were able to characterize the expressed transcriptome under our specific study conditions. Moreover, our deeply sequenced RNA-Seq libraries provided ample data for transcript identification and quantitation. For this manuscript, we chose to focus our RNA analyses to only strains from the HXB/BXH recombinant inbred panel rather than the full HRDP because splice variants and alternative polyadenylation sites that are unique to either progenitor strains will likely be represented by approximately half of the RI strains. This decreases the likelihood of identifying a transcript variant that is exclusive to a single RI strain in the analysis thus increasing our power for detection. A secondary goal of this manuscript was to re-examine the relationship of alcohol consumption in the two-bottle choice paradigm to brain RNA expression using an updated and expanded transcriptome data set.

Because the rat Ensembl transcriptome is under annotated compared to humans and other species such as mouse (Ji et al., 2020), many of transcripts in the DABG transcriptome were identified by the computational approaches that utilized RNA-Seq data (Table 1) and were not included in the rat Ensembl transcriptome (v.99), highlighting the importance of annotating transcriptomes in the context of the conditions. Additionally, the comparable expression heritabilities of StringTie and aptardi transcripts to Ensembl transcripts

indicates these algorithms annotate transcripts that demonstrate significant genetic influences and robust expression similar to those transcripts that are well annotated.

Unsurprisingly, we found that the transcript:gene ratio in the DABG transcriptome was much greater than existing rat Ensembl reference annotation (Table 1), and many more genes in the DABG transcriptome expressed more than one isoform compared to the Ensembl reference annotation (Supplementary Figure S5). This aligns with the literature that many genes from higher order eukaryotic organisms express alternative splicing and/or alternative polyadenylation transcripts (Nilsen and Graveley, 2010; Tian and Manley, 2017) and, in particular, that brain expresses the greatest mRNA diversity compared to other tissues due to alternative splicing and alternative polyadenylation (MacDonald, 2019). Furthermore, a recent study also observed an increase in the transcript:gene ratio in rat when including RNA-Seq data to generate the transcriptome compared to Ensembl annotation (Ji et al., 2020). In the DABG transcriptome, a significant portion of transcripts were derived from each of the three sources (i.e., StringTie, aptardi, and Ensembl), demonstrating the importance of both StringTie and aptardi in our transcript reconstruction pipeline.

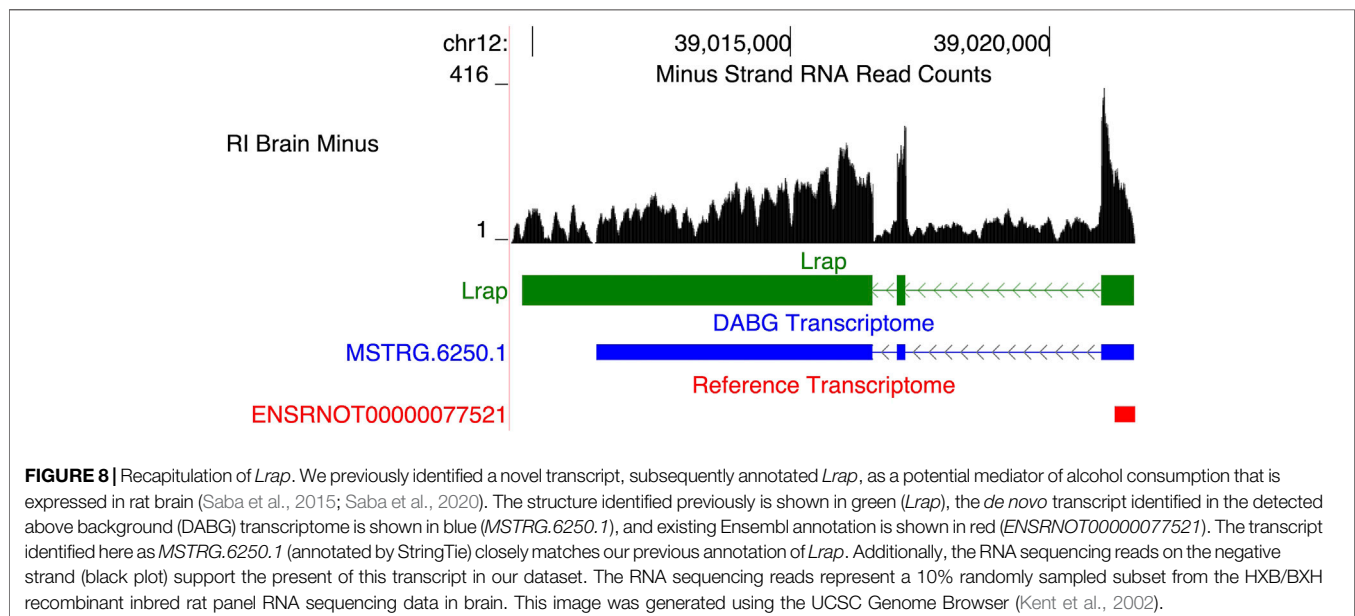
Also of note, we suggest that our transcriptome generation pipeline, including the filtering procedure, provides a means to generate a high-quality, representative transcriptome. In the DABG transcriptome, many genes did not include a Ensembl transcript. We hypothesize this is because many isoforms identified by StringTie and/or aptardi more accurately annotated the transcripts expressed by those genes. Specific examples of this include *Ift81* and *Aldh1a7*, where the Ensembl transcript was removed after filtering in favor of the StringTie and/or aptardi transcripts, and these computationally identified transcripts are better supported by the RNA-Seq data (Figure 7 and Figure 4).

### 4.2 Evaluation of Genes Previously Identified as Associated With Voluntary Alcohol Consumption in the HXB/BXH Recombinant Inbred Rat Panel

We previously performed WGCNA on brain expression data in the HXB/BXH RI panel to identify networks of genes associated with the same phenotype (voluntary alcohol consumption) (Saba et al., 2015). The major difference was in the technology used to generate expression data and, as a result, the capacity to quantitate individual transcripts in the HXB/BXH RI panel. Specifically, we currently utilized RNA-Seq data (as opposed to Affymetrix exon microarray data used earlier) for the quantitative measurement of transcript expression in the full HXB/BXH RI panel. For most genes, the array was not capable of unambiguously estimating the expression of individual transcript isoforms. It is well-documented that RNA-Seq has a broader dynamic range than microarrays (Marioni et al., 2008). With RNA-Seq data from the full RI panel, we were not only able to estimate expression for each individual transcript of a gene for

**TABLE 4 |** Comparison of results from microarrays to results from RNA-Seq for genes whose brain expression was previously identified as associated with voluntary alcohol consumption in the HXB/BXH recombinant inbred rat panel. Correlations were determined using Spearman's rank correlation and strain mean gene level normalized expression estimates or strain mean transcript level normalized expression estimates and strain mean alcohol consumption values for the gene and transcript correlations, respectively. Genes are ordered by intramodular connectivity in the original microarray-based coexpression module. The number of transcripts identified for each gene in the detected above background transcriptome is shown with its source of identification. The intramodular connectivity values of genes in the candidate module from the previous study (Saba et al., 2015; Saba et al., 2020) are shown, along with their rank within the module.

Gene symbol	Gene description	From microarray data (Saba et al. (2015), Saba et al. (2020))		From HXB/BXH RNA-Seq data		
		Correlation with alcohol consumption in microarray data [correlation coefficient (p-Value)]	Connectivity-based intramodular connectivity (rank within module)	Number of transcripts identified in HXB/BXH panel in the DABG transcriptome	Number of Ensembl/StringTie/apartardi transcripts	Most significant transcript correlation with alcohol consumption [correlation coefficient (p-value)]
Lrap	Locus regulating alcohol preference	-0.55 (0.011)	2.99 (1)	1	0/1/0	-0.45 (0.042)
Ift81	Intraflagellar transport 81	-0.43 (0.051)	2.66 (2)	3	0/1/2	-0.44 (0.049)
Coq5	Coenzyme Q5, methyltransferase	-0.50 (0.021)	2.24 (3)	2	1/0/1	0.13 (0.59)
Txnip	Thioredoxin interacting protein	0.61 (0.003)	2.20 (4)	1	1/0/0	0.41 (0.068)
P2rx4	Purinergic receptor P2X 4	-0.63 (0.002)	2.15 (5)	2	1/1/0	-0.58 (0.006)
Tmem116	Transmembrane protein 116	0.34 (0.133)	2.00 (6)	1	1/0/0	0.52 (0.017)
Cfap91 (formerly Maats1)	Cilia and flagella associated protein 91	-0.56 (0.008)	1.95 (7)	2	1/0/1	0.21 (0.37)
GENE_27603	Unannotated gene	-0.51 (0.021)	1.74 (8)	Not included in DABG transcriptome		



each individual strain, but we were also able to filter individual transcripts for their heritability across the RI panel.

The previous candidate coexpression module's meQTL also overlapped a voluntary alcohol consumption pQTL on chromosome 12. Similarly, here we identified a single

candidate coexpression module (out of 215 modules) with its meQTL/pQTL overlap also on chromosome 12. Of the six transcripts in the new candidate transcript module, genes of three were present in our previous candidate gene module—*P2rx4*, *Lrap*, and *Ift81*. Additionally, the genes of

these transcripts had some of the greatest intra-modular connectivity values in the previous gene module; *Lrap*, *Ift81*, and *P2rx4* had the first, second, and fifth greatest intra-modular connectivity values, respectively.

Many other genes from the original candidate coexpression module—especially those with high intra-modular connectivity values—displayed correlation with voluntary alcohol consumption at the individual transcript level (Table 4). More specifically, we examined the genes from the previous candidate coexpression module that were either significantly associated with alcohol consumption ( $p < 0.05$ ) in the microarray analysis or were within the top eight most highly connected genes within the original module. The RNA-Seq data from the HXB/BXH RI panel replicated the association with voluntary alcohol consumption (correlation in the same direction and  $p$ -value  $< 0.05$ ) for four of the eight genes (Table 4). For *Txnip*, the association with alcohol was only suggestive ( $p = 0.068$ ) in the current analysis. The two remaining genes (*Cfap91* and *Coq5*) both had two transcripts each in the RNA-Seq data and neither transcript was associated with alcohol consumption in this analysis.

Among the genes in the original module, a long, potentially non-coding RNA transcript, *Lrap*, was identified as the hub gene and key modulator of voluntary alcohol consumption in the HXB/BXH RI panel, initially using a systems genetics approach and subsequently using genetically manipulated rats (Saba et al., 2015, 2020). This originally unannotated transcript was initially identified using short read RNA sequencing from the progenitor strains only and its splicing structure was confirmed using PCR. In this study, we assessed whether it was present within the full HXB/BXH RI panel through our transcriptome reconstruction methods (i.e., StringTie and aptardi). A similar transcript (transcript ID = *MSTRG.6520.1*; associated gene name = *AABR07036336.2*)—identified by StringTie—was observed (Figure 8). *MSTRG.6520.1* was the only isoform of this gene, i.e., Gene ID *MSTRG.6520*. Both *MSTRG.6520.1* and the original *Lrap* are on the negative strand of chromosome 12 and possess three exons with similar locations in the genome (Original *Lrap*: 39,009,809–39,016,585, 39,017,055–39,017,223, and 39,021,009–39,021,641; *MSTRG.6520.1*: 39,011,243–39,016,585, 39,017,056–39,017,223, and 39,021,010–39,021,635). There are dramatic differences in the transcription stop site as expected based on the lack of precision in the initial reconstruction, yet the transcription start sites were within six base pairs of each other. The two exon junctions in *Lrap* also differed by one base pair each. Although the exon junctions were previously validated via PCR, we note that the precise locations of the 3' and 5' ends have not been validated (Saba et al., 2015). As a result, this gene/transcript was hereafter labeled *Lrap*. With the new RNA-Seq data from the entire HXB/BXH RI panel, *Lrap* remained significantly negatively associated with alcohol consumption (correlation coefficient =  $-0.45$ ;  $p$ -value =  $0.042$ ; Table 4). Furthermore, it was identified in the candidate coexpression network where it had the second highest intra-modular connectivity.

Overall, these results indicate, in this instance, that the major genes/transcripts in candidate coexpression modules (i.e., those

with the greatest intra-modular connectivity values) are robust across diverse data acquisition methods and data analyses.

## 4.3 Candidate Coexpression Module and Candidate Individual Transcripts

### 4.3.1 Characterization of Transcripts in the Current Candidate Coexpression Module

Existing Ensembl annotation possessed a single transcript structure for *Ift81*; here we identified three alternative transcripts (Figure 7). Moreover, filtering to yield the DABG transcriptome removed the Ensembl transcript (due to low estimated read counts), but the three new structures remained. The RNA-Seq data support the presence of these structures, exemplifying how the transcriptome generation procedure can not only annotate new transcripts, but also potentially improve annotation of existing transcripts. Furthermore, while *Ift81* was identified in the previous candidate gene module and was present in the current candidate transcript module, only a single isoform of *Ift81* was present in the current candidate transcript module, thereby enabling greater granularity as to the exact transcript that is associated with alcohol consumption. Likewise, a second, previously unannotated isoform of *P2rx4* was identified, but the Ensembl transcript of this gene was present in the current candidate transcript module. Of note, both transcripts were the predominantly expressed isoforms for their respective genes.

*P2rx4* encodes the P2X purinoceptor 4 receptor, which is a subtype of the purinergic system of ligand-gated ion channels (Köles et al., 2007) that, when activated, exerts excitatory effects in the central nervous system (Lalo et al., 2007). Several studies have demonstrated that alcohol inhibits the excitatory effects of this receptor (Li et al., 2000; Davies et al., 2002; Xiao et al., 2008; Asatryan et al., 2010). Moreover, alcohol preferring P rats show lower functional expression of this gene in brain compared to alcohol nonpreferring NP rats (Kimpel et al., 2007), and alcohol modulates receptor expression (Gofman et al., 2014). Likewise, our previous work found a negative correlation between expression of the *P2rx4* gene as a whole and voluntary alcohol consumption in rats (as observed here) (Tabakoff et al., 2009), and others have likewise corroborated that higher levels of alcohol consumption are associated with lower levels of *P2rx4* gene expression (Kimpel et al., 2007; Tabakoff et al., 2009). In rats treated with alcohol, self-administration was inhibited by a *P2rx4* receptor agonist in rats (Kosten, 2011). These receptors also regulate neuro-inflammatory processes (Gofman et al., 2014). The functional role of *Ift81*—and its potential link with voluntary alcohol consumption—is less clear, although it is a component of cilium formation in astrocytes and neurons (Bhogaraju et al., 2013). Furthermore, cilia, which are neurites, play an important role in brain development including neurogenesis and neuronal migration (Karunakaran et al., 2020).

Beyond *Ift81*, *P2rx4*, and *Lrap*, the other transcripts in the current candidate module include isoforms/transcripts of *Mapkapk5*, *Oas3*, and *AABR07065438.1*.

The *Mapkapk5* (MAPK activated protein kinase 5) transcript in the current candidate module was annotated by StringTie (*MSTRG.6281.1*). MAPK activated protein kinases are enzymes

whose activation is mediated by mitogen-activated protein kinases (Cargnello and Roux, 2011). Notably, *Mapkapk5* is a downstream target of *Mapk14* (New et al., 1998), which was shown to be a central regulator of the immunological response in astrocytes (Lo et al., 2014). *Mapk14* was also differentially expressed in alcohol preferring AA (alko, alcohol) vs alcohol-avoiding (alko, non-alcohol) rats (Arlinde et al., 2004; Sommer et al., 2005). Furthermore, *Mapk14* was expressed at lower levels in alcohol preferring iP rats compared to the alcohol non preferring iNP rats in the caudate-putamen of brain (Rodd et al., 2007). Combining transcripts from the individual transcript analysis and from the current candidate coexpression module, the protein product of *Map3k7*—a candidate individual transcript—is an upstream regulator of *Mapk14* (Martín-Blanco, 2000), providing a common biological pathway for *Mapkapk5* and *Map3k7*.

The single transcript for *Oas3*, 2'-5'-oligoadenylate synthetase 3, in the current candidate module was annotated by Ensembl. A genome-wide association study of alcohol consumption in Korean male drinkers identified a SNP in *OAS3* with genome-wide significance (Baik et al., 2011). Similar to *Mapkapk5*, *OAS3* plays a role in immunity, namely the antiviral immune response (Lee et al., 2019, 1). Expression of *Oas3* was shown to be enriched in infiltrating macrophages relative to homeostatic brain microglia during virus-induced neuroinflammation (DePaula-Silva et al., 2019).

The final transcript was derived from the *AABR07065438.1* gene and was identified by StringTie. The single Ensembl annotated transcript for this gene was removed from the DABG transcriptome due to low expression estimates and, therefore, was not included in WGCNA. The Ensembl and StringTie transcripts have identical 5' and 3' ends but differ in that the Ensembl transcript has as a single exon, whereas StringTie identified a splice junction and therefore annotated two exons. Ensembl describes the Ensembl transcript as ribosomal protein L6, pseudo 1. Pseudogenes have similar sequence to another gene but are often defective (Vanin, 1985); however, pseudogenes can be transcribed (Kalyana-Sundaram et al., 2012).

Overall, the function of the transcripts in the current candidate module can be linked to inflammation/the immune response. Such an observation is consistent with our previous findings (Saba et al., 2015; Saba et al., 2020).

#### 4.3.2 Candidate Individual Transcripts

Notable candidate transcripts include *Aldh1a7* and *Map3k7*. The individual candidate transcript of *Map3k7* was identified *de novo* and differed from the existing Ensembl transcript for this gene in that exon 12 was skipped (Figure 3). Previous literature has reported that *Map3k7* expresses an exon 12 skipping isoform of the gene (Martinez et al., 2012; Martinez and Lynch, 2013), providing credence for the transcript structure identified here. Specifically, the exon skipping isoform was observed to be differentially expressed in the JSL1 human T-cell line when stimulated to elicit an immune response (Martinez et al., 2012). Regarding alcohol, differences in brain expression of *Map3k7* between high and low alcohol preferring mice have been reported (Hoffman et al., 2014).

The human *ALDH1* family consists of six genes (Black et al., 2009). *Aldh1a7* is an additional rodent-specific gene for this family (Touloupi et al., 2019) that is a paralogue of *Aldh1a1* (Jackson et al., 2011). Here we annotated a novel transcript for this gene, *ENSRNOT00000024093.1*, which was identified by aptardi. This transcript was present in the DABG transcriptome, while the Ensembl transcript for this gene (*ENSRNOT00000024093*), was removed during filtering. The transcripts shared splice junctions but differ in that the aptardi transcript has a longer 3' exon. The RNA-Seq reads support the presence of the aptardi transcript (Figure 4). *Aldh1a7* is the cytosolic aldehyde dehydrogenase, which metabolizes acetaldehyde and also catalyzes the irreversible conversion of retinaldehyde to retinoic acid (Singh et al., 2013). Retinoic acid can act on immune cells and is involved in neuroinflammation (Oliveira et al., 2018).

These candidate individual transcripts further point towards the role of inflammation and immunity as predisposing factors associated with voluntary alcohol consumption.

### 4.4 Limitations and Future Directions

One limitation of this work is the relatively small sample size for mapping voluntary alcohol consumption ( $n = 21$ ) and for genetic correlations with voluntary alcohol consumption. No individual transcripts were significantly associated with alcohol consumption when correcting for multiple testing (false discovery rate  $< 0.05$ ). However, the fact that inclusion of other data sources enabled the use of multiple, diverse filtering criteria and many of the correlations observed with microarray data were further validated in the RNA-Seq data is evidence for a robust signal.

A second limitation was the ambiguity of the physical location of *Map3k7* and whether *MSTRG.23809.1* and *MSTRG.17584.2* were truly separate transcripts with important difference in the 3' UTR or if they represent the same transcript. This type of genomic ambiguity often complicates short read RNA-Seq quantitation and further validation of untranslated regions of *Map3k7* may be warranted.

Finally, whole brains were used to generate RNA-Seq libraries. Since alternative splicing and alternative polyadenylation display region- and cell-specific expression, whole brain samples may dilute these transcripts to a degree that their abundance is undetectable. However, including entire brains allows for capture of pervasive alternative splicing and alternative polyadenylation in this tissue under our conditions, and future work could complement this study by focusing on particular regions and cell types.

## 5 CONCLUSION

Current studies on the genetic components of complex traits such as voluntary alcohol consumption often rely on existing annotation. Here we provide a pipeline that enables identification of previously unannotated alternative splicing and alternative polyadenylation transcripts from RNA-Seq data. In the case of the rat brain, we showed that many transcripts are not present in existing annotation and,

furthermore, that these previously unknown transcripts may provide important insights into genetic predisposition to voluntary alcohol consumption.

## DATA AVAILABILITY STATEMENT

The alcohol consumption data, the genotype dataset used from mapping alcohol consumption and module eigengenes, the normalized RNA expression levels for the DABG transcriptome, the Gene Transfer File (GTF) for the DABG transcriptome, and the strain-specific genomes for the RI strains that were used for RNA-Seq alignment are on the PhenoGen website [<https://phenogen.org/web/sysbio/resources.jsp>]. The RNA-Seq data generated and analyzed for this study can be found in the Sequence Read Archive [BioProject ID PRJNA810034]. The single molecule RNA sequencing data is also available through the Sequence Read Archive [BioProject ID: PRJNA801761].

## ETHICS STATEMENT

The animal study was reviewed and approved by the Ethics Committee of the Institute of Physiology, Czech Academy of Sciences, Prague.

## REFERENCES

- Abiola, O., Angel, J. M., Avner, P., Bachmanov, A. A., Belknap, J. K., Bennett, B., et al. (2003). The Nature and Identification of Quantitative Trait Loci: a Community's View. *Nat. Rev. Genet.* 4, 911–916. doi:10.1038/nrg1206
- Arlinde, C., Sommer, W., Björk, K., Reimers, M., Hyytiä, P., Kiianmaa, K., et al. (2004). A Cluster of Differentially Expressed Signal Transduction Genes Identified by Microarray Analysis in a Rat Genetic Model of Alcoholism. *Pharmacogenomics J.* 4, 208–218. doi:10.1038/sj.tpj.6500243
- Asatryan, L., Popova, M., Perkins, D., Trudell, J. R., Alkana, R. L., and Davies, D. L. (2010). Ivermectin Antagonizes Ethanol Inhibition in Purinergic P2X4 Receptors. *J. Pharmacol. Exp. Ther.* 334, 720–728. doi:10.1124/jpet.110.167908
- Baik, I., Cho, N. H., Kim, S. H., Han, B.-G., and Shin, C. (2011). Genome-wide Association Studies Identify Genetic Loci Related to Alcohol Consumption in Korean Men. *Am. J. Clin. Nutr.* 93, 809–816. doi:10.3945/ajcn.110.001776
- Beaudoing, E., and Gautheret, D. (2001). Identification of Alternate Polyadenylation Sites and Analysis of Their Tissue Distribution Using EST Data. *Genome Res.* 11, 1520–1526. doi:10.1101/gr.190501
- Bhogaraju, S., Cajanek, L., Fort, C., Blisnick, T., Weber, K., Taschner, M., et al. (2013). Molecular Basis of Tubulin Transport within the Cilium by IFT74 and IFT81. *Science* 341, 1009–1012. doi:10.1126/science.1240985
- Black, W. J., Stagos, D., Marchitti, S. A., Nebert, D. W., Tipton, K. F., Bairoch, A., et al. (2009). Human Aldehyde Dehydrogenase Genes: Alternatively Spliced Transcriptional Variants and Their Suggested Nomenclature. *Pharmacogenet. Genomics* 19, 893–902. doi:10.1097/FPC.0b013e3283329023
- Broman, K. W., and Sen, S. (2009). *A Guide to QTL Mapping with R/qtl*. New York: Springer-Verlag. doi:10.1007/978-0-387-92125-9
- Bullard, J. H., Purdom, E., Hansen, K. D., and Dudoit, S. (2010). Evaluation of Statistical Methods for Normalization and Differential Expression in mRNA-Seq Experiments. *BMC Bioinformatics* 11, 94. doi:10.1186/1471-2105-11-94
- Cargnello, M., and Roux, P. P. (2011). Activation and Function of the MAPKs and Their Substrates, the MAPK-Activated Protein Kinases. *Microbiol. Mol. Biol. Rev.* 75, 50–83. doi:10.1128/MMBR.00031-10

## AUTHOR CONTRIBUTIONS

Study design: BT, PH, RL, and LS. Quantitation: SM and RL. Analysis: RL and LS. Animal tissues: MP and JS. Single molecule RNA sequencing analysis: SM, HS, SR, and LS. Writing: RL and LS with input from all authors.

## FUNDING

Sponsored by the following NIH grants: NIAAA (F31AA027430), NIAAA (R24AA013162), and NIDA (P30DA044223), as well as the Banbury Fund, the Czech National Science Foundation (Grant 13-044205) and Academic Premium Award (AP1502).

## ACKNOWLEDGMENTS

The authors thank Richard A. Radcliffe, Katerina Kechris, and Peter L. Anderson for their helpful discussions.

## SUPPLEMENTARY MATERIAL

The Supplementary Material for this article can be found online at: <https://www.frontiersin.org/articles/10.3389/fgene.2022.821026/full#supplementary-material>

- Churchill, G. A., and Doerge, R. W. (1994). Empirical Threshold Values for Quantitative Trait Mapping. *Genetics* 138, 963–971. doi:10.1093/genetics/138.3.963
- Dafne Giammartino, D. G., Nishida, K., and Manley, J. L. (2011). Mechanisms and Consequences of Alternative Polyadenylation. *Mol. Cell* 43, 853–866. doi:10.1016/j.molcel.2011.08.017
- Davies, D. L., Machu, T. K., Guo, Y., and Alkana, R. L. (2002). Ethanol Sensitivity in ATP-Gated P2X Receptors Is Subunit Dependent. *Alcohol. Clin. Exp. Res.* 26, 773–778. doi:10.1111/j.1530-0277.2002.tb02604.x
- Dawson, D. A., and Grant, B. F. (2011). The "Gray Area" of Consumption between Moderate and Risk Drinking\*. *J. Stud. Alcohol. Drugs* 72, 453–458. doi:10.15288/jsad.2011.72.453
- DePaula-Silva, A. B., Gorbea, C., Doty, D. J., Libbey, J. E., Sanchez, J. M. S., Hanak, T. J., et al. (2019). Differential Transcriptional Profiles Identify Microglial- and Macrophage-specific Gene Markers Expressed during Virus-Induced Neuroinflammation. *J. Neuroinflammation* 16, 152. doi:10.1186/s12974-019-1545-x
- Derti, A., Garrett-Engle, P., Macisaac, K. D., Stevens, R. C., Sriram, S., Chen, R., et al. (2012). A Quantitative Atlas of Polyadenylation in Five Mammals. *Genome Res.* 22, 1173–1183. doi:10.1101/gr.132563.111
- Dredge, B. K., Polydorides, A. D., and Darnell, R. B. (2001). The Splice of Life: Alternative Splicing and Neurological Disease. *Nat. Rev. Neurosci.* 2, 43–50. doi:10.1038/35049061
- Faustino, N. A., and Cooper, T. A. (2003). Pre-mRNA Splicing and Human Disease. *Genes Dev.* 17, 419–437. doi:10.1101/gad.1048803
- Garcia-Blanco, M. A., Baraniak, A. P., and Lasda, E. L. (2004). Alternative Splicing in Disease and Therapy. *Nat. Biotechnol.* 22, 535–546. doi:10.1038/nbt964
- Gibbs, R. A., Weinstock, G. M., Metzker, M. L., Muzny, D. M., Sodergren, E. J., Scherer, S., et al. (2004). Genome Sequence of the Brown Norway Rat Yields Insights into Mammalian Evolution. *Nature* 428, 493–521. doi:10.1038/nature02426
- Gofman, L., Cenna, J. M., and Potula, R. (2014). P2X4 Receptor Regulates Alcohol-Induced Responses in Microglia. *J. Neuroimmune Pharmacol.* 9, 668–678. doi:10.1007/s11481-014-9559-8
- Grant, J. D., Agrawal, A., Bucholz, K. K., Madden, P. A. F., Pergadia, M. L., Nelson, E. C., et al. (2009). Alcohol Consumption Indices of Genetic Risk for Alcohol Dependence. *Biol. Psychiatry* 66, 795–800. doi:10.1016/j.biopsych.2009.05.018

- Harrall, K. K., Kechris, K. J., Tabakoff, B., Hoffman, P. L., Hines, L. M., Tsukamoto, H., et al. (2016). Uncovering the Liver's Role in Immunity through RNA Co-expression Networks. *Mamm. Genome* 27, 469–484. doi:10.1007/s00335-016-9656-5
- Hartley, C. A., McKenna, M. C., Salman, R., Holmes, A., Casey, B. J., Phelps, E. A., et al. (2012). Serotonin Transporter Polyadenylation Polymorphism Modulates the Retention of Fear Extinction Memory. *Proc. Natl. Acad. Sci.* 109, 5493–5498. doi:10.1073/pnas.1202044109
- Havlak, P., Chen, R., Durbin, K. J., Egan, A., Ren, Y., Song, X.-Z., et al. (2004). The Atlas Genome Assembly System. *Genome Res.* 14, 721–732. doi:10.1101/gr.2264004
- Hermesen, R., de Ligt, J., Spee, W., Blokzijl, F., Schäfer, S., Adami, E., et al. (2015). Genomic Landscape of Rat Strain and Substrain Variation. *BMC Genomics* 16, 357. doi:10.1186/s12864-015-1594-1
- Hoffman, P. L., Saba, L. M., Flink, S., Grahame, N. J., Kechris, K., and Tabakoff, B. (2014). Genetics of Gene Expression Characterizes Response to Selective Breeding for Alcohol Preference. *Genes, Brain Behav.* 13, 743–757. doi:10.1111/gbb.12175
- Hong, M., Zhukareva, V., Vogelsberg-Ragaglia, V., Wszolek, Z., Reed, L., Miller, B. I., et al. (1998). Mutation-specific Functional Impairments in Distinct Tau Isoforms of Hereditary FTDP-17. *Science* 282, 1914–1917. doi:10.1126/science.282.5395.1914
- Hoque, M., Ji, Z., Zheng, D., Luo, W., Li, W., You, B., et al. (2013). Analysis of Alternative Cleavage and Polyadenylation by 3' Region Extraction and Deep Sequencing. *Nat. Methods* 10, 133–139. doi:10.1038/nmeth.2288
- Hutton, M., Lendon, C. L., Rizzu, P., Baker, M., Froelich, S., Houlden, H., et al. (1998). Association of Missense and 5'-Splice-Site Mutations in Tau with the Inherited Dementia FTDP-17. *Nature* 393, 702–705. doi:10.1038/31508
- Jackson, B., Brocker, C., Thompson, D. C., Black, W., Vasilou, K., Nebert, D. W., et al. (2011). Update on the Aldehyde Dehydrogenase Gene (ALDH) Superfamily. *Hum. Genomics* 5, 283–303. doi:10.1186/1479-7364-5-4-283
- Ji, X., Li, P., Fuscoe, J. C., Chen, G., Xiao, W., Shi, L., et al. (2020). A Comprehensive Rat Transcriptome Built from Large Scale RNA-Seq-Based Annotation. *Nucleic Acids Res.* 48, 8320–8331. doi:10.1093/nar/gkaa638
- Johnson, W. E., Li, C., and Rabinovic, A. (2007). Adjusting Batch Effects in Microarray Expression Data Using Empirical Bayes Methods. *Biostatistics* 8, 118–127. doi:10.1093/biostatistics/kxj037
- Kalyana-Sundaram, S., Kumar-Sinha, C., Shankar, S., Robinson, D. R., Wu, Y.-M., Cao, X., et al. (2012). Expressed Pseudogenes in the Transcriptional Landscape of Human Cancers. *Cell* 149, 1622–1634. doi:10.1016/j.cell.2012.04.041
- Karunakaran, K. B., Chaparala, S., Lo, C. W., and Ganapathiraju, M. K. (2020). Cilia Interactome with Predicted Protein-Protein Interactions Reveals Connections to Alzheimer's Disease, Aging and Other Neuropsychiatric Processes. *Sci. Rep.* 10, 15629. doi:10.1038/s41598-020-72024-4
- Kawasawa, Y. I., Mohammad, S., Son, A. I., Morizono, H., Basha, A., Salzberg, A. C., et al. (2017). Genome-wide Profiling of Differentially Spliced mRNAs in Human Fetal Cortical Tissue Exposed to Alcohol. *Alcohol* 62, 1–9. doi:10.1016/j.alcohol.2017.05.001
- Kelmen, O., Convertini, P., Zhang, Z., Wen, Y., Shen, M., Falaleeva, M., et al. (2013). Function of Alternative Splicing. *Gene* 514, 1–30. doi:10.1016/j.gene.2012.07.083
- Kent, W. J. (2002). BLAT-the BLAST-like Alignment Tool. *Genome Res.* 12, 656–664. doi:10.1101/gr.229202
- Kent, W. J., Sugnet, C. W., Furey, T. S., Roskin, K. M., Pringle, T. H., Zahler, A. M., et al. (2002). The Human Genome Browser at UCSC. *Genome Res.* 12, 996–1006. doi:10.1101/gr.229102
- Kim, D., Langmead, B., and Salzberg, S. L. (2015). HISAT: a Fast Spliced Aligner with Low Memory Requirements. *Nat. Methods* 12, 357–360. doi:10.1038/nmeth.3317
- Kimpel, M. W., Strother, W. N., McClintick, J. N., Carr, L. G., Liang, T., Edenberg, H. J., et al. (2007). Functional Gene Expression Differences between Inbred Alcohol-Preferring and -Non-Preferring Rats in Five Brain Regions. *Alcohol* 41, 95–132. doi:10.1016/j.alcohol.2007.03.003
- Kosten, T. A. (2011). Pharmacologically Targeting the P2rx4 Gene on Maintenance and Reinstatement of Alcohol Self-Administration in Rats. *Pharmacol. Biochem. Behav.* 98, 533–538. doi:10.1016/j.pbb.2011.02.026
- Lalo, U., Verkhatsky, A., and Pankratov, Y. (2007). Ivermectin Potentiates ATP-Induced Ion Currents in Cortical Neurones: Evidence for Functional Expression of P2X4 Receptors? *Neurosci. Lett.* 421, 158–162. doi:10.1016/j.neulet.2007.03.078
- Lander, E., and Kruglyak, L. (1995). Genetic Dissection of Complex Traits: Guidelines for Interpreting and Reporting Linkage Results. *Nat. Genet.* 11, 241–247. doi:10.1038/ng1195-241
- Langfelder, P., and Horvath, S. (2008). WGCNA: an R Package for Weighted Correlation Network Analysis. *BMC Bioinformatics* 9, 559. doi:10.1186/1471-2105-9-559
- Langmead, B., and Salzberg, S. L. (2012). Fast Gapped-Read Alignment with Bowtie 2. *Nat. Methods* 9, 357–359. doi:10.1038/nmeth.1923
- Lau, A. G., Irier, H. A., Gu, J., Tian, D., Ku, L., Liu, G., et al. (2010). Distinct 3'UTRs Differentially Regulate Activity-dependent Translation of Brain-Derived Neurotrophic Factor (BDNF). *Proc. Natl. Acad. Sci.* 107, 15945–15950. doi:10.1073/pnas.1002929107
- Lee, W.-B., Choi, W. Y., Lee, D.-H., Shim, H., Kim-Ha, J., and Kim, Y.-J. (2019). OAS1 and OAS3 Negatively Regulate the Expression of Chemokines and Interferon-Responsive Genes in Human Macrophages. *BMB Rep.* 52, 133–138. doi:10.5483/bmbrep.2019.52.2.129
- Leek, J. T., Johnson, W. E., Parker, H. S., Jaffe, A. E., and Storey, J. D. (2012). The Sva Package for Removing Batch Effects and Other Unwanted Variation in High-Throughput Experiments. *Bioinformatics* 28, 882–883. doi:10.1093/bioinformatics/bts034
- Li, B., and Dewey, C. N. (2011). RSEM: Accurate Transcript Quantification from RNA-Seq Data with or without a Reference Genome. *BMC Bioinformatics* 12, 323. doi:10.1186/1471-2105-12-323
- Li, C., Xiong, K., and Weight, F. F. (2000). Ethanol Inhibition of Adenosine 5'-Triphosphate-Activated Current in Freshly Isolated Adult Rat Hippocampal CA1 Neurons. *Neurosci. Lett.* 295, 77–80. doi:10.1016/s0304-3940(00)01586-x
- Li, H., Handsaker, B., Wysoker, A., Fennell, T., Ruan, J., Homer, N., et al. (2009). The Sequence Alignment/Map Format and SAMtools. *Bioinformatics* 25, 2078–2079. doi:10.1093/bioinformatics/btp352
- Li, H. (2018). Minimap2: Pairwise Alignment for Nucleotide Sequences. *Bioinformatics* 34, 3094–3100. doi:10.1093/bioinformatics/bty191
- L. Koles, L., S. Furst, S., and P. Illes, P. (2007). Purine Ionotropic (P2X) Receptors. *Cpd* 13, 2368–2384. doi:10.2174/138161207781368747
- Lo, U., Selvaraj, V., Plane, J. M., Chechneva, O. V., Otsu, K., and Deng, W. (2014). p38α (MAPK14) Critically Regulates the Immunological Response and the Production of Specific Cytokines and Chemokines in Astrocytes. *Sci. Rep.* 4, 7405. doi:10.1038/srep07405
- Love, M. I., Huber, W., and Anders, S. (2014). Moderated Estimation of Fold Change and Dispersion for RNA-Seq Data with DESeq2. *Genome Biol.* 15, 550. doi:10.1186/s13059-014-0550-8
- Lusk, R., Saba, L. M., Vanderlinden, L. A., Zidek, V., Silhavy, J., Pravenec, M., et al. (2018). Unsupervised, Statistically Based Systems Biology Approach for Unraveling the Genetics of Complex Traits: A Demonstration with Ethanol Metabolism. *Alcohol. Clin. Exp. Res.* 42, 1177–1191. doi:10.1111/acer.13763
- Lusk, R., Stene, E., Banaei-Kashani, F., Tabakoff, B., Kechris, K., and Saba, L. M. (2021). Aptardi Predicts Polyadenylation Sites in Sample-specific Transcriptomes Using High-Throughput RNA Sequencing and DNA Sequence. *Nat. Commun.* 12, 1652. doi:10.1038/s41467-021-21894-x
- MacDonald, C. C. (2019). Tissue-specific Mechanisms of Alternative Polyadenylation: Testis, Brain, and beyond (2018 Update). *WIREs RNA* 10, e1526. doi:10.1002/wrna.1526
- Manning, K. S., and Cooper, T. A. (2017). The Roles of RNA Processing in Translating Genotype to Phenotype. *Nat. Rev. Mol. Cell Biol.* 18, 102–114. doi:10.1038/nrm.2016.139
- Marioni, J. C., Mason, C. E., Mane, S. M., Stephens, M., and Gilad, Y. (2008). RNA-seq: An Assessment of Technical Reproducibility and Comparison with Gene Expression Arrays. *Genome Res.* 18, 1509–1517. doi:10.1101/gr.079558.108
- Martin, M. (2011). Cutadapt Removes Adapter Sequences from High-Throughput Sequencing Reads. *EMBnet j.* 17, 10–12. doi:10.14806/ej.17.1.200
- Martin-Blanco, E. (2000). p38 MAPK Signalling Cascades: Ancient Roles and New Functions. *Bioessays* 22, 637–645. doi:10.1002/1521-1878(200007)22:7<637::AID-BIES6>3.0.CO;2-E
- Martinez, N. M., and Lynch, K. W. (2013). Control of Alternative Splicing in Immune Responses: many Regulators, many Predictions, Much Still to Learn. *Immunol. Rev.* 253, 216–236. doi:10.1111/immr.12047
- Martinez, N. M., Pan, Q., Cole, B. S., Yarosh, C. A., Babcock, G. A., Heyd, F., et al. (2012). Alternative Splicing Networks Regulated by Signaling in Human T Cells. *RNA* 18, 1029–1040. doi:10.1261/rna.032243.112
- Miura, P., Sanfilippo, P., Shenker, S., and Lai, E. C. (2014). Alternative Polyadenylation in the Nervous System: To what Lengths Will 3' UTR Extensions Take Us? *Bioessays* 36, 766–777. doi:10.1002/bies.201300174
- New, L., Jiang, Y., Zhao, M., Liu, K., Zhu, W., Flood, L. J., et al. (1998). PRAK, a Novel Protein Kinase Regulated by the P38 MAP Kinase. *EMBO J.* 17, 3372–3384. doi:10.1093/emboj/17.12.3372

- Nilsen, T. W., and Graveley, B. R. (2010). Expansion of the Eukaryotic Proteome by Alternative Splicing. *Nature* 463, 457–463. doi:10.1038/nature08909
- Nissim-Rafinia, M., and Kerem, B. (2002). Splicing Regulation as a Potential Genetic Modifier. *Trends Genet.* 18, 123–127. doi:10.1016/s0168-9525(01)02619-1
- Oliveira, L. d. M., Teixeira, F. M. E., and Sato, M. N. (2018). Impact of Retinoic Acid on Immune Cells and Inflammatory Diseases. *Mediators Inflamm.* 2018, 1–17. doi:10.1155/2018/3067126
- Pan, Q., Shai, O., Lee, L. J., Frey, B. J., and Blencowe, B. J. (2008). Deep Surveying of Alternative Splicing Complexity in the Human Transcriptome by High-Throughput Sequencing. *Nat. Genet.* 40, 1413–1415. doi:10.1038/ng.259
- Perteu, M., Perteu, G. M., Antonescu, C. M., Chang, T.-C., Mendell, J. T., and Salzberg, S. L. (2015). StringTie Enables Improved Reconstruction of a Transcriptome from RNA-Seq Reads. *Nat. Biotechnol.* 33, 290–295. doi:10.1038/nbt.3122
- Petrucelli, E., Brown, T., Waterman, A., Ledru, N., and Kaun, K. R. (2020). Alcohol Causes Lasting Differential Transcription in Drosophila Mushroom Body Neurons. *Genetics* 215, 103–116. doi:10.1534/genetics.120.303101
- Pravenec, M., Klír, P., Kren, V., Zicha, J., and Kunes, J. (1989). An Analysis of Spontaneous Hypertension in Spontaneously Hypertensive Rats by Means of New Recombinant Inbred Strains. *J. Hypertens.* 7, 217–221. doi:10.1097/00004872-198903000-00008
- Pravenec, M., Saba, L. M., Zidek, V., Landa, V., Mlejnek, P., Šilhavý, J., et al. (2018). Systems Genetic Analysis of Brown Adipose Tissue Function. *Physiol. Genomics* 50, 52–66. doi:10.1152/physiolgenomics.00091.2017
- Ren, F., Zhang, N., Zhang, L., Miller, E., and Pu, J. J. (2020). Alternative Polyadenylation: a New Frontier in post Transcriptional Regulation. *Biomark Res.* 8, 67. doi:10.1186/s40364-020-00249-6
- Rhinn, H., Qiang, L., Yamashita, T., Rhee, D., Zolin, A., Vanti, W., et al. (2012). Alternative  $\alpha$ -synuclein Transcript Usage as a Convergent Mechanism in Parkinson's Disease Pathology. *Nat. Commun.* 3, 1084. doi:10.1038/ncomms2032
- Risso, D., Schwartz, K., Sherlock, G., and Dudoit, S. (2011). GC-content Normalization for RNA-Seq Data. *BMC Bioinformatics* 12, 480. doi:10.1186/1471-2105-12-480
- Rodd, Z. A., Bertsch, B. A., Strother, W. N., Le-Niculescu, H., Balaraman, Y., Hayden, E., et al. (2007). Candidate Genes, Pathways and Mechanisms for Alcoholism: an Expanded Convergent Functional Genomics Approach. *Pharmacogenomics J.* 7, 222–256. doi:10.1038/sj.tpj.6500420
- Saba, L. M., Flink, S. C., Vanderlinden, L. A., Israel, Y., Tampier, L., Colombo, G., et al. (2015). The Sequenced Rat Brain Transcriptome - its Use in Identifying Networks Predisposing Alcohol Consumption. *Febs J.* 282, 3556–3578. doi:10.1111/febs.13358
- Saba, L. M., Hoffman, P. L., Homanics, G. E., Mahaffey, S., Daulatabad, S. V., Janga, S. C., et al. (2020). A Long Non-coding RNA (Lrap) Modulates Brain Gene Expression and Levels of Alcohol Consumption in Rats. *Genes Brain Behav.* 20, e12698. doi:10.1111/gbb.12698
- Sanfilippo, P., Wen, J., and Lai, E. C. (2017). Landscape and Evolution of Tissue-specific Alternative Polyadenylation across Drosophila Species. *Genome Biol.* 18, 229. doi:10.1186/s13059-017-1358-0
- Sasabe, T., and Ishiura, S. (2010). Alcoholism and Alternative Splicing of Candidate Genes. *Ijeph* 7, 1448–1466. doi:10.1390/ijeph7041448
- Sen, S., and Churchill, G. A. (2001). A Statistical Framework for Quantitative Trait Mapping. *Genetics* 159, 371–387. doi:10.1093/genetics/159.1.371
- Shannon, P., Markiel, A., Ozier, O., Baliga, N. S., Wang, J. T., Ramage, D., et al. (2003). Cytoscape: A Software Environment for Integrated Models of Biomolecular Interaction Networks. *Genome Res.* 13, 2498–2504. doi:10.1101/gr.1239303
- Singh, S., Brocker, C., Koppaka, V., Chen, Y., Jackson, B. C., Matsumoto, A., et al. (2013). Aldehyde Dehydrogenases in Cellular Responses to Oxidative/electrophilic stress. *Free Radic. Biol. Med.* 56, 89–101. doi:10.1016/j.freeradbiomed.2012.11.010
- Smit, A., Hubley, R., and Green, P. (1996). RepeatMasker Open-3.0.1996. Available at: <http://www.repeatmasker.org> (Accessed November 22, 2018).
- Sommer, W., Arlinde, C., and Hellig, M. (2005). The Search for Candidate Genes of Alcoholism: Evidence from Expression Profiling Studies. *Addict. Biol.* 10, 71–79. doi:10.1080/13556210412331327821
- Spillantini, M. G., Murrell, J. R., Goedert, M., Farlow, M. R., Klug, A., and Ghetti, B. (1998). Mutation in the Tau Gene in Familial Multiple System Tauopathy with Presenile Dementia. *Proc. Natl. Acad. Sci.* 95, 7737–7741. doi:10.1073/pnas.95.13.7737
- STAR Consortium (2008). SNP and Haplotype Mapping for Genetic Analysis in the Rat. *Nat. Genet.* 40, 560–566. doi:10.1038/ng.124
- Tabakoff, B., Saba, L., Saba, L., Printz, M., Flodman, P., Hodgkinson, C., et al. (2009). Genetical Genomic Determinants of Alcohol Consumption in Rats and Humans. *BMC Biol.* 7, 70. doi:10.1186/1741-7007-7-70
- Tabakoff, B., Smith, H., Vanderlinden, L. A., Hoffman, P. L., and Saba, L. M. (2019). Networking in Biology: The Hybrid Rat Diversity Panel. *Methods Mol. Biol.* 2018, 213–231. doi:10.1007/978-1-4939-9581-3\_10
- Tian, B., and Manley, J. L. (2017). Alternative Polyadenylation of mRNA Precursors. *Nat. Rev. Mol. Cell Biol.* 18, 18–30. doi:10.1038/nrm.2016.116
- Touloupi, K., Küblbeck, J., Magkara, A., Molnár, F., Reinisalo, M., Konstandi, M., et al. (2019). The Basis for Strain-dependent Rat Aldehyde Dehydrogenase 1A7 (ALDH1A7) Gene Expression. *Mol. Pharmacol.* 96, 655–663. doi:10.1124/mol.119.117424
- Van Booven, D., Mengying Linull, Sunil Rao, J., Sunil Rao, J., Blokhin, I. O., Dayne Mayfield, R., Barbier, E., et al. (2021). Alcohol Use Disorder Causes Global Changes in Splicing in the Human Brain. *Transl Psychiatry* 11, 2. doi:10.1038/s41398-020-01163-z
- Vanderlinden, L. A., Saba, L. M., Printz, M. P., Flodman, P., Koob, G., Richardson, H. N., et al. (2014). Is the Alcohol Deprivation Effect Genetically Mediated? Studies with HXB/BXH Recombinant Inbred Rat Strains. *Alcohol. Clin. Exp. Res.* 38, 2148–2157. doi:10.1111/acer.12471
- Vanin, E. F. (1985). Processed Pseudogenes: Characteristics and Evolution. *Annu. Rev. Genet.* 19, 253–272. doi:10.1146/annurev.ge.19.120185.001345
- Verhulst, B., Neale, M. C., and Kendler, K. S. (2015). The Heritability of Alcohol Use Disorders: a Meta-Analysis of Twin and Adoption Studies. *Psychol. Med.* 45, 1061–1072. doi:10.1017/S0033291714002165
- Wang, E. T., Sandberg, R., Luo, S., Khrebukova, I., Zhang, L., Mayr, C., et al. (2008). Alternative Isoform Regulation in Human Tissue Transcriptomes. *Nature* 456, 470–476. doi:10.1038/nature07509
- Wang, G.-S., and Cooper, T. A. (2007). Splicing in Disease: Disruption of the Splicing Code and the Decoding Machinery. *Nat. Rev. Genet.* 8, 749–761. doi:10.1038/nrg2164
- Winkler, A., Mahal, B., Kianmaa, K., Ziegglänsberger, W., and Spanagel, R. (1999). Effects of Chronic Alcohol Consumption on the Expression of Different NR1 Splice Variants in the Brain of AA and ANA Lines of Rats. *Mol. Brain Res.* 72, 166–175. doi:10.1016/s0169-328x(99)00218-1
- Xiao, C., Zhou, C., Li, K., Davies, D. L., and Ye, J. H. (2008). Purinergic Type 2 Receptors at GABAergic Synapses on Ventral Tegmental Area Dopamine Neurons Are Targets for Ethanol Action. *J. Pharmacol. Exp. Ther.* 327, 196–205. doi:10.1124/jpet.108.139766
- Yates, A. D., Achuthan, P., Akanni, W., Allen, J., Allen, J., Alvarez-Jarreta, J., et al. (2020). Ensembl 2020. *Nucleic Acids Res.* 48, D682–D688. doi:10.1093/nar/gkz966
- Yeh, H.-S., and Yong, J. (2016). Alternative Polyadenylation of mRNAs: 3'-Untranslated Region Matters in Gene Expression. *Mol. Cell* 39, 281–285. doi:10.14348/molcells.2016.0035
- Yoon, O. K., Hsu, T. Y., Im, J. H., and Brem, R. B. (2012). Genetics and Regulatory Impact of Alternative Polyadenylation in Human B-Lymphoblastoid Cells. *Plos Genet.* 8, e1002882. doi:10.1371/journal.pgen.1002882
- Yoon, Y., McKenna, M. C., Rollins, D. A., Song, M., Nuriel, T., Gross, S. S., et al. (2013). Anxiety-associated Alternative Polyadenylation of the Serotonin Transporter mRNA Confers Translational Regulation by hnRNPK. *Proc. Natl. Acad. Sci.* 110, 11624–11629. doi:10.1073/pnas.1301485110
- Zhang, B., and Horvath, S. (2005). A General Framework for Weighted Gene Co-expression Network Analysis. *Stat. Appl. Genet. Mol. Biol.* 4, Article17. doi:10.2202/1544-6115.1128
- Zhang, H., Lee, J., and Tian, B. (2005). Biased Alternative Polyadenylation in Human Tissues. *Genome Biol.* 6, R100. doi:10.1186/gb-2005-6-12-r100

**Conflict of Interest:** The authors declare that the research was conducted in the absence of any commercial or financial relationships that could be construed as a potential conflict of interest.

**Publisher's Note:** All claims expressed in this article are solely those of the authors and do not necessarily represent those of their affiliated organizations, or those of the publisher, the editors and the reviewers. Any product that may be evaluated in this article, or claim that may be made by its manufacturer, is not guaranteed or endorsed by the publisher.

Copyright © 2022 Lusk, Hoffman, Mahaffey, Rosean, Smith, Silhavy, Pravenec, Tabakoff and Saba. This is an open-access article distributed under the terms of the Creative Commons Attribution License (CC BY). The use, distribution or reproduction in other forums is permitted, provided the original author(s) and the copyright owner(s) are credited and that the original publication in this journal is cited, in accordance with accepted academic practice. No use, distribution or reproduction is permitted which does not comply with these terms.



# Cocaine-Induced Locomotor Activation Differs Across Inbred Mouse Substrains

## OPEN ACCESS

### Edited by:

Peter Kalivas,  
Medical University of South Carolina,  
United States

### Reviewed by:

Camron D. Bryant,  
Boston University, United States  
Ryan K. Bachtell,  
University of Colorado Boulder,  
United States  
Andrew Tapper,  
University of Massachusetts Medical  
School, United States

### \*Correspondence:

Lisa M. Tarantino  
lisat@med.unc.edu

†These authors have contributed  
equally to this work and share first  
authorship

### Specialty section:

This article was submitted to  
Addictive Disorders,  
a section of the journal  
Frontiers in Psychiatry

**Received:** 22 October 2021

**Accepted:** 22 March 2022

**Published:** 06 May 2022

### Citation:

Gaines CH, Schoenrock SA,  
Farrington J, Lee DF,  
Aponte-Collazo LJ, Shaw GD,  
Miller DR, Ferris MT, Pardo-Manuel de  
Villena F and Tarantino LM (2022)  
Cocaine-Induced Locomotor  
Activation Differs Across Inbred  
Mouse Substrains.  
Front. Psychiatry 13:800245.  
doi: 10.3389/fpsy.2022.800245

Christiann H. Gaines<sup>1,2†</sup>, Sarah A. Schoenrock<sup>1†</sup>, Joseph Farrington<sup>1</sup>, David F. Lee<sup>1,3</sup>,  
Lucas J. Aponte-Collazo<sup>3,4</sup>, Ginger D. Shaw<sup>1,5</sup>, Darla R. Miller<sup>1,5</sup>, Martin T. Ferris<sup>1</sup>,  
Fernando Pardo-Manuel de Villena<sup>1,5</sup> and Lisa M. Tarantino<sup>1,6\*</sup>

<sup>1</sup> Department of Genetics, School of Medicine, University of North Carolina at Chapel Hill, Chapel Hill, NC, United States,

<sup>2</sup> Neuroscience Curriculum, University of North Carolina at Chapel Hill, Chapel Hill, NC, United States, <sup>3</sup> Pharmacology Curriculum, University of North Carolina at Chapel Hill, Chapel Hill, NC, United States, <sup>4</sup> Department of Pharmacology, School of Medicine, University of North Carolina at Chapel Hill, Chapel Hill, NC, United States, <sup>5</sup> Lineberger Comprehensive Cancer Center, School of Medicine, University of North Carolina at Chapel Hill, Chapel Hill, NC, United States, <sup>6</sup> Division of Pharmacotherapy and Experimental Therapeutics, Eshelman School of Pharmacy, University of North Carolina at Chapel Hill, Chapel Hill, NC, United States

Cocaine use disorders (CUD) are devastating for affected individuals and impose a significant societal burden, but there are currently no FDA-approved therapies. The development of novel and effective treatments has been hindered by substantial gaps in our knowledge about the etiology of these disorders. The risk for developing a CUD is influenced by genetics, the environment and complex interactions between the two. Identifying specific genes and environmental risk factors that increase CUD risk would provide an avenue for the development of novel treatments. Rodent models of addiction-relevant behaviors have been a valuable tool for studying the genetics of behavioral responses to drugs of abuse. Traditional genetic mapping using genetically and phenotypically divergent inbred mice has been successful in identifying numerous chromosomal regions that influence addiction-relevant behaviors, but these strategies rarely result in identification of the causal gene or genetic variant. To overcome this challenge, reduced complexity crosses (RCC) between closely related inbred mouse strains have been proposed as a method for rapidly identifying and validating functional variants. The RCC approach is dependent on identifying phenotypic differences between substrains. To date, however, the study of addiction-relevant behaviors has been limited to very few sets of substrains, mostly comprising the C57BL/6 lineage. The present study expands upon the current literature to assess cocaine-induced locomotor activation in 20 inbred mouse substrains representing six inbred strain lineages (A/J, BALB/c, FVB/N, C3H/He, DBA/2 and NOD) that were either bred in-house or supplied directly by a commercial vendor. To our knowledge, we are the first to identify significant differences in cocaine-induced locomotor response in several of these inbred substrains. The identification of substrain differences allows for the initiation of RCC populations to

more rapidly identify specific genetic variants associated with acute cocaine response. The observation of behavioral profiles that differ between mice generated in-house and those that are vendor-supplied also presents an opportunity to investigate the influence of environmental factors on cocaine-induced locomotor activity.

**Keywords:** cocaine sensitivity, initial cocaine response, genetics, reduced complexity cross, rodent behavior, addiction, rodent model, mice models

## INTRODUCTION

Recent data indicate that cocaine use, the prevalence of cocaine use disorder (CUD) and cocaine-related overdose deaths have been increasing in the United States (1–4). Although cocaine use and abuse remain a significant public health concern, there are currently no FDA approved therapies for CUD. The lack of treatment options is due, in part, to gaps in our knowledge about the etiology of this complex and devastating disorder.

Not all who use cocaine will go on to develop a CUD, suggesting that individual differences contribute to risk. Twin studies yield heritability estimates of approximately 0.70 for cocaine dependence indicating a significant genetic contribution to risk of developing a CUD (5). CUD risk is also heavily influenced by the environment and gene by environment interactions (5–9). Human genome wide association studies (GWAS) have been successful in identifying specific loci and genes associated with nicotine dependence and alcohol use disorders (10–13). The few GWAS studies that have been published for cocaine dependence or CUD have suffered from insufficient sample sizes, limiting discovery of loci and genes that contribute to CUD risk (14–16). Identifying genetic and molecular pathways implicated in CUD would provide insight into individuals at increased risk and generate novel targets that could be investigated for development of effective therapeutics.

Genetic mapping studies and follow-up of loci identified in human GWAS using rodent models provides complementary approaches to human GWAS studies of CUD. One notable example is the identification of the family with sequence similarity 53, member B (*FAM53B*) gene as a risk variant for cocaine dependence in a human CUD GWAS and a mouse mapping study of self-administration of cocaine (14, 17). The use of rodent models offers several advantages, including the ability for the genetic background, environment, and drug exposure regimens to be controlled and manipulated. While rodent models cannot fully recapitulate the range of symptoms observed in human CUD, they do allow for measurement of specific addiction-relevant behaviors, including initial drug sensitivity. Retrospective and longitudinal studies in humans have shown that individual differences in initial subjective drug responses can predict subsequent drug use (18–21). In mice, acute locomotor response to an initial dose of cocaine is a well-established model of initial sensitivity (22, 23).

Genetic mapping studies in inbred mouse strains have successfully identified genomic regions, termed quantitative trait loci (QTL), that are associated with cocaine-induced locomotor activation (17, 24–30). Traditional mapping approaches typically involve crossing genetically and phenotypically diverse pairs of inbred strains and intercrossing or backcrossing the resulting

F1s to generate F2 or N2 mapping populations, respectively. The resulting QTL identified in these studies typically span tens of megabases containing hundreds of genes and thousands of potential causal polymorphisms. Therefore, identifying the specific variant(s) that affect cocaine-induced locomotor activation and other complex behavioral traits has been extremely challenging.

Reduced Complexity Crosses (RCC) between inbred mouse substrains offer a significant advantage over traditional genetic mapping strategies. Substrains are nearly isogenic inbred strains derived from the same founder strain that have been bred independently for multiple generations (typically >20). An RCC is generated in the same fashion as an F2 or N2 population described above, by crossing two substrains that differ for a phenotype of interest. QTL identified in RCCs are similarly sized in comparison to those identified using traditional F2 mapping populations, but causal polymorphisms in the region are limited to those that were still segregating at the time the strains were separated or arose spontaneously since that time (31, 32). This feature of RCCs dramatically facilitates detection of polymorphisms within the QTL region and identification of the causative polymorphism (32). Additionally, a recently developed genotyping array captures polymorphisms between inbred mouse substrains, facilitating rapid and reliable genotyping of RCCs (33). RCCs have been used successfully to identify genetic polymorphisms that impact psychostimulant response, binge eating, binge alcohol consumption, thermal nociception and brain weight (34–38).

Genetic differences between substrains are likely to influence any number of phenotypes, offering a powerful tool with which to expand our knowledge about the genetic loci that affect addiction-relevant behaviors. However, the literature describing substrain differences in locomotor response to drugs of abuse has been limited primarily to the C57BL/6 substrains. In this study, we measured cocaine-induced locomotor activation across 20 substrains derived from A/J, BALB/c, DBA/2, FVB/N, NOD and C3H/He inbred mouse strains. We report significant substrain differences in acute cocaine locomotor activation in response to an acute exposure to 20 mg/kg cocaine. Our data significantly expand the current knowledge about substrain differences in cocaine locomotor response and offer the opportunity to pursue genetic studies to identify genes that contribute to this behavior.

## MATERIALS AND METHODS

### General Methods

Mice were all housed in a pathogen-free facility at UNC. This facility consisted of a 12-h light/dark cycle with lights on at 7:00 AM. All animal care and protocols were approved by the

University of North Carolina at Chapel Hill (UNC) Institutional Animal Care and Use Committee and followed guidelines that were implemented by the National Institutes of Health Guide for the Care and Use of Laboratory Animals, 8th Edition. Mice were maintained in AAALAC-accredited, specific pathogen free (SPF) barrier colony in ventilated cages (Tecniplast, Buguggiate, Italy). Food (PicoLab Rodent Diet 20, Purina, St. Louis, Missouri) was provided *ad libitum* and throughout the duration of behavioral testing. Edstrom carbon filtered; reverse osmosis hyper-chlorinated water was provided *ad libitum* except during behavioral testing.

Two groups of mice were used for behavioral testing (see **Supplementary Table 1** for a summary of substrains, origin, housing, and vendor). The first group consisted of six sets of substrains that were originally purchased from their respective vendors and bred in the vivarium at UNC. Mice bred at UNC were either group-housed with cagemates of the same substrain or co-housed at weaning (postnatal day 21) with mice from other substrains within their strain group (i.e. DBA/2J, DBA/2Ncrl and DBA/2NTac mice in the same cage). The second group consisted of four sets of substrains that were purchased directly from their respective commercial vendors, delivered to our vivarium at 6–7 weeks of age and maintained in group housing throughout testing. Since these substrains were received close to testing age, they were maintained in substrain-specific cages and not co-housed due to concerns about aggressive behavior among males that had not been previously co-housed.

Vendor supplied substrains were an average age of 62 days old at the start of testing. Mice bred in-house were an average age of 65 days old at the start of testing. All mice were weighed on the day prior to testing and weights were used to determine the volume of saline or cocaine administered during testing. Mice were transported to the procedure room located within the same vivarium immediately prior to the start of testing. Behavioral testing occurred during the light cycle from 8:00 AM to 12:00 PM with the time that a mouse was tested being consistent across the three test days. All vendor-supplied substrains were tested by the same experimenter (female) whereas those bred in-house were tested by 5 different experimenters (male and female).

## Vendor Supplied Substrains

Information on all inbred substrains including source and cage environment (cohousing vs not cohousing) is provided in **Supplementary Table 1**. A/J, BALB/c, FVB/N and DBA/2 substrains were purchased from their respective commercial vendors and housed in substrain specific cages throughout testing. Mice were an average of 27 days old upon arrival to UNC and were acclimated to the vivarium for 5 weeks after arrival before behavioral testing. A/J substrains were A/J (The Jackson Laboratory, 000646), A/JCr (Charles River Laboratories, 563) and A/JOlA<sup>Hsd</sup> (Envigo, 049). BALB/c substrains were BALB/cJ (The Jackson Laboratory, 000651), BALB/cByJ (The Jackson Laboratory, 001026), BALB/cAnNCrl (Charles River Laboratories, 028) and BALB/cAnNHsd (Envigo, 047). FVB/N substrains were FVB/NJ (The Jackson Laboratory, 001800), FVB/NCrl (Charles River Laboratories, 207), FVB/NHsd (Envigo, 118), and FVB/NTac (Taconic Biosciences, FVB-F/FVB-M). DBA/2 substrains were DBA/2J (The Jackson

Laboratory, 000671), DBA/2NCrl (Charles River Laboratories, 026) and DBA/2NTac (Taconic Biosciences, DBA2-F/DBA2-M).

## Substrains Bred In-house

Another cohort of inbred mouse substrains were purchased from commercial vendors but test animals were bred in-house at UNC. The following substrains were tested in this cohort: DBA/2J, DBA/2NCrl, DBA/2NTac, A/J, A/JOlA<sup>Hsd</sup>, BALB/cByJ, BALB/cJ, FVB/NJ, FVB/NTac, NOD/MrkTac (Taconic Biosciences, NOD-F/NOD-M), NOD/ShiLtJ (The Jackson Laboratory, #001976), C3H/HeJ (The Jackson Laboratory, #000659), C3H/HeNTac (Taconic Biosciences, C3H-F/C3H-M), C3H/HeNHsd (Envigo, 040) and C3H/HeNCrl (Charles River Laboratories, 025). Some of these mice were cohoused with cagemates that included at least two different substrains from a single progenitor strain.

## Drugs

Cocaine hydrochloride (HCl) was purchased from Sigma-Aldrich (St. Louis, MO, USA; C5776-5G). A solution of cocaine HCl was prepared fresh daily. Cocaine HCl was dissolved in physiological saline at a concentration of 2 mg/ml and administered via intraperitoneal (i.p.) injection at a volume of 0.01 ml/g resulting in a dose of 20 mg/kg of body weight administered to mice for behavioral testing. Saline was purchased from Fisher Scientific (Waltham, MA, USA; 297753).

## Open Field Apparatus

The open field (OF) arena (ENV-515-16, Med Associates, St. Albans, VT, USA), measured 17 x 17 x 13cm and consisted of four clear Plexiglas walls and a white Plexiglas floor. The walls are surrounded by infrared detection beams on the X, Y, and Z axes used to detect horizontal and vertical activity of the animal throughout the duration of the test session. The OF chamber is placed within a sound attenuating box (73.5 x 59 x 59 cm) that has two overhead light fixtures containing 28-V lamps. Light levels on the arena floor were 24 lux in the center, 10 lux in the corners and 13 lux along the walls. Eight identical OF arenas were used for testing with a mouse being tested in the same arena each test day.

## Acute Cocaine-Induced Locomotor Activity Test

On Day 1, behaviorally naïve mice were given an i.p. injection of saline at a volume of 0.01 ml/g body weight and immediately placed into the OF for 30 min to habituate to the arena. On Day 2, mice were again given an i.p. injection of saline and placed into the OF for 30 min. On Day 3, mice were given an i.p. injection of 20 mg/kg of cocaine and placed into the OF chamber for 30 min. Locomotor behavior was measured as total distance moved (in centimeters) for the entire 30-min test period each day using the manufacturers data acquisition software (Activity Monitor v5.9.725; Med Associates). Locomotor activity recorded during day 2 was used as a baseline measurement for comparison with cocaine-induced locomotor activity on Day 3. At the end of each test session, mice were placed back into their home cages and the OF chambers were cleaned with 0.25% bleach solution.

## Statistical Analyses

All statistical analyses were performed using SPSS v28 for Mac (IBM Inc). Due to normality of data variables, a Box-Cox transformation of locomotor activity data for each substrain was performed and the resulting transformation used for each strain group is reported in **Supplementary Table 2**. For each set of substrains, we performed an ANOVA that included day of testing, substrain and sex as independent variables and locomotor activity as the dependent variable. In cases where multiple individuals tested animals within the same strain cohorts, we added experimenter as a covariate in the ANOVA model. Significant main effects ( $p < 0.05$ ) were followed up with *post-hoc* Tukey's HSD or independent samples T-tests.

## RESULTS

Experimental data for all inbred mouse substrains including origin of the mice, number of mice tested, cage environment, strain means and standard deviations are provided in **Supplementary Table 1**. We observed significant substrain differences in basal and/or cocaine-induced locomotor activity in all 6 strain groups we examined (**Supplementary Table 2**). C3H/He and DBA/2 substrain differences were fairly stable across experimental cohorts. We also observed substrain differences (i.e., A/J and FVB/N) that were not replicated across experimental groups (vendor-supplied vs in-house). Sex differences also varied across and within strain groups and experimental cohorts. Results presented individually by substrain are described below.

### A/J Substrains Are Not Activated Upon Acute Exposure to 20 mg/kg Cocaine Vendor Supplied

Overall, the locomotor activity of the vendor-supplied A/J substrains did not increase significantly after exposure to cocaine ( $F_{(2, 126)} = 0.17$ ;  $p = 0.846$ ; **Figure 1A**), although increased cocaine-induced locomotor activity can be observed in the A/JCr substrain. There was a significant main effect of substrain ( $F_{(2, 126)} = 4.1$ ;  $p = 0.019$ ). A/JCr mice were significantly more active than A/JOlaHsd mice ( $p = 0.014$ ), but this appears to be mostly driven by several high-responding A/JCr mice (data not shown). No significant sex ( $F_{(1, 126)} = 0.73$ ;  $p = 0.396$ ) or interaction effects were observed.

### Bred In-house

Two A/J substrains were bred in-house at UNC for 1–2 (A/JOlaHsd) or 3–4 (A/J) generations. These mice showed a different behavioral profile than those obtained from commercial vendors. We observed a significant decrease in locomotor activity across all 3 days, including Day 3 after exposure to cocaine (**Figure 1B**;  $F_{(2, 206)} = 30.5$ ;  $p = 2.5 \times 10^{-12}$ ). We also observed significant substrain ( $F_{(1, 206)} = 34.9$ ;  $p = 1.4 \times 10^{-8}$ ) and sex [ $F_{(1, 206)} = 7.1$ ;  $p = 0.009$ ] effects. The A/J substrain showed significantly higher locomotor activity regardless of day ( $t(217) = 5.2$ ;  $p = 4.1 \times 10^{-7}$ ; **Figure 1C**). Overall, male mice were significantly more active than female mice ( $t(217) = 2.5$ ;  $p =$

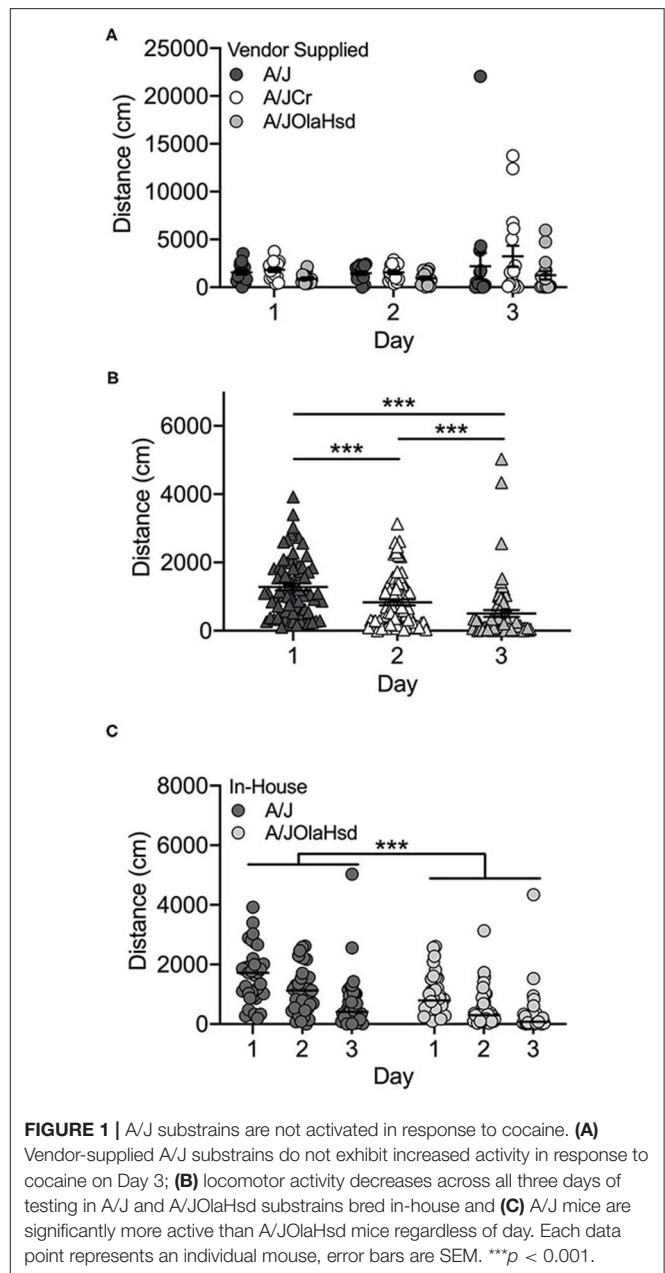
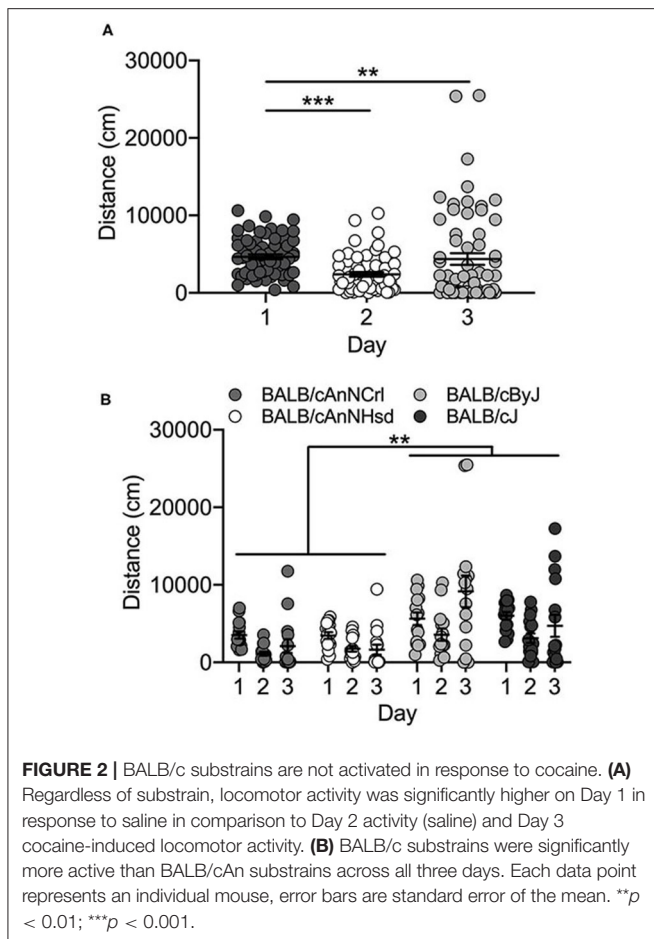


**FIGURE 1 |** A/J substrains are not activated in response to cocaine. **(A)** Vendor-supplied A/J substrains do not exhibit increased activity in response to cocaine on Day 3; **(B)** locomotor activity decreases across all three days of testing in A/J and A/JOlaHsd substrains bred in-house and **(C)** A/J mice are significantly more active than A/JOlaHsd mice regardless of day. Each data point represents an individual mouse, error bars are SEM. \*\*\* $p < 0.001$ .

0.013; data not shown). There were no significant interactions among any of the independent variables tested.

### Locomotor Response to Cocaine Differs in BALB/c Substrains From the “J” Lineage in Comparison With Substrains From the “AnN” Lineage Vendor Supplied

Vendor-supplied BALB/c substrains showed no locomotor activation in response to cocaine exposure on Day 3. Rather, locomotor activity decreased across the three days of testing in the four substrains [ $F_{(2, 162)} = 10.8$ ;  $p = 3.9 \times 10^{-5}$ ]. Collapsed across substrains, locomotor activity on Day 1 is significantly



higher than either Day 2 ( $p = 3.7 \times 10^{-5}$ ) or Day 3 ( $p = 0.004$ ) (Figure 2A). We also observed a significant main effect of substrain [ $F_{(3, 162)} = 13.6$ ;  $p = 6.2 \times 10^{-8}$ ]. Mice of both J substrains (BALB/cJ and BALB/cByJ) are significantly more active than both BALB/cAnNHsd and BALB/cAnNCrI mice (all  $p < 0.01$ ; Figure 2B). Female mice were significantly more active than male mice [ $F_{(1, 162)} = 5.9$ ;  $p = 0.016$ ; data not shown].

### Bred In-house

BALB/cJ and BALB/cByJ mice were generated in-house and we tested offspring from the 1st and 2nd generations of breeding from the initial vendor stock. We observed no significant day [ $F_{(2, 27)} = 2.4$ ;  $p = 0.106$ ] or substrain [ $F_{(1, 27)} = 0.12$ ;  $p = 0.731$ ] differences. We did observe a sex difference [ $F_{(1, 27)} = 4.5$ ;  $p = 0.043$ ], but it should be noted that our experimental cohort was limited to only 2 BALB/cByJ males and no BALB/cJ males (data not shown).

## C3H/HeNTac Mice Are More Active Than Other C3H/He Substrains

### Bred In-house

All C3H/He substrains were bred in-house. The initial cohort was limited to C3H/HeJ and C3H/HeNTac substrains that were the first generation of offspring from vendor-supplied mice

(C3H/HeJ) or offspring of crosses between mice from the third generation bred at UNC (C3H/HeNTac). These animals were cohoused such that mice from each substrain were weaned into cages together and maintained in that manner throughout testing. The second cohort of mice included C3H/HeNCrI and C3H/HeNHsd substrains in addition to C3H/HeNTac and C3H/HeJ, and were produced by breeding vendor-supplied mice at UNC for one generation. These mice were weaned into and maintained in substrain-specific caging throughout testing.

Both C3H/HeJ and C3H/HeNTac substrains in the cohoused cohort were significantly more active in response to cocaine (Day 3) vs saline (Days 1 and 2) [ $F_{(2, 104)} = 246.3$ ;  $p = 3.6 \times 10^{-40}$ ]. We also observed a significant substrain effect [ $F_{(1, 104)} = 52.5$ ;  $p = 7.9 \times 10^{-11}$ ]. C3H/HeNTac mice were significantly more active than C3H/HeJ mice ( $t(115) = 3.3$ ;  $p = 0.001$ ; Figure 3A). No sex differences [ $F_{(1, 104)} = 0.0003$ ;  $p = 0.986$ ] or interaction effects were observed.

In the non-cohoused cohort comparing all four C3H/He substrains, we observed a significant effect of substrain [ $F_{(3, 527)} = 27.0$ ;  $p = 3.0 \times 10^{-16}$ ] and day [ $F_{(2, 527)} = 277.5$ ;  $p = 4.7 \times 10^{-83}$ ]. Cocaine-induced locomotor activity on Day 3 was significantly higher than activity on Days 1 and 2 (both  $p < 0.001$ ). As in the cohoused cohort, C3H/HeNTac mice were significantly more active than C3H/HeJ ( $p = 2.3 \times 10^{-12}$ ) and both C3H/HeNCrI ( $p = 1.2 \times 10^{-12}$ ) and C3H/HeNHsd ( $p = 1.3 \times 10^{-12}$ ) substrains (Figure 3B; all  $p < 0.001$ ). We also observed a significant substrain by sex interaction; C3H/HeNCrI males are significantly more active than females ( $p = 0.013$ ) whereas the opposite is true for C3H/HeNHsd ( $p = 0.01$ ). Two different individuals tested mice in this cohort and we identified experimenter as a significant covariate ( $p = 2.0 \times 10^{-6}$ ). The experimenter effect reflects higher locomotor activity across all substrains following cocaine administration on Day 3 in mice tested by one experimenter vs the other (data not shown).

The availability of data from both cohoused and non-cohoused C3H/HeJ and C3H/HeNTac mice allowed us to examine the effects of housing on behavior in these two substrains. An ANOVA including housing (cohoused vs. non-cohoused) as well as day, strain and sex as independent variables yielded no significant main effect of housing [ $F_{(1, 300)} = 2.4$ ;  $p = 0.120$ ]. A significant housing by day interaction [ $F_{(2, 300)} = 4.9$ ;  $p = 0.008$ ] suggested that non-cohoused mice were significantly less active than cohoused mice in response to an acute exposure to cocaine on Day 3, but *post hoc* tests revealed no significant difference (data not shown).

## DBA/2NTac Mice Were Significantly Less Active Than DBA/2J and DBA/2NCrI Mice Vendor Supplied

We observed significant day [ $F_{(2, 126)} = 18.2$ ;  $p = 1.2 \times 10^{-7}$ ] and substrain [ $F_{(2, 126)} = 25.0$ ;  $p = 7.1 \times 10^{-10}$ ] differences among the three vendor-supplied DBA/2 substrains – DBA/2J, DBA/2NTac and DBA/2NCrI. Cocaine-induced locomotor activity on Day 3 was significantly higher than activity

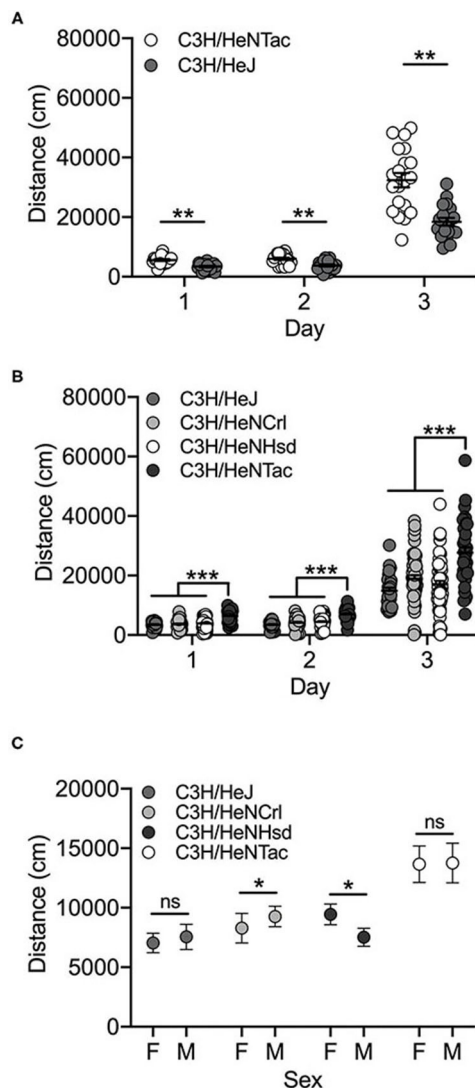


**FIGURE 3 |** C3H/HeN mice are more active than other C3H/He substrains. **(A)** Cohoused C3H/HeJ and C3H/HeN mice are significantly activated by cocaine on Day 3 and C3H/HeN mice are significantly more active than C3H/HeJ mice regardless of treatment (saline, cocaine). **(B)** Non-cohoused C3H/He substrains are significantly activated in response to cocaine on Day 3 and C3H/HeN mice are significantly more active than C3H/HeJ, C3H/HeNcr and C3H/HeNsd substrains. **(C)** C3H/HeNcr males are significantly more active than females and C3H/HeNsd females are significantly more active than males. Each data point represents an individual mouse, error bars are standard error of the mean. \* $p < 0.05$ ; \*\* $p < 0.01$ ; \*\*\* $p < 0.001$ .

following saline administration on Days 1 and 2 (both  $p < 0.001$ ; **Figure 4A**). DBA/2NTac mice were significantly less active than both DBA/2J and DBA/2Ncr (both  $p < 0.001$ ). No significant sex differences were observed.

### Bred In-house

The same set of DBA/2 mice were bred in-house at UNC and mice from the first generation were tested for cocaine-induced locomotor activity. As with the vendor-supplied DBA/2

substrains, we observed significant day [ $F_{(2, 288)} = 23.5$ ;  $p = 3.6 \times 10^{-10}$ ] and substrain [ $F_{(2, 288)} = 10.5$ ;  $p = 3.8 \times 10^{-5}$ ] effects. We also observed a significant day  $\times$  substrain interaction [ $F_{(4, 288)} = 4.1$ ;  $p = 0.003$ ]. Although none of the substrains differed for locomotor activity on Day 1, DBA/2NTac mice had significantly lower locomotor activity than both DBA/2J ( $p = 0.014$ ) and DBA/2Ncr ( $p = 0.028$ ) mice on Day 2. DBA/2NTac mice also differed from DBA/2J ( $p = 0.003$ ) and DBA/2Ncr ( $p = 0.002$ ) mice on Day 3 (**Figure 4B**).

## Basal and Cocaine-Induced Locomotor Behavior Differs Across FVB/N Mice Bred In-house but Not the Vendor-Supplied Cohort

### Vendor Supplied

We identified significant day [ $F_{(2, 72)} = 207.8$ ;  $p = 1.2 \times 10^{-30}$ ] and substrain [ $F_{(3, 72)} = 4.7$ ;  $p = 0.005$ ] effects but no substrain by day interaction for the vendor-supplied FVB/N substrains. All FVB/N substrains showed significantly increased locomotor activity on Day 3 after exposure to cocaine (**Figure 5A**). FVB/Ncr mice are significantly less active than FVB/NHsd mice ( $p = 0.002$ ; data not shown). No significant sex differences or interactions were observed.

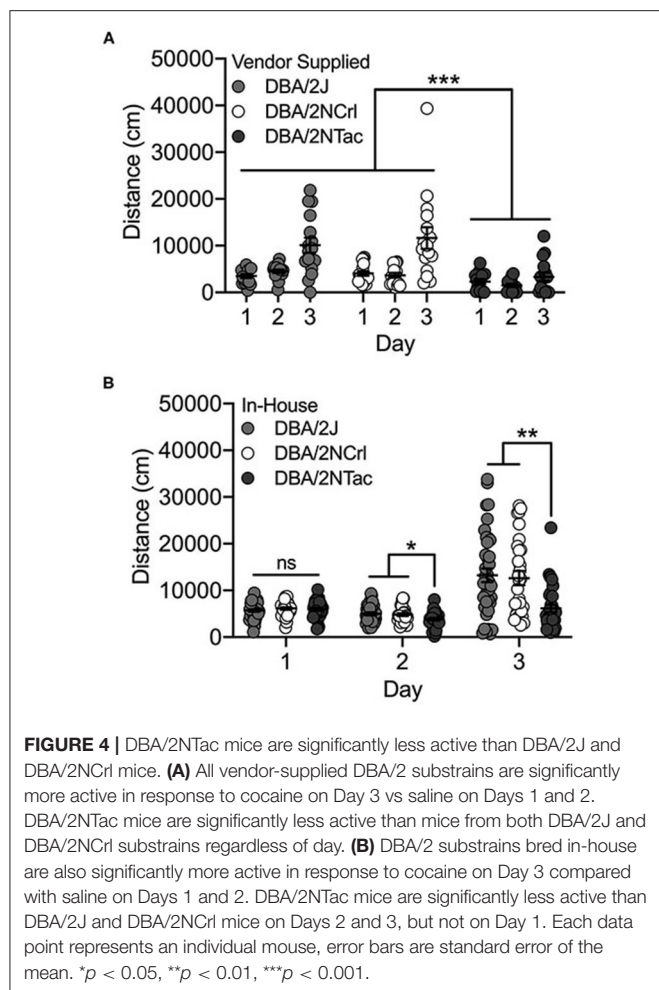
### Bred In-house

Significant day [ $F_{(2, 107)} = 35.7$ ;  $p = 1.3 \times 10^{-12}$ ], substrain [ $F_{(2, 107)} = 30.4$ ;  $p = 2.5 \times 10^{-7}$ ] and sex [ $F_{(1, 107)} = 4.7$ ;  $p = 0.032$ ] effects as well as substrain by day ( $F_{(2, 107)} = 3.5$ ;  $p = 0.034$ ) and substrain by sex [ $F_{(1, 107)} = 8.3$ ;  $p = 0.005$ ] interactions were observed for FVB/NJ and FVB/NTac substrains that were bred in-house for 1–2 generations. The two substrains differed significantly for locomotor activity on Days 1 [ $t(38) = 6.1$ ;  $p = 3.4 \times 10^{-7}$ ] and 2 [ $t(38) = 3.4$ ;  $p = 0.002$ ] but not cocaine-induced locomotor activity on Day 3 [ $t(38) = 0.706$ ;  $p = 0.485$ ] (**Figure 5B**). FVB/NJ females are significantly more active than FVB/NJ males ( $t(58) = 2.0$ ;  $p = 0.045$ ) but male and female FVB/NTac mice do not differ ( $t(44) = 0.943$ ;  $p = 0.351$ ) (data not shown).

FVB substrains in this cohort were tested by two different individuals and experimenter was a significant covariate in the ANOVA ( $p = 0.009$ ). The experimenter effect reflects decreased locomotor activity following cocaine exposure on Day 3 as well as increased variability in data collected by one experimenter vs the other (data not shown).

## Locomotor Response to Cocaine Did Not Differ Across 2 NOD Substrains Bred In-house

Characterization of cocaine-induced locomotor activation in NOD substrains was limited to those that were bred in-house at UNC. We observed a significant effect of both substrain [ $F_{(1, 239)} = 4.2$ ;  $p = 0.04$ ] and day [ $F_{(2, 239)} = 139.0$ ;  $p = 9.0 \times 10^{-41}$ ] as well as a significant substrain by day interaction [ $F_{(2, 239)} = 5.1$ ;  $p = 0.007$ ]. NOD/MrkTac mice were significantly more active than NOD/ShiLtJ mice on Days 1 ( $t(82) = 3.0$ ;  $p = 0.003$ ) and 2 ( $t(82)$

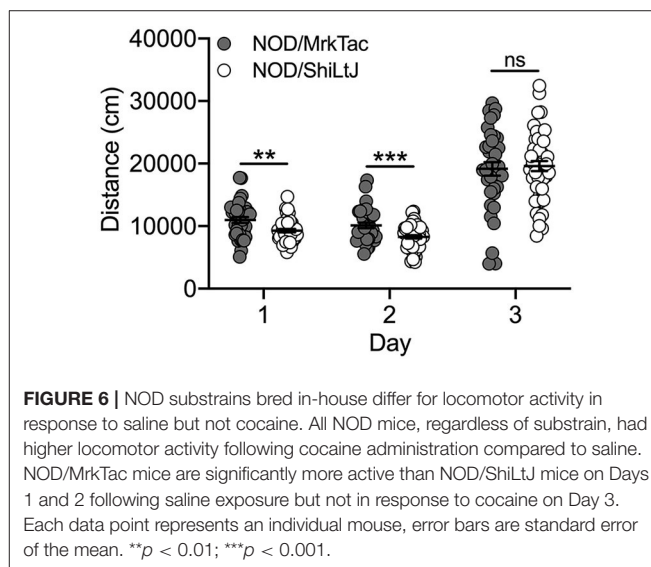
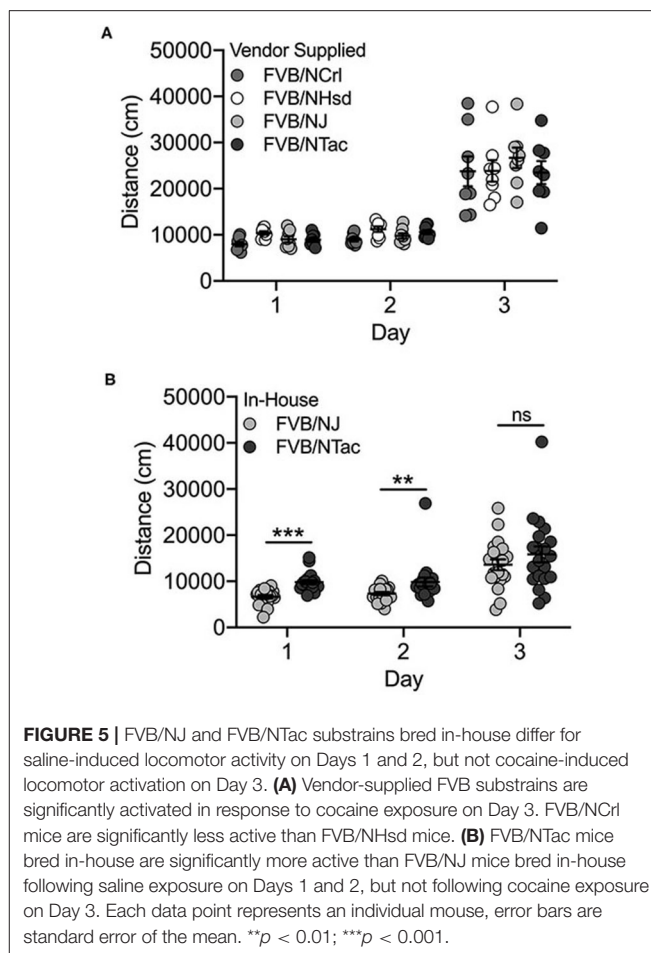


= 3.5;  $p = 7.7 \times 10^{-4}$ ) but not following cocaine exposure on Day 3 (Figure 6). No significant sex differences were detected.

## DISCUSSION

Laboratory mice are invaluable tools in biomedical research and have contributed greatly to our understanding of biological and disease processes. Inbred strains, in particular, have been used for decades in studies aimed at identifying genes that contribute to behavioral phenotypes, including responses to various drugs of abuse (27, 39–41). These studies have been very successful in identifying chromosomal regions that likely harbor causal genetic variants. However, the genetic diversity present in mapping crosses between any two standard inbred strains and the sheer number of potential causal genes and polymorphisms in mapped loci has hindered progress. Thus, these strategies rarely progress to identifying a specific causal gene or variant. The reduced genetic complexity in inbred mouse substrains offers the opportunity to overcome this hurdle and more rapidly and efficiently identify the causative gene and specific genetic variant.

In order to use the RCC approach to identify causal genes and genetic variants, one needs to identify substrains that exhibit



phenotypic differences in the trait of interest. This approach has been used successfully to identify the *Cyfp2* gene as a regulator of basal and cocaine-induced locomotor activity, behavioral sensitization and binge-eating in two C57BL/6 substrains,

C57BL/6J and C57BL/6NJ (34, 42). The study of addiction-related behaviors, and specifically initial locomotor sensitivity to psychostimulants, has been mostly limited to the C57BL/6 inbred substrains. We assessed differences in cocaine-induced locomotor response across 20 inbred mouse substrains from 6 different strains. Our data represent the first behavioral characterization of cocaine-induced locomotor activation in most of these substrains.

Two sets of strains showed particularly robust substrain differences that were replicated across experimental cohorts. C3H/HeNTac mice had significantly higher basal and cocaine-induced locomotor activity than C3H/HeNCrl and C3H/HeNHsd mice in one experimental cohort and C3H/HeJ mice in both cohorts (**Figures 3A,B**). The similarity of the behavioral phenotype in C3H/HeJ, C3H/HeNCrl and C3H/HeNHsd substrains suggests that the causal variant(s) may have become fixed in the C3H/HeNTac substrain after it diverged from the other C3H/HeN lines in 1974 (C3H/HeNCrl) and 1983 (C3H/HeNHsd). However, we must also consider the possibility that C3H/HeNCrl and C3H/HeNHsd behavioral phenotypes result from a different variant or variants. We also observed consistent substrain differences in behavior in DBA/2 mice that were supplied by commercial vendors and bred in-house. DBA/2NTac mice had significantly lower basal and cocaine-induced locomotor activity compared to DBA/2J and DBA/2NCrl in both cohorts (**Figures 4A,B**). These data suggest that the causal variant(s) likely arose in the DBA/2NTac substrain after it diverged from DBA/2N in 1981.

Correspondence of significant substrain differences across the two cohorts suggests a strong genetic component and supports the use of the RCC to identify specific causal variants that influence basal locomotor activity and response to cocaine. Our observation of significant substrain differences in basal and/or cocaine-induced locomotor behavior in all of the strain sets examined (**Supplementary Table 2**) does suggest that a complex genetic landscape underlies these behaviors. The presence of more than one causal polymorphism and/or background genetic factors that contribute to behavioral differences may make it necessary to produce larger mapping crosses that are adequately powered to detect QTL.

We also identified different behavioral phenotypes in vendor-supplied substrains vs. those bred in-house. For example, FVB/NTac mice bred in-house were significantly more active than FVB/NJ mice bred in-house across all three days of testing (**Figure 5B**) whereas vendor-supplied FVB substrains showed similar locomotor behavior across all three test days (**Figure 5A**). Neither A/J nor A/JolaHsd substrains bred in-house were significantly activated in response to cocaine and in fact, locomotor behavior in these two substrains decreased significantly across all 3 days of testing (**Figures 1B,C**). Similarly, vendor-supplied A/J and A/JolaHsd substrains were not significantly activated in response to cocaine, but we observed no significant decrease in locomotor activity across test days (**Figure 1A**). It is important to highlight that cross-cohort comparisons, especially those highlighting behavioral differences, must be made with caution as these differences may be driven in part by confounding factors.

The availability of cohoused C3H/HeNTac and C3H/HeJ substrains vs those maintained in substrain-specific housing allows us to examine indirect genetic effects that might influence basal and cocaine-induced locomotor activity. Indirect genetic effects are environmental effects that result from the genetic background of interacting conspecifics (43, 44). We tested the hypothesis that C3H/HeJ mice housed in mixed substrain cages were behaviorally different than C3H/HeJ mice from substrain-specific cages (and similarly for C3H/HeNTac). Our analyses yielded no significant effect of housing demonstrating that cage-level interactions among C3H/He substrains did not contribute to behavioral differences.

The observation of behavioral differences in the same substrain based on the source from which mice were obtained suggests that other environmental factors could be responsible. Multiple studies have systematically examined environmental factors that might affect behavioral phenotypes including, but not limited to diet, type of cage, cage density, season, time of day, transportation and experimenter effects (45–49). However, previous studies have generally assessed behavioral differences in mice tested across multiple sites. We examined behavior in all mice, independent of the source, in the same behavioral facility (and same testing room) at UNC. As such, we were able to control, to the extent possible, the environment to which the mice were exposed in the 5-week period leading up to testing. Mice were maintained on the same light cycle, tested during the same time of day, provided the same diet and water and housed in the same caging and animal holding room prior to and throughout testing.

The stress of transportation is an obvious difference between vendor-supplied mice and those bred in-house. We don't believe transportation stress could fully explain behavioral differences between mice from different sources. Previous studies have shown that transportation has very little effect on behavioral outcomes (45, 48). Moreover, vendor-supplied mice arrived at UNC very close to weaning age and were habituated to our vivarium conditions for approximately 5 weeks prior to testing.

Experimenter effects can also have an impact on behavioral outcomes. All mice supplied directly from the vendor were tested by the same animal handler (a female), whereas substrains bred in-house were tested by a group of 5 animal handlers including males and females. At least two studies have established that experimenter effects (49) and even the sex of the individual testing the mice (47) can significantly affect the outcome of behavioral tests. Although not widely observed, our analyses support significant behavioral differences due to experimenter in two substrain cohorts. However, drawing broader conclusions from these results is confounded by experimental parameters. For example, experimenters were not distributed evenly across all batches for all substrains and although we tried to balance substrains across all test batches, the composition of substrains included in each batch varied such that experimenter differences might also reflect substrain differences.

The gut microbiome has been implicated in numerous behavioral traits including locomotor response to psychostimulants (50, 51). Composition of the gut microbiota, even in the same inbred strain background, can vary across time,

from vendor to vendor, and even between different facilities and animal holding rooms at the same vendor or institution (52, 53). These differences can be attributed to a host of environmental factors including diet, caging, bedding and water supply (54–56). Host genetic background also plays a significant role in the composition of the gut microbiota (57). Profound or even subtle changes in the gut microbiota in response to relocation from vendors to our vivarium could interact with different genetic backgrounds to significantly impact behavior. The relationship between genetic background and behavior becomes even more complicated when one considers that substrain behaviors attributable to stable differences in the gut microbiota could be erroneously ascribed solely to genetics. Shifts in the gut microbiota in response to changing environments could alter phenotypes and impact replicability from study to study. Recent studies have also established that the maternal microbiome can affect offspring neurodevelopment and impact behavior in adulthood (58–60). Thus, it is important to consider not only the source of the mice being tested, but the composition of the maternal microbiome during neurodevelopment.

Finally, an important caveat of our study is the limitation of using a single, acute dose of 20 mg/kg cocaine. These data represent a first step for future work involving a more in-depth behavioral analyses of these substrains. Testing at additional doses is certainly warranted as dose dependent effects may reflect differences in drug sensitivity. It is also important to examine activity across the session as substrain differences in timing of the response, shifts in peak cocaine-induced locomotor activation and other behavioral patterns may not be adequately captured by collapsing across the entire 30-min session (**Supplementary Figure 1**). It is also important to note that dose-specific differences in cocaine sensitivity may not be fully captured using locomotor activity as the primary behavioral measure. Other behaviors, such as stereotypy, should also be assessed in an expanded range of doses. Finally, a full pharmacokinetic profile of these substrains will be essential in determining potential differences in drug metabolism that may be responsible for any observed behavioral differences.

In summary, this study expands the knowledge of phenotypic differences in locomotor activity and initial response to cocaine in 6 sets of inbred mouse substrains which had previously not been characterized. All six strain lineages displayed substrain differences in either basal- or cocaine-induced locomotor behavior and can be utilized in RCCs to identify causal genetic variants. Expanded behavioral testing in these substrains to characterize the rewarding and reinforcing effects of cocaine is an

important next step. Environmental factors also warrant follow-up, as differences in behavior were observed across the same inbred substrains obtained from different sources. Substrains from C3H/He and DBA/2 lineages demonstrated stable and robust differences in cocaine-induced locomotor behavior, and are good candidates for additional studies to investigate genetic and environmental factors that contribute to initial cocaine sensitivity. Future studies can utilize these data to increase our understanding of the complex factors that increase CUD and potentially lead to new therapeutic targets.

## DATA AVAILABILITY STATEMENT

The raw data supporting the conclusions of this article will be made available by the authors, without undue reservation.

## ETHICS STATEMENT

The animal study was reviewed and approved by UNC Institutional Animal Care and Use Committee.

## AUTHOR CONTRIBUTIONS

CG, SS, MF, FP-M, and LT: conception and design of work and revising/editing manuscript. CG, SS, JF, DL, and LA-C: data collection. CG, SS, and LT: data analysis and drafting the manuscript. CG, SS, JF, DL, LA-C, GS, DM, MF, FP-M, and LT: approval of manuscript. SS, GS, DM, MT, FP-M, and LT: provided resources. All authors contributed to the article and approved the submitted version.

## FUNDING

This study was supported by pilot funding from NIDA P50 039841 to SS and LT. Pilot funding was used to purchase research materials and support personnel conducting studies. Funding from R21 DA052171 to LT was used to support personnel conducting studies and purchase research material. U24 HG010100, U19 AI100625, and P01 AI132130 to FP-M and MF provided funding to maintain inbred mouse substrain colonies that provided research subjects for the work.

## SUPPLEMENTARY MATERIAL

The Supplementary Material for this article can be found online at: <https://www.frontiersin.org/articles/10.3389/fpsy.2022.800245/full#supplementary-material>

## REFERENCES

- Karila L, Petit A, Lowenstein W, Reynaud M, and consequences of cocaine addiction. *Curr Med Chem.* (2012) 19:5612–8. doi: 10.2174/092986712803988839
- John WS, Wu LTrends T, and correlates of cocaine use and cocaine use disorder in the United States from 2011 to 2015. *Drug Alcohol Depend.* (2017) 180:376–84. doi: 10.1016/j.drugalcdep.2017.08.031
- Jalal H, Buchanich JM, Roberts MS, Balmert LC, Zhang K, Burke DS. Changing dynamics of the drug overdose epidemic in the United States from 1979 through 2016. *Science.* (2018) 361. doi: 10.1126/science.aau1184
- Bentzley BS, Han SS, Neuner S, Humphreys KM, Kampman K, Halpern CH. Comparison of Treatments for Cocaine Use Disorder Among Adults, A Systematic Review and Meta-analysis. *JAMA Netw Open.* (2021) 4:e218049. doi: 10.1001/jamanetworkopen.2021.8049

5. Ducci F, Goldman D. The genetic basis of addictive disorders. *Psychiatr Clin North Am.* (2012) 35:495–519. doi: 10.1016/j.psc.2012.03.010
6. Merikangas KR, Avenevoli S. Implications of genetic epidemiology for the prevention of substance use disorders. *Addict Behav.* (2000) 25:807–20. doi: 10.1016/S0306-4603(00)00129-5
7. Goldman D, Oroszi G, Ducci F. The genetics of addictions, uncovering the genes. *Nat Rev Genet.* (2005) 6:521–32. doi: 10.1038/nrg1635
8. Thatcher DL, Clark DB. Adolescents at risk for substance use disorders, role of psychological dysregulation, endophenotypes, environmental influences. *Alcohol Res Health.* (2008) 31:168–76.
9. Mennis J, Stahler GJ, Mason MJ. Risky substance use environments and addiction, a new frontier for environmental justice research. *Int J Environ Res Public Health.* (2016) 13. doi: 10.3390/ijerph13060607
10. Bierut LJ, Madden PA, Breslau N, Johnson EO, Hatsukami D, Pomerleau OF, et al. Novel genes identified in a high-density genome wide association study for nicotine dependence. *Hum Mol Genet.* (2007) 16:24–35. doi: 10.1093/hmg/ddl441
11. Hancock DB, Markunas CA, Bierut LJ, Johnson EO. Human Genetics of Addiction, New Insights and Future Directions. *Curr Psychiatry Rep.* (2018) 20:8. doi: 10.1007/s11920-018-0873-3
12. Sullivan PF, Agrawal A, Bulik CM, Andreassen OA, Borglum AD, Breen G, et al. Psychiatric genomics, an update and an agenda. *Am J Psychiatry.* (2018) 175:15–27. doi: 10.1176/appi.ajp.2017.17030283
13. Walters RK, Polimanti R, Johnson EC, McClintick JN, Adams MJ, Adkins AE, et al. Transancestral GWAS of alcohol dependence reveals common genetic underpinnings with psychiatric disorders. *Nat Neurosci.* (2018) 21:1656–69. doi: 10.1038/s41593-018-0275-1
14. Gelernter J, Sherva R, Koesterer R, Almasy L, Zhao H, Kranzler HR, et al. Genome-wide association study of cocaine dependence and related traits, FAM53B identified as a risk gene. *Mol Psychiatry.* (2014) 19:717–23. doi: 10.1038/mp.2013.99
15. Cabana-Dominguez J, Shivalikanji A, Fernandez-Castillo N, Cormand B. Genome-wide association meta-analysis of cocaine dependence, Shared genetics with comorbid conditions. *Prog Neuropsychopharmacol Biol Psychiatry.* (2019) 94:109667. doi: 10.1016/j.pnpbp.2019.109667
16. Sun J, Kranzler HR, Gelernter J, Bi J. A genome-wide association study of cocaine use disorder accounting for phenotypic heterogeneity and gene-environment interaction. *J Psychiatry Neurosci.* (2020) 45:34–44. doi: 10.1503/jpn.180098
17. Dickson PE, Miller MM, Calton MA, Bubier JA, Cook MN, Goldowitz D, et al. Systems genetics of intravenous cocaine self-administration in the BXD recombinant inbred mouse panel. *Psychopharmacology (Berl).* (2016) 233:701–14. doi: 10.1007/s00213-015-4147-z
18. Haertzen CA, Kocher TR, Miyasato K. Reinforcements from the first drug experience can predict later drug habits and/or addiction, results with coffee, cigarettes, alcohol, barbiturates, minor and major tranquilizers, stimulants, marijuana, hallucinogens, heroin, opiates and cocaine. *Drug Alcohol Depend.* (1983) 11:147–65. doi: 10.1016/0376-8716(83)90076-5
19. Davidson ES, Finch JF, Schenk S. Variability in subjective responses to cocaine, initial experiences of college students. *Addict Behav.* (1993) 18:445–53. doi: 10.1016/0306-4603(93)90062-E
20. Lambert NM, McLeod R, Schenk S. Subjective responses to initial experience with cocaine, an exploration of the incentive-sensitization theory of drug abuse. *Addiction.* (2006) 101:713–25. doi: 10.1111/j.1360-0443.2006.01408.x
21. de Wit H, Phillips TJ. Do initial responses to drugs predict future use or abuse? *Neurosci Biobehav Rev.* (2012) 36:1565–76. doi: 10.1016/j.neubiorev.2012.04.005
22. Thomsen M, Caine SB. Psychomotor stimulant effects of cocaine in rats and 15 mouse strains. *Exp Clin Psychopharmacol.* (2011) 19:321–41. doi: 10.1037/a0024798
23. Wiltshire T, Ervin RB, Duan H, Bogue MA, Zamboni WC, Cook S, et al. Initial locomotor sensitivity to cocaine varies widely among inbred mouse strains. *Genes Brain Behav.* (2015) 14:271–80. doi: 10.1111/gbb.12209
24. Tolliver BK, Belknap JK, Woods WE, Carney JM. Genetic analysis of sensitization and tolerance to cocaine. *J Pharmacol Exp Ther.* (1994) 270:1230–8.
25. Miner LL, Marley RJ. Chromosomal mapping of the psychomotor stimulant effects of cocaine in BXD recombinant inbred mice. *Psychopharmacology (Berl).* (1995) 122:209–14. doi: 10.1007/BF02246541
26. Phillips TJ, Huson MG, McKinnon CS. Localization of genes mediating acute and sensitized locomotor responses to cocaine in BXD/Ty recombinant inbred mice. *J Neurosci.* (1998) 18:3023–34. doi: 10.1523/JNEUROSCI.18-08-03023.1998
27. Jones BC, Tarantino LM, Rodriguez LA, Reed CL, McClearn GE, Plomin R, et al. Quantitative-trait loci analysis of cocaine-related behaviours and neurochemistry. *Pharmacogenetics.* (1999) 9:607–17. doi: 10.1097/00008571-199910000-00007
28. Boyle AE, Gill K. Sensitivity of AXB/BXA recombinant inbred lines of mice to the locomotor activating effects of cocaine, a quantitative trait loci analysis. *Pharmacogenetics.* (2001) 11:255–64. doi: 10.1097/00008571-200104000-00009
29. Gill KJ, Boyle AE. Confirmation of quantitative trait loci for cocaine-induced activation in the AcB/BcA series of recombinant congenic strains. *Pharmacogenetics.* (2003) 13:329–38. doi: 10.1097/00008571-200306000-00004
30. Boyle AE, Gill KJ. A verification of previously identified QTLs for cocaine-induced activation using a panel of B6.A chromosome substitution strains (CSS) and A/J x C57BL/6J F2 mice. *Psychopharmacology (Berl).* (2009) 207:325–34. doi: 10.1007/s00213-009-1656-7
31. Bryant CD, Ferris MT, De Villena FPM, Dama MI, Kumar V. Reduced complexity cross design for behavioral genetics academic press(molecular-genetic and statistical techniques for behavioral and neural research. (2018) 165–90. doi: 10.1016/B978-0-12-804078-2.00008-8
32. Bryant CD, Smith DJ, Kantak KM, Nowak TS, Williams RW, Damaj MI, et al. Facilitating complex trait analysis via reduced complexity crosses. *Trends Genet.* (2020) 36, 549–562. doi: 10.1016/j.tig.2020.05.003
33. Sigmon JS, Blanchard MW, Baric RS, Bell TA, Brennan J, Brockmann GA, et al. Content and Performance of the MiniMUGA Genotyping Array, A New Tool To Improve Rigor and Reproducibility in Mouse Research. *Genetics.* (2020) 216:905–30. doi: 10.1534/genetics.120.303596
34. Kumar V, Kim K, Joseph C, Kourrich S, Yoo SH, Huang HC, et al. C57BL/6N mutation in cytoplasmic FMRP interacting protein 2 regulates cocaine response. *Science.* (2013) 342:1508–12. doi: 10.1126/science.1245503
35. Yao EJ, Babbas RK, Kelliher JC, Luttik KP, Borrelli KN, Damaj MI, et al. Systems genetic analysis of binge-like eating in a C57BL/6J x DBA/2J-F2 cross. *Genes Brain Behav.* (2021) e12751. doi: 10.1111/gbb.12751
36. Jimenez Chavez CL, Bryant CD, Munn-Chernoff MA, Szumlanski KK. Selective inhibition of PDE4B reduces binge drinking in two C57BL/6 substrains. *Int J Mol Sci.* (2021) 22. doi: 10.3390/ijms22115443
37. Beierle JA, Yao EJ, Goldstein SI, Scotellaro JL, Sena KD, Linnertz CA, et al. Genetic basis of thermal nociceptive sensitivity and brain weight in a BALB/c reduced complexity cross. *Mol Pain.* (2022) 17448069221079540. doi: 10.1177/17448069221079540
38. Goldberg LR, Yao EJ, Kelliher JC, Reed ER, Wu Cox J, Parks C, et al. A quantitative trait variant in Gabra2 underlies increased methamphetamine stimulant sensitivity. *Genes Brain Behav.* (2021) 20:e12774. doi: 10.1111/gbb.12774
39. Tarantino LM, McClearn GE, Rodriguez LA, Plomin R. Confirmation of quantitative trait loci for alcohol preference in mice. *Alcohol Clin Exp Res.* (1998) 22:1099–105. doi: 10.1111/j.1530-0277.1998.tb03707.x
40. Philip VM, Duvvuru S, Gomero B, Ansah TA, Blaha CD, Cook KM, et al. High-throughput behavioral phenotyping in the expanded panel of BXD recombinant inbred strains. *Genes Brain Behav.* (2010) 9:129–59. doi: 10.1111/j.1601-183X.2009.00540.x
41. Yazdani N, Parker CC, Shen Y, Reed ER, Guido MA, Kole LA, et al. Hnrnp1 Is A Quantitative Trait Gene for Methamphetamine Sensitivity. *PLoS Genet.* (2015) 11:e1005713. doi: 10.1371/journal.pgen.1005713
42. Kirkpatrick SL, Goldberg LR, Yazdani N, Babbas RK, Wu J, Reed ER, et al. Cytoplasmic FMR1-Interacting Protein 2 Is a Major Genetic Factor Underlying Binge Eating. *Biol Psychiatry.* (2017) 81:757–69. doi: 10.1016/j.biopsych.2016.10.021
43. Baud AFP, Casale AM, Barkley-Levenson N, Farhadi C, Montillot B, Yalcin J, et al. Dissecting indirect genetic effects from peers in laboratory mice. *Genome Biol.* (2021) 22:216. doi: 10.1186/s13059-021-02415-x

44. Baud AS, McPeck N, Chen K, Hughes A. Indirect Genetic Effects, A Cross-disciplinary Perspective on Empirical Studies. *J Hered.* (2021). doi: 10.1093/jhered/esab059
45. Crabbe JC, Wahlsten D, Dudek BC. Genetics of mouse behavior, interactions with laboratory environment. *Science.* (1999) 284:1670–2. doi: 10.1126/science.284.5420.1670
46. Wahlsten D, Metten P, Phillips TJ, Boehm, Burkhart-Kasch S, Dorow J, et al. Different data from different labs, lessons from studies of gene-environment interaction. *J Neurobiol.* (2003) 54, 283–311. doi: 10.1002/neu.10173
47. Sorge RE, Martin LJ, Isbester KA, Sotocinal SG, Rosen S, Tuttle AH, et al. Olfactory exposure to males, including men, causes stress and related analgesia in rodents. *Nat Methods.* (2014) 11:629–32. doi: 10.1038/nmeth.2935
48. Chesler EJ, Wilson SG, Lariviere WR, Rodriguez-Zas SL, Mogil JS. Identification ranking of genetic and laboratory environment factors influencing a behavioral trait, thermal nociception, via computational analysis of a large data archive. *Neurosci Biobehav Rev.* (2002) 26:907–23. doi: 10.1016/S0149-7634(02)00103-3
49. Chesler EJ, Wilson SG, Lariviere WR, Rodriguez-Zas SL, Mogil JS. Influences of laboratory environment on behavior. *Nat Neurosci.* (2002) 5:1101–2. doi: 10.1038/nn1102-1101
50. Kiraly DD, Walker DM, Calipari ES, Labonte B, Issler O, Pena CJ, et al. Alterations of the host microbiome affect behavioral responses to cocaine. *Sci Rep.* (2016) 6:35455. doi: 10.1038/srep35455
51. Meckel KR, Kiraly DD. A potential role for the gut microbiome in substance use disorders. *Psychopharmacology (Berl).* (2019) 236:1513–30. doi: 10.1007/s00213-019-05232-0
52. Servick K. Of mice and microbes. *Science.* (2016) 353:741–3. doi: 10.1126/science.353.6301.741
53. Ericsson AC, Franklin CL. The gut microbiome of laboratory mice, considerations and best practices for translational research. *Mammalian Genome.* (2021). doi: 10.1007/s00335-021-09863-7
54. Lundberg R, Bahl MI, Licht TR, Toft MF, Hansen AK. Microbiota composition of simultaneously colonized mice housed under either a gnotobiotic isolator or individually ventilated cage regime. *Sci Rep.* (2017) 7:42245. doi: 10.1038/srep42245
55. Ericsson AC, Gagliardi J, Bouhan D, Spollen WG, Givan SA, Franklin CL. The influence of caging, bedding, and diet on the composition of the microbiota in different regions of the mouse gut. *Sci Rep.* (2018) 8:4065. doi: 10.1038/s41598-018-21986-7
56. Bidot WA, Ericsson AC, Franklin CL. Effects of water decontamination methods and bedding material on the gut microbiota. *PLoS ONE.* (2018) 13:e0198305. doi: 10.1371/journal.pone.0198305
57. Bubier JA, Chesler EJ, Weinstock GM. Host genetic control of gut microbiome composition. *Mamm Genome.* (2021) 32:263–81. doi: 10.1007/s00335-021-09884-2
58. Codagnone MG, Stanton C, O'Mahony SM, Dinan TG, Cryan JF. Microbiota neurodevelopmental trajectories. role of maternal and early-life nutrition. *Ann Nutr Metab.* (2019) 74 Suppl 2:16–27. doi: 10.1159/000499144
59. Warner BB. The contribution of the gut microbiome to neurodevelopment and neuropsychiatric disorders. *Pediatr Res.* (2019) 85:216–24. doi: 10.1038/s41390-018-0191-9
60. Vuong HE, Pronovost GN, Williams DW, Coley EJJ, Siegler EL, Qiu A, et al. The maternal microbiome modulates fetal neurodevelopment in mice. *Nature.* (2020) 586:281–6. doi: 10.1038/s41586-020-2745-3

**Conflict of Interest:** The authors declare that the research was conducted in the absence of any commercial or financial relationships that could be construed as a potential conflict of interest.

**Publisher's Note:** All claims expressed in this article are solely those of the authors and do not necessarily represent those of their affiliated organizations, or those of the publisher, the editors and the reviewers. Any product that may be evaluated in this article, or claim that may be made by its manufacturer, is not guaranteed or endorsed by the publisher.

Copyright © 2022 Gaines, Schoenrock, Farrington, Lee, Aponte-Collazo, Shaw, Miller, Ferris, Pardo-Manuel de Villena and Tarantino. This is an open-access article distributed under the terms of the Creative Commons Attribution License (CC BY). The use, distribution or reproduction in other forums is permitted, provided the original author(s) and the copyright owner(s) are credited and that the original publication in this journal is cited, in accordance with accepted academic practice. No use, distribution or reproduction is permitted which does not comply with these terms.



# Glucocorticoid Receptor-Regulated Enhancers Play a Central Role in the Gene Regulatory Networks Underlying Drug Addiction

Sascha H. Duttke<sup>1,2</sup>, Patricia Montilla-Perez<sup>1</sup>, Max W. Chang<sup>1</sup>, Hairi Li<sup>1</sup>, Hao Chen<sup>3</sup>, Lieselot L. G. Carrette<sup>4</sup>, Giordano de Guglielmo<sup>4</sup>, Olivier George<sup>4</sup>, Abraham A. Palmer<sup>4,5</sup>, Christopher Benner<sup>1\*</sup> and Francesca Telese<sup>1\*</sup>

<sup>1</sup> Department of Medicine, University of California, San Diego, La Jolla, CA, United States, <sup>2</sup> School of Molecular Biosciences, College of Veterinary Medicine, Washington State University, Pullman, WA, United States, <sup>3</sup> Department of Pharmacology, Addiction Science and Toxicology, University of Tennessee Health Science Center, Memphis, TN, United States, <sup>4</sup> Department of Psychiatry, University of California, San Diego, La Jolla, CA, United States, <sup>5</sup> Institute for Genomic Medicine, University of California, San Diego, La Jolla, CA, United States

## OPEN ACCESS

### Edited by:

Gary T. Hardiman,  
Queen's University Belfast,  
United Kingdom

### Reviewed by:

Andreas Pfenning,  
Carnegie Mellon University,  
United States  
Katia Gysling,  
Pontificia Universidad Católica  
de Chile, Chile

### \*Correspondence:

Francesca Telese  
ftelese@ucsd.edu  
Christopher Benner  
cbenner@ucsd.edu

### Specialty section:

This article was submitted to  
Neurogenomics,  
a section of the journal  
Frontiers in Neuroscience

**Received:** 20 January 2022

**Accepted:** 25 April 2022

**Published:** 16 May 2022

### Citation:

Duttke SH, Montilla-Perez P,  
Chang MW, Li H, Chen H,  
Carrette LLG, Guglielmo G,  
George O, Palmer AA, Benner C and  
Telese F (2022) Glucocorticoid  
Receptor-Regulated Enhancers Play  
a Central Role in the Gene Regulatory  
Networks Underlying Drug Addiction.  
Front. Neurosci. 16:858427.  
doi: 10.3389/fnins.2022.858427

Substance abuse and addiction represent a significant public health problem that impacts multiple dimensions of society, including healthcare, the economy, and the workforce. In 2021, over 100,000 drug overdose deaths were reported in the US, with an alarming increase in fatalities related to opioids and psychostimulants. Understanding the fundamental gene regulatory mechanisms underlying addiction and related behaviors could facilitate more effective treatments. To explore how repeated drug exposure alters gene regulatory networks in the brain, we combined capped small (cs)RNA-seq, which accurately captures nascent-like initiating transcripts from total RNA, with Hi-C and single nuclei (sn)ATAC-seq. We profiled initiating transcripts in two addiction-related brain regions, the prefrontal cortex (PFC) and the nucleus accumbens (NAc), from rats that were never exposed to drugs or were subjected to prolonged abstinence after oxycodone or cocaine intravenous self-administration (IVSA). Interrogating over 100,000 active transcription start regions (TSRs) revealed that most TSRs had hallmarks of bonafide enhancers and highlighted the KLF/SP1, RFX, and AP1 transcription factors families as central to establishing brain-specific gene regulatory programs. Analysis of rats with addiction-like behaviors versus controls identified addiction-associated repression of transcription at regulatory enhancers recognized by nuclear receptor subfamily 3 group C (NR3C) factors, including glucocorticoid receptors. Cell-type deconvolution analysis using snATAC-seq uncovered a potential role of glial cells in driving the gene regulatory programs associated with addiction-related phenotypes. These findings highlight the power of advanced transcriptomics methods to provide insight into how addiction perturbs gene regulatory programs in the brain.

**Keywords:** transcription, transcriptional enhancer, transcription factor, gene regulation, brain function, addiction, self-administration, glucocorticoid receptor

## INTRODUCTION

Drug addiction and related health problems impact millions of lives in the United States and impose an enormous medical, social, and economic burden on society (Fan et al., 2019). Addiction is a chronic relapsing disorder characterized by diminished control over drug-seeking, compulsive consumption despite negative consequences resulting from drug use, and relapse to drug-taking even after years of abstinence. These enduring effects suggest that chronic drug exposure causes persistent changes in the brain that underlie the development of addiction-related behaviors. The transition from recreational to compulsive drug-seeking is associated with the recruitment of brain reward and stress systems (Koob et al., 2014), including the corticostriatal circuitry that involves the prefrontal cortex (PFC) and the nucleus accumbens (NAc) (Koob and Volkow, 2016). This transition is a critical step in the emergence of compulsivity, which leads to loss of inhibitory control over drug use by recruitment of neuronal populations in the prefrontal cortex (PFC) (Koob and Volkow, 2016).

Numerous studies have demonstrated that long-lasting changes in gene expression patterns in brain regions of the reward pathway are a critical mechanism by which substances of abuse lead to persistent drug-induced neuroadaptations (Russo et al., 2010; Gipson et al., 2014). These neuroadaptations manifest as changes in excitability, synaptic function, and structure, ultimately contributing to the increased risk of relapse after prolonged abstinence (Dong et al., 2017). It is well known that different drugs of abuse act through distinct receptors but engage convergent pathways that activate or repress the activity of transcriptional factors (TFs) or epigenetic regulators, which in turn drive changes in gene expression patterns (Pierce et al., 2018; Hamilton and Nestler, 2019; Teague and Nestler, 2021; Werner et al., 2021). Numerous studies have elucidated the role of crucial TFs in regulating gene expression patterns altered by repeated exposure to addictive drugs, including opioids and cocaine. These TFs include AMP response element-binding protein (CREB),  $\Delta$ FOSB, nuclear factor  $\kappa$ B (NF $\kappa$ B), early growth response protein 3 (EGR3), and nuclear receptor subfamily 4 group a member 1 (NR4A1) (Hope et al., 1994; Carlezon Jr., Thome et al., 1998; Barrot et al., 2002; McClung and Nestler, 2003; Zachariou et al., 2006; Chandra et al., 2015; Carpenter et al., 2020). In parallel, numerous studies have begun to uncover chromatin-mediated mechanisms that contribute to behavioral responses to addictive drugs, such as drug-induced post-translational modification of histone proteins (Stewart et al., 2021).

Despite this knowledge, remarkably little is known about the gene regulatory mechanisms responsible for driving these changes. Mammalian gene expression programs are orchestrated by the collective action of tens or even hundreds of thousands of regulatory elements, most of which are annotated as putative enhancers and located in regions far from the promoter regions of genes (Sheffield et al., 2013). Enhancers recruit key TFs and other cofactors to influence the transcription of nearby genes, are usually cell type- and stimulus-specific (Ong and Corces, 2011; Heinz et al., 2015), and play an essential role in brain development and function (Carullo and Day, 2019).

While the mapping of open chromatin by DNase/ATAC-seq or the epigenetic landscape (e.g., H3K4me1, H3K27ac) by ChIP-seq have provided a wealth of information about potential enhancers (Ernst et al., 2011), discerning their activity or function in different contexts remains challenging.

To improve our understanding of gene regulation underlying addiction-related behaviors, we profiled the activity of regulatory elements in the brains of rats exhibiting addiction-like behaviors using a recently developed technique called capped small(cs)RNA-seq (Duttke et al., 2019). csRNA-seq captures short initiating (20–60 nt) RNAs with a 5' cap structure synthesized during the earliest stages of transcription initiation by RNAP II. The method reveals the genome-wide transcription start sites (TSSs) of both stable and unstable transcripts and, thus, all active regulatory elements, including promoters and enhancers, which we will collectively refer to as transcription start regions (TSRs). Since changes in enhancer RNA transcription serve as one of the most reliable markers for nearby gene regulation (Mikhaylichenko et al., 2018), csRNA-seq profiles can provide critical information about the state of regulatory networks in the cell (Duttke et al., 2019; Lim et al., 2021). Furthermore, the single-nucleotide resolution of csRNA-seq data provides a high-resolution mapping of regulatory elements and can reveal spacing relationships between individual transcription start sites (TSS) and TF binding sites (Duttke et al., 2019).

Here, we compared transcription initiation profiles by csRNA-seq using brain tissues isolated from rats that were not exposed to drugs or were subjected to a well-validated extended access model of intravenous self-administration (IVSA) of oxycodone or cocaine (Ahmed and Koob, 1998; Ahmed et al., 2000, 2002; George et al., 2008; Chen et al., 2013; Koob et al., 2014; de Guglielmo et al., 2019; Carrette et al., 2021). Tissues were collected after five weeks of prolonged abstinence to study the long-term effects of voluntary drug intake and were obtained from a tissue repository (Carrette et al., 2021). We selected NAc for its role in mediating the reinforcing effects of substances of abuse and the prefrontal cortex (PFC) for its role in inhibitory control behavior altered in addiction (Everitt, 2014). We integrated active TSR profiles with bulk and single-cell epigenomic data from rat brains to characterize active regulatory elements genome-wide. By comparing drug-exposed versus control samples, we identified potential TFs binding sites differentially transcribed at key enhancer elements in rats with a history of addiction-like behavior. Overall, these findings show the advantage of profiling initiating transcripts to facilitate the identification of upstream regulators of addiction-like phenotypes.

## RESULTS

### Identification of Transcribed Regulatory Elements in the Rat Brain

To probe if substance abuse can alter gene regulatory programs in the brain, we comprehensively profiled active regulatory elements in two brain regions implicated in addiction: the prefrontal cortex (PFC) and nucleus accumbens (NAc, **Figure 1A**). Samples from

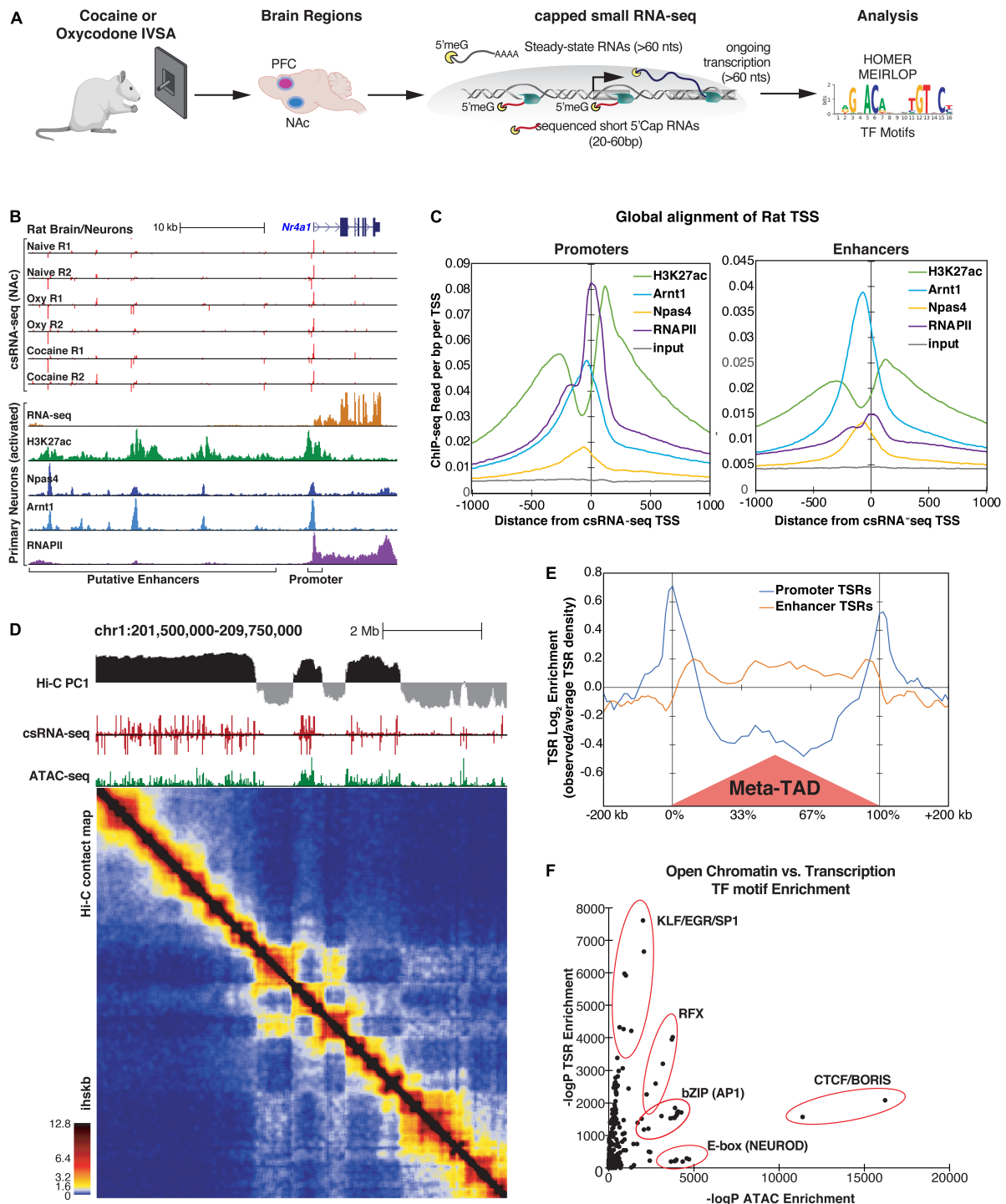


**FIGURE 1 |** Identification of Transcriptional Start Regions (TSRs) by csRNA-seq in rat brain tissues. **(A)** Diagram of study design. **(B)** An example of csRNA-seq data generated from naive, cocaine-, and oxycodone-exposed rat brains at the *Nr4a1* locus (top) showing overlap with previously published transcriptomic and epi-genomic data from rat hippocampal neurons (bottom). **(C)** Distribution of various histone marks and TFs from primary rat hippocampus neurons with respect to promoter-associated (left) or enhancer-associated (right) TSRs identified by csRNA-seq in rat brains. Regions are aligned to the primary transcription start site (TSS) in the TSR. **(D)** Genome browser tracks from a representative region of chr1 showing (from top to bottom) A/B chromatin compartments (PC1 from Hi-C), TSRs (csRNA-seq), open chromatin regions (ATAC-seq), and the corresponding contact map of chromatin interactions (Hi-C) from rat PFC tissues. lkskb = interactions per hundred square kilobases per billion mapped reads. **(E)** Histogram showing the relative distribution of promoter and enhancer-associated TSRs around TAD regions identified by Hi-C. **(F)** Relationship between ATAC and csRNA motif enrichment for known TF motifs. Motifs recognized by key TFs sharing common DNA binding domains are highlighted.

six animals were obtained from a tissue repository (Carrette et al., 2021), including two naive rats, two rats subjected to oxycodone intravenous self-administration (IVSA), and two rats subjected to cocaine IVSA (Arnold et al., 2019; Adhikary et al., 2021; Carrette et al., 2021). We further generated total small RNA-seq libraries used as input in csRNA-seq peak calling to mitigate the identification of false TSS from potential RNA degradation-related biases or other high abundance short RNA species. Except for one of the libraries prepared from the NAc of a rat exposed to oxycodone, which failed QC and was discarded from the analysis, csRNA-seq worked as expected by enriching 5'-capped initiating short transcripts (**Supplementary Table 1** and **Supplementary Figure 1**). As such, the methodological advance of csRNA-seq allowed us to define actively transcribed enhancer RNAs from the banked tissues, which enabled us to explore changes in gene regulatory networks associated with addiction-like behavior.

Across 11 csRNA-seq libraries, we identified 131,647 and 96,563 genomic regions in the PFC and NAc, respectively, with one or more transcription start sites (TSSs) which we refer to as Transcriptional Start Regions (TSRs). While 15.7% TSRs (20,693 total) in PFC and 19.5% TSRs (18,878 total) in NAc were within or proximate to annotated gene promoter regions, the majority were at promoter-distal sites within introns and intergenic regions of the genome (61% in PFC and 57% in NAc; **Supplementary Figure 2A**). These promoter-distal TSRs commonly overlapped with markers of active promoters and enhancers from available rat epigenetic data (**Supplementary Figure 2B**), as exemplified for the *Nr4a1* locus (**Figure 1B**). Notably, as seen for the *Nr4a1* locus, distal TSRs were largely bidirectionally transcribed, a common enhancer feature (**Figure 1B**; De Santa et al., 2010; Kim et al., 2010; Telese et al., 2015). Analysis of all TSRs genome-wide displayed an architecture typical for vertebrates, with the summit of open chromatin just upstream of the TSSs where the strongest transcription factor ChIP-seq signals can be found (**Figure 1C**). At the same time, H3K27ac modified nucleosomes were distributed just downstream or upstream of the regulatory region (**Figure 1C**). Together these data show that csRNA-seq captures active promoters and distal enhancers with high fidelity and accuracy.

The three-dimensional (3D) genome organization can be an essential factor in gene regulation (Andrey et al., 2013; Benabdallah and Bickmore, 2015). To place our identified TSRs in the context of chromatin structure, we generated Hi-C data for the PFC of one rat. 83% of TSRs overlapped with A compartments ( $PC > 0$ ), which define the active region of the genome (**Figure 1D**; Lieberman-Aiden et al., 2009). Notably, the association with the A compartment was significantly stronger ( $p < 1e-16$ ) for transcribed accessible regions ( $n = 91323$  ATAC-seq peaks that overlapped a TSR) compared to those that were not transcribed ( $n = 45389$  ATAC-seq peaks that did not overlap a TSR, **Supplementary Figure 2C**). In addition, TSRs associated with promoters versus enhancers showed a distinct distribution pattern around topological domains (TAD, **Figure 1E**). While promoter-associated TSRs were enriched at TAD boundaries, enhancer-associated TSRs

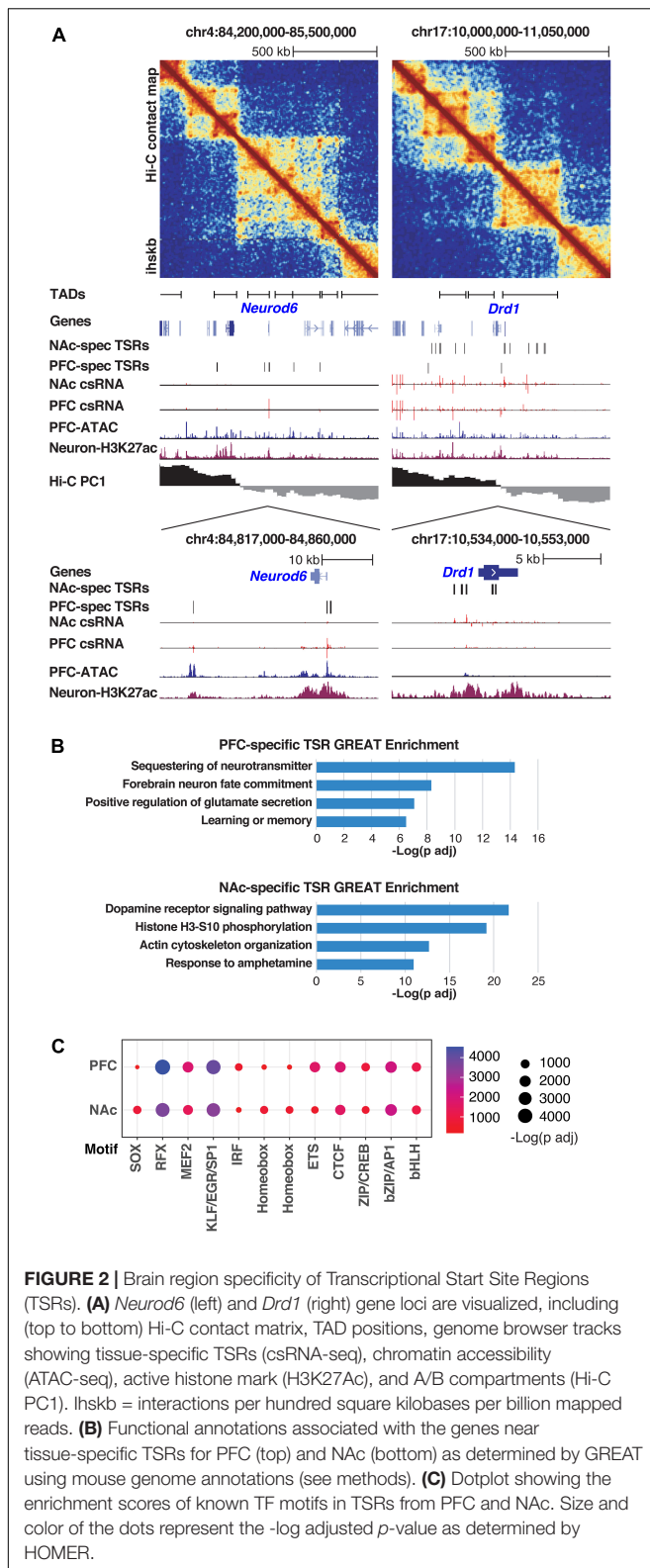
were enriched within TADs (**Figure 1D**), which supports the role of promoters and enhancers in defining the TAD boundaries genome-wide (Dixon et al., 2012). In support of this observation, TSRs also overlapped with the enrichment of H3K27Ac and ATAC-seq peaks at topological domains (TAD) boundaries (**Supplementary Figure 2D**). Contrasting transcribed and untranscribed open chromatin regions revealed the enrichment of CTCF or helix-loop-helix (bHLH) TFs (e.g., NEUROD1 or OLIG2) in regions with little or no transcription (**Figure 1F** and **Supplementary Figure 2E**). At the same time, KLF/SP1, RFX, and AP1 motifs were highly enriched in actively transcribed ones (**Figure 1F** and **Supplementary Figure 2E**), suggesting that these TFs may act as critical activators of brain transcriptional programs. Together, these data emphasize the advantage of capturing enhancer RNAs through methods such as csRNA-seq to define active enhancers over a more basic definition of enhancers simply based on open chromatin or ATAC-seq peaks.

## Brain Region Specificity of TSRs

Enhancers play a critical role in regulating tissue-specific gene expression (Levine, 2010). To identify specific transcriptional signatures for each brain region, we therefore compared TSRs from PFC and NAc, which identified 2,967 PFC-specific and 5,991 NAc-specific TSRs ( $>2$ -fold difference, FDR  $<10\%$ ). Differential TSRs were commonly found near genes typically expressed in the specific brain region. For example, TSRs at the *Neurod6* gene locus were highly transcribed in the PFC but not in the NAc, while the dopamine receptor-1 (*Drd1*) gene locus was highly transcribed in the NAc but not in the PFC (**Figure 2A**). These results are consistent with the known cellular composition of these brain regions, with the PFC enriched in NEUROD6-expressing glutamatergic excitatory neurons and the NAc enriched in DRD1-expressing medium spiny projection neurons. In addition, this analysis showed that the tissue-specific TSRs are often located adjacent to one another and map within the same TAD (**Figure 2A**), suggesting that distal TSRs might preferentially function within a TAD. Brain region-specific changes in TSRs also correlated with changes in gene expression measured by RNA-seq in the same samples, with a stronger correlation for proximal versus distal regulatory elements (**Supplementary Figure 2F**).

These results were corroborated by pathway analysis of genes found in the vicinity of tissue-specific TSRs. TSRs specifically regulated in PFC were enriched near genes involved in glutamate receptor signaling and learning and memory, supporting the known function of cortical areas in cognitive functions (**Figure 2B**, upper panel). On the other hand, the TSRs specifically regulated in NAc were enriched near genes in the dopamine receptor signaling pathway and response to psychostimulants, which support the role of NAc in mediating the rewarding effects of substances of abuse (**Figure 2B**, bottom panel).

The tissue specificity of TSRs was also confirmed by the motif enrichment analysis (**Figure 2C** and **Supplementary Table 2**). In both regions, TSRs were highly enriched in motifs recognized by general TFs, including the KLF/EGR/SP1 family TFs, basic



leucine-zipper (bZIP) TFs (e.g., CREB and AP1 family members) as well as more brain-specific TFs such as MADS-box TFs (e.g., MEF2 family members), and RFX family members (Di Bella et al.,

2021; Li et al., 2021; Yao et al., 2021; Zhang et al., 2021; Ziffra et al., 2021). However, these results differed slightly between PFC and NAc. Specifically, PFC-specific TSRs were enriched preferentially for ETS and ISRE motifs, while NAc-specific TSRs were enriched preferentially for RFX, SOX, and Homeobox motifs (Figure 2C).

These results show that TSRs profiling from repository tissue is a valid approach to decoding tissue-specific regulatory networks, which may be crucial to identifying the TFs driving addiction-related transcriptional programs in a brain region-specific manner.

## Comparison of Oxycodone/Cocaine/Naive Rats Reveals Activated and Repressed Regulatory Programs Associated With Addiction-Like Behaviors

We next sought to identify regulatory elements associated with a history of addiction-like behavior. We limited our analysis to comparing conditions within the same brain regions because normalized csRNA-seq read counts across all samples segregated most strongly based on their brain region of origin (Supplementary Figure 3A). Using a statistical threshold of  $> 2$ -fold difference and FDR  $< 10\%$ , we identified 317 and 90 differentially regulated TSRs associated with addiction-like behavior in NAc and PFC, respectively (Figure 3A, Supplementary Figures 3B,C and Supplementary Table 3). Notably, oxycodone IVSA resulted in more differential TSRs than cocaine IVSA in both regions (Figure 3A and Supplementary Figures 3B,C). In addition, a subset of regulated TSRs were shared between brain regions and conditions (Supplementary Figure 3D). These shared TSRs included several near *Hif3a* and *Fkbp5* loci (Figure 3A and Supplementary Figure 3B). Moreover, differential TSRs were also enriched near genes that have been previously linked to addiction processes [*Foxo3* (Ferguson et al., 2015), *Tlr4* (Wu and Li, 2020)] or addiction vulnerability [*Nat1* (Comings et al., 2000), *Ppm1k* (Carr et al., 2007; Liang et al., 2010), *Pknox2* (Zuo et al., 2014)].

To gain insights into the TFs that may mediate changes in gene expression networks in response to a history of substance abuse, we identified TF motifs enriched in TSRs regulated by oxycodone or cocaine exposure in each brain region. We used MEIRLOP (Brigidi et al., 2019; Delos Santos et al., 2020), a DNA motif analysis approach that associates motifs with the magnitude of regulation at TSRs across conditions based on logistic regression. This analysis identified a strong and consistent association between the glucocorticoid response element (GRE) and TSRs down-regulated in brain tissue from rats with addiction-like phenotypes versus controls (Figure 3B and Supplementary Figure 4A). Our identification of GRE-binding TFs as potential key regulators of addiction-related reprogramming of gene regulatory networks is consistent with the well-established role of glucocorticoid signaling in addiction (Srinivasan et al., 2013; Koob et al., 2014). Furthermore, our analysis identified bZIP motifs for AP1 family members (e.g., CREB, JUN, FOS) as enriched in TSRs up-regulated in both brain

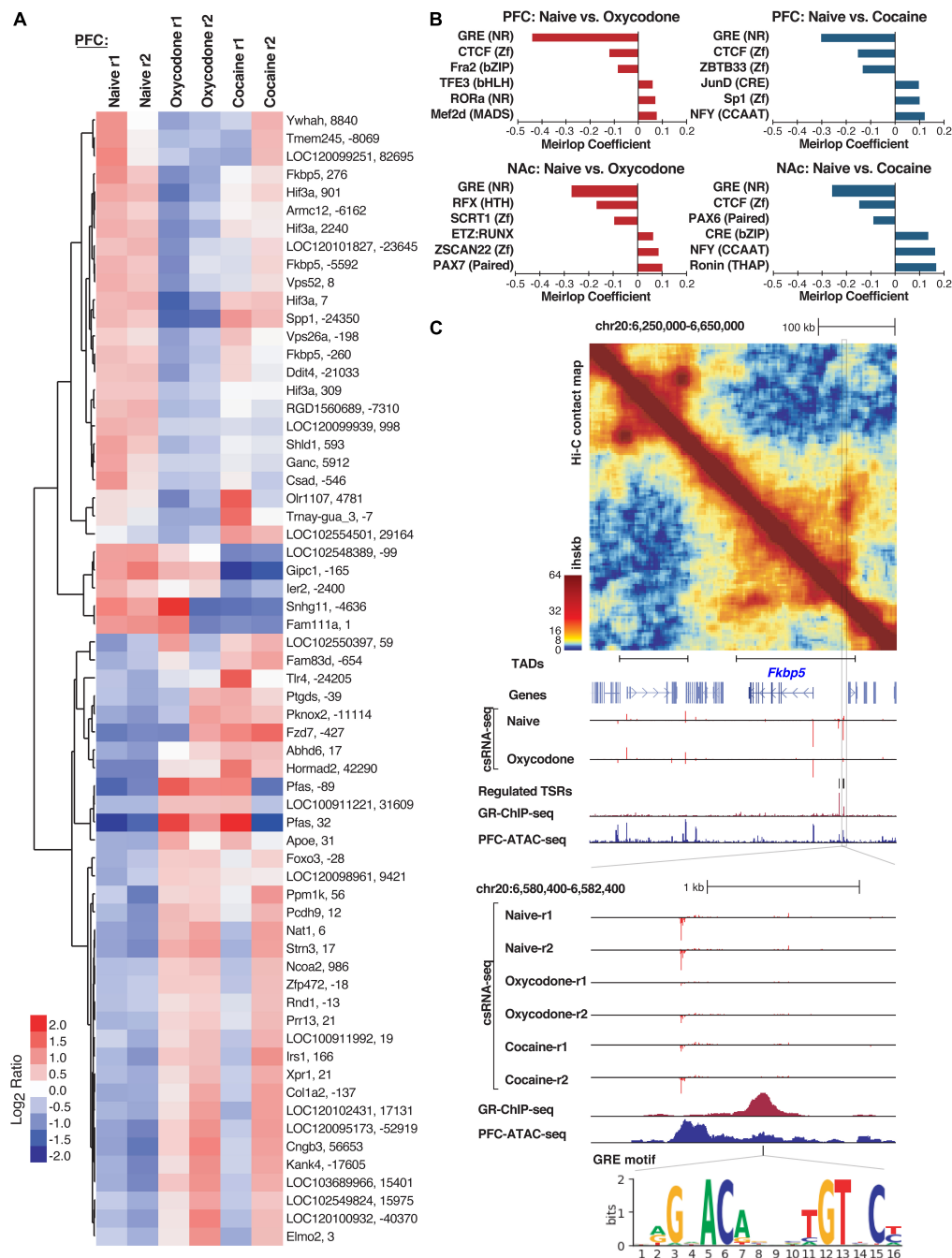


**FIGURE 3 |** Differentially regulated Transcriptional Start Sites (TSRs) in naive versus cocaine or oxycodone exposed rat brains. **(A)** Heatmap of transcription initiation levels from differential TSRs in PFC naive, oxycodone- and cocaine-exposed rats based on mean-centered log2 ratios; each row shows the closest gene and the TSR position relative to that gene's annotated TSS. **(B)** Barplot of significant logistic regression MEIRLOP coefficients for top-ranked motifs associated with regulated TSRs between naive and oxycodone or cocaine conditions in PFC and NAC. **(C)** Example of regulation at the *Fkbp5* gene locus, including (top to bottom) Hi-C contact matrix with TAD positions, genome browser tracks showing regulated TSRs (csRNA-seq), GR binding (ChIP-seq), chromatin accessibility (ATAC-seq), and GRE motif location. lnsk = interactions per hundred square kilobases per billion mapped reads.

regions from rats exposed to cocaine compared to naive rats (Figure 3B), which is consistent with previous findings showing activation of members of the AP1 family in addiction-related processes, such as  $\Delta$ FOSB or CREB (Teague and Nestler, 2021).

To validate the motif enrichment predictions, we next overlapped regulated TSRs with GR binding sites previously identified in the rat hippocampal neurons (Buurstede et al., 2021). We found that 12 of the 32 TSRs

down-regulated in oxycodone-exposed PFC were within 1 kb of a GR ChIP-seq peak ( $p < 0.0002$ ). To further support GR's potential role in regulating these TSRs, several downregulated TSRs were found in the intergenic region upstream of *Fkbp5* (Figure 3C), a well-known GR target gene. Analysis of Hi-C data in this region identified a TAD that encompasses the *Fkbp5* locus and includes the cluster of regulated TSRs associated with addiction-like behavior (Figure 3C), which provides evidence for GR binding and GRE motifs in the nearby regulatory DNA. These results are corroborated by the evidence of enhanced enrichment of GR ChIP signal in TSRs downregulated in brains with addiction-like behaviors (Supplementary Figure 4B).

Together, the unbiased discovery of TSRs, combined with motif analysis, uncovered TF-driven gene regulatory programs associated with addiction-like phenotypes in rats.

### Cell Type Specificity of TSRs Associated With Addiction-Like Behaviors

Enhancers often function in a highly cell type-specific manner (Levine, 2010). Understanding the specific cell types of the brain in which enhancers are active may be critical to unlocking important regulatory mechanisms underlying addiction-like behavior. To this aim, we used a cell type-specific reference of chromatin accessibility sites that we generated by snATAC-seq using the PFC of a naive rat (Figure 4A and Supplementary Figures 4C,D). First, we annotated different classes of brain cell types based on the chromatin accessibility of known cell markers, including excitatory and inhibitory neurons, astrocytes, oligodendrocytes, oligodendrocytes precursor cells, microglia, and endothelial cells, showing that this dataset successfully captured known cell types of the rat PFC. Supporting this result, motif enrichment analysis with HOMER (Figure 4B) showed that motifs for lineage-specific TFs are enriched in their expected cell types (e.g., AP1/MEF2C/TBR1 in neurons, PU.1 in microglia, SOX10 in oligodendrocytes). By cross-referencing TSRs with the snATAC-seq, we assigned expressed genes and their active regulatory elements identified by csRNA-seq to specific cell types (Figure 4C). For example, regulatory elements at gene loci of known cell type-specific markers (e.g., *Olig2*, *Ctss*, *Slc32a1*, *Neurod6*) showed accessible chromatin exclusively in the expected cell types that directly overlapped TSRs identified in the bulk csRNA-seq experiments (Figure 4B).

To address the cell-type specificity of the gene regulatory networks associated with addiction-like behavior, we sought to map the addiction-regulated TSRs to the different cell types identified by snATAC-seq. We analyzed the oxycodone-repressed TSRs in the PFC and NAc, which were strongly enriched in GRE motifs (Figure 3B). This analysis revealed that the downregulated TSRs overlapped accessible regions enriched in non-neuronal cells, such as astrocytes, microglia, and oligodendrocytes (Figure 4D), suggesting the involvement of glial cells in the regulatory programs underlying addiction-like behaviors. When we mapped the GR ChIP-seq peaks corresponding to the downregulated TSRs to cell type-specific accessible sites, we also observed the enrichment of most GR binding sites in

non-neuronal cell types (Supplementary Figure 4E). Given that the repressed TSR were enriched in GRE motifs, this result also suggests a role of GR in regulating transcriptional responses to opioids in glial cells.

These results highlight the advantage of integrating csRNA-seq with snATAC-seq data to probe the cellular specificity of gene regulatory mechanisms and highlight the role of glial cells in modulating addiction-related behavior.

## DISCUSSION

Here we report the active transcriptional landscape of the PFC and NAc from rats with a history of addiction-like behaviors. By integrating transcriptional initiation (csRNA-seq) with genome structure (HiC) and single-cell epigenomic data (snATAC-seq), the analysis of the regulatory landscape not only provided a comprehensive catalog of eRNAs but also identified TFs that are likely to play important regulatory roles. Using this approach, we discovered that GR-bound enhancers are strongly down-regulated during prolonged abstinence from oxycodone or cocaine IVSA, and that many of the impacted sites are specific to glial cells.

There is firm evidence supporting the role of cell type- or stimulus-specific enhancers in the gene regulation (Ostuni et al., 2013; Heinz et al., 2015; Joo et al., 2016), but determining whether an enhancer is active in specific cellular or biological states remains a significant challenge in the field. Recent studies using nascent transcriptional profiling suggest that the transcriptional states of enhancers are better predictors of active chromatin states than open chromatin or histone modifications (Wang et al., 2021). However, many nascent transcriptional methods have technical limitations, including the requirement of intact nuclei and large numbers of cells. csRNA-seq overcomes these limitations by quantifying the level of transcription initiation at regulatory elements, such as enhancers, from total RNA, which can be easily obtained from frozen tissues (e.g., samples from a tissue repository). Using csRNA-seq on  $< 1 \mu\text{g}$  of total RNA isolated from repository brain tissues, we identified  $> 100\text{k}$  TSRs across PFC and NAc from naive rats or rats with addiction-like behavior following oxycodone or cocaine IVSA (Carrette et al., 2021). Most TSRs represent eRNAs as they initiate transcripts in regions associated with known features of enhancer elements, including open chromatin, histones harboring the H3K27ac mark, and bidirectional transcription. Although the function of eRNAs is still controversial (Li et al., 2016), converging lines of evidence show that their abundance is highly correlated with the expression of proximal genes and precedes stimulus-dependent transcription of the mRNA of these genes (Kaikkonen et al., 2013; Arnold et al., 2019). Thus, identifying active enhancers is likely important to decipher the gene regulatory basis of addiction. Furthermore, combining csRNA-seq with TF motif discovery provides different and complementary information than traditional transcriptomic or epigenetic data (e.g., ATAC-seq). As such, it can be used as an unbiased functional assay for TF activity.

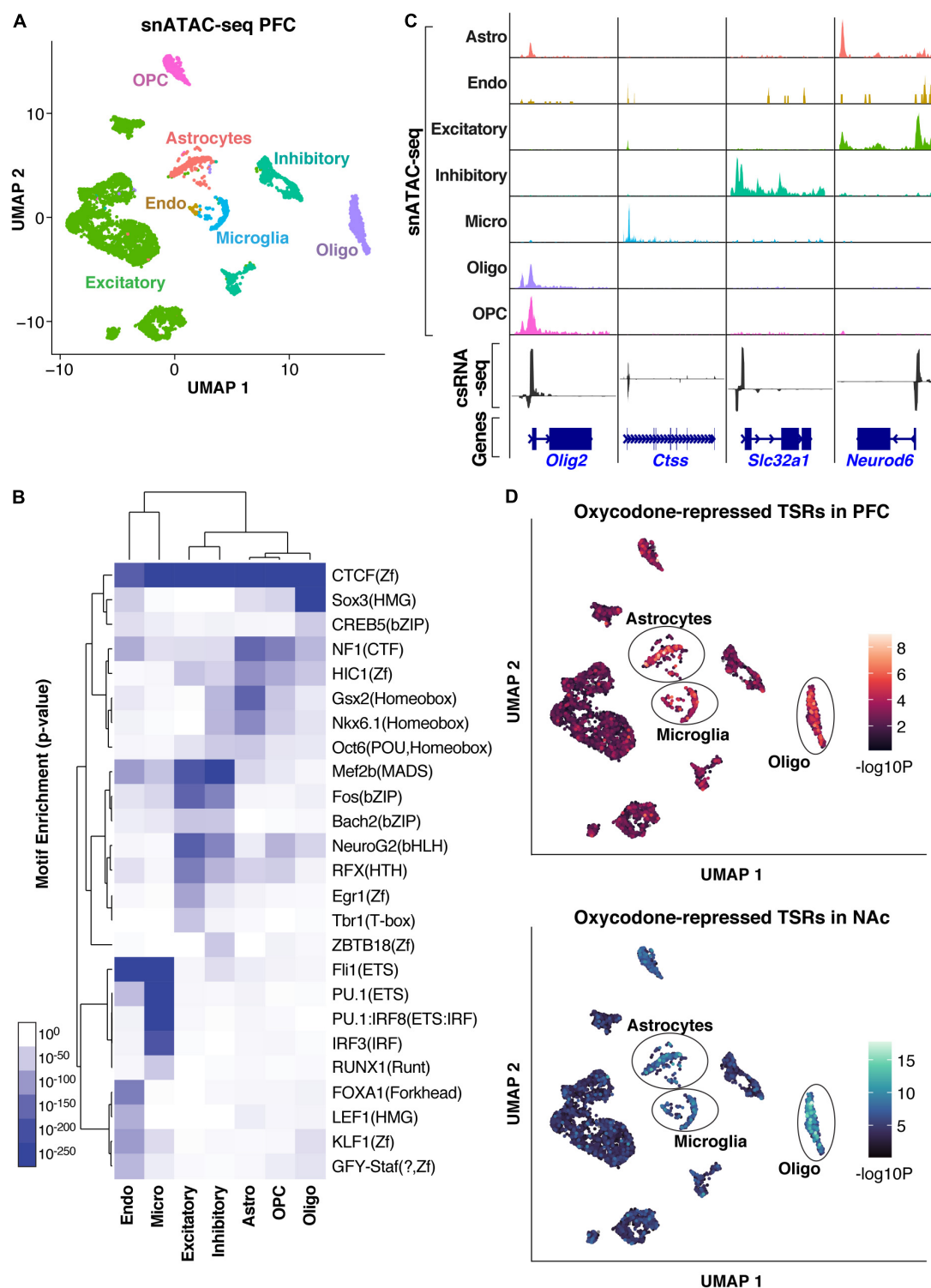


**FIGURE 4 |** Cell-type assignment of active regulatory elements (TSRs). **(A)** UMAP clustering of cells based on snATAC-seq of the PFC. Clusters are colored based on cell types inferred from the accessibility patterns near known marker genes. **(B)** Genome browser tracks of pseudo bulk ATAC-seq read densities showing genes with cell-type-specific snATAC-seq profiles and csRNA-seq from bulk tissue. **(C)** TF motif enrichment across accessible regions from specific cell types in the snATAC-seq data. **(D)** UMAP visualization of oxycodone-associated repressed TSRs enriched in individual cells identified by snATAC-seq in PFC and NAc, showing consistent enrichment in astrocyte, microglia, and oligodendrocyte populations.

The major finding of this study is the identification of TF-regulatory networks associated with a history of addiction-like behavior. The analysis of drug-altered TSRs revealed that GR-regulated enhancers were consistently repressed in PFC and NAc from rats with a history of oxycodone and cocaine addiction-like behavior compared to controls. This result is consistent with converging evidence that the brain stress system involving glucocorticoid signaling plays a critical role in the development of addiction in humans and rodent models of addiction-like phenotypes (Deroche et al., 1997; Deroche-Gamonet et al., 2003; Ambroggi et al., 2009; George and Koob, 2010; Vendruscolo et al., 2012, 2015; Koob et al., 2014). The cell-type deconvolution analysis also showed that repressed TSRs in the PFC and NAc were enriched in glial cells, consistent with findings suggesting that alterations of neuroimmune mechanisms such as neuroinflammation or synaptic remodeling by glial cells can contribute to the liability of addiction (Lacagnina et al., 2017). Furthermore, a recent single-cell transcriptomic study found a robust transcriptional response to acute morphine treatment in oligodendrocytes and astrocytes of the mouse NAc (Avey et al., 2018). Several morphine-induced genes identified in this study were GR targets, supporting the role of GR in regulating transcriptional responses to opioids. In line with this notion, GR has been shown to modulate opioid reward processing by regulating genes essential for astrocytic metabolism (Slezak et al., 2013; Skupio et al., 2020). However, our results show an opposite direction of transcriptional regulation that the different treatment protocols may explain (acute versus chronic exposure), or it may reflect negative feedback mechanisms of glucocorticoid signaling during stress responses associated with addiction-related phenotypes (prolonged abstinence vs. acute withdrawal) (Srinivasan et al., 2013). It is also important to note that our results do not entirely preclude the involvement of neuronal cell types or different TFs that recognize similar motifs, including mineralocorticoid, androgen, or progesterone receptors. Further experiments targeting GR or its targets in specific cell types of rodent models of addiction will be necessary to validate the cell type-specific role of GR in different addiction-like behaviors.

Our study has several limitations. First, we used a limited number of samples ( $n = 2/\text{condition}$ ), which may lead to a low statistical power to detect differentially expressed TSRs and could explain why, despite identifying over 100,000 TSRs across two brain regions, we only detected a relatively small number of differentially regulated TSRs in both PFC and NAc. A study with a larger cohort of rats would be ideal for confirmation. Second, the control animals used in this study are rats that were never exposed to drugs; thus, our study design does not consider environmental factors associated with the behavioral protocol (e.g., surgery, foot-shock, pharmacokinetics factors). Including rats with a low addiction index subjected to the same behavioral protocol but do not develop addiction-like phenotypes would serve as important control to provide more substantial evidence that the differences we observe reflect molecular changes associated with addiction-related processes rather than other phenomena. Third, different subregions of the PFC (e.g., medial vs. orbital) (Porrino and Lyons, 2000; Volkow

et al., 2015; Goldstein and Volkow, 2011) and NAc (e.g., core vs. shell) (Di Chiara, 2002) are known to play distinct roles in addiction-related processes. Thus, analyzing the entire PFC and NAc could mask specific signals from these subregions. Lastly, our study only includes male rats, which precludes the analysis of sex differences in regulatory networks associated with the known sexual dimorphism of addiction-like behaviors (Fattore and Melis, 2016).

In summary, we used an unbiased and highly sensitive method to identify active enhancers by measuring levels of initiating transcripts from brain tissues of rats with addiction-like phenotypes. We identified TF-centered regulatory mechanisms implicated in addiction, including those regulated by GR in glial cells. Overall, our study demonstrates that transcriptional initiation profiling has the potential to dissect the gene regulatory mechanisms driving addiction-related phenotypes in an unbiased and quantitative manner.

## MATERIALS AND METHODS

### Brain Samples

Brain samples from male heterogeneous stock (HS) rats (2 naive, 2 cocaine, 2 oxycodone) were obtained from the cocaine oxycodone<sup>1,2</sup> tissue repositories at UCSD and are part of an extensive and ongoing study of addiction that uses outbred HS rats<sup>3</sup> (Solberg Woods and Palmer, 2019). We selected samples collected during prolonged abstinence after the last session of extended access to oxycodone or cocaine IVSA (Carrette et al., 2021). In this model, male Heterogeneous Stock (HS) rats were trained to self-administer drugs in short access conditions (2 h/day for 4 days for oxycodone or 2 h/day for 10 days for cocaine) followed by long access conditions (12 h/day for oxycodone and 6 h/day for cocaine) for 14 days to develop escalation of drug intake. Following the escalation phase, the rats from the oxycodone cohort were characterized for motivation (progressive ratio responding), withdrawal-induced hyperalgesia (mechanical nociception, von Frey test), and development of tolerance to the analgesic effect of opioids (tail immersion test). For the cocaine cohorts, rats were characterized for motivation (progressive ratio responding), compulsive-responding to drug use (contingent footshock), and irritability-like behavior (bottle-brush test). An Addiction Index was computed by integrating all the behavioral measures (Kallupi et al., 2020; Carrette et al., 2021; Sedighim et al., 2021). HS rats classified as having a high Addiction Index were used for this study. Age-matched naive male rats that were not exposed to any drug were used as control. Lastly, brain punches of PFC and NAc tissues were collected after 5 weeks of abstinence. Brain tissue was extracted and snap-frozen (at  $-30^{\circ}\text{C}$ ). Cryosections of approximately 500 microns were used to dissect PFC and NAc punches on a  $-20^{\circ}\text{C}$  frozen stage. Bregma for PFC: 4.20–2.76 mm, and for NAc: 2.28–0.72 mm (3 sections were combined for each).

<sup>1</sup>[www.oxycodonebiobank.org](http://www.oxycodonebiobank.org)

<sup>2</sup>[www.cocainebiobank.org](http://www.cocainebiobank.org)

<sup>3</sup>[www.ratgenes.org](http://www.ratgenes.org)

## csRNA-Seq Library Preparation

We extracted total RNA from PFC and NAc tissues dissected from 6 rat brains using Trizol Reagent (Invitrogen, Cat. num. 15596018) and Zirconium Beads RNase Free (Next Advance, Cat. num. ZrOB05-RNA 0.5 mm) with the Bullet Blender Blue (Next Advance, Model. num. BBX24B) at speed 6 for 1 min. The RNA was purified according to the manufacturer's instructions (Invitrogen).

csRNA-seq was performed as described previously (Duttke et al., 2019). Briefly, small RNAs of ~15–60 nt were size selected from 0.3–1.0 microgram of total RNA by denaturing gel electrophoresis. A 10% input sample was taken aside, and the remainder enriched for 5'-capped RNAs. Monophosphorylated RNAs were selectively degraded by Terminator 5'-phosphate-dependent exonuclease (Lucigen). Subsequent 5' dephosphorylation by quickCIP (NEB) followed by decapping with RppH (NEB) augments Cap-specific 5' adapter ligation by T4 RNA ligase 1 (NEB) (Hetzel et al., 2016). Thermostable quickCIP was used instead of rSAP, and hence the bead clean-up step was skipped before heat denaturation before the second round of CIP treatment. The 3' adapter was ligated using truncated T4 RNA ligase 2 (NEB) before 3' repair to select against degraded RNA fragments. Following cDNA synthesis, libraries were amplified for 11–14 cycles and sequenced SE75 on the Illumina NextSeq 500 sequencer.

## mRNA-Seq Library Preparation

RNA sequencing libraries were generated using the Illumina® Stranded mRNA Prep (Illumina, San Diego, CA). Samples were processed following the manufacturer's instructions. The resulting libraries were multiplexed and sequenced with 100 basepairs (bp) Paired-End reads (PE100) to a depth of approximately 25 million reads per sample on an Illumina NovaSeq 6000. Samples were demultiplexed using bcl2fastq Conversion Software (Illumina, San Diego, CA, United States).

## Hi-C Library Preparation

One adult SHR/OlaIpcv naive rat was used to generate the Hi-C data. This rat was bred at the University of Tennessee Health Science Center using breeders provided by the Hybrid Rat Diversity Program at the Medical College of Wisconsin. The animal was fully anesthetized by using isoflurane before the brains were removed. Brain tissue was extracted and rapidly frozen. Cryosections of approximately 120 microns were obtained in a cryostat set at −11°C. PFC punches were dissected on a −20°C frozen stage. Tissues were then pulverized in liquid nitrogen. The Arima-Hi-C kit was used to construct the Hi-C libraries (#A410231, Arima Genomics). Sequencing of the libraries was conducted on an Illumina Novaseq S4 instrument by Novogen Inc. The use of rodents was approved by UTHSC IACUC.

## Single-Nuclei ATAC-Seq Library Preparation

PFC brain tissue from one naive male HS rat was used to generate a single-nuclei ATAC-seq library. Nuclei were isolated from

brain tissue as previously described (Corces et al., 2018). Briefly, frozen tissue was homogenized using a 2 ml glass dounce with 1 ml cold 1x Homogenization Buffer (HB). The cell suspension was filtered using a 70 µm Flowmi strainer (BAH136800070, Millipore Sigma) and centrifuged at 350g for 5 min at 4°C. Nuclei were isolated by iodixanol (D1556, Millipore Sigma) density gradient. The nuclei iodixanol solution (25%) was layered on top of 40% and 30% iodixanol solutions. Samples were centrifuged in a swinging bucket centrifuge at 3,000g for 20 min at 4°C. Nuclei were isolated from the 30–40% interface. Library preparation targeting the capture of ~6000 nuclei was carried out as detailed in the Chromium Next GEM Single Cell ATAC v1.1 manual (10x Genomics). Library sequencing was performed using the Illumina NovaSeq.

## csRNA-Seq and RNA-Seq Analysis

Sequencing reads were trimmed for 3' adapter sequences using HOMER ("homerTools trim -3 AGATCGGAAGAGCACACGTCT -mis 2 -min Match Length 4 -min 20") and aligned to the rat mRatBN7.2/rn7 genome assembly using STAR (Dobin et al., 2013) with default parameters. Sequencing statistics are included in **Supplementary Table 1**. Only reads with a single, unique alignment (MAPQ > = 10) were considered in the downstream analysis. Furthermore, reads with spliced or soft clipped alignments were discarded (the latter often removes erroneous alignments from abundant snRNA species). Transcription Start Regions (TSRs), representing 150 bp sized loci with significant transcription initiation activity (i.e., 'peaks' in csRNA-seq), were defined using HOMER's findPeaks tool using the '-style tss' option, which uses short input RNA-seq to eliminate loci with csRNA-seq signal arising from non-initiating, high abundance RNAs that nonetheless are captured and sequenced by the method (full description is available in Duttke et al. (2019)). To lessen the impact of outlier samples across the data collected for this study, csRNA-seq samples were first pooled into a single META-experiment per brain tissue region to collectively identify TSRs in each tissue. The resulting TSRs were then quantified in all samples by counting the 5' ends of reads aligned at each TSR on the correct strand. The raw read count table was then normalized using DESeq2's rlog variance stabilization method (Love et al., 2014).

The resulting normalized data was used for all downstream analyses. Normalized genome browser visualization tracks were generated using HOMER's makeMultiWigHub.pl tool (Heinz et al., 2010). TSR genomic DNA extraction, nucleotide frequency analysis relative to the primary TSS, general annotation, and other general analysis tasks were performed using HOMER's annotatePeaks.pl function. Overlaps between TSRs and other genomic features (including peaks from published studies and annotation to the 5' promoter using RefSeq defined transcripts), was performed using HOMER's mergePeaks tool. When defining promoter and enhancer TSRs, promoter TSRs were defined as TSRs overlapping annotated gene TSS in the sense direction within 200 bp, while enhancer TSRs were defined as TSRs found greater than 3 kb from any annotated gene TSS. Functional enrichment analysis of regulated regions was performed using

GREAT (McLean et al., 2010) by identifying homologous regions for each TSR in the mouse genome (mm10) using UCSC Genome Browser's liftOver tool and running GREAT using the mm10 database.

To identify differential TSRs between brain regions or conditions (naive vs. cocaine or oxycodone), we used DESeq2 with FDR < 10% PFC vs. NAc, Naive vs. Oxycodone, Naive vs. Cocaine, or Oxycodone vs. Cocaine, and 2-fold change, as cutoffs. DESeq2 log2 fold change, p-value, and adj. P-value for all differentially regulated TSRs in response to addiction-like behaviors in each tissue are reported in **Supplementary Table 3**. Because one of the NAc-oxycodone samples failed QC, we estimated variability using pooled replicate variance from the duplicate naive samples during the differential calculation.

For RNA-seq analysis, sequencing reads were aligned to the rat mRatBN7.2/rn7 genome assembly using STAR (Dobin et al., 2013) with default parameters. Gene expression values were calculated using feature Counts and normalized using DESeq2's rlog function. To compare changes in RNA-seq gene expression values to change in csRNA-seq levels (**Supplementary Figure 2F**), csRNA-seq TSRs were first assigned to the nearest annotated gene TSS using HOMER's annotatePeaks.pl program. Log2 ratios between PFC and NAc naive tissues for both csRNA-seq and RNA-seq were then stratified across TSR-promoter sets based on the distance of the TSR to the annotated gene TSS.

## Analysis of Previously Published ChIP-Seq and ATAC-Seq Data

Raw FASTQ files associated with public ChIP-seq and ATAC-seq datasets were downloaded from NCBI's Short Read Archive and processed in a consistent manner to ensure differences in data processing were minimized for downstream analysis. Reads from ChIP-seq or ATAC-seq datasets were analyzed in a consistent manner. Reads were first trimmed for adapter sequences and then aligned to the rat genome using STAR (Dobin et al., 2013) with default parameters. Only reads with a single, unique alignment (MAPQ > = 10) were considered in the downstream analysis. ChIP/ATAC-seq peaks were identified using HOMER's findPeaks tool using "-style factor" and "-style atac," respectively. Normalized genome browser tracks were generated using HOMER's makeMultiWigHub.pl tool. Peak annotations and normalized read density counts were calculated using HOMER's annotatePeaks.pl tool. Overlapping peaks were determined using HOMER's mergePeaks.

Datasets used in the study include GR ChIP-seq GSE160806 from the rat hippocampus (Buurstede et al., 2021). ATAC-seq GSE134935 from rat PFC (Scherma et al., 2020); histone marks and TF ChIP-seqs GSE127793 from rat hippocampal neurons (Brigidi et al., 2019).

## Hi-C Analysis

Hi-C reads were first trimmed for sequences downstream of the restriction/ligation site ("GATCGATC") and aligned to the rat genome using STAR with default parameters. Normalized interaction contact maps were then generated using

HOMER. PCA compartment analysis and topological domain (TAD) calls were generated using HOMER's runPCAhic.pl and findTADsAndLoops.pl scripts (Heinz et al., 2018). The significant association of the A compartment (PC > 1) with ATAC-seq peaks and/or TSRs was calculated using the Mann-Whitney non-parametric Ranksum test.

## DNA Motif Analysis

Known motif enrichment and *de novo* motif discovery of TSRs were performed using HOMER's findMotifsGenome.pl tool using 200 bp sequences centered on [-150,+50] relative to TSR primary initiation sites (e.g., strongest TSS in the region) or from -100,100 relative to the center of ATAC-seq peaks (Heinz et al., 2010). When performing *de novo* motif discovery, sequences were compared to a background set of 50,000 random genomic regions matched for overall GC-content. Nucleotide frequency and motif density plots were created using HOMER's annotatePeaks.pl tool (Heinz et al., 2010). When analyzing ATAC-seq peaks from cell types identified by snATAC-seq, the top 25,000 peaks were selected from each cell type to avoid comparing motif enrichment from sets with large differences in the number of regions that can impact the absolute enrichment levels.

To analyze motif enrichment associated with changes in transcription levels, we analyzed regulated TSRs with MEIRLOP (Delos Santos et al., 2020). Sequences were scored based on their shrunken log2 fold change between treatment conditions (e.g., naive vs. cocaine or oxycodone exposed) and analyzed with MEIRLOP using HOMER's known transcription factor motif library. Based on their regression coefficients, the top 3 motifs associated with up- and down-regulation are reported for each comparison (adj. *p*-values < 0.05).

Furthermore, we provide the BigWig track with the map of transcription factor binding site predictions in the rat genome (rn7), which can be uploaded as a custom track on the UCSC browser as follow:

```
track type=bigBed name="HOMER Known Motifs rn7 (210922)"
description="HOMER Known Motifs rn7 (210922)"
bigDataUrl=http://homer.ucsd.edu/homer/data/motifs/homer.
KnownMotifs.rn7.210922.bigBed visibility=3
```

## Single Nuclei ATAC-Seq Analysis

Sequencing reads were processed using Cell Ranger ATAC 2.0 with a custom reference for *Rattus norvegicus*, built from the Ensembl Rnor 6.0 release 103 genome and annotation. The filtered results were subsequently analyzed using Signac 1.4.0 (Stuart et al., 2021). Only peaks present in at least 10 cells and cells with at least 200 peaks were considered. Further filtering was performed to retain only cells with between 3,000 and 25,000 fragments, at least 30% of reads in peaks, a blacklist ratio less than 0.05, nucleosome signal less than 4, and TSS enrichment of at least 2.5. Based on these criteria, we retained 7,065 of 7,694 initial nuclei. Normalization and linear dimensionality reduction were performed using TFIDE, identifying top features with no minimum cutoff and SVD. Nonlinear dimensionality reduction with UMAP and neighbor finding used LSI components 2 through 30, and clustering was performed with the SLM

algorithm (Blondel et al., 2008). Cell types were assigned using inferred gene activity. The following cell marker genes were used: *Slc17a* for excitatory neurons, *Gad2* for inhibitory neurons, *Gjai* for astrocytes, *C1qa* for microglia, *Mobp* for oligodendrocytes, *Pdgfra* for oligodendrocytes precursor cells (OPC), *Flt1* for endothelial cells. Pseudo bulk peak positions for each cell type were identified using MACS2 (Zhang et al., 2008). In addition, we used Amulet (Thibodeau et al., 2021) to detect multiplets, which identified 532 nuclei (~7.5%) as multiplets. These nuclei were removed to visualize the read coverage and TSR enrichment plots. Per-cell TSR enrichment significance was calculated using a one-tailed hypergeometric test and corrected for multiple hypothesis testing using the Bonferroni-Hochberg method.

## DATA AVAILABILITY STATEMENT

The datasets presented in this study can be found in online repositories. The names of the repository/repositories and accession number(s) can be found below: <https://www.ncbi.nlm.nih.gov/geo/>, GSE193757.

## ETHICS STATEMENT

The animal study was reviewed and approved by the institutional Animal Care and Use Committee at the University of California, San Diego.

## AUTHOR CONTRIBUTIONS

FT conceived, designed, and coordinated the study. CB conceived, designed, conducted the overall bioinformatic analysis. SD generated the csRNA-seq data. PM-P assisted with the csRNA-seq data generation. MC conducted the snATAC-seq analysis. HL generated snATAC-seq data. HC generated the HiC data. LC dissected the brain tissues. GG, OG, and AP contributed expertise important for the study design. FT, CB, and SD wrote the manuscript with input from all authors.

## FUNDING

This work was supported by NIH (R00GM135515 to SD; DA050239 to FT; DA051972 to FT and CB; GM134366 to CB; U01DA047638 to HC; P50DA037844 to AP.; DA043799, DA037844 to OG. This publication includes data generated at the UC San Diego IGM Genomics Center utilizing an Illumina NovaSeq 6000 that was purchased with funding from a National Institutes of Health SIG grant (#S10 OD026929). A version of this manuscript is hosted on BioRxiv <https://doi.org/10.1101/2022.01.12.475507>.

## REFERENCES

- Adhikary, S., Roy, S., Chacon, J., Gadad, S. S., and Das, C. (2021). Implications of enhancer transcription and enhancers in cancer. *Cancer Res.* 81, 4174–4182. doi: 10.1158/0008-5472.CAN-20-4010
- Ahmed, S. H., and Koob, G. F. (1998). Transition from moderate to excessive drug intake: change in hedonic set point. *Science* 282, 298–300.
- Ahmed, S. H., Kenny, P. J., Koob, G. F., and Markou, A. (2002). Neurobiological evidence for hedonic allostasis associated with escalating cocaine use. *Nat. Neurosci.* 5, 625–626. doi: 10.1038/nn872

## ACKNOWLEDGMENTS

We want to thank Lisa Maturin for her technical assistance.

## SUPPLEMENTARY MATERIAL

The Supplementary Material for this article can be found online at: <https://www.frontiersin.org/articles/10.3389/fnins.2022.858427/full#supplementary-material>

**Supplementary Figure 1** | csRNA-seq data in rat brain tissues. (A) Variation in csRNA-seq levels at each Transcriptional Start Site (TSR) between tissues (NAc vs. PFC) or between replicates (PFC r1 vs. r2) in samples from naive rat brains. (B) Read length distribution for input libraries (left) and csRNA-seq libraries (right). Input libraries show a strong spike at 21 nt corresponding to mature miRNA. (C) Nucleotide frequencies at csRNA-seq reads shown for the PFC naive-r1 library. (D) Read counts at the annotated promoters (5' end of transcripts  $\pm$  200bp) with blue dots indicating miRNA transcripts, red dots mRNA transcripts, and grey dots other transcripts (snRNAs, snoRNAs, etc.). csRNA-seq and input data corresponding to the PFC naive-r1 sample is shown.

**Supplementary Figure 2** | Identification and characterization of Transcriptional Start Sites (TSRs) from csRNA-seq data. (A) Pie charts showing the distribution of TSRs in different genomic regions. (B) Fraction (%) of promoter- and enhancer-associated TSRs that overlap peaks identified from ATAC-seq or ChIP-seq for several histone marks. The total numbers of overlapping peaks are reported. (C) Violin plot showing the distribution of Hi-C PC1 values for ATAC-seq peaks that are not transcribed or overlapping a TSR. (D) Histogram showing the distribution of TSRs, H3K27Ac and ATAC-seq peaks around TAD regions identified by Hi-C. (E) Location of several TFs motifs with respect to the primary TSS from csRNA-seq TSRs and the center of ATAC peaks genome-wide. (F) Scatter plots of transcript level differences (Log2 ratio) between NAc and PFC in RNA-seq vs csRNA-seq for TSRs located at different distances from gene TSS.

**Supplementary Figure 3** | Differentially regulated Transcriptional Start Sites (TSRs) in naive versus cocaine- or oxycodone- exposed rat brains. (A) Hierarchical clustering of csRNA-seq samples shows segregation based on brain regions. (B) Heatmap of differential TSRs in NAc naive, oxycodone- and cocaine-exposed rats based on log2 ratios relative to the mean; each row showing the closest gene, TSR position relative to TSS, and chromosomal coordinates. (C) Number of differentially regulated TSRs ( $>2$  fold, FDR  $< 10\%$ ) across naive and drug-exposed conditions. (D) Venn diagram showing the number of overlapping TSRs between different brain regions and drug treatment conditions. P-values for the Fisher Exact Test are reported for each Venn diagram.

**Supplementary Figure 4** | Relationship of GR enhancers with cell type-specific open chromatin regions: (A) Fraction of TSR containing the GRE motif in TSRs regulated by oxycodone showing that ~20% of downregulated TSRs are enriched in GRE motifs. (B) GR binding based on ChIP-seq is enriched in downregulated TSRs in oxycodone-treated vs control rats. (C) Insert size distribution of transposase accessible fragments sequenced showing expected periodicity (~150bp). (D) Large TSS enrichment score of ~10 is computed from the transposable sites per base in a window of 2,000 bases around annotated TSSs and shows the expected high accessibility of TSSs compared to flanking regions.

**Supplementary Table S1** | Alignment Stats.

**Supplementary Table S2** | Motif Enrichment Results.

**Supplementary Table S3** | Differential TSRs.

- Ahmed, S. H., Walker, J. R., and Koob, G. F. (2000). Persistent increase in the motivation to take heroin in rats with a history of drug escalation. *Neuropsychopharmacology* 22, 413–421. doi: 10.1016/S0893-133X(99)00133-5
- Ambroggi, F., Turiault, M., Milet, A., Deroche-Gamonet, V., Parnaudeau, S., Balado, E., et al. (2009). Stress and addiction: glucocorticoid receptor in dopaminergic neurons facilitates cocaine seeking. *Nat. Neurosci.* 12, 247–249. doi: 10.1038/nn.2282
- Andrey, G., Montavon, T., Mascres, B., Gonzalez, F., Noordermeer, D., Leleu, M., et al. (2013). A switch between topological domains underlies HoxD genes collinearity in mouse limbs. *Science* 340:1234167. doi: 10.1126/science.1234167
- Arnold, P. R., Wells, A. D., and Li, X. C. (2019). Diversity and emerging roles of enhancer RNA in regulation of gene expression and cell fate. *Front. Cell Dev. Biol.* 7:377. doi: 10.3389/fcell.2019.00377
- Avey, D., Sankararaman, S., Yim, A. K. Y., Barve, R., Milbrandt, J., and Mitra, R. D. (2018). Single-cell RNA-Seq uncovers a robust transcriptional response to morphine by glia. *Cell Rep.* 24, 3619–3629.e4. doi: 10.1016/j.celrep.2018.08.080
- Barrot, M., Olivier, J. D. A., Perrotti, L. I., DiLeone, R. J., Berton, O., Eisch, A. J., et al. (2002). CREB activity in the nucleus accumbens shell controls gating of behavioral responses to emotional stimuli. *Proc. Natl. Acad. Sci. U.S.A.* 99, 11435–11440. doi: 10.1073/pnas.172091899
- Benabdallah, N. S., and Bickmore, W. A. (2015). Regulatory domains and their mechanisms. *Cold Spring Harb. Symp. Quant. Biol.* 80, 45–51.
- Blondel, V. D., Guillaume, J.-L., Lambiotte, R., and Lefebvre, E. (2008). Fast unfolding of communities in large networks. *J. Stat. Mech.* 2008:10008. doi: 10.1103/PhysRevE.83.036103
- Brigidi, G. S., Hayes, M. G. B., Delos Santos, N. P., Hartzell, A. L., Texari, L., Lin, P.-A., et al. (2019). Genomic decoding of neuronal depolarization by stimulus-specific npas4 heterodimers. *Cell* 179, 373–391.e27. doi: 10.1016/j.cell.2019.09.004
- Buurstede, J. C., van Weert, L. T. C. M., Colucci, P., Gentenaar, M., Viho, E. M. G., Koorneef, L. L., et al. (2021). Hippocampal glucocorticoid target genes associated with enhancement of memory consolidation. *Eur. J. Neurosci.* 00:1–18. doi: 10.1111/ejn.15226
- Carlezon, W. A. Jr., Thome, J., Olson, V. G., Lane-Ladd, S. B., Brodtkin, E. S., Hiroi, N., et al. (1998). Regulation of cocaine reward by CREB. *Science* 282, 2272–2275.
- Carpenter, M. D., Hu, Q., Bond, A. M., Lombroso, S. I., Czarnecki, K. S., Lim, C. J., et al. (2020). Nr4a1 suppresses cocaine-induced behavior via epigenetic regulation of homeostatic target genes. *Nat. Commun.* 11:504. doi: 10.1038/s41467-020-14331-y
- Carr, L. G., Kimpel, M. W., Liang, T., McClintick, J. N., McCall, K., Morse, M., et al. (2007). Identification of candidate genes for alcohol preference by expression profiling of congenic rat strains. *Alcohol. Clin. Exp. Res.* 31, 1089–1098. doi: 10.1111/j.1530-0277.2007.00397.x
- Carrette, L. L. G., de Guglielmo, G., Kallupi, M., Maturin, L., Brennan, M., Boomhower, B., et al. (2021). The cocaine and oxycodone biobanks, two repositories from genetically diverse and behaviorally characterized rats for the study of addiction. *eNeuro* 8, 1–12. doi: 10.1523/ENEURO.0033-21.2021
- Carullo, N. V. N., and Day, J. J. (2019). Genomic enhancers in brain health and disease. *Genes (Basel)* 10:43. doi: 10.3390/genes10010043
- Corces, M. R., Granja, J. M., Shams, S., Louie, B. H., Seoane, J. A., Zhou, W., et al. (2018). The chromatin accessibility landscape of primary human cancers. *Science* 362:eaav1898.
- Chandra, R., Francis, T. C., Konkalmatt, P., Amgalan, A., Gancarz, A. M., Dietz, D. M., et al. (2015). Opposing role for Egr3 in nucleus accumbens cell subtypes in cocaine action. *J. Neurosci.* 35, 7927–7937. doi: 10.1523/JNEUROSCI.0548-15.2015
- Chen, B. T., Yau, H.-J., Hatch, C., Kusumoto-Yoshida, I., Cho, S. L., Hopf, F. W., et al. (2013). Rescuing cocaine-induced prefrontal cortex hypoactivity prevents compulsive cocaine seeking. *Nature* 496, 359–362. doi: 10.1038/nature12024
- Comings, D. E., Muhleman, D., Wu, S., and MacMurray, J. (2000). Association of the N-acetyltransferase I gene (NAT1) with mild and severe substance abuse. *Neuroreport* 11, 1227–1230. doi: 10.1097/00001756-200004270-00017
- de Guglielmo, G., Kallupi, M., Sedighim, S., Newman, A. H., and George, O. (2019). Dopamine d3 receptor antagonism reverses the escalation of oxycodone self-administration and decreases withdrawal-induced hyperalgesia and irritability-like behavior in oxycodone-dependent heterogeneous stock rats. *Front. Behav. Neurosci.* 13:292. doi: 10.3389/fnbeh.2019.00292
- De Santa, F., Barozzi, I., Mietton, F., Ghisletti, S., Polletti, S., Tusi, B. K., et al. (2010). A large fraction of extragenic RNA pol II transcription sites overlap enhancers. *PLoS Biol.* 8:e1000384. doi: 10.1371/journal.pbio.1000384
- Delos Santos, N. P., Texari, L., and Benner, C. (2020). MEIRLOP: improving score-based motif enrichment by incorporating sequence bias covariates. *BMC Bioinformatics* 21:410. doi: 10.1186/s12859-020-03739-4
- Deroche, V., Marinelli, M., Le Moal, M., and Piazza, P. V. (1997). Glucocorticoids and behavioral effects of psychostimulants. II: cocaine intravenous self-administration and reinstatement depend on glucocorticoid levels. *J. Pharmacol. Exp. Ther.* 281, 1401–1407.
- Deroche-Gamonet, V., Sillaber, I., Aouizerate, B., Izawa, R., Jaber, M., Ghazizadeh, S., et al. (2003). The glucocorticoid receptor as a potential target to reduce cocaine abuse. *J. Neurosci.* 23, 4785–4790. doi: 10.1523/JNEUROSCI.23-11-04785.2003
- Di Bella, D. J., Habibi, E., Stickels, R. R., Scalia, G., Brown, J., Yadollahpour, P., et al. (2021). Molecular logic of cellular diversification in the mouse cerebral cortex. *Nature* 595, 554–559.
- Di Chiara, G. (2002). Nucleus accumbens shell and core dopamine: differential role in behavior and addiction. *Behav. Brain Res.* 137, 75–114.
- Dixon, J. R., Selvaraj, S., Yue, F., Kim, A., Li, Y., Shen, Y., et al. (2012). Topological domains in mammalian genomes identified by analysis of chromatin interactions. *Nature* 485, 376–380. doi: 10.1038/nature11082
- Dobin, A., Davis, C. A., Schlesinger, F., Drenkow, J., Zaleski, C., Jha, S., et al. (2013). STAR: ultrafast universal RNA-seq aligner. *Bioinformatics* 29, 15–21. doi: 10.1093/bioinformatics/bts635
- Dong, Y., Taylor, J. R., Wolf, M. E., and Shaham, Y. (2017). Circuit and synaptic plasticity mechanisms of drug relapse. *J. Neurosci.* 37, 10867–10876. doi: 10.1523/JNEUROSCI.1821-17.2017
- Duttke, S. H., Chang, M. W., Heinz, S., and Benner, C. (2019). Identification and dynamic quantification of regulatory elements using total RNA. *Genome Res.* 29, 1836–1846. doi: 10.1101/gr.253492.119
- Ernst, J., Kheradpour, P., Mikkelsen, T. S., Shores, N., Ward, L. D., Epstein, C. B., et al. (2011). Mapping and analysis of chromatin state dynamics in nine human cell types. *Nature* 473, 43–49. doi: 10.1038/nature09906
- Everitt, B. J. (2014). Neural and psychological mechanisms underlying compulsive drug seeking habits and drug memories—indications for novel treatments of addiction. *Eur. J. Neurosci.* 40, 2163–2182. doi: 10.1111/ejn.12644
- Fan, A. Z., Chou, S. P., Zhang, H., Jung, J., and Grant, B. F. (2019). Prevalence and correlates of past-year recovery from DSM-5 alcohol use disorder: results from national epidemiologic survey on alcohol and related conditions-III. *Alcohol. Clin. Exp. Res.* 43, 2406–2420. doi: 10.1111/acer.14192
- Fattore, L., and Melis, M. (2016). Sex differences in impulsive and compulsive behaviors: a focus on drug addiction. *Addict. Biol.* 21, 1043–1051. doi: 10.1111/adb.12381
- Ferguson, D., Shao, N., Heller, E., Feng, J., Neve, R., Kim, H.-D., et al. (2015). SIRT1-FOXO3a regulate cocaine actions in the nucleus accumbens. *J. Neurosci.* 35, 3100–3111. doi: 10.1523/JNEUROSCI.4012-14.2015
- George, O., and Koob, G. F. (2010). Individual differences in prefrontal cortex function and the transition from drug use to drug dependence. *Neurosci. Biobehav. Rev.* 35, 232–247. doi: 10.1016/j.neubiorev.2010.05.002
- George, O., Mandyam, C. D., Wee, S., and Koob, G. F. (2008). Extended access to cocaine self-administration produces long-lasting prefrontal cortex-dependent working memory impairments. *Neuropsychopharmacology* 33, 2474–2482. doi: 10.1038/sj.npp.1301626
- Gipson, C. D., Kupchik, Y. M., and Kalivas, P. W. (2014). Rapid, transient synaptic plasticity in addiction. *Neuropharmacology* 76 Pt B, 276–286. doi: 10.1016/j.neuropharm.2013.04.032
- Goldstein, R. Z., and Volkow, N. D. (2011). Dysfunction of the prefrontal cortex in addiction: neuroimaging findings and clinical implications. *Nat. Rev. Neurosci.* 12, 652–669.
- Hamilton, P. J., and Nestler, E. J. (2019). Epigenetics and addiction. *Curr. Opin. Neurobiol.* 59, 128–136.

- Heinz, S., Benner, C., Spann, N., Bertolino, E., Lin, Y. C., Laslo, P., et al. (2010). Simple combinations of lineage-determining transcription factors prime cis-regulatory elements required for macrophage and B cell identities. *Mol. Cell* 38, 576–589. doi: 10.1016/j.molcel.2010.05.004
- Heinz, S., Romanoski, C. E., Benner, C., and Glass, C. K. (2015). The selection and function of cell type-specific enhancers. *Nat. Rev. Mol. Cell Biol.* 16, 144–154. doi: 10.1038/nrm3949
- Heinz, S., Texari, L., Hayes, M. G. B., Urbanowski, M., Chang, M. W., Givarkes, N., et al. (2018). Transcription elongation can affect genome 3D structure. *Cell* 174, 1522–1536.e22. doi: 10.1016/j.cell.2018.07.047
- Hetzl, J., Duttke, S. H., Benner, C., and Chory, J. (2016). Nascent RNA sequencing reveals distinct features in plant transcription. *Proc. Natl. Acad. Sci. U.S.A.* 113, 12316–12321. doi: 10.1073/pnas.1603217113
- Hope, B. T., Nye, H. E., Kelz, M. B., Self, D. W., Iadarola, M. J., Nakabeppu, Y., et al. (1994). Induction of a long-lasting AP-1 complex composed of altered Fos-like proteins in brain by chronic cocaine and other chronic treatments. *Neuron* 13, 1235–1244.
- Joo, J.-Y., Schaukowitz, K., Farbiak, L., Kilaru, G., and Kim, T.-K. (2016). Stimulus-specific combinatorial functionality of neuronal c-fos enhancers. *Nat. Neurosci.* 19, 75–83. doi: 10.1038/nn.4170
- Kaikkonen, M. U., Spann, N. J., Heinz, S., Romanoski, C. E., Allison, K. A., Stender, J. D., et al. (2013). Remodeling of the enhancer landscape during macrophage activation is coupled to enhancer transcription. *Mol. Cell* 51, 310–325. doi: 10.1016/j.molcel.2013.07.010
- Kallupi, M., Carrette, L. L. G., Kononoff, J., Solberg Woods, L. C., Palmer, A. A., Schweitzer, P., et al. (2020). Nociceptin attenuates the escalation of oxycodone self-administration by normalizing CeA-GABA transmission in highly addicted rats. *Proc. Natl. Acad. Sci. U.S.A.* 117, 2140–2148. doi: 10.1073/pnas.1915143117
- Kim, T.-K., Hemberg, M., Gray, J. M., Costa, A. M., Bear, D. M., Wu, J., et al. (2010). Widespread transcription at neuronal activity-regulated enhancers. *Nature* 465, 182–187. doi: 10.1038/nature09033
- Koob, G. F., and Volkow, N. D. (2016). Neurobiology of addiction: a neurocircuitry analysis. *Lancet Psychiatry* 3, 760–773. doi: 10.1016/S2215-0366(16)00104-8
- Koob, G. F., Buck, C. L., Cohen, A., Edwards, S., Park, P. E., Schlosburg, J. E., et al. (2014). Addiction as a stress surfeit disorder. *Neuropharmacology* 76 Pt B, 370–382. doi: 10.1016/j.neuropharm.2013.05.024
- Lacagnina, M. J., Rivera, P. D., and Bilbo, S. D. (2017). Glial and neuroimmune mechanisms as critical modulators of drug use and abuse. *Neuropsychopharmacology* 42, 156–177. doi: 10.1038/npp.2016.121
- Levine, M. (2010). Transcriptional enhancers in animal development and evolution. *Curr. Biol.* 20, R754–R763. doi: 10.1016/j.cub.2010.06.070
- Li, W., Notani, D., and Rosenfeld, M. G. (2016). Enhancers as non-coding RNA transcription units: recent insights and future perspectives. *Nat. Rev. Genet.* 17, 207–223. doi: 10.1038/nrg.2016.4
- Li, Y. E., Preissl, S., Hou, X., Zhang, Z., Zhang, K., Qiu, Y., et al. (2021). An atlas of gene regulatory elements in adult mouse cerebrum. *Nature* 598, 129–136.
- Liang, T., Kimpel, M. W., McClintick, J. N., Skillman, A. R., McCall, K., Edenberg, H. J., et al. (2010). Candidate genes for alcohol preference identified by expression profiling in alcohol-preferring and -nonpreferring reciprocal congenic rats. *Genome Biol.* 11:R11. doi: 10.1186/gb-2010-11-2-r11
- Lieberman-Aiden, E., van Berkum, N. L., Williams, L., Imakaev, M., Ragoczy, T., Telling, A., et al. (2009). Comprehensive mapping of long-range interactions reveals folding principles of the human genome. *Science* 326, 289–293. doi: 10.1126/science.1181369
- Lim, J.-Y., Duttke, S. H., Baker, T. S., Lee, J., Gambino, K. J., Venturini, N. J., et al. (2021). DNMT3A haploinsufficiency causes dichotomous DNA methylation defects at enhancers in mature human immune cells. *J. Exp. Med.* 218:e20202733. doi: 10.1084/jem.20202733
- Love, M. I., Huber, W., and Anders, S. (2014). Moderated estimation of fold change and dispersion for RNA-seq data with DESeq2. *Genome Biol.* 15:550. doi: 10.1186/s13059-014-0550-8
- McClung, C. A., and Nestler, E. J. (2003). Regulation of gene expression and cocaine reward by CREB and  $\Delta$ FosB. *Nat. Neurosci.* 6, 1208–1215. doi: 10.1038/nn1143
- McLean, C. Y., Bristor, D., Hiller, M., Clarke, S. L., Schaaf, B. T., Lowe, C. B., et al. (2010). GREAT improves functional interpretation of cis-regulatory regions. *Nat. Biotechnol.* 28, 495–501. doi: 10.1038/nbt.1630
- Mikhaylichenko, O., Bondarenko, V., Harnett, D., Schor, I. E., Males, M., Viales, R. R., et al. (2018). The degree of enhancer or promoter activity is reflected by the levels and directionality of eRNA transcription. *Genes Dev.* 32, 42–57. doi: 10.1101/gad.308619.117
- Ong, C.-T., and Corces, V. G. (2011). Enhancer function: new insights into the regulation of tissue-specific gene expression. *Nat. Rev. Genet.* 12, 283–293. doi: 10.1038/nrg2957
- Ostuni, R., Piccolo, V., Barozzi, I., Polletti, S., Termanini, A., Bonifacio, S., et al. (2013). Latent enhancers activated by stimulation in differentiated cells. *Cell* 152, 157–171. doi: 10.1016/j.cell.2012.12.018
- Porrino, L. J., and Lyons, D. (2000). Orbital and medial prefrontal cortex and psychostimulant abuse: studies in animal models. *Cereb. Cortex* 10, 326–333.
- Pierce, R. C., Fant, B., Swinford-Jackson, S. E., Heller, E. A., Berrettini, W. H., and Wimmer, M. E. (2018). Environmental, genetic and epigenetic contributions to cocaine addiction. *Neuropsychopharmacology* 43, 1471–1480. doi: 10.1038/s41386-018-0008-x
- Russo, S. J., Dietz, D. M., Dumitriu, D., Morrison, J. H., Malenka, R. C., and Nestler, E. J. (2010). The addicted synapse: mechanisms of synaptic and structural plasticity in nucleus accumbens. *Trends Neurosci.* 33, 267–276. doi: 10.1016/j.tins.2010.02.002
- Scherma, M., Qvist, J. S., Asok, A., Huang, S.-S. C., Masia, P., Deidda, M., et al. (2020). Cannabinoid exposure in rat adolescence reprograms the initial behavioral, molecular, and epigenetic response to cocaine. *Proc. Natl. Acad. Sci. U.S.A.* 117, 9991–10002. doi: 10.1073/pnas.1920866117
- Sedighim, S., Carrette, L. L., Venniro, M., Shaham, Y., de Guglielmo, G., and George, O. (2021). Individual differences in addiction-like behaviors and choice between cocaine versus food in Heterogeneous Stock rats. *Psychopharmacology* 238, 3423–3433. doi: 10.1007/s00213-021-05961-1
- Sheffield, N. C., Thurman, R. E., Song, L., Safi, A., Stamatoyannopoulos, J. A., Lenhard, B., et al. (2013). Patterns of regulatory activity across diverse human cell types predict tissue identity, transcription factor binding, and long-range interactions. *Genome Res.* 23, 777–788. doi: 10.1101/gr.152140.112
- Skupio, U., Tertilt, M., Bilecki, W., Barut, J., Korostynski, M., Golda, S., et al. (2020). Astrocytes determine conditioned response to morphine via glucocorticoid receptor-dependent regulation of lactate release. *Neuropsychopharmacology* 45, 404–415. doi: 10.1038/s41386-019-0450-4
- Slezak, M., Korostynski, M., Gieryk, A., Golda, S., Dzbek, J., Piechota, M., et al. (2013). Astrocytes are a neural target of morphine action via glucocorticoid receptor-dependent signaling. *Glia* 61, 623–635. doi: 10.1002/glia.22460
- Solberg Woods, L. C., and Palmer, A. A. (2019). Using heterogeneous stocks for fine-mapping genetically complex traits. *Methods Mol. Biol.* 2018, 233–247. doi: 10.1007/978-1-4939-9581-3\_11
- Srinivasan, S., Shariff, M., and Bartlett, S. E. (2013). The role of the glucocorticoids in developing resilience to stress and addiction. *Front. Psychiatry* 4:68. doi: 10.3389/fpsy.2013.00068
- Stewart, A. F., Fulton, S. L., and Maze, I. (2021). Epigenetics of drug addiction. *Cold Spring Harb. Perspect. Med.* 11, a040253. doi: 10.1101/cshperspect.a040253
- Stuart, T., Srivastava, A., Madad, S., Lareau, C. A., and Satija, R. (2021). Single-cell chromatin state analysis with Signac. *Nat. Methods* 18, 1333–1341. doi: 10.1038/s41592-021-01282-5
- Teague, C. D., and Nestler, E. J. (2021). Key transcription factors mediating cocaine-induced plasticity in the nucleus accumbens. *Mol. Psychiatry* 27, 687–709. doi: 10.1038/s41380-021-01163-5
- Telesse, F., Ma, Q., Perez, P. M., Notani, D., Oh, S., Li, W., et al. (2015). LRP8-reelin-regulated neuronal enhancer signature underlying learning and memory formation. *Neuron* 86, 696–710. doi: 10.1016/j.neuron.2015.03.033
- Thibodeau, A., Eroglu, A., McGinnis, C. S., Lawlor, N., Nehar-Belaid, D., Kursawe, R., et al. (2021). AMULET: a novel read count-based method for effective multiplex detection from single nucleus ATAC-seq data. *Genome Biol.* 22:252. doi: 10.1186/s13059-021-02469-x
- Vendruscolo, L. F., Barbier, E., Schlosburg, J. E., Misra, K. K., Whitfield, T. W. Jr., Logrip, M. L., et al. (2012). Corticosteroid-dependent plasticity mediates compulsive alcohol drinking in rats. *J. Neurosci.* 32, 7563–7571. doi: 10.1523/JNEUROSCI.0069-12.2012
- Vendruscolo, L. F., Estey, D., Goodell, V., Macshane, L. G., Logrip, M. L., Schlosburg, J. E., et al. (2015). Glucocorticoid receptor antagonism decreases alcohol seeking in alcohol-dependent individuals. *J. Clin. Invest.* 125, 3193–3197. doi: 10.1172/JCI79828

- Volkow, N. D., Wang, G.-J., Ma, Y., Fowler, J. S., Wong, C., Ding, Y.-S., et al. (2015). Activation of orbital and medial prefrontal cortex by methylphenidate in cocaine-addicted subjects but not in controls: relevance to addiction. *J. Neurosci.* 25, 3932–3939.
- Wang, Z., Chivu, A. G., Choate, L. A., Rice, E. J., Miller, D. C., Chu, T., et al. (2022). Prediction of histone post-translational modification patterns based on nascent transcription data. *Nat. Genet.* 54, 295–305.
- Werner, C. T., Altshuler, R. D., Shaham, Y., and Li, X. (2021). Epigenetic mechanisms in drug relapse. *Biol. Psychiatry* 89, 331–338. doi: 10.1016/j.biopsych.2020.08.005
- Wu, R., and Li, J.-X. (2020). Toll-like receptor 4 signaling and drug addiction. *Front. Pharmacol.* 11:603445. doi: 10.3389/fphar.2020.603445
- Yao, Z., Liu, H., Xie, F., Fischer, S., Adkins, R. S., Aldridge, A. I., et al. (2021). A transcriptomic and epigenomic cell atlas of the mouse primary motor cortex. *Nature* 598, 103–110.
- Zachariou, V., Bolanos, C. A., Selley, D. E., Theobald, D., Cassidy, M. P., Kelz, M. B., et al. (2006). An essential role for  $\Delta$ FosB in the nucleus accumbens in morphine action. *Nat. Neurosci.* 9, 205–211. doi: 10.1038/n1636
- Zhang, Y., Liu, T., Meyer, C. A., Eeckhoutte, J., Johnson, D. S., Bernstein, B. E., et al. (2008). Model-based analysis of ChIP-Seq (MACS). *Genome Biology* 9, R137. doi: 10.1186/gb-2008-9-9-r137
- Zhang, Z., Zhou, J., Tan, P., Pang, Y., Rivkin, A. C., Kirchgessner, M. A., et al. (2021). Epigenomic diversity of cortical projection neurons in the mouse brain. *Nature* 598, 167–173.
- Ziffra, R. S., Kim, C. N., Ross, J. M., Wilfert, A., Turner, T. N., Haeussler, M., et al. (2021). Single-cell epigenomics reveals mechanisms of human cortical development. *Nature* 598, 205–213.
- Zuo, L., Lu, L., Tan, Y., Pan, X., Cai, Y., Wang, X., et al. (2014). Genome-wide association discoveries of alcohol dependence. *Am. J. Addict.* 23, 526–539. doi: 10.1111/j.1521-0391.2014.12147.x

**Conflict of Interest:** The authors declare that the research was conducted in the absence of any commercial or financial relationships that could be construed as a potential conflict of interest.

**Publisher's Note:** All claims expressed in this article are solely those of the authors and do not necessarily represent those of their affiliated organizations, or those of the publisher, the editors and the reviewers. Any product that may be evaluated in this article, or claim that may be made by its manufacturer, is not guaranteed or endorsed by the publisher.

Copyright © 2022 Duttke, Montilla-Perez, Chang, Li, Chen, Carrette, Guglielmo, George, Palmer, Benner and Telese. This is an open-access article distributed under the terms of the Creative Commons Attribution License (CC BY). The use, distribution or reproduction in other forums is permitted, provided the original author(s) and the copyright owner(s) are credited and that the original publication in this journal is cited, in accordance with accepted academic practice. No use, distribution or reproduction is permitted which does not comply with these terms.

# Advantages of publishing in Frontiers



## OPEN ACCESS

Articles are free to read  
for greatest visibility  
and readership



## FAST PUBLICATION

Around 90 days  
from submission  
to decision



## HIGH QUALITY PEER-REVIEW

Rigorous, collaborative,  
and constructive  
peer-review



## TRANSPARENT PEER-REVIEW

Editors and reviewers  
acknowledged by name  
on published articles

## Frontiers

Avenue du Tribunal-Fédéral 34  
1005 Lausanne | Switzerland

**Visit us:** [www.frontiersin.org](http://www.frontiersin.org)

**Contact us:** [frontiersin.org/about/contact](http://frontiersin.org/about/contact)



## REPRODUCIBILITY OF RESEARCH

Support open data  
and methods to enhance  
research reproducibility



## DIGITAL PUBLISHING

Articles designed  
for optimal readership  
across devices



## FOLLOW US

@frontiersin



## IMPACT METRICS

Advanced article metrics  
track visibility across  
digital media



## EXTENSIVE PROMOTION

Marketing  
and promotion  
of impactful research



## LOOP RESEARCH NETWORK

Our network  
increases your  
article's readership